

Society of Earth Scientists Series

Harendra Nath Bhattacharya
Soma Bhattacharya
Balai Chandra Das
Aznarul Islam *Editors*

Himalayan Neotectonics and Channel Evolution



 Springer

Society of Earth Scientists Series

Series Editor

Satish C. Tripathi, Lucknow, India

The Society of Earth Scientists Series aims to publish selected conference proceedings, monographs, edited topical books/text books by leading scientists and experts in the field of geophysics, geology, atmospheric and environmental science, meteorology and oceanography as Special Publications of The Society of Earth Scientists. The objective is to highlight recent multidisciplinary scientific research and to strengthen the scientific literature related to Earth Sciences. Quality scientific contributions from all across the Globe are invited for publication under this series. Series Editor: Dr. Satish C. Tripathi

More information about this series at <https://link.springer.com/bookseries/8785>

Harendra Nath Bhattacharya · Soma Bhattacharya ·
Balai Chandra Das · Aznarul Islam
Editors

Himalayan Neotectonics and Channel Evolution



 Springer

Editors

Harendra Nath Bhattacharya
Department of Earth Sciences
Techno India University
Kolkata, India

Soma Bhattacharya 
Department of Geography
Vivekananda College for Women
Kolkata, India

Balai Chandra Das 
Department of Geography
Krishnagar Government College
Krishnanagar, India

Aznarul Islam 
Department of Geography
Aliah University
Kolkata, India

ISSN 2194-9204

ISSN 2194-9212 (electronic)

Society of Earth Scientists Series

ISBN 978-3-030-95434-5

ISBN 978-3-030-95435-2 (eBook)

<https://doi.org/10.1007/978-3-030-95435-2>

© The Editor(s) (if applicable) and The Author(s), under exclusive license to Springer Nature Switzerland AG 2022

This work is subject to copyright. All rights are solely and exclusively licensed by the Publisher, whether the whole or part of the material is concerned, specifically the rights of translation, reprinting, reuse of illustrations, recitation, broadcasting, reproduction on microfilms or in any other physical way, and transmission or information storage and retrieval, electronic adaptation, computer software, or by similar or dissimilar methodology now known or hereafter developed.

The use of general descriptive names, registered names, trademarks, service marks, etc. in this publication does not imply, even in the absence of a specific statement, that such names are exempt from the relevant protective laws and regulations and therefore free for general use.

The publisher, the authors and the editors are safe to assume that the advice and information in this book are believed to be true and accurate at the date of publication. Neither the publisher nor the authors or the editors give a warranty, expressed or implied, with respect to the material contained herein or for any errors or omissions that may have been made. The publisher remains neutral with regard to jurisdictional claims in published maps and institutional affiliations.

This Springer imprint is published by the registered company Springer Nature Switzerland AG
The registered company address is: Gewerbestrasse 11, 6330 Cham, Switzerland

Series Editor Foreword

The picturesque Andaman and Nicobar Islands of India is a chain of N-S trending islands at the juncture of the Bay of Bengal in the west and the Andaman Sea in the east. This archipelago attracted the geoscientists because the Andaman Sea is an active backarc basin lying above and behind the Sunda subduction zone where convergence between the overriding Southeast Asian plate and the subducting Australian plate is highly oblique. The geological and tectonic history of the Andaman Sea cannot be separated from Myanmar (Burma) on the north and Sumatra on the south, as such representing an important sector of India–Asia collision and its timing and evolution when compared with the Himalayan belt. The book on geology, tectonics and Palaeoclimate of the Andaman Islands and adjoining offshore will certainly open new vistas for future researches.

The mega-event of 36th International Geological Congress 2020 in India opened a new chapter on the Geology of India. On such an occasion Society of Earth Scientist Series by Springer decided to bring out 36th IGC Commemorative Volumes on various recent geological and geophysical studies of India. As such veteran geoscientists were requested to prepare comprehensive accounts as monographs or edited volumes. I am personally thankful to all the editors and authors for the timely submission of high-quality manuscripts for inviting interest of the global community of geoscientists.

Lucknow, India

Satish C. Tripathi
Series Editor

Foreword

Once Sara Jeannette Duncan uttered ‘When God gave men tongues, He never dreamed that they would want to talk about the Himalayas; there are consequently no words in the world to do it with’. Yet hundreds of geoscientists across the world are endeavouring to have those words! They have not only dated back to the birth of the Himalayas but also spotted the light on the processes of differential folding, faulting, inverted metamorphism, thrusting, napping, etc. Explorations from time to time sometimes strengthen the older findings, while in some other cases making prominent doubts. As the Himalayas is a tectonically active everchanging face of the earth, not only its structural geology has become complex to more complex but also its landforms show a convoluted mode of evolution. In the direction of river channel evolution under the impact of the Himalayan neotectonics, some veteran authors garlanded this volume with their precious contributions.

The mega-event of the 36th International Geological Congress 2020 in India opened a new chapter on the Geology of India. On such an occasion, the Society of Earth Scientist Series by Springer decided to bring out 36th IGC Commemorative Volumes on various recent geological and geophysical studies of India. As such veteran geoscientists were requested to prepare comprehensive accounts as monographs or edited volumes. I am personally thankful to all the editors and authors for the timely submission of high-quality manuscripts for inviting the interest of the global community of geoscientists.

Lucknow, India

Satish C. Tripathi
Series Editor

Preface

Tectonic forces and subaerial processes are working in opposite directions to shape the earth's surface forms. More recent is the tectonics more prominent imprints of it are on the forms of landscape. On the other side, most of the solid earth's surface (except permafrost and too dry areas) is under the impact of fluvial processes and being highly sensitive to slope, structure and lithology rivers are good geomorphic markers. Therefore, most of the earth's surface forms bear the fused expression of tectonics and fluvial processes. The Himalaya is tectonically the most perturbed belt in the Indian subcontinent where fluvial processes are also the most active subaerial process. River channel forms (plan form and cross-sectional form) through the course of their evolution bear the signature of both tectonics and fluvial actions. The Foreland Basin, the Ganga-Brahmaputra-Meghna Basin are also under the influence of neotectonics. In these regions of low-magnitude landforms, river terraces, channel avulsions, crisscrossed river lines, etc. follow direct or indirect dictates of the tectonics of the recent past.

The importance of understanding the channel evolution under the impact of sub-surface tectonics is long felt and decoding of sub-surface tectonics using tools of surface fluvial features is widely used practice. A recent study of earth science is of cross-knowledge nature. Understanding of the earth's surface from the viewpoint of morpho-tectonics is only grasped when knowledge of geomorphology and geology fuses. Having this acute urge in mind, Dr. Aznarul Islam took the key initiative to frame a board of editors of four fusing geology and geography to address issues on Himalayan Neotectonics and Channel Evolution.

We invited chapters from scholars with expertise in the field. After a long process of 1.5 years, we collected all 15 chapters on Himalayan Neotectonics and Channel Evolution of different river basins. We hope the reader's thirst for tectonic geomorphology of the Indian Himalayan region will achieve contentment in this volume. Academicians from a wide group of disciplines such as earth science, geology, geography, geomorphology, river science and river engineering, who are keen to know about tectonic fluvial geomorphology of the region will be benefited from the volume.

We acknowledge our heartiest gratitude to authors who offered their best for this volume. We acknowledge our deepest gratitude to them. Special thanks to

our colleagues and friends for their sincere support. We are thankful to all our students who helped in the field and the lab for the successful completion of this book. Finally, we acknowledge our sincere gratitude to the Springer Nature Switzerland AG, especially Dr. Annett Büttner, Executive Editor of Geology, Geochemistry, Volcanology, Mineralogy, Geophysics, Interdisciplinary Geosciences, Springer Heidelberg; Dieter Merkle, Vice President, Springer Nature Switzerland AG and Guido Zosimo-Landolfo, Editorial Director/Asset Manager, and their team for their interest in working with us.

West Bengal, India
30 April 2021

Harendra Nath Bhattacharya
Soma Bhattacharya
Balai Chandra Das
Aznarul Islam

Contents

Neotectonic Movements and Channel Evolution in the Indian Subcontinent: Issues, Challenges and Prospects	1
Soma Bhattacharya, Harendra Nath Bhattacharya, Balai Chandra Das, and Aznarul Islam	
Effects of Differential Tectonic Uplift on Steepness and Concavity Indices and Erosion Rates in Between the Major Thrusts in Bhagirathi-Alaknanda Catchments, NW Himalayas, India	51
Sumit Das and Satish J. Sangode	
Spatial Variability of Topographic Attributes and Channel Morphological Characteristics in the Ladakh Trans-Himalayas and Their Tectonic and Structural Controls	67
Priyank Pravin Patel, Shantamoy Guha, Debsmita Das, and Madhurima Bose	
Geomorphic Response of the Solani River Basin to Neotectonics: A Study from the Western Himalayan Foothills, India	111
Narendra K. Patel and Pitambar Pati	
Tectonic Control on the Meanders Pattern of Alaknanda River in Srinagar Valley, Garhwal Himalaya, India	133
Sapna Semwal and D. D. Chauniyal	
Significance of Channel Planform Change and Morphometric Indices in the Buri River Basin, India and Bangladesh	151
Saheli Bhattacharjee, Sunando Bandyopadhyay, and Sunil Kumar De	
Morphotectonic Expressions of the Drainage Basins and Channel Long Profile Forms on a Selected Part of Sikkim-Bhutan Himalayas ...	175
Ujwal Deep Saha, Nilanjana Biswas, Sushonova Mondal, and Soma Bhattacharya	

Development of the Dharala River Course and Its Response to Neotectonic Indentations-Evidences from Old Data Inventory, Satellite Images and Sedimentary Architecture	207
Ujwal Deep Saha, Soma Bhattacharya, Harendra Nath Bhattacharya, and Sanjana Dutt	
Preliminary Study of the Manabhum Anticline: A Possible Key to Better Understanding the Quaternary Tectonics of the Eastern Himalayan Syntaxial Zone	239
Chandreyee Goswami Chakrabarti, Belligraham Narzary, John C Weber, Prasun Jana, Somhrita Bhattacharjee, and Manoj Jaiswal	
Assessment of Neotectonic Effect on Quaternary Deposits in Darjeeling Himalayas	261
Sunipa Mandal and Pinaki Roy	
Himalayan Foredeep Neotectonics and Deformed Riverscape Landforms: An Integrated Discussion, West Bengal, India	289
Adrija Raha and Mery Biswas	
Evaluating the Relative Tectonic Response of the Fluvial Systems Using Multicriteria Entropy Method: A Case Study of the Rangit Catchment, Eastern Himalayas, India	315
Lopamudra Roy, Somasis Sengupta, Sayantan Das, and Arindam Sarkar	
Role of Active Tectonism and Geomorphic Drivers on Channel Oscillation of the Raidak-I River in the Eastern Himalayan Foothills, India	345
Md. Hasanuzzaman, Pravat Kumar Shit, and Aznarul Islam	
Morphotectonics of the Chel River Basin, Eastern Himalaya, India: Insights from Shuttle Radar Topography Mission Digital Elevation Model- Based Geomorphic Indices	367
Sonam Lama and Ramkrishna Maiti	
Influence of Neotectonics on Channel Evolution of Kameng River, North-East Himalaya	397
Balai Chandra Das, Suman Deb Barman, and Aznarul Islam	

Editors and Contributors

About the Editors



Dr. Harendra Nath Bhattacharya born in 1954, is presently Professor of Earth Sciences, Techno India University, West Bengal, Salt Lake, Kolkata 700091, India with ongoing Department of Science and Technology (DST) projects. He was formerly a Professor and Head in the Department of Geology, Presidency University, Kolkata. He stood first class first in B.Sc. Honours in Geology from Jadavpur University, Kolkata. He did his Master's in Applied Geology (first class first) from Jadavpur University, Kolkata. He did his Ph.D. in Ore Geology from the same University. His field of specialization is Ore Geology and Sedimentology. He has already supervised 13 Ph.D. and another 06 pursuing. He visited as a Scientist, Johannesburg University, Johannesburg, South Africa, 2003, for 3 months to do research on Iron Ore Deposits. Further, he visited as scientist, Centre of Ore Deposit Research, University of Tasmania, Australia, 2003–2004 for 6 months. He taught Economic Geology in the Department of Geology, Kumaun University, Uttarakhand as Visiting Professor (March 2012). He also visited Department of Geology, University of Pretoria, South Africa as Visiting Professor (May–June 2013). He delivered a lecture series on 'Crustal Evolution and Metallogeny of India'. He visited Indonesia several times to perform exploration work for Manganese and Coal. He is a member of some academic/professional bodies including West Bengal Academy of Science and

Technology (WAST, the International Sedimentological Association, Geological Society of India, Bangalore, Editorial Board member, Indian Journal of Geo-sciences (published by Geological Survey of India). He is a recipient of national awards including '*National Mineral Award, Government of India*, for significant contributions in Geology in the year 2004', Prof. N. N. Chatterjee Medal (1987) from *The Asiatic Society*, Kolkata for contribution to the knowledge of Economic Geology.



Dr. Soma Bhattacharya a distinguish scholar, did her M.Phil. from North Eastern Hill University, Shillong, Meghalaya, India and Ph.D. from University of Calcutta, West Bengal, India. She is a student of Geomorphology with special interest in Neotectonics and foothill Geomorphology particularly in Eastern Himalayas. She also has profound research experience in Anthropogenic Geomorphology and did research work on micro- and meso-level landforms developed due to various anthropogenic activities. Her speciality is detailed fieldwork-based studies. With scholarly presentation she has attended many national and international conferences and symposiums over the world and conducted three research projects funded by University Grants Commissions. She has 12 published papers in books and journals of national and international repute. She is life member of Geographical Society of India and Indian Institute of Geomorphologists. She is also enlisted Reviewer of Elsevier. Presently, she is the Principal of Vivekananda College for Women, Barisha, Kolkata-700008, India, working also as Professor of Post-graduate Department and Research Centre in Geography of the same college affiliated to University of Calcutta.



Dr. Balai Chandra Das born in 1970, earned his Bachelor's degree (1992) and Master's degree (1994) in Geography from the University of Burdwan and was awarded Ph.D. degree in geography from the University of Calcutta. He has published more than 30 research articles in journals/edited volumes of national and international repute. He is the corresponding Editor of two books *Neo-Thinking on Ganges Brahmaputra Basin Geomorphology* and *Quaternary Geomorphology in India—Case Studies from the Lower Ganga Basin*, Springer International Publishing, Switzerland and another book 'Anthropogeomorphology of Bhagirathi-Hooghly River System in India', Taylor & Francis Group. Reviewed manuscripts of five International Earth Science Journals of *Springer* and *Current Science* in India. He is an editorial board member of two international journals. He was one of the members of the *Scientific Committee of IWC-2016* and *WRAA-2020 held at Sultan Qaboos University, Oman*. His current research interest is on the fundamental geomorphology of rivers and lakes.



Dr. Aznarul Islam is an Applied Fluvial Geomorphologist with M.Sc. degree in Geography from Kalyani University, West Bengal and M.Phil. and Ph.D. in Geography from the University of Burdwan, West Bengal. He is currently engaged as an Assistant Professor in the Department of Geography, Aliah University, Kolkata. Previously, he was engaged in teaching and research at the Department of Geography, Barasat Govt. College, West Bengal. He has already published more than 20 research papers in different journals of national and international repute. He has contributed four book chapters in edited volumes and one conference proceedings. He is an Editor of *Neo-Thinking on Ganges Brahmaputra Basin Geomorphology*, Springer International Publishing, Switzerland. He has presented papers in more than 20 national and international seminar and conferences. He had delivered several invited lectures and special lectures in different national and regional programmes. He has been performing the role of a reviewer of Environment, Development and Sustainability, Springer; Modelling Earth System science and Environment, Springer and Spatial Information Research, Springer. He is a life member of Indian

Geographical Foundation (IGF), Kolkata and National Association of Geographers, India (NAGI), New Delhi. He was an Assistant Convenor of the 2-day national seminar: Geography of Habitat (26–27 February 2016), organized by foundation of practicing geographer. Till date he has successfully supervised more than 25 dissertations on various topics of geomorphology at master's level. Currently, he is supervising four Ph.D. students in Geomorphology. His principal area of research includes channel shifting and river bank erosion. Currently, he is deeply engaged in the analysis of channel shifting and bank erosion of the River Bhagirathi, West Bengal and its impact on society and economy.

Contributors

Sunando Bandyopadhyay Department of Geography, University of Calcutta, Kolkata, India

Suman Deb Barman Independant Researcher, Barasat, India

Somhrita Bhattacharjee Department of Geology, University of Calcutta, Kolkata, India

Harendra Nath Bhattacharya Department of Earth Sciences, Techno India University Kolkata, Kolkata, West Bengal, India

Soma Bhattacharya Vivekananda College for Women, Barisha, Kolkata, India

Saheli Bhattacharjee Department of Geography, University of Calcutta, Kolkata, India

Mery Biswas Department of Geography, Presidency University, Kolkata, West Bengal, India

Nilanjana Biswas Vivekananda College for Women, Kolkata, India

Madhurima Bose Department of Geography, Presidency University, Kolkata, West Bengal, India

Chandreyee Goswami Chakrabarti Department of Geology, University of Calcutta, Kolkata, India;
Department of Neotectonics and ThermoChronology, Institute of Rock Structure and Mechanics, Prague, Czech Republic

D. D. Chauniyal Department of Geography, Nitya Nand Himalayan Research and Study Center, Doon University, Dehra Dun, India

Balai Chandra Das Department of Geography, Krishnagar Government College, Krishnagar, West Bengal, India

Debsmita Das Department of Geography, University of California, Santa Barbara, CA, USA

Sayantana Das Department of Geography, Dum Dum Motijheel College, Kolkata, India

Sumit Das Department of Geography, Savitribai Phule Pune University, Pune, India

Sunil Kumar De Department of Geography, North Eastern Hill University, Shillong, India

Sanjana Dutt Department of Geography, University of Calcutta, Kolkata, India

Shantamoy Guha Department of Earth Sciences, Indian Institute of Technology, Gandhinagar, Gujarat, India

Md. Hasanuzzaman PG Department of Geography, Raja N. L. Khan Women's College (Autonomous), Midnapore, India

Aznarul Islam Department of Geography, Aliah University, Kolkata, West Bengal, India

Manoj Jaiswal Department of Earth Science, Indian Institute of Science Education and Research, Kolkata, India

Prasun Jana Geological Survey of India, Northern Region, Lucknow, India

Sonam Lama Department of Geography, Darjeeling Govt. College, Darjeeling, West Bengal, India

Ramkrishna Maiti Department of Geography, Vidyasagar University, Medinipur, West Bengal, India

Sunipa Mandal Department of Geological Sciences, Jadavpur University, Kolkata, West Bengal, India

Sushonova Mondal SACT-I, Surendranath College for Women, Kolkata, India

Belligraham Narzary Department of Earth Science, Indian Institute of Science Education and Research, Kolkata, India

Narendra K. Patel Department of Earth Sciences, Indian Institute of Technology, Roorkee, Uttarakhand, India

Priyank Pravin Patel Department of Geography, Presidency University, Kolkata, West Bengal, India

Pitambar Pati Department of Earth Sciences, Indian Institute of Technology, Roorkee, Uttarakhand, India

Adrija Raha Department of Geography, Presidency University, Kolkata, West Bengal, India

Lopamudra Roy Department of Geography, Pakuahat Degree College, Malda, India

Pinaki Roy Department of Geology, Durgapur Government College, Durgapur, West Bengal, India

Ujwal Deep Saha University of Calcutta, Kolkata, India;
Department of Geography, Vivekananda College for Women, Barisha, Kolkata, India

Satish J. Sangode Department of Geology, Savitribai Phule Pune University, Pune, India

Arindam Sarkar Department of Geography, P.K.H.N. Mahavidyalaya, Howrah, India

Sapna Semwal Department of Geography, Nitya Nand Himalayan Research and Study Center, Doon University, Dehra Dun, India

Somasis Sengupta Department of Geography, The University of Burdwan, Bardhaman, India

Pravat Kumar Shit PG Department of Geography Raja N. L, Khan Women's College (Autonomous), Midnapore, India

John C Weber Department of Geology, Grand Valley State University, Allendale, MI, USA

Neotectonic Movements and Channel Evolution in the Indian Subcontinent: Issues, Challenges and Prospects



Soma Bhattacharya, Harendra Nath Bhattacharya, Balai Chandra Das, and Aznarul Islam

Abstract Neotectonics keeps its prominent signatures on river channel evolution. This chapter reviewed emergence, flourishing and advancement of the study of neotectonics, adjustment of fluvial forms and processes to neotectonics within the territory of Indian Subcontinent. Based on this review, we confirm the theme of the volume and suggest profuse scope of further research on the Himalayan Neotectonics and Channel Evolution in the Indian Subcontinent ranging from basin-scale to channel-site scale. We also introduced other chapters of the book.

Keywords Neotectonics · Quaternary evolution · Morphotectonic signatures · Dating techniques · Cratonic blocks · Pericratonic Basin · Early Proterozoic mobile belts · The Himalaya · The Indogangetic plain · The Ganga-Brahmaputra-Meghna delta · Indian Peninsular

1 Introduction

Neotectonics is a comparatively new branch of study dealing with the earth's deformation process continuing from recent geological time. Obruchev (1948) who used the term 'neotectonic' first "recognised the importance of the recent and active geological processes and proposed a new independent branch of Geosciences" (Pavlidis 1989). The study of neotectonics flourished since the last quarter of the twentieth century, being carried by researchers from different scientific disciplines

S. Bhattacharya (✉)

Vivekananda College for Women, Kolkata, West Bengal, India

H. N. Bhattacharya

Department of Earth Sciences, Techno India University Kolkata, Kolkata, West Bengal, India

B. C. Das

Post Graduate Department of Geography, Krishnagar Government College, Krishnagar, West Bengal, India

A. Islam

Department of Geography, Aliah University, Kolkata, West Bengal, India

like geology, geodesy, seismology, geomorphology, etc. and the subject is gaining popularity day by day as it permits detailed observation and analysis.

Definitions of neotectonics are varied where scientists try to emphasize the term from different angles; some try to define it from the point of view of time, either relative or absolute; some others from its structural and topographic implications. Such definitions arouse two questions: first, from when exactly neotectonic activity starts and second whether it is really possible to make a distinction between old and recent tectonics.

1.1 Definition of Neotectonics

If we arrange the definitions of neotectonics provided by various scientists and researchers chronologically we can recognise a trend. Instead of explaining the driving mechanism workers are more interested to define the term on the basis of its manifestation time either absolute or relative. The age of commencement as specified by different scientists for neotectonics varies widely. Obrutschow fixed the age of commencement to early Neogene, (Murawski 1972) whereas Gary et al. (1972) assigned it to Pliocene which was subsequently supported by Bates and Jackson (1980). On the other hand Bloom (1998) also assumed Neogene as the starting age of neotectonism and Vita-Finzi (1986) attributed it to Late Cenozoic. Diebold and Muller (1985) assigned neotectonics to the Quaternary epoch only. However, all these definitions extend the period of neotectonics up to the present time. Therefore, it appears that there is a lack of consciousness among the scientists regarding the actual period of neotectonic activity, as it is really tough to separate Neotectonic from Paleotectonic in field observations.

As a result, the later definitions describe the neotectonics in a relative time frame such as neotectonics start at a different time in different regions. As a consequence, the phrases like, ‘the recent geological past’ (Stewart 2005), ‘current tectonic regime’ (Stewart 2005), after ‘last significant tectonic reorganisation’ (Pavlides 1989), ‘contemporary stress field’ (Blenkinsop 1986), after completion of ‘the present day configuration of relative plate boundaries and motion’ (Hancock 1986); were used to demarcate the relative age and characteristics of neotectonics.

The International Union of Quaternary Research (INQUA) defines neotectonics “as any earth movements or deformation of the geodetic reference level, their mechanisms, their geological origin, their implications for various practical purposes and their future extrapolations”. According to Pavlides (1989) “neotectonics is the study of young tectonic events which have occurred or are still occurring in a given region after final orogeny or more precisely after its last significant tectonic reorganisation”. Stewart (2005) defines neotectonics “as the study of horizontal and vertical crustal movements that have occurred in the geologically recent past and which may be ongoing today”.

Therefore in conclusion it can be said that the neotectonics explain movements and structural deformations active when ‘contemporary stress field’ of a region is

established after the 'significant tectonic reorganisation' of the area. This implies that it occurred at different regions at different times. Often active tectonics is used as a synonym of 'neotectonics', though according to Wallace (1986) "active tectonics are tectonic movements which are expected to occur within a future time span of concern to society".

1.2 Implications of Neotectonics

Neotectonics involves both regional and isostatic deformations. As a result, they are common along the young orogenic mountain belts lying at active plate boundaries. The vertical crustal movements occur due to seismic displacements, glacio-hydro and sediment isostatic movements and also from anthropogenic changes. Mainly recent sediments bear their signature. Neotectonic movement of studies comprises a wide range of timescale. As Morner (1980) says, it includes movements from "instantaneous (seismic), $10-10^2$ (geodetic), 10^2-10^4 yr (Holocene studies), 10^4-10^6 yr (Pleistocene studies), up to about 10^7 yr if it is necessary to enable us to understand the origins of recorded movements". Neotectonic activities and their effects are generally smaller in scale than the paleo-tectonic activity. Neotectonics and seismological studies are supplementary to each other. It gives ample opportunity to study the role of tectonic activity on landform features through morphometric analysis. Quantitative techniques and analysis of remote sensing data are widely used in neotectonic and morphotectonic studies. Being recent they provide a scope of the investigation, measuring and monitoring of landscape evolution through field observation. Migration or lateral displacement of stream courses, abrupt deflection of streams, dissection and displacement of sub-recent or recent geomorphic feature, valley asymmetry, linear scarp, fan terraces, river terraces, increasing incision of rivers, formation of paleolakes due to ponding of rivers are some of the geomorphic indicators of neotectonics.

1.3 Determination of Age

Dating of features by field study and laboratory experiment is an important part of neotectonic studies. There are different dating processes- some deriving the relative age and some other the absolute age. Relative age is determined by the laws like the principle of superimposition, the principle of cross-cutting relationship, the principle of horizontality, the principle of lateral continuity, the principle of unconformity and through paleontological studies. Such features are generally identified on exposed vertical sections where the depth of rock mantle or soil cover is very little or they are completely absent. Boring is also done to decipher the stratigraphic relationship. The clast seismic velocity method, the study of weathering rinds, the study of obsidian hydration rind, depth of soil cover, the study of carbonate coatings

and other pedogenic indicators also help to derive the relative age of the surface and near-surface materials. Lichenometry is also a long-used technique of relative dating in geomorphology. All these are qualitative derivation.

To deduct absolute age several methods are used some of them are biological or geological and the remaining techniques are radiometric dating, luminescence dating, cosmogenic dating, chemical dating and paleomagnetic dating. The following table gives an idea regarding these dating techniques (see Table 1).

2 Neotectonics and Channel Morphology in Indian Subcontinent

Being highly dynamic in nature the fluvial systems bear signatures of adjustments to the latest phase of tectonic deformation of the area. As a result, the effect of neotectonics is displayed widely over the drainage basins of the world, though it is very difficult to discrete it from those of paleotectonics and other allogenic changes. Through appropriate analysis of such features, the tectonic and geomorphic evolutionary history of landscapes are summarised, which is the prime aim of this edited volume. The papers accrued in this volume incorporate interesting morphometric analysis to establish the influences rendered by neotectonic movements on channel evolution in the Indian subcontinent.

2.1 Physiographic and Geotectonic Divisions of Indian Subcontinent

Indian Subcontinent lies in the collision zone of Asian Plate with Indian Plate comprising of the countries of India, Pakistan, Bangladesh, Nepal and Bhutan. It is a surprising land mass embodying rigid and consolidated Paleo-Achaean Cratonic blocks; the Early Proterozoic mobile belts, the lofty Tertiary mountain chain, the Quaternary plains and deltas. The Himalayas, the world's highest mountain containing 10 out of 14 eight-thousander peaks of the world separates Indian Subcontinent from the rest of Asia. The Peninsular India comprises the southern block. In between, there are the largest alluvial plains and deltas of the world—the Indo Gangetic plains and the Ganga–Brahmaputra–Meghna delta (Fig. 1). The subcontinent is highly active tectonically as the Tertiary tectonic evolution has not been seized yet and the Indian plate is still moving towards the Asian Plate (at a rate of $58 + 4$ mm/year, Freymueller et al. 1996) and to the Sundaland. (at a rate of $34 + 6$ mm/year, Sahu et al. 2006). The neotectonic activity in the Indian subcontinent can be broadly classified into two—(i) Interplate tectonic activities are those associated with the Himalayas and the Indo-Gangetic Plains which are the direct products of inter plate collision of the Tertiary Era and (ii) Intraplate tectonic activities are those

Table 1 Different dating techniques

Method	Useful range	Materials needed	References
Radioisotopic ^{14}C	35 ka	Wood, shell	Libby (1955), Stuiver (1970)
U-Th	10–350 ka	Carbonate (corals speleothems) Silicate (zircon, mica)	Ku (1976)
Thermoluminescence (TL)	30–300 ka	Quartz or feldspar silt	Berger (1988)
Optically stimulated luminescence (OSL)	30–300 ka	Quartz silt	Aitken (1998)
Cosmogenic	0–4 Ma	Quartz	Lal (1988), Nishiizumi et al. (1991)
In situ ^{10}Be , ^{26}Al			
He, Ne	unlimited	Olivine, quartz	Cerling and Craig (1994)
^{36}Cl	0–4 Ma		Phillips et al. (1986)
Fission Track analysis	1 Ky–5 Ma	Apatite, Zircon sphene and Mica	
Chemical Tephrochronology	0–several Ma	Volcanic ash	Westgate and Gorton (1981), Sarna-Wojcicki et al. (1991)
Amino acid racemization	0–300 ka, temperature dependent	–	
Paleomagnetic Identification of reversals	>700 ka	Fine sediments, volcanic flows	Cox et al. (1964)
Secular variation	0–several Ma	Fine sediments	Creer (1962, 1967) Lund (1996)
Biological	0–10 ka, depending upon existence of a local master chronology	Wood	Fritts (1976), Jacoby et al. (1988), Yamaguchi and Hoblitt (1995)
Dendrochronology			
Sclerochronology	0–1000 yr	Coral	Buddemeier and Taylor (2000)

After Burbank and Anderson (2016)

associated with the reactivation of old fold and shear zones of the Indian Peninsular due to breaking, migration and collision of plates.

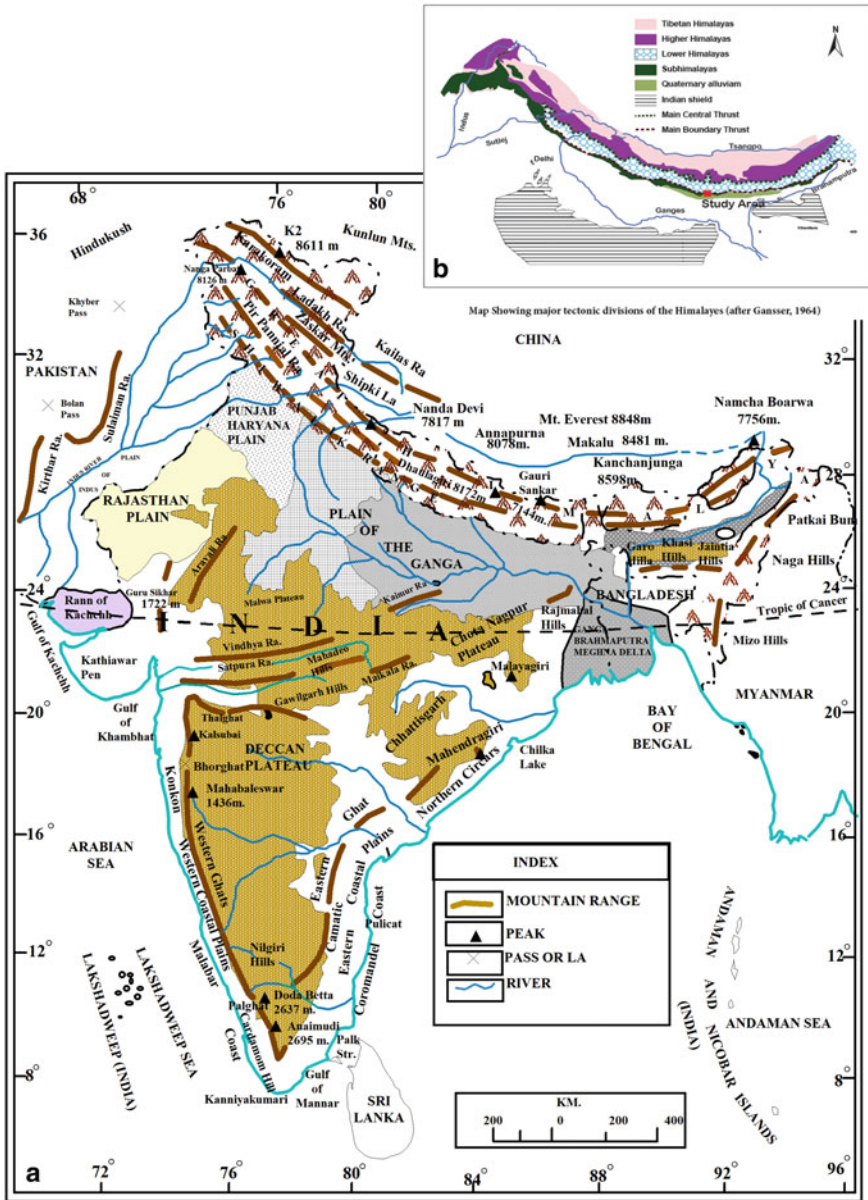


Fig. 1 a Physiography of India (modified from Khuller); b Tectonic divisions of India (after Gansser 1964)

2.2 Interplate Neotectonic Movements in the Himalayan Region and Resultant Landforms

It is difficult to specify the age of neotectonic movement in the Himalayan region and separate it from the long continuous paleo-tectonic activity of the region and resultant landforms.

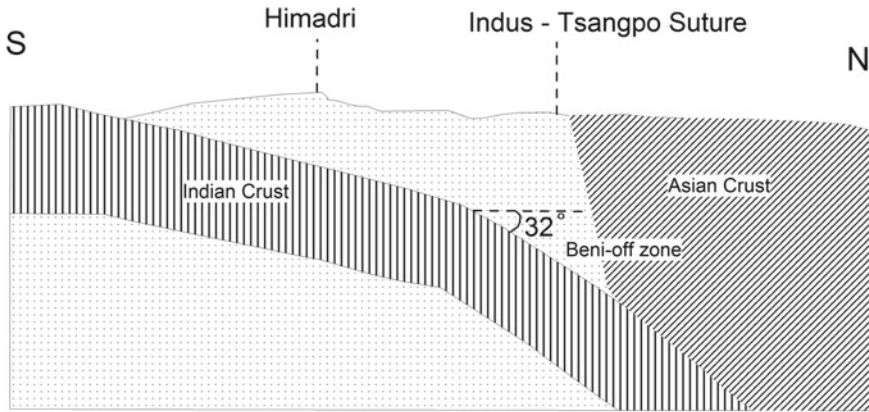
If we follow the definition of Pavlides (1989) as mentioned earlier the 'neotectonic age' of India may be considered as started from Late Quaternary after the Siwalik orogeny and formation of Indo Gangetic plain (126 Ma) But for practical purposes, most of the studies on neotectonics are of the Quaternary period extending over Pleistocene through Holocene to Anthropocene age.

The Pleistocene and Holocene earth movements and structural deformations have been termed as neotectonic movements by a group of scientists whereas others prefer to use the term active tectonic though this term is specifically associated with repeated recent or sub-recent earthquakes whose results are directly compatible with seismic analysis and their future extrapolations. The reactivation of old and traditional faults is manifested through different geomorphic markers among which adjustment of drainage lines/systems, terrace building, channel deflection, paleochannels, formation of knick points, waterfalls, lakes, etc. are noteworthy. Analysis of the evolution of such features with the help of different morphometric techniques, topographical sheets and remote sensing data, different dating processes, and study of micro-sedimentological, paleontological and paleoseismic evidence help us to derive the age and character of tectonic deformation. All these geomorphic features not only bear the evidence of structural deformation but also bear the evidence of Pleistocene climatic change. Therefore in searching the clues of earth movement and structural deformation one should be careful about the evaluation of climatic influences also. Quaternary Developments in India, neotectonics, active tectonics and resultant structural and geomorphic deformation can be summarized as follows.

2.2.1 A Great Himalaya or Himadri

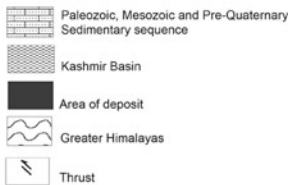
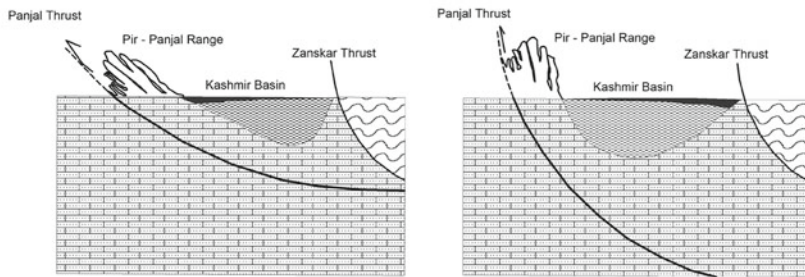
During Quaternary, the Great Himalayas or Himadri was rising at a very fast rate. The rate of uprising in its northwestern part was variable. In Nanga Parbat-Harmosh Massif it was 3–4 mm/year (Whittington 1996), in Karakoram region, it was 2 mm/year (Zeitler et al. 1982) and in intermountain Karewa basin along Pir Panjal range it was 3.5–10 mm/year (Burbank and Jhonson 1982). The rate of erosion was also high though variable from region to region with variation in structure, lithology and climate. The river Indus curved a deep valley in the Nanga Parbat Massif through an incision along the active thrust boundary creating deep gorges (Valdiya 2016). The uplift along the PirPanjal thrust system about 4 million years ago originated the Karewa Paleo Lake ponding the course of the Jhelum River (Valdiya 2016). Valley of Rambiassa in the Southern part of Kashmir valley shows unpaired fluvial terraces and the basin is cut by three northeast dipping faults (Ahmad and Bhat 2012).

These faults have affected the recently deposited soft sediments. It was subjected to subsequent sedimentation of a thickness of 1300 m at a rate of 16 cm/1000 year to 64 cm/1000 year deposited by fluvio-lacustrine or glacio-fluvio-lacustrine and aeolian processes and the thickness of sediment in the basin changed its location due to the movement along Panjal Thrust (Agarwal et al. 2002; Fig. 2) The sedimentation was triggered by the landslides and debris flows activated by the movements along



SCHEMATIC SECTION

a



b

Fig. 2 **a** A model depicting the collision and subsequent bending of Indian crust against the Asian crust (after Makovsky et al. 1996, From Valdiya, 2016); **b** Schematic diagrams showing (i) deposition taking place towards south and (ii) towards north of Karewa basin due to movement along Panjal Thrust (after Agarwal et al. 2018)

thrust planes. The faulting of the southern part of Karewa resulted in the formation of finger liketerraces occurring at an elevation of 2700–3000 m (Valdiya 2016). These terraces are known as marg e.g. Gulmarg and Khillanmarg. Around 20,000 yr BP continuing movements on faults formed an opening (Baramula gorge) which resulted in the draining of the substantial part of the lake (Agarwal et al. 1989). The remnants are the Dal and Wular lakes. The area is subjected to subsequent neotectonic movements resulting in the formation of the fold, fault, sand dykes, terraces, etc. The earthquakes changed and reoriented the geomorphic features. Drainage in the area comprises dendritic, anastomosing and parallel. A sudden decrease in the gradient of the area resulted in the development of anastomosing drainage pattern while parallel drainage indicates the presence of linear faults and ridges (Agarwal et al. 2018).

Displacement of debris-flow deposits and offsetting of 1–2 km fan indicates reactivation of Karakoram fault in recent past. The rate of incision of the Indus river in Pakistan increased in the recent past and there are left out strath terraces produced in the process of incision. With the help of in situ cosmogenic ^{10}B and ^{26}Al exposure Leland et al. (1998) stated that the rate of incision has profusely increased upto 9–12 mm/year in last 7000 yr before which the rate was 1–6 mm/year. This obviously indicates the occurrences of tectonic movement in the recent past.

Ladakh is a barren land with rugged topography where most of the area lies above the tree line. Unlike other areas Ladakh experienced a decreased rate of the incision. Since 15,000 years BP the region experiences an incision rate of 0.3–0.4 mm/year compared to 2 mm/year in the period between 15,000–22,000 year B.P. (Sharma et al. 1998). This rate is the lowest in Quaternary Himadri of northwest. Huge alluvial fans, talus and scree cones, deep gorges (Fig. 3a), waterfalls, scarp faces, fan terraces dominate the local relief (Phartiyal et al. 2005). A number of lakes of fresh or brackish water are found on either side of the Indus–Tsangpo Suture zone. These lakes probably are the result of tectonic reactivation in the Holocene. Tso Morari Lake is the largest among such lakes. It has a length of about 25 km and an average width of 6–8 km indicating damming of north-northwest-south-southeast trending river and its tributaries by debris avalanches (Shukla et al. 2012). The water from the surrounding region drains into the lake. West of Leh damming of the river Lamayuru by a tectonically induced landslide produced a lake during 35,000–45,000 yr B.P. (Bagati et al. 1996; Phartiyal et al. 2005). Subsequent sedimentation under fluvial and lacustrine environments has turned it into a delta (Mathur and Kotlia 1999).

Spiti Valley in Himadri shows a mature topography with uninterrupted sedimentary cover (outwash plains, alluvial fans, debris cones, fluvial terraces and lake deposits) which holds very good potential to study the Quaternary history, palaeo climate, neotectonic and earth surface processes (Phartiyal et al. 2009). The valley is located in the extensional regime with MCT (Ni and Barazangi 1985; Bhargava and Bassi 1998) in the south and Indus -Tsangpo Suture Zone in the north with several north-south and north northeast-south-southwest trending faults. According to Phartiyal et al. (2009) the north-south trending normal faults (Kaurik-Chango and Leo-Kargil Horst) and their conjugate faults are the cause of slope failure and landslides leading to blockade of river intermittently converting a fluvial regime into lacustrine phase. Tso Lake is another paleolake along the upper course of Yunam

**a****b**

Fig. 3 Deep Gorge of the river **a** Zaskar in Ladakh; **b** Alakananda in Uttarakhand

Tso river formed due to damming of the river in response to neotectonic activity during Quaternary times (Bohra and Kotlia 2008). Phartiyal et al. (2009) recognized evidence of recurrent earthquakes along the ShyokSuture zone through the study of multiple lenses of paleoseismites in the paleolake at Khalsar. The uplifted and incised fluvial sediments in SekoNascongPaleolake in the upper reaches of the Spiti river

indicate two phases of active tectonic movements in 12,000 year BP and 7000 yr B.P. respectively. In Spiti valley, the N-S trending Smudo fault is one of the very active transverse faults which has displaced fluvial and lacustrine sediments (Shah and Virdi 1997). Mohindra and Bagati (1996) noticed 90,000–26,000 ka old eight levels of seismites in a 120 m thick sedimentary column. In 1975 an earthquake of 6.5 magnitude occurred along this fault. Chamba fault with sinistral strike-slip movement along Ravi river was also a very active fault being subjected to earthquake in 1975, 1945, 1968, 1986 and 1995 (Joshi 2004; Valdiya 2016).

Deflection of the river along lineaments, incision forming deep gorges due to river rejuvenation, formation and disappearance of lakes are geomorphic features found along the great Himalayas in Himachal Pradesh and Uttarakhand due to reactivation of Main Central Thrust and Trans Himadri Detachment fault. Deflection of the Sutlej river in the vicinity of NS trending lineament proves the active nature of the basin (Joshi and Kathyari 2008). A number of lakes have formed along the rivers Gori, western and eastern Dhauli and Kali in Uttarakhand due to damming by landslides and huge moraines and upward movement of footwall made up of Vaikrita crystalline rocks. (Valdiya 2016). At least three lakes have formed due to tectonic reactivation in the eastern Kumaon sector (lake Garbyang studied by Kotlia and Rawat (2004); lake Goting studied by Juyal et al. (2009) and lake Burfu studied by Pant et al. 2006, Kotlia and Joshi (2013). According to their studies, Garbyanglake has formed by movements between 17,000 and 20,000 B.P and 13,000–14,000 year B.P; Goting paleolake has formed earlier than 40,000 yr BP and Burfu were active in between 11,000–16,000 year B.P. Draining of these lakes produced waters cut gorges on downstream of fault crossings (Valdiya 2016).

In Nepal, the movements along the reactivated MCT have generated a youthful, rugged topography with deep gorges and high ranges. In northwest Nepal, tectonic movements have reactivated portions of MCT. The Darma Fault, the Talphi Fault, the Tibrikot Fault and the Dhaulagiri fault are right stepping en echelon faults forming a 170 km long fault system extending from north west to south east (Nakata 1989) resulting in the right lateral displacement of stream courses and ridges. Fluvial terraces, scarps, alluvial fans and fan terraces indicate vertical displacement.

All the major rivers Yamuna, Ganga, Alakananda, Kali, Gandok, Kosi etc. have maintained their courses through rejuvenation. They show nearly vertical deep gorges (Fig. 3b) knick points, waterfalls and rapids along their courses in the southern zone related to MCT. River Tsangpo Brahmaputra has cut a deep valley near Namcha Barwa along the syntaxial bend. In its long course from Tibet to eastern India, it has majestically developed amazingly deep gorges cutting the entire width of the Himalayas through the zone of weakness near the bend.

2.2.2 The Lesser Himalaya

The lesser Himalaya presents a gentle relief with wide valleys and meandering rivers indicating a mature topography in between the MCT and MBT. Crossing the Greater Himalayas in deep gorges as soon as the rivers enter the undulating lesser Himalayas

they flow through wide and open valleys. The tributary streams also full of twists and turns, excepting where they enter the trunk stream at a lower level. The wide-open valleys are transformed into narrow gorges of 200–300 m depth in areas of active tectonics of the MBT e.g. Nainital Massif (Valdiya 1988). In many sections, nappes of crystalline rocks overlie the sedimentary rocks. These nappe zones are ideal places for mass movements with resultant ponding of streams into the lake. South central Kumaon is dotted with a number of lakes whose origin can be attributed to faulting along the MBT. The Nainital and Bhimtal are the results of movements along a conjugate pairs of NW–SE and NEN–SWS trending faults showing right lateral and left lateral displacement respectively (Valdiya 2016).

The Bhimtal and Nakuchiyatal, now separated by 52 m thick deposits of lacustrine sediment was once continuous as revealed from paleontological studies (Kotlia 1995; Kotlia et al. 1997). The Dulampaleolake, formed about 30,000 year BP on Saryu River (Kotlia and Sanwal 2004) and Wadda paleolake near Pithoragrah formed about 35,000 years BP (Kotlia et al. 2000) are lakes of the same origin active during the Late Quaternary. Six levels of aggradational terraces along both sides of the Alakananda river in Uttarakhand, structure governed course, fast cascading and deeply incised tributary streams indicate neotectonic movements along North Almora Thrust (Chaudhary et al. 2008; Kothyari and Pant 2008).

There is growing evidence of neotectonics and seismicity in the Lesser Himalayas in Nepal. According to Jackson and Bilham (1994) the rate of uplift is 3 mm/year. Active faults trending NNW and ESE direction are found along older fault lines. Barigad Fault and Sun Kosi–RosiKhola fault show right-lateral strike-slip displacements (Naktala 1989). Some NS trending normal faults are also found. The results of uplift and displacements along such active faults are seen in the rejuvenation and superimposition of young topography on the overall mature topography of lesser Himalayas with offsetting of rivers and ridges, formation of terraces and alluvial fans. The courses of the Bari Gad, Nishi Khola, ThuloKhola and SaniBheri rivers lie along these active faults for about 140 km (Nakata 1989). Fault scarps, elongated depressions are also found. Almost all the streams exhibit paired or unpaired terraces. Generally, three and occasionally six aggradational terrace levels are found (Khan et al. 1982), indicating different pulses of Pleistocene Holocene earthquakes. Such six levels of terraces are also found upstream of the Tehri dam near Srinagar, Uttarakhand along the river Bhagirathi (Valdiya 2016). Active faults with repeated Quaternary slip are relatively straight in nature in Nepal suggesting a near surface steep dip.

Pokhra and Rar lakes are the results of river ponding. The Kathmandu paleolake essentially a paleotectonic feature was formed in the late Pliocene, as revealed from paleontological studies (Yoshida and Gautam 1988; Sakai 2001), by ponding of Bagmati river due to uplift of Chandragiri Hill along an east–west trending fault (Valdiya 2016). Subsequent movement along a tear fault resulted in the draining of the lake 11,000 years ago (Valdiya 2016).

Neotectonic activity in the lesser Himalayas of Darjeeling and Sikkim are not uncommon. The Tistariver has migrated about 150 m east ward (average rate 13 mm/year) and incised its valley for about 48 m (vertically average rate

4.4 mm/year) creating unpaired strath terraces between 11,000 and 14,000 years (Mukul et al. 2007). Quaternary unsorted deposits are found along the northern and southern part of Kali Khola a tributary of the Tista at a height of 4 m from the present channel suggests a very recent activity on the MBT (Mukul 2000). Darjeeling sector, the imbricate structure extends southward over a width of more than 30 km (Valdiya 2016). This imbrication has raised the bed of the river Tista leading to the formation of a bar upstream (Fig. 4) (Valdiya 1976). The Lesser Himalayan Duplex is an active structure in the Darjeeling Sikkim, Himalaya with a very pronounced cluster of earthquake epicentres (Kellet et al. 2014). The clustering is prominent along the traces of surface exposures between MCT and MBT (Pandey et al. 1999). The observed seismicity in the Lesser Himalayan Duplex is dominated by moderate frequent thrust and strike-slip earthquakes (Kellet et al. 2014) whereas eastern Nepal records moderate to micro earthquakes along the entire length of Himalayan Wedge (Pandey et al. 1999; de la Torre et al. 2007).

2.2.3 The Sub-Himalayas or Siwaliks

The entire sub-Himalaya with foothills lying to the south of MBF is the result of Quaternary tectonic movements. During the late Pleistocene the resurgence of tectonic movement led to the reactivation of MBT and structural development of Siwalik sediments, derived from the subaerial wastes of the mountains, swept down by the numerous rivers and streams. The process was alike that of what present day rivers and their tributaries are doing. Reactivation of MBT and associated reverse fault system brought the older rocks from north to rest over the Siwaliks. The Siwalik sediments were deformed to a series of simple open folds which become more complex as one moves towards the north. Such open synclines west of 79° east longitude form longitudinal intermontane piggy back valleys later filled up to form duns e.g. Pinjaur Dun in Punjab, Dehra Dun in Uttarakhand and Kota Dun in Kumaun and Dung Dun in Nepal separated by piedmont type of foothills. Dun type foothills are the most common features along the sub-Himalayan zone of the central Himalayas including Kumaon and Nepal Himalayas (Nakata 1972) (Fig. 5). The Duns are good archives of alluvial fans and fluvial deposits. Pinjore Dun, a 45 km long and 8–10 km wide valley lying near Chandigarh is drained by longitudinally flowing major tributaries of Sutlej and the Ghaggar Rivers. Aggradation under alluvial fan environment by the processes of mass movement is the prime cause of the initial formation of the Dun later shaped by the streams. The subsequent confinement of the streams into channelized flow due to increased erosion and resultant incision formed different terrace levels. Increased erosion and the subsequent incision may occur both due to climatic change and tectonic movement during Quaternary. Five terrace levels were observed in the Pinjore Dun and along the Ghaggar river as studied by Malik and Nakata (2003). The Kota Dun lies in the eastern part of the Kumaon Himalayas in Uttarakhand. Between the river, Kosi in the west and Baur in the east lies 21 km long Kota Dun with an average width of 5 km. Most of the streams here form antecedent gorges with straight escarpments running in the WNW-ESE direction parallel to each

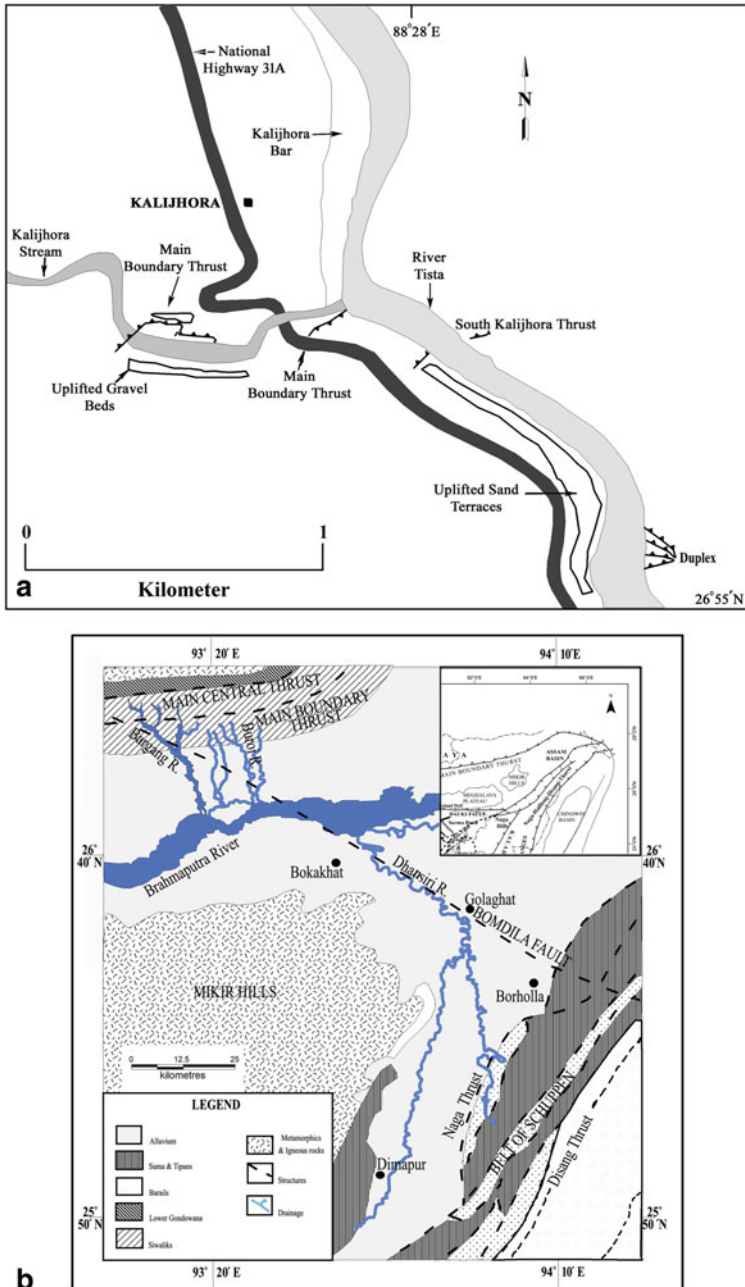


Fig. 4 **a** Map showing the tectonic features and associated landforms as uplifted sand terrace and gravel beds in and around Kalijhora in Darjeeling Himalayas, India (after Mukul 2000). **b** Map showing fault guided course of river Subansiri a tributary to Brahmaputra river, Brahmaputra planes, India (after Sarma and Sharma 2018)

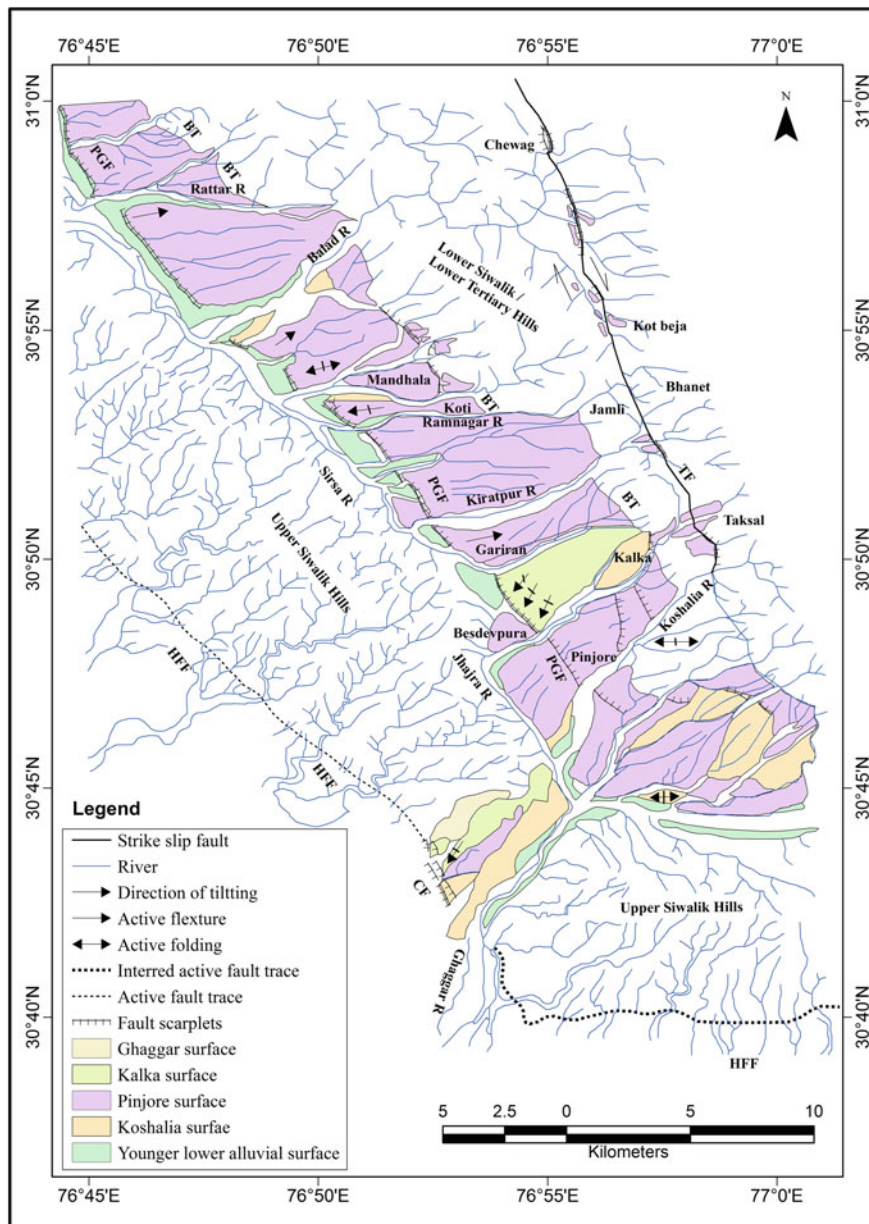


Fig. 5 An example of Dun type of foothill in north western Himalayas (after Malik and Nakata 2003)

other when they cut through the uplifted ridges near the plain (Nakata 1972). Middlemiss (1890) designated these escarpments as warped cliffs. The sedimentation and evolution process of the Kota Dun is more or less similar to that of Pinjore Dun. Dehra Dun is located in the northwestern part of Uttarakhand with an average length of 90 km and an average width of 25 km. The Dun is drained by two major rivers Ganga and Yamuna both of which exhibit a series of river terraces along their course. The characteristic deposits of all the Duns are designated as Dun Gravel, deposited during Late Pleistocene and early Holocene as tectonic movements decreased the gradient of rivers and streams (Valdiya 2018). Reactivation of these faults caused tilting and deformation of the Dun gravel at 15° – 20° (Nakata 1972; Valdiya et al. 1992; Rautela and Sati 1996; Thakur and Pandey 2004).

Reactivation also formed newer Duns (Rao 1977) in the Late Holocene after a decrease in stream gradient. All these are related to the neotectonics of the Himalayan Frontal Thrust (HFT). Originating about 1.6ma ago HFT is a series of reverse faults that demarcates the boundary of the Himalayas against the vast expanse of the Indo-Gangetic plain. At someplaces, it is covered by younger alluvium. According to Valdiya (2003), 'where the hidden ridges of the Indo-Gangetic basement impinge the Himalayas, the mountain fronts are ruptured. At these places, HFT is repeatedly reactivated'. But in the sectors where the basement does not touch the Himalayas, there is no surface expression of HFT and the ground of adjoining Indo-Gangetic plain is sinking with the lateral shifting of the river courses, and large tracts of marshy and water logged lands are formed (Valdiya 2003). Whatever it may be the HFT is the tectonically most active part of the Himalayas.

The recent rate of convergence as measured by Wesnousky et al. (1999) based on geological studies of deformed terraces is 14 ± 4 mm/year in western Himalaya near DehraDun. Powers et al. 1998 suggested a rate of convergence of 1 ± 5 mm/yr across the Himalayan Front in Dehra Dun and 14 ± 2 mm/yr in the northwest of Dehra Dun. The rate is 15 mm/year in the central Himalayas (Yeats and Thakur 1998). Numerous faults have been traced in recent investigations along the HFF. In Pinjore Dun the active Chandigarh Fault, Pinjore Garden Fault and Barsar Thrust have vertically dislocated, warped and back tilled the fluvial and alluvial fan surfaces of late Pleistocene and Holocene time (Malik and Nakata 2003). A right lateral offset of streams and younger quaternary terraces proves a prominent right lateral movement along the Taksal Fault in the same region. Black Mango Tear fault in the same region resulted in two large surface rapture earthquakes in the last 650 years (Kumar et al. 2001) as revealed by paleoseismic studies. Oatney et al. (2001) through paleoseismic analysis concluded that two earthquakes have struck along the Sirmurital fault in DehraDun.

Sinuosity along the strike is another conspicuous characteristic of HFT which occurs due to differential movements of different thrust sheets. The convex part of HFT is known as salient whereas the concave part is known as recess. The lift over portions of the thrust sheet is thus connected with the lateral ramps or connecting splays which appear on the surface as transverse faults or tear faults (Srivastava et al. 2012). Yamuna tear fault forced the Giri, Bata and Sukha Rao rivers to take sharp southward bend from their normal south east flow (Srivastava et al. 2012) Such

transverse faults are obviously younger in age than HFT. Between the Yamuna and Markanda river exists the Dhanura anticline grew by the merging of three HFT segments and formed a barrier to the drainage arising from the initial northern topography forcing them to get deflected (Sharma et al. 2019).

Simple folds cut by faults, branching off from a decollement are the characteristics of Siwaliks in Nepal, rising abruptly from the Gangetic plain to about 2000 m. South eastern Nepal is characterized by active tectonics along MBF and HFF. An active fault near the River TumniKhola on the MBF locally strikes northwest–south east and crosses the east–west active faults on the HFT and extends upto the plains (Nakata 1989). This results in the development of three levels of terraces along TumniKhola. The average slip as calculated by the vertical displacement of terraces is about 1.7 mm/1000 year along HFF (Nakata 1989). A very recent earthquake along an active fault produced a small scarplet of 4.5 m height. Duns are not uncommon in Nepal also like Surkhet-Ghorahi Dun and Dang Dun. Active faulting on the MBF in this region is typically represented by Surkhet-Ghorahi fault which demarcates the northern margin of Surkhet-Ghorahi Dun and extends upto north of Dang Dun (Nakata 1989). Yamanaka and Yogi (1984) deduced the age of terraces of Dang Dun based on radio carbon dating and placed it 20,000–27,000 yr B.P. Gully type of debris flow is a common feature of Siwaliks in Nepal. High rainfall induced mass movement along the steep and precipitous slopes resulted in the development of such features. Sometimes active faulting plays important role in their formation e.g. the region near and along Malai Thrust (Bhandari and Dhakal 2019).

The Siwalik belt is narrow or altogether absent in the eastern Himalayas being buried by metamorphic rocks of the lesser Himalayas (Starkel et al. 2008; Gansser 1964). Nakata (1972) stated that the eastern Himalayas are fringed by piedmont type Foot Hills; which is called Duars and characterized by the formation of Quaternary alluvial fans and fluvial terraces along deeply incised major and minor rivers lying between river Tista in the west and river Jayanti in the east. The major rivers are deeply incised than the minor rivers and discharge their loads in the adjacent alluvial plains. In eastern Himalaya, another pair of salient and recess has been recognized the Dharan salient and Garubathan recess (Mukul 2010) which is a great repository of quaternary alluvium (Fig. 6). This salient recess pair is Non-Dun type which opens to the foreland and the rivers carrying sediments from the recess flush out directly into the foreland (Srivastava et al. 2017). The Garubathan recess (Fig. 7) is an ideal unit to study the deformation of Quaternary sediments as its northern boundary is defined by the Ramgarh Thrust (previously termed as Garubathan Jiti fault (Nakata 1989) and the presence of blind faults 35 km south of the mountain front (Martin and Mukul 2010; Nakata 1989; Guha et al. 2007; Goswami et al. 2012). The Ramgarh thrust bifurcates to the east forming escarpments along Matiali surface, Rangamati and Sumshing surfaces (Nakata 1989). Guha et al. (2007) placed the date of activation of Ramgarh Thrust through radio carbon dating to 34 kybp.

The Matiali scarp shows a dislocation of Quaternary sand and gravel beds of Matiali surface for about 90 m, whereas the uplift along the Rangamati surface is about 70 m and 40 m along samshing surface. These surfaces as designated by Nakata (1972) are nothing but old and abandoned alluvial fans being deeply incised

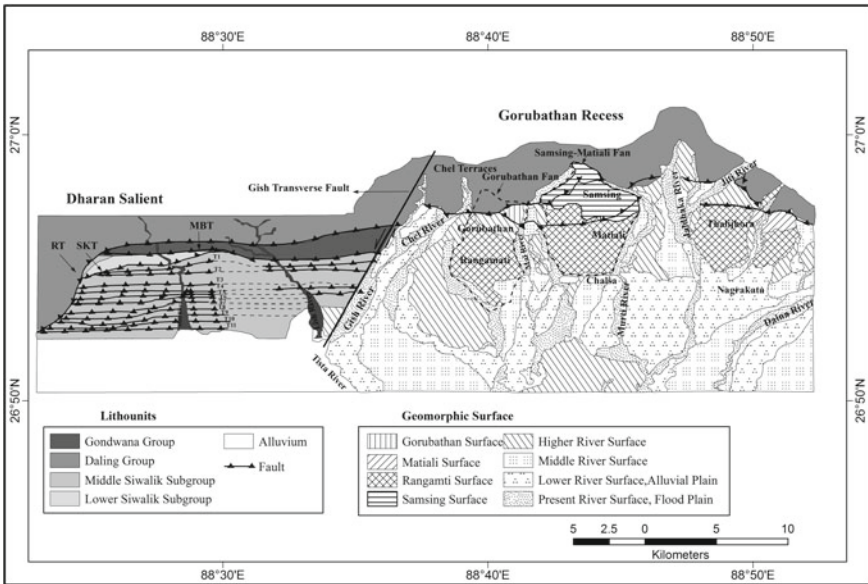


Fig. 6 Showing Lithofacies and Geomorphic surfaces of Garubathan Recess and Dharan Salient area at Darjeeling Himalayan Foothill. (after Srivastava et al. 2017)

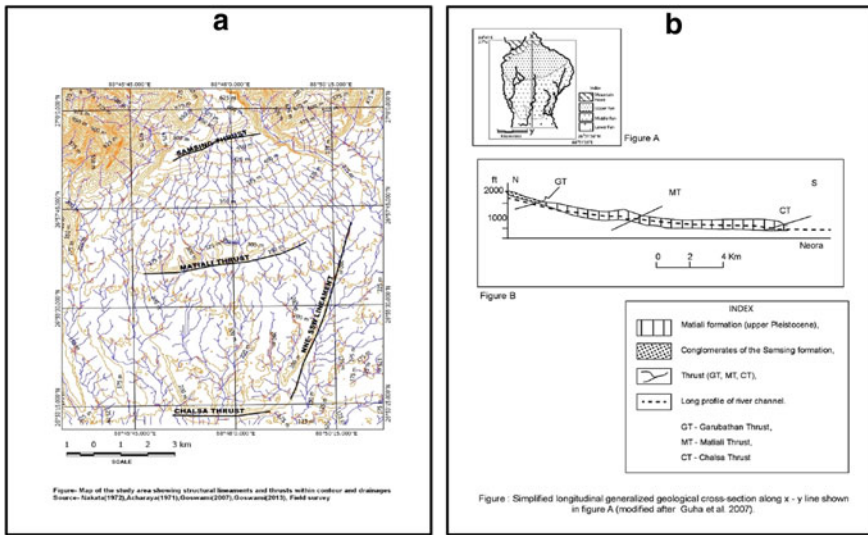


Fig. 7 Map of Darjeeling foothill region **a** (Survey of India topographical sheet no. 78 B/13) showing structural lineaments, thrusts and sudden disappearance and resurgence of streams in Tarai region; **b** Generalised geologic cross section along the line NS

by Chel, Mal, Neora and Murti rivers. The Ramgarh Thrust or Garubathan Jiti fault further extends eastward crossing Jaldhaka River upto Jiti river. South of this line lies the Chalsa thrust which has been attributed to MFT by Nakata (1989) again demarcated by an escarpment (Fig. 8). These east–west propagating faults have not only dissected the alluvial fans but also responsible for the rejuvenation of rivers cutting near vertical terraces along their course.

The Matiali fault was probably active between 24,000 and 11,000 yr B.P (Kar et al. 2014) and whereas repeated activation along Chalsa thrust has been envisaged by Singh et al. (2016), between 41,000 and 48,000 yr B.P; Guha et al. (2007) after 22,000 yr B.P and around 11,000–6000 yr. BP by Kar et al. (2014). Another fault was identified by Nakata (1989). South of Chalsa Fault known as Baradighi fault which tentatively is a blind fault equivalent to MFT (Srivastava et al. 2017). The Righ River terrace of Jaldhaka has been dislocated by Chalsa fault vertically for about 20 m indicating an average slip rate of about 1 m or more per 1000 yr, which is similar to that of Matiali fault. (Nakata 1989). No lateral displacement has been recorded along these active faults of the Himalaya Frontal zone (Nakata 1989).

The Siwalik or the Sub Himalayan tectonics in the east has been studied less compared to the west or north western part. Burgess et al. (2012) have studied a part of the eastern Himalayan MFT zone in detail in Bhalukpong area in eastern Bhutan. Using the age and geometry of uplifted terraces they established a minimum Holocene slip rate of 23 ± 6.2 mm/yr along 10 km wide MFT zone which has been partitioned on three structures–Bhalukpong thrust in the north, growing Bilpara anticline in the middle and Nameri thrust in the south (Burgess et al. 2012).

Strath terraces in the hanging wall of the Bhalukpong thrust, river terraces across the growing Bilpara anticline are the resultant geomorphic features. Bomdila fault is a major tectonic feature in Assam Himalaya extending in NW–SE trend from the Eastern Himalayas to the Naga Hills and directly the courses of rivers Brahmaputra, Dhansiri, Bargang and many others (Sarma and Sharma 2013). An unusually straight course of the river, Dhansiri, north-west ward deflection, knick points, faults scarp are some of the results of neotectonic movements along Bomdila Fault (Fig. 4B). Along Kale river a tributary of the Subansiri river, there was a 15 km long and 5 km wide north–south oriented lake which was formed due to ponding of Kale river by a fault about 20–22 Ka B.P (Valdiya 2016). The reactivation of this fault about 21 Ka B.P. terminated the life of the lake (Srivastava et al. 2009).

Some active faults have been identified in the sub-Himalayan region of Arunachal Pradesh. Devi (2007) detected unpaired terraces along Sinkhi and Dokhoso river and wind gap at a height of about 35 m from the present channel of Senkhi river, linear arrangements of ponds along NW SW indicating paleo channel of Dokhoso river all of which indicates neotectonic activity in the region. There are two active faults along HFT in Arunachal Himalayas; the Banderdewa Fault and the Churachandpur fault have been identified using the GPS Geodetic measurement. (Kumalet et al. 2011). The northward deflection of the south-flowing Singra, Kimin and Ranga rivers along fault lines indicate the presence of active tectonic in the region of Arunachal Pradesh (Devi 2008).

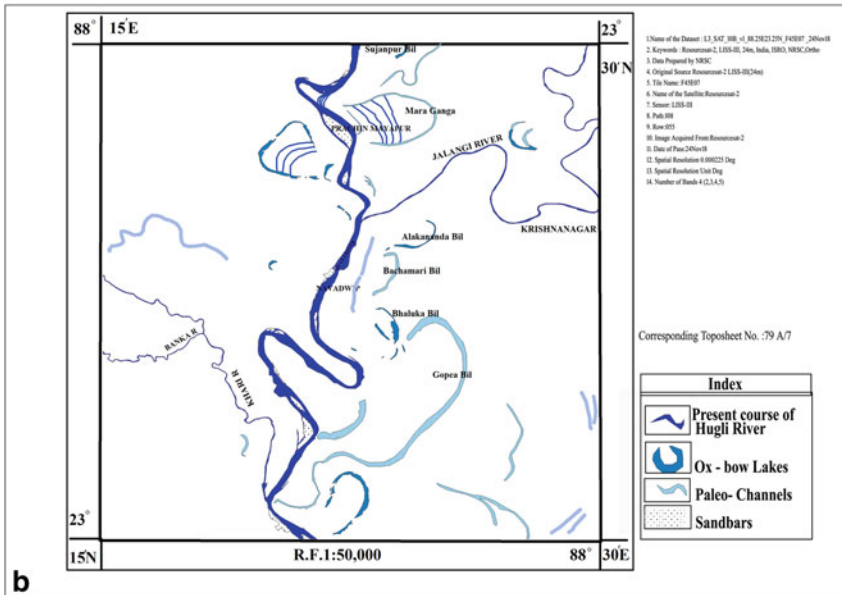
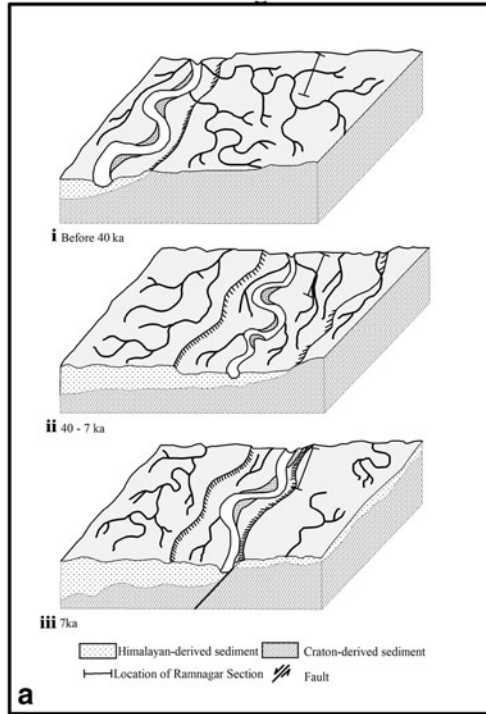


Fig. 8 **a** Channel Migration and incision of river Ganges near Varanasi (i) 40,000 year, (ii) between 40,000 and 7,000 year and (iii) before 7,000 year. **b** Lateral migration of river Ganga with Paleo channels, Ox-bows and Bils, a part of Ganga, Brahmaputra, Meghna Delta, West Bengal, India

The Indian plate bends down as it underthrusts the Himalayas and the slip rate has been calculated from seismic evidence of great earthquakes. The rate is highly variable. In Arunachal Himalayas, the rate of slip has been estimated to 23 ± 6.2 mm/yr whereas the rate varies from 1.5 to 8 mm in the Nagaland and Tripura Mizoram salient and Manipur recess (Jade et al. 2007).

2.3 *The Indo-Gangetic Plain*

The Indo Gangetic plain is a fore-deep in front of the rising Himalayas that came into existence in Late Quaternary, due to the breaking of the Siwalik basin into two unequal halves by the Himalayan Frontal Thrust (HFT) or the Main Frontal Thrust (MFT) (Das et al. 2019). The northern 25–45 km wide part evolved to the rising Siwalik Ranges and the southern 200–450 km wide part became a subsiding basin (Valdiya 1998, 2001, 2016) with variable depth, later filled up by the simple process of alluviation.

The highly monotonous plain covers an area of about 777,000 km² extending over the largest portion of Sindh province of Pakistan, northern Rajasthan, Punjab, Uttar Pradesh, Bihar, Bengal, Assam in India and the whole of Bangladesh being the largest alluvial plain of the world. The plain is the widest in the west (about 500 km wide) from where the width decreases eastward (about 280 km near Allahabad and 160 km near Rajmahal hills). The plain widens again in Bengal (about 460 km) and narrows in Assam (about 60–100 km). The gradient of the plain is highly imperceptible, the average gradient being only 25 cm per km. The floor of the basin is not uniform structurally being intercepted by ridges or highs and depressions or lows, all of which dip steeply to the north (Wadia 1976). Magnetic, gravity and seismic surveys along with deep drilling have indicated that the floor of the basin is also dissected by faults (Sastri et al. 1971; Fuloria 1996). The basins and depressions extend transversely from northeast to southwest in the central sector and from northwest to southeast in the western sector and are closely associated with faults of considerable extent (Valdiya 2016). Generally, the basin deepens towards north which indicates the bending of the Indian plate under the Eurasian plate. The northern margin of the basin is under considerable tectonic strain. There is evidence of a considerable amount of flexure and dislocation at the northern margin of the trough passing into the zone of various boundary faults at the foot of the Himalayas (Wadia 1976).

The Sindhu basin deepens westward giving rise to Sulaiman and Kirthar Depressions, naturally, the depth of alluvium also increases westward. The eastern part of the plain is intercepted with occasional residual hills of Pre-Cambrian rocks, probably being the extended stumps of the Aravalli Mountain.

The river Indus, according to Wadia (1976) shifted westward for about 130 km as revealed from the records of third century B.C. The past channel now exists as a dried course extending upto Rann of Kutch. The westering of the Indus with all Punjab rivers is a very pronounced phenomena for which different causes have been suggested including neotectonism.

The line joining Mount Kailas, Mount Abu with Mount Girnar seems to have served like a water-divide (Valdiya 2016). It separates the east southeast following Bay of Bengal rivers from the southwest and south-flowing rivers, discharging in the Arabian Sea. This buffer area between the Sutlej river in the west and Yamuna in the east does not have any perennial river and is known as the Punjab Hariyana plain (Singh 1996; Singh and Ghosh 1994). This area is drained by some ephemeral streams. To the east the drainage basins are PathralaNadi and Somb river, whereas Khairikakhala; Fandi Rao, Sukar Rao, Chautang 1, Chautang 2 and Saraswati are the basins towards west (Shrivastava et al. 2011). According to Shrivastava et al. (2011) the area was subjected to neotectonic uplifting and tilting along the Delhi Ambala Subsurface Basement High (a subsurface continuation of Aravalli Delhi Massif) and along HFT. Shallow subsurface sand bodies have been identified by several geologists who reconstructed the ancient channel system of the Punjab and Hariyana plain and provided OSL dates to the buried channels (Saini et al. 2009; Saini and Mujtaba 2010) which is responsible for the youthful nature of the basins. Strong structural control exercised by the northeast southwest and northwest southeast lineaments and resultant various fluvial anomalies as reflected by long straightened course, abrupt changes in the flow direction, water gaps, sharp knee shaped bends have been observed along river Sutlej and Beas and their tributaries along with seasonal rivulets in Bistdoab region. (Bhatt et al. 2008).

A high scarp running along the western side of the Beas river and presence of paleo channels, oxbow lakes, compressed meanders etc. in the west indicate a upliftment of the western side and the upliftment along the HFT is evident in the form of elongated and asymmetric water sheds (Bhatt et al. 2008).

Late Tertiary and Quaternary reactivation resulted in a horst like raising of the Aravallis and a slow rise of the area to NW and W (Ahmad 1986; Valdiya 2016, 1984; Sinha-Roy et al. 1993; Sinha-Roy 2001, Bakliwal and Grover 1988) north–south, northeast–southwest and northwest–southeast trending faults and fractures among which the Sardar Sahar fault, Luni Saki fault, Jaisalmer-Barwani fault are of considerable extent (Sinha- Roy et al. 1993; Balkiwal and Ramasamy 1987; Ramasamy 1999). This tectonic deformation led to drainage disruption including deflection of channels, formation of lakes and ultimate disappearance to the west of Aravalli in Rajasthan and adjoining regions of Hariyana and Gujrat. This tract is the driest part of India and may be described as the Thar Domain. This region which was once fertile riverine land and seat of very old and rich civilisation along the course of the river Saraswati has been converted into a dry land over a period of 10,000 yr or more due to past climatic change and the above mentioned tectonic activity which disrupted the entire drainage pattern of the area. The disappearance of the river Saraswati has been attributed to this tectonic movement which must have caused the deflection of the two Himalayan rivers Yamuna and Satadru, two important feeders of the river (Valdiya 2002, 2016). Due to westward deflection, Satradru finally joined the Beas and the Yamuna with an eastward shift joined the river Ganga. The abandoned course of the river Saraswati is traceable as curvilinear or meandering segments of dry channels as concluded by a good number of researchers from the study of satellite images, the study of paleo-sediments and OSL dating (Ghose et al. 1979; Yashpal et al. 1980;

Ramasamy et al. 1991; Bakliwal and Grover 1988; Valdiya 2002). The present day Ghaghra, the Hakra and the Nara rivers probably occupied the old and abandoned channel of the Saraswati (Valdiya 2016). The drainage of the Luni river was also controlled by E-W, NE-SW, and NW-SE trending fault as revealed by a study of sediments (Valdiya 2016). Neotectonic activity related to block faulting also resulted in changes in recharge of fresh water from base flow and surface flow leading to a drastic change in salinity in the Mendha basin, an important river flowing to Lake Sambhar (Rathore et al. 2008).

The Ganga Basin as a whole exhibits a low geomorphic relief through which the river and its tributaries are flowing in the incised valley with a relatively narrow flood plain. This is a unique feature of the river. Over the Bhangar section (composed of beds of clays of yellow and brownish red colour with calcareous or ferruginous concretions) there is a chain of upland with 14 m high escarpment on the southern bank of the Ganga, which is possibly the result of active fault (Valdiya 2016). Similar escarpments with greater height (20–60 m) are also found along Yamuna in Sengarh Valley which has been attributed to Middle and Upper Holocene time (Singh et al., 1997; Agarwal et al. 2002). In the northern part of Ganga Plain the region lying to the east of the river Ghaggar and west of the river Kosi neotectonic faulting events are associated with the terminal fans, which has been correlated with the segmentation of Indo Gangetic plain (Pati et al. 2015). This area is characterised by coalescing alluvial fans of the rivers Yamuna, Ganga, Sharda, Gondok and the river Kosi formed of very coarse detritus materials predominantly gravels. Pati et al. (2015) refer to the segmentation of the region into blocks and subblocks by fault-guided rivers. The fans are incised and the development of terraces is common. The stratigraphy of the upland interfluvium (Ganga Yamuna Doab) shows deposits that are made up of sloping surfaces, flat areas, small channels, ponds and lakes which are exposed at cliff sections and the ravines of the rivers (Singh et al. 1997). In this doab, the river Ganga made deep incision in response to tectonic activity in the peripheral bulge (Shing et al. 1997). Similar features are also found in the Sikkim-Darjeeling foothill zone along Garubathan recess as discussed earlier in connection with Siwalik Gap. TL dating has revealed that the age of the Ganga mega-fan is in between 3000 and 8000 yr. B.P. and the age of fan terraces developed on it is in between the last 3000–1100 yr. BP (Srivastava et al. 2003).

Near Varanasi on the right bank of river Ganga there is a 750 m long cliff the Ramnagar section; the lithofacies study of which indicates recent tectonic deformation (Shukla et al. 2012). River Gomati also shows the development of such a cliff. The river Ganga here is also subjected to shifting and incision as shown (Fig. 8) by Shukla et al. (2012).

Holocene tectonic activity in and around Kanpur at 2.5, 5 and 8.5 ka controlled the Ganga river and the drainage pattern of the area as a whole (Pati et al. 2006). The change in the course of the river Ganga by about 90° is probably due to the block tectonics and diagonal slip faults (Pati et al. 2006). The long profiles of river Ganga near Patna suggest the presence of a knick zone that has shifted upstream due to incision (Sahu and Saha 2014).

Further east the Gondok and Kosi rivers are tectonically active (Pati et al. 2006). The Gondak mega fan formed by episodic tilting of tectonic blocks followed by an eastward shift leaving natural waterlogs and paleo channels as observed from the study of satellite images, GPR study, OSL dating, morphometry and Pedology (Pati et al. 2015). The Gondak shifted about 105 km east leaving behind the paleo channel of Buri Gondak in between 1735 and 1975. The Kosi mega fan is a flat country like any other flood plain covering an area of 16,000 km². The monotony of the landscape being broken by features like old courses now occupied by much smaller streams, old channel courses, oxbow lakes and in places dunes like mounds. (Gohin and Prakash 1990). The shift in case of the river Kosi is about 105 km over its own mega fan between 1736 and 1964 (Valdiya 2016).

Brahmaputra plain, the north eastern extension of the Gangetic plain is a narrow corridor of 80–100 km width compressed between the eastern syntaxis and the Meghalaya Massif. Geologically it is a part of the Assam Arakan Basin, Assam Plain forming its shelf area while the Naga Patkoi Hills represent the mobile area (Sharma and Sarma 2013; Dasgupta and Biswas, 2000). The Precambrian basement of the Basin is faulted with structural 'highs' and 'lows' and deepens southeastward (Valdiya 1999, 2016). Major tectonic features of the area are the northeast-south west trending belt of Schuppen and nearly east–west trending Jorhat fault (Dasgupta 1977; Narula et al. 2000). The area is tectonically active with north-east south-west trending active faults crisscrossed by another group as revealed by seismic survey of the area (Narula et al. 2000; Kent et al. 2002).

Neotectonic activity along the active faults has grossly affected the drainage pattern and characteristics of the upper Brahmaputra Basin. The overall drainage pattern is parallel and sub-parallel with exceptions indicating immediate response to neotectonism. The annular drainage pattern of the river Dikhu and Jhanzi, paleochannels of Mori Namdang and Mori Dikhou, compressed meanders of Dikhu, Mori Dikhou and Namdang, sharp right angle bends along the rivers Thanzi, Namdang, Dimou Jan, Dorika and Disang and low lying swampy areas along their downstream reaches where they meet the axial river the Brahmaputra all indicate active tectonics (Sharma and Sarma 2013). Most of the major tributaries joining the Brahmaputra from the north have distinct paleochannels as revealed from the study of historical maps and recent satellite imageries (Lahiri and Sinha 2012). Evidence of shifting of river courses and confluences are also not uncommon. As Lahiri and Sinha (2012) concluded that the confluence point of the river Siang, Dibang and Lohit, (from where the river Brahmaputra starts) as shown in the topographical maps of 1915 experienced a shift of about 16 km downstream by 1975 and further 129 km downstream by 1975 and further 19 km in 2005. The recent bank erosion of the Majuli island has also been attributed to neotectonics activity (Lahiri and Sinha 2014).

The drainage pattern over the plains of Bengal is highly dynamic. This is partly due to fluvial adjustment in a land of imperceptible gradient and partly due to neotectonic changes in land level, eustatic changes of sea level due to Quaternary climate change and sediment-isostatic adjustments.

The rivers of North Bengal plain namely Mahananda, Tista, Jaldhaka, and Torsa along with their tributaries, after crossing the pediment zone in deeply incised valleys



Fig. 9 Deeply incised course of river Murti with fan terraces in North Bengal plane, India

meet the plain in wide open braided channels (Fig. 9). Following the regional eastward dip they are also migrating eastward through avulsions leaving behind paleochannels, oxbows, etc. (Fig. 10 a–d). The river Tista in 1787 shifted eastward and joined the river Brahmaputra leaving its previous course meeting the river Ganges (Valdiya 2016). Further south in between river Tista and Mahananda there is another group of rivers namely Punarvaba, Kulic, Tangon and their tributaries show structural adjustment and response to the domal uplift of Barind tract and movements along 40 m long Maldah-Kishanganj fault. The Atreyee and Punarbhaba rivers flow through entrenched valleys over Barind tract. The rivers of the western part of the Bengal basin flowing from the eastern flank of Chhotonagpur plateau like Ajoy, Mayurakhi and Damodar along with their innumerable tributaries also show markers of neotectonic adjustments (Barman et al. 2019). An ancient fan delta was developed by the river Damodar, lying at 6–10 m high above the present sea level exists here. This part of Bengal Basin is characterised by numbers of north–south trending normal faults shifting river courses.

The Rajmohol Pahar and the Meghalaya massive with Rangpur saddle in between divide the South Bengal and North Bengal plain. The tectonic settings of South Bengal are highly complex as this is the area where the North or North-East ward migration of the Indian plate gradually changes its direction to East and South-East. Among the major structural and tectonic features is the Hinge zone which marks the periphery of the Indian craton where the Indian plate gradually slopes down to be destroyed ultimately, below the Asian Plate (Bandopadhyay 2019). The Hinge zone is 25 km wide and extends roughly along the line running between Kolkata and Maymensingh. The angle of subsidence varies from 2° – 3° to 6° – 12° and again decreasing to 1° – 2° (Rudra 2018). The Bengal Basin, the Sylhet Trough, Faridpur

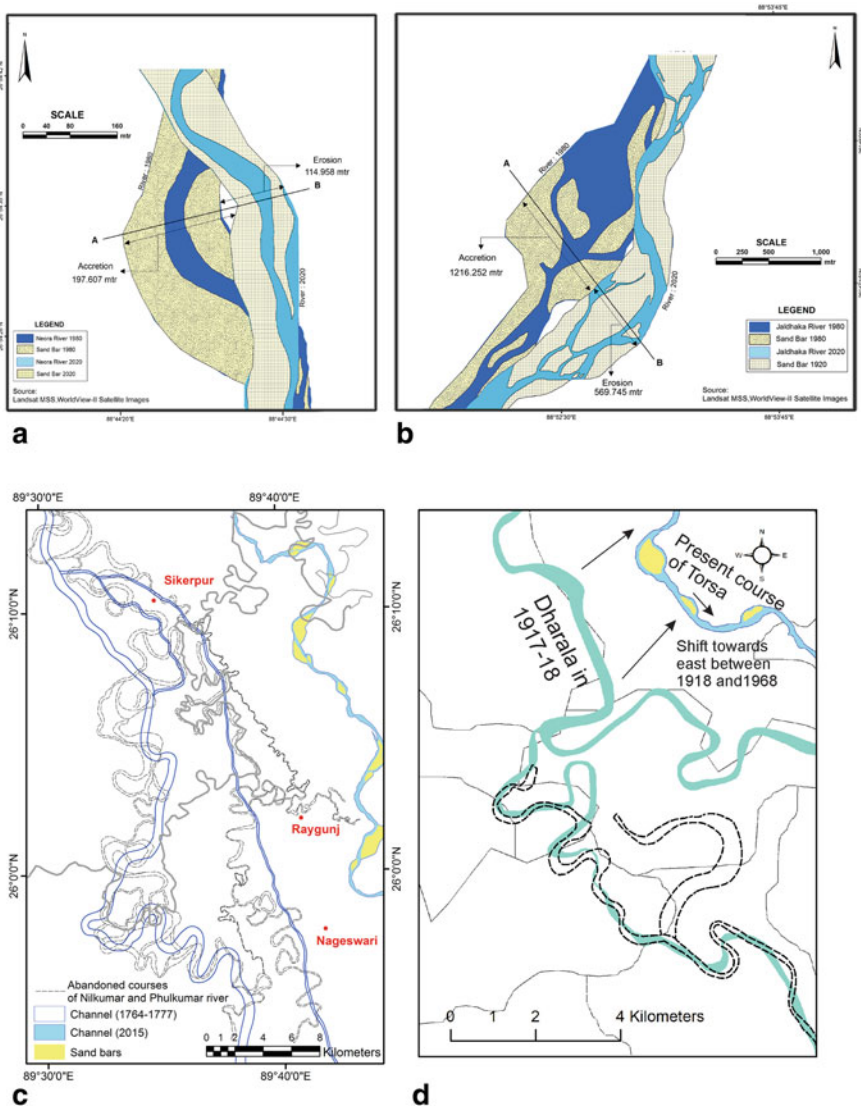


Fig. 10 East ward shift of rivers across North Bengal plane leaving paleo channels and bills

Trough and Hatiya Trough lies over the Benioff zone and Barishal Chandpur gravity high marks the point from where Oceanic crust starts. The Chittagone Tripura fold belt and Chittagone and Coxbazar Fault marks the line approximately along which is present subduction is going on (Alam et al.2003). Dauki Fault marks the Southern end of the Meghalaya massif. A number of NNW SSE trending fault runs roughly between the Rajmohol Pahar and Meghalaya massif, extending up to Sylhet Basin (Fig. 11).

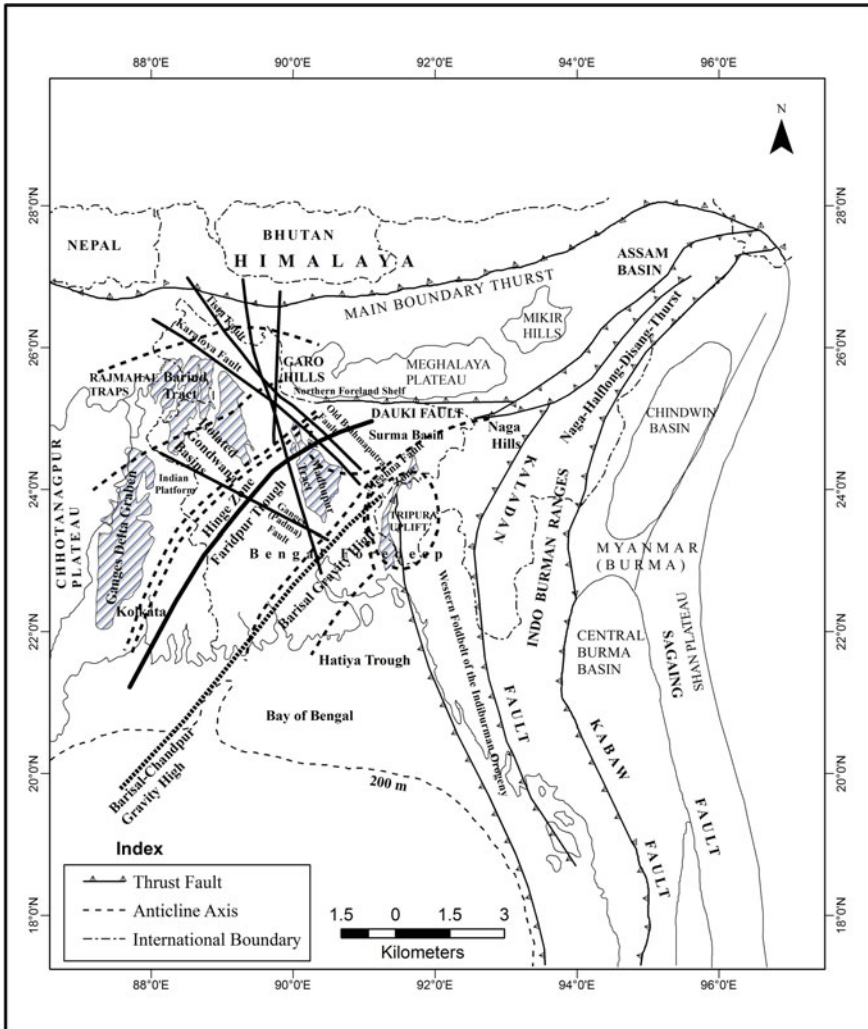


Fig. 11 Geotectonic setup of Bengal Basin (compiled from various sources: Rudra 2018; Rashid et al. 2015; Bandyopadhyay 2019)

Physiographically the Bengal Basin is marked by an uninterrupted plain. The river Brahmaputra and the Ganga enter the deltaic part of Bengal through Rajmahal-Garogap. The monotony of the plain is interrupted by the elevated terraces of old alluviums: the barind Tract and the Madhupur tract. The entire Bengal Plain is marked by innumerable distributary channels of the main rivers, paleo channels and abandoned channels indicating lateral shifting, meander bend cut off, oxbow lakes, pools, bills, waterlogged marshy areas (Fig. 8b). Such features though normal in any deltaic region as a part of fluvial adjustment in areas of imperceptible gradient in

case of the Bengal Basin tectonic deformation also plays a vital role in the lateral shifting of rivers and abrupt switching of course through avulsion (Reitz et al. 2015) as it lies over an active plate margin. The subsidence rate has been estimated at 2–4 mm/a by Goodbred and Kuehl (2000). Due to the subsidence of Sylhet Basin and associated reactivation of Dawki Fault the river Brahmaputra frequently (5 times) shifted its course on either side of the Madhupur Tract in the last 8000 years presently flowing between Barind and Madhupur Tract. Goodbred and Kuehl (2000) as revealed by sedimentological analysis of facies. The old course is marked by the river old Brahmaputra on the East of Barind Tract.

The Ganga Brahmaputra Delta is the largest delta in the world covering about 15,000 km². The southern and southeastern part of Bengal Basin, being enclosed by the rivers Bhagirathi Hoogly, Ganga, Padma, Brahmaputra and Meghna is the deltaic part of Bengal Basin. This delta is the output of high sediment influx by the major perennial rivers and their tributaries draining through the highly tectonically active hinterland. The delta building processes are going on Goodbred and Kuehl (2000) established a subsidence of the order of 2–4 mm /yr for the central and coastal part of Ganga Brahmaputra Delta. This subsidence is the obvious result of huge sedimentation and following isostatic adjustments and vis-a-vis. Stanley and Hait (2000) calculated a subsidence of 5 mm/yr against sediment accumulation of upto 7 mm/yr for the western Sundarban Delta.

3 Intraplate Tectonic Activity—The Indian Peninsula

Peninsular India is a landmass of great antiquity and is formed of the conjunction of four stable cratonic blocks which remained practically undeformed through the ages. “The cratons are the Dharwar Craton in South India, the Bastar Craton in central India, the Singbhum Craton in eastern India and the Bundelkhand Craton in northern India (Valdiya 2016). These Cratons are separated from one another by the Eastern ghat mobile belt borders the Dharwar and Bastar Craton, the Satpura-Aravalli Mobile belt encompassing the Bundelkhand Craton, and the Chhotonagpur Shingbhum Mobile belt demarcating northern margin of the Singbhum Craton” (Valdiya 2016). This unified and stabilized land mass in the early Permian was subjected to block faulting leading to the development of elongated grabens or basins now occupied by the rivers Damodar, Mahanadi, Son Narmada, Pranhita and Godavari. During the Cretaceous the Indian Peninsular was put through stupendous volcanic eruptions. Lava flows coming out from fissures covered almost the whole of Maharashtra and adjoining regions in Gujrat, Madhya Pradesh, Karnatak and Telengana. Rajmahal Hills, Southern Meghalaya and parts of Sylhet in Bangladesh also bear segregated remnants of Deccan Basalt.

Subsidence due to faulting along the coasts of Peninsular resulted in the formation of Peri Cratonic basins subsequently filled up by marine and fluvial sediments ranging in age from upper Jurassic to Quaternary. They are the seat of Mahanadi, Godavari, Krishna and Cauvery delta, Khambat Bay and the Kutch region. Therefore,

from the Cretaceous, the Peninsular Shield practically did not suffer from any type of major tectonic deformations being subjected to unrelenting activities of exogenous forces turning it into a region of subdued relief excepting the formation and filling of the Pericratonic Basins along the Coast.

3.1 Neotectonics and Associated Channel Adjustments

As outlined by Plate tectonic theory, it is known that the plate interiors are relatively free from major tectonic disturbances. The Peninsular Shield suffered both from paleo and neotectonic movements. Presently the Shield is also experiencing earthquakes of different magnitudes. The neotectonics and active tectonic deformation have resulted in drainage adjustments as reflected by their anomalous geomorphic indices. The neotectonic movements in the Peninsular area are mainly concentrated along its boundaries.

Quaternary revival of tectonic activity of the Aravalli region has already been dealt in detail in the previous section in connection with the rivers Saraswati and Luni. Ali and Ikbal (2020) from their studies on Ahar watershed area near Udaypur located in the Southern front of the Aravalli Hills concluded that this watershed area is tectonically active.

In the south-east of Aravalli, this uplift rejuvenated the river Chambal which through headward erosion captured the Banas catchment and resulted in 25–30 km shifting of Banas watershed along the Vindhya hills (Sinha-Roy 2001). About 10,000 yr. B.P. the fluvial activity of the river Mahi increased due to neotectonic uplift which is manifested by deeply incised (40–50 m deep) meanders and ravines popularly known as the Badlands of Mahi Valley (Chamyal et al. 2003). The Orang river in the Southern part of Mahi basin deflected southward to join Narmada river leaving its paleochannel as Dhadar river (Raj 2004). River Sabarmati in northern Gujrat also deflected its course southward and met the Gulf of Khambat, leaving its paleochannel now occupied by Rupen River (Sridhar et al. 1994; Ramasamy et al. 1991).

The neotectonic activity of the Aravalli and Vindhyan region is going on. The WNW and ESE and NE-SW lineaments are more persistent pairs of lineaments and have maximum control in the evolution of Quaternary landforms (Roy and Jakhar 2002). The GPS measurements of 2007–2011 of a permanent GPS site at Udaypur suggest that the site moves at a rate of 49 mm/yr towards northeast (Bhu et al. 2014).

The Kachchh (also spelt as Kutch) region is too a tectonically sensitive region and is cut by some major faults. Reactivation of such zones is common and is revealed by river responses like—the reactivation of Kachchh Mainland Fault have resulted in debris flow deposition and formation of colluvial fans towards the north of Northern Hill Ranges (Malik et al. 2001). These fans are deeply incised by youthful streams. South Wagad Fault also is tectonically active which is manifested by the development of strath terraces along the rivers; incised alluvial fans and deflection of channels

(Mukul and Sing 2016). Kachchh region is seismotectonically active being the site of recent and subrecent earthquakes.

The Narmada, Son, Tapi Fault zone also known as Central Indian Tectonic zone extends for about 1000 km from the west southwest to east northeast travelling through the Central part of India is a spectacular structural feature of Indian subcontinent. The zone nurtures the west-flowing Narmada and Tapi rivers and north east-flowing Son river. The region represents a horst-graben structure with Satpura Ranges as a horst separating the Narmada and Tapi valley. The northern margin of Narmada graben is marked by Son Narmada North Fault and southern margin by Son Narmada South Fault and the Gavailgarh Fault marks the northern limit of Tapi graben. This paleo-rift region of Precambrian origin suffered repeated tectonic deformation through ages (Fig. 12).

During Quaternary, the north south compression due to continued northward movement of Indian Plate folded the Tertiary sediments south of Narmada Son Fault into anticlines with steep reverse fault running in east north east to west south west direction (Joshi et al. 2013). Quaternary deformation and reactivation of reverse faults have also been suggested by Mulchandani et al. (2007) through their study of the Kim river basin south of the Narmada Son Fault.

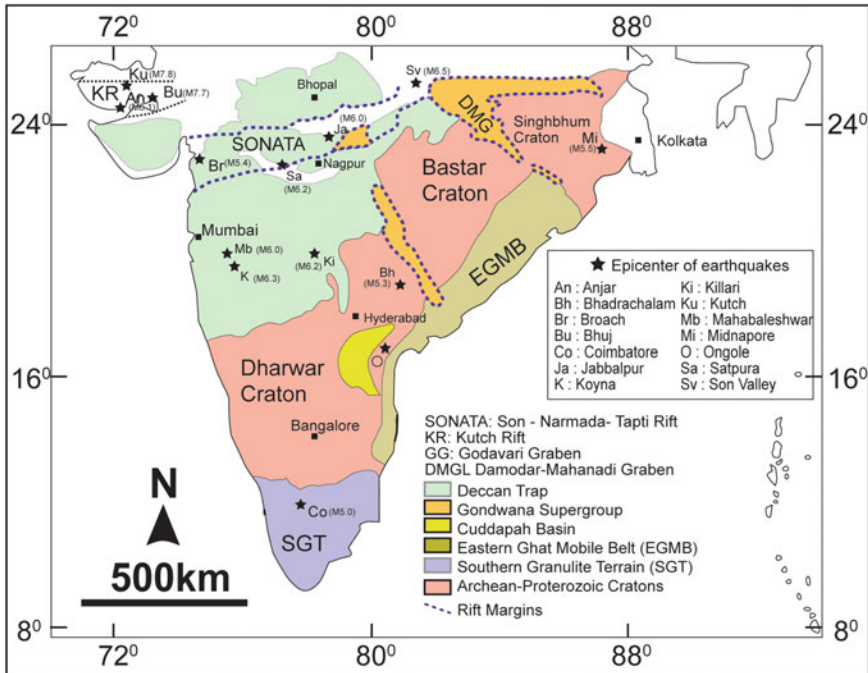


Fig. 12 Precambrian Cratonic Fragments and mobile belts with major paleo rift zones and earthquake epicenters (after Chattopadhyay et al. 2020)

Parallel drainage, knick points and associated waterfalls, incised meanders, and deep ravines (indicating gully erosion) are the geomorphological indicators of neotectonics along the north-flowing tributaries of the Narmada river (Joshi et al. 2013). However, based on the quantitative morphometric study, they concluded a spatial variation in neotectonic activity. The north south compression in Son Narmada Fault zone in the upper course of the river Narmada near Jabalpur is represented by the shifting river channel near Amarkantak, the Dhuandhar waterfalls, the vertical incision in Bhedaghat (Kothyari and Rastogi 2013). The lower reaches of Narmada also suffered from tectonic deformation during Holocene (Chamyal et al. 2002). Terrestrial Cosmogenic Radionuclide Dating places the age of deep gorges near Dardi waterfalls in Gujrat at about 40,000 yr (Gupta et al. 2007). The Relative Index of Active Tectonics of the Son sub-basin, Bijul sub-basin, Rihand sub-basin and Kanhar sub-basin in Son valley also suggests reactivation of Son Narmada North Fault and Son Narmada South Fault (Dubey and Shankar 2019).

Geomorphic analysis of longitudinal profile, river pattern, valley width valley depth ratio, hypsometric curve and OSL dating of the terraces of the rivers Wardha, Maru, Purna and Arna and their tributaries crossing the Gavilgarh Fault indicates that the fault zone is tectonically active and repeated deformation occurred at about 65–80 ka, 50 ka and 14 ka (Bhattacharjee et al. 2016). The Son Narmada fault zone also suffered from a number of recent earthquakes which roughly associates with Son, Narmada Valley (Choubey 1971) and also Tapi Valley (Copley et al. 2014).

The Sahyadri or Western Ghats stands as a high escarpment on the coastal plain rising abruptly from a height of about 80 m to a height of about 1200 m with a gentle undulating surface topography. The Sahyadri is divided into longitudinal blocks by NW and SSE trending echelon faults which are cut by WNW and ESE trending lineaments (Valdiya 2001). These are all active faults. The west flowing rivers exhibit wide valley, gentle slope, low gradient, meandering course over ridges, cutting into deep gorges with waterfalls and rapids over the escarpment face and flowing in an incised meandering valley with terraces over the coastal plains (Fig. 13). These fluvial features indicate that the Western Ghat and associated coastal area is tectonically active. The Valapattanam river along with its tributaries flowing through the Precambrian terrain of Western Ghat in north Kerala also shows signatures of neotectonic activity of variable magnitude as revealed by analysis of Digital Elevation Model (DEM) and morphotectonic analysis (Jayappa et al. 2012).

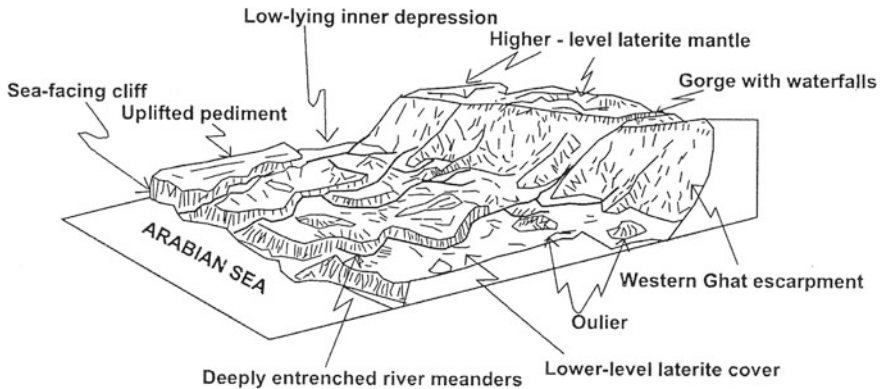


Fig. 13 A schematic section across Western Ghat to Arabian Sea in Konkan-Kanara coastal belt showing landscape differences (after Widdowson 1977)

The Bharathapuzha Basin in the vicinity of Palaghat Gap near Palghat Cauvery Shear Zone exhibits tectonic drainage disruptions along a WNW-ESE fault suggesting that the area is affected by the episodic neotectonic movement since middle Quaternary (Jhon and Rajendran 2008).

The continuous shift of the courses of the Cauvery, Palar and Ponnaiyar rivers indicate ongoing tectonism along (Valdiya 2016) Coromandal Coast.

The Godavari Krishna Delta shows the evolution in four stages, the oldest one dates back to 65,000 Yr BP (Rengamannar and Pradhan 1991). The Mahanadi Delta also shows a developmental history of more than one stage (Bharaii et al. 1991). The Cauvery Delta shows a recession in the delta building process due to Quaternary movement and the morphology of the delta being dominated by paleochannel and distributaries suggesting the presence of neotectonism (Ramasamy et al. 2006).

In Mysore plateau, the tectonic reactivation of persistently weak fault and shear zones resulted in fluvial anomalies along the rivers Cauvery, Bedti, Sharavati etc. being represented by waterfalls, cascades and rapids, upstream ponding of rivers Cauvery, Shimsha, the Kabini and Suvarnabati and deformation of fluvial and lacustrine sediments (Valdiya 2001; Valdiya and Rajagopalon 2000).

Along 13°N parallel between Pulki and Pulicat there is a water divide separating the north flowing and south-flowing streams which indicate crustal buckling (Subrahmanya 1994, 2002). Moreover, the tectonic resurgence of the western edge of the plateau is evidenced by a case of stream piracy by west-flowing Sharavati River (Radhakrishna 1964).

In the Deccan Volcanic Province of Andhra Pradesh and Maharashtra the fluvial characteristics show neotectonic activity on local and regional scale due to intense loading of basalt (Veeraswamy and Raval 2005) and erosional unloading of the same (Sangode et al. 2013). The courses of the Godavari and its tributary Kaddam bear signatures of such neotectonism. The sharp knee bend deflection of the river Godavari and distinctly linear course of the river Kaddam is definitely fault-guided

(Sangode et al. 2013). The rivers also show paleochannels and paleo-confluence location of which is now occupied by Kaddam reservoir lake (Sangode et al. 2013). The lineament guided Terna river basin (a tributary to the Manjra river of Maharashtra) with sharp deflections in the course and other fluvial anomalies indicate the presence of neotectonic activity (Babar and Chunchekar 2008).

Geomorphic analysis of the streams of Deccan Basaltic Region flowing to the east of the Western Ghat was done by Kale and Shejwalkar 2008. They observed, “some well known knick points with scablands, inner channels, waterfalls and potholes occur on the Godavari river near Gangapur and Punlamba, on the Pravara river at Randha, on the Mandvi river near Chilewadi, on the Kas river near Bote, on the Mula river near Mandwe, on the Indrayani river at Shelarwadi on the Kukdi river near Nighoj and on the Shivaganga river at Baneswar”. These features are common markers of tectonic adjustment by fluvial channels (Fig. 14).

4 Modern Earthquakes Effecting Indian Subcontinent

Indian Subcontinent comprising of the Cratonic Blocks with Peri-Cratonic Basins, ‘Early Proterozoic Mobile Belts’, the Tertiary Orogenic Arc and vast alluvial plains evolved from filling of Fore-Deep Basin, is one of the most seismically active areas of the world. Earthquakes of variable magnitudes are frequent with disastrous effects to human society, but earthquakes producing detectable surface deformation are not so frequent. Earthquakes are the result of reactivation of preexisting faults, thrust and shear zones (Fig. 15). They are most common with dense epicenter distribution in the Himalayan Chain particularly in Lesser Himalayas between MCT and MBT (Fig. 16). Verma and Bansal (2016) researchers of Centre for Seismology and Geosciences Division of Ministry of Earth Sciences identified 67 tectonically active faults in India out of which 15 is in the Himalayas, 17 in the Indus Gangetic Plain and as much as 30 in the long-accepted region of stability in Peninsular. The list of major earthquakes with their surface effects is given in Table 2.

5 Introducing the Other Chapters

The previous discussion is just an overview which has tried to sum up partly the areas of the Indian subcontinent experiencing neo and active tectonic movements and the resultant drainage evolution and adjustments. In General, it appears that majority of the Neotectonic movements are associated with the evolution of the Himalaya. Thus, we intended to trace out the role of Himalayan Neotectonics on channel evolution in India through this volume—‘Himalayan Neotectonics and Channel Evolution’. To address all corners of the selected topic—‘Himalayan Neotectonics and Channel Evolution’ in detail will need more than an epic volume. The following chapters are the detailed description and analysis of some particular areas with spectacular

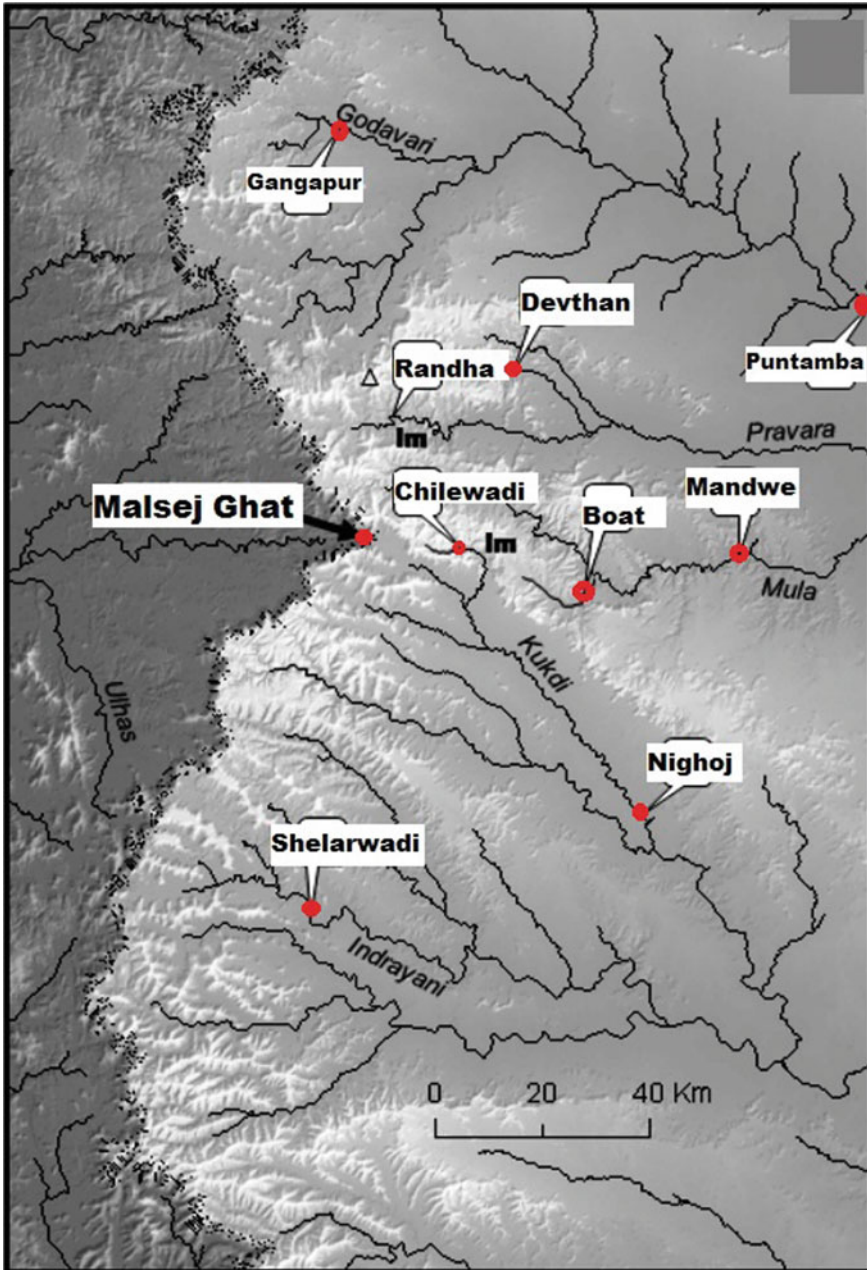


Fig. 14 Map showing the approximate location of major knick points on Upland river (1) near Gangapur on Godavari, (2) near Puntamba on Godavari, (3) near Devthan on Adula, (4) at Radha on Pravara, (5) near Chilewadi on Mandvi, (6) near Bote on Kas, (7) near Mandwe on Mula, (8) near Nighoj on Kukdi, (9) at Shelarwadi on Indrayani, Im represents incised meanders (After Kale and Shejwalkar 2008)

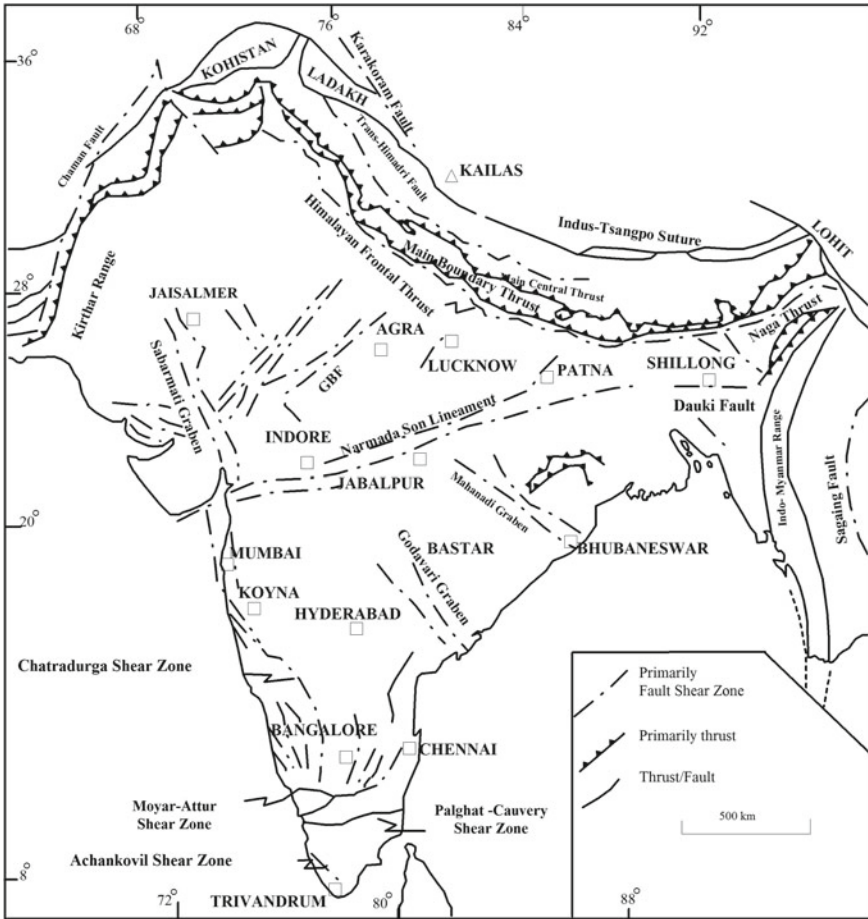


Fig. 15 Map showing thrusts, faults and shear zones of India some of which are currently active. (from Valdiya 2016)

impressions of neotectonics which can be used as identical examples for the others with minor local variations.

The book contains fifteen chapters all together including the present one. All the chapters disclose different issues related to neotectonics and channel evolution of different parts of the region with the help of modern techniques and methodology.

The Chap. 2 intends to comprehend the role of tectonics and differential uplift in landscape dynamics and erosion rates of the Bhagirathi-Alaknanda catchment. The authors suggested a higher recurrence of landslides and profound fluvial incision as a consequence of tectonics and upliftment between major thrusts.

Tectonic controls on spatial variability of topographic attributes and channel morphological characteristics in the Ladakh Trans-Himalayas are illuminated in

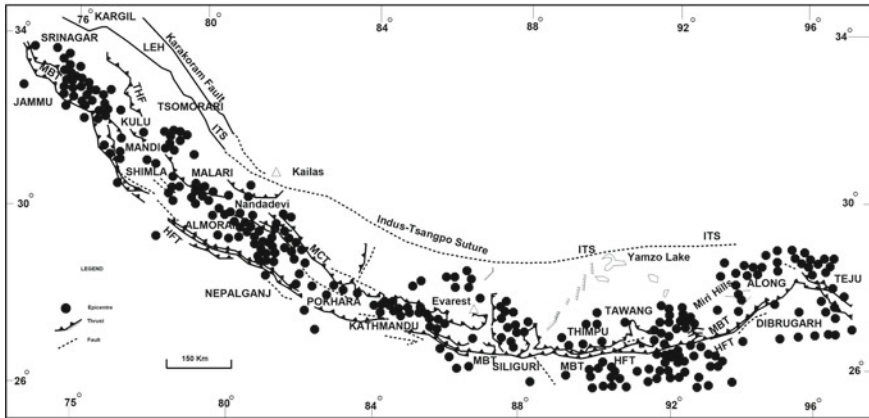


Fig. 16 Distribution of earthquake epicentres between MCT and MBT (after Valdiya 2016)

Chap. 3. Authors used the ALOS PALSAR Digital Elevation Model (DEM) to elicit watershed and channel parameters related to tectonics.

‘Geomorphic response of the Solani river basin to neotectonics: A study from the western Himalayan foothills, India’, the Chap. 4, investigates the influence of neotectonic on the Solani river basin, using morphometric parameters, seismic events, field evidences, and OSL chronology.

‘Tectonic Control on the Meanders Pattern of Alaknanda River in Srinagar Valley (Garhwal Himalaya), India’ constitutes the Chap. 5 and investigates tectonic control on the meander pattern of Alaknanda River in Lesser Garhwal Himalaya. Using remotely sensed data, AOI map and field survey authors confirm the structural and lithological controls on the abrupt change in the flow direction, incised meandering, offset river channels, paleo-channels, multi-level terraces, knick points, pools in longitudinal profile. Meanders are controlled by faults and lineaments.

The Chap. 6 ‘Significance of Channel Planform Change and Morphometric Indices in the Buri River Basin, India and Bangladesh’ used Shuttle Radar Topography Mission elevation data (3 arc second tiles) to bring out the structural signature on drainage using profile shape, normalized stream length-gradient (SLk) index and basin asymmetry factor (AF). Moreover, χ -map and long-term rainfall records were analyzed to show that the Buri is antecedent to all anticlinal axes along its course. The chapter also found that the Buri basin has been tilted to the north and water divides are shifting towards the basin.

The Chap. 7 disclosed the ongoing adjustment of river valleys and channels with the active tectonism of lesser Himalaya. The basin-scale neotectonic signature for some selected rivers in the eastern Himalayan region is mined in the chapter ‘Morpho-tectonic expressions of the drainage basins and channel long profile forms on a selected part of Sikkim-Bhutan Himalayas’.

With the help of “Old Data Inventory, Satellite Images and Sedimentary Architecture” the Chap. 8 analysed the sudden deflections in channel direction around

Table 2 Major earthquakes in Indian subcontinent since 1819

Date	Location	Magnitude	Epicentre	Effect
2001-01-26	Gujarat	7.7 M _w	9 km south-southwest of the village of <u>Chobari</u> in <u>Kuchchh District</u> of <u>Gujarat</u>	0.5 km rupturing along Kuchchh Mainland Fault and some other transverse lineaments (Pande et al. 2003)
1999-03-29	Chamoli district-Uttarakhand	6.8 M _w	–	Strike-slip motion along north west south east trending Nandprayag fault (Valdiya 1976–1980) Deformation features in fluvial soft sediments (Pande and Pande 2004)
1993-09-30	Latur, Maharashtra	6.2 M _w	–	Deformed the ground surface in a 100 m wide zone (Gupta et al. 1996)
1991-10-20	Uttarkashi, Uttarakhand	6.8 M _w	–	Low-angle thrust faulting with varying amounts of strike-slip movement (Ali and Ikbal 2020)
1988-08-06	Myanmar, India	7.3 M _w	–	Landslides were reported in India and Bangladesh <u>subsidence of 20 cm</u> (7.9 in) was recorded in <u>Gauhati, India</u>
1967-12-11	Maharashtra	6.6 M _w	The 1967 Koynanagar earthquake occurred near <u>Koynanagar</u> town in <u>Maharashtra</u>	Probably Anthropocene in origin caused a 10–15 cm (3.9–5.9 in) fissure in the ground which spread over a length of 25 km (16 mi). S
1950-08-15	Assam, Tibet	8.6 M _w	The epicentre was located in the <u>Mishmi Hills</u> ,	200 km long rapture and 8 m slip (Khattri 1987, 1998)

(continued)

Table 2 (continued)

Date	Location	Magnitude	Epicentre	Effect
1905-04-04	Kangra	7.8 M_s	epicenter of the earthquake lies within the zone of <u>thrusts</u>	More than 120 km long rapture and 8 m slip (Khattri 1987 and 1998)
1897-06-12	Shillong, India	8.0 M_w	–	Two new faults resulting in 18 km long with up through upto 10 m A series of waterfalls and pools along the stream About 11 km long zone marked by surface cracks
1833-08-26	Bihar, Kathmandu	8.0 M_s	epicentre located in eastern Nepal about 9.5 km south of <u>Mount Everest</u> (Agarwal et al. 1989)	sand and water vents appeared throughout the central vents of the earthquake area, ground around these sand fissures subsided
1819-06-16	Gujarat	7.7–8.2 M_w	–	a 80 km long (possibly as much as 150 km) and 6 m high natural dam across the Puran river known as the Allah Bund, or Dam of God formation of Sindri Lake covering an area of more than 1,000 km ² due to subsidence of up to 3 m south of the Allah Bund which was later drained out

lineaments or fault lines and intense meandering with sinuosity ranging from 1.20 to 3.12. The existence of micro-terraces and entrenched channel segments encountered structural confinements and certified the positive controls of neotectonics on development of Dharala River.

The Chap. 9 is a ‘Preliminary Study of the Manabhum Anticline: A Possible Key to Better Understanding the Quaternary Tectonics of the Eastern Himalayan Syntaxial Zone’. In this chapter, a detailed geomorphic and geological study of NNW-SSE trending Manabhum Anticline of Naga-Schuppen belt and Mishmi hill has been done to establish the tectonic scenario during Quaternary time. The authors interpret

that the present-day drainage is mainly controlled by the ENE'ly dipping thrust with the considerable effect of the strike-slip fault. They also opined that as Manabhum Anticline is one of the most tectonically active regions during the Quaternary time in South East Asia, it may act as a key to understand the movement of the Indian Plate along the Eastern Syntaxial zone.

The Chap. 10 'Assessment Of Neotectonic Effect On Quaternary Deposits In Darjeeling Himalayas' detected signals of neotectonism from landform and sediments of Darjeeling-Jalpaiguri Sub-Himalayas and southerly adjacent piedmont. A quantitative approach is adopted in this chapter. Sinuosity value less than 1.4 in most of its straight channel segments, minimum gradient on the crest of the Mountain Front Thrust (MFT), the frequent presence of mass-flow products and increase in clast size and share of distal crystalline rocks in clast composition but stable climate indicate towards the uplift of MFT.

Tectonic events of Himalayan Foredeep and its effects on the fluvial landscape with special emphasis on scarps and fans has been discussed in 'Himalayan Foredeep Neotectonics and Deformed Riverscape Landforms: An Integrated Discussion, West Bengal, India', the Chap. 11.

The Chap. 12 'Evaluating the relative tectonic response of the fluvial systems using multi-criteria Entropy Method: A case study of the Rangit Catchment, Eastern Himalayas, India' assess the tectonic response in the fluvial systems using several indices such as the asymmetric factor, hypsometric integral, elongation ratio, stream gradient index and valley width-height ratio for all 16 sub-catchments along with the trunk-stream of the Rangit River. Authors suggest that the left bank tributaries show a higher degree of tectonic control than the right bank tributaries. The Main Central Thrust (MCT), which was active in the Holocene period has prominent control on the basin and channel evolution.

The Chap. 13 'Role of geomorphic drivers and active tectonism on channel oscillation of the Raidak-I River in the eastern Himalayan foothills, India' illuminates the relationship between the riverbank erosion-deposition and geomorphological and tectonic adjustment.

'Morphotectonics of the Chel river basin, Eastern Himalaya, India: Insights from Shuttle Radar Topography Mission digital elevation model-based geomorphic indices' comprises the Chap. 14 which examined the implications of Neotectonic activity on channel characteristics and landform development of Chel river basin. Authors analyzed Shuttle Radar Topography Mission (SRTM) DEM based geomorphic indices and uncovered how the elongated basin shape, hypsometric integral value, basin asymmetry factor, irregular mountain front, presence of V-shaped valleys, and knick points point towards neotectonism and the senile stage of the basin.

The Chap. 15, 'Influence of Neotectonics on Channel Evolution of Kameng River, North-East India' used morphometric and statistical tools and pointed towards the signature of neotectonism on the channel evolution of the Kameng River of North-East India. Due to neotectonic perturbations and associated inclinations of different parts of the basin into different directions, sub-basins became significantly asymmetric. Direction of flow paths of channel links are associated with the orientation of fault lines and lineaments.

6 Conclusions

The subject tectonic geomorphology (Morphotectonic Studies) attracted the attention of geologists and geomorphologists in the last few decades starting its journey from the last century, with the overwhelming Davisian concept—‘Landscape is a function of structure, process and stage’, which grasped the central concept of tectonic geomorphology in a very incipient form. This Davisian concept had to wait a long to be tested in the field due to a lack of proper identification tools, age determining techniques and quantification methods and is now gaining popularity day by day.

Studies on neotectonic activity and landform started with the refinement of tectonic geomorphology as a subject. Identification and analysis of geomorphic markers from secondary data are required in the field of neotectonic study obviously being followed by field observations. Innovative tools for identification of such geomorphic markers were not available to the researchers even in seventies and eighties of the last century. Presently high resolution remotely sensed data of different satellite systems of different countries and highly sophisticated software to identify the geomorphic markers are easily available. Now a day remote sensing data is mostly available in digital formats, like Landsat MSS, Landsat TM, Landsat ETM+, SPOT, QuickBird, Cartosat, IKONOS, etc. These digital images are processed with appropriate hardware and software like ER Mapper, Ilwis, Erdas, Geomatica, ArcGis, TNTmips etc. Geo referencing helps to derive the location of the feature on earth and map overlays helps to derive the pattern of change through time. Then ground checking is done to determine the location and exact characteristics of the features on real earth. All these are opening the scope of the subject day by day and young researchers are becoming interested in such studies. Moreover the modernisation of dating techniques is also helping more accurate prediction of data and time which is making the subject more fascinating and innovative. All these undoubtedly indicate a profusely expanding arena of the subject though inaccessibility will remain as a natural hinderance in the field verification and study.

Neotectonic events are in operation in the Himalayas, the peninsular plateau and Indo-Gangetic-Brahmaputra plain with deltaic part of the Indian subcontinent, and river channels in these areas show striking imprints of tectonism in their evolution. Though the Indian subcontinent is much diversified in geological evolution and fluvial response, the tools and techniques to explore the non-linear fluvial behavior in response to geology and stratigraphy are strikingly insufficient compared to the Anglo-European nations of the world. However, in the recent decades developments in high resolution imageries and the GISciences is backing the earth scientists to some extent to explore the newer areas. With this backdrop, present volume initiated fused-avenue of tectonic geology and fluvial geomorphology for a better understanding of rivers and sub-surface tectonics of the Indian subcontinent with special reference to the Himalayan Neotectonics. We hope that this initiation directs to the vast scope and paves the way of further research ranging from basin-scale to channel-site scale on each and every basins, and their sub-basins of different orders in different

hydro-meteorological and tectonic regions of the world in general and in the Indian subcontinent in particular.

References

- Agarwal K, Singh I, Sharma M, Rajagopalan G (2002) *Int J Earth Sci* 91(5):897–905
- Agarwal KK, Shah RA, Achyuthan H, Singh DS, Srivastava S, Khan I (2018) Neotectonic activity from Karewa sediments, Kashmir Himalaya, India. *Geotectonics* 52(1):88–99
- Agarwal DP, Dodia R, Kotlia BS, Razdan H, Sahni A (1989) The Plio- Pleistocene geologic and climatic record of the Kashmir Valley, A review and new data. *Palaeogeogr Palaeoclimatol Palaeoecol* 73:267–286
- Ahmad S, Bhat MI (2012) Tectonic geomorphology of the Rambiasa basin, SW of Kashmir valley reveals emergent out-of-sequence active fault system. *Himalayan Geol* 33:162–172
- Ahmad F (1986) Geological evidence bearing on the origin of Rajasthan desert. *Proc Indian Natl Sci Acad* 52A:1285–1306
- Ali SA, Iqbal J (2020) Assessment of relative active tectonics in parts of Aravalli mountain range, India: Implication of geomorphic indices, remote sensing and GIS. *Arabian J Geosci* 1–16
- Alam M, Alam MM, Curray JR, Chowdhury MLR, Gani MR (2003) An overview of sedimentary geology of the Bengal Basin in relation to the regional framework and basin-fill history. *Sed Geol* 155:179–208
- Aitken MJ (1998) *An introduction to optical dating: the dating of quaternary sediments by the use of photon stimulated luminescence*. Oxford University Press, New York
- Babar SMD, Chunchekar RV (2008) Neotectonic and geomorphic characteristics of Terna River Basin, West Central India. In: *International association for Gondwana research conference series*, vol 5, pp 114
- Bagati TN, Mazari RK, Rajagopalan G (1996) Palaeotectonic implication of Lamayuru Lake (Ladakh). *Curr Sci* 71:479–482
- Bandopadhyay S (2019) *Sundarban: a review of evolution & geomorphology*. World Bank Report, p 36
- Bakliwal PC, Grover AK (1988) Signature and migration of Saraswati river in Thar desert, western India, vol 116. *Records of Geological Survey of India*, pp 77–86
- Barman SD, Islam A, Das BC, Mandal S, Pal SC (2019) Imprints of Neo-tectonism in the evolutionary record along the course of Khari river in Damodar fan delta of lower Ganga basin. In: Das B, Ghosh S, Islam A (eds) *Quaternary Geomorphology in India*. *Geography of the Physical Environment*. Springer, Cham, pp 105–126
- Bates RL, Jackson JA (1980) *Glossary of geology*. American Geological Institute, Falls Springs, Virginia, p 751
- Berger GW (1988) Dating quaternary events by luminescence. In: Easterbrook DJ (ed) *Dating quaternary sediments*, special paper 227. Geological Society of America, Boulder, CO, pp 13–50
- Bharali B, Rath S, Sarma R (1991) A brief review of Mahanadi delta and the deltaic sediments in Mahanadi basin. In: Vaidyanadhan R (ed) *Quaternary deltas of India*. Geological Society of India, Bangalore, pp 31–47
- Bhatt CM, Litoria PK, Sharma PK (2008) Geomorphic signatures of active tectonics in Bist Doab interfluvial Tract of Punjab, NW India
- Bhattacharjee D, Jain V, Chattopadhyay A., Biswas RH, Ashok KS (2016). Geomorphic evidence and chronology of multiple neotectonic events in a crato area: results from Gavilgarh Fault Zone, central India. *Technophysics* 1–45
- Bhandari BP, Dhakal S (2019) *J Nepal Geol Soc* 59:89–94
- Bhargava ON, Bassi UK (1998) *Geology of Spiti-Kinnaur, Himachal Himalaya*, vol 124. Geological Survey of India Memories, pp 1–210

- Bohra A, Kotlia BK (2008) Neotectonics of upper Yunam River Valley, Lahul-Spiti, NW Himalaya, vol 5. International Association for Gondwana Research, p 44
- Bhu H, Purohit R, Ram J, Sharma P, Jakhar SR (2014) Neotectonic activity and the parity in movements of Udaipur block of the Arvalli Craton and Indian Plate. *J Earth Syst Sci* 123(2):343–350
- Blenkinsop TG (1986) In: Hancock PL, Williams GD (1986) Neotectonics (Conf.rep.). *J geol Soc Lond* 143:325–326
- Bloom AL (1998) Geomorphology: a systematic analysis of late Cenozoic landforms (No. 551.79 BLO)
- Buddemeier RW, Taylor FW (2000) Sclerochronology. In: Noller JS, Sowers JM, Lettis WR (eds) Quaternary geochronology: methods and applications. American geophysical union, Washington, DC, pp 25–40
- Burbank DW, Anderson RS (2016). Tectonic geomorphology, 2nd edn. WILEY Blackwell
- Burbank DW, Johnson GD (1982) Intermontanebasin development in the past 4 Myr in the northwest Himalaya. *Nature* 289:432–436
- Burgess WP et al (2012) Holocene shortening across the Main Frontal Thrust zone in eastern Himalaya. *Earth Planet Sci Lett* 152–167
- Cerling TE, Craig H (1994) Geomorphology and in-situ cosmogenic isotopes. *Annu Rev Earth Pl Sc* 22:273–317
- Chamyal LS, Maurya DM, Bhandari S, Rachna R (2002) Late Quaternary geomorphic evolution of the lower Narmada Valley, western India: implications for neotectonic activity along the Narmada-Son Fault. *Geomorphology* 46:177–202
- Chamyal LS, Maurya DM, Raj R (2003) Fluvial systems of the drylands of western India: a synthesis of Late Quaternary environmental and tectonic changes. *Quat Int* 104:69–86
- Chattopadhyay A, Bhattacharjee D, Srivastava S (2020) Neotectonic fault movement and intraplate seismicity in the central Indian shield: a review and reappraisal. *J Miner Petrol Sci* 115:138–151
- Chaudhary S et al (2008) Neotectonic Activity in Monsoon Dominated Lower Alakananda Valley, Central Himalaya: implication towards landform evolution. In: International association for Gondwana research conference series, vol 46. Japan
- Choubey VD (1971) Narmada-son lineament, India. *Nature* 232:38–40
- Copley A et al (2014) Active faulting in the apparently stable peninsular India: rift inversion and a Holocene-age great earthquake on the Tapi Fault. *J Geophys Res Solid Earth* 6650–6666
- Cox A, Doell RR, Dalrymple GB (1964) Reversals of the earth's magnetic field. *Science* 144:1537–1543
- Creer KM (1962) The dispersion of the geomagnetic field due to secular variation and its determination for remote times from paleomagnetic data. *J Geophys Res* 67:3461–3476
- Creer KM (1967) Application of rock magnetism to investigations of the secular variation during geological time. In: Magnetism and the cosmos, NATO advanced study institute on planetary and stellar magnetism, University of Newcastle upon Tyne, 1965, Oliver and Boyd, Edinburgh, pp 45–59
- Das BC, Ghosh S, Islam A (2019) Quaternary geomorphology in India: concepts, advances and applications. In: Das B, Ghosh S, Islam A (eds) Quaternary geomorphology in India. Geography of the physical environment. Springer, Cham, pp 1–24
- Dasgupta AB, Biswas AK (2000) Geology of Assam. Geological Society of India, Bangalore, pp 45–83
- Dasgupta AB (1977) Geology of Assam Arakan region. *Mining Metall Soc India Q J* 49:1–54
- De la Torre TL, Monsalve G, Sheehan AF, Sapkota S, Wu F (2007) Earthquake processes of the Himalayan collision zone in eastern Nepal and the southern Tibetan Plateau. *Geo-Phys J Int* 171:718–738
- Devi RKM (2007) Geomorphic appraisals of active tectonics associated with the uplift of the Gohpur-Ganga section in Itanagar, Arunachal Pradesh, India. *Geomorphology* 99:76–89
- Devi RKM (2008) Tectono-geomorphic forcing of the frontal sub-Himalayan streams along the Kimin section of Arunachal Himalaya. *J Geol Soc India* 72:253–262

- Diebold P, Muller WH (1985) Szenarium der geologischen Langzeitsicherheit: Risikoanalysen für ein Endlager für hochaktive Abfälle in der Nordschweiz. NAGRA Techn Ber 84–26: 110 pp
- Dubey RK, Shankar R (2019) Drainage pattern and its bearing on relative active tectonics of a region: a study in Son Valley, Central India. *J Geol Soc India* 93:693–703
- Freyemueller J, Bilham R, Burgmann R, Larson KM, Paul J, Jade S et al (1996) Global positioning system measurements of Indian plate motion and convergence across the Lesser Himalaya. *Geophys Res Lett* 23:3107–3110
- Fritts HC (1976) Tree rings and climate. Academic Press, New York
- Fuloria RC (1996) Geology and hydrocarbon prospects of the Vindhyan sediments in Ganga valley. In: *Memoirs of the Geological Society of India*, vol 36, pp 235–256
- Gansser A (1964) The geology of the Himalaya. Wiley Interscience, New York, p 189
- Gary M, McAfee R, Wolf CL (1972) Glossary of geology. American Geological Institute, Washington, DC, p 805
- Ghose B, Kar A, Hussain Z (1979) The lost courses of the Saraswati river in the Great Indian Desert: New evidence from LND SAT imagery. *Geograph. J Lond* 145(3):446–451
- Goodbred SL Jr, Kuehl SA (2000) The significance of large sediment supply, active tectonism, and eustasy on margin sequence development: late Quaternary stratigraphy and evolution of the Ganges-Brahmaputra delta. *Sed Geol* 133(3–4):227–248
- Gohin, K, Prakash B (1990) Morphology of the Kosi Megafan. In: Rachocki, AM, Church M (eds) *Alluvial fan a field approach*. Wiley, pp 151–178
- Goswami C, Mukhopadhyay D, Poddar BC (2012) Tectonic control on the drainage system in a piedmont region in tectonically active eastern Himalayas. *Front Earth Sci* 6(1):29–38
- Guha D, Bardhan S, Basir SR, De AK, Sarkar A (2007) Imprints of Himalayan thrust tectonics on the Quaternary piedmont sediments of the Neora-Jaldhaka Valley. Darjeeling-Sikkim Sub-Himalayas, India. *J Asian Earth Sci* 30:464–473
- Gupta A, Kale VS, Owen LA, Singhvi AK (2007) Late Quaternary bedrock incision in the Narmada River at Dardi Falls. *Curr Sci* 93:564–567
- Gupta HK, Sarma SVS, Harinarayana T, Virupakshi G (1996) Fluids below the hypocentral region of Latur Earthquake, India: geophysical indicators. *Geophys Res Lett* 23(13):1569–1572
- Hancock PL, Williams GD (1986) Neotectonics (conf. rep.). *J Geol Soc Lond* 143:325–326
- Jackson M, Bilham R (1994) Constraints on Himalayan deformation inferred from vertical velocity fields in Nepal and Tibet. *J Geophys Res* 99:13897–13912
- Jacoby GC, Sheppard PR, Sieh KE (1988) Irregular recurrence of large earthquakes along the San Andreas fault: evidence from trees. *Science* 241:196–199
- Jade S, Mukul M, Bhattacharya AK, Vijayan MSM, Jagannathan S, Kumar A et al (2007) Estimates of interseismic deformation in northeast India from GPS measurements. *Earth Planet Sci Lett* 263:221–234
- Jayappa KS, Markose VJ, Nagaraju M (2012) Identification of geomorphic signatures of neotectonic activity using DEM in the Precambrian terrain of Western Ghats, India, vol XXXIX-B8, *International archives of the photogrammetry, Remote sensing and spatial information sciences*, p 6
- Jhon B, Rajendran CP (2008) Geomorphic indicators of neotectonism from Precambrian Terrain of Peninsular India: a study from the Bharathapuzha Basin, Kerala. *J Geol Soc India* 71:827–840
- Joshi DD (2004) A seismogenic active fault in the western Himalaya. *Curr Sci* 87:863–864
- Joshi M, Kothiyari GC (2008) Morphotectonic evidence of Rejuvenation in Satluj River Basin, Kinnaur Himalaya, vol 5. *International Association for Gondwana Research*, p 54
- Joshi PN, Maurya DM, Chamyal LS (2013) Morphotectonic segmentation and spatial variability of neotectonic activity along the Narmada-Son Fault, Western India: Remote sensing and GIS analysis. *Geomorphology* 292–306
- Juyal N, Pant RK, Basavalah N, Bhushan R, Jain M, Saini NK, Yadava MG, Singhvi AK (2009) Reconstruction of Last Glacial to early Holocene monsoon variability from relict lake sediments of the Higher Central Himalaya, Uttarakhand, India. *J Asian Earth Sci* 34:437–449

- Kar R, Chakraborty T, Chakraborty C, Ghosh P, Tyagi AK, Singhvi AK (2014) Morpho-sedimentary characteristics of the Quaternary Matiali fan and associated river terraces, Jalpaiguri, India: Implications for climatic controls. *Geomorphology* 227:137–152
- Kale VS, Shejwalkar N (2008) Uplift along the western margin of the Deccan Basalt Province: Is there any geomorphic evidence? *J Earth Syst Sci* 6:959–971
- Kellet DA, Mottram C, Grujic D, Mukul M (2014) Virtual Field Guide for the Darjiling- Sikkim Himalaya, India. *J Virtual Explor* 47(5):1–38
- Kent WN, Hickman RG, Das Gupta U (2002) Application of a ramp/flat-fault model to interpretation of the Naga thrust and possible implications for petroleum exploration along the Naga Thrust front. *Am Asso Petrol Geol Bull* 86(12):2023–2045
- Khan AA, Dubey US, Sehgal MN, Awasthi SC (1982) Terraces in the Himalayan tributaries of the Ganga in Uttar Pradesh. *J Geol Soc India* 23:392–401
- Khattri KN (1987) Great earthquakes, seismicity gaps and potential for earthquake disaster along the Himalaya plate boundary. *Tectonophysics* 138(1):79–92
- Kothyari GC, Pant PD (2008) Evidence of active deformation in northwest part of Almora in Kumaun Lesser Himalaya: a geomorphic perspective. *J Geol Soc India* 72:353–364
- Kothyari GC, Rastogi GC (2013) Tectonic control on drainage network evolution in the Upper Narmada Valley: implication to neotectonics. *Geography J* 1–9
- Kotlia BS, Joshi LM (2013) Neotectonic and climatic impressions in the zone of Trans Himadri Fault (THF), Kumaun Tethys Himalaya, India: a case study of palaeolake deposits. *Zeitschrift für Geomorphologie* 57(3):289–303
- Kotlia BS, Rawat KS (2004) Soft sediment deformation structures in the Garbyang palaeolake: evidence from the past shaking events in the Kumaun Tethys Himalaya. *Curr Sci* 87(3):377–379
- Kotlia BS (1995) Upper Pleistocene Soricidae and Muridae from Bhimtal-Bilaspur deposits, Kumaun Himalaya. *J Geol Soc India* 46:177–190
- Kotlia BS, Sanwal J (2004) Fauna and palaeoenvironment of a late Quaternary fluviolacustrine basin in central Kumaun Himalaya. *Curr Sci* 87:1295–1299
- Kotlia BS, Bhalla MS, Sharma C, Rajagopalan G, Ramesh R, Chauhan MS et al (1997) Palaeoclimatic conditions in the upper Pleistocene and Holocene Bhimtal-Naukuchiatal lake basin in southcentral Kumaun, India. *Palaeogeogr Palaeoclimatol Palaeoecol* 130:307–322
- Kotlia BS, Sharma C, Bhalla MS, Rajagopalan G, Subrahmanyam K, Bhattacharya A et al (2000) Palaeoclimatic conditions in the late Pleistocene Wadda Lake (Pithoragarh), Kumaun Himalaya. *Palaeogeogr Palaeoclimatol Palaeoecol* 162:105–118
- Ku TL (1976) The uranium-series methods of age determination. *Annu Rev Earth Pl Sc* 4:347–379
- Kumar S, Wesnousky SG, Rockwell TK, Ragona D, Thakur VC, Seitz GG (2001) Earthquake recurrence and rupture dynamics of Himalayan Frontal Thrust, India. *Science* 294:2323–2331
- Lahiri SK, Sinha R (2012) Tectonics controls on the morphodynamics of Brahmaputra River system in the upper Assam valley, India. *Geomorphology* 1–12
- Lahiri SK, Sinha R (2014) Morphometric evolution of Majuli Island in the Brahmaputra valley of Assam, India inferred from the geomorphic and geophysical analysis. *Geomorphology* 227:101–111
- Lal D (1988) In situ produced cosmogenic isotopes in terrestrial rocks and some applications to geochronology. *Annu Rev Earth Pl Sc* 16:355–388
- Lund SP (1996) A comparison of Holocene paleomagnetic secular variation records from North America. *J Geophys Res* 101:8007–8024
- Leland J, Reid MR, Burbank DW, Finkel R, Caffee M (1998) Incision and differential bedrock uplift along the Indus River near Nanga Parbat, Pakistan Himalaya, from ¹⁰Be and ²⁶Al exposure age dating of bedrock straths. *Earth Planet Sci Lett* 154:93–107
- Libby WF (1955) Radiocarbon dating. University of Chicago Press, Chicago
- Malik JN, Sohoni P, Merh SS, Karanth RV (2001) Active tectonic control on alluvial fan architecture along Kachchh mainland hill range western India. *Zeitschrift für Geomorphologie*, NF 45:81–100
- Malik JN, Nakata T (2003) Active faults and related Late Quaternary deformation along the Northwestern Himalayan Frontal Zone, India. *Ann Geophys* 46(5):917–935

- Makovsky Y et al (1996) Structural elements of the southern Tethys Himalayan crust from wide-angle seismic data. *Tectonics* 15:997–1005
- Mathur PP, Kotlia BS (1999) Late Quaternary microvertebrate assemblage from glaciolacustrine sediments of the Lamayuru basin, Ladakh Himalaya. *J Geol Soc India* 53:173–180
- Middlemiss CS (1890) Physical geology of the sub-Himalaya of Garhwal and Kumaon Mem. Geol Surv India 24(2):59–200
- Mohindra R, Bagati TN (1996) Seismically induced soft-sediment deformation structures (seismites) around Sumdo in the Lower Spiti valley (Tethys Himalaya). *Sediment Geol* 101:69–83
- Morner NA (1980) The INQUA neotectonic commission. *Bull INQUA Neotectonic Comm* 3:1
- Mukul M (2000) The geometry and kinematics of the Main Boundary Thrust and related neotectonics in the Darjiling Himalayan fold-and-thrust belt, West Bengal, India. *J Struct Geol* 22:1261–1283
- Mukul M (2010) First-order kinematics of wedge-scale active Himalayan deformation: insights from Darjiling-Sikkim-Tibet (DaSiT) wedge. *J Asian Earth Sci* 39:645–657
- Mukul M, Jaiswal M, Singhvi AK (2007) Timing of recent out-of-sequence active deformation in the frontal Himalayan wedge: insights from the Darjiling sub-Himalaya, India. *Geology* 35:999–1003
- Mukul M, Singh V (2016) Active tectonics and geomorphological studies in India during 2012–2016. *Proc Indian Natl Sci Acad* 82(3 July Spl):727–735
- Murawski H (1972) *Geologisches Wörterbuch*. Enke, Stuttgart, p 260
- Mulchandani N, Patidar AK, Vaid SJ, Maurya DM (2007) Late Cenozoic geomorphic evolution in response to inversion: evidence from Weld and GPR studies in Kim drainage basin, western India. *J Asian Earth Sci* 30:33–52
- Nakata T (1972) Geomorphic history and crustal movements of the foot-hills of the Himalayas Sendai, Japan
- Nakata, T. (1989). Active faults of the Himalaya of India and Nepal. *Geol Soc Am* 232(Special paper):243–264
- Narula PL, Acharyya SK, Banerjee J (2000) Seismotectonic atlas of India and its environs. Special publication, vol 59. Geological Survey of India, pp 1–40
- Ni J, Barazangi M (1985) Active tectonics of western tethyan Himala above the underthrusting Indian plate: the upper Sutluj river basin as a pull apart structure. In: Kobayashi K, Sacks IS (eds) Structures and processes in subduction zones. *Tectonophysics*, vol 112, pp 277–295
- Nishiizumi K, Kohl CP, Arnold JR, Klein J, Fink D, Middleton R (1991) Cosmic ray produced ¹⁰Be and ²⁶Al in Antarctic rocks: exposure and erosion history. *Earth Planet Sc Lett* 104:440–454
- Oatney EM, Virdi NS, Yeats RS (2001) Contribution of Trans-Yamuna Active Fault System to wards hanging wall strain release above the decollement, Himalayan foothills of Northwest India. *Himal Geol* 22(2):9–27
- Obruchev VA (1948) Osnovnye cherty kinetiki i plastiki neotektonik. *Izv. Akad. Nauk. Ser. Geol.* 5:13–24
- Pandey P, Pandey AK (2004) Soft sediment deformation features in the meizoseismal region of 1999-Chamoli earthquake of Garhwal Himalaya and their significance. *Himal Geol* 25(1):79–87
- Pande P, Kayal JR, Joshi YC, Ghevariya ZG (2003) Lithotectonic framework of Gujarat and adjoining regions, in Kutch (Bhu) earthquake 26 January, 2001. *Geol Surv India Sp Pub* 76:5–11
- Pandey MR, Tandulkar RP, Avouac JP, Vergne J, Heritier T (1999) Seismotectonics of the Nepal Himalaya from a local seismic network. *J Asian Earth Sci* 17:703–712
- Pant RK, Juyal N, Basavalah N, Singhvi AK (2006) Later Quaternary glaciation and seismicity in the Higher Central Himalaya: evidence from Shalang basin (Gori-ganga), Uttaranchal. *Science* 90(11):1500–1505. (current)
- Pati JK, Malviya VP, Prakash K (2006) Basement reactivation and its relation to neotectonic activity in and around Allahabad, Ganga plain. *J Indian Soc Remote Sens* 34(1):47–56
- Pati P, Mohan PR, Dash C, Prakash B, Awasthi AK (2015) Terminal fans and the Ganga plain tectonism: a study of neotectonism and segmentation episodes of the Indo-Gangetic foreland basin, India. *Earth Sci Rev* 148:134–149

- Pavlidis SB (1989) Looking for a definition of neotectonics. *Terra Nova* 1(3):233–235. <https://doi.org/10.1111/j.1365-3121.1989.tb00362.x>
- Phartiyal B, Sharma A, Srivastava P, Ray Y (2009) Chronology of relict lake deposits in the Spiti River, NW Trans Himalaya: implications to Late Pleistocene-Holocene climate-tectonic perturbations. *Geomorphology* 108:264–272
- Phartiyal B, Sharma A, Upadhyay R, Awatar R, Sinha AK (2005) Quaternary geology, tectonics and determination of palaeo- and present fluvio-glacio-lacustrine deposits in Ladakh, NW Indian Himalaya—a study based on field observations. *Geomorphology* 65:241–256
- Phillips FM, Leavy BD, Jannik NO, Elmore D, Kubik PW (1986) The accumulation of cosmogenic chlorine-36 in rocks: a method for surface exposure dating. *Science* 231:41–43
- Powers PM, Lille RJ, Yeats RS (1998) Structure and shortening of the Kangra and Dehra Dun re-entrants, Sub-Himalaya, India. *Bull Geol Soc Am* 110:1010–1027
- Rao DP (1977) A note on recent movements and origin of some piedmont deposits of Dehradun Valley. *Photonirvachak* 5:4–40
- Radhakrishna BP (1964) Evolution of the Sharavati drainage, Mysore State, South India. *J Geol Soc India* 5:72–79
- Raj R (2004) Fluvial response to Later Quaternary tectonic changes in the Dhadhar River basin, Mainland Gujarat. *J Geol Soc India* 64:666–676
- Ramasamy SM (1999) Neotectonic controls on the migration of Sarasvati River of the Great Indian desert. *Mem Geol Soc India* 42:153–162
- Ramasamy SM, Bakliwal PC, Verma RP (1991) Remote sensing and river migration in western India. *Int J Remote Sens* 12:2597–2609
- Ramasamy SM, Saravanavel J, Selvakumar R (2006) Late Holocene geomorphic evolution of Cauvery Delta, Tamil Nadu. *J Geol Soc India* 67(5):649–657
- Rathore VS, Nathawat MS, Ray PKC (2008) Influence of neotectonic activity on groundwater salinity and playa development in the Mendha river catchment, western India. *Int J Remote Sens* 29(13):3975–3986
- Rashid B, Islam SU, Islam B (2015) Sub-Surface geology and evolution of the 263 Barind Tract, Bangladesh. *Am J Earth Sci* 2(2):22–38
- Rautela P, Sati D (1996) Recent crustal adjustments in Dehradun Valley, western Uttar Pradesh, India. *Curr Sci* 71:776–780
- Reitz MD, Pickering JL, Goodbred SL Jr, Paola C, Steckler MS, Seeber L, Akhter SH (2015) Effects of tectonic deformation and sea level on river path selection: theory and application to the Ganges-Brahmaputra-Meghna River Delta. *J Geophys Res Earth Surf* 120:671–689
- Rengamannar V, Pradhan PK (1991) Geomorphology and evolution of Godavari delta. *Mem Geol Soc India* 22:51–56
- Roy AB, Jakhar SR (2002) *Geology of Rajasthan (Northwest India) Precambrian to recent*, vol 349. Scientific Publishers, Jodhpur
- Rudra K (2018) *Rivers of the Ganga-Brahmaputra-Meghna Delta, A Fluvial account of Bengal*. Springer International Publishing AG part of Springer Nature
- Sakai H (2001) Stratigraphic division and sedimentary facies of the Kathmandu Basin Group central Nepal. *J Nepal Geol Soc* 25:19–32
- Sarna-Wojcicki AM, Lajoie KR, Meyer CE, Adam DP, Rieck HJ (1991) Tephrochronology correlation of upper Neogene sediments along the Pacific margin, conterminous United States. In: Morrison RB (ed) *Quaternary nonglacial geology: conterminous U.S. (The geology of North America, vol. K-2)*. Geological Society of America, Boulder, CO, pp 117–140
- Shah MP, Virdi NS (1997) Geomorphic signatures of neotectonic activity along the Sumdo Fault, Spiti valley, district Kinnaur, H.P. *Himalayan Geol* 18:81–92
- Sahu S, Saha D (2014) Geomorphologic, stratigraphic and sedimentologic evidences of tectonic activity in Sone-Ganga alluvial tract in Middle Ganga Plain, India. *J Earth Syst Sci* 6:1335–1347
- Sahu VK, Gahalaut VK, Rajput S, Chadha RK, Laishram SS, Kumar A (2006) Crustal deformation in the Indo-Burmese arc region: implications from the Myanmar and southeast Asia GPS measurements. *Curr Sci* 90:1688–1693

- Saini HS, Tandon SK, Mujtalia SAI, Pant NC, Khorana RK (2009) Reconstruction of buried channel-floodplain system of northwestern Haryana Plains and their relation to the Vedic Saraswati. *Curr Sci* 97:1634–1693
- Saini HS, Mujtalia SAI (2010) Luminescence dating of the sediments from a buried channel loop in Fatehabad area, Haryana: Insight into Vedic Saraswati. *Geochronometria* 37:29–35
- Sangode SJ, Meshram DC, Kulkarni YR, Gudadhe SS, Malpe DB, Herlekar MA (2013) Neotectonic response of the Godavari and Kaddam Rivers in the Andhra Pradesh, India: implication of quaternary reactivation of Old Fracture System. *J Geol Soc India* 81:459–471
- Sarma JN, Sharma S (2018) Neotectonic activity of the Bomdila Fault in the northeastern India from geomorphological evidences using remote sensing and GIS. *J Earth Syst Sci* 127(9):113
- Sastry VV, Bhandari LL, Raju ATR, Datta AK (1971) Tectonic framework and subsurface stratigraphy of the Ganga Basin. *J Geol Soc India* 12:222–233
- Sharma KK, Gu, ZY, Pal D, Caffè MW, Southon J (1998) Late quaternary morphotectonic evolution of Upper Indus valley: a cosmogenic radionuclide study of river polished surfaces. *Curr Sci* 75:366–369
- Sharma S, Sarma JN (2013) Drainage analysis in a part of the Brahmaputra Valley. *J Indian Soc Remote Sens* 1–10
- Sharma M, Divyadarshini A, Singh V (2019) Morphotectonic evolution of the Siwalik Hills between the Yamuna and the Markanda River Exits, NW Himalaya. *J Geol Soc India* 94:453–463
- Shukla UK, Srivastava P, Singh IB (2012) Migration of Ganga River and development of cliffs in the Varanasi region, India during the late Quaternary: role of active tectonics. *Geomorphology* 101–113
- Singh IB (1996) Tectonic control of sedimentation in Ganga Plain—an overview. *J Palaeontol Soc India* 41:272–282
- Singh IB, Ghosh DK (1994) Geomorphology and neotectonic features of Indo-Gangetic plain. In: Dixit KR, Kale VS, Kaul MN (eds.) *Geomorphological diversity. Essays in honour of Prof. A. B. Mukerji*. Rawat Publications, Jaipur and New Delhi, pp 270–286
- Singh AK, Jaiswal MK, Pattanaik JK, Dev M (2016) Luminescence chronology of alluvial fan in North Bengal, India: implications to tectonics and climate. *Geochronometria* 43:102–112
- Singh IB, Rajagopalan G, Agarwal KK, Srivastava P, Sharma M, Sharma S (1997) Evidence of Middle to Late Holocene neotectonic activity in the Ganga Plain. *Curr Sci* 73(12):1114–1117
- Sinha-Roy S (2001) Neotectonically controlled catchment capture: an example from the Banas and Chambal drainage basins, Rajasthan. *Curr Sci* 80:293–298
- Sinha-Roy S, Mohanty M, Guha DB (1993) Banas dislocation zone in Nathadwara- Khannor area Udaipur District, Rajasthan and its significance on the basement-cover relations in the Aravali fold belt. *Curr Sci* 65:68–72
- Sridhar V, Chamyal LS, Merh SS (1994) North Gujarat rivers: remnants of super fluvial system. *J Geol Soc India* 44:427–434
- Srivastava V, Mukul M (2017) Quaternary deformation in the Gorubathan recess: Insights on the structural and landscape evolution in the frontal Darjiling Himalaya. *Quatern Int* 462:138–161
- Srivastava GS, Kulshrestha AK, Agarwal KK (2012) Morphometric evidences of neotectonic block movement in Yamuna Tear Zone of Outer Himalaya, India. *Zeitschrift für Geomorphologie* 57(4):471–484
- Srivastava P, Ray Y, Sundriyal Y (2009) Himalayan Rivers: responses to past climatic changes. *Indian Geophysical Union*, pp 764–778
- Srivastava GS, Singh IB, Kulshrestha AK (2011) Neotectonic activity along Ganga-Indus water divide in Haryana-Punjab plain: inferences from drainage morphometry. *Him Geol* 32(2):113–121
- Srivastava P, Singh IB, Sharma S, Shukla UK, Singhvi AK (2003) Late Pleistocene- =Holocene hydrologic changes in the interfluve areas of the central Ganga Plain India. *Geomorphology* 54:279–292
- Stanley DJ, Hait AK (2000) Holocene depositional patterns, neotectonics and sundarban mangroves in the Western Ganges-Brahmaputra Delta. *J Coast Res* 16(1):26–39

- Starkel L, Sarkar S, Soja R, Prokop P (2008) Present-day evolution of the Sikkimese-Bhutanese Himalayan Piedmont, *Geographical Studies*: No 219
- Stewart I (2005) *Encyclopedia of geology*
- Stuiver M (1970) Tree ring, varve and carbon-14 chronologies. *Nature* 228:454–455
- Subrahmanya KR (1994) Post-Gondwana tectonics of Indian Peninsula. *Curr Sci* 67:527–530
- Subrahmanya KR (2002) Deformation-related lineaments in the Indian Peninsula near 13°N. *Indian J Geophys* 23:59–68
- Thakur VC, Pandey AK (2004) Active deformation of Himalayan frontal thrust and piedmont zone south of Dehra Dun in respect of seismotectonics of Garhwal Himalaya. *Himal Geol* 25:23–31
- Valdiya KS (1976) Himalayan transverse faults and folds and their parallelism with subsurface structures of North Indian plains. *Tectonophysics* 32:353–386
- Valdiya KS (1988) *Geology and natural environment of Nainital Hills*. Nainital: Gyanodaya Prakashan, p 155
- Valdiya KS (2001) Reactivation of terrane-defining boundary thrusts in central sector of the Himalaya: implications. *Curr Sci* 81:1418–1431
- Valdiya KS, Rajagopalan G (2000) Large palaeolakes in Kaveri basin in Mysore Plateau: late Quaternary fault reaction. *Curr Sci* 78:1138–1142
- Valdiya KS, Rana RS, Sharma PK, Dey P (1992) Active Himalayan frontal fault, main boundary Thrust and Ramgarh Thrust in Southern Kumaun. *J Geol Soc India* 40:509–528
- Valdiya KS (1999) Why does river Brahmaputra remain untamed? *Curr Sci* 76:1301–1303
- Valdiya KS (2016) *The Making of India Geodynamic Evolution*. Springer
- Valdiya KS (1998). Late Quaternary movements on landscape rejuvenation in southeastern Karnataka adjoining Tamil Nadu in Southern Indian shield. *J Geol Soc India* 51:139–166
- Valdiya KS (2002) *Saraswati: the river that disappeared*. Universities Press, Hyderabad, p 116
- Valdiya, K S (1984) *Aspects of tectonics: focus on South–Central Asia*, (pp 270–272). Tata MacGraw Hill, New Delhi, pp 319
- Valdiya KS (2003) Reactivation of Himalayan frontal fault: Implication. *Curr Sci* 85(7):1031–1040
- Veerawamy K, Raval U (2005) Remobilization of the palaeoconvergent corridors hidden under the Deccan trap cover and some major stable continental region earthquakes. *Curr Sci* 89(3):522–530
- Verma M, Bansal BK (2016). Active fault research in India: achievements and future perspective. *Geomat Nat Hazards Risk* 7(1):65–84
- Vita-Finzi C (1986) *Recent earth movements, an introduction to neotectonics*. Academic Press, London, p 226
- Wadia DN (1976) *Geology of India*. Tata MC Graw-Hill Publishing Co., New Delhi
- Wallace RE (Panel chairman) (1986) *Active tectonics*. Studies in geophysics. National Academy Press, Washington D.C
- Wesnousky SG, Kumar S, Mohindra R, Thakur VC (1999): Uplift and convergence along the Himalayan Frontal Thrust. *Tectonics* 18(6):967–976
- Westgate JA, Gorton MP (1981) Correlation techniques in tephra studies. In: Self S, Sparks RSJ (eds) *Tephra studies*, NATO advanced studies institute series C. Reidel, Dordrecht, pp 73–94
- Whittington AG (1996) Exhumation over-reted at Nangpa Parbat northern Pakistan. *Tectonophysics* 206:215–226
- Yashpal SB, Sood RK, Agarwal DP (1980) Remote sensing of the lost Saraswati river. *Proc Ind Acad Sci (earth & Planet Sci)* 89:317–337
- Yamaguchi DK, Hoblitt RP (1995) Tree-ring dating of pre-1980 volcanic flowage deposits at Mount St. Helens, Washington. *Geol Soc Am Bull* 107:1077–1093
- Yamanaka H, Yagi H (1984) Geomorphic development of Dang Dun, Sub-Himalayan Zone, southwestern Nepal. *Nepal Geol Soc J* 4:149–157
- Yeats RS, Thakur VC (1998) Reassessment of earthquake hazard based on a fault-bend fold model of the Himalayan plate-boundary fault. *Curr Sci* 74:230–233

- Yoshida M, Gautam P (1988) Magnetostratigraphy of Plio-Pleistocene lacustrine deposits in the Kathmandu Valley, central Nepal. In: Palaeoclimatic and Palaeoenvironmental Changes in Asia during the last 4 million years. Indian National Science Academy, New Delhi, pp 78–85
- Zeitler PK, Johnson NM, Naeser CW, Tahirkheli RAK (1982) Fission-track evidence for Quaternary uplift of the Nanga Parbat region, Pakistan. *Nature* 298:255–257

Effects of Differential Tectonic Uplift on Steepness and Concavity Indices and Erosion Rates in Between the Major Thrusts in Bhagirathi-Alaknanda Catchments, NW Himalayas, India



Sumit Das  and Satish J. Sangode

Abstract Geomorphology of the Bhagirathi-Alaknanda catchments draining across the northwest Himalayas was studied to understand the role of differential tectonic uplifts over landscape erosional rates and landscape shaping. We plotted longitudinal profiles of Bhagirathi and Alaknanda and identified the major thrust zones along these trunk streams. For the comprehension of differential uplift, steepness and concavity indices were computed in between major thrusts along the longitudinal profiles. The regions experiencing very high erosion were recognized through anomalously high normalized steepness index (k_{sn}) and dense distribution of knick-points on the drainage network. Further estimation of average erosion and deposition rates between the major thrusts was done through establishing linear correlation of average normalized steepness index and readily available in-situ ^{10}Be cosmogenic dating-derived erosion rate data. Our results indicated a very high erosion rate (2.87 mm/yr) between Main Central Thrust I and II (Vaikrita Thrust), related to intense uplift, high recurrence of landslides and profound fluvial incision. Regions from MBT to further south towards Ganga plain showed strong aggradation at an average rate of 3.03 mm/yr.

Keywords Tectonic uplift · Steepness index · Erosion rate · Longitudinal profile · Alaknanda · Himalayas

1 Introduction

The mighty Himalayas politically shares a considerable area of north India, Nepal, and Bhutan and forms an arc-shaped series of high mountains, showing the highest peak (Mount Everest—8848.86 m a.s.l.) of the world and several peaks that have elevation above 7000 m above sea level [a.s.l.] (e.g. Kanchenjunga, Nanga Parbat, Nanda Devi, Makalu etc.) (Fig. 1). A large number of geological-geomorphic

S. Das (✉)

Department of Geography, Savitribai Phule Pune University, Pune 411007, India

S. J. Sangode

Department of Geology, Savitribai Phule Pune University, Pune 411007, India

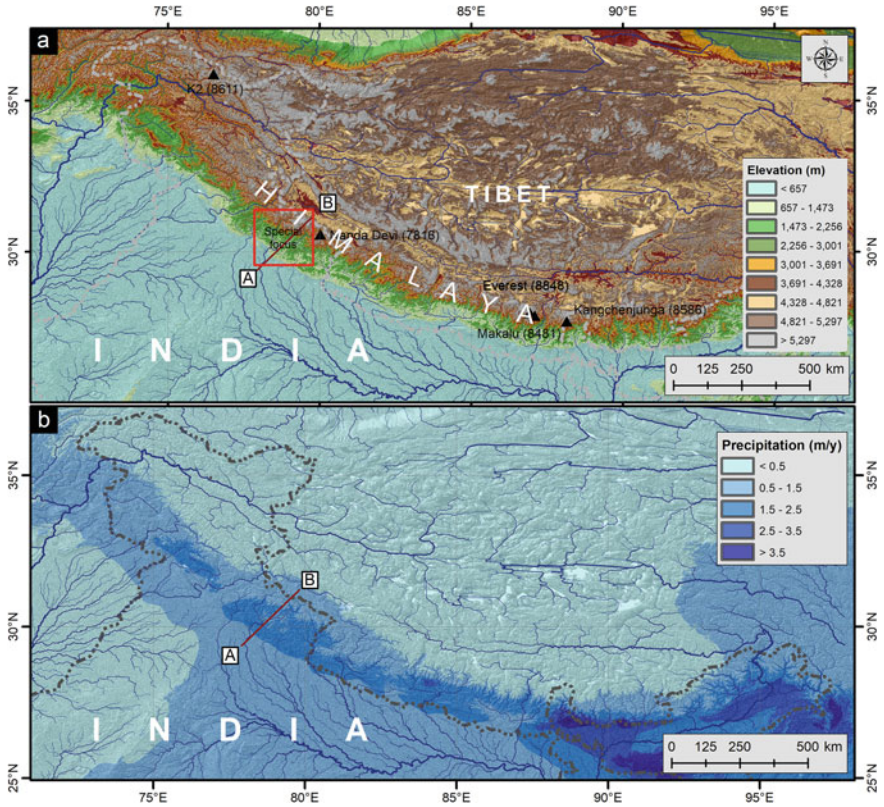


Fig. 1 **a** DEM is showing variation in elevation along the Himalayas and surrounding regions with major drainage networks. **b** Spatial distribution of rainfall along the Himalayas (*Source* <https://www.worldclim.org/>)

processes (both endogenetic and exogenetic) led to shape and reshape the landscape of the Himalayas, what we see presently. Created by continent–continent collision, the Himalayas is one of the best classic examples of the orogenic system (Dewey and Bruke 1973). To understand the geomorphic processes and diversity in the Himalayas, it is essential to look back in time and understand the continental framework that led to the rise of such massive and spectacular high ranges.

About 180 Ma ago, the Indian continent started breaking from the Gondwana land and drifted northwards at rates varying from ~4 to 20 cm/yr (Seeber et al. 1981; Patriat and Achache 1984; Pichon et al. 1992). The relatively fast, inexorable drift of the South Asian continent then nearly 50 Ma ago collided with the Eurasian plate and resulted in uplifting of huge compressed seafloor (the Tethys) and formation of an extraordinary gigantic range of fold mountains named the Himalayas that stands

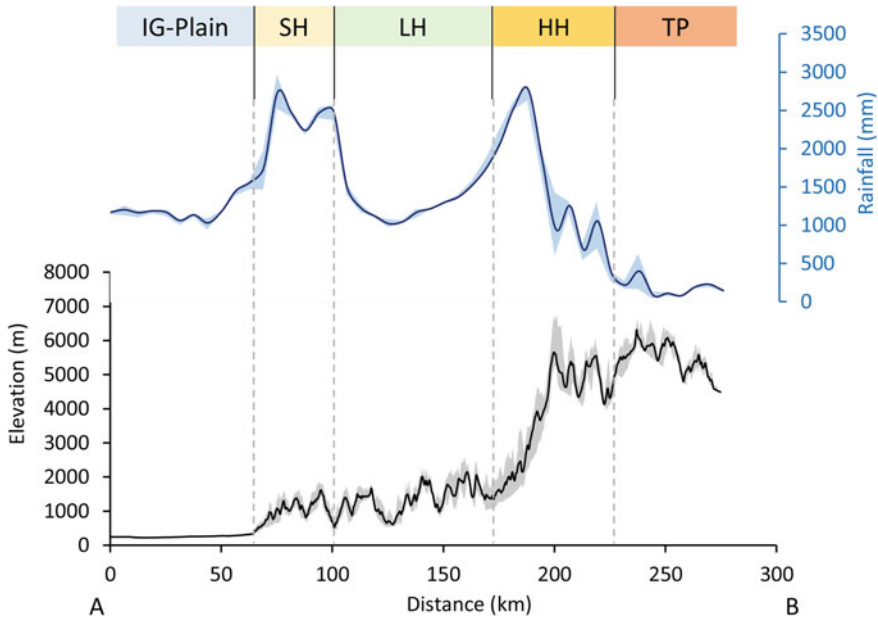


Fig. 2 Generalized broad physiographic divisions and variation in precipitation in the Himalayas (Alaknanda catchment) from south (a) to north (b). See Fig. 1. For the swath line, IG: Indo-Gangetic plain, SH: Sub-Himalayas, LH: Lesser Himalayas, HH: Higher Himalayas, TP: Tibetan Plateau

above all other places in the world (Patriat and Achache 1984). The abundant distribution of fossils of ancient sea creatures, for example, ammonites on the Himalayan sedimentary rocks indicates that the region once was beneath the ocean.

Based on the range's orientation and structure, the Himalayas can be divided into four major broad physiographic divisions (Fig. 2). The southern section comprises an Indo-Gangetic plain made of alluvium brought by the Himalayan Rivers (Singh et al. 2015). The low, frontal sub-Himalayas form the foothill region. These foothills have an average height of about 900–1500 m (Whitehouse 1990). North of the sub-Himalayas, the hill ranges within the lesser Himalayas show elevation between 700 and 2500 m. The higher Himalayas forms the highest relative relief (~6000 m) with several peaks above 8000 m. The Tibetan marginal range forms a 6000–7000 m high Tibetan plateau north of the higher Himalayas.

The Indian Summer Monsoon (ISM) modulates the process of erosion and its rates along the southern margin of the Himalayan topographic front (Bookhagen and Burbank 2006). The rainy season in the Himalayas starts from early June and continues till September; therefore, this orographic rainfall has a significant role in the erosional mechanism (Fasullo and Webster 2003). The topographic and rainfall distribution was poorly understood until the work of Bookhagen and Burbank (2006). They showed the relationship between rainfall and topographic (elevation) distribution across the Himalayas through a number of swath profiles. The monsoons, while

moving northward, experience the first significant topographic barrier due to the Lesser Himalayas, where intense orographic rainfall occurs. Once the cloud crosses Lesser Himalayas, rainfall intensity becomes less until it once again reaches the Higher Himalayas and the second phase of rainfall occurs in front of this massive topographic front. The Higher and Tethyan Himalayas receives the majority of its precipitation from the Western Disturbances responsible for the winter snow accumulation (Rees and Collins 2006; Dimri et al. 2015).

Landscapes of the Himalayas are mainly formed by the collision of continental blocks that uplifted the landmass; and the intense and variable summer monsoon precipitation shaped the modern topography in Lesser and Outer Himalayas (Abrahami et al. 2016; Sinha and Sinha 2016). The Himalayas has become a natural laboratory to understand the complex relationship between tectonic uplift and climate on erosion for the past several decades. While a large number of studies only focus on the role of uplift (e.g. Kothyari and Luirei 2016; Bhakuni et al. 2017; Sharma et al. 2018), several studies indicate a combination of climate and tectonics to play a crucial role in differential erosion rates (e.g. Vence et al. 2003; Thide et al. 2005) through geological time. Since the antecedent river response is simultaneous to both tectonic and climatic variability across the cross-sections of the Himalayas, they are ideal locales for detailed studies.

Bhagirathi and Alaknanda are two major rivers that flow across the Himalayas covering the major section of Lesser and Outer Himalayas and forming the mega river Ganga in the foothills. In the past few decades, these two rivers and the areas within the catchment have become the interests of geomorphologists to understand the complex geomorphic processes (e.g. Valdiya 1988; Tyagi et al. 2009; Ray and Srivastava 2010; Rana et al. 2016). The geomorphic processes in this region are genetically related to structural and tectonic complexities within Kumaun Lesser Himalayas as described in classical literature (Valdiya 1988). Nonetheless, the influence of climate in the formation of river terraces and stratigraphic development is very well described (e.g., Ray and Srivastava 2010). Rana et al. (2016) earlier elaborated the significance of tectonic geomorphology within the Alaknanda valley through morphometric analysis. Tyagi et al. (2009) made a remarkable discussion by identifying of differentially uplifted areas using the steepness index of the Alaknanda River profile. These workers (Tyagi et al. 2009) divided the longitudinal profiles into several reaches to compute the normalized steepness index (k_{sn}). Although considering a single longitudinal profile merely provides some instances of differential uplift and erosion at local scale, for the regional tectonic framework, it is essential to estimate k_{sn} for all the available drainages as well, and correlate the average k_{sn} with erosion rate for a robust conclusion. Therefore, the aim of this present study is set to understand the role of tectonics in the formation of anomalies on the longitudinal profiles, variation in steepness and concavity index and estimation of erosion rates in between major Himalayan thrust belts in the Alaknanda-Bhagirathi catchment. In the event of an emerging climate change scenarios marked by heavy rainfall, cloud burst triggered flash-floods or the Glacial Lake Outburst Floods (GLOF), an assessment of the longitudinal profiles across these Himalayan states is essential to anticipate their response.

2 Study Area

2.1 Location

The Alaknanda and Bhagirathi Rivers (Fig. 3) flow over the active orogeny of the Himalayas (Ray and Srivastava 2010). These two rivers cross the Himalayan thrust belts in the northern section while the southern section is characterized by the vast Ganga plain (Singh et al. 2007, 2015). River Alaknanda originates from the Satopanth glacier at an elevation of 3641 m, and the Bhagirathi originates from the Gangotri glacier near Gaumukh at an elevation of 3892 m a.s.l. These two rivers meet near Devprayag and form the sacred river Ganga. Geomorphological breaks that are marked by a series of knick points in Bhagirathi and Alaknanda show deep incision and gorges in the upper and middle reaches. Geomorphologically, these two rivers show three distinct reaches: (a) the glaciated, semi-arid U-shaped valley in the upper section; (b) steep V-shaped deep gorges in the middle reach and this section forms the main orographic barrier of the ISM and shows intense precipitation marked by numerous geomorphic processes (Bookhagen and Burbank 2006; Wasson et al. 2008); and (c) gentle slope with sediment-filled wide valley in the lower reaches.

2.2 Geology

The Alaknanda-Bhagirathi catchment shows two major geomorphic divisions: (i) the Himalayan active terrain and (ii) the Ganga foreland plain (Ray and Srivastava 2010). Himalayan thrust belt, located in the northern section of Alaknanda- Bhagirathi catchment shows several parallel thrusts marked by distinct lithology groups. The major lithology in this catchment from north to south are (i) Tethyan sedimentary, (ii) upper higher Himalayan crystalline (Vaikrita group), (iii) lower higher Himalayan crystalline (Munsiari formation), (iv) inner lesser Himalayan sedimentary, (v) outer lesser Himalayan sedimentary, and (vi) Quaternary sediment. While flowing over the Himalayas, Alaknanda river crosses the South Tibetan Detachment (STD) in the northernmost region of catchment, followed by Main Central Thrust (MCT) II and I, Main Boundary Thrust (MBT), and Main Frontal Thrust (MFT) in the south before reaching the vast Gangetic Plain.

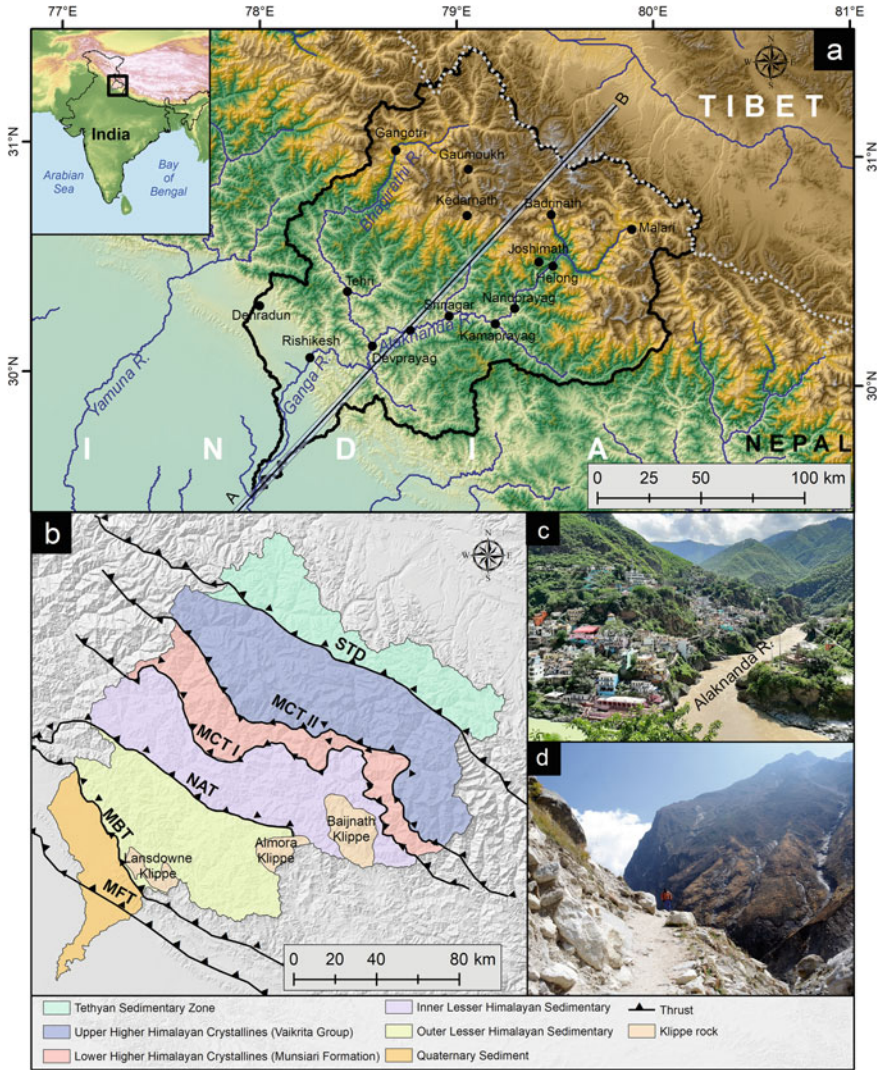


Fig. 3 Location of the Alaknanda-Bhagirathi catchment. **a** Major rivers and locations in the study area. See Fig. 2 for the swath profile of A-B. **b** Simplified geological map of the study area (reproduced after Singh 2018). Note that the thrusts are not limited as shown in this figure but continuous features along the Himalayas from west to east. **c** The confluence of Alaknanda and Bhagirathi near Devprayag. **d** Landscape configuration at the upper Alaknanda catchment

3 Data and Methodology

3.1 Data Processing

High-resolution digital elevation models are often considered in quantitative landscape evolution studies around the world. In this study, we utilized the Shuttle Radar Topographic Mission (SRTM) digital elevation model (DEM) of 90 m spatial resolution (<http://srtm.csi.cgiar.org>). The DEM was processed in ArcGIS 10.1 to fill data gaps, generating Alaknanda-Bhagirathi catchment and streams, utilizing hydrology tools. We also delineated sub-catchments by carefully selecting all the tributaries that have streams of 4th order while joining the trunk stream. Then we computed relief, slope, and hypsometric integral [mean elevation-min elevation/max elevation- min elevation] for all the sub-catchments.

We plotted longitudinal profiles in MATLAB (<https://www.mathworks.com>) based stream profiler tool (<https://geomorphtools.geology.isu.edu>). Then normalized steepness index (k_{sn}) for the entire stream network was estimated in TopoToolbox (Schwanghart and Kuhn 2010).

Pixel-based TRMM precipitation data (www.geog.ucsb.edu/~bodo/TRMM) was utilized for swath profiling and rainfall- k_{sn} correlation.

3.2 Longitudinal Profile and Steepness-Concavity Analysis

The effect of spatially varying rock uplift rates on the bedrock river profiles can be understood from the steepness index (Howard et al. 1994; Kirby and Whipple 2001). The river profile evolution can be expressed as an equation through the incision modeling of the power-law function of channel gradient and drainage area (Howard and Kerby 1983; Howard 1994; Kirby and Whipple 2001):

$$\frac{dz}{dt} = U(x, t) - K A^m S^n \quad (1)$$

where dz/dt indicates the changes in the bedrock elevation through time, U indicates the rate of bedrock uplift while the base-level is constant, S is the local channel gradient, A is the upstream drainage area and K is the coefficient of erosion. The constants m and n are positive and are closely related to erosion, hydraulic geometry, and hydrology (Howard et al. 1994; Whipple and Tucker 1999). For equilibrium condition, the above equation can be rewritten as:

$$S_c = \left(\frac{U}{K} \right)^{1/n} A^{-\left(\frac{m}{n}\right)} \quad (2)$$

and

$$S = k_s A^{-\theta} \quad (3)$$

where S denotes the slope, k_s is the steepness index and θ indicates the concavity index. Since past decades, several studies have suggested a close relationship between erosion rate and the steepness index. As differential uplift has different erosion rates along the channel, as a proxy, this index can be used to determine the variable uplift of a catchment. Although the steepness index is a good indicator of varying uplift, k_s can significantly be affected by lithological variation (Das 2020). Moreover, departures from the normal concavity ($\theta = 0.5 \pm 0.2$) may indicate tectonic uplift by disrupting the longitudinal profile (Burbank and Anderson 2012). In this study, the k_s values are normalized using a reference concavity (θ) of 0.45 for comparison of the steepness in different reaches, tributaries and sub-tributaries.

4 Neo-Tectonic Movement and Channel Evolution

4.1 Longitudinal Profiles of Bhagirathi-Alaknanda

Figure 4 shows longitudinal profiles of the Bhagirathi and Alaknanda rivers. It can be clearly observed that characterized by the glacier domain, first few kilometers of Alaknanda show a very steep gradient. Later, the river shows a series of knickpoints in between the Himalayan thrusts (STD and MCTs). These thrusts closely match with the knickpoints in Alaknanda (Fig. 4). From the source to the MCT I, the Alaknanda forms the knick zone. After crossing the MCT I, the gradient becomes very low. Compared to the Alaknanda, the Bhagirathi river shows a lesser gradient and fewer knick points. While Alaknanda shows prominent knicks in between MCT I and MCT II (MCT II is also known as Vaikrita thrust), such knicks are not very common in the Bhagirathi. Most of the major steep sections on the longitudinal profile are located above the MCT II.

4.2 Steepness-Concavity Index and Influence of Major Thrusts

In the present study, k_{sn} and θ are calculated for reaches in between major thrusts or distinct steeper topography. The longitudinal profile of Alaknanda is divided into four sections for the steepness concavity analysis. The normalized steepness index (k_{sn}) above STD is 121 ($\theta = 0.23 \pm 0.076$), followed by 792 ($\theta = -0.54 \pm 0.3$) in between STD and MCT II, 446 ($\theta = -17 \pm 40$) between MCT II and MCT I,

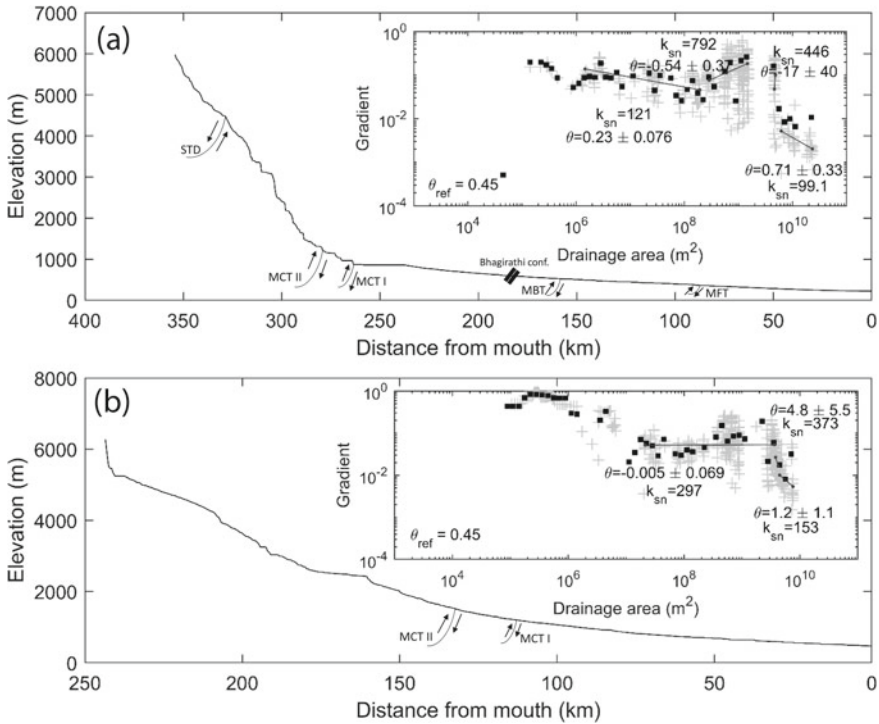


Fig. 4 Longitudinal profiles and the steepness-concavity index in between thrusts and major steep reaches. **a** Alaknanda; **b** Bhagirathi

and 99.1 ($\theta = 0.71 \pm 0.33$) from MCT I to Ganga plain, respectively, from north to south. A careful observation indicates that most of the knickpoints in the study area are distributed between MCT I and STD.

For the Bhagirathi, k_{sn} was calculated for three reaches (a) the irregular elevated, steeper topography in the upper-middle section above MCT II (VT), (b) between MCT II and MCT I and (c) relatively gentle middle-downstream reach. The k_{sn} value in the upper Bhagirathi above MCT II is 297 ($\theta = -0.005 \pm 0.16$), between MCT II and MCT I is 373 ($\theta = 4.8 \pm 5.5$) in, and in the gentler plain section below MCT I until Alaknanda confluence the k_{sn} is 153 ($\theta = 1.2 \pm 1.1$).

Several workers have reported that during the Pleistocene to Holocene periods, major boundary thrusts and faults (e.g. MBT, North Almora Thrust, MCT Alaknanda fault etc.) were active in this region (Sundriyal et al. 2007). Considering this, it is obvious that the geomorphology of this region is highly influenced by the tectonic perturbation by modifying the paleo-landscape. The active landscape has been directed to form some remarkable geomorphic features such as deep incision, changes in river courses and meanders, deformed and uplifted sequential fluvial terraces etc. (Sati et al. 2008) as a result of the recent mountain building process.

Vance et al. (2003) studied the erosion and exhumation rates in the Bhagirathi-Alaknanda catchment using in-situ ^{10}Be cosmogenic dating. In this study, besides longitudinal profile, a k_{sn} map for all the tributaries and sub-tributaries was prepared for the study area (Fig. 5a) for correlating the erosion rates at different thrust regions using the data produced by Vance et al. (2003). A significant positive correlation between k_{sn} and erosion rate is observed (Fig. 6) and therefore, any conclusion drawn from the k_{sn} may be considered as valid. Vance et al. (2003) showed a very

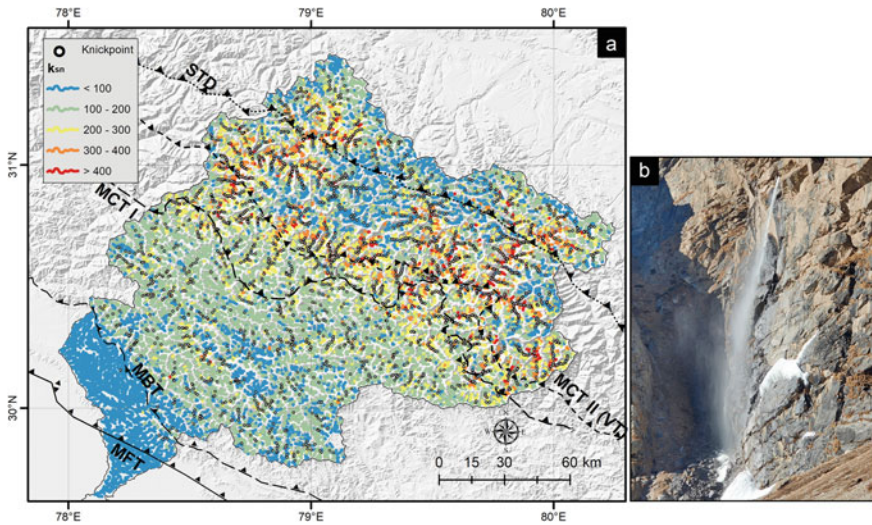
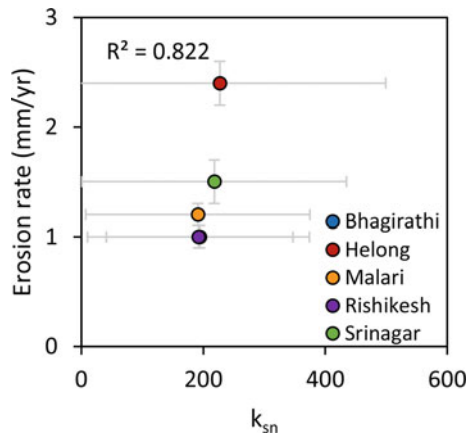


Fig. 5 a Variation of the normalized steepness index (k_{sn}) and knickpoint distribution in the Bhagirathi-Alaknanda catchment. Knickpoints are identified mathematically in MATLAB based Topotoolbox algorithm. The mathematical algorithm identified 2466 knickpoints in the study area. b Vasudhara knickpoint in the upper Alaknanda catchment

Fig. 6 Correlation between normalized steepness index (k_{sn}) and ^{10}Be derived erosion rates at upstream of several locations. ^{10}Be derived erosion rates for the study area are taken from Vance et al. (2003). Note that the data of Bhagirathi and Rishikesh are overlapping on the graph



high erosion rate in upstream of Helong ($2.4 \pm 0.2 \text{ mm yr}^{-1}$), followed by Srinagar ($1.5 \pm 0.2 \text{ mm yr}^{-1}$), Malari ($1.2 \pm 0.1 \text{ mm yr}^{-1}$), Bhagirathi and Rishikesh (both $1.0 \pm 0.1 \text{ mm yr}^{-1}$). This study shows a very consistent values of average k_{sn} in the upstream of Helong ($k_{sn} = 227$), Srinagar ($k_{sn} = 218$), Malari ($k_{sn} = 191$), Bhagirathi ($k_{sn} = 194$) and Rishikesh ($k_{sn} = 192$).

4.3 Estimation of Erosion Rates Between Thrusts

The integrated study of the longitudinal profile, steepness index and concavity index gives good insights into spatial distribution of differential erosion in Bhagirathi-Alaknanda basins. The upstream regions of the Alaknanda-Bhagirathi catchment in between MCTs show deep incisions and steeper gradients compared to the other reaches. Therefore, it may be said that in the study area, differential rock-uplift rate exerts a critical control on the channel gradient and that makes a difference in the steepness and concavity of the channels in different reaches.

Using the linear regression equation derived from the relationship between k_{sn} (this study) and erosion rate (Vance et al. 2003), a further estimation of the average erosion–deposition rates between thrust are calculated by the following equation:

$$\text{Erosion rate} = (0.0314 \times k_{sn}) - 5.0075 \quad (4)$$

while the regression showed $R = 0.91$, and $p \text{ value} = 0.03$.

Table 1 shows that the average k_{sn} value above STD (toward Tibet) is 178 while the derived average erosion rate is 0.58 mm/yr . Although the Tethyan sediment is more erodible than Himalayan crystalline rocks, the dominance of glacial activity over the fluvial process is the main reason behind the lower erosion rate above STD. Most of the landscape in this region is covered by Alpine and Valley glaciers that make a

Table 1 Average normalized steepness index (k_{sn}) and erosion/deposition rates at regions in between major thrusts

Region	Average k_{sn}	Erosion (+) or deposition (–) rate (mm/yr)
Above STD	178	0.58
Between MCT II and STD	237	2.43
Between MCT I and MCT II	251	2.87
Between MBT and MCT I	146	–0.42
Between MFT and MBT	30	–4.07
Ganga plain	13	–4.60

thick veneer on the rocky substrate and prevent intensive erosion. Consequently, the region between MCT I and II show the maximum estimated rate of erosion ($k_{sn} = 251$; erosion rate = 2.87 mm/yr). This region is found to have differential exhumation rates through geological past with a rapid exhumation of garnet rock as high as 9 mm/yr reported after reactivation of MCT during Miocene (~8 Myr) (Harrison et al. 1997; Catlos et al. 2001; Vance et al. 2003). Several studies suggest that in tectonically active landscape, differential k_{sn} values between faults indicate differential uplift (Kirby and Whipple 2001). Tyagi et al. (2009) suggested that the MCT region of the Alaknanda falls under a higher rate of uplift. Hence, based on results from this study, it can be said that the higher erosion rate between MCT I and MCT II may be a result of a higher uplift rate which is reflected by a higher frequency of landslides (Sarkar et al. 2015). Also, the MCT region shows high relief topography compared to the region above STD, which could be possibly another reason behind active incision and higher erosion rate. However, the negative values southwards of MBT (Table 1) indicate dominant depositional regime although, the present inferences are purely based on a statistical correlation between the erosion rate and k_{sn} , demanding further validation. Based on the above information, the average rates of deposition between MBT-MCT I, MFT-MBT and on the frontal plain are estimated as 0.42, 4.07 and 4.59 mm/yr, respectively.

4.4 Correlation of Landscape Variables and Rainfall with k_{sn}

Correlation between geomorphic parameters that are related to erosion (e.g. elevation, relief, slope, hypsometry etc.), rainfall, and lithology as independent factors and the normalized steepness index (k_{sn}) as dependent factor provides critical quantitative information about the potential control of the erosion in a given area (Abrahami et al. 2016). Therefore, although our study mainly focused on understanding differential uplift with respect to varying uplift rates in between major thrusts, in addition, we correlated major potentially controlling factors of the varying erosion rate in the Alaknanda-Bhagirathi catchment (Fig. 7). Among five variables (mean elevation, relief, slope, hypsometric integral, and rainfall) only relief is found to have a significant relation with k_{sn} ($R = 0.698$, $\alpha = 0.05$). It implies that, in the Alaknanda-Bhagirathi catchment, regions with a great elevation range experience greater erosion. Moreover, all these high relief catchments were found to have fluvially dominant processes contributing a large area between MCT I and II.

The evolution of the Indian Summer Monsoon in the Himalayan region is hand in hand with the evolution of mountain building processes which are marked by the thrust reactivations in this region. The absence of any correlation between the spatial distribution of precipitation and k_{sn} indicates the landscape processes and erosion rates are more controlled by tectonics than climate. Abrahami et al. (2016) showed a similar observation in Sikkim Himalayas, where they concluded that while erosion rates are highly correlated to k_{sn} and primarily controlled by tectonic uplift, precipitation only has a secondary control.

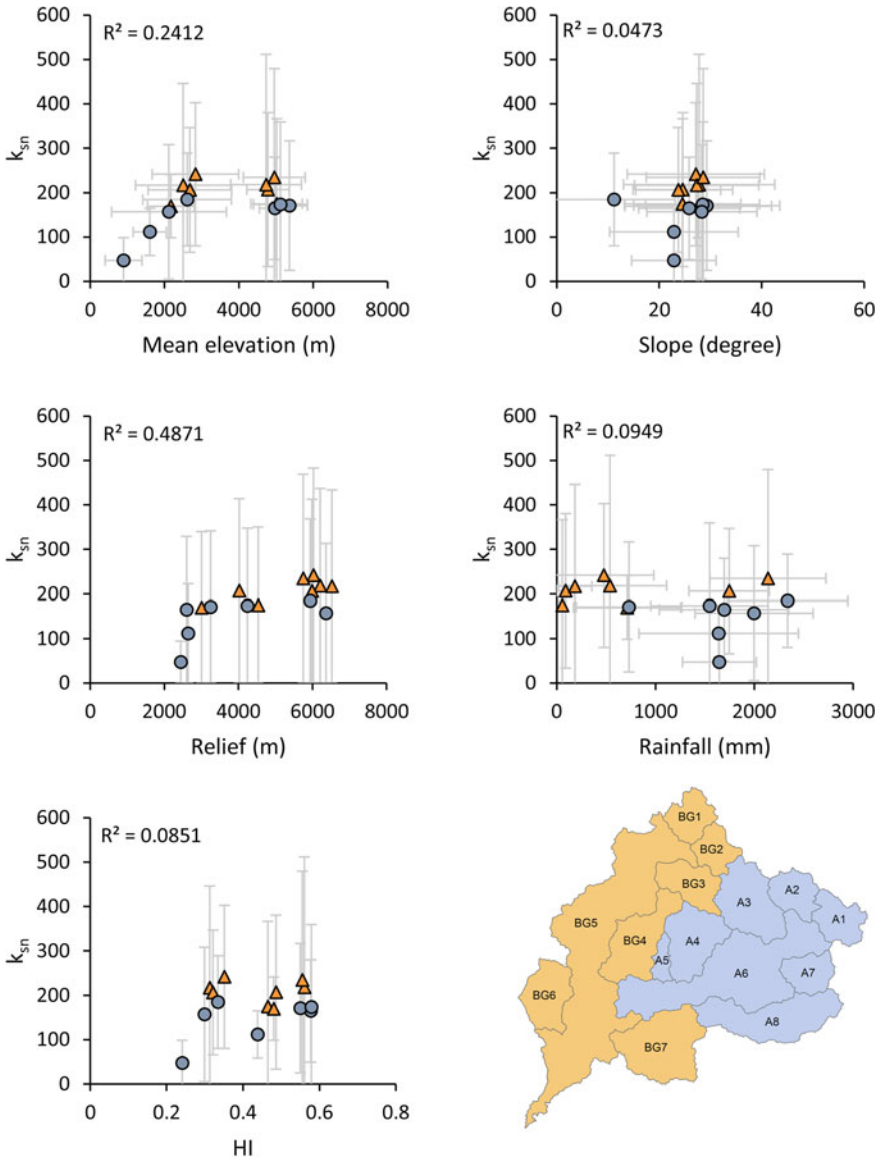


Fig. 7 Correlation between major driving factors with k_{sn} . Blue and orange dots indicate subcatchments in Alaknanda and Bhagirathi-Ganga respectively

In understanding the complex nature of coupled tectonic and climatic influence on the evolution of post-orogenic mountains, rock uplift, and erosion; k_{sn} have been extensively considered as a proxy of erosion rate because of its strong correlation with in-situ based erosion rate data (e.g. Abrahami et al. 2016; Dey et al. 2016; Scherler et al. 2017; Nennewitz et al. 2018; Adams et al. 2020). The k_{sn} data is proven to be efficient in comprehending such external perturbations on the landscape dynamics and varying erosion rates in a systematic way. Based on the outcomes of our study and the previously published studies, this method can be considered as one of the simplest approaches that may be applicable in other regions in the Himalayas to understand the impact of tectonics and monsoon climate on topographic evolution even for the regions where in-situ based erosion rate data are unavailable.

5 Conclusion

River longitudinal profiles and distribution of normalized steepness index (k_{sn}) provide significant insight into the landscape evolution and erosion potential of a region. Our study demonstrates a systematic analysis of river longitudinal profiles and k_{sn} to comprehend the role of varying uplift rate, geomorphic indices and monsoon rainfall in differential erosion rates in between major thrusts in the Alaknanda-Bhagirathi catchment. A significant correlation between ^{10}Be derived erosion rate and k_{sn} indicated high rate of erosion (2.87 mm/yr) between MCT I and II. Fluvial processes may have a dominant role in erosion as the maximum erosion rate is found between MCT I and II where the region is under transition from the glacial to the fluvial regime with intense headward erosion. Though topographic relief has significant control on erosion rate in this region, because of no correlation between rainfall and k_{sn} , we conclude that differential tectonic uplift is the main driving factor in topographic evolution while rainfall exerts a secondary control.

Acknowledgements S.D. wishes to thank UGC-India for financial support. The authors wish to thank Heads, Department of Geography and Geology, Savitribai Phule Pune University for providing necessary facilities to carry out this study. Constructive comments from two anonymous reviewers improved the final chapter significantly. We thank the editors of this book for their generous helps and supports during the entire editorial process.

References

- Abrahami R, Beek PVD, Huyghe P, Hardwick E, Carcaillet J (2016) Decoupling of long-term exhumation and short-term erosion rates in the Sikkim Himalayas. *Earth Planetary Sci Lett* 433:76–88
- Adams BA, Whipple KX, Forte AM, Heimsath AM, Hodges KV (2020) Climate controls on erosion in tectonically active landscapes. *Sci Adv* 6:eaa3166

- Bhakuni SS, Luirei K, Kothiyari GC, Imsong W (2017) Transverse tectonic structural elements across Himalayan mountain front, eastern Arunachal Himalayas, India: implication of superposed landform development on analysis of neotectonics. *Geomorphology* 282:176–194
- Bookhagen B, Burbank DW (2006) Topography, relief and TRMM-derived rainfall variation along the Himalayas. *Geophys Res Lett* 35:L08405
- Burbank DW, Anderson RS (2012) *Tectonic geomorphology*. Blackwell Science, Oxford
- Catlos EJ, Harrison TM, Kohn MJ, Grove M, Ryerson FJ, Manning CE, Upreti BN (2001) Geochronologic and thermobarometric constraints on the evolution of the Main Central Thrust, central Nepal Himalayas. *J Geophys Res* 106:16177–16204
- Das S (2020) Koyana-Warna shallow seismic region, India: Is there any geomorphic expression of active tectonics? *J Geol Soc India* 96:217–231
- Dewey J, Bruke K (1973) Tibetan, Variscan and Precambrian basement reactivation: products of continental collision. *J Geol* 81:683–692
- Dey S, Thiede RC, Schildgen TF, Wittmann H, Bookhagen B, Scherler D, Strecker MR (2016) Holocene internal shortening within the northwest Sub-Himalayas: out-of-sequence faulting of the Jwalamukhi Thrust, India. *Tectonics* 35:2677–2697
- Dimri AP, Niyogi D, Barros AP, Ridley J, Mohanty UC, Yasunari T, Sikka DR (2015) Western disturbances: a review. *Rev Geophys* 53:225–246
- Fasullo J, Webster PJ (2003) A hydrological definition of Indian monsoon onset and withdrawal. *J Clim* 16:3200–3211
- Harrison TM, Ryerson FJ, Le Fort P, Yin A, Lovera OM, Catlos EJ (1997) A late Miocene-Pliocene origin for the central Himalayan inverted metamorphism, Earth Planet. Sci Lett 146:E1–E7
- Howard AD (1994) A detachment-limited model of drainage basin evolution. *Water Resour Res* 30:2261–2285
- Howard AD, Kerby G (1983) Channel changes in badlands. *Geol Soc Am Bull* 94:739–752
- Howard AD, Seidl MA, Dietrich WE (1994) Modeling fluvial erosion on regional to continental scales. *J Geophys Res* 99:13971–13986
- Kirby E, Whipple K (2001) Quantifying differential rock-uplift rates via stream profile analysis. *Geology* 29:415–418
- Kothiyari GC, Luirei K (2016) Late quaternary tectonic landforms and fluvial aggradation in the Saryu River Valley: Central Kumaun Himalayas. *Geomorphology* 268:159–176
- Nennewitz M, Thiede RC, Bookhagen B (2018) Fault activity, tectonic segmentation and deformation pattern of the western Himalayas on Ma timescale inferred from landscape morphology. *Lithosphere* 10:632–640
- Patriat P, Achache J (1984) India-Eurasia collision chronology has implications for crustal shortening and driving mechanism of plates. *Nature* 311:615–621
- Pichon XL, Fournier M, Jolivet L (1992) Kinematics, topography, shortening, and extrusion in the India-Eurasia collision. *Tectonics* 11:1085–1098
- Rana N, Singh S, Sundriyal YP, Rawat GS, Juyal N (2016) Interpreting the geomorphometric indices for neotectonic implications: an example of Alaknanda valley, Garhwal Himalayas, India. *J Earth Sys Sci* 125:841–854
- Ray Y, Srivastava P (2010) Widespread aggradation in the mountainous catchment of the Alaknanda-Ganga river systems: timescales and implications to Hinterland-foreland relationships. *Quatern Sci Rev* 29:2238–2260
- Rees HG, Collins DN (2006) Regional differences in response of flow in glacier-fed Himalayan Rivers to climatic warming. *Hydrol Process* 20:2157–2169
- Sarkar S, Kanungo DP, Sharma S (2015) Landslide hazard assessment in the upper Alaknanda valley of Indian Himalayas. *Geomat Nat Hazard Risk* 6:308–325
- Sati SP, Rana N, Kumar D, Reddy DV, Sundriyal YP (2008) Pull-apart origin of wider segments of the Alaknanda Basin Uttarakhand Himalayas, India. *Himal Geol* 29:89–90
- Scherler D, DiBiase RA, Fisher GB, Avouac J (2017) Testing monsoonal controls on bedrock river incision in the Himalayas and Eastern Tibet with a stochastic-threshold stream power model. *J Geophys Res Earth Surf* 122:1389–1429

- Schwanghart W, Kuhn NJ (2010) TopoToolbox: a set of Matlab functions for topographic analysis. *Environ Model Softw* 25:770–781
- Seeber L, Armbruster JG, Quittmeyer RC (1981) Seismicity and continental subduction in the Himalayas Arc. In: Gupta HK, Delany FM (eds) *Zagros, Hindukush, Himalayas, geodynamic evolution*. Geodynamic series, vol 3. American Geophysical Union, Washington, pp 215–242
- Sharma G, Champati ray PK, Mohanty S (2018) Morphotectonic analysis and GNSS observations for assessment of relative tectonic activity in Alaknanda basin of Garhwal Himalayas, India. *Geomorphology* 301:108–120
- Singh S (2018). Alaknanda-Bhagirathi river system. https://doi.org/10.1007/978-981-10-2984-4_8
- Singh M, Singh IB, Muller G (2007) Sediment characteristics and transportation dynamics of the Ganga River. *Geomorphology* 86:144–175
- Singh DS, Gupta AK, Sangode SJ, Clemens SC, Prakasam M, Srivastava P, Prajapati SK (2015) Multiproxy record of monsoon variability from the Ganga Plain during 400–1200 A.D. *Quatern Int* 371:157–163
- Sinha S, Sinha R (2016) Geomorph evolution of Dehra Dun, NW Himalayas: tectonics and climate coupling. *Geomorphology* 266:20–32
- Sundriyal YP, Jayant T, Sati SP, Rawat GS, Srivastava P (2007) Landslide dammed lakes in the Alaknanda basin, Lesser Himalayas: causes and implications. *Curr Sci* 93(4):568–574
- Thiede RC, Arrowsmith JR, Bookhagen B, McWilliams MO, Sobel ER, Strecker MR (2005) From tectonically to erosionally controlled development of the Himalayas orogen. *Geology* 33:689–692
- Tyagi AK, Chaudhary S, Rana N, Sati SP, Juyal N (2009) Identifying areas of differential uplift using steepness index in the Alaknanda basin, Garhwal Himalayas, Uttarakhand. *Curr Sci* 97:1473–1477
- Valdiya KS (1988) Tectonics and evolution of the central sector of the Himalayas. *Phil Trans R Soc Lond A* 326:151–175
- Vance D, Bickle M, Ivy-Ochs S, Kubik PW (2003) Erosion and exhumation in the Himalayas from cosmogenic isotope inventories of river sediments. *Earth Planet Sci Lett* 206:273–288
- Wasson RJ, Juyal N, Jaiswal M, Culloch M, Sarin MM, Jain V, Srivastava P, Singhvi AK (2008) The mountain-lowland debate: deforestation and sediment transport in the Upper Ganges catchment. *J Environ Manage* 88:53–61
- Whipple KX, Tucker GE (1999) Dynamics of the stream-power river incision model: implications for height limits of mountain ranges, landscape response timescales, and research needs. *J Geophys Res* 104:17661–17674
- Whitehouse IE (1990) Geomorphology of the Himalayas: a climate-tectonic framework. *NZ Geogr* 46:75–85

Spatial Variability of Topographic Attributes and Channel Morphological Characteristics in the Ladakh Trans-Himalayas and Their Tectonic and Structural Controls



Priyank Pravin Patel, Shantamoy Guha, Debsmita Das,
and Madhurima Bose

Abstract The Trans-Himalayas in India comprise of the Ladakh, Karakoram and Zaskar (also spelled as Zaskar) ranges. These ranges are marked out by the presence of several active major thrust faults, which are epicenters of recurrent seismic activity. Their alignments control the main stream courses of the area, resulting in sharp bends, obtuse junctions, steep defiles and abrupt changes in channel morphology, wherever streams transition across different morpho-structural units. The present study focuses on the drainage composition and topographic characteristics of the Leh and Nubra valleys in the Ladakh region, along the courses of the Indus, Zaskar, Shyok and Nubra rivers. The morphometric attributes and spatial variation in terrain aspects of the basins developed within the aforementioned three ranges and draining into these four rivers are examined using the ALOS PALSAR Digital Elevation Model (DEM) to elicit watershed and channel parameters related to tectonics. Thrust faults digitized from the available geological maps of the region are compared with the principal streams extracted from the above DEM dataset through an overlay analysis to discern the influence exerted by the principal thrust faults and other structural lineaments on the drainage alignment. Segment-wise stream gradient indices reveal the abrupt changes in longitudinal profile and resultant changes in channel morphological characteristics as the rivers traverse these various structural and lithological entities. These attributes of the drainage character are compared with the various lithological and geomorphic entities of the area, to elicit the river character in each physiographic unit.

Keywords Ladakh · Trans-Himalayas · Karakoram · Indus · Nubra · Morphometry · Stream gradient · Tectonics · Channel planform

P. P. Patel (✉) · M. Bose

Department of Geography, Presidency University, 86/1, College Street, Kolkata, West Bengal 700073, India

S. Guha

Department of Earth Sciences, Indian Institute of Technology, Gandhinagar, Gujarat, India

D. Das

Department of Geography, University of California, Santa Barbara, CA, USA

1 Introduction

Tectonic signatures are often observed on natural landscapes that bear the marks of relative movement of the surface (England and Molnar 1990). Identifying these tectonic signatures along rivers is quite difficult since the morphological signatures are subtler, wherein the appearance of river courses and the paths taken by them from source to mouth depends on the natural setting of the environment through which they flow (Nag and Chakraborty 2003; Strecker et al. 2003). Tectonic signatures along streams can thus be identified using associative attributes like angular drainage patterns, channel sinuosity, abandoned channels, anomalous river flow, compressed meanders, abrupt change in flow directions and the asymmetry of river bends, to mention a few (Guha and Patel 2017). The strong controls exercised by the various mountain fronts all over the Himalayas are evident from the courses of the rivers that flow through it (e.g. Duncan et al. 2003). Such rivers are generally characterized by straightened courses, v-shaped valleys, asymmetric and oval-shaped watersheds and sharp knee-bend turns of seasonal rivulets and incised meanders (Burbank et al. 1996).

In this respect, the best description of the shape of a river's longitudinal profile is its slope or gradient, which is the graphic representation of the ratio of the fall of the elevation along the channel to its length over a given reach. It is thus the configuration of the channel bed or bottom in longitudinal view (Knighton 1998). In most cases and particularly in humid regions and for steady-state conditions, it is concave-upwards (Seeber and Gornitz 1983). Yet, the longitudinal profiles of natural rivers, though concave upward, rarely tend to be smooth and they often contain breaks (Oguchi 1997). Such local steepening of the channel gradient can result from one of several causes like more transitions in the lithology, the introduction of a coarser or larger bedload or from tectonic activity (Bhat et al. 2008). This 'concave up' shape of the long profile has also often been described in terms of the graded profile or profile of equilibrium for stable channels. Thus, the longitudinal profile of a river represents its long-term morphologic adjustment to the varying conditions of climate, lithology and tectonic activity (Burbank and Anderson 2011).

In a steady-state system, erosion keeps pace with uplift (Guha and Patel 2017). River gradients, which are a driving factor of erosion, are adjusted to the external forcings. Thus abrupt changes in slope along river profiles may indicate active faults encountered by these rivers (Seeber and Gornitz 1983). River channels, therefore, have a lot of controlling factors behind their evolutionary trajectories, which include topography, climate and geology. However, most often it is the tectonics of the area that plays the most crucial role of all, especially in high mountain regions. The aim of the work presented is to discern the tectonic signatures that appear in the landscape using geospatial and quantitative methods, along with their likely influence on the examined river forms in the studied area.

2 Concepts and Parameters Related to Morphotectonic Indices and River Longitudinal Profile Analysis

The availability of several of GIS technologies as well as a large range of geospatial data have led to their wide-ranging applications in geomorphology (Remondo and Oguchi 2009). These technologies allow precise quantification and mapping of geomorphic features at a range of spatial scales. Therefore, they have become an integral part of Geomorphometry, defined as the science of quantitative land surface analysis (Pike 2000; Pike et al. 2009; Sofia 2020). Geomorphometry has found applications in a variety of fields but the largest applications have been in river basin analyses (Evans, et al. 2009; Sofia 2020). A number of morphometric variables or parameters may be identified and these provide information about the land surface and hydrology of an area either in itself or in the form of indices (i.e. combinations of various parameters) (Olaya 2009; Gruber and Peckham 2009; Florinsky 2017; Patel 2012; Sofia 2020).

One such morphological parameter group includes various morpho-tectonic indices, which allow us to understand how rock resistance, tectonics and climate interact and affect the evolution of landforms and drainage in an area (Doornkamp 1986; Ramirez-Herrera 1998; Keller and Pinter 2002; Bull 2007; Brocklehurst 2010). Various morphotectonic indices have been devised over the years but the most common ones used are the hypsometric curve and integral (HI, Strahler 1952), mountain front sinuosity index (S_{mf} , Bull and McFadden 1977), valley floor to valley height ratio (V_f , Bull 1977, 1978), stream length gradient index (SL, Hack 1973), normalized stream index (NSL, Seeber and Gornitz 1983; Whipple and Tucker 2002), basin asymmetry factor (A_f , Hare and Gardner 1985), transverse topography symmetry factor (T, Cox 1994), S_t Index (Sklar and Dietrich 1998) and channel steepness index (k_{sn} , Wobus et al. 2006; Castillo et al. 2014). All these indices have been used in a number of studies dealing with tectonic geomorphology. The hypsometric integral/curve is especially important as it describes the distribution of elevations across a land surface (e.g. a basin) and the HI is the area under the curve (Strahler 1952). Based on the shape of the curve and HI values, the landscape may be divided into classical stages of youth, maturity and old, with progressively declining HI values indicating increased senility (Strahler 1952; Keller and Pinter 2002; Patel and Sarkar 2007). The skewness and kurtosis of the hypsometric curve are geomorphologically significant (Sarkar and Patel 2011) as a large, positive value of skewness indicates increased erosion in the upper reaches of a basin, whereas larger values of kurtosis indicate higher erosion in both the upper and lower reaches (Harlin 1978; Perez-Pena et al. 2008; Radaideh and Mosar 2019). However, the hypsometric curve and its integral value may also be influenced by the dimensions of the basins rather than erosion and uplift alone and Radaideh and Mosar (2019) suggested that care must be employed while using the hypsometric approach.

In contrast to the abovementioned indices that discern the tectonic influences at the landscape (basin) scale, are those which derive such information directly from the

channel itself. A river's long profile is indicative of the occurring long-term adjustments by the channel and its resultant morphology to climatic, structural, lithological and tectonic variations, perturbations and forcings. The easiest and most comprehensive way of its analysis is via methods like the Stream Length (SL) Gradient Index and its direct correlation with the geology of the study area. While the numerical calculations provide an idea about the steepness of the river, this index can be directly connected to the underlying lithology to assess the ambient stream power (Kale et al. 2010). For computing the SL Index, Hack (1973) devised a semi-logarithmic relation connecting the channel length and elevation, as:

$$H = C - k \ln(L)$$

where, H = elevation, L = distance from the source, C = an empirical constant and k = slope of the idealized profile, or the Gradient Index. Furthermore, a graded stream's long profile can be taken to be in a state of equilibrium and this would then appear as a straight line on a semi-logarithmic plot. Consequently, any notable deviations from the plotted or theoretically expected straight line can be taken to be indicative of forcings or disturbances along/across the stream course. Thus, Hack (1973) further provided a morphotectonic index, which is known as the Stream Length Gradient Index. This is computed as:

$$SL = \frac{(e_1 - e_2)}{[\ln(D_2) - \ln(D_1)]}$$

where, e_1 = elevation of the first point from the source, e_2 = elevation of the second point of the source, D_1 = distance of the first point from the source and D_2 = distance of the second point from the source.

The above SL index is also commonly referred to as the Stream Gradient Index (SGI). The SGI refers to a range of values that indicate the gradient of a stream. It is calculated using the fall in elevation of the stream and its change in the logarithmic value of cumulative length. Essentially, it tries to draw a relation between the amount of elevation drop and the traversed distance (Patel et al. 2021). These values are generally not bound by any range and tend to represent the geomorphic conditions of the region. Higher values are indicative of a greater change in elevation, rugged relief and steeper slopes, possibly as a result of uplift or marked variation in the local lithology (Lee and Tsai 2010), while lower values indicate flatter relief and gentler slopes. The SL to k ratio is referred to as the Normalized Stream Index (NSL) and this indicates the range of channel steepness (Seeber and Gornitz 1983; Whipple and Tucker 2002). Mathematically, it is expressed as:

$$NSL = SL/k.$$

where, SL = gradient index of a reach and k = slope of the stream's graded profile.

The NSL has a similar, if not almost identical graphs to the original SL Index and is representative of the same characteristics of the area, only reducing the scale of the values to more easily comprehensible and comparable range by dividing the originally derived values by the ideal value of the region. Seeber and Gornitz (1983) studied various Himalayan rivers and suggested that $NSL \geq 2$ indicates steep reaches, whereas values >10 indicate extremely steep reaches. Since channels in tectonically active areas are generally steep, they considered SL and NSL to be indicators of neotectonics within the drainage basin. However, high SL and NSL values might also result from differential erodibility of the various lithounits (Patel et al. 2021) or mass movements like landslides, debris flows and slumps (Troiani and Della Seta 2008).

Another good indicator of the steepness or gentleness of a channel reach and the inherent effect of the local structure/tectonics/topography on the channel form is the change in the SGI or the SL change rate. In either case, a river when steeper has a greater SGI value and when gentler has a lesser SGI value. Naturally, when moving from a gentler to a steeper territory, the SGI value of the river increases and the change value calculated is a positive number. However, when moving from a steeper to a gentler territory, the river's SGI value falls as a result of which the change in SGI value returns a negative number, helping us immediately identify those places that have a significantly gentler gradient than its neighbours. It furthermore helps in correlating the reasons for such changes in gradient with the possibly concomitant changes in lithology, presence of faults and lineaments or simply the geomorphology. Using the normalized elevation and cumulative downstream distance parameters, plotted graphs can be fitted with linear, exponential, logarithmic and power form trendlines. According to Lee and Tsai (2010), when the calibre of load in the river is larger than the carrying capacity of the stream, thereby choking the river in turn, the long profile of the river has a better linear function fit. As the river downstream reaches dynamic equilibrium, it has a better exponential fit. Further downstream when the load calibre becomes even smaller, the river reaches a graded condition and the long profile is a better logarithmic fit. With increased downstream concavity of the river, the long profile fits the power function the best. Thus an indicator of the geomorphic evolutionary stage of the channel (and likely its basin) can be obtained from such trendline fitting (following Kale et al. 2010).

The various morphotectonic indices mentioned above have been used to understand the tectonic influences on landscape and drainage evolution throughout the active orogens of the world, including the Himalayas and Trans-Himalayan mountains. Seeber and Gornitz (1983) pioneered this through their work on the SGI and NSL and that paved the way for multiple studies in the region (Jamieson et al. 2004; Robl et al. 2008; Singh and Tandon 2008; Dortch et al. 2010; Phartiyal and Kothiyari 2012; Mahmood and Gloaguen 2012; Dar et al. 2013; Munack et al. 2014; Kumar and Srivastava, 2017; Prerna et al. 2018; Anand and Pradhan 2019, Nag et al. 2021; Sarkar et al. 2021). Within the Ladakh region, however, such studies are somewhat limited. Dortch et al. (2010) combined the use of morphometric parameters, longitudinal profile analysis and cosmogenic radionuclide dating to conclude that the Ladakh range is eroding asymmetrically, with the southern part of the range eroding

at almost twice the rate at which the northern part is, implying that there is an imbalance between uplift and erosion in the northern catchments. The Indus basin, of which Ladakh is a part, was divided into upper, middle and lower segments through analysis of morphometric parameters and longitudinal profiles by Prerna et al. (2018), where they concluded that a third of the basin is in a state of tectonic stability. However, their finding stands in conflict with those of a recent study along a 225 km long stretch of the River Indus (Nag et al. 2021), which concluded that the upper Indus is yet to reach tectonic stability and has continued to have tectonic disturbances throughout the late Quaternary. This suggests that tectonic disturbances rather than climate driven changes are the dominant *raison d'être* for the present configuration of the landscape in Ladakh.

3 Study Area

Ladakh ($32^{\circ}15'N$ – $36^{\circ}N$ and $75^{\circ}15'$ – $78^{\circ}15'E$; approx. 119,820 km² in area) may be considered as the western extension of the Tibetan Plateau (Fielding 1996; Sharma 2003). Due to its remote location, rugged topography, inclement weather conditions and strategic position, studies on this region were scarce till the 1990s. Some notable works (e.g. Cunningham 1854; Drew 1875; Gansser 1964), nevertheless, did exist. However, the proliferation of research since the 1990s has shed a wealth of information about the geology and geomorphology of Ladakh. The entire Ladakh region may be divided into four tectonic zones, namely, from south to north, the Zaskar (or Zaskar) Suture Zone, the Indus-Tsangpo Suture Zone (ITSZ), the Shyok Suture Zone and the Karakoram Plutonic Complex (Thakur 1981). Parallel to these, run three major mountain ranges, the Zaskar Range, the Ladakh Range and the Karakoram Range. The study areas, the Leh and Nubra valleys, lie on either side of the Ladakh Range. Numerous studies have documented the glacial geomorphology of Ladakh (summarized by Dortch et al. 2013). Though glaciers in the Ladakh region only made small advances from their present positions during the Late Glacial (Owen 2011, 2014; Owen and Dortch 2014), their retreat has left a remarkable assemblage of landforms that are essentially paraglacial (*sensu* Church and Ryder 1972) in nature. The main components of this landscape include glacial troughs, moraines, cirques, fluvial terraces, alluvial fans, sand dunes and palaeo-lacustrine deposits (Juyal 2014).

In terms of climate, this region lies in the rain-shadow zones of successive Himalayan and Trans-Himalayan ranges, and as such the prevailing climatic conditions are typical of a high altitude cold desert. At Leh, the maximum and minimum temperature in January is $-2.8^{\circ}C$ and $-14.0^{\circ}C$, while those in July are $24.7^{\circ}C$ and $10.2^{\circ}C$, respectively (Osmaston 1994). Though the average annual precipitation is <500 mm (Bookhagen and Burbank 2006; Hedrick et al. 2011), the precipitation regime is affected by the altitude, the Indian summer monsoon streams and mid-latitude westerly disturbances (Benn and Owen 1998; Dortch et al. 2010, 2013). While the 30-year average precipitation at Leh is 115 mm/year, only a small percentage of it is in the form of snow (Osmaston 1994). A recent study has found

that over a period of 89 years (1901–1989), both the total annual precipitation and winter precipitation in Leh have been showing a declining trend (Bhutiyanani et al. 2010). Very little climatic data exists for the Nubra Valley. However, it is distinctly colder and wetter (precipitation is mostly in form of snow) as it lies between the Ladakh and Karakoram ranges, where the temperature is below 0 °C for significant parts of the year (Bhutiyanani 2014). Most of the precipitation is received from the western disturbances that hit the region during the winter months (September to April). During this period, the temperature can drop to –25 °C (Nagar and Ahmed 2007). After April, the weather improves and July is the hottest month when the temperature in the valley can be as high as 32 °C (Nagar and Ahmed 2007; Ganjoo et al. 2014).

Another climatic parameter that has an important control on geomorphic processes in Ladakh, including the two study areas, is insolation. Due to its high elevation and consequent, low temperature and pressure (510 mm of Hg at Leh [Bharadwaj et al. 1973]), the atmosphere here is rarified. As a consequence, Ladakh receives a large amount of insolation, approximately 320 days of sunshine in a year (Lohan and Sharma 2012). Ramachandra et al. (2011) found that on average, the Ladakh area receives between 4.7 and 5.0 KWh/m²/day of insolation throughout the year, but during the summer months (May to August), the range increases to between 5.7 and 6.7 KWh/m²/day. Additionally, Jacobson (2000) reported that during 1996–1998, Leh received 5530 Wh/m²/day of solar energy, whereas Sumoor in the Nubra Valley received 5300 Wh/m²/day. These studies suggest that insolation is a potent force that can exacerbate thermal weathering in the study area.

The Indus is the main river of the region. As an antecedent stream that was formed in the Eocene (Searle and Owen 1999), it initially follows the strike of the Karakoram Fault before taking a westward turn to flow along the east–west trending Indus-Tsangpo Suture Zone (ITSZ) (Clift 2002). Together with its tributaries (the Dras, Zaskar, Shyok and Nubra rivers), it forms the lifeline of Ladakh. The town of Leh (34°17' N; 77°58' E) is situated on the right bank of the Indus, on the southern foot slopes of the Ladakh Range. One of the longest tributaries of the Indus, the River Shyok, flows parallel to the Indus, on the northern side of the Ladakh Range, before joining it near Skardu. The confluence of the Shyok and its tributary, the Nubra, near the village of Diskit (34°33' N; 77°32' E) has given rise to a barbed drainage pattern due to stream piracy (Juyal 2014). The chosen study area in this paper comprises the Zaskar–Indus–Shyok–Nubra valleys and their intervening mountain ranges (Fig. 1).

4 Datasets and Methods

The present study has used several of different datasets that are listed and described below:

- a. The terrain attributes of the area studied were mapped from the ALOS (Advanced Land Observing Satellite) PALSAR (Phased Array type L-band

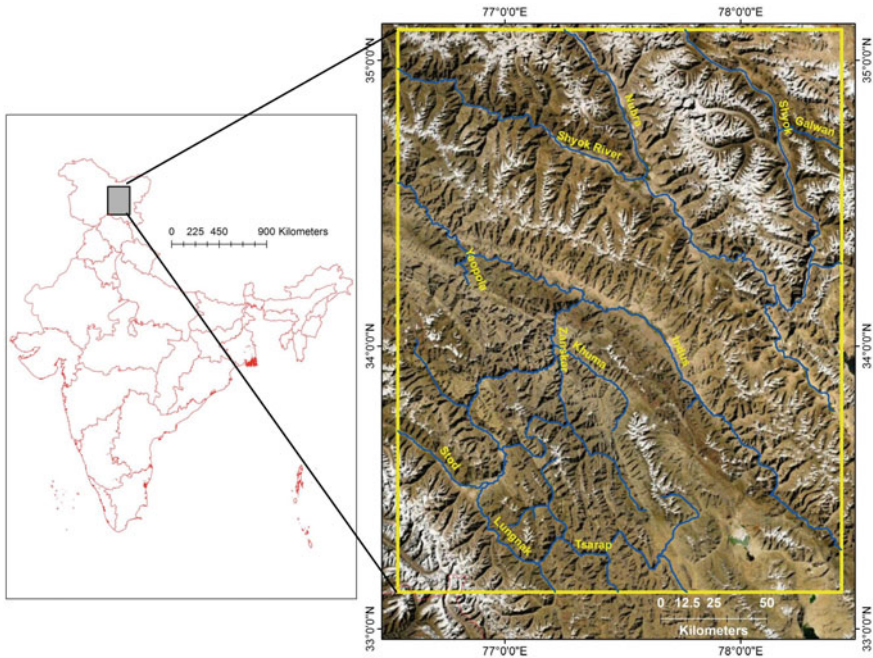


Fig. 1 Location of the study area within Ladakh

Synthetic Aperture Radar) Digital Elevation Model (DEM) of spatial resolution 12.5 m, obtained from the Alaska Satellite Facility. This is at present the highest resolution freely available global DEM (as a re-sampled by-product of the SRTM 30 m DEM) and its use was preferred since DEM resolution has been shown to have a significant effect on the terrain attributes derived (Das et al. 2016). Since this DEM is of an ellipsoidal nature, the required conversion of the elevation values from the reference ellipsoid to the required geoidal heights was done using the $1' \times 1'$ interval Earth Gravity Undulations Model (EGM2008) dataset that was interpolated for the study area. The finally corrected DEM with proper elevation values (Fig. 2) was obtained using the equation:

$$H = h - N$$

where, H = corrected elevation or orthometric height, h = ellipsoidal height and N = geoid height.

- b. The corrected DEM was processed for any data gaps and voids and to remove any inadvertent data peaks and pits in the Geospatial WhiteBox software environment. Subsequently, standard D-8 flow routing and flow accumulation algorithms were used to extract the principal drainage lines and their tributary networks and perform Strahler order classification of streams (see Patel and

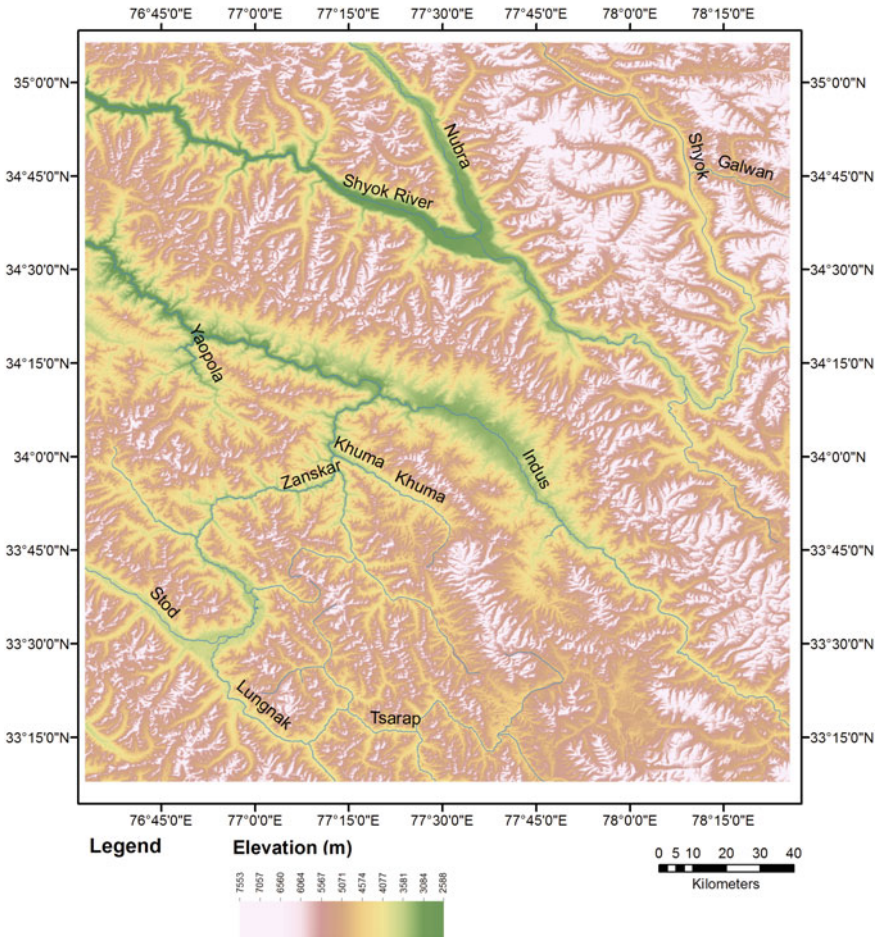


Fig. 2 The corrected DEM representing the elevation values in the study area

Sarkar 2009, 2010 for full details on these methods and their utility). The drainage basins of the ascertained stream segments (Fig. 3) were extracted using the classified flowlines and the entire raster datasets thus elicited were converted to vector shapefiles for ease of mapping and parameter extraction. Once the principal drainage lines were discerned in the above manner (i.e. the courses of the Zaskar, Shyok (its upper and lower segments, situated before and after its great bend), Nubra and Indus), we identified all the river basins that drained directly into these channels. Leaving out the very minor stream segments, all basins of Strahler Order 2 and higher (which went up to Order 5) were thus mapped (Fig. 4). In all, 177 such basins were identified and each of these were assigned a numerical code to differentiate them from each other (Fig. 5) and also the relative position of each basin (i.e. which river it drained

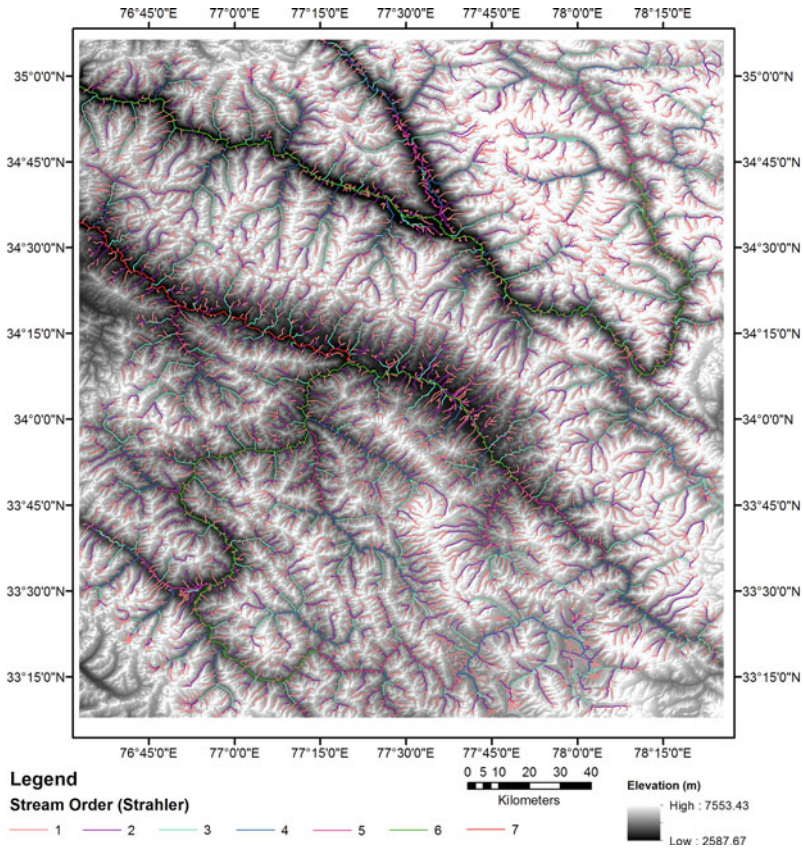


Fig. 3 Classified streams according to the Strahler (1952) stream segment ordering scheme

into and whether its location was on the right or left flank of the main channel) was ascertained and input into its respective database (Fig. 5).

- c. A range of terrain parameters were directly extracted from the DEM and enumerated for each of the river basins. These comprised of the maximum, minimum and mean basin elevation and its standard deviation, the mean basin slope, hypsometric integrals, ruggedness and dissection indices (for details of their enumeration methods see Patel 2012, 2013 and Sarkar and Patel 2009, 2012). Alongside these, the basin geometric attributes (area and perimeter) and shape (circularity ratio) were also computed. Enumeration of the basin-wise stream frequency and drainage density parameters was done by overlaying the stream segments on each basin and clipping their extents, followed by stream number counts and total length estimates.
- d. The reach-wise channel steepness index (SL index) was measured and mapped for the principal rivers, using the method outlined in the prior section. It is to be noted that some of these streams are international rivers and as such only a

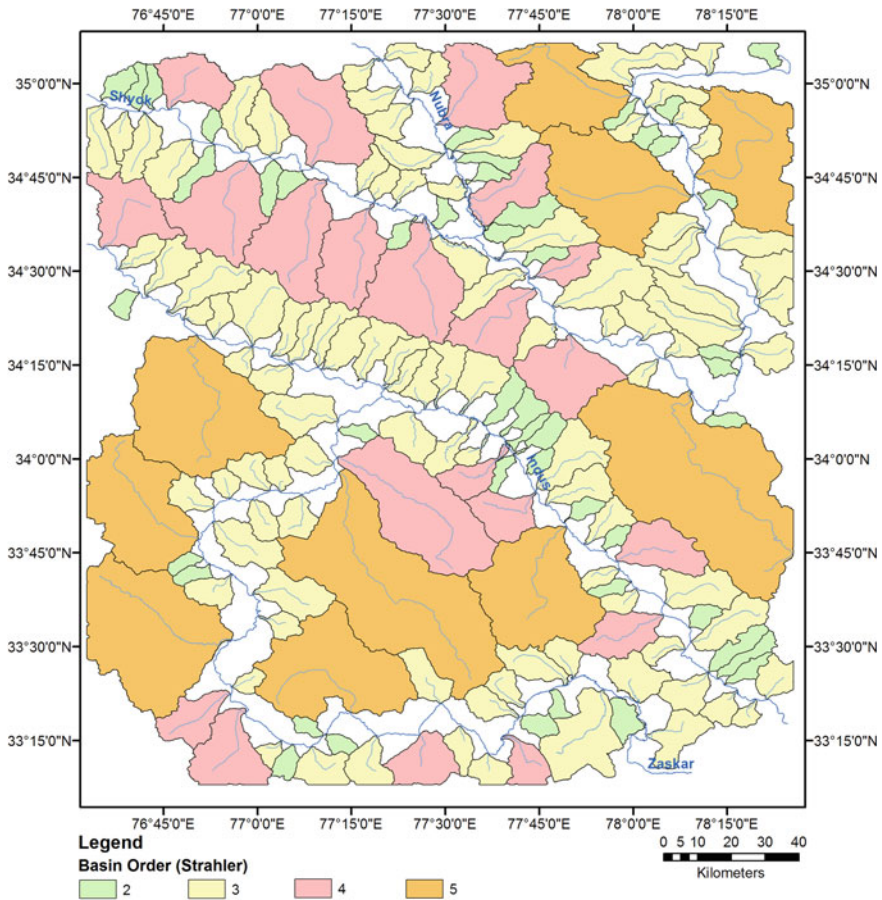


Fig. 4 The demarcated basins of Strahler second order and higher that drain directly into the four principal drainage lines of Indus, Shyok, Nubra and Zaskar

portion of their courses lie within India. Therefore instead of looking into the longitudinal profile character of the whole stream, we have constrained ourselves to simply examining it within the demarcated study area, in which these river valleys are in close juxtaposition to each other. The long profiles of these partial courses were extracted from the corrected DEM and an 11-pixel smoothing window (following Kale et al. 2010) was used to remove any irregularities in their plots. Each stream was divided into segments of 5 km each for the SL Index enumeration. This created 66 segments for the Indus, 105 segments for the Shyok (comprising its upper and lower portions, before and after its great bend within the study area), 24 segments for the Nubra and 82 segments for the Zaskar. Subsequently, their respective fall in elevation was calculated and each segment slope was found out, with a combination of these eliciting the SGI

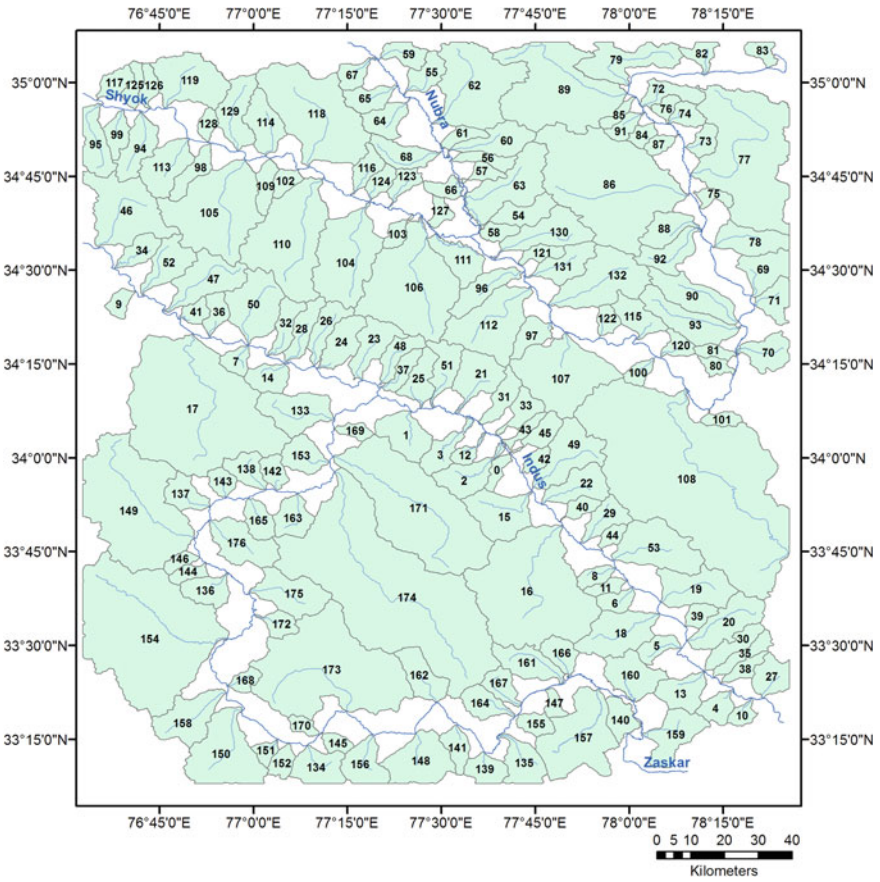


Fig. 5 The coded drainage basins for subsequent morphometric analysis

value per segment of the river. When overlain on the DEM and geological maps, a clear insight into the possible role of the lithology/structure on the channel morphology could be ascertained.

- e. Breaks along the longitudinal profile are indicators of lithological or structural changes. In order that the studied rivers could be compared, despite their different lengths and different elevation differences along their courses, a normalization or standardization procedure was applied (cf. Guha and Patel 2017). Four mathematical functions were then used to compare and derive a best-fit curve on the respective profiles to ascertain the stage of development of the respective basins, as well as inculcate a process-based understanding, as previously described (cf. Kale et al. 2010).
- f. Langbein's (1964) Concavity plots were used to further the argument about the shape of the river longitudinal profile curves. According to this concept, when the value is 0, the channel is straight. As the value increases, the channel starts

to curve or meander and the calibre of its load tends to decrease. The greater the relief of a given basin, the straighter the profile. Simply put, the greater the length of a basin for a given relief, the more concave it is and the river is characterised by an increase in discharge downstream with relative crustal stability.

- g. A number of topographical and geological maps were used to obtain the surface lithological attributes. The toposheets of the area were obtained from the US-AMS collection and were at 1:250,000 scale. The geological maps were obtained from the Geological Survey of India (GSI) Quadrangles and the information present in these sheets were mapped and overlain on the DEM derived parameters for visual correlations.
- h. High-resolution Google Earth images, in planform and tilted 3-D views, were used to examine the minor geomorphic units present in the study area. For select reaches of the principal streams, their respective stream corridor morphologic attributes (cf. Banerji and Patel 2019) could thus be ascertained and using similar information present in the GSI maps, these were outlined.

5 Results and Discussions

5.1 *Ambient Structural and Geologic Characteristics*

The study area reports elevations ranging from 2588 to 7553 m (Fig. 2). This almost 5000 m elevation change within this region markedly influences the terrain character and geomorphic attributes. This great elevation difference is a result of Himalayan and Trans-Himalayan tectonics and repeated movements that characterise the entire region (Burbank and Anderson 2011). The Zaskar cuts across the mountain range that bears its name while the Ladakh Range forms the water divide between the Indus and Shyok rivers, with rivers draining its southern face flowing into the Indus and those arising on the northern flanks eventually meeting the Shyok. The Great Karakoram Range abuts between the Shyok and Nubra valleys and carries on further to the east.

A number of lithologic groups and formations are present herein (Fig. 6), with all of them exhibiting a linear pattern, aligned from NW–SE, highlighting both the compressional tectonics that have occurred here, resulting in a series of parallel ranges and the melange of rocks that have been crumpled and uplifted along the main suture zones that trend in the aforementioned direction. A greater heterogeneity of these rock groups/formations is apparent in the Zaskar zone, on the left flank of the Indus. Typical metamorphics and crystallines associated with continental subduction and suture zones (ophiolites and acidic intrusives) abound. Notable is the presence of patches of undifferentiated recent sediments (mixture of coastal, glacial, aeolian and fluvial origin). This denotes the complex evolutionary history of the area and these sediment patches occupy locations where the valley floors have broadened out to accommodate them, resulting from the infilling taking place along the suture

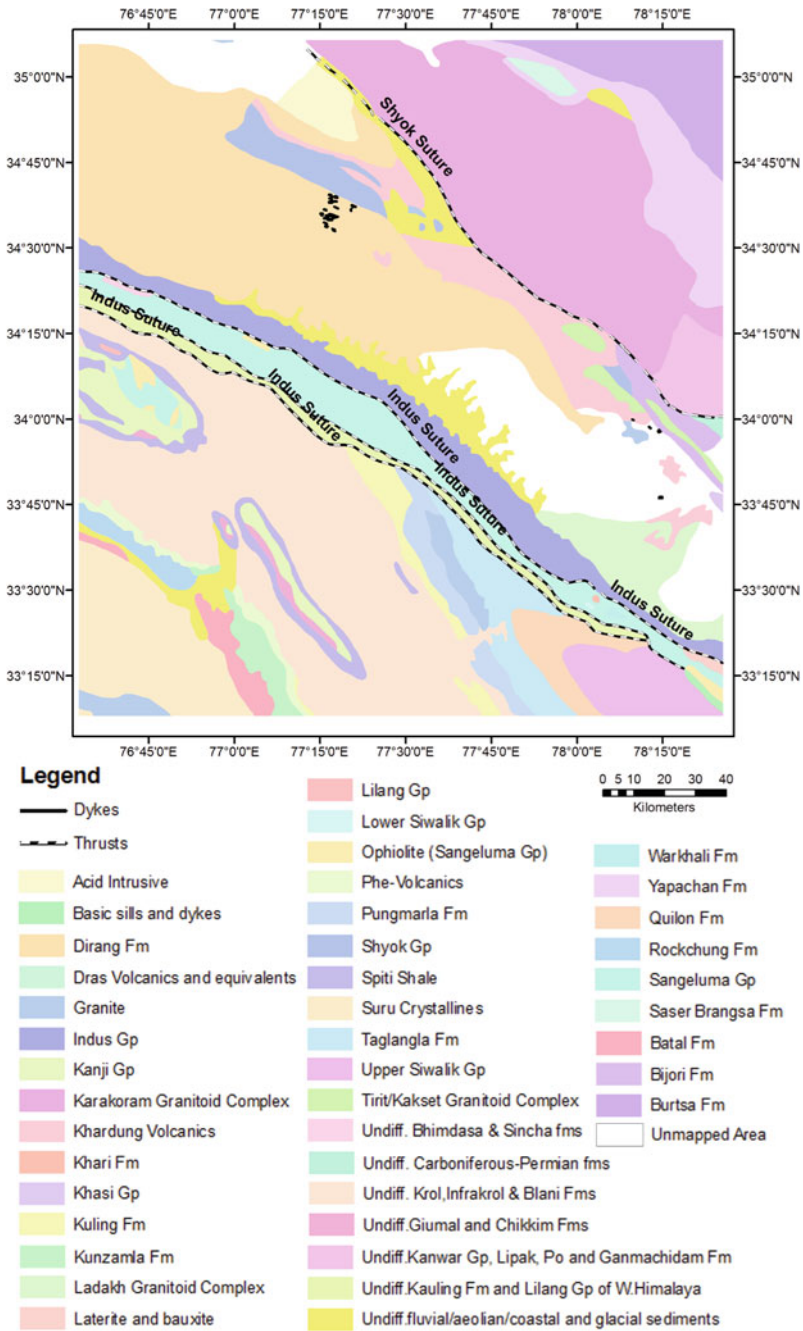


Fig. 6 Major geological formations and rock groups in the study area

zones (especially the Indus and Shyok sutures). These valley fills extend upslope as finger-like projections that represent the tributary valleys (Fig. 7) that meet these main drainage lines, as can be seen prominently along the Ladakh Range and on the eastern flank of the Nubra. By bringing rocks of very different geologic ages in close juxtaposition, these two suture zones typify the sharp lithological changes that

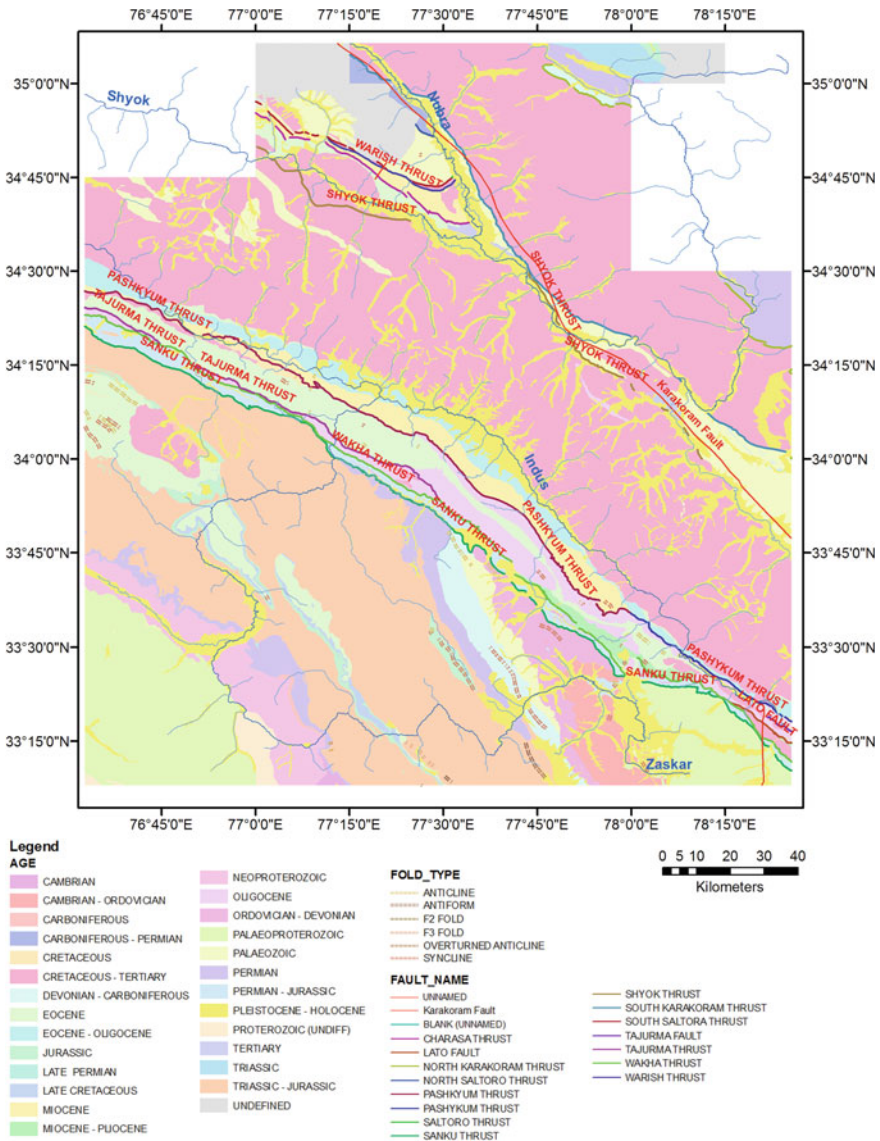


Fig. 7 Geological time periods when the constituent rock formations developed and major structural elements

are characteristic of continental subduction zones and the associated chaotic rock complex. A classic example of the intense upwarping and tilting of the constituent rocks is seen along the Indus' left flank at Stok and Choglamsar, with seemingly large-scale uniclinal and folded formations being present here (see Fig. 26k).

Such intense rock décollement also gives rise to multiple faults and folded structures alongside the main sutures and these are seen abundantly in the study area, with a variety of anticlines, synclines and folded forms present along with series of different thrusts, lineaments and faults. Simple visual comparison of their position and alignment with the overlain drainage lines makes it apparent that they exert marked control over the courses of not only the main rivers but also influence the formation of structural meanders, obtuse tributary junctions and sharp course changes throughout the entire drainage network of the area (Fig. 8). In the northern part of the map, the upper section of the Shyok initially flows to the south but then executes a sharp turn of more than 90° towards the NW on meeting the Karakoram Fault. This confined channel then courses towards the NW and occupies the Shyok Suture and then the Shyok Thrust further to the west. The alignment of the Shyok's main tributary, the Nubra, is entirely controlled by the NW–SE trending Shyok Thrust that results in these two rivers forming a remarkable obtuse barbed junction at their confluence. In the central part of the area, the course of the Indus is also constrained and controlled by the adjacent SE–NW trending Indus Suture and its associated Pashkyum, Wakha and Tajurma Thrusts (cf. Phartiyal et al. 2005; Kumar and Srivastava 2018). While the Zaskar region does not have any of the markedly developed thrusts, it has a number of folded and structural lineaments that have influenced the alignment of the main channels and its tributaries. That these faults are quite active and have influenced tectonic movements in the recent past also becomes clear when the seismicity map of the area is examined (Fig. 9). The NE and SW zones of the study area have a preponderance of earthquake epicentres. Most of these are shallow focus earthquakes and are generally above 4 MW, reflecting the ongoing tectonic movements in this area.

5.2 Spatial Variability of Basin-Wise Topographic Attributes

The mapped basins draining directly into each main channel were examined next. Of the total of 177 such basins that are of Strahler second to fifth orders, 54 drained into the Indus (19 on its left flank and 35 on its right), 44 into the Zaskar (26 left and 18 right), 64 into the Shyok (30 left and 34 right) and 15 into the Nubra (10 left and 5 right) (Table 1). The markedly unequal distribution of drainage basins on either flank is possibly due to the respective alignments of the main water divides and the courses these streams have cut through them. The mean basin size is 158.52 km² with the Zaskar region reporting the highest mean basin size and the Nubra the lowest (Table 1).

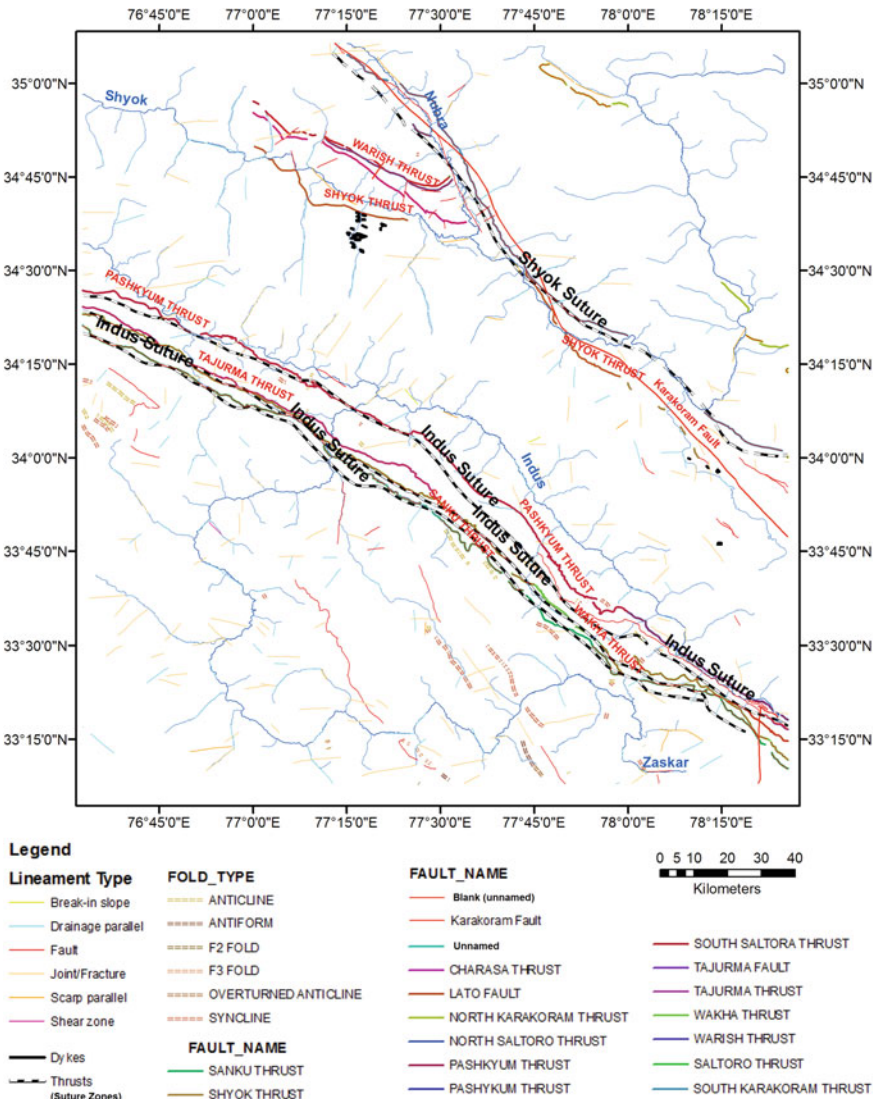


Fig. 8 Different types of structural elements present in the area and their overlay with drainage lines

We observed that the basin-average relief varies between ~1000 m and 4000 m (Fig. 10). The highest relief is observed in the northern part of the region along various tributaries of the Shyok and Nubra rivers. These regions exhibit high relief because there are topographic and chronological signatures of the displacement along the Karakoram Fault (Phartiyal et al. 2005; Imsong et al. 2017). The high standard deviation among the elevation values (Table 1) within each basin (these are often

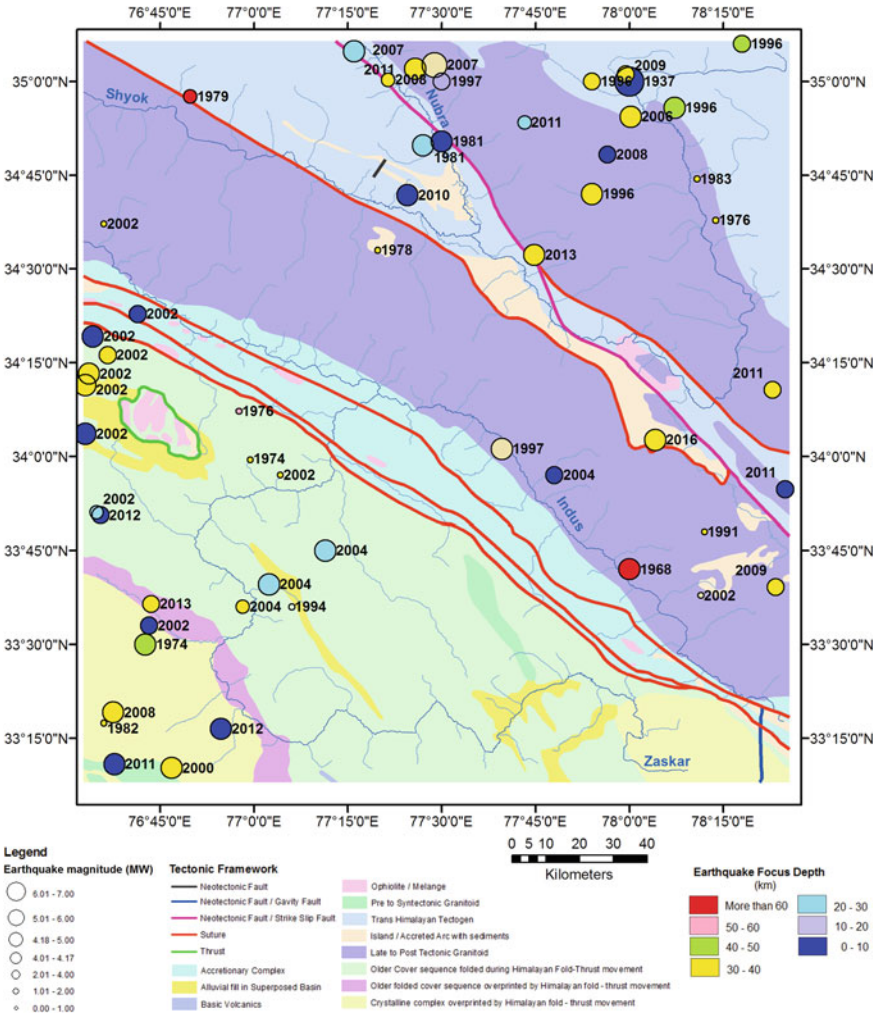


Fig. 9 Recent seismicity map of the area

1/4th or 1/5th of the mean basin relief) indicates the rugged nature of the terrain and the marked changes in elevation (and consequently surface slope) within short distances. The basin-average slope varies between 7° and 35° (Fig. 11), however, its spatial variability is not distinctly discernable. We observed that the basin-average slope is mostly high in the entire region whereas it is highest in the tributaries of the Zaskar in the southwest part and the tributaries of Shyok in the northeast part of the region. It is clearly observed that the basin-average slope is highest in the small tributaries across the region. Usually, the slope values are derived locally from the neighbourhood analysis that inherently introduces a scale-factor dependent on the

Table 1 Mean values of select morphometric parameters enumerated for basins in the Leh–Nubra region

Basin location	No. of basins	Area(km ²)	Perimeter (km)	Circularity ratio	Mean Elevation (m)	Basin relief (m)	Std. dev. elevation (m)	Avg. stream nos in basins
All basins	177	158.52	75.22	0.27	4879.80	2572.12	514.83	41
Indus all	54	123.40	69.58	0.26	4657.71	2500.80	542.65	32
Indus left Flank	19	158.52	75.22	0.27	4879.80	2572.12	514.83	41
Indus right flank	35	99.61	69.03	0.25	4630.70	2507.24	561.33	25
Zanskar all	44	198.21	78.77	0.30	4805.27	2098.48	415.16	52
Zanskar left flank	26	161.82	70.26	0.32	4779.46	2084.16	417.58	42
Zanskar Right Flank	18	250.77	91.07	0.28	4842.53	2119.17	411.68	65
Shyok all	64	175.02	79.32	0.26	5089.10	2813.48	535.41	45
Shyok left flank	30	223.90	87.40	0.27	5007.22	2825.00	556.20	55
Shyok right flank	54	131.88	72.19	0.25	5161.35	2803.33	517.08	36
Nubra all	15	98.17	67.63	0.24	5004.98	3188.37	619.22	26
Nubra left flank	10	113.32	72.90	0.23	5026.53	3268.78	642.24	30
Nubra right flank	5	67.88	57.10	0.26	4961.89	3027.56	573.18	19

(continued)

Table 1 (continued)

Avg. total stream length (km)	Stream frequency (no./km ²)	Drainage density (km/km ²)	Mean slope (°)	Std. dev. slope (°)	Ruggedness index	Dissection index	Hypsometric integral
79.59	0.26	0.50	26.65	11.76	1.29	0.42	0.53
62.65	0.27	0.52	25.29	10.42	1.30	0.43	0.53
79.59	0.26	0.50	26.65	11.76	1.29	0.42	0.53
50.88	0.25	0.52	25.28	10.38	1.29	0.43	0.53
95.90	0.25	0.47	26.12	10.62	0.97	0.36	0.48
79.02	0.25	0.46	26.59	10.84	0.96	0.36	0.48
120.30	0.26	0.47	25.44	10.30	0.99	0.36	0.47
88.23	0.26	0.49	28.09	12.94	1.39	0.45	0.57
108.55	0.26	0.48	27.88	12.27	1.36	0.46	0.57
70.31	0.25	0.50	28.27	13.54	1.42	0.44	0.57
55.88	0.25	0.55	26.98	14.93	1.79	0.50	0.57
64.37	0.24	0.55	26.61	14.28	1.82	0.50	0.57
38.91	0.28	0.57	27.71	16.22	1.73	0.48	0.56

Source Enumerated by the authors

spatial resolution of the dataset. Therefore, the hillslope dominated regions primarily depict higher slope, which is consistent in the study region.

Basin circularity ratio values are all on the lower side (all values are below 0.50) (Fig. 12). Higher values, nearer 1.00, indicate a more circular and developed basin with well-integrated drainage lines and usually having a dendritic drainage pattern developing over gentler terrain. These lower values again indicate the ambient structural control and segmented, parallel linear drainage lines that have developed on the steep flanks of the intervening high mountains between the main rivers. Overall, drainage density values are again on the lower side, possibly due to the scant rainfall received in this region. Relatively, drainage density is highest in the tributary basins of Shyok and Nubra in the northeast part of the region (Fig. 13). However, high values are also observed in the tributary basins of the Indus. The major rivers are generally oriented according to the main tectonic structures (e.g. Karakoram Fault and Indus Suture). Therefore, the relative movement of these structures results in disturbances in the tributaries of these rivers. Previously, researchers have characterised the slope angle as a factor of drainage density (e.g. Schumm 1956). However, high-resolution DEM studies have suggested that direct correlation seldom exists and corresponds to the channelization stages (Lin and Oguchi 2004). We also observed that there is no direct relationship between drainage density and the mean basin slope.

The basin hypsometric integral (HI) values again attest to the predominantly youthful nature of the landscape. Most of the HI values range between 0.4 to 0.6

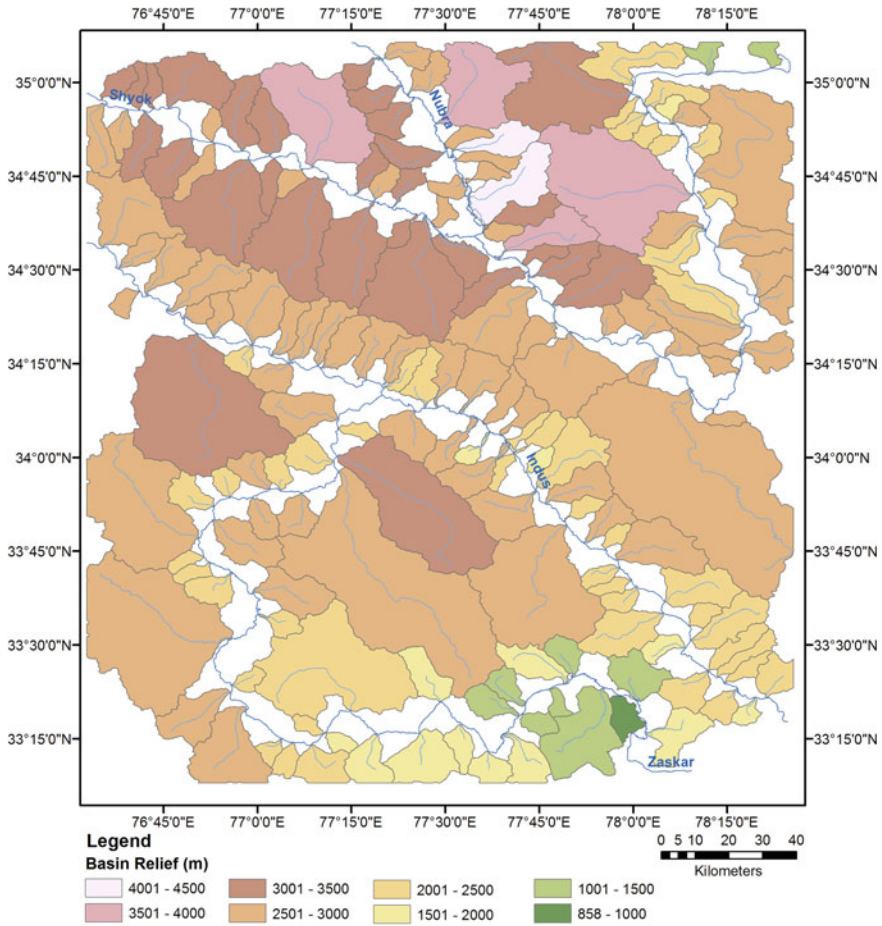


Fig. 10 Basin Relief Map

or between 0.6 to 0.8 (Fig. 14), with these higher values indicating a landscape that has suffered relatively less net dissection (uplift and/or incision). A strong spatiality is observed in this aspect. The basins flanking the Karakoram Range between the Shyok and Nubra valleys show higher values, as do the basins located around the remarkable great bend of the Shyok in the eastern part of the study area (see Table 1 for comparison of region-wise mean HI values for the constituent basins). Most basins of the Indus and Zaskar region show values between 0.4 - 0.6, being in the mature stage of geomorphic evolution. The fact that these basins still report such higher values from landscapes that are essentially millions of years old, amply attest to the ongoing uplift and increase in surface elevation that has occurred here over millennia. Consequently, the mean ruggedness index and dissection index values are also greater for the basins along the Shyok and Nubra in the northern part of the

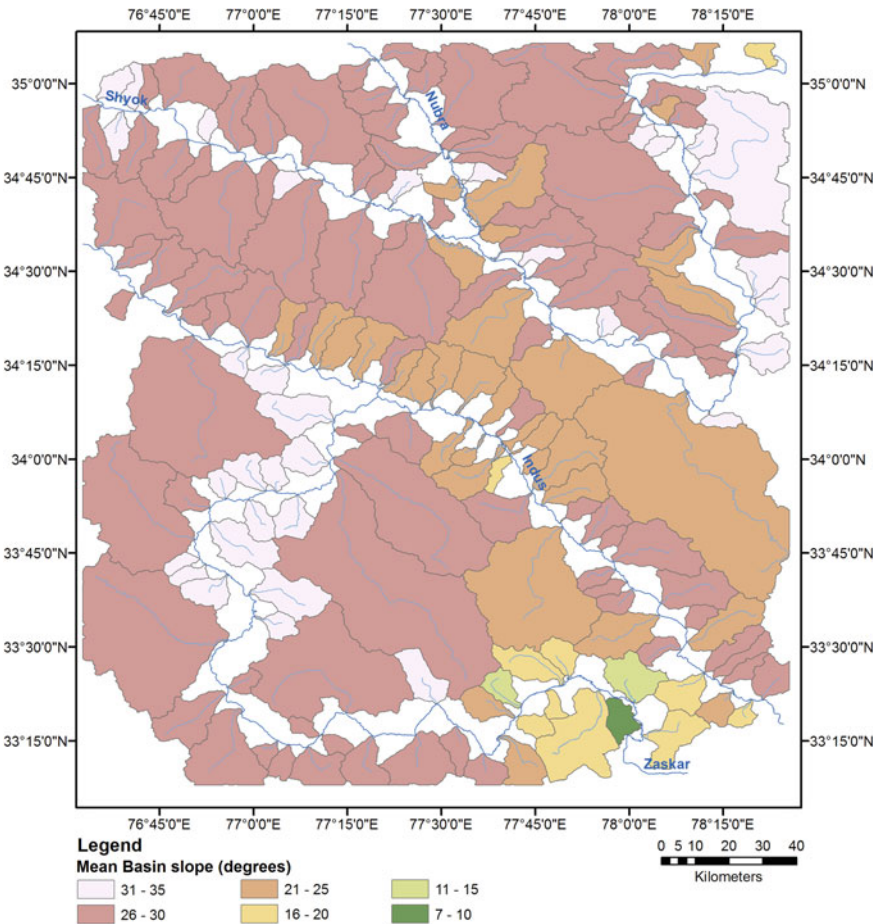


Fig. 11 Mean Basin Slope Map

study area (see Table 1 for comparison) than for the basins in the central part along the Indus or in the southern portion within the Zaskar's province.

The respective basin morphometric parameters were collated for all the 177 basins and a hierarchical clustering analysis was done through a dendrogram (Fig. 15). We could identify some distinct groupings of the basins in this manner (Fig. 16), based on the respective basin morphometric parameters. In all, 23 such basin groups were differentiated (see Table 2 for details). Most basin groups are situated on any one flank of the different ranges and water divides that cut across the study area (e.g. Groups II, I2, M). These groupings further reveal the possible influence of the local structural elements, lithology and basin position/alignment on its formed geometric and morphological attributes.

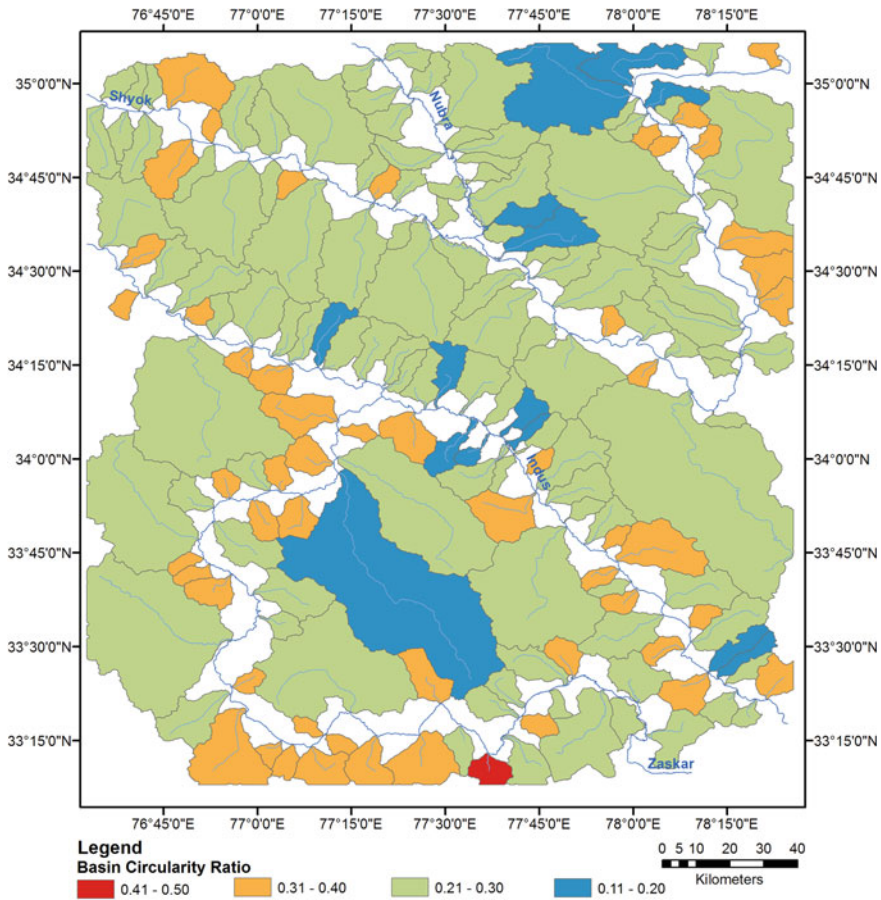


Fig. 12 Circularity Ratio values for the mapped basins

5.3 Long Profile Characteristics of the Main Rivers

The longitudinal profile of a river is highly sensitive to changes in the underlying lithology over which it courses or to any sudden relative elevation change arising from tectonic disturbances (Lin and Oguchi 2006; Ambili and Narayana 2014). SL index changes generally indicate the elevation drop per unit length in a region. Higher values mean that the slope is steeper while a lower value means that the slope is gentle. Sudden changes in values are indicative of tectonic occurrences, often where knick-points are located or other anomalies take place. Knick-points are longitudinally steepened sections of river reaches that bear the unmistakable signatures of tectonic activities among other factors (they can also arise due to lithological variations). They cause an abrupt change in the downstream gradient of the river and have a

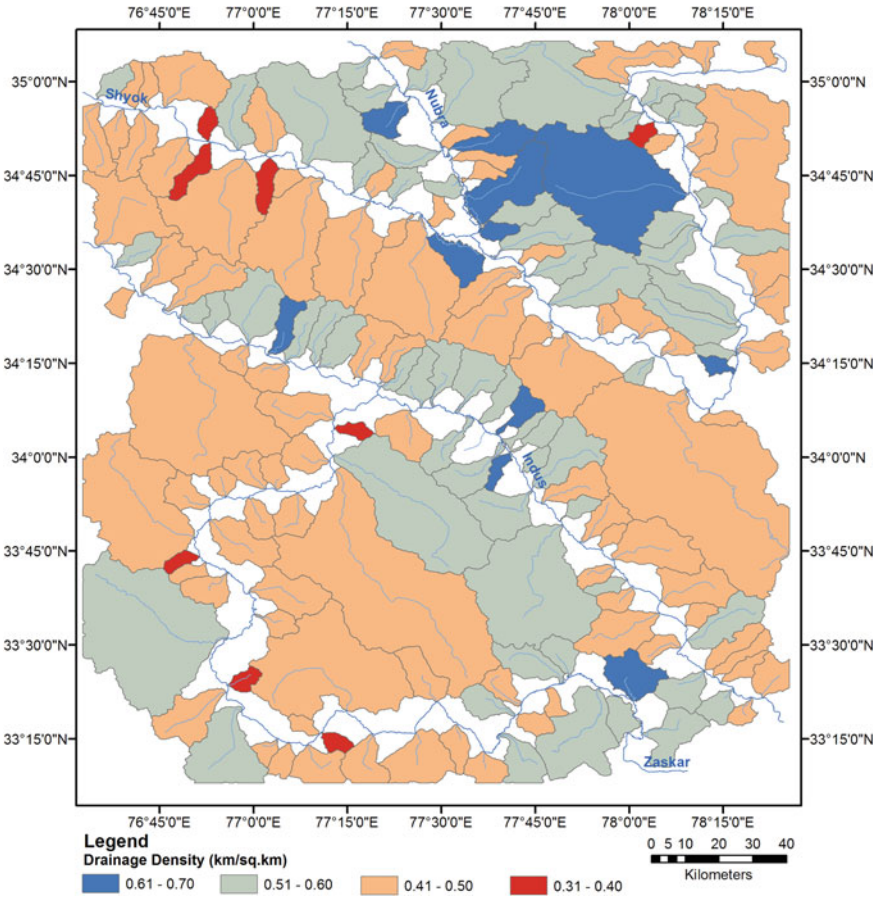


Fig. 13 Basin-wise Drainage Density Map

direct effect on the local base level of the area. Knick-points are thus a source of identification of change in a transient landscape.

Calculating the stream gradient index and the normalised stream gradient index along with their rate of change and fitting the resultant curves reveals the extent and result of the tectonism that occurs in the region. We can thus see a relationship where the more confined a stream is, the lesser opportunity it has to adjust to the local geological setting, making the reach steeper and straighter with higher SL values and lower channel sinuosity values. Contrarily, when the streams are less confined and more able to shifting across the valley, they adjust to the local setting better, making the reach gentler and are more meandering in nature, returning a lower SL value and higher channel sinuosity value. Higher SL values are seen along segments of the Zaskar and western part of the Shyok (Fig. 17), that are situated within gorges. SL index values are the lowest along the central part of the Indus, near Leh, and around

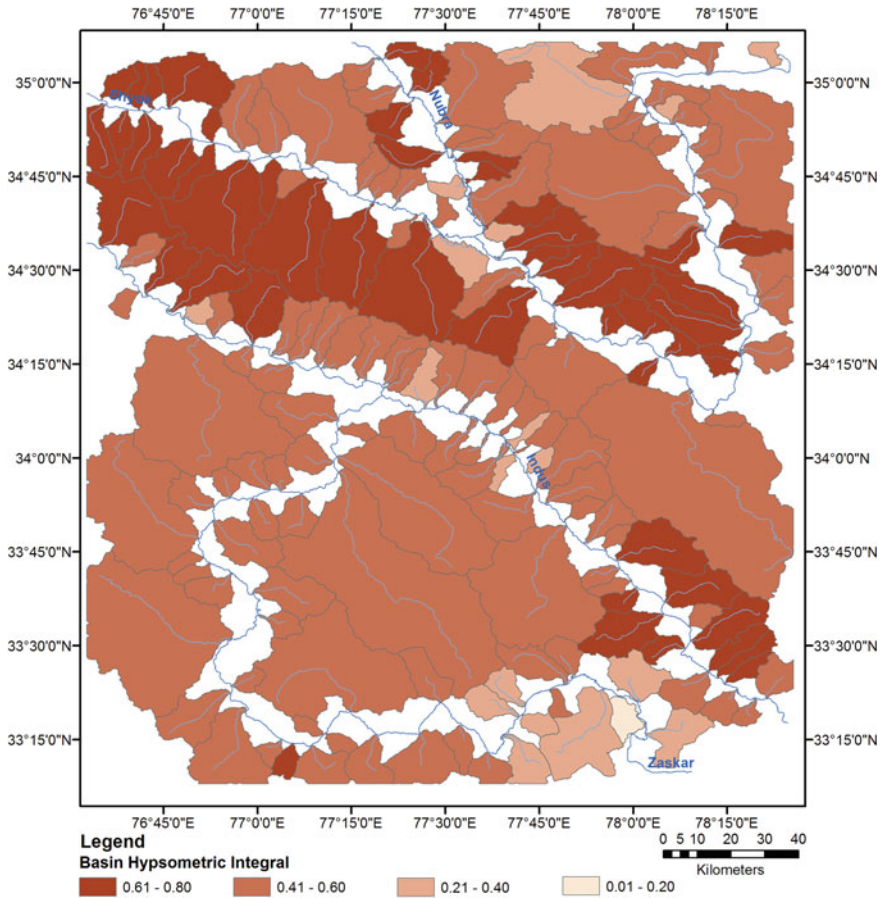


Fig. 14 Hypsometric Integrals for the mapped basins

the Nubra-Shyok confluence zone. It is exactly these channel segments that display a wide braided planform morphology, and thus the link between channel slope and form is apparent. The NSL values (Fig. 18) reflect the same picture. NSL values higher than 2.0 reflect steep courses while those higher than 10.0 are usually taken to reflect extremely steep courses, usually formed by uplift induced incision (Seeber and Gornitz 1983). Most segments here report values higher than 2.0 and the highest values are seen along the courses of the Shyok and Indus in the western part of the study area, where these rivers transition into gorges after earlier occupying broader valley floors further to the east.

Examined individually, each of the main rivers' longitudinal profiles elicit pertinent information about its course. The initial part of the Indus's long profile (Fig. 19) shows a gently declining course before this translates into a steep fall in its latter half, dropping by about 1400 m over 350 km. The marked rise in the segment SL

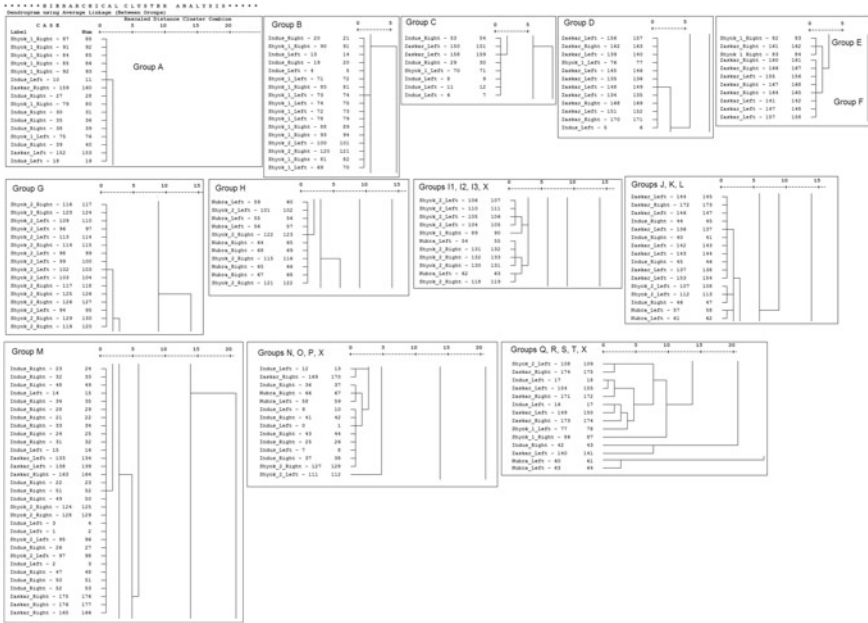


Fig. 15 Clusters formed on the basis of basin morphometric properties using a dendrogram. *Note* The figure presented here has been segmented out into smaller fragments due to its large size. The unbroken image can be supplied if required, upon request

values reflects this pertinently. Due to this steep course, the river profile shows little concavity in its course (the concavity value is 0.44). The mathematical curve that best fit its normalised profile was the exponential one ($R^2 = 0.975$). For the Zanskar (Fig. 20), the semi-log river long profile shows a number of sharp breaks. After an initial less steep segment, the curve falls sharply before again straightening out. This portion corresponds to the gentle middle section of the river, just after its confluence with its principal tributary, the Stod. Here the valley widens and a variety of depositional features have formed. Beyond this, the river enters a gorge that continues till its confluence with the Indus, and this is reflected in the steeply falling last portion of its long profile curve. The above changes are apparent in its markedly changing segment-wise SL values, being below 500 initially, then shooting up to four times that before dropping to the initial levels and then shooting up again. The exponential curve also best-fits the normalised long profile of this river. Of all the four studied rivers, the Zanskar's profile has developed possibly the greatest concavity (value is 0.54), due to its sharp fall in the upper reaches and then continued fall post the gentle middle segment. The semi-log plot of the Shyok's long profile (Fig. 21) also shows a number of breaks in the river's course. Its segment-wise SL index values show a steadily rising trend before dropping markedly between 350 and 450 km along its course. This portion corresponds to the broad valley that has formed at Diskit–Hunder and where the Nubra flows into it. Given the semi-confined nature of the river and

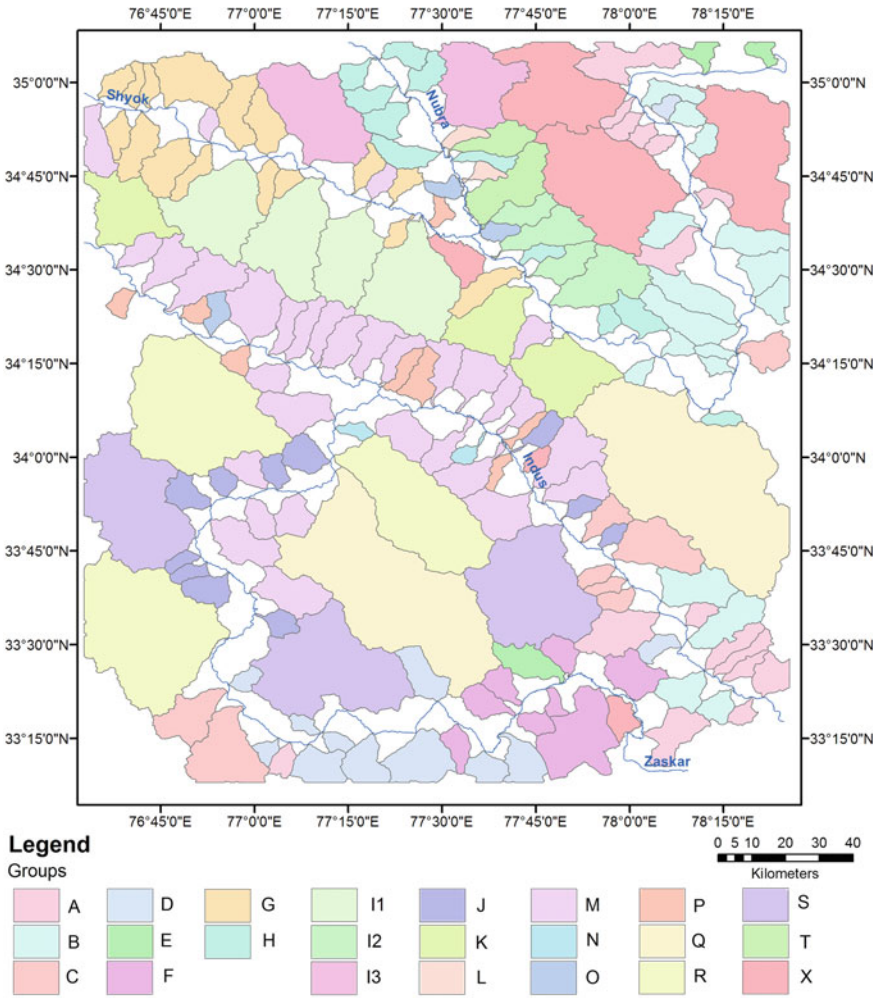


Fig. 16 Mapped basin clusters on basis of the devised dendrogram

the abundant supply of detritus from the surrounding terrain, an extensive braided channel planform has evolved herein (Fig. 25c). After this segment, the Shyok transitions into a gorge further to the west and this is reflected in its sharply rising SL index values. The exponential curve is again the best fit for its normalised profile form, while its constant drop has developed some measure of concavity in the profile (value is 0.34). The semi-log profile plot of the Nubra (Fig. 22) shows the least variations, compared to the other three rivers, due to its shorter length and the fact that it entirely occupies the Shyok Suture for the duration of its course. The river drops down at an almost constant rate and steepens slightly in its lowermost segments, just before its confluence with the Shyok. This is reflected in its segment-wise SL Index

Table 2 Basin groups ascertained through hierarchical cluster analysis based on basin morphological attributes

Basin group	No. of basins	Remarks
A	16	Scattered basins in the Zaskar region, mostly concentrated around its headwater reaches, amidst heavily dissected hill ranges
B	17	Basins that are mostly clustered along the upper section of the Shyok, just prior to and after its great bend and which drain both flanks of it
C	8	Basins that cluster in the upper sections of the Zaskar and around the eastern section of the Indus' course
D	12	These basins cluster around the upper to middle course of the Zaskar, primarily draining its right flank
E	3	These basins are scattered around the headwater reaches of the Zaskar and Shyok
F	8	Located within the medium to highly dissected structural hills around the upper reaches of the Zaskar
G	16	Clustered around the steepest segments of the Shyok in the westernmost part of its course in the study area, draining down both its flanks
H	11	Basins mostly clustered around the upper course of the Nubra, on its right flank
I1	4	Larger basins that arise on the northern flank of the Karakoram and drain into the Nubra on its right flank
I2	4	Smaller and elongated basins that arise in the Karakoram and drain the left flank of the Nubra and the Shyok's right flank just before they meet
I3	2	These are larger sized basins that drain either into the upper section of the Nubra or the steep western segments of the Shyok
J	11	This is a group of some of the smallest sub-basins, that are often located on the extensive piedmonts, between the mouths or larger sub-basins. The mostly drain into the Zaskar, in its central section, where its valley has widened considerably
K	3	Medium sized basins that drain into the Shyok just after its sharp turn towards the northwest and into the steeper western segment of the Indus
L	2	Quite small sub-basins that are present between the lower sections of larger basins and drain the left flank of the Nubra into it
M	31	The Group with the largest number of sub-basins, almost all of which are of smaller dimensions, arise from the southern flank of the Ladakh Range and flow into the left flank of the Indus. Some of these arise from the opposite flank too, particularly over the extensively dissected northern flank of the Zaskar Range and the substantial pediment surfaces that have formed opposite Leh and Choglamsar and near Stok. These basins are essentially steep mountain flank originating small parallel basins

(continued)

Table 2 (continued)

Basin group	No. of basins	Remarks
N	2	Very small, narrow basins lying between larger members, that drain the southern face of the Zaskar Range into the Indus and Zaskar rivers
O	3	Quite small, elongated sub-basins situated between larger members and mostly flowing into the Nubra-Shyok near their confluence zone
P	8	Small confined basins that lie on either side of the Indus Thrust and Suture Zone and drain into this river
Q	2	This group denotes the largest sub-basins in the study area, one of which drains into the Zaskar and the other into the Indus in its eastern section
R	3	This group contains the next largest sub-basins in terms of size, after Group Q and all of these drain into the Zaskar, on both its left and right flanks
S	3	Medium to large sized sub-basins situated in the dissected hill ranges of the Zaskar Basin and draining into it or into the Indus towards the north
T	2	Small group that is present by the Nubra's left flank
X	6	Singular basins, without any group members. These are scattered across the study area

variations and the near-constant drop has made the linear trendline the best-fit for its normalised long profile curve. The concavity value is low at 0.39.

Thus, the two more southern rivers, the Indus and the Zaskar, have higher concavity values, indicating a possibly greater ongoing erosion process. Situated within the Karakoram, the Shyok and Nubra have slightly lower concavities, indicating possibly a greater incidence of uplift that has kept channel segments steeper. Comparison of the best fit curves show that in three cases the logarithmic trendline was the best fit while the linear trendline was the best fit in one case. However, in each case, the R^2 values of the logarithmic and linear trendlines were quite close to each other. This is indicative of the coarse bedload that characterise these rivers and cause braiding to occur in certain stretches, while also hinting at a yet to be achieved equilibrium condition for these streams, possibly due to the ongoing tectonic movements that perturb the channel. However, these conclusions are mere surmises and no generalisations should be drawn on the basis of a single parameter or index-based evaluation, without ancillary data and field information. What is undeniable, however, is the role that the regional geological structures and tectonics have had in influencing the channel morphologies and alignments. This is examined in more detail in the next section.

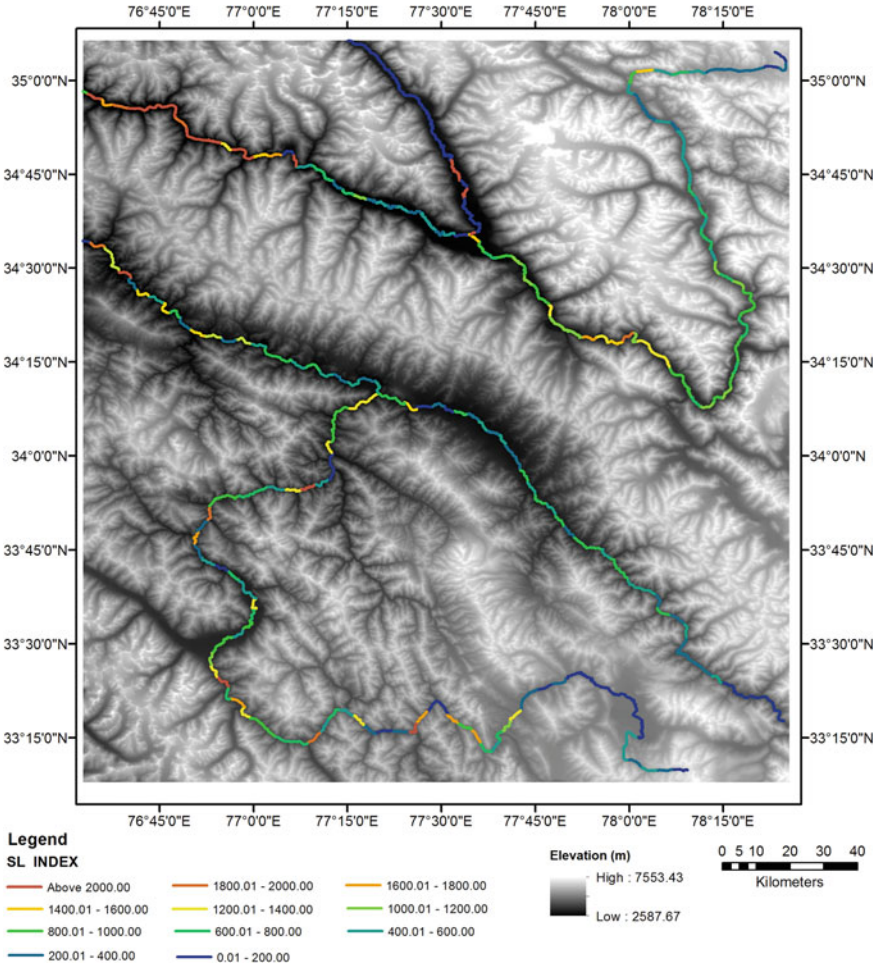


Fig. 17 Mapped SL Index values for the principal drainage lines

5.4 *Principal Drainage Lines, Valley Form and Channel Morphology*

The strong controls exercised by the various mountain fronts all over the Himalayas is evident from the courses of the rivers that flow through it. Such rivers are generally characterised by straightened courses, v-shaped valleys, asymmetric and oval-shaped watersheds and sharp knee bend turns of seasonal rivulets and incised meanders, as channels adjust to the surface they are flowing over and these are directly related to the lithology and geology of the area. The channels carve out their landforms and vary diversely from an alluvial channel to a bedrock channel. O'Brien et al. (2019) defined channel confinement as the percentage of the length of a channel margin that

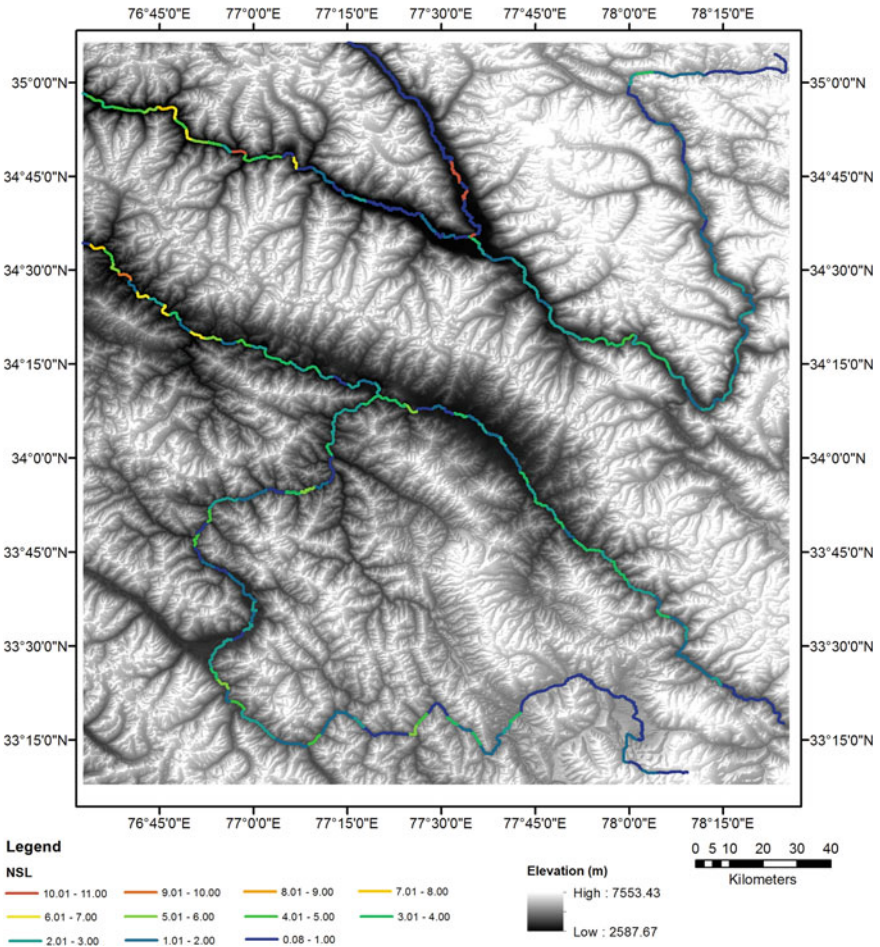


Fig. 18 Mapped NSL values for the principal drainage lines

abuts a confining margin on either bank. Channel confinement gives us an idea as to what degree the channel has the freedom to move and adjust to the rocks beneath it. Channel slope and scale is often used to determine the level of adjustment of a river but in most cases, the simplest way is by comparing the channel width to the valley width. (O'Brien et al. 2019). When the channel width is equal to the valley width, it means that the channel is flowing across the entire valley with no space for the stream to move and hence adjust to the local setting. Such channels are generally geometrically straighter with little to no bends and both flanks of the channel are in contact with the valley edge. In other cases, when the river is meandering within the valley, the channel width is always lesser than that of the valley width allowing the stream to roll over from one edge of the valley to another and giving the stream enough space to adjust to the local setting. In such cases, either end of the stream

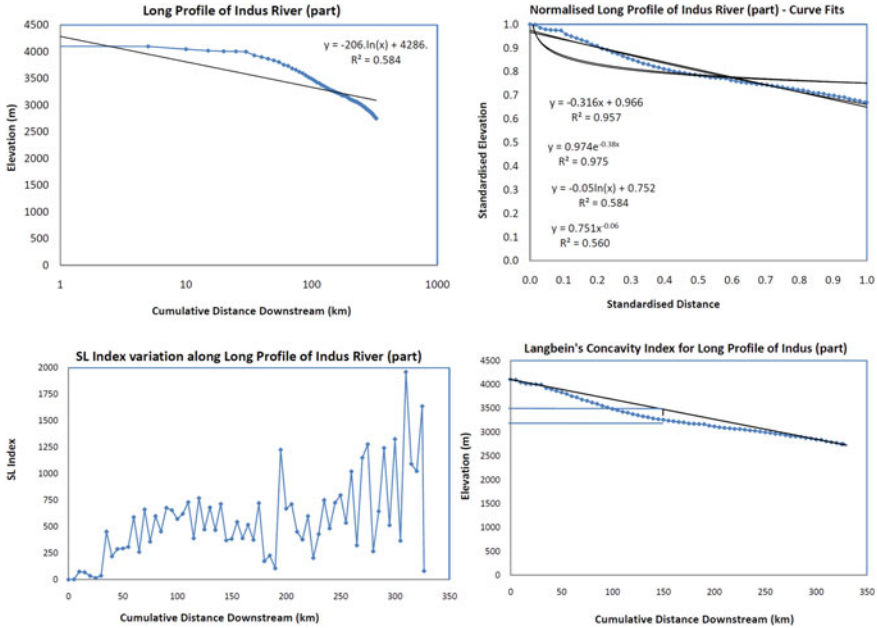


Fig. 19 Long profile plot and curve-fitting for the River Indus, along with reach-wise SL Index variations and computation of the Langbein's concavity parameter

might be in contact with the valley edge or may have both ends of the stream freely flowing within the valley. These channels are generally not straight and can have considerable sinuosity to them.

The above structural control induced channel confinement aspect is seen to markedly influence the valley form, channel morphology and formed geomorphic units in the study area along its principal rivers. Here, the main valleys stand out as broad lower elevation ribbons, especially the confluence zone of the Nubra and Shyok rivers and the Indus at Leh, and have wider river corridors. The Indus flows southeast to northwest across the central part of the area and is joined on its left flank by the Zaskar river near Nimo Peak. The gradual widening of the Indus valley can be observed from its narrow linear form towards the east and subsequent increase in width in the central portion alongside the settlements of Leh, Stok and Choglamsar, just before it is met by the Zaskar and then the Yappola (Fig. 23). Beyond this, the valley width is maintained almost uniformly, though to a lesser extent than was seen in the central portion. This wide central portion is characterised by extensive piedmont surfaces (Fig. 26c), valley margin alluvial fans, high fan-talus (cf. Wadia 1919) and scree deposits and the braided character of the main channel (Fig. 24a, Fig. 25a–d). The Zaskar forms by the meeting of the Tsarap-Lungnak and Stod rivers, at which point its valley widens considerably to the greatest extent along its course, in the south-western portion of the study area. This short wide section of the Zaskar valley contains the greatest diversity of geomorphic forms along its course,

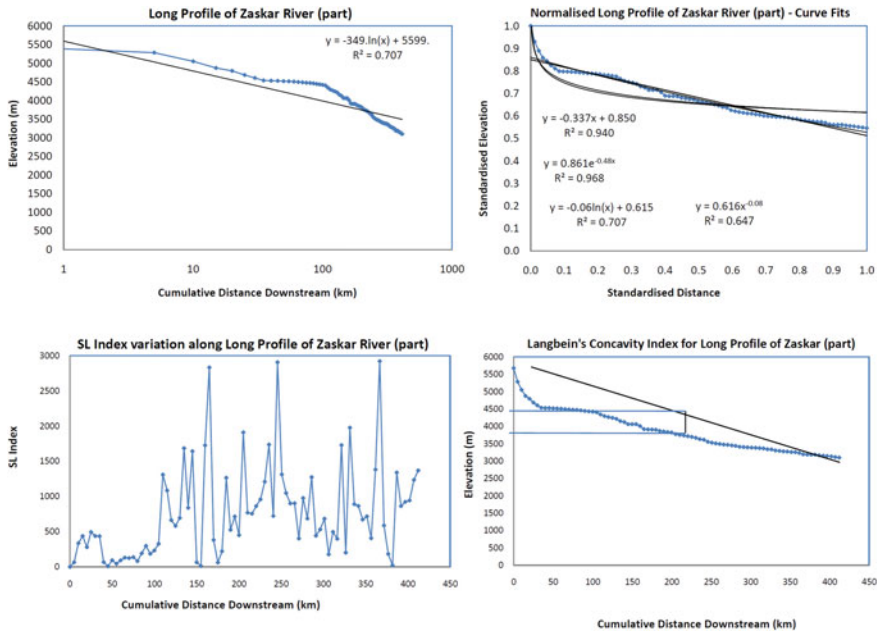


Fig. 20 Long profile plot and curve-fitting for the River Zaskar, along with reach-wise SL Index variations and computation of the Langbein’s concavity parameter

being occupied by several small alluvial fans, large mid-channels bars that cause extensive braiding in this stretch, talus deposits and abutting dissected hill ranges (Fig. 24c). After this, the river flows through a gorge for almost the entire extent of its remaining course before debouching into the Indus (Fig. 24b). The Nubra arises from the Siachen Glacier which is just to the north of the demarcated study area. It flows through a broad glacial valley and is a markedly braided river for its entire course (Fig. 23). Its valley sides are occupied by a number of alluvial fans formed by the steeply dropping streams along either flank. These alluvial fans have been further incised due to repeated regional uplift and thus are flanked by paired terraces along their margins, formed of past deposits. Often the surface of the present fan is occupied by small settlements (Fig. 25b and c). A considerable length of the Shyok is present in the study area and its course most aptly depicts the strong structural control exerted by the parallel Trans-Himalayan ranges and their associated suture zones and fault lines. The Shyok enters the study area at its upper right corner, flows due south in a narrow valley, before taking a sharp but pronounced bend to turn all the way towards the northwest, by an angle of $>90^\circ$ (Fig. 24d). After this turn, the river is flanked by extensive piedmont slopes as the valley widens out manifold times towards its confluence with the Nubra.

The confluence zone of the Nubra and Shyok rivers is the largest lower elevation zone in the entire region along with the Leh town piedmont surface and is discernable by its valley widths of around 2.5–3.0 km (Fig. 24e). This wide floodplain represents

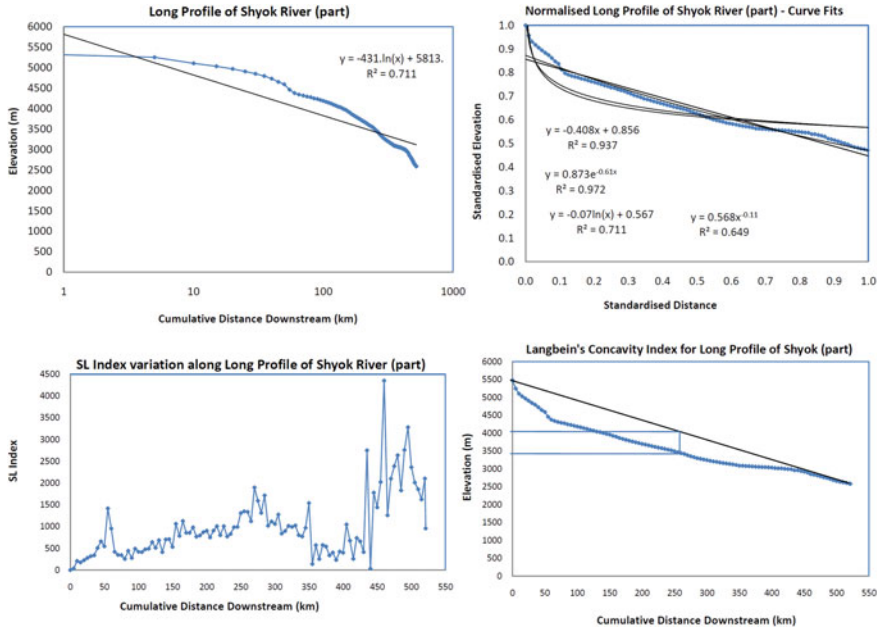


Fig. 21 Long profile plot and curve-fitting for the River Shyok, along with reach-wise SL Index variations and computation of the Langbein's concavity parameter

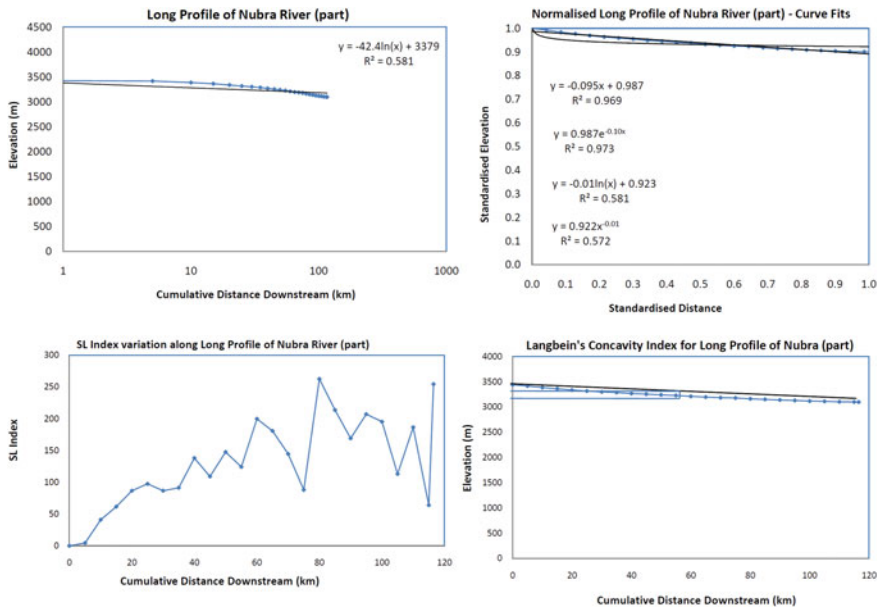


Fig. 22 Long profile plot and curve-fitting for the River Nubra, along with reach-wise SL Index variations and computation of the Langbein's concavity parameter

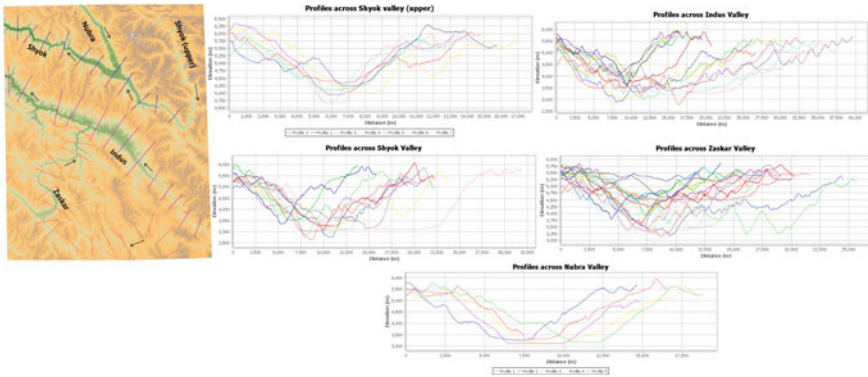


Fig. 23 Valley cross-sections across the principal rivers

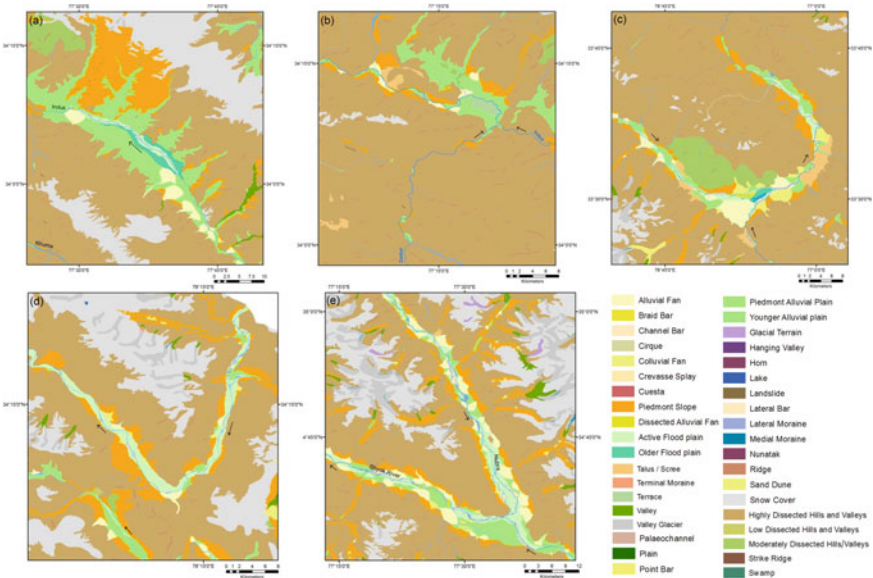


Fig. 24 Different geomorphic units present in the landscape and associated channel morphology in select reaches of the principal rivers. **a** Central part of the Indus’ course around Leh. **b** Confluence of the Zaskar with Indus. **c** Confluence of the Stod and Zaskar, with resultant wide valley segment with diverse geomorphic forms. **d** The great bend of the Shyok, turning from going towards due south to towards the northwest, after occupying the Karakoram Fault. **e** The confluence zone of the Nubra and Shyok rivers in an obtuse barbed meeting and the resultant wide valley floor formation

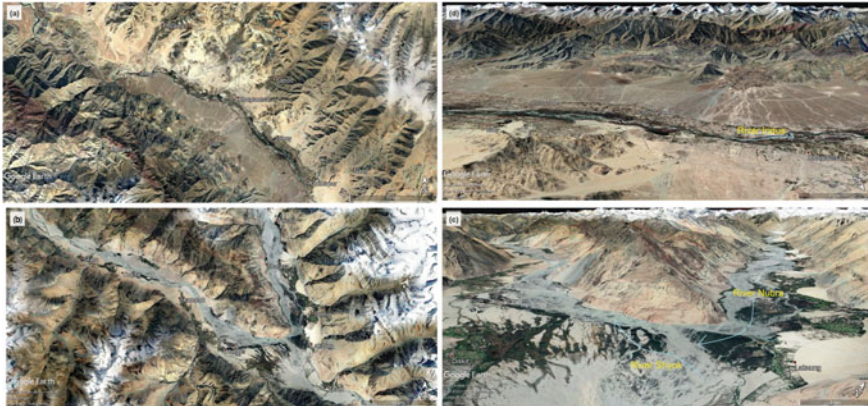


Fig. 25 Google earth views of the channel morphology and adjacent valley geomorphic features in plan view and in tilted 3D view—**a** and **d** for the central part of the Indus valley near Leh, Stok and Choglamsar, with extensive pediments on the southern flank and valley fills and alluvial fans on the northern side wherein banded and inclined rock formations are also discernable along the dissected triangular scarp facets; **b** and **c** the obtuse/barded confluence zone of the Nubra and Shyok rivers near the village of Diskit, with the two valleys being separated by the intervening Great Karakoram Range

the obtuse and barbed drainage confluence of these two rivers, with the Nubra flowing in almost a completely opposite direction to the Shyok, as both of these rivers occupy their respective fault zones (Fig. 25b and c). Their confluence zone around the villages of Diskit and Hunder is also unique in having some high-altitude wetlands and barchanoid sand dunes that have developed in the broad space created by these two rivers via sediment infilling of the Karakoram fault and Shyok Sutures (Fig. 26n). The broad nature of the Shyok valley (Fig. 26o) is retained for some duration after this confluence as the river occupies a central position and extensively braids over the rest of its course here before it transitions into a narrower channel and then moves into a gorge further west.

The highly braided nature of some of these main channel segments is typically what happens in the Himalayan region when adequate valley width is available, usually due to tectonic and warping processes and then infilling of these zones by laid down deposits and the marked sediment supply from hillslopes and river discharge variability (Rajbanshi et al. 2022). It also points to the marked denudation that occurs throughout this region, not only by fluvial processes but also by substantial physical weathering due to the great extremities of the weather elements in daily and seasonal timescales and the intense insolation received here, as pointed out before. The exposed timescales and bare hillslopes, which are almost entirely devoid of any vegetation, often have thick weathered angular rock fragments at their base. Adding to this is the sheetflow and rill erosion that occurs along these slopes. Thus large fan-talus forms are seen to occupy the valley margin areas and their materials are gradually worked into the main channels by tributaries. The other source of sediment supply comes



Fig. 26 Field photographs of the Ladakh region and the study area. **a** Sharp anticlines in the Zaskar Range. **b** Large fan-talus deposits near Dras. **c** Extensive bare pediment surface along the southern flank of the Indus opposite Leh. **d** Re-incised alluvial fan surface and fan front margin near Dras indicating possible latter day uplift after initial deposition. **e** Glacial valley near Khardung La. **f** Meeting of two former glacial valleys that then form a piedmont zone near Leh. **g** Moraine near Khardung village that has been partly levelled and used for cultivation. **h** Apparent recumbent fold in the Zaskar range. **i** Moonland at Lamayuru, possibly indicating a former lake that has been uplifted, drained and heavily dissected. **j** Possible white salina surface, resulting from evaporation of a playa lake, along the Muree Plains within the Zaskar Range. **k** Possible homoclinal rock attitude along the Zaskar Range opposite Choglamsar indicating the great uplift and tilting that has occurred. **l** Folded and vertical rock alignments in the Zaskar Range of many hues. **m** Looking across the Shyok valley at Hunder village, with the seasonal wetlands in the foreground and the dissected surface of a portion of the Great Karakorams in the background. **n** High altitude barchans in the foreground that have formed along the Shyok plains near Hunder village, with the braided Shyok River in the background. **o** The extensive braided nature of the Shyok River, which is occupying the Karakoram Fault and the wide valley floor across which it traverses. **p** A tributary arising from the Great Karakoram range confluent with the Shyok River, having cut down through its past deposits that are present as paired terraces on either flank of its present lower vegetated alluvial fan surface. *Note* All the photographs have been taken by the first author

from reworked past glacial deposits, with a number of moraines present in this area (e.g. the moraine deposits at Khardung village- Fig. 26g). Past and ongoing uplift can also result in hydrological changes, by raising lake beds, leading to their dissection (e.g. what has occurred in the Moonlands of Lamayuru (Kotlia et al. 1997)—Fig. 26i). Conversely, the basins formed within the uplifted ranges can also house extensive piedmont zones and low-lying playas (Fig. 26j) where local runoff can accumulate

and form lakes, which usually dry up and leave behind salinas, while along the main channels like the Shyok and Indus, particularly where their tributaries flow in, local seasonal grasslands/wetlands also arise that are usually used as pasturelands.

6 Conclusions

This paper has tried to briefly bring out the notable lithologic and structural elements of a part of the Ladakh region and relate them with the enumerated terrain parameters and ambient river character. The high mountain landscape and the associated tectonic and structural elements have abetted the formation of very confined to partly unconfined river channels. While the main rivers have some wider valley segments, occupied by extensive channel braids, the tributaries are incised and of bedrock character. Both erosional and depositional forms are seen, with the former being more extensive and manifesting as numerous dissected ridges of varying degrees and substantial pediment surfaces. The depositional features are more localised, whether they be in-channel bars or channel adjacent alluvial fans. The extent to which such depositional elements have formed largely rests on the available valley floor space, which is in turn dependent on the compressional/extensional and shearing movements that have occurred herein. In-filling of such available spaces by unconsolidated deposits borne by the principal rivers and supplied by their many tributaries have enabled the formation of sustained flatter surfaces in some locations, which serve as settlement points (e.g. on valley floors or lower fan surfaces). The alignments of almost all streams are controlled by the underlying sutures, faults and their associated thrust elements. Greater insight into the evolutionary history of the drainage and its linkages with the ambient past and present tectonic elements can be better ascertained through detailed sediment/rock dating, reach-scale denudation rates and facies analysis of the deposited sediment profiles along the main and tributary channels.

Acknowledgements The authors are grateful to Mr. Rajarshi Dasgupta of the Department of Geography, East Calcutta Girls' College, Kolkata and Dr. Somasis Sengupta of the Department of Geography, The University of Burdwan, Bardhaman, for their inputs regarding the paper.

References

- Allamano A, Claps P, Laio F (2009) Global warming increases flood risk in mountainous areas. *Geophys Res Lett* 36:L24404. <https://doi.org/10.1029/2009GL041395>
- Ambili V, Narayana AC (2014) Tectonic effects on the longitudinal profiles of the Chaliyar River and its tributaries, southwest India. *Geomorphology* 217:37–47
- Anand AK, Pradhan SP (2019) Assessment of active tectonics from geomorphic indices and morphometric parameters in part of the Ganga basin. *J Mt Sci* 16:1943–1961. <https://doi.org/10.1007/s11629-018-5172-2>

- Ashrit R (2010) Investigating the Leh 'Cloudburst'. National Centre for Medium Range Weather Forecasting, Ministry of Earth Sciences, Government of India. http://www.ncmrwf.gov.in/Cloudburst_Investigation_Report.pdf. Accessed 26 April 2016
- Banerji D, Patel PP (2019) Morphological aspects of the Bakreshwar River Corridor, West Bengal, India. In: Das B, Ghosh S, Islam A (eds) *Advances in micro geomorphology of lower Ganga Basin—Part I: Fluvial geomorphology*. Springer International Publishing, Cham, pp 155–189. https://doi.org/10.1007/978-3-319-90427-6_9
- Barnett TP, Adam JC, Lettenmaier DP (2005) Potential impacts of a warming climate on water availability in snow-dominated regions. *Nature* 438:303–309
- Benn DI, Owen LA (1998) The role of Indian summer monsoon and the mid-latitude westerlies in Himalayan glaciation: review and speculative discussion. *J Geol Soc London* 155:353–363
- Bhan SC, Devrani AK, Sinha V (2015) An analysis of monthly rainfall and the meteorological conditions associated with cloudburst over the dry region of Leh (Ladakh), India. *Mausam* 66:107–122
- Bharadwaj H, Singh AP, Malhotra MS (1973) Body comparison of the high-altitude natives of Ladakh: a comparison with sea-level residents. *Hum Biol* 45:423–434
- Bhatt CM, Litoria PK, Sharma PK (2008) Geomorphic signatures of active tectonics in Bist Doab interfluvial tract of Punjab, NW India. *J Indian Soc Remote Sens* 36(4):361–373
- Bhutiyan MK (2014) The Siachen Glacier: the second longest glacier outside the polar regions. In: Kale VS (ed) *Landscapes and Landforms of India*. Springer, Dordrecht, pp 105–113
- Bhutiyan MK, Kale VS, Pawar NJ (2010) Climate change and the precipitation variations in the northwestern Himalaya: 1866 to 2006. *Int J Climatol* 30:535–548
- Bookhagen B, Burbank DW (2006) Topography, relief and TRMM-derived rainfall variations along the Himalaya. *Geophys Res Lett* 33:L08405. <https://doi.org/10.1029/2006GL026037>
- Brocklehurst SH (2010) Tectonics and geomorphology. *Prog Phys Geogr* 34:357–383. <https://doi.org/10.1177/0309133309360632>
- Bull WB (2007) *Tectonic geomorphology of mountains: a new approach to paleoseismology*. Wiley-Blackwell, Oxford
- Bull WB, McFadden L (1977) Tectonic geomorphology north and south of the Garlock fault, California. In: Doehring DO (eds) *Geomorphology in arid regions. Proceedings of the 8th Annual Geomorphology Symposium*, State University of New York, Binghamton, pp 115–138
- Bull WB (1977) Tectonic geomorphology of the Mojave Desert. U.S. Geological Survey Contract Report 14-08-001-G-394. Office of Earthquakes, Volcanoes, and Engineering, Menlo Park, California
- Bull WB (1978) Geomorphic tectonic classes of the south front of the San Gabriel Mountain, California. U.S. Geological Survey Contract Report 14-08-001-G-394. Office of Earthquakes, Volcanoes, and Engineering, Menlo Park, California
- Burbank DW, Anderson RS (2011) *Tectonic geomorphology*. Wiley, New Jersey
- Burbank DW, Leland J, Fielding E, Anderson RS, Brozovic N, Reid MR, Duncan C (1996) Bedrock incision, rock uplift and threshold hillslopes in the northwestern Himalayas. *Nature* 379:505–510
- Castillo M, Munoz-Salinas E, Ferrari L (2014) Response of a landscape to active tectonics using channel steepness indices (k_{sn}) and OSL: a case study from the Jalisco block, western Mexico. *Geomorphology* 221:204–214. <https://doi.org/10.1016/j.geomorph.2014.06.017>
- Church M, Ryder JM (1972) Paraglacial sedimentation: a consideration of fluvial processes conditioned by glaciation. *Geol Soc Am Bull* 83:3059–3072
- Clift PD (2002) A brief history of the Indus River. In: Clift PD, Kroon D, Gaedicke C, Craig J (eds) *The tectonic and climatic evolution of the Arabian Sea region*, vol 195. Geological Society of London Special Publications. Geological Society of London, London, pp 237–258
- Cox RT (1994) Analysis of drainage-basin symmetry as a rapid technique to identify areas of possible Quaternary tilt-block tectonics: an example from the Mississippi Embayment. *Geol Soc Am Bull* 106(5):571–581. [https://doi.org/10.1130/00167606\(1994\)1062.3.CO;2](https://doi.org/10.1130/00167606(1994)1062.3.CO;2)
- Cunningham A (1854) *Ladak, physical, historical and statistical*. W.H. Allen & Company, London

- Dar RA, Chandra R, Romshoo SA (2013) Morphotectonic and lithostratigraphic analysis of intermontane Karewa basin of Kashmir Himalayas, India. *J Mt Sci* 10:1–15. <https://doi.org/10.1007/s11629-013-2494-y>
- Das S, Patel PP, Sengupta S (2016) Evaluation of different digital elevation models for analyzing drainage morphometric parameters in a mountainous terrain: a case study of the Supin. Upper Tons Basin, Indian Himalayas. *SpringerPlus*, vol 5, p 1544. <https://doi.org/10.1186/s40064-016-3207-0>
- Doomkamp JC (1986) Geomorphological approaches to the study of neotectonics. *J Geol Soc* 143:335–342. <https://doi.org/10.1144/gsjgs.143.2.0335>
- Dortch JM, Owen LA, Caffee MW (2010) Quaternary glaciation in the Nubra and Shyok valley confluence, northernmost Ladakh, India. *Quatern Res* 74:132–144
- Dortch JM, Owen LA, Caffee MW (2013) Timing and climatic drivers for glaciation across semi-arid western Himalaya-Tibetan orogen. *Quatern Sci Rev* 78:188–208
- Drew F (1875) *The Jummoo and Kashmir territories: a geographical account*. Edward Stanford, London
- Duncan C, Masek J, Fielding E (2003) How steep are the Himalaya? Characteristics and implications of along-strike topographic variations. *Geology* 31:75–78
- England P, Molnar P (1990) Surface uplift, uplift of rocks, and exhumation of rocks. *Geology* 18:1173–1177
- Evans IS, Hengl T, Gorsevski P (2009) Applications in geomorphology. In: Hengl T, Reuter HI (eds) *Geomorphometry: concepts, software, applications*. *Developments in soil science*, vol 33, pp 497–525. [https://doi.org/10.1016/S0166-2481\(08\)00022-6](https://doi.org/10.1016/S0166-2481(08)00022-6)
- Fielding EJ (1996) Tibet uplift and erosion. *Tectonophysics* 260:55–84
- Florinsky IV (2017) An illustrated introduction to general geomorphometry. *Prog Phys Geogr* 41:723–752
- Ganjoo RK, Koul MN, Bahuguna IM, Ajai (2014) The complex phenomenon of glaciers of Nubra Valley, Karakorum (Ladakh), India. *Nat Sci* 6:733–740
- Gansser A (1964) *Geology of the Himalaya*. Wiley-Interscience, London
- Gruber S, Peckham S (2009) Land surface parameters and objects in hydrology. In: Hengl T, Reuter HI (eds) *Geomorphometry: concepts, software, applications*. *Developments in soil science*, vol 33, pp 171–194. [https://doi.org/10.1016/S0166-2481\(08\)00007-X](https://doi.org/10.1016/S0166-2481(08)00007-X)
- Guha S, Patel PP (2017) Evidence of topographic disequilibrium in the Subarnarekha River Basin, India: a digital elevation model based analysis. *J Earth Syst Sci* 126:106. <https://doi.org/10.1007/s12040-017-0884-1>
- Hack JT (1973) Stream profile analysis and stream-gradient index. *J Res US Geol Surv* 1:421–429
- Hare PW, Gardner TW (1985) Geomorphic indicators of vertical neotectonism along converging plate margins, Nicoya Peninsula, Costa Rica. In: Morisawa M, Hack JT (eds) *Tectonic geomorphology*. *Proceedings of the 15th Annual Binghamton Geomorphology Symposium*. Allen and Unwin, Boston, MA, pp 123–134
- Harlin JM (1978) Statistical moments of the hypsometric curve and its density function. *Int J Assoc Math Geol* 10:59–72
- Hedrick KA, Seong YB, Owen LA, Caffee MW, Dietsch C (2011) Towards defining the transition in style and timing of Quaternary glaciation between the monsoon-influenced Greater Himalaya and the semi-arid Transhimalaya of northern India. *Quatern Int* 236:21–33
- Hobley DEJ, Sinclair HD, Mudd SM (2012) Reconstruction of a major storm event from its geomorphic signature: the Ladakh floods, 6 August 2010. *Geology* 40:483–486
- Imson W, Bhattacharya F, Mishra RL, Phukan S (2017) Geomorphic evidence of late Quaternary displacement of the Karakoram Fault in Nubra and Shyok valleys, Ladakh Himalaya. *Curr Sci* 2295–2305
- Jacobson A (2000) Solar energy measurements for Ladakh, India. In: Banerjee R, Nayak JK, Fernandes BG (eds) *Renewable energy technology for the new millennium*, *Proceedings of the 24th national renewable energy convention*. Allied Publishers Limited, New Delhi

- Jamieson SSR, Sinclair HD, Kirstein LA, Purves RS (2004) Tectonic forcing of longitudinal valleys in the Himalaya: morphological analysis of the Ladakh batholith, north India. *Geomorphology* 58:49–65
- Juyal N (2010) Cloud burst-triggered debris flow around Leh. *Curr Sci* 99:1166–1167
- Juyal N (2014) Ladakh: the high-altitude Indian cold desert. In: Kale VS (ed) *Landscapes and Landforms of India*. Springer, Dordrecht, pp 115–124
- Kale VS, Achyuthan H, Sengupta S (2010) Reconstruction of late quaternary fluvio-sedimentary response of Kaveri and Palar Rivers: based on Chronostratigraphy, Digital geomorphometry and remote sensing analysis. University of Pune, Pune
- Keller EA, Pinter N (2002) *Active tectonics: earthquakes, uplift and landscape*, 2nd edn. Prentice Hall, Upper Saddle River, New Jersey
- Knighton D (1998) *Fluvial forms and processes: a new perspective*. Routledge
- Kotlia BS, Shukla UK, Bhalla MS, Mathur PD, Pant CC (1997) Quaternary fluvio-lacustrine deposits of the Lamayuru Basin, Ladakh Himalaya: preliminary multidisciplinary investigations. *Geol Mag* 134(6):807–812
- Kumar A, Srivastava P (2018) Landscape of the Indus River. In: Singh D (ed) *The Indian Rivers*. Springer, pp 47–59
- Kumar MS, Shekhar MS, Rama Krishna SSVS, Bhutiyani MR, Ganju A (2012) Numerical simulation of cloud burst event on August 05, 2010, over Leh using WRF mesoscale model. *Nat Hazards* 62:1261–1271
- Langbein WB (1964) Profiles of rivers of uniform discharge. *US Geol Surv Prof Pap* 501B:119–122
- Lee CS, Tsai LL (2010) A quantitative analysis for geomorphic indices of longitudinal river profile: a case study of the Choushui River, Central Taiwan. *Environ Earth Sci* 59:1549–1558
- Lin Z, Oguchi T (2004) Drainage density, slope angle, and relative basin position in Japanese bare lands from high-resolution DEMs. *Geomorphology* 63(3–4):159–173
- Lin Z, Oguchi T (2006) DEM analysis on longitudinal and transverse profiles of steep mountainous watersheds. *Geomorphology* 78:77–89
- Lohan SK, Sharma S (2012) Present status of renewable energy resources in Jammu & Kashmir state of India. *Renew Sustain Energy Rev* 16:3251–3258
- Mahmood SA, Gloaguen R (2012) Appraisal of active tectonics in Hindu Kush: insights from DEM derived geomorphic indices and drainage analysis. *Geosci Front* 3:407–428. <https://doi.org/10.1016/j.gsf.2011.12.002>
- Munack H, Korup O, Resentini A, Limonta A, Garsanti E, Blothe JH, Scherler D, Wittman H, Kubik PW (2014) Postglacial denudation of western Tibetan plateau margin outpaced by long-term exhumation. *Bull Geol Soc America* 126:1580–1594. <https://doi.org/10.1130/B30979.1>
- Nag SK, Chakraborty S (2003) Influence of rock types and structures in the development of drainage network in hard rock area. *J Indian Soc Remote Sens* 31:25–35
- Nag D, Phartiyal B, Joshi M (2021) Late Quaternary tectono-geomorphic forcing vis-a-vis topographic evolution of Indus catchment, Ladakh, India. *Catena* 199:105103. <https://doi.org/10.1016/j.catena.2020.105103>
- Nagar DP, Ahmed Z (2007) Biological spectrum of Nubra Valley (Ladakh). *Indian J Forest* 30:479–481
- O'Brien GR, Wheaton JM, Fryirs K, Macfarlane WW, Brierley G, Whitehead K, Gilbert J, Volk C (2019) Mapping valley bottom confinement at the network scale. *Earth Surf Proc Land* 44(9):1828–1845
- Oguchi T (1997) Drainage density and relative relief in humid steep mountains with frequent slope failure. *Earth Surf Proc Land* 22:107–120. [https://doi.org/10.1002/\(SICI\)1096-9837\(199702\)22:2%3c107::AID-ESP680%3e3.0.CO;2-U](https://doi.org/10.1002/(SICI)1096-9837(199702)22:2%3c107::AID-ESP680%3e3.0.CO;2-U)
- Olaya V (2009) Basic land-surface parameters. In: Hengl T, Reuter HI (eds) *Geomorphometry: concepts, software, applications*. Developments in soil science, vol 33, pp 141–69. [https://doi.org/10.1016/S0166-2481\(08\)00006-8](https://doi.org/10.1016/S0166-2481(08)00006-8)

- Osmaston H (1994) The geology, geomorphology and Quaternary history of Zangskar. In: Crook J, Osmaston H (eds) *Himalayan Buddhist villages: environment, resources, society and religious life in Zangskar, Ladakh*. University of Bristol Press, Bristol, pp 1–36
- Owen LA (2014) Himalayan landscapes of India. In: Kale VS (ed) *Landscapes and landforms of India*. Springer, Dordrecht, pp 41–52
- Owen LA, Dortch JM (2014) Nature and timing of Quaternary glaciation in the Himalayan-Tibetan orogen. *Quatern Sci Rev* 88:14–54
- Owen LA (2011) Quaternary glaciation of northern India. In: Elhers J, Gibbard P, Hughes PD (eds) *Quaternary glaciations: extent and chronology: a closer look*. Developments in quaternary science, vol 15. Elsevier, Amsterdam, pp 929–942
- Palmer TN, Räisänen J (2002) Quantifying the risk of extreme seasonal precipitation events in a changing climate. *Nature* 415:512–514
- Patel PP (2012) An exploratory geomorphological analysis using modern techniques for sustainable development of the Dulung river basin. Unpublished Ph.D. thesis, University of Calcutta, Kolkata. <https://sg.inflibnet.ac.in/handle/10603/156681>
- Patel PP (2013) GIS techniques for landscape analysis—case study of the Chel River Basin, West Bengal. In: Proceedings of state level seminar on geographical methods in the appraisal of landscape, held at Department of Geography, Dum Dum Motijheel Mahavidyalaya, Kolkata, 20 March 2012, pp 1–14
- Patel PP, Sarkar A (2007) Hypsometric analysis of the Dulung N. Basin and its sub-basins. *Geograph Rev India* 69(4):409–422
- Patel PP, Sarkar A (2009) Application of SRTM data in evaluating the morphometric attributes: a case study of the Dulung River Basin. *Pract Geographer* 13(2):249–265
- Patel PP, Sarkar A (2010) Terrain characterization using SRTM data. *J Indian Soc Remote Sens* 38(1):11–24. <https://doi.org/10.1007/s12524-010-0008-8>
- Patel PP, Dasgupta R, Chanda S, Mondal S (2021) An investigation into longitudinal forms of gullies within the “Grand Canyon” of Bengal, Eastern India. *Trans GIS* 25(5):2501–2528. <https://doi.org/10.1111/tgis.12828>
- Perez-Pena JV, Azanon JM, Azor A (2008) CalHypso: an ArcGIS extension to calculate hypsometric curves and their statistical moments. *Comput Geosci* 35:1214–1223
- Phartiyal B, Kothiyari GC (2012) Impact of neotectonics on drainage network evolution reconstructed from morphometric indices: case study from NW Indian Himalaya. *Zeitschrift Fur Geomorphologie* 56:121–140. <https://doi.org/10.1127/0372-8854/2011/0059>
- Phartiyal B, Sharma A, Upadhyay R, Sinha AK (2005) Quaternary geology, tectonics and distribution of palaeo-and present fluvio/glacio lacustrine deposits in Ladakh, NW Indian Himalaya—a study based on field observations. *Geomorphology* 65(3–4):241–256
- Pike RJ (2000) Geomorphometry: diversity in quantitative surface analysis. *Prog Phys Geogr* 24:1–20
- Pike RJ, Evans IS, Hengl T (2009) Geomorphometry: a brief guide. In: Hengl T, Reuter HI (eds) *Geomorphometry: concepts, software, applications*. Developments in soil science, vol 33, pp 3–30. [https://doi.org/10.1016/S0166-2481\(08\)00001-9](https://doi.org/10.1016/S0166-2481(08)00001-9)
- Prerna R, Pandey DK, Mahender K (2018) Longitudinal profiling and elevation-relief analysis of the Indus. *Arab J Geosci* 11:343. <https://doi.org/10.1007/s12517-018-3657-5>
- Radaideh OMA, Mosar J (2019) Tectonic controls on fluvial landscapes and drainage development in the westernmost part of Switzerland: insights from DEM-derived geomorphic indices. *Tectonophysics* 768:228179
- Rajbanshi J, Das S, Patel PP (2022) Planform changes and alterations of longitudinal connectivity caused by the 2019 flood event on the braided Brahmaputra River in Assam, India. *Geomorphol* 403:108174. <https://doi.org/10.1016/j.geomorph.2022.108174>
- Ramachandra TV, Jain R, Krishnadas G (2011) Hotspots of solar potential in India. *Renew Sustain Energy Rev* 15:3178–3186
- Ramirez-Herrera MT (1998) Geomorphic assessment of active tectonics in the Acambay graben, Mexican volcanic belt. *Earth Surf Proc Land* 23:317–332

- Rasmussen KL, House RA Jr (2012) A flash-flooding storm at the steep edge of high terrain. *Bull Am Meteor Soc* 93:1713–1724
- Remondo J, Oguchi T (2009) Editorial- GIS and SDA applications in geomorphology. *Geomorphology* 111:1–3. <https://doi.org/10.1016/j.geomorph.2009.04.015>
- Robl J, Stuwe K, Hergarten S (2008) Channel profiles around Himalayan river anticlines: constraints on their formation from digital elevation model analysis. *Tectonics* 27:TC3010. <https://doi.org/10.1029/2007TC002215>
- Sarkar A, Patel PP (2011) Topographic analysis of the Dulung R Basin. *Indian J Spat Sci* II(1):2
- Sarkar A, Patel PP (2012) Terrain classification of the Dulung Drainage Basin. *Indian J Spat Sci* III 1:6
- Sarkar A, Roy L, Das S, Sengupta S (2021) Fluvial response to active tectonics: analysis of DEM-derived longitudinal profiles in the Rangit River Basin, Eastern Himalayas India. *Environ Earth Sci* 80:258. <https://doi.org/10.1007/s12665-021-09561-2>
- Sarkar A, Patel PP (2009) Drainage analysis of the dulung basin. In: Sharma HS, Kale VS (ed) *Geomorphology in India*. Prayag Pustak Bhavan, Allahabad, pp 133–154
- Schumm SA (1956) Evolution of drainage systems and slopes in badlands at Perth Amboy, New Jersey. *Geol Soc Am Bull* 67:597–646
- Searle MP, Owen LA (1999) The evolution of the Indus River in relation to topographic uplift, climate and geology of western Tibet, the Trans-Himalayan and High-Himalayan Range. In: Meadows A, Meadows PS (eds) *The Indus River: biodiversity, resources and humankind*. Oxford University Press, Oxford, pp 210–230
- Seeber L, Gornitz V (1983) River profiles along the Himalayan arc as indicators of active tectonics. *Tectonophysics* 92:335–367. [https://doi.org/10.1016/0040-1951\(83\)90201-9](https://doi.org/10.1016/0040-1951(83)90201-9)
- Sharma J (2003) *Architectural heritage: Ladakh*. Haranand Publications, New Delhi
- Singh V, Tandon SK (2008) The Pinjaur dun (intermontane longitudinal valley) and associated active mountain fronts, NW Himalaya. *Tectonic geomorphology and morphotectonic evolution*. *Geomorphology* 102:376–394. <https://doi.org/10.1016/j.geomorph.2008.04.008>
- Sklar L, Dietrich W (1998) River longitudinal profiles and bedrock incision models: stream power and the influence of sediment supply. In: Tinkler KJ, Wohl EE (eds) *Rivers over rocks: fluvial processes in bedrock channels*. American Geophysical Union Geophysical Monograph Series, vol 107, pp 207–230
- Sofia G (2020) Combining geomorphometry, feature extraction techniques and earth-surface processes research: the way forward. *Geomorphology* 355:107055. <https://doi.org/10.1016/j.geomorph.2020.107055>
- Strahler AN (1952) Hypsometric (area-altitude) analysis of erosional topography. *GSA Bull* 63(11):1117–1142
- Strahler AN (1957) Quantitative analysis of watershed geomorphology. *Trans Am Geophys Union* 38(6):913–920. <https://doi.org/10.1029/TR038i006p00913>
- Strecker MR, Hilley GE, Arrowsmith JR, Coutand I (2003) Differential structural and geomorphic mountainfront evolution in an active continental collision zone: the northwest Pamir, southern Kyrgyzstan. *Geol Soc Am Bull* 115:166–181
- Thakur VC (1981) Regional framework and geodynamic evolution of the Indus-Tsangpo suture zone in the Ladakh Himalayas. *Trans Royal Soc Edinburgh: Earth Sci* 72:87–97
- Thayyen RJ, Dimri AP, Kumar P, Agnihotri G (2013) Study of cloudburst and flash floods around Leh, India, during August 4–6, 2010. *Nat Hazards* 65:2175–2204
- Troiani F, Della Seta M (2008) The use of the stream length–gradient index in morphotectonic analysis of small catchments: a case study from Central Italy. *Geomorphol* 102(1):159–168. <https://doi.org/10.1016/j.geomorph.2007.06.020>
- Wadia, DN (1919) *Geology of India*. Macmillan Publishers.
- Whipple KX (2004) Bedrock rivers and the geomorphology of active orogens. *Annu Rev Earth Planet Sci* 32:151–185. <https://doi.org/10.1146/annurev.32.101802.1203556>

- Whipple KX, Tucker GE (2002) Implications of sediment flux dependent river incision models for landscape evolution. *J Geophys Res-Solid Earth* 107:2039. <https://doi.org/10.1029/2001JB000162>
- Wobus CW, Whipple KX, Kirby E, Snyder NP, Johnson J, Spyropolu K, Crosby BT, Sheehan D (2006) Tectonics from topography: procedure, promise and pitfalls. In: Willet SD, Hovius N, Brandon MT, Fisher DM (eds) *Tectonics, climate and landscape evolution*. Geological Society of America Bulletin Special Paper, vol 398, pp 55–74

Geomorphic Response of the Solani River Basin to Neotectonics: A Study from the Western Himalayan Foothills, India



Narendra K. Patel and Pitambar Pati

Abstract This study investigates the influence of neotectonics on the Solani River basin, using morphometric parameters, seismic signatures, and field-based study of unpaired river terraces. Morphometric parameters such as linear, areal, relief parameters, slope, aspect, stream-length (SL) index, and longitudinal river profile (LRP) suggest that the neotectonic activity triggered by the Himalayan tectonics affect the Solani River basin. Local convexity in the LRP indicates differential uplift along the associated faults. However, minor variation in knick points in LRP has been interpreted as rapid erosion due to unconsolidated to semi-consolidated nature of the sediments. The SL index of the Solani River ranges from 29.4 to 5233.2. The SL values along the river length indicates anomalies around the active fault zones. Mountain front sinuosity (S_{mf}) adjacent to the river basin ranges from 1.04 to 1.13, suggesting tectonically active nature of the region. Unpaired terraces reported at Roorkee and Toda-Kalyanpur at the right bank of the river are evidence of neotectonics. Three unpaired terraces reported at Roorkee, have riser-height of 1, 1.5, and 3 m and tread-width of 50, 40, and 70 m. While the riser and tread could not be measured at Toda-Kalyanpur due to their deformed nature. These E-W aligned terraces present 1.5 km south of the present river course dated back to 2.5 Ka (T_1) and 1.6 Ka (T_2). These terraces were formed due to the river shifting in response to the uplift of the river basin along with the Ganga plain. The upliftment rate along the Himalaya in the area shows a good coherency with few of the morphotectonic signatures of the basin. Other morphometric parameters such as hypsometry, asymmetry, valley width height ratio, did not yield supporting result, probably due to the DEM error and the unconsolidated nature of the sediments.

Keywords Solani River · Terraces · Neotectonics · Himalaya

N. K. Patel · P. Pati (✉)

Department of Earth Sciences, Indian Institute of Technology, Roorkee, Uttarakhand, India

e-mail: pitambar.pati@es.iitr.ac.in

N. K. Patel

e-mail: npatel@es.iitr.ac.in

1 Introduction

Landscape geomorphology epitomizes the balance between processes that produce and destroy topographic relief by uplifting and erosion (D'Arcy and Whittaker 2014). The landform evolution mechanism is regulated by various processes, such as lithology, tectonics, and climate change (Solanki et al. 2020). In high-level terrain, active tectonics during the recent geological period can be reflected by river incisions and sediment yields; diversion of channels, the formation of hanging tributaries and so on (Bull and McFadden 1977; Molin and Fubelli 2005; Kale and Shejwalkar 2008; Pati et al. 2018; Das 2020). However, alluvial plains like the Ganga plain respond to the neotectonics by abandoned river terraces, forming terminal fans, change in soil properties, and morphometric variations of the present and paleochannels. Morphometric analysis has widely been used to investigate the relationship between landform geometry and active faults (Kale and Shejwalkar 2008; Singh and Tandon 2008; Raj 2012; Pati et al. 2018; Gailleton et al. 2019; Das 2020). Quantitative landscape measurements may provide important information on geomorphic evolution and the degree of tectonic activity during recent geological times. Geomorphic indices are highly convenient tools for understanding active tectonics as these indices provide insights into particular sites that are rapidly adapting to variable tectonic deformation. The morphotectonic and field-based studies are widely used to locate undergoing tectonic deformation (Azor et al. 2002; Kirby and Whipple 2012; Han et al. 2017; Moodie et al. 2018; Pati et al. 2019; Patel et al. 2020).

The Solani, a tributary of the river Ganga has experienced frequent seismic activity with moderate-size earthquakes, epicentered around 10 km depth. Several studies have been performed to understand geology, stratigraphy, earthquake recurrence, and GPS measurements in the area (Jade 2004; Bhosle et al. 2008; 2009; Patel et al. 2020). The scale and methodology used in the earlier studies are highly generalized to apprehend the tectonic deformation of the area. However, a geomorphic evaluation supporting to the ongoing tectonic uplift is lacking in this area. Besides, any response to the neotectonic activity of the Himalayan segment can be studied along the respective foothill segments and their river systems. This study investigates the impact of the neotectonic activity on the Solani River basin using morphometric analysis, OSL chronology of alluvial terraces, and seismicity.

2 Study Area

2.1 Location

The study area lies between latitude 29–31°N and longitude 77–79°E. Politically it partly falls in Uttarakhand and Uttar Pradesh state of India. Thus, its northern extent is up to the Himalaya and southern extent is up Bijnor Uttar Pradesh. The Solani River is a tributary of the Ganga River, which originates from the Himalayan foothills

(Fig. 1). This monsoon-fed river has a catchment area of ~2009 km². It's ~150 km course passes through the Himalayan piedmont, consisting of boulders, pebbles, and

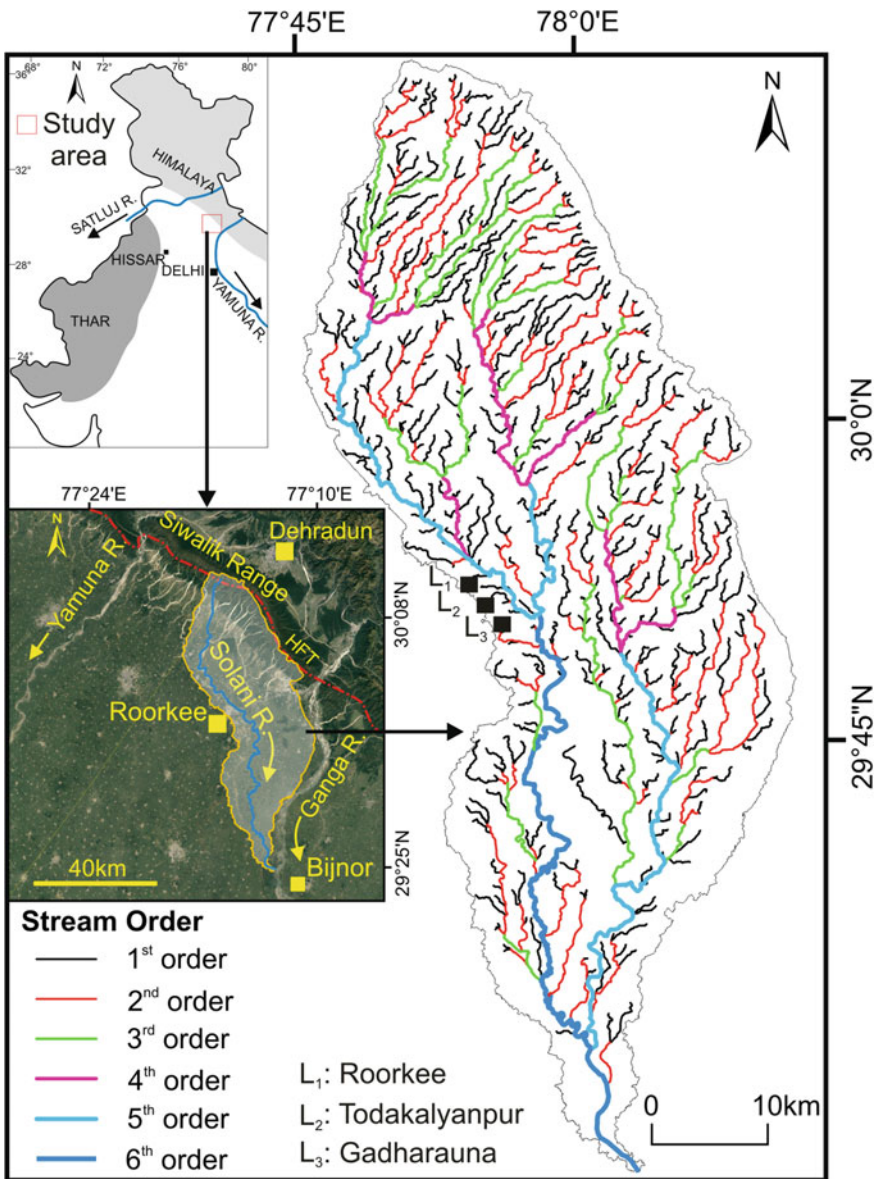


Fig. 1 Drainage map of the Solani River basin showing different orders of streams. The inset map shows the location of the study area

massive sandstones of Mio-Pliocene age and sandy to loamy Quaternary soils of the Ganga plain, until meeting the Ganga River.

2.2 Geology

The Solani River basin is a part of the western Ganga plain and lies in the Yamuna-Ganga interfluve (Fig. 2). The Solani River originates from the Himalaya foothills at Mohand. This incised river flows through a longitudinal fault (Solani fault), where the lower order tributaries follow less distance, and the trunk river continues further south and merges with the Ganga River near Bijnor of Uttar Pradesh. The river basin is restricted by the Ganga River in the east, the Yamuna River in the west, and the Siwalik in the north. Seismically active, the Mahendragarh-Dehradun Fault (MDF) following the Delhi-Haridwar ridge (Patel et al. 2020), passes along the western boundary of the basin (Fig. 3). Except the steep slope along the northern foothill piedmonts, running along the Siwalik's foothills, the river basin lacks any topographic prominence. The piedmont in the northern end is a narrow (10–25 km vast), elongated landscape, drained by several parallel to sub-parallel ephemeral streams. The piedmont is composed of gravel, sand, and clays, whereas the abundance of gravels decreases significantly from north to south. The river basin experiences semi-arid to sub-humid climate where annual precipitation varies from 500 to 1200 mm, out of which 80–85% is received between July and September (Kumar et al. 1996).

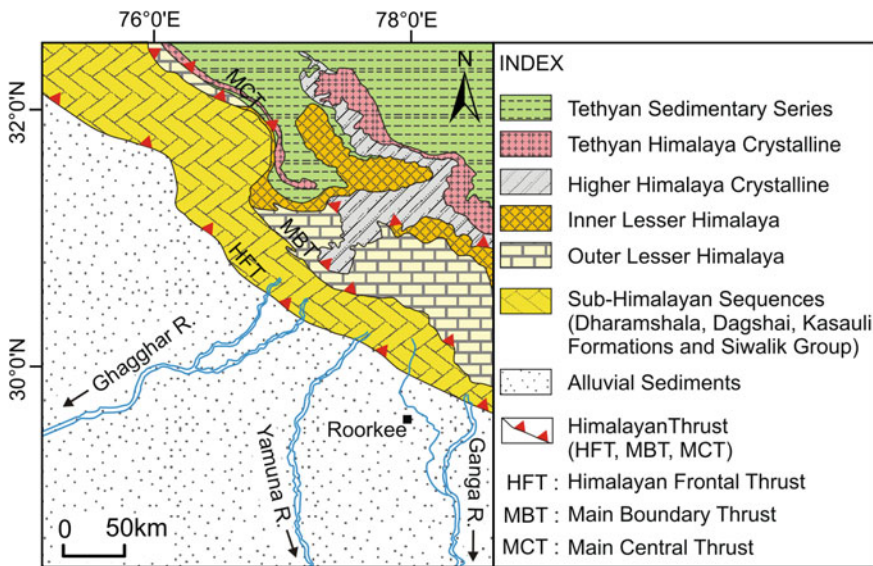


Fig. 2 Simplified geological map of NW Himalaya (modified after Singh et al. 2016)

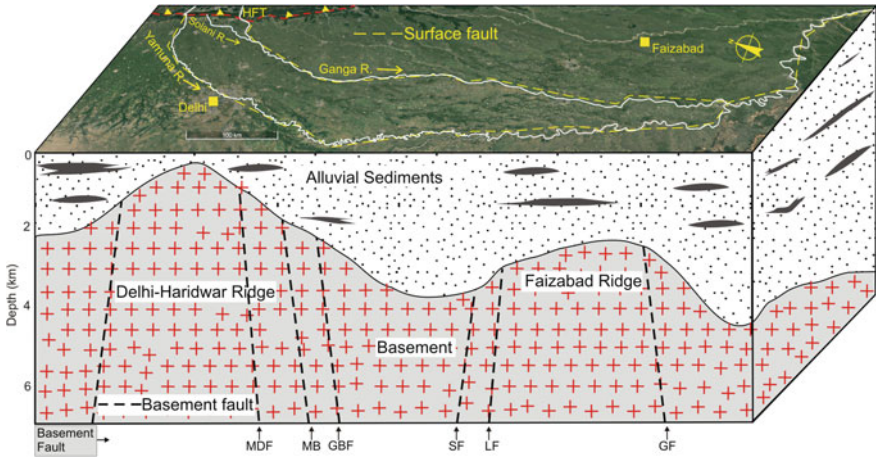


Fig. 3 Schematic diagram showing the basement configuration of the western Ganga plain. The Delhi–Haridwar ridge passes through the western boundary of the Solani River basin (modified after Gahalaut and Kundu 2012; MDF: Mahendragarh-Dehradun Fault, GBF: Great Boundary Fault, LF: Lucknow Fault, MF: Moradabad Fault, SF: Saharanpur Fault, GF: Gorakhpur Fault)

3 Materials and Methodology

Methodology followed in this study includes morphometric analysis, field study, and seismic data analysis.

3.1 Morphometric Analysis

We used ALOS data of 12.5 m resolution to evaluate the morphotectonics of the Solani River basin (Fig. 4). The datasets were validated using the Survey of India (SOI) topographic maps (1:50,000 scale) and Google Earth image. For the morphostructural analysis, the datasets were processed in ArcGIS 10.8 software on WGS 1984 datum. Field studies were carried out to validate the observations from the remote sensing based studies.

3.1.1 Bifurcation Ratio (R_b)

R_b is defined as the ratio of the number of streams in any given order to the number of streams in the next higher-order in the basin (Schumm 1956). It is a significant parameter that denotes the basin’s water-carrying ability and related flood potential (Mahala 2020). A higher R_b value indicates a steep slope with impermeable or less permeable lithology, and a lower R_b value indicates the geological heterogeneity,

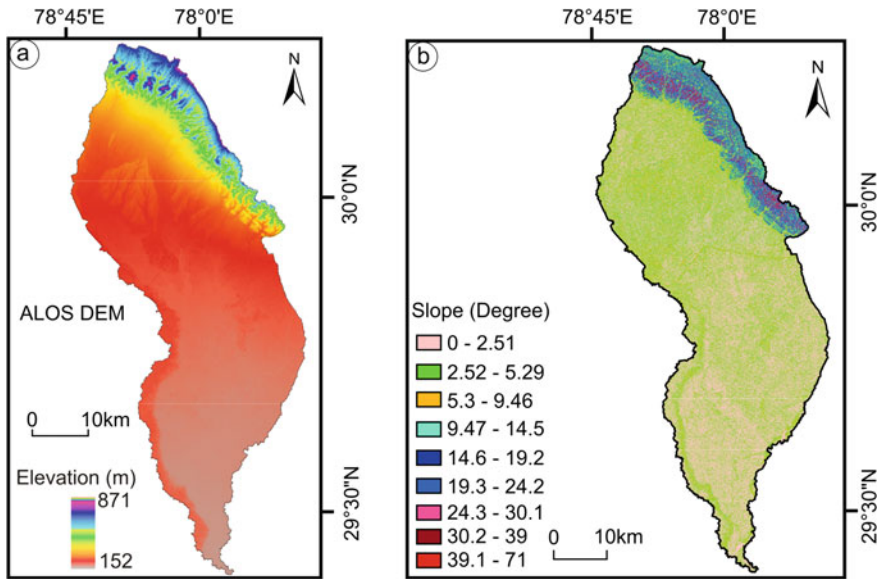


Fig. 4 a ALOS DEM of the Solani River basin showing topographic perception, b Slope map

higher permeable rocks with less structural control (Hajam et al. 2013). The R_b varies from 2.33 to 4.36, with a mean R_b of 3.46 for the Solani River basin (Table 1). This indicates that the basin falls under the normal category (Pandey and Das 2016). The high bifurcation ratio is found between 1st (4.36) and 2nd (4.04) order, and streams up to the 2nd order flow through strongly dissected and steep gradient of the piedmont area.

3.1.2 Stream-Length Ratio (R_L)

R_L is the ratio of the average length of the stream to one order to the next lower order (Horton 1945). It is an essential link between the discharge of the surface flow and the erosion of the basin. R_L for the Solani basin varies from 0.68 to 3.77, with an average R_L of 1.85 (Table 1). Higher values observed in the ratio of 1st and 2nd (1.95), 2nd and 3rd (1.77), and 3rd and 4th (3.37), which are strongly dependent on topography and slope, and in turn are controlled by the tectonic activity.

3.1.3 Elongation Ratio (R_e)

R_e is the ratio between the diameter of the circle of the same area as the drainage basin and the maximum length of the basin (Schumm 1956). It is believed that the elongated shapes of the basins are due to the guiding effect of thrusting and faulting

Table 1 Different geomorphic parameters studied for the Solani River basin

<i>Basin parameters</i>		
Basic parameter	Basin area	2009.27 km ²
	Basin perimeter	318.14 km
<i>Linear parameters</i>		
Number of streams	Number of first order streams (N1)	440
	Number of second order streams (N2)	447
	Number of third order streams (N3)	25
	Number of fourth order streams (N4)	7
	Number of fifth order streams (N5)	3
	Number of sixth order streams (N6)	1
	Total number of streams	577
Stream length (Lu)	Total length of first order streams (LT1)	870.83 km
	Total length of second order streams (LT2)	447 km
	Total length of third order streams (LT3)	252.38 km
	Total length of fourth order streams (LT4)	74.83 km
	Total length of fifth order streams (LT5)	109.62 km
	Total length of sixth order streams (LT6)	74.78 km
	Total length of the streams	1829.45 km
Mean stream length (Lsm)	Mean length of first order streams (L1)	1.98 km
	Mean length of second order streams (L2)	4.43 km
	Mean length of third order streams (L3)	10.10 km
	Mean length of fourth order streams (L4)	10.69 km
	Mean length of fifth order streams (L5)	36.54 km
	Mean length of sixth order streams (L6)	74.78 km
Bifurcation ratio (R _b)	1st/2nd order	4.36
	2nd/3rd order	4.04
	3rd/4th order	3.57
	4th/5th order	2.33
	5th/6th order	3.00
	Mean	3.46
Stream length ratio (R _L)	6th/5th	1.95
	5th/4th	1.77
	4th/3rd	3.37
	3rd/2nd	0.68
	2nd/1st	1.47
	Mean	1.85

(continued)

Table 1 (continued)

<i>Basin parameters</i>		
Basic parameter	Basin area	2009.27 km ²
	Basin perimeter	318.14 km
Rho coefficient (RHO)		0.53
Areal parameters	Drainage density (Dd)	0.91 km/km ²
	Stream frequency (Fs)	0.29
	Infiltration ratio	0.26
	Drainage texture (Dt)	1.81
	Form factor (Rf)	0.21
	Elongation ratio (Re)	0.52
	Circulatory ratio (Rc)	0.25
	Length of overland flow (Lo)	2.19
Relief aspect	Basin relief (Bh)	0.72 km
	Relief ratio (Rr)	0.0074
	Ruggedness number (Rn)	0.65
	Gradient ratio (Rg)	0.0054

in the basin (Zaidi 2011). The basins with lower Re values are susceptible to erosion (Sreedevi et al. 2009) because of moderate to high relief of the basin. The elongation ratio for the Solani River basin is 0.52 (Table 1).

3.1.4 Longitudinal River Profile (LRP)

LRP is a very sensitive linear feature of tectonic deformation in the earth's crust (Holbrook and Schumm 1999; Whittaker et al. 2007; Viveen et al. 2012; Fekete and Vojtko 2013; Goren et al. 2014). Convex segments of LRP are called knickpoints or knickzones depending upon their length, which can be examined to determine their coincidence with tectonic disruptions (Molin and Fubelli 2005). Knickpoints in the LRP could serve as useful indicators of active structures along a river (Wobus et al. 2005). Fault movements will produce several small knick points in the channel profile (Zhang et al. 2011). In this study, LRP has been prepared for the Solani River (Fig. 5) using ALOS DEM. Avoiding the river confluences, the river shows multiple other local convexities along the LRP. Hence we interpret these knick points are related to tectonics.

3.1.5 Stream Length Gradient Index (SL Index)

Hack (1973) proposed a parameter known as the SL index to determine the geomorphological equilibrium. The SL index describes a stream network's morphology

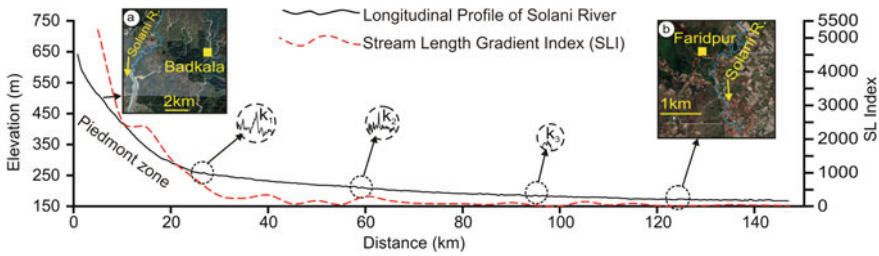


Fig. 5 Longitudinal river profiles and SL Index along the Solani River plotted together. **a** Google Earth image of the piedmont zone shows many first-order streams, **b** confluence of the river in the lower part of the basin shows minor knickpoints, k_1 , k_2 , and k_3 are the major knickpoints in the river profile

using the distribution of the topographic gradients along rivers (Font et al. 2010). It is sensitive to slope changes and allows to evaluate the tectonic activity, rock resistance, and topography (Keller and Pinter 2002) and is strictly related to the stream power (Moussi et al. 2018). A high SL index value may indicate if a particular region is experiencing tectonic activity or has any structural control. The SL index values of the Solani River range from 29.4 to 5233.2 (Fig. 5). The maximum value of SL index for the Solani River is 5233.2 (Piedmont region), and the minimum value is 29.4 (Plain region).

3.1.6 Mountain-Front Sinuosity Index (S_{mf})

Mountain-front sinuosity has been applied to study mountain front tectonics by several researchers (Ramírez-Herrera 1998; Frankel and Pazzaglia 2005; Azañón et al. 2012; Mahmood and Gloaguen 2012; Dar et al. 2013; Elias 2015; Topal et al. 2016; Bhakuni et al. 2017; Giaconia et al. 2012) in different parts of the globe (Bull and McFadden 1977; Keller and Pinter 2002; Silva et al. 2003; Pérez-Peña et al. 2010; Giaconia et al. 2012). Along the active mountain fronts, uplift prevails over erosional processes, yielding straight fronts with low values of S_{mf} . Along less active fronts, erosional processes generate irregular or sinuous fronts with high values of S_{mf} (Azañón et al. 2012; Topal et al. 2016). Bull and McFadden (1977) defined mountain front sinuosity (S_{mf}) as an index that reflects the balance between erosional forces and tectonic processes that control the embayment of the mountain front to make it linear.

Mountain-front sinuosity was defined by Bull (1977) as $S_{mf} = L_{mf} / L_s$.

Where, S_{mf} : mountain front sinuosity.

L_{mf} : length of the mountain front along the foot of the mountain along the pronounced break in slope.

L_s : length of the mountain front measured along a straight line.

S_{mf} reflects the balance between erosion forces that tend to cut embayment into a mountain front and tectonic forces that tend to produce a straight mountain front

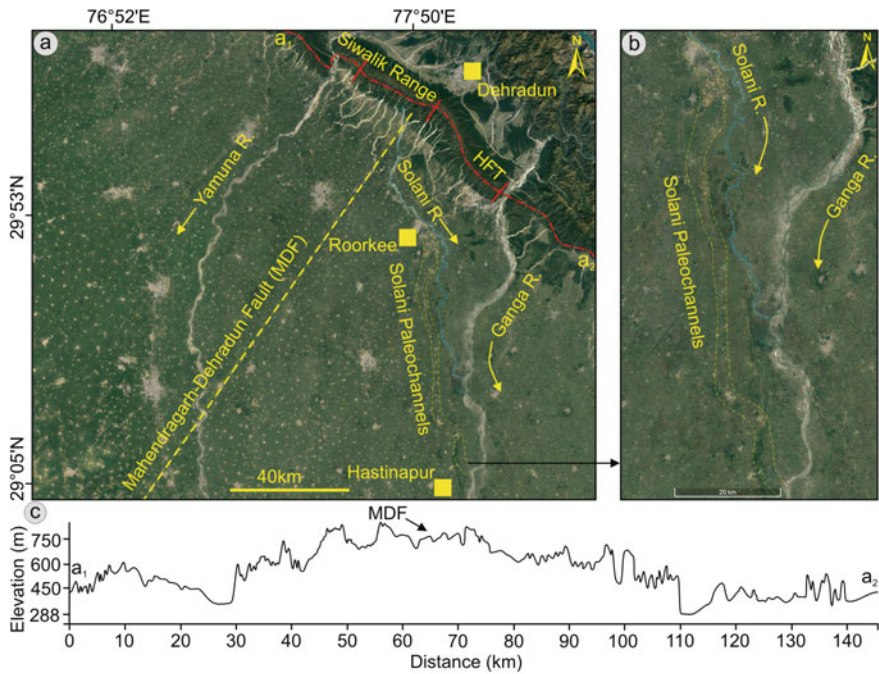


Fig. 6 a Piedmont zone showing many first and second-order streams, b major paleochannels in the area, c profile along the HFT shows upliftment

coincident with an active range-bounding fault (Verriou et al. 2004). S_{mf} of highly active mountain fronts generally ranges from 1.0 to 1.5, that of moderately active fronts ranges from 1.5 to 3, and that of inactive fronts ranges from 3 to more than 10 (Elias 2015). Some other studies have proposed that the values of the S_{mf} index lower than 1.4 are indicative of tectonically active fronts (Silva et al. 2003). It is possible to understand tectonic activity and Quaternary landscape evolution through the application of such geomorphic analyses. Young mountain fronts tend to have low values of S_{mf} , as they have not experienced significant range-front erosion and are responding to active tectonic uplift on a relatively steep fault, keeping it approximately straight (Topal et al. 2016). In the present study, the S_{mf} varies from 1.1 to 1.2, indicating the active nature of the region with pronounced uplift (Fig. 6).

3.2 Field Study

The Solani River basin was studied by detailed fieldwork. During the fieldwork, three unpaired terraces at Roorkee, and two unpaired terraces at Toda Kalyanpur have been studied (Figs. 7 and 8).

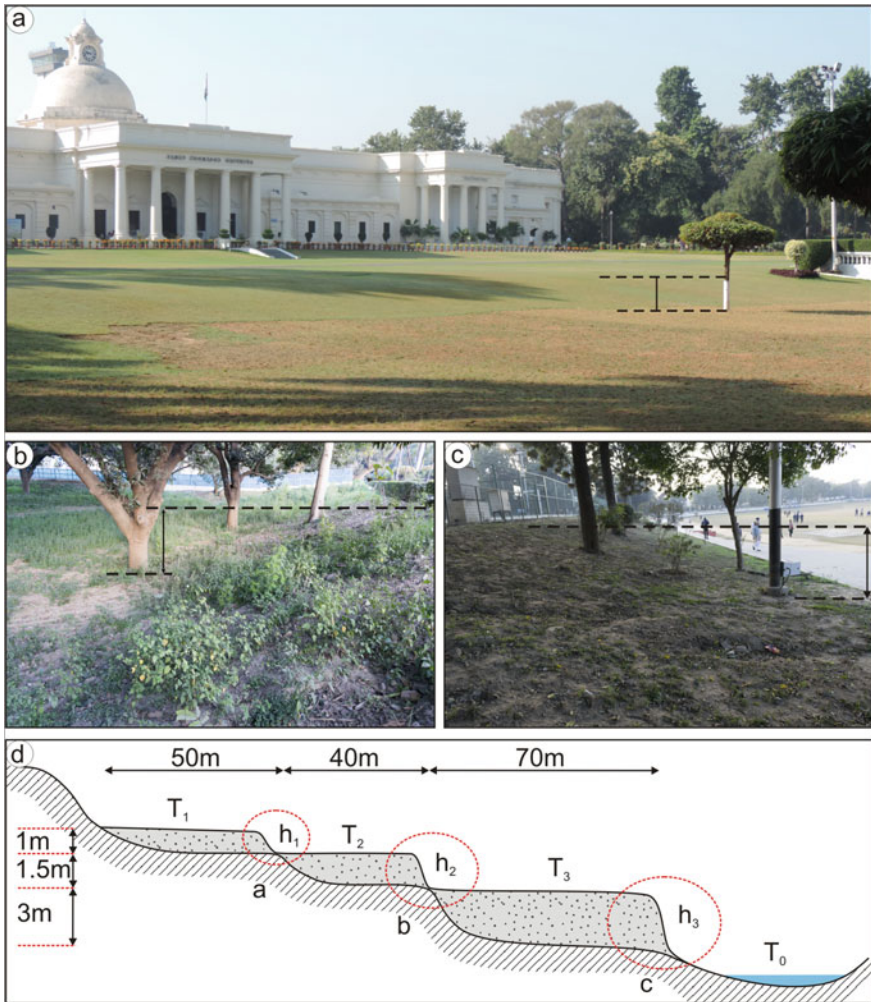


Fig. 7 a–c are the field photos of terraces, **d** schematic diagram of the Solani River terraces at Roorkee

3.3 Seismic Activity

Paleoseismology uses elements of tectonic geomorphology, sedimentology and stratigraphy to assess the position timing and displacement of past earthquakes (Kondo and Owen 2013). Recent technological advances including remote sensing, geodesy, fault trenching and computational dating have helped to accelerate knowledge and analysis of past earthquakes. Efficient seismic hazard mapping requires the creation of ground acceleration maps based on high resolution, accurate geomorphic and quaternary geological mapping. Geomorphology is the primary tool for

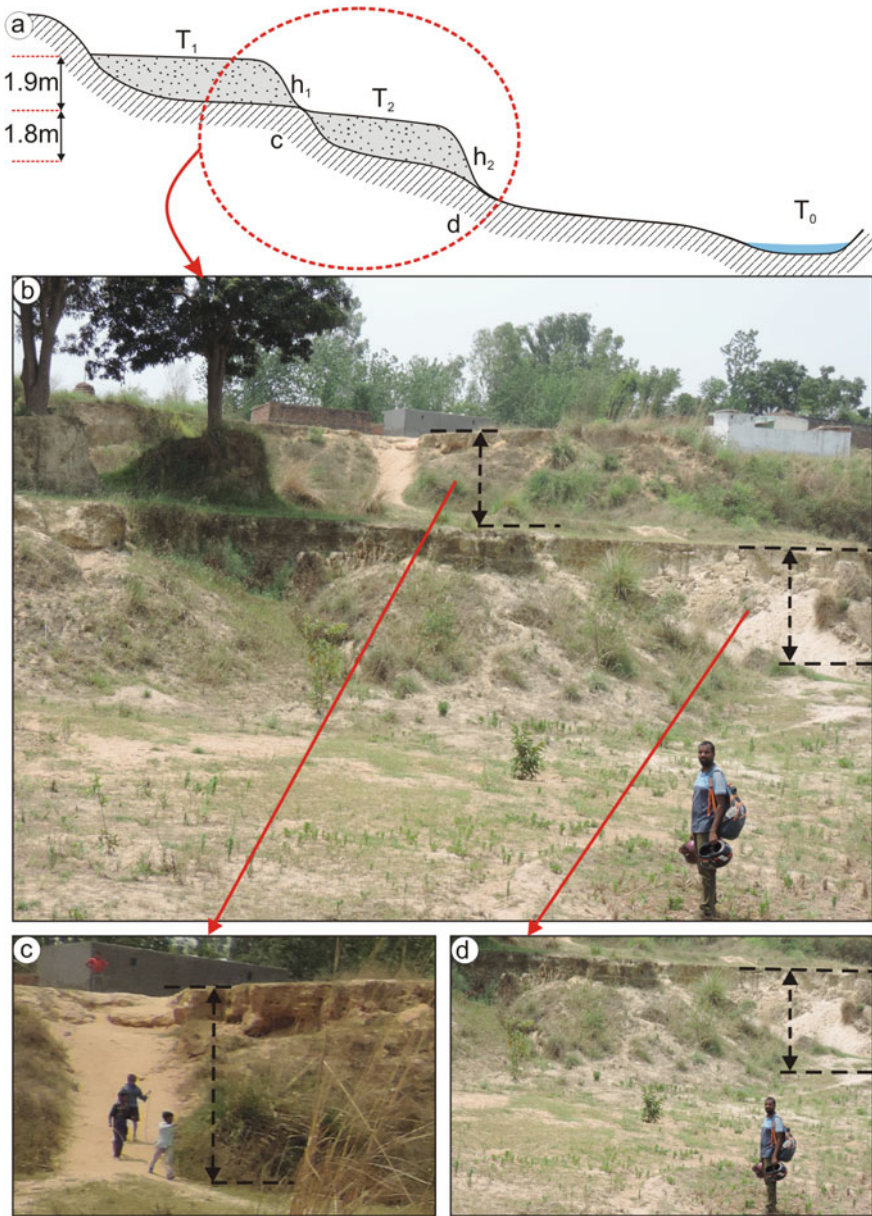


Fig. 8 a Schematic diagram of the Solani River terraces at Todakalyanpur, b–d are the field photos of the terraces

neotectonics, earthquake geology, paleoseismology studies and evaluation of seismic hazards. The geomorphology of active fault plays a dominant role in the collection of such data (Kondo and Owen 2013). Neotectonic activity in the present area of study has been well recorded by several seismic events in recent years (Fig. 9). These seismic events indicate active tectonics in the area.

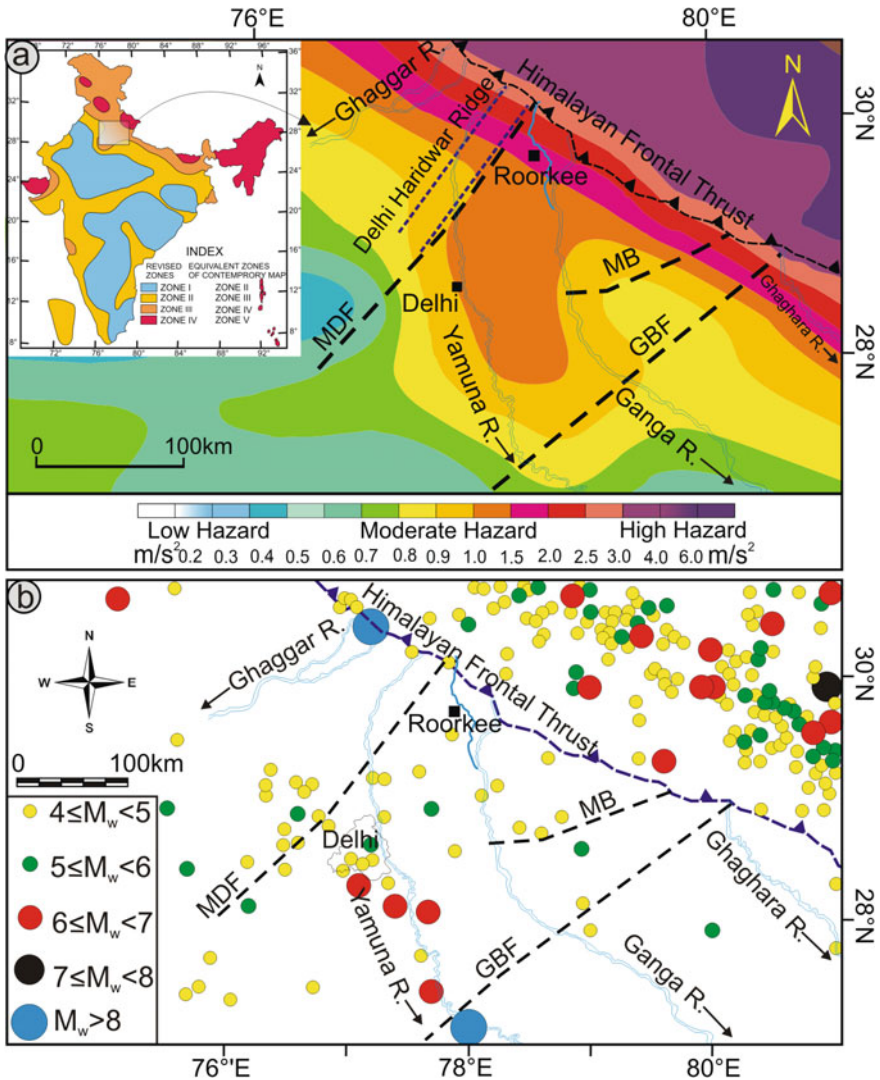


Fig. 9 Seismicity map of the western Ganga plain shows seismicity pattern in and around the Solani River basin. **a** Seismic Hazard map (data compiled from <http://asc-india.org>, inset shows seismic zone of India with the location of the study area), **b** Distribution of faults and seismic pattern (for abbreviations refer to Fig. 3, seismic data taken from Prabhu and Raghukanth 2015)

4 Neotectonic Movements and Channel Evolution

It is difficult to describe any parameter that would systematically isolate the tectonic effect on a river basin. However, the morphometric analysis of the Solani basin has provided evidence for the influence of neotectonics. Kumar et al. (1996) delineated many paleochannels on a regional scale, which shows the river's northeastward shift of channel. Modern channels also show meandering and northeastward shifting (Fig. 10). This long-term unidirectional shift may be due to tilting of the tectonic clock due to the ongoing NE-SW compression. LRP shows the local convexity corresponds the knickpoints and tributary junction. However, ignoring the confluences, all other local convexities are due to local structural perturbations. The SL index plotted along the LRP is showing a good correlation. The stream length gradient index and LRP corroborate each other, indicating neotectonic influence in the river basin.

Paleochannels in the area begin near to Roorkee and end near to Hastinapur (Fig. 10). The "folklore", as verbally stated by the natives, are the Burhi (Old) Ganga channel (Kumar et al. 1996) (through depicted by the Aeolian ridges and without any significant channels, Fig. 11). The Hindu epic Mahabharat states that Hastinapur was the capital of the Kaurava-King Prikhsit, and he had to shift his

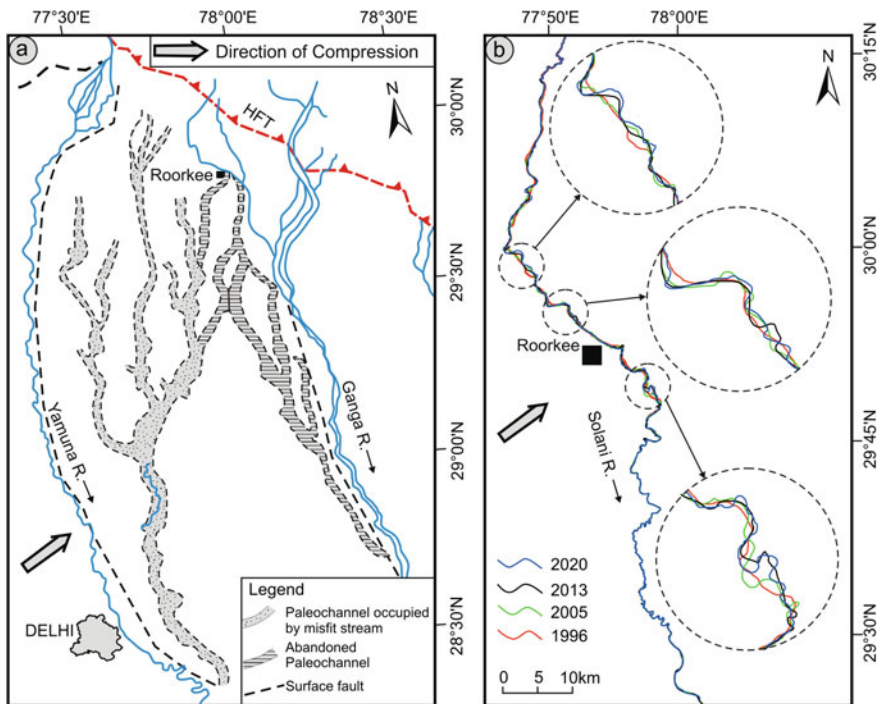


Fig. 10 a Mapping of paleochannels shows river shifting towards the east (modified after Kumar et al. 1996), b the migration of recent Solani channels

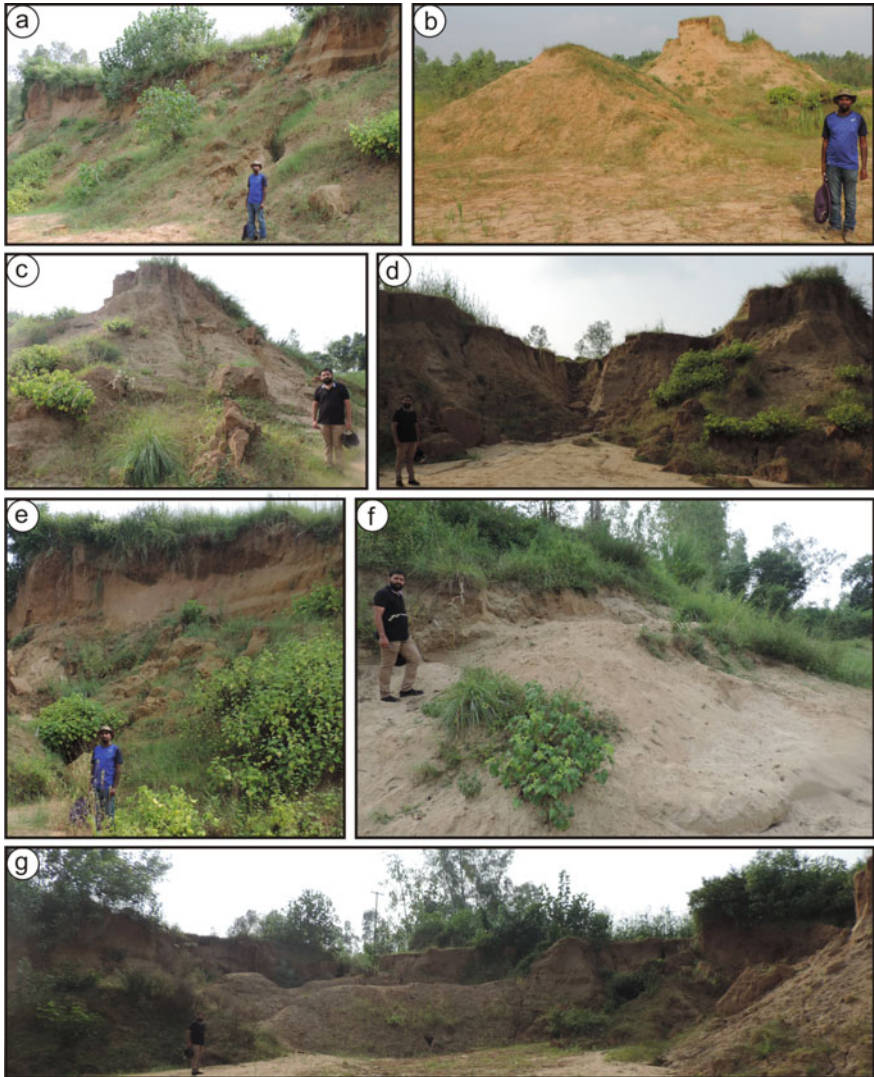


Fig. 11 Field photographs of the alluvial ridges in the Solani River deposits around Gadharauna

capital from Hastinapur due to floods in the Ganga (Thaper 1966). The Mahabharat Era is closely related to the Painted Gray Ware (PGW) culture, and the later dated back to 600–1000 B.C. (Lal 1954–55, 1981). The flooding time of Hastinapur was dated 800 B.C. (Thaper 1966). This suggests the Ganga River flowed on this upland region (about 15 m higher than the Ganga flood plain, where the present Ganga River flows) sometime before 600 B.C.

The Solani River basin records neotectonic activities in the Ganga plain along its course. Unpaired tectonic terraces at Roorkee and Toda Kalyanpur at the river's right bank are evidence of faulting and river shifting (Figs. 7 and 8). At Roorkee, three terraces have been identified, having riser of 1, 1.5, and 3 m height and tread of 50, 40, and 70 m width, respectively, while riser and tread cannot be measured at Toda-Kalyanpur due to the deformation. These terraces are about 2 km south from the present river course. Different generations of river terraces in the Ganga plain are generally distinguished by their respective degree of soil development. However, the presently studied terraces have no signature of soil development, indicating that they are very recently developed. These terraces were formed by upliftment of the Ganga plain due to compression along the Himalayan front and subsequent river shifting. The Ganga plain is tectonically active by its coupled nature with the Himalaya (Parkash et al. 2011). River courses in the Ganga plain are continuously shifting in one direction due to the area's compression and upliftment. The results allow in reconstructing the Holocene evolution of the river valley and correlating the processes that led to the terrace formation.

Four unpaired terraces (T_0 – T_3), were recognized along the right bank of the Solani River (Vorha 1987). The T_3 lies 14–18 m above the present Solani River bed (T_0), Terrace T_3 and T_2 were dated using the Thermo Luminescence (TL) technique by Vhora (1987) and assigned ages 2500 and 1600 cal. B.P., respectively. The date for the T_3 terrace is the same order of magnitude, as indicated by the PGW culture. Unpaired tectonic terraces and the morphometric parameters suggest temporal activity of the Solani fault.

Unpaired terraces and different faults are indicative of the ongoing tectonic activity in the area. These terraces, composed of fluvial deposits, prominently stand above the modern river channel. Morphotectonic parameters indicate tectonic movements along the MDF, which is close to the Solani basin (Patel et al. 2020). Paleochannels of Solani River are linear in nature, associated with terraces, are indicative of migration of the river (Fig. 6b).

The Himalaya along with the Solani basin experience strong compressional stress (Zoback 1992). Due to the tectonic activity along the Solani, Yamuna, and Ganga faults, the upper Ganga-Yamuna block was raised, and the Ganga-Ramganga block was thrown down (Kumar et al. 1996, Fig. 12). This is clear evidence of the tectonic upliftment of the area. Since its origin, the Ganga plain has undergone numerous geomorphic changes due to tectonic activity (Mohindra et al. 1992). Finite element modelling of the Ganga plain by Parkash et al. (2000) indicates that SW compression (Fig. 12) develops longitudinal faults (parallel to sub-parallel with the Himalayan trend) and extensional transverse normal faults (an angle to the Himalayans trend). Using the Global Positioning System (GPS), Jade (2004) indicates the displacement of the Indian plate to the northwest. The above works support the mechanism for the creation of longitudinal and transverse faults in the Ganga plain studied by several researchers (Singh et al. 2006; Bhosle et al. 2007, 2008; Pati et al. 2018, 2019; Verma et al. 2017; Patel et al. 2020). The present study confirms the existence of active tectonics in the area and highlights its role in shaping the Solani River basin.

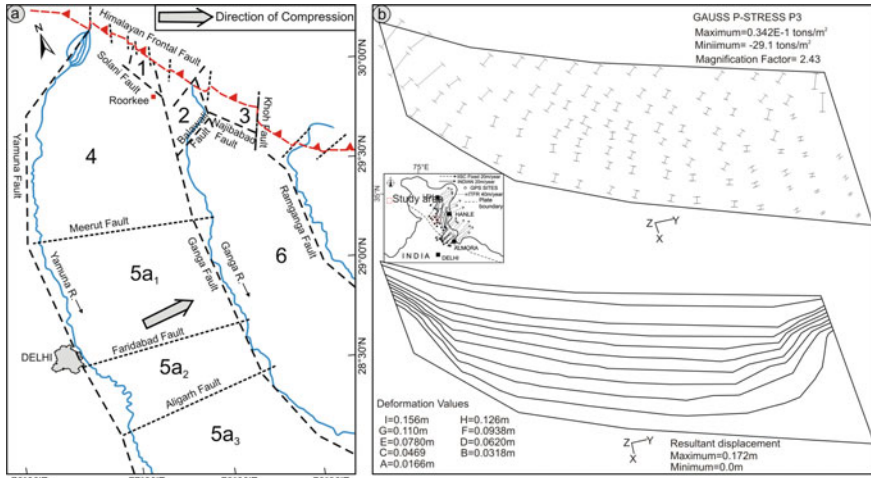


Fig. 12 a Surficial faults and tectonic blocks in the area. 1—Solani block, 2—Ganga Solani block, 3—Koh block, 4—Upper Ganga-Yamuna block, 5a₁—Modinagar subblock, 5a₂—Khurja sub-block, 5a₃—Etah sub-block, and 6—Ganga-Ramganga block (modified after Kumar et al. 1996), b Finite element model after Parkash et al. (2000) shows compression from SW develops longitudinal faults in the area. GPS movement was taken from Jade (2004) (Inset figure)

5 Conclusions

The tectono-geomorphic investigations of the Solani River basin was conducted in the western Ganga plain on the basis of ALOS DEM analysis. The morphometric analysis, seismic, and field-based study helps us to reach the following conclusions.

1. The Solani River basin is a sixth-order river basin with the dominance of lower-order streams.
2. The unpaired terraces at Roorkee and Toda Kalyanpur are evidence of neotectonics.
3. Seismicity and morphometric parameters indicate the river basin is tectonically influenced.
4. Tectonic influence in the Solani River basin is due to its position adjacent to a highly compressed zone of the Himalayan front, where significant upliftment has been recorded.

References

Azañón JM, Pérez-Peña JV, Giaconia F, Booth-Rea G, Martínez-Martínez JM, Rodríguez-Peces MJ (2012) Active tectonics in the central and eastern Betic Cordillera through morphotectonic

- analysis: the case of Sierra Nevada and Sierra Alhamilla. *J Iber Geol* 38:225–238. https://doi.org/10.5209/rev_JIGE.2012.v38.n1.39214
- Azor A, Keller EA, Yeats RS (2002) Geomorphic indicators of active fold growth: South Mountain-Oak Ridge anticline, Ventura basin, southern California. *Bull Geol Soc Am* 114:745–753. [https://doi.org/10.1130/0016-7606\(2002\)114%3c0745:GIOAFG%3e2.0.CO;2](https://doi.org/10.1130/0016-7606(2002)114%3c0745:GIOAFG%3e2.0.CO;2)
- Bhakuni SS, Luirei K, Kothiyari GC, Imsong W (2017) Transverse tectonic structural elements across Himalayan mountain front, eastern Arunachal Himalaya, India: implication of superposed landform development on analysis of neotectonics. *Geomorphology* 282:176–194. <https://doi.org/10.1016/j.geomorph.2016.12.025>
- Bhosle B, Parkash B, Awasthi AK, Singh VN, Singh S (2007) Remote sensing-GIS and GPR studies of two active faults, Western Gangetic Plains, India. *J Appl Geophys* 61:155–164. <https://doi.org/10.1016/j.jappgeo.2006.10.003>
- Bhosle B, Parkash B, Awasthi AK, Pati P (2009) Use of digital elevation models and drainage patterns for locating active faults in the Upper Gangetic Plain, India. *Int J Remote Sens* 30:673–691
- Bhosle B, Parkash B, Awasthi AK, Singh S, Khan MSH (2008) Role of extensional tectonics and climatic changes in geomorphological, pedological and sedimentary evolution of the Western Gangetic Plain (Himalayan Foreland Basin), India. *Himalayan Geol* 29:1–24
- Bull WB (1977) The alluvial-fan environment. *Progr Phys Geogr: Earth Environ* 1:222–270. <https://doi.org/10.1177/030913337700100202>
- Bull WB, McFadden LD (1977) Tectonic geomorphology north and south of the Garlock fault, California. *Geomorphol Arid Reg* 115–138
- Dar RA, Chandra R, Romshoo SA (2013) Morphotectonic and lithostratigraphic analysis of intermontane Karewa Basin of Kashmir Himalayas, India. *J Mt Sci* 10:1–15. <https://doi.org/10.1007/s11629-013-2494-y>
- Das S (2020) Koyna-Warna Shallow seismic region, India: is there any geomorphic expression of active tectonics? *J Geol Soc India* 96:217–231. <https://doi.org/10.1007/s12594-020-1541-x>
- D'Arcy M, Whittaker AC (2014) Geomorphic constraints on landscape sensitivity to climate in tectonically active areas. *Geomorphology* 204:366–381. <https://doi.org/10.1016/j.geomorph.2013.08.019>
- Elias Z (2015) The neotectonic activity along the lower Khazir River by using SRTM image and geomorphic indices. *Earth Sci* 4:50. <https://doi.org/10.11648/j.earth.20150401.15>
- Fekete K, Vojtko R (2013) Neotectonic activity of the Pravno fault in the area of the Ziar Mts. *Acta Geologica Slovaca* 5:117–127
- Font M, Amorese D, Lagarde JL (2010) DEM and GIS analysis of the stream gradient index to evaluate effects of tectonics: the Normandy intraplate area (NW France). *Geomorphology* 119:172–180. <https://doi.org/10.1016/j.geomorph.2010.03.017>
- Frankel KL, Pazzaglia FJ (2005) Tectonic geomorphology, drainage basin metrics, and active mountain fronts. *Geogr Fis Din Quat* 28:7–21
- Gahalaut VK, Kundu B (2012) Possible influence of subducting ridges on the Himalayan arc and on the ruptures of great and major Himalayan earthquakes. *Gondwana Res* 21:1080–1088. <https://doi.org/10.1016/J.GR.2011.07.021>
- Gailleton B, Mudd SM, Clubb FJ, Peifer D, Hurst MD (2019) A segmentation approach for the reproducible extraction and quantification of knickpoints from river long profiles. *Earth Surf Dyn* 7:211–230. <https://doi.org/10.5194/esurf-7-211-2019>
- Giaconia F, Booth-Rea G, Martínez-Martínez JM, Azañón JM, Pérez-Peña JV, Pérez-Romero J, Villegas I (2012) Geomorphic evidence of active tectonics in the Sierra Alhamilla (eastern Betics, SE Spain). *Geomorphology* 145–146:90–106. <https://doi.org/10.1016/j.geomorph.2011.12.043>
- Goren L, Fox M, Willett SD (2014) Tectonics from fluvial topography using formal linear inversion: theory and applications to the Inyo Mountains, California. *J Geophys Res F: Earth Surf* 119:1651–1681. <https://doi.org/10.1002/2014JF003079>
- Hack JT (1973) Stream-profile analysis and stream-gradient index. *J Res US Geol Surv* 1:421–429

- Hajam RA, Hamid A, Bhat S (2013) Application of morphometric analysis for geo-hydrological studies using geo-spatial technology—a case study of Vishav Drainage Basin. *Hydrol Curr Res* 4:1–12. <https://doi.org/10.4172/2157-7587.1000157>
- Han Z, Xusheng LI, Wang N, Chen G, Wang X, Huayu LU (2017) Application of river longitudinal profile morphometrics to reveal the uplift of Lushan Mountain. *Acta Geol Sin* 91:1644–1652. <https://doi.org/10.1111/1755-6724.13403>
- Holbrook J, Schumm SA (1999) Geomorphic and sedimentary response of rivers to tectonic deformation: a brief review and critique of a tool for recognizing subtle epeirogenic deformation in modern and ancient settings. *Tectonophysics* 305:287–306. [https://doi.org/10.1016/S0040-1951\(99\)00011-6](https://doi.org/10.1016/S0040-1951(99)00011-6)
- Horton RE (1945) Erosional development of streams and their drainage basins, hydrographical approach to quantitative morphology. *Geol Soc Am Bull* 56:275–370. [https://doi.org/10.1130/0016-7606\(1945\)56\[275:EDOSAT\]2.0.CO;2](https://doi.org/10.1130/0016-7606(1945)56[275:EDOSAT]2.0.CO;2)
- Jade S (2004) Estimates of plate velocity and crustal deformation in the Indian subcontinent using GPS. *Curr Sci* 86:1143–1448
- Kale VS, Shejwalkar N (2008) Uplift along the western margin of the Deccan Basalt Province: is there any geomorphometric evidence? *J Earth Syst Sci* 117:959–971. <https://doi.org/10.1007/s12040-008-0081-3>
- Keller E, Pinter N (2002) *Active tectonics: earthquakes, uplift and landscape*. New Jersey
- Kirby E, Whipple KX (2012) Expression of active tectonics in erosional landscapes. *J Struct Geol* 44:54–75
- Kondo H, Owen LA (2013) 5.12 Paleoseismology. In: Shroder JF (ed) *Treatise on geomorphology*. Academic Press, Cambridge, pp 267–299
- Kumar S, Parkash B, Manchanda ML, Singhvi AK, Srivastava P (1996) Holocene landform and soil evolution of the western gangetic plains: implications of neotectonics and climate. *Zeitschrift Fur Geomorphologie, Supplementband* 103:283–312
- Lal BB (1954–55) Excavations at Hastinapur and other explorations in the Upper Ganga and Sutlej Basins. *Ancient India* 10–11:5–151
- Lal BB (1981) The two Indians epics vis-à-vis Indian Archeology. *Antiquity* 55:27–34
- Mahala A (2020) The significance of morphometric analysis to understand the hydrological and morphological characteristics in two different morpho-climatic settings. *Appl Water Sci* 10:1–16. <https://doi.org/10.1007/s13201-019-1118-2>
- Mahmood SA, Gloaguen R (2012) Appraisal of active tectonics in Hindu Kush: Insights from DEM derived geomorphic indices and drainage analysis. *Geosci Front* 3:407–428. <https://doi.org/10.1016/j.gsf.2011.12.002>
- Mohindra R, Parkash B, Prasad J (1992) Historical geomorphology and pedology of the Gandak Megafan, middle gangetic plains, India. *Earth Surf Proc Land* 17:643–662. <https://doi.org/10.1002/esp.3290170702>
- Molin P, Fubelli G (2005) Morphometric evidence of the topographic growth of the central Apennines. *Geogr Fis Din Quat* 28:47–61
- Moodie AJ, Pazzaglia FJ, Berti C (2018) Exogenic forcing and autogenic processes on continental divide location and mobility. *Basin Res* 30:344–369. <https://doi.org/10.1111/bre.12256>
- Moussi A, Rebaï N, Chaieb A, Saâdi A (2018) GIS-based analysis of the stream length-gradient index for evaluating effects of active tectonics: a case study of Enfidha (North–East of Tunisia). *Arab J Geosci* 11:123
- Pandey PK, Das SS (2016) Morphometric analysis of Usri River basin, Chhotanagpur Plateau, India, using remote sensing and GIS. *Arab J Geosci* 9:240. <https://doi.org/10.1007/s12517-015-2287-4>
- Parkash B, Kumar S, Rao MS, Giri SC, Kumar CS, Gupta S, Srivastava P (2000) Holocene tectonic movements and stress field in the western Gangetic plains. *Curr Sci* 79:438–449
- Parkash B, Rathor RS, Pati P, Jakhmola RP, Singh S (2011) Convergence rates along the Himalayan Frontal Thrust inferred from terraces at Chandidevi Temple Hill, Hardwar, Northwestern Himalaya. *Curr Sci* 100:1426–1432

- Patel NK, Pati P, Verma AK, Dash C, Gupta A, Sharma V (2020) Seismicity around the Mahendragarh-Dehradun basement fault in the western Ganga plain, India: a neotectonic perspective. *Int J Earth Sci* 109:689–706. <https://doi.org/10.1007/s00531-020-01826-8>
- Pati P, Acharya V, Verma AK, Patel NK, Jakhmola RP, Dash C, Sharma V, Gupta A, Parkash B, Awasthi AK (2018) Holocene tectono-geomorphic evolution of Haryana plains, Western Ganga plain, India. *Arab J Geosci* 11:361. <https://doi.org/10.1007/s12517-018-3714-0>
- Pati P, Verma AK, Dash C, Patel NK, Gupta A, Sharma V, Jakhmola R, Parkash B, Awasthi AK, Saraf AK (2019) Influence of neotectonism on geomorphology and depositional architecture of the Gandak megafan, middle Ganga plain, India. *Geomorphology* 327:489–503. <https://doi.org/10.1016/j.geomorph.2018.11.029>
- Prabhu M, Raghukanth STG (2015) Development of surface level probabilistic seismic hazard map of Himachal Pradesh. *Advances in structural engineering: dynamics*, vol 2. Springer India, New Delhi. https://doi.org/10.1007/978-81-322-2193-7_60
- Pérez-Peña JV, Azor A, Azañón JM, Keller EA (2010) Active tectonics in the Sierra Nevada (Betic Cordillera, SE Spain): Insights from geomorphic indexes and drainage pattern analysis. *Geomorphology* 119:74–87. <https://doi.org/10.1016/j.geomorph.2010.02.020>
- Raj R (2012) Active tectonics of NE Gujarat (India) by morphometric and morphostructural studies of Vatrak River basin. *J Asian Earth Sci* 50:66–78. <https://doi.org/10.1016/j.jseaes.2012.01.010>
- Ramírez-Herrera MT (1998) Geomorphic assessment of active tectonics in the acambay graben, Mexican volcanic belt. *Earth Surf Proc Land* 23:317–332. [https://doi.org/10.1002/\(SICI\)1096-9837\(199804\)23:4%3c317::AID-ESP845%3e3.0.CO;2-V](https://doi.org/10.1002/(SICI)1096-9837(199804)23:4%3c317::AID-ESP845%3e3.0.CO;2-V)
- Schumm SA (1956) Evolution of drainage systems and slopes in badlands at Perth Amboy, New Jersey. *Bull Geol Soc Am* 67:597–646. [https://doi.org/10.1130/0016-7606\(1956\)67:597:EODSASJ2.0.CO;2](https://doi.org/10.1130/0016-7606(1956)67:597:EODSASJ2.0.CO;2)
- Seismic Hazard Data (2020) <http://asc-india.org/maps/hazard/haz-cdh.htm>. Accessed 7 Sept 2020
- Silva PG, Goy JL, Zazo C, Bardají T (2003) Fault-generated mountain fronts in southeast Spain: geomorphologic assessment of tectonic and seismic activity. *Geomorphology* 50:203–225. [https://doi.org/10.1016/S0169-555X\(02\)00215-5](https://doi.org/10.1016/S0169-555X(02)00215-5)
- Singh S, Parkash B, Rao MS, Arora M, Bhosle B (2006) Geomorphology, pedology and sedimentology of the Deoha/Ganga–Ghaghara Interfluve, Upper Gangetic Plains (Himalayan foreland basin)-extensional tectonic implications. *Catena* 67:183–203. <https://doi.org/10.1016/j.catena.2006.03.013>
- Singh A, Paul D, Sinha R, Thomsen KJ, Gupta S (2016) Geochemistry of buried river sediments from Ghaggar Plains, NW India: Multi-proxy records of variations in provenance, paleoclimate, and paleovegetation patterns in the Late Quaternary. *Palaeogeogr Palaeoclimatol Palaeoecol* 449:85–100. <https://doi.org/10.1016/j.palaeo.2016.02.012>
- Singh V, Tandon SK (2008) The Pinjaur dun (intermontane longitudinal valley) and associated active mountain fronts, NW Himalaya: Tectonic geomorphology and morphotectonic evolution. *Geomorphology* 102:376–394. <https://doi.org/10.1016/j.geomorph.2008.04.008>
- Solanki T, Solanki PM, Makwana N, Prizomwala S, Kothiyari GC (2020) Geomorphic response to neotectonic instability in the Deccan volcanic province, Shetrunji River, western India: insights from quantitative geomorphology. *Quatern Int*. <https://doi.org/10.1016/j.quaint.2020.06.015>
- Sreedevi PD, Owais S, Khan HH, Ahmed S (2009) Morphometric analysis of a watershed of South India using SRTM data and GIS. *J Geol Soc India* 73:543–552. <https://doi.org/10.1007/s12594-009-0038-4>
- Thapar R (1966) *A history of India*, vol I. Penguin Book Ltd., Middlesex, England
- Topal S, Keller E, Bufe A, Koçyiğit A (2016) Tectonic geomorphology of a large normal fault: Akşehir fault, SW Turkey. *Geomorphology* 259:55–69
- Verma AK, Pati P, Sharma V (2017) Soft sediment deformation associated with the East Patna Fault south of the Ganga River, northern India: influence of the Himalayan tectonics on the southern Ganga plain. *J Asian Earth Sci* 143:109–121. <https://doi.org/10.1016/j.jseaes.2017.04.016>
- Verros S, Zygori V, Kokkalas S (2004) Morphotectonic analysis in the Eliki fault zone (Gulf of Corinth, Greece). *Bull Geol Soc Greece* 36:1706–1715

- Vhora MS (1987) Thermoluminescence dating of fluvial terraces: a feasibility study. Unpublished M. Tech. dissertation, University of Roorkee (Present IIT Roorkee)
- Viveen W, van Balen RT, Schoorl JM, Veldkamp A, Temme AJAM, Vidal-Romani JR (2012) Assessment of recent tectonic activity on the NW Iberian Atlantic Margin by means of geomorphic indices and field studies of the Lower Miño River terraces. *Tectonophysics* 544–545:13–30. <https://doi.org/10.1016/j.tecto.2012.03.029>
- Whittaker AC, Cowie PA, Attal M, Tucker GE, Roberts GP (2007) Bedrock channel adjustment to tectonic forcing: implications for predicting river incision rates. *Geology* 35:103–106. <https://doi.org/10.1130/G23106A.1>
- Wobus C, Helmsath A, Whipple K, Hodges K (2005) Active out-of-sequence thrust faulting in the central Nepalese Himalaya. *Nature* 434:1008–1011. <https://doi.org/10.1038/nature03499>
- Zaidi FK (2011) Drainage basin morphometry for identifying zones for artificial recharge: a case study from the Gagas River Basin, India. *J Geol Soc India* 77:160–166. <https://doi.org/10.1007/s12594-011-0019-2>
- Zhang HP, Zhang PZ, Fan QC (2011) Initiation and recession of the fluvial knickpoints: a case study from the Yalu River-Wangtian'e volcanic region, northeastern China. *Sci China Earth Sci* 54:1746–1753. <https://doi.org/10.1007/s11430-011-4254-6>
- Zoback ML (1992) First and second-order patterns of stress in the lithosphere: the world stress map project. *J Geophys Res* 97:11703. <https://doi.org/10.1029/92JB00132>

Tectonic Control on the Meanders Pattern of Alaknanda River in Srinagar Valley, Garhwal Himalaya, India



Sapna Semwal and D. D. Chauniyal

Abstract The present study deals with the study of tectonically regulated landform development within the meander pattern of the Alaknanda River in Lesser Garhwal Himalaya. We used high-resolution satellite imageries supplemented by field investigation to identify landform features exclusively regulated because of tectonic forces. The style of geomorphic landform and deformation pattern reveals the presence of strike-slip transverse faults within a zone of North Almora Thrust (NAT). The structural and lithological controls on the Alaknanda River system in Srinagar valley are manifested by steepness changes and deviations of drainage patterns. We identified several geomorphic anomalies such as an abrupt change in the flow direction, incised meandering, offset river channels, paleo-channels, multi-levels of terraces, knick points, and pools in the longitudinal profile associated with active tectonic in the area. Furthermore, we used morphotectonic landforms and a digital terrain model to generate a litho-tectonic map of the Srinagar valley. The results of the study show that the sinuosity index of the river is 1.34 which shows a sinuous to meandering trend. All 8 sets of meander segments are controlled by tectonic features i.e. fault, and lineaments. Six levels of terraces are the results of episodic upliftment. The meandering course is correlated with tectonic features hence it concluded that the river channel is closely controlled by structural features in the study area.

Keywords Tectonic control · Meander · Channel pattern · Structure · NAT · Transverse

1 Introduction

In the Himalayan range, the neo-tectonic movements occurred in the upper part of the Tertiary (Neocene) and Quaternary periods which have attributed to topographic development across the Himalaya (Obruchev 1948; Valdiya 2001). The

S. Semwal · D. D. Chauniyal (✉)

Department of Geography, Nitya Nand Himalayan Research and Study Center, Doon University, Dehra Dun, India

transverse faults across the major Himalayan thrusts are providing excellent transects to understand tectonic movement during the Quaternary (Kothyari et al. 2019, 2020a, b). The reactivation of fault rejuvenated the mature geomorphology of the Lesser Himalayan very dramatically (Kothyari and Luirei 2016). The differential upliftment across the Himalaya during the Quaternary period was also responsible for crustal adjustment (Valdiya 2001; Kothyari and Pant 2007; Kothyari et al. 2017; 2019). Sati et al. (2007) are also identified geomorphic expressions of tectonic landforms in the Srinagar (Garhwal) area. In the mountainous region, rivers are extremely sensitive. The complex changes in their course are caused by tectonic activities and associated features. Tectonic effects on rivers and their resultant landforms may be a very useful tool for identifying the faulting, folding, and fractures associated with smaller-scale deformation in channel settings. Tectonic warping and faulting may result in either longitudinal (parallel to channel orientation) or transverse (normal to meanders orientation) tilting of river profiles.

In the mountain belt, several studies have been conducted in the past to determine the behaviour of river profiles and patterns of active deformation (Hack 1957; Lavé and Avouac 2001). The river terrace provides information on incision rates, where rivers are forced to cut down into rising base rocks and have abandoned numerous strath terraces in the valleys (Lavé and Avouac 2001). Duvall et al. (2004) assessed the manner and degree to which bedrock channels respond to variations in rock strength and tectonic forcing within the Santa Ynez Mountains of California. The structure also plays an important role in controlling the longitudinal profiles of channels (Kothyari et al. 2017). Channels in the Catalina-Rincon core complex are characterized by structurally controlled knick points with a wide distribution of heights and spacing's in metamorphic core complexes in Arizona (Jon and Pelletier 2009). Bedrock Rivers set much of the relief structure of active origins and dictate rates and patterns of denudation (Whipple 2003). The spatial changes in the rock-upliftment rate and rock strength in different bedrock channels and their morphological responses in the northwest Himalayan front are investigated by Allen et al. (2013), Kothyari et al. (2019).

Active tectonic control on the morphology in the Bagmati river of Bihar was observed by Jain and Sinha (2005). The active tectonic faults were characterized by the association of fluvial anomalies and morphological changes. The multi-channel pattern developed in bedrock was initiated by block or domal upliftment and its effects can be observed on the channel morphology of the stream (Kale et al. 1996). The impact of active tectonic on the characterization of the fluvial landscape has been investigated on the strike-slip fault of the Ajay-Damodar interfluves in India by Roy and Sahu (2015). Sahu et al. (2010) provided a detailed description of the Son-Ganga River to active tectonics and geomorphology in an alluvial tract of India. There are several intensive works related to the tectonic control in the Ajay-Damodar interfluves of eastern India. In the Himalayan region, Bawa et al. (2014) has investigated the natural and anthropologic controls on the spatial morphological variability of the Yamuna River. Valdiya (2018) has expressed his view that it has been qualified to the reactivation of the WNW-ESE trending faults and lineaments in the recent and sub recent time. Furthermore, it is attributed that the formation of deep gorges, uplifted

terraces, landslides, and debris avalanches along faults, anomalies in stream courses are attributed to the recent movement along North Almora Thrust (NAT) in the Lesser Himalaya (Kothyari and Pant 2008; Kothyari et al. 2017; Kothyair and Luirei 2016). Srinagar section of the NAT has been attributed to the reactivation along transverse and longitudinal faults which have been taken into consideration. The main objective of the present study is to describe the tectonic control on the meander pattern of the Alaknanda River in Srinagar valley.

2 Study Area

2.1 Location

The area investigated lies in the lower basin of Alaknanda River between Supana to Kirtinagar of Garhwal Lesser Himalaya. Srinagar valley is formed by the River Alaknanda in Lesser Himalaya. Alaknanda rises from the snout of Satopant Glacier at the height of 3760 m and after traveling 191 km it joins the Bhagirathi River at Devprayag (442 m). The average gradient of the river is about 17.3 m/km from source to mouth (Nand and Kumar 1989). After passing the distance of 161 km downstream from the source it enters in 11.5 km long and 2.5 km wide sinuous meandering river valley of Srinagar (Fig. 1). Geographically the valley is bounded between $78^{\circ} 45' 16''$ E to $78^{\circ} 49' 43''$ E Long and $30^{\circ} 12' 36''$ N to $30^{\circ} 15' 47''$ N Lat. which covers 41.29 km² area. About 600^m contour line demarcates its valley bottom. Out of the total area, about 13.27km² is occupied by Quaternary sediments. The River Alaknanda flows in the centre along with bow shape meander. The average gradient of the river is very low (0.0054) from Supana to Kirtinagar. After passing 11.5 km (channel length) distance further it enters a narrow shape gorge at Kirtinagar in the west (Fig. 1).

2.2 Structural Setting and Geology

The study area is located in the central portion of the tectonically active Lesser Himalayan domain. The Lesser Himalaya lies between the Main Central Thrust (MCT) in the north and the Main Boundary Thrust (MBT) in the south. It has made an extremely rugged landscape characterized by complex topography. This terrain is made up of Precambrian rocks older than 540 million years in age (Valdiya 1980, 2001). The North Almora Thrust (NAT) is one of the major tectonic units in the Lesser Himalaya which passes through NW to SE direction near Srinagar (Fig. 2). This regional thrust is also known as Tons Thrust (TT) and Srinagar Thrust (Valdiya 1980) or NAT (Kumar and Agarwa 1975; Srivastava and Ahmed 1979). Within the NAT zone because of the horizontal and vertical shear stress, a large number of

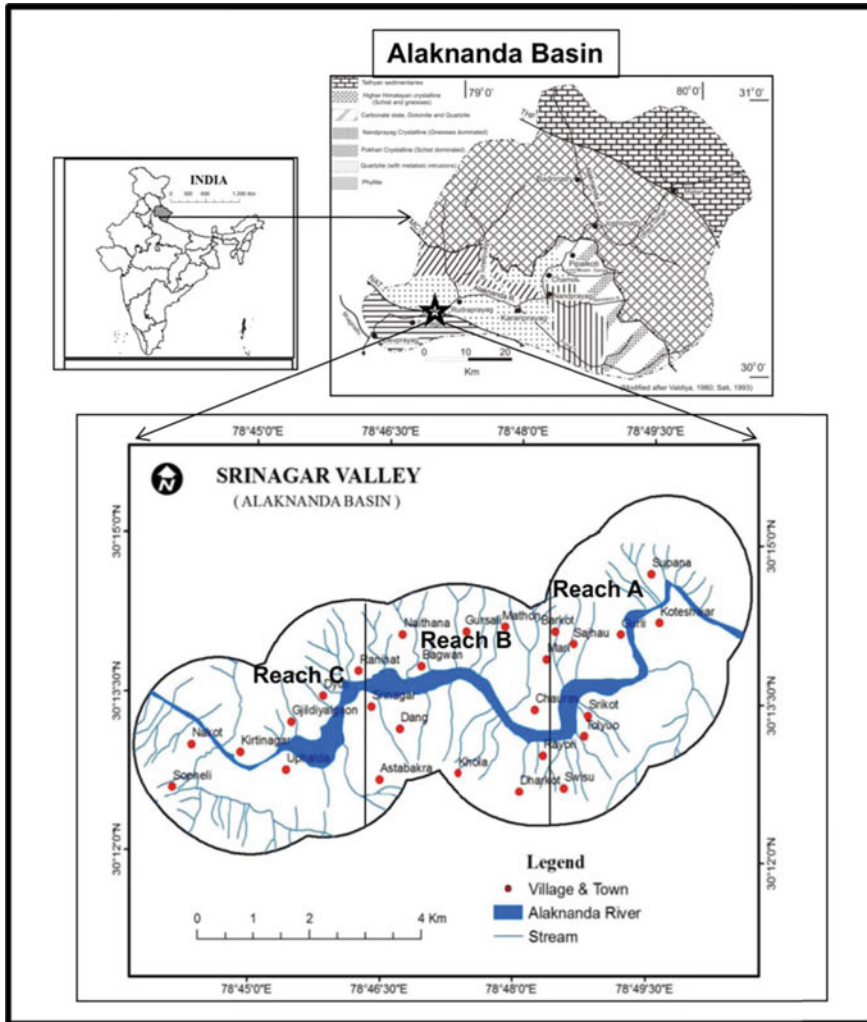


Fig. 1 Location map of the Srinagar valley along with reaches (a, b, and c) and geological map of Alaknanda basin in Garhwal Himalaya

transverse and oblique faults have been generated. Out of those two local faults/lineaments, the SCKF Fault in the centre and Dhobi ghat-Kirtinagar-Maletha Faults (DKMF) in the SW also exist in the study area. The Dhobighat-Kirtinagar-Maletha Fault is inferred from lineaments viewed in aerial photography on a local scale (Sati et al. 2007) (Figs. 2 and 3).

The NAT separates the Garhwal group of rocks in the north from the Chandpur group of rocks in the south (Kumar and Agrawal 1975). The Chandpur phyllite is predominant in the present study area. Upper proterozoic rocks on both sides of

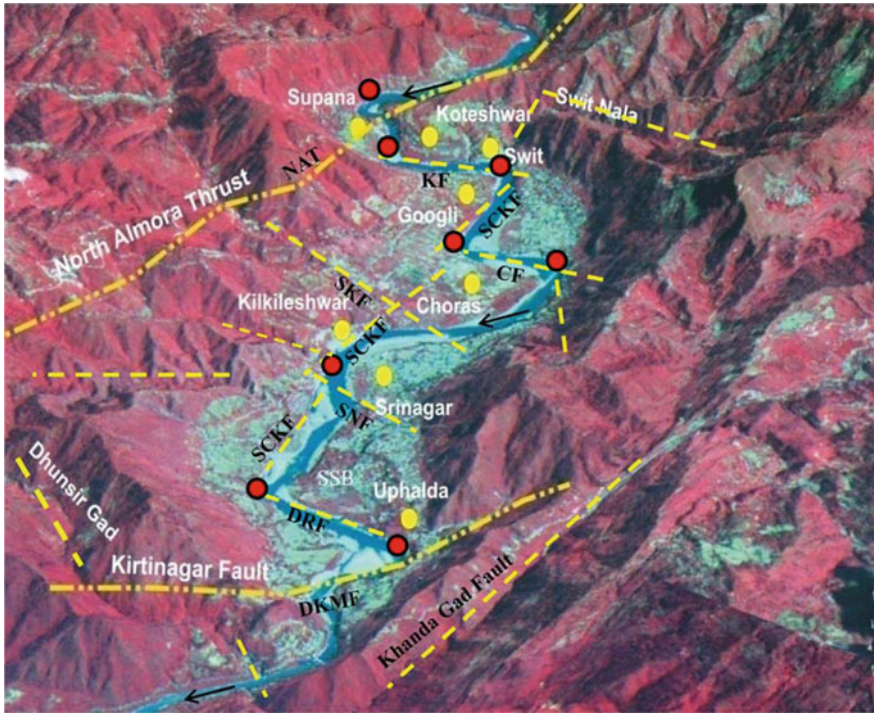


Fig. 2 Tectonic setting of the Srinagar valley along North Almora Thrust (NAT). Red dots are showing the meander bends, yellow dots are localities and dashed lines are faults and lineaments. Faults DRF = Dhobighat-Ranihat-Fault, SCKF = Sweet–Chauras-Kilkileswar Fault, SNF = Srinagar-Naithana Fault, SKF = Srinagar-Badkot Fault, CF = Chauras Fault, DKMF = Dhobighat-Kirtinagar-Maletha Fault. SCKF is a longitudinal lineament/fault parallel to NAT but displaced by transverse faults in places

the thrust are directly overlain by quaternary deposits consisting of boulder and gravel beds along with sandy and clayey horizons, contained in several depositional terraces. The phyllite is tightly folded, fractured, and weathered in nature. Enter bedded flaggy quartzite between phyllite is very common near Chauras suspension bridge and Kirtinagar locality. The study area is situated very near to NAT so that it is characterized by a wide shear zone (Kumar and Agrawal 1975).

3 Material and Methodology

The present research work is essentially based on the interpretation made on a topographical map, large-scale aerial photographs (1/40000 scale), Digital Elevation Model, Satellite image LISS III, Google images, and field investigations. The base map of the study area has been prepared on 1:50,000 topographical sheets.

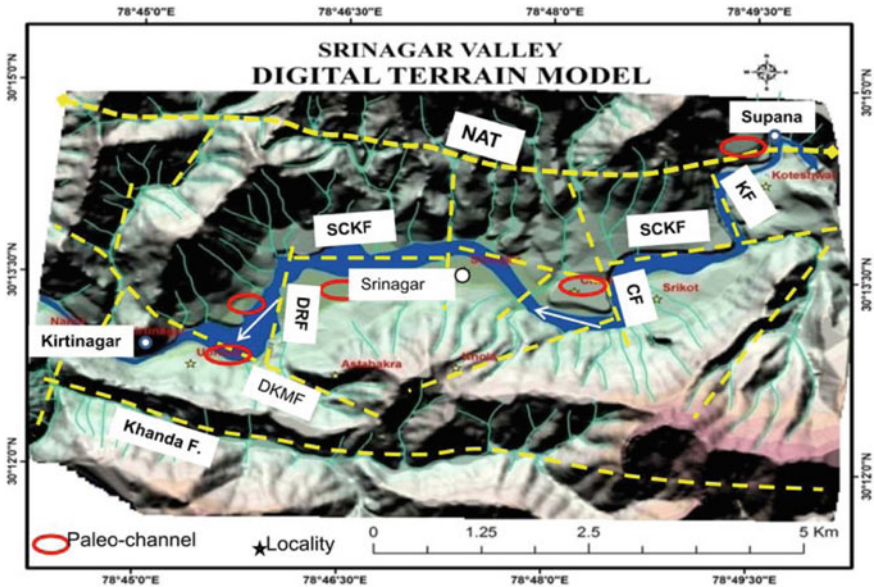


Fig. 3 Digital Terrain Model is showing the location of meander bends control by transverse faults in the Srinagar valley. The longitudinal lineament in the center is displaced by transverse faults. Red oval-shaped marks are showing the location of paleochannels. Meander bends are showing the hogback features from Supana to Chauras

The survey of India (SOI) topographical sheets and satellite images were georeferenced in Arc GIS 10.1. The terraces are demarcated by large-scale 1:40,000 aerial photographs. Thrust, faults, major and minor lineaments are marked based on satellite imageries, SOI map, DTM, and drainage pattern using the software ARC GIS and datum system. Furthermore, geomorphic anomalies such as terrace scarps, faulted cliffs, offset drainage, hogback and rapids are identified during longitudinal and transverse field traverses. A dumpy level, plane table, and GPS surveys have been conducted for the measurement of meander bends and stream gradient. The depth of pools has been measured by measuring tape and rope in the deepest portion of the pool. The depth of pools upward and the downward stream is less than the deepest portion.

In addition, the vertical and lateral extent of the previous (2013) flood level was also identified on the ground. Paleo-valleys were identified and differentiated from terraces, based on their morphology and association with incised bedrock. For the analysis of channel pattern and meander geometry, the 11.5 km long Alaknanda River channel course in Srinagar valley is divided into hierarchical geomorphic units. A geomorphic unit is a portion of the river that shows different forms of physical features that can be summarized by properties. On the basis of uniform gradient, shape and width, the geomorphic unit is classified into three reaches (Fig. 1c). The reach is a section of geomorphic unit in which not only the river shape and energy

flow are relatively uniform but also other conditions such as meandering pattern, bank properties and bed sediments. Each river reach can contain one to several meander segments. Thus on the basis of meander pattern and morpho-tectonic characteristics, three reaches are further classified into 8 meander segments (Table 1). A single segment includes one or several hydraulic elements such as rapids, pools, point bars, sediment particles, bank erosion etc. On the basis of 1:50,000 SOI map sinuosity index and other geometrical parameters such as length, width, depth, amplitude, radius and w/d ratio (Table 1) have been measured according to Leopold (1964), Leopold and Wolman (1957). Stream sinuosity means deviation channel course from the straight channel. It is the ratio of channel length and valley length. A Digital Elevation Model of the Srinagar valley is constructed using 20-m contours from SOI topographical maps (Fig. 3). Extensive longitudinal and transverse field traverses were carried out to identify and check the morpho-tectonic features.

4 Neotectonic Movement and Channel Evolution

4.1 *Morpho-Tectonics and Channel Evolution*

The mountainous region of Garhwal is influenced by Himalayan tectonics. Large-scale morpho-tectonic activities occurred in the south of NAT during the Quaternary (Kothyari and Pant 2008; Luirei et al. 2016; Kothyari et al. 2017, 2018). Evidence suggests that the Srinagar Thrust (ST) is a subsidiary branch of NAT was reactivated during the Late Quaternary (Sati et al. 2005). Quaternary episodic movement along the tectonic plan has rejuvenated the old mature topography of the Lesser Himalayan terrain. The horizontal and vertical shear and stress to the south of the NAT are responsible for recent active deformation in the region (Valdiya et al. 1992). The major and minor longitudinal and transverse faults and lineaments indicate that the area was passing through differential upliftment. Dhobighat-Kirtinagar-Maletha Fault (DKMF) and Sweet-Chauras-Kilkileswar-Ranihat Fault (SCKF) are two longitudinal linear features parallel to NAT in the study area (Fig. 3). After crossing NAT at Supana village the general trend of Alaknanda valley is an east–west direction parallel to NAT (Fig. 3). It shows that the river was followed the trend of SCKF lineament from Supana to Kirtinagar. Due to the continuous episodic upliftment and shear and stress, strike-slip/ transverse faults were activated. The incision of the valley along these lineaments was more active and simultaneously river followed the trends of transverse faults. Numbers of tributaries streams are also developed along these fault lines on both sides of the river. The prominent streams are Sweet Gadhera along with SCKF, Badkot Gadhera along with CF, Naithana Gadhera along with SN, and Dhobighat along with DKM, Nauli Gad, Dhundir Gad and Khanda Gad (Figs. 2 and 3). The N-S transverse faults or lineaments are the second and third-generation deformation features which displaced the earlier linear features at

Table 1 Channel morphological parameters

Reach	Segment	Meander width ratio	Meander length ratio	W/D ratio	Wave length (km)	Amplitude (km)	Radius (km)	Sinuosity Index	Width (m)	Depth (km)
A	Supana	7.0	20.0	1.43	1.0	0.35	0.38	1.18	10	7
	Koteswar	4.67	11.67	3.33	1.25	0.8	0.43	1.4	30	9
	Surasu	6.67	16.67	2.86	1.5	1.0	0.4	1.43	20	7
	Srikot	2.29	7.14	6.25	1.5	0.8	0.43	1.29	50	8
B	Chauras	5.5	15.0	2.73	1.25	1.15	0.5	1.41	30	11
	Srinagar	2.8	10.0	4.37	1.75	0.8	0.4	1.18	35	8
C	SSB	2.12	6.25	8.33	1.5	0.9	0.4	1.25	50	6
	SriyantraTapu	1.9	5.0	9.17	1.5	1.0	0.5	1.34	55	6
Average	Alaknanda (Supana to Kirtinagar)	4.12	11.47	4.83	1.4	0.86	0.43	1.34	35	7.25

Source The table generated from 1/50000 SOI topographical sheet by the authors

the junction (Fig. 2). The prominent transverse and strike-slip faults/lineaments are shown in Figs. 2 and 3.

Srinagar valley has a tectonic origin between NAT and Dhobighat-Kirtinagar-Maletha fault (DKMF) because of the flexure slip faulting (Sati et al. 2007). Few Quaternary tectonic features are reported by Sati et al. (2005) in the Srinagar valley. The presence of unpaired terraces preserved along the Sweet Nala-Chauras-Kilkleswar Fault (SCKF) is considered to be uplifted along with the NAT (Semwal 2018). The Alaknanda River flows through a bow-shaped meandering course in Srinagar valley and meander bends are either controlled by transverse fault or lineaments (Figs. 2 and 3). Juyal et al. (2010) have also identified that most of the meander bends are control by tectonic features in the Srinagar valley. At the junctions of morpho-tectonic features, landslide, undercut by river, terrace scarp, and talus cone are prominent features (Photo 5 A and B) while channel bars, boulder bed, pools, and riffles are channel bed features along the river course.

In the Himalayan terrain, the evolution of streams/rivers and their pattern are characterized by episodic upliftment, litho-stratigraphy, and steepness of the terrain, water discharge, and sediment load. These factors have been interpreted as indications of the presence of structure in the region bounded by thrust and faults. The sinuosity index of the Alaknanda River is calculated at 1.34 which advocated a sinuous to the meandering pattern. Based on tectonic features and sinuosity index, it can be inferred that fault pattern, sinuous to meander pattern, and straight pattern of the three reaches are found in the study area. From Supana to Srikot (reach A) the river formed a sinuous to meanders pattern controlled by faults and lineaments in which the sinuosity index is 1.4. From Chauras to Ranihat (reach B) the river formed nearer to the straight pattern which the sinuosity index is 1.18 while Ranihat to Kirtinagar (reach C) sinuosity index is 1.33 which shows sinuous to meanders pattern. Similarly, the sinuosity index of 8 meander segments has been calculated to range from 1.18 to 1.43 (Table 1).

Srinagar valley is well known for its intermountain-wide basin with a multi-level of terraces and ingrown meanders develop along the longitudinal course of the Alaknanda River. The aerial photo interpretation shows the development of six levels of fluvial terraces preserved along the longitudinal course of the Alaknanda River. Genetically debris fill, valley fill, and strath three types of terraces are identified in the Srinagar valley (Juyal et al. 2010). The sequence of six-generation terraces and their sub-levels are demarcated at Chauras localities (Fig. 4a, b).

4.2 *Tectonic Control in the Formation of Meander*

Regional seismic records indicate that the Garhwal region is tectonically very active. Transverse faults have played a significant role in the recurrence of seismic events along with the NAT (Valdiya 1976; Dasgupta 1987). These tectonic movements have also influenced the fluvial dynamics in the region. A large number of evidence of geomorphic expressions associated with tectonic activity has been documented along

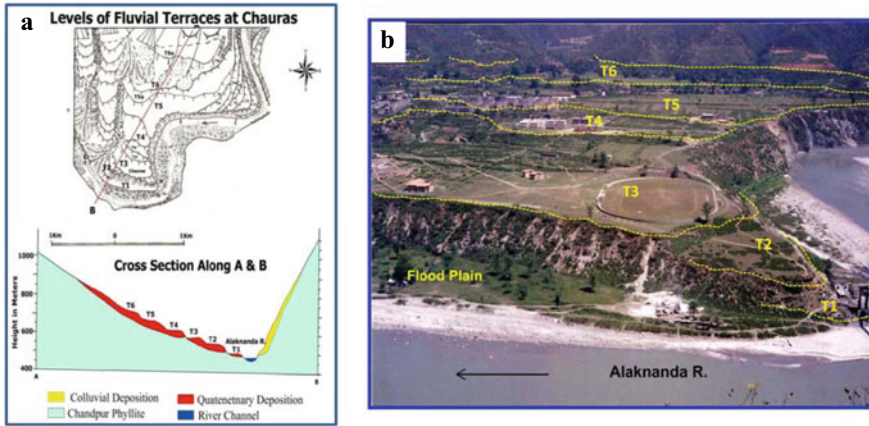


Fig. 4 a A geomorphological map at Chauras locality is showing the sequence of six levels of river terraces and their schematic cross section along a–b. The cross section is also showing unpaired terraces and asymmetrical valley. b Field photograph is the true evidence of 6 levels of terraces at Chauras locality

the Alaknanda River. These geomorphic expressions are 6 levels of river terraces (Fig. 4a, b), fault scarp (Fig. 5a) offset drainage (hogback) (Figs. 2 and 3), deformation of earlier generation fault and lineament (Fig. 2, SCKF), valley incision in undercut side (pools), tilting of beds (Fig. 5b) and landslide on terrace scarp (Fig. 5a, b). The most remarkable geomorphic expressions are associated with tectonic activity.

During the reactivation of the NAT, numbers of longitudinal and transverse faults, fractures and lineaments have been formed along with the thrust. Simultaneously major and minor drainage lines were also developed with these structural features. Tectonic control is reflected in the formation of meanders of the Alaknanda River

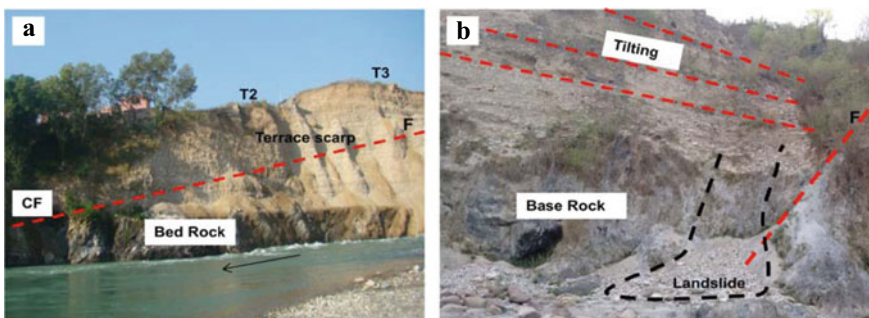


Fig. 5 a Active fault (CF) scarps extending from N-S along with landslide on terrace scarp at Chauras. It was exposed during the 2013 Kedarnath flood. b Quaternary sedimentary beds are tilted eastward on terrace scarp which inferred the active tectonic along the transverse fault. It is an undercut side of the river which is prone to landslides. The newly generated fault is showing the displacement of Quaternary beds and bedrock near the transverse fault (CF)

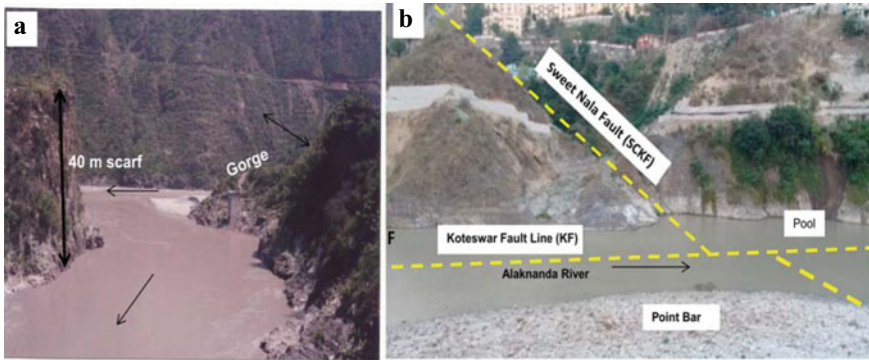


Fig. 6 The River suddenly changes her direction at Supana and is flowing through a narrow passage (a). Here the river formed a hogback feature along with a 40 m vertical rocky fault scarp. (b) Field photograph is showing the junction of Koteswar fault and the Sweet Nala fault. The Alaknanda River formed a 10 m deep pool (b) and hogback feature at the junction point

in Srinagar valley. The offset drainage pattern is clearly indicating the displacement and deformation (Figs. 2 and 3). Reconstruction of channel configuration indicates that the river followed east–west along longitudinal SCKF line parallel to the NAT prior to the meandering course in the Srinagar valley. SCKF is one of the earlier generated longitudinal lineaments parallels to NAT. In the latter episodic stages, this was deformed and displaced by a number of north–south trending transverse faults and lineaments in the area. Just after crossing the NAT at Supana village the river turns towards the southwest direction and formed a hogback feature (Figs. 2 and 3). The sinuosity of the meander bend is calculated at 1.18 while the width and depth ratio is 1.43. The 40 m deep narrow gorge on the quartzite rock indicates that the river has been shifted toward the left along the transverse fault plane (Fig. 6a).

At the right bank near Supana village, a paleochannel also proofs the fact that the river shifted towards the left along the newly activated fault line (Fig. 2). After flowing a half km distance it further follows the pattern of the Koteswar fault (KF) which extended from north to south direction up to Sweet Nala (Fig. 6b). The important lithology of the area is phyllite and inter-bedded quartzite which is folded in many places (Srivastava and Ahmad 1979). The sinuosity of the Koteswar meander is 1.4 which width and depth ratio is 3.33. It is compressed by the Koteswar fault. At the junction point of the Koteswar Fault (KF) and Sweet Nala Fault (SNF), the river suddenly turns towards the west direction along longitudinal lineament (SCKF) and forms a hogback feature (Fig. 6a). The offset drainage pattern is attributed due to differential tectonic movement in the region. Mostly junction of two lineaments becomes the unstable part that tends to fast vertical and lateral erosion. It advocated that the valley incision was deepest near the junction point where a 10 m deep pool is formed at the meander bend (Fig. 6b). The Surasu meander segment is compressed by Koteswar Fault (KF) and Sweet-Chauras-Kilkileswar fault (SCKF) (Fig. 7). The sinuosity index of the Surasu meander is 1.43 which indicates the sinuous to the meandering pattern.

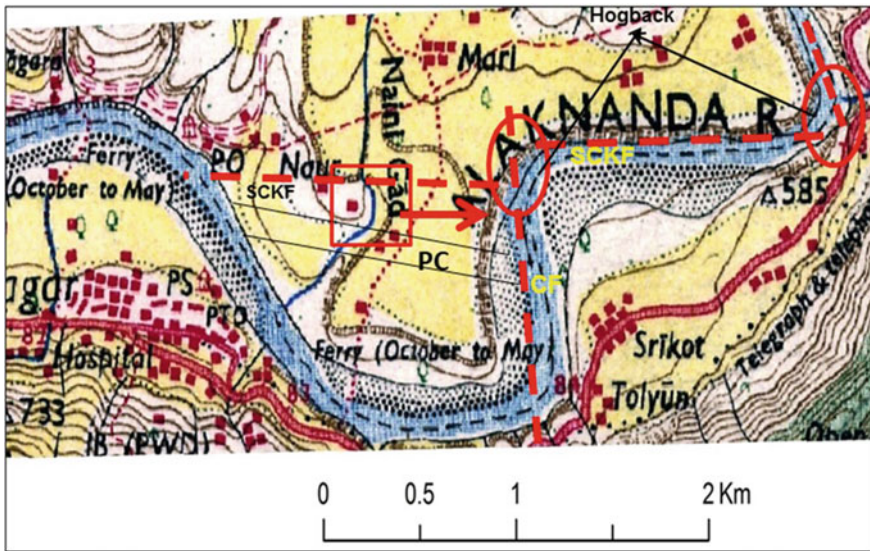


Fig. 7 Topo map is showing the faulted pattern of the river (SCKF and CF). Earlier generation fault SCKF (red dashes lines) displaced by latter generation transverse fault CF at Chauras. Red circles are showing the meander bends and hogback feature control by faults. The red squire is showing the deflection of Nauni Gad towards the east direction. Two black parallel lines are showing the buried paleo-channel (PC) course under T3 at Chauras

Opposite of the Chauras bend the Alaknanda River formed a prominent Srikot meander (Figs. 2 and 3) which is compressed between SCKF and CF. At Chauras E-W flowing Alaknanda River suddenly turned towards the south direction along the younger generation Chauras transverse fault (CF). Hogback feature is advocating the offset drainage pattern (Figs. 7 and 8). Paleo channel course is also one of the evidence of shifting of the river. The paleo-channel (PC) was identified during field observation which was exposed during the 2013 Kedarnath flood by undercutting at Chauras terrace scarp (Fig. 7). It was 1.25 km long and 0.75 km wide. Potholes and polished rock surfaces on quartzite rocks are the ground evidence in the exposed paleo channel course. The sinuosity index of the Srikot meander is 1.29 which shows sinuous to meandering pattern of which the width/ depth ratio is 6.25. Here the valley is quite wide with numerous channel morphological features (Pools, riffles, braided channel and knick points) (Fig. 8). Channel morphology in this segment confirms to hydrological characteristics and therefore, external control such as active tectonic is implied. The detailed characteristics of the meander geometry are given in Table 1. After running 500 m south direction, the river further turns to south-west direction through 154 m narrow rocky passage at Chauras suspension bridge (Fig. 8). Opposite of this bend there are 6 levels of river terraces (Fig. 4).

Figure 7 reveals that earlier generation east–west trending longitudinal fault (SCKF) is displaced by north–south trending transverse fault (CF). As the latter generation transverse fault reactivated continue due to the episodic upliftment, the

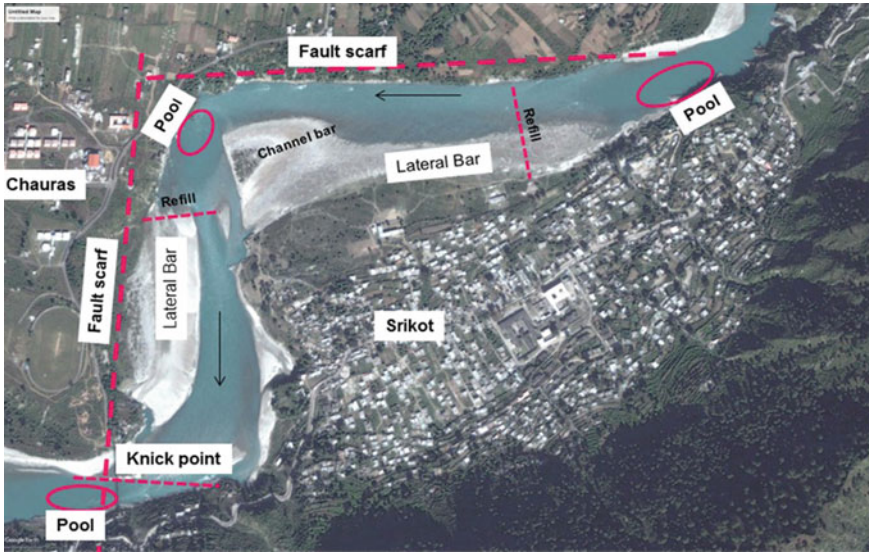


Fig. 8 Google earth image is showing the tectonic (faults and fault scarps) and channel morphological features (lateral and channel bars, pools knick points and refills)

river followed the trend of that lineaments and shifted eastward. In addition, the channel course of Naudi Gad a small tributary rivulet of Alaknanda is also deflated towards the east direction (Fig. 7 in box) which manifested that the deflation force was from W to E direction by the differential rate of upliftment). It also indicates that that episodic upliftment is not rejuvenated the main river but also tributary streams in the area that manifested in the epigenetic gorges, knick points (Fig. 8) and steepness of gradient in the streams,

Srinagar and SSB meander segments are also controlled by tectonics. Srinagar-Gorsali Gadhera lineament is passing from N to S direction and formed a Srinagar wide meander bend. The sinuosity of the meander bend is very low (1.18) and higher width and depth ratio (8.33) which indicates a straight course to a sinuous course. SSB meander is formed between Naithana Gadhera and Dhobighat-Ranihat (DRF) transverse faults. The low sinuosity index (1.25), high width and depth ratio (8.33) braided channel and aggradations of the meander indicates the wide meander segment (Table1).

Sriyantra Tapu meander segment displays a number of features that are suggestive of tectonic control in the development of meander and channel pattern. This investigation was supplemented with topographic sheet, Google earth image and field verification (Fig. 9a, b). At Ranihat village the Alaknanda River suddenly change its flow direction toward the south which seems to be the manifestation of a fault pattern. Reconstruction of channel configuration in this area shows that the river followed the usually east–west course prior to following the trend of DRF (Fig. 9a, b). The abandoned channel course is 500 m long, 125 m wide and 25 m above the present

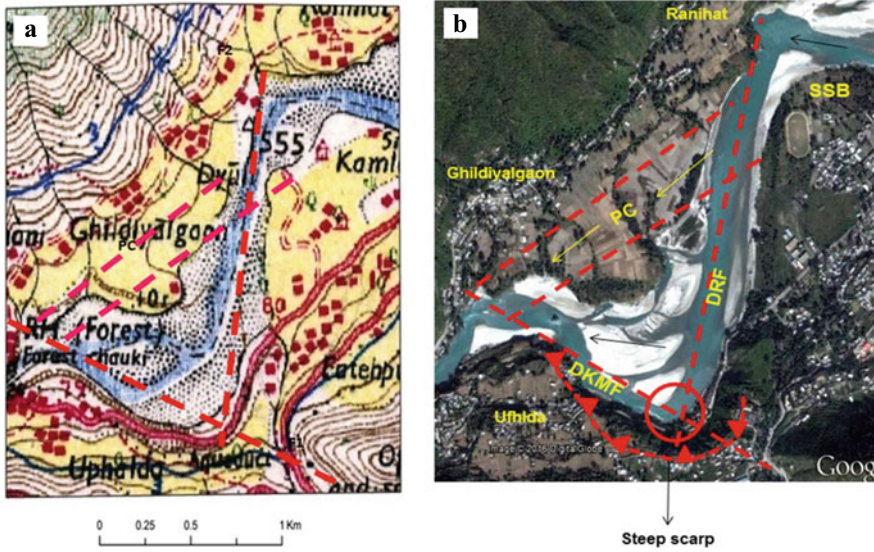


Fig. 9 Topo map (a) and Google earth image (b) both are showing the two faults line DRF and DKMF along the Alaknanda River by red dashes line. Red circle showing the junction of two faults line and meander bend of Sriyantra Tapu. It is the most sensitive zone and prone to landslide in concave undercut side (B). PC is showing the paleo channel. The general trend of the river valley is showing east–west direction but due to the activation of DRF the river followed the trend of fault from north to south. Similarly river followed the trend of DKMF and forming a 60 m steep faulted site at the undercut site

river level. Two sets of river terraces are clearly identified at the Gildiyalgaon. This proves that as well as the fault reactivated up, the river continued to shift along the fault line by incision of the river. Latter on old river channel course has been filled by mega-flood events and remained as a buried channel. Rounded quartzite and granite boulders exposed polished rock surfaces with potholes are the field evidence on the paleochannel course. A major flood can be generated during the interglacial period and phases of deglaciation because of the very high transport capacity and steep gradient of the Alaknanda River (Chodhary et al. 2015). The fault notch is the most sensitive zone prone to landslides and, undercutting by the river. The high sinuosity index (1.34) of the meander segment is showing the tight bend compressed by DRF and DKMF. The high width and depth ratio (9.17) indicates a wide channel course in which braided channel, lateral and channel bars are identified in different shapes and sizes. (Fig. 9a, b).

5 Discussion

Detection of structural features and geomorphic anomalies in the Alaknanda River has provided tools for recognizing the tectonic control in the meandering pattern of the study area. The trends of closely spaced transverse faults along the major thrusts are sufficient to relate active tectonic movements in the Himalayan terrain (Fig. 2). This approach using remote sensing imagery and DTM coupled with repeated field observations have provided information on the nature of the fault (Figs. 2 and 3). River response to neo-tectonics depends upon the nature and rate of vertical movement and the trend of faults with respect to the direction of flow of the river. In the Srinagar valley, most of the transverse faults are across the Alaknanda River channel near the North Almora Thrust (Figs. 2 and 3). Differential movements along the strike-slip faults have produced river terraces, tilting of Quaternary sediment beds (Fig. 5b), hogback features, faulted scarp, and shifting of river channel course. Out of these features riverbank erosion, aggravation behaviour of the channel, channel pattern, channel widening, overbank flooding, and channel morphology are also some of the geomorphologic expressions of tectonic control in the meander pattern of the Alaknanda River. Most of the transverse faults are identified in the Srinagar valley where the Precambrian phyllite of Chandpur formation is the main lithology. One of the longitudinal lineaments parallel to NAT in the center of the valley is displaced by latter generation transverse faults or lineaments which are responsible for turning of river channel course, formation of terraces, paleochannels, and other morpho-tectonic features.

The formation of compressed meanders is due to the two closely related faults i.e. Koteswar fault (KF) Sweetnala-Chauras-Kilkileswar fault (SCKF). SSB and Sriyantra Tapu meander segment zone are characterized by flooding because of lowering the channel gradient. Typical geomorphic signature of tectonic movement and shifting of the river along the faults can be seen in the Supana, Chauras, Ufald, and Ghildiyalgaon localities. Paleo channels are the results of upliftment of the terrain, valley incision, and shifting of the river towards active tectonic faults. At Supana village the river crosses the North Almora Thrust (NAT) and enters the Srinagar valley. Here the paleochannel is 400 m long parallel to the present river course. The incision phase has been inferred that the Supana paleo channel formed around 8 Ka (Chaudhary et al. 2015). A typical paleo channel pattern is observed at Chauras. The buried paleo-channel was exposed during the 2013 Kedarnath flood. It was parallel to the SCKF but after the activation of CF, the river shifted toward the newly generated fault line by the valley incision. At Ufald village, there are two sets of paleochannels extending from NE to SW direction lie at an elevation of 35 m and 55 m above the river bed respectively. The narrow bedrock passages are carved by fluvial action. It shows that the river shifted northwards along the Dhubighat-Kirtinagr-Maletha fault (DKMF). An isolated erosion-resistant rock mass in the middle of the channel bed at Sriyantra Tapu also indicates the river shifted towards the north along with the active tectonic fault (DKMF) (Fig. 9b). Below the Ufald village, the river crosses the DKMF and enters into a narrow bedrock gorge. At Kirtinagar the Srinagar valley becomes closed.

Another important point that emerged from this study is the development of 6 sets of river terraces at Chauras locality. The paleochannels and river terraces are closely associated with transverse faults. At Chauras 6 levels of fill, terraces are well exposed along the transverse fault which is formed during -15, 8 Ka valley aggradations (Juyal et al. 2010). It can be inferred that the Paleo channels are formed due to the turning of the river eastward along the transverse faults by the action tectonic movements (Fig. 7). Supana, Chauras, Ghildiyalgaon, and Ufhlda are prominent examples of paleochannels along a transverse fault in the study area. The digital elevation model of the valley area has been generated for comparison of tectonic setting, the slope of the terrain, and direction of flow. The major tectonic landforms identified in the study area are associated not only with tectonic activities related to NAT, but are modified by the recent tectonic activities of the latter-formed transverse fault. Therefore, we must take into account the role of transverse tectonics while analysing the neotectonics in the Himalayan region. The results obtained from the tectonic control on the meanders pattern of Alaknanda River in the Srinagar Valley and confirmed with field evidence indicating that the transverse faults along the North Almora Thrust (NAT) is tectonically active. The drainage pattern of the region is controlled by thrusts, faults and lineaments.

6 Conclusion

Based on the above geomorphic investigations following conclusions have been drawn.

- 1 The present study reveals that the landform development and the deformation pattern within the NAT zone are a result of the late Quaternary tectonic movement.
- 2 Further, based on geomorphic anomalies we strongly argued that the transverse faults play a significant role in the development of landforms as evident from the offset drainage patterns, meandering of the river, paleochannels, knick-points, and steeping of river gradient.
- 3 However, a river that follows the transverse faults in substrate rock display a sudden change in river profile form. The channel morphological features such as paleochannel, knick points, refills, pools, undercut sites; meander scars; and hogback all are associated and controlled by tectonic activities.
- 4 Based on detailed satellite data interpretation and geomorphic analysis we infer the presence of NW–SE oriented strike-slip faults, genetically associated North Almora Thrust.
- 5 The present course of the Alaknanda River in the Srinagar valley is being deflected in many places by tectonic forces. Meanders' patterns, size, and shape are controlled by different phases of tectonic activities.
- 6 Channel incision under differential upliftment rate and slope gradient display sinuosity indices is consistent with the channel pattern. The Alaknanda River

in the study area appears to adjust both gradient and width in response to the increased tectonic moment.

- 7 Finally, it is concluded that the structure plays an important role in controlling the river riches, meander segments and longitudinal profile of rivers in the study area.

References

- Allen GH et al. (2013) Lithologic and tectonic controls on bedrock channel form at the northwest Himalayan front. *J Geophys Res Earth Surface (JSR)* 1181–20
- Bawa N et al. (2014) Controls on morphological variability and role of stream power distribution pattern, Yamuna River, western India. *Geomorphology* 227:60–72
- Chaudhary S et al. (2015) Formation of paleo-valleys in the central Himalaya during valley. *Quat Int* 371:255
- Dasgupta S et al. (1987) Active transverse features in the central portions of the Himalaya. *Tectonophysics* 136:255–264
- Duval A et al. (2004) Tectonic and lithological controls on bedrock channel profiles and processes in coastal California. *J Geophys* 109(F3): 1
- Hack JT (1957) Studies of longitudinal stream profiles in Virginia and Maryland, US Geol Surv Prof Pap, 45–97
- Jain V, Sinha R (2005) Response of active tectonics on the alluvial Bagmati river, Himalayan foreland basin, eastern India. *Geomorphology* 70(3–4):339–356
- Juyal N et al. (2010) Late Quaternary fluvial aggradation and incision in the monsoon-dominated Alaknanda valley, Central Himalaya, Uttarakhand, India. *J Quat Sci* 25(8):1293–1304
- Kale et al. (1996) Multi-channel pattern of Bedrock river: an example from the central Narmada basin, India. *Catena* 26(1–2): 85–98
- Kothiyari G et al. (2017) Morphotectonic records of neotectonic activity in the vicinity of North Almora Thrust Zone, Central Kumaun Himalaya. *Geomorphology* 285:272–286
- Kothiyari G et al. (2018) Response: Discussion of ‘Morphotectonic records of neotectonic activity in the vicinity of North Almora Thrust Zone, Central Kumaun Himalaya’ *Geomorphol* 285:272–286
- Kothiyari GC et al. (2019) Landscape evolution and deduction of surface deformation in the Soan Dun, NW Himalaya, India. *Quat Int* 10,1016/j.Quaint 02, 016
- Kothiyari GC et al. (2020a) Evidences of neotectonic activity along Goriganga River, higher central Kumaun Himalaya, India. *Geol J* <https://doi.org/10.1002/gj.3791>
- Kothiyari GC, Pant PD (2007) Neotectonics of northwestern part of Almora district around Dwarahat-Chaukhutia area in central Kumaun Himalaya: a geomorphic perspective
- Kothiyari G, Pant PD (2007) Geomorphological and geological investigation of Neotectonic activity of Saryu River Fault (SRF), a Part of North Almora Thrust (NAT) in Seraghat-Basauli area in Central Kumaun, Uttarakhand
- Kothiyari G et al. (2019) Quaternary landform study in Kosi and Dabka river valleys in Kumaun sub-Himalaya: implication of reactivation of thrusts. *Geol J*. <https://doi.org/10.1002/gj.3705>
- Kothiyari G et al. (2017) Discussion of Morphotectonic records of neotectonic activities in the vicinities of North Almora Thrust Central Kumaun Himalaya. *Geomorphology* 285:272–285
- Kothiyari G, Pant PD (2008) Evidences of active deformation in the Northwestern part of Almora, in Kumaun Lesser Himalaya: a geomorphic perspective. *J Geol Soc India* 72(3):353–364
- Kothiyari G, Luirei K (2016) Late quaternary tectonic landforms and fluvial aggradations in Saryu River valley in Kumaun Lesser Himalaya. *Geomorphology* 268:159–176

- Kumar G, Agarwal NC (1975) Geology of the Srinagar Nandprayag area (Alaknanda Valley) Chamoli Garhwal and Tehri Garhwal districts, Kumaun Himalaya, Uttar Pradesh. *Himalayan Geol* 5:29–59
- Lavé J, Avouac JP (2001) Fluvial incision and tectonic uplift across the Himalayas of central Nepal
- Leopold LB et al. (1964) *Fluvial processes in geomorphology*. Freeman, London
- Leopold LB, Wolman MG (1957) River channel pattern: braided, meandering and straight. USGS Professional paper, 282-B
- Luirei K et al. (2016) Quaternary extensional and compression tectonics revealed from Quaternary landforms along Koshi River valley, outer Kumaun Lesser Himalaya. *Uttarakhand Int J Earth Sci* 105:965–981
- Nand N, Kumar K (1989) *Holy Himalaya: a geographical interpretation of Garhwal*. Daya Publisher, New Delhi
- Obruchev VA (1948) “Osnovnye cherty kinetiki i plastiki neotektonik”. *Izv. Akad. Nauk. Ser Geol* 5:13–24
- Pelletier JD, Jon D et al. (2009) Tectonic and structural control of fluvial channel morphology in metamorphic core complexes: The example of the Catalina-Rincon core complex, Arizona. *Geosphere* 5(4):363–384
- Roy S, Sahu AS (2015) Quaternary tectonic control on channel morphology over Sedimentary low land: a case Study in the Ajay-Damodar interfluvies of eastern India. *Geosciences* 6(6):927–946
- Sahu S et al. (2010) Active tectonics and geomorphology in the Sone-Ganga alluvial tract in mid-Ganga Basin, India. *Quat Int* 227:116–126
- Sati SP et al. (2005) Neo-tectonic features and related hazards along Srinagar thrust in Alaknanda Valley, Garhwal Himalay. geological aspect of environment. *Bull Ind Geol Assoc Spl* 38(1&2):53–59
- Sati SP et al. (2007) Geomorphic indicators of neotectonic activity around Srinagar (Alaknanda basin), Uttarakhand. *Curr Sci* 92:824–829
- Semwal S (2018) Channel morphology of the Alaknanda river in Srinagar valley. Unpublished PhD Thesis. HNB Garhwal University, Srinagar (Garhwal), Uttarakhand
- Srivastava RN, Ahmed A (1979) Geology and structure of Alaknanda Valley. *Himalayan Geol* 9:225–254
- Valdiya KS (1976) Himalayan transverse faults and folds and their parallelism with subsurface structures of North Indian Plains. *Tectonophysics* 32, pp 353–386
- Valdiya KS et al. (1992) Active himalayan frontal fault, boundary thrust and Ramgarh thrust. *Southern Kumaun J. Geol Soc India* 40:509–528
- Valdiya KS (2001) Reactivation of terrane-defining boundary thrusts in central sector of the Himalaya: implications. *Curr Sci* 81:1418–1430
- Valdiya KS (1980) *Geology of Kumaon lesser Himalaya*. Wadia Institute of Himalayan Geology Publication, p 291
- Whipple KX (2003) Bedrock river and the geomorphology of active organs. *Rev Earth Planetary Sci* 32:151–185

Significance of Channel Planform Change and Morphometric Indices in the Buri River Basin, India and Bangladesh



Saheli Bhattacharjee, Sunando Bandyopadhyay, and Sunil Kumar De

Abstract The Indian state of Tripura and the adjacent parts of eastern Bangladesh are characterised by six N–S aligned westerly arcuate anticlinal ridges of the Chitragong–Tripura Fold Belt (CTFB), uplifted during the Pleistocene. The Buri (107 km in 2017) originates from the western flank of the CTFB’s Baramura Range (247 m) and drains into the Meghna system of the Ganga–Brahmaputra–Meghna Delta. Maps and images of 1931–34 (Survey of India ‘inch’ maps), 1962 (Corona photos), 1975 (Landsat-1 MSS image), and 2017 (Resourcesat-2 L4-fmx image) show that the river markedly changed its planform during the last 84.5 years. Based on valley directions and characteristics, the Buri is divided into 37 reaches. Of these, sinuosity indices (SI) of 36 are calculated for the four survey/imaging years to determine the extent of change. Shuttle Radar Topography Mission elevation data (3 arc second tiles) of the region are utilised to bring out structural signature on drainage using profile shape, normalised stream length-gradient (SLk) index, and basin asymmetry factor (AF). χ -map of the Buri and its surrounding basins is taken into consideration to observe the topographic stability of this region. Finally, long-term rainfall records close to the Buri Basin (932 km²) are analysed as proxies for change in discharge. The results show that the Buri is antecedent to all anticlinal axes along its course. Overall, its 1931–34–2017 SI decreased in 64% of the reaches (1.58–2.76 to 1.02–1.17). Within the hills, increase in 1931–34–2017 channel SI coincided with high SLk values (>2) as well as profile convexity in two stretches, suggesting neotectonic uplift. In two other convexity zones, the 1931–34–2017 SI decreased contradictorily, possibly due to local aggradation or modification. An AF of 31 indicates that the Buri Basin has a probable tilt to the north. The χ -map of the area shows that the water divide is migrating towards the basin at its headwater region. Any statistically significant change in long-term rainfall records close to the basin is not present. Landuse alterations in the basin is also small, and unlikely to impact planform changes. In its deltaic stretch, the reasons for drastic change in the Buri’s sinuosity index (1.40–4.13

S. Bhattacharjee · S. Bandyopadhyay (✉)
Department of Geography, University of Calcutta, Kolkata 700019, India
e-mail: sunando@live.com

S. K. De
Department of Geography, North Eastern Hill University, Shillong 793022, India

to 1.08–1.26) can principally be ascribed to channelisation that reduced its length by 55% between 1931–34 and 1962; sinuosity of the river is slowly increasing thereafter.

1 Introduction

Among the geomorphic elements of a landscape, river networks are most sensitive to any change in the existing balance between tectonics, climate, and catchment area landuse. In an unstable region, changes in planform of a river are often caused by spurts in subtle tectonic or isostatic activity. Therefore, progressive alterations in channel planforms are widely used as reliable indicators of orogenic or epeirogenic movements in many parts of the world (Seeber and Gornitz 1983; Ouchi 1985; Burbank and Anderson 2012). River planform changes can also be induced by variations in water and sediment discharge due to changes in climatic forcings or landuse characteristics in the basin (Kiss and Blanka 2012); or by a combination of all these factors (Goudie and Viles 2010). Besides channel planform changes, morphotectonic indices, derived from basin elevation and channel gradient characteristics, are commonly used for detecting active deformations, even in a region with a low rate of tectonic activity (Pedrera et al. 2009; Ntokos et al. 2016).

‘Neotectonics’ refers to the study of crustal movements that occurred in the geologically recent past and that may be ongoing today (Stewart 2004). The term ‘Neotectonics’, emerged from the papers of Obruchev in 1936 and 1948, used to denote crustal structures created during the Neogene. It currently purviews to ‘fully explain all the characteristics of the contemporary relief of the land surface of the entire globe’ (Beckinsale and Chorley 1991:171, Chandra 2012).

This article traces the changes in the planform of the Buri, a sixth order stream of the western Chittagong–Tripura Fold Belt (CTFB) during 1931–34—2017 and analyses selected morphometric indices to assess the nature of neotectonic and climatic imprints on the river. Although some previous works exist on tectonic geomorphology on some parts of the CTFB (Bandyopadhyay and De 2009; Dey et al. 2009; De and Bandyopadhyay 2011; Bandyopadhyay et al. 2013; Valdiya and Sanwal 2017), the Buri has been taken up for study for the first time.

2 Study Area

2.1 Location

The 107-km Buri drains some 932 km² between 90°57′–91°35′ E and 23°28′–57′ N. It emanates from the 247-m Baramura Range at an altitude of ~200 m, takes up a general west-southwestward course for its first 72 km (2017 length) up to its debouchment into the deltaic plains through the Rakhia Range at Nayanpur. In this section, the

Buri's course is marked by confined passages towards the source, gradually giving way to broad intervening alluvial and colluvial valleys below 70 m. Bishalgarh, an important town of the Indian state of Tripura (Sepahijala District), is located in this section. As the river enters the Ganga–Brahmaputra–Meghna Delta (GBMD) plains at 10 m, it crosses over into the Bangladeshi district of Comilla and takes up a northwestward course of 35 km up to its outfall into a partially cut-off meander of the Pagla (lower Titas), a spill channel of the Meghna, near Nabinagar (Fig. 1). The course of this cut-off, upstream of its confluence with the Buri, largely degenerated during 1931–34—1962. Its lower part is now maintained by the discharge from the latter. This effectively increased the length of the Buri by 4.6 km. The final 22 km of its course between Kuti and the outfall used to be tidal in 1931–34. Stretches of the Buri is also known as the Bijai in Tripura and the Saida in Bangladesh.

2.2 Geology

After India separated from the eastern Gondwanaland and started to drift north in the early Cretaceous (Lawver et al. 1985), the Indian plate started an oblique and rotational subduction beneath the Burmese microplate that formed the Indo-Burman Ranges (IBR) in the Cenozoic. The remnant ocean basin at the western edge of the Burmese plate was subjected to a 'zipper-like' closure from north to south (Biswas and Agrawal 1992; Steckler et al. 2016). The sediments eroded from the Barail and Naga Hills on the north and the IBR on the east formed an accretionary prism in its arc-trench setting and eventually got folded, faulted, and uplifted in form of the CTFB, mostly during the Pleistocene (Nandy 2001; Maurin and Rangin 2009) (Fig. 2). From west to east, this fold belt is comprised of six major westerly convex anticlinal ridges of increasing altitude and age of deformation—Rakhia, Baramura, Atharamura, Longtarai, Machhlithum and Jampui—separated by the synclinal valleys of Agartala, Khowai, Dhalai, Manu, and Juri–Deo, respectively (Fig. 1b). On its western edge, the Buri flows across the structural grain of the CTFB.

The CTFB is mainly characterised by repetitive successions of fine- and coarse-grained poorly consolidated flysch sediments of four discernible formations belonging to Miocene–Pleistocene with Quaternary alluvial and colluvial deposits in the valleys (Fig. 3). Most anticlines have older formations exposed along their crests (Alam et al. 1990; Nandy 2001; GSI 2011). Sedimentation and tectonic activity of the area initiated from the east and gradually migrated towards the west. Consequently, the intensity of folding and structural complexities also decreases westward, and finally disappears under the alluvial silts and clays of the deltaic plains (Maurin and Rangin 2009; Wang et al. 2014).

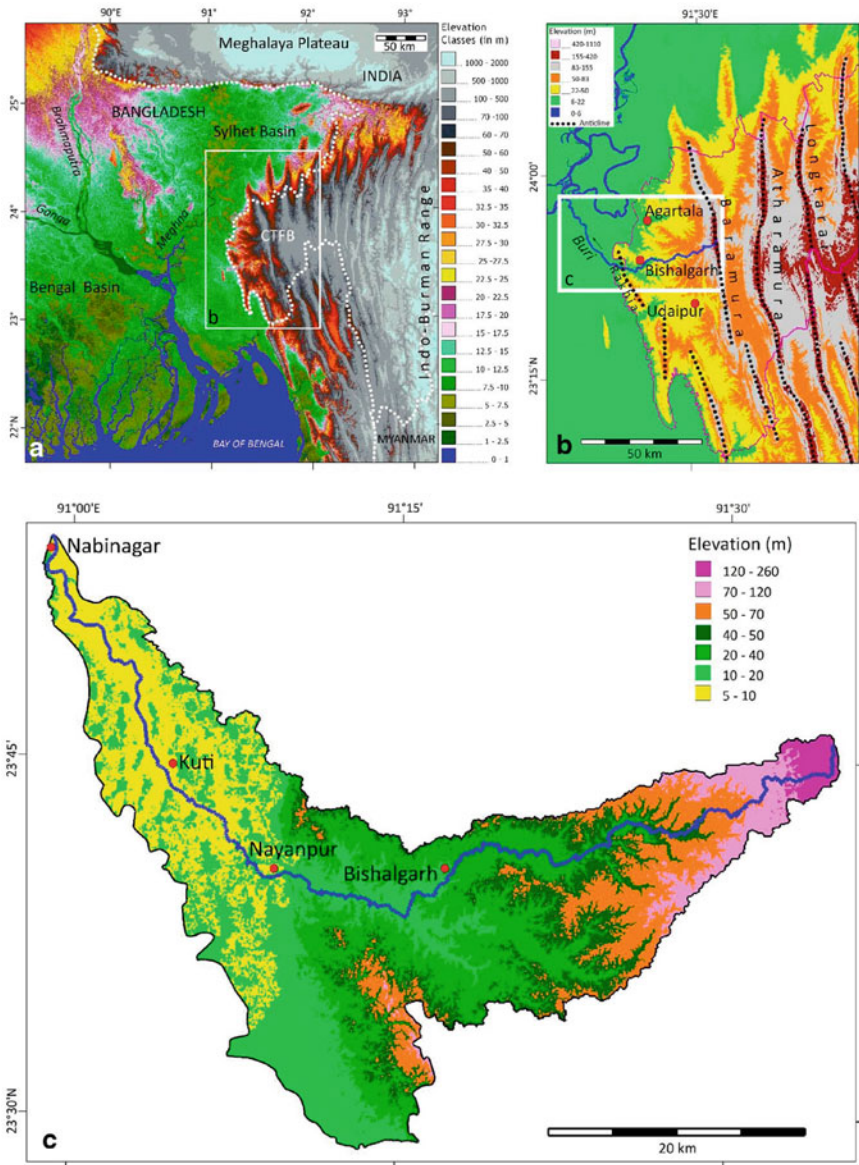


Fig. 1 Physiographic setting of the Buri basin. **a** Chittagong–Tripura Fold Belt (CTFB) located at the eastern margin of the Ganga–Brahmaputra–Meghna Delta. **b** The principal anticlinal ridges forming the northern portion of CTFB. **(c)** The course of the Buri and elevation distribution in its basin. Scales of the maps increase clockwise from upper left; positions of enlarged area shown by white rectangles. *Source* Based on SRTM 3 arc second data of 2000

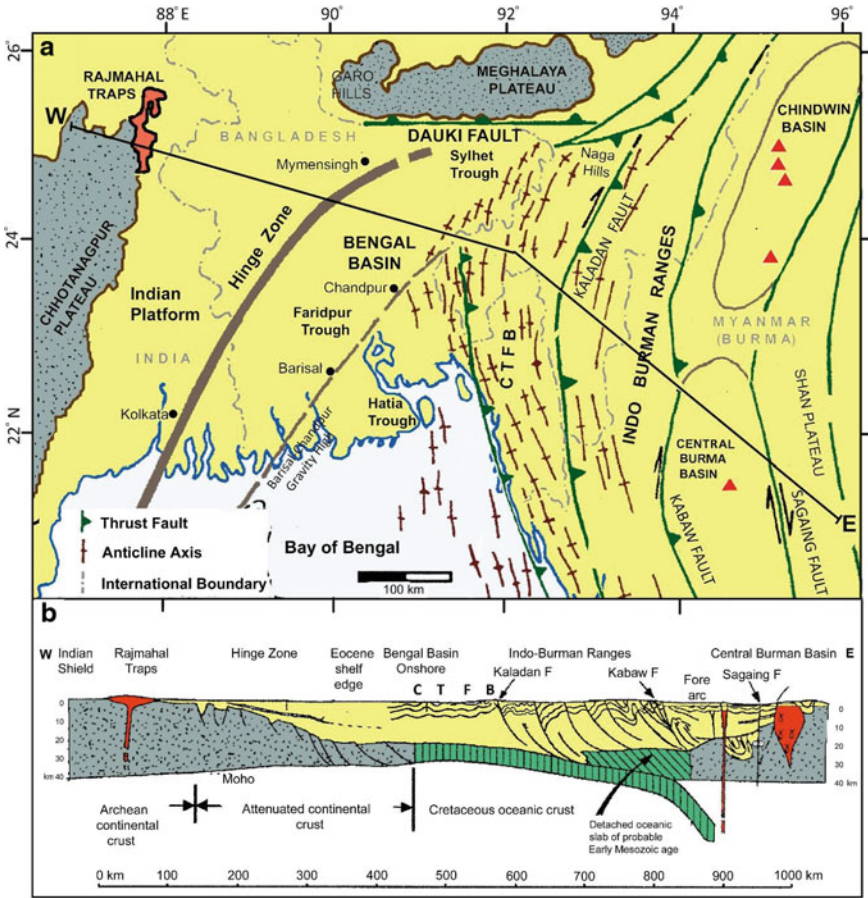


Fig. 2 Tectonic setting of the Chittagong–Tripura Fold Belt (CTFB). **a** Major tectonic and geological features of the Bengal Basin and its surrounding highlands. The Hinge Zone represents the edge of the continental shelf of India. The Barisal-Chandpur Gravity High (BCGH) indicates the transition between the continental and oceanic crusts of the subducting Indian plate. Red triangles denote tertiary volcanic centres. **b** Schematic W–E cross section shows the CTFB region as folded and uplifted sedimentaries formed at the arc-trench location. *Source* Based on Alam et al. (2003). Some elements are incorporated from Nandy (2001), Gani and Alam (2003), and Bandyopadhyay (2007)

3 Materials and Methods

3.1 Maps and Images: Availability

To study the planform change of the Buri, four datasets spanning 84.5 yr have been considered with an average interval of 28 yr. The details of these are shown in

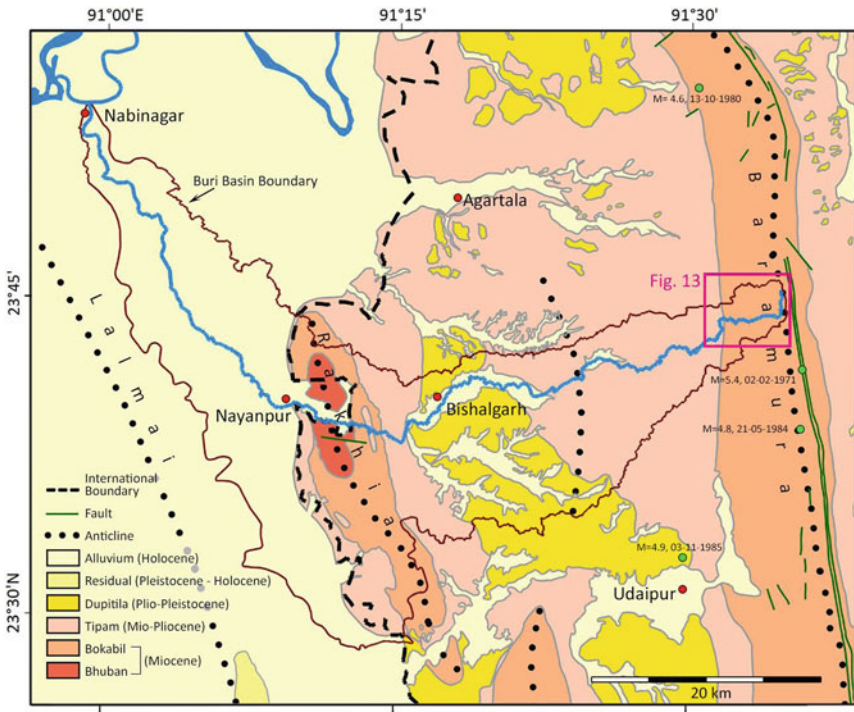


Fig. 3 Geology of the Buri basin and its surrounding area. *Source* Compiled from Alam et al. (1990), Persits et al. (2001), GSI (2011), Wang et al. (2014)

Table 1. Besides these, vector χ (chi) maps of the Buri and its surrounding basins, were retrieved from <https://www.nature.com/articles/sdata2018127> (Giachetta and Willett 2018).

3.2 Maps and Images: Processing and Digitisation

The six Survey of India ‘one inch’ toposheets surveyed in 1931–34 were individually georeferenced using graticule intersections and mosaiced to a file pertaining to Everest spheroid and Universal Transverse Mercator (UTM, zone 46-Q) projection. The available 1974–75 Survey of India ‘metric’ toposheet was similarly rectified. The MSS scene was georeferenced at source and the LISS-4 scenes were obtained as precision orthorectified products on WGS-84 spheroid and UTM projection. These were reprojected to Everest datum and mosaiced where necessary. The three Corona space-photos were orthorectified and mosaiced on the basis of the georectified LISS-4 fmx mosaic. Finally, the SRTM 90-m (3 arc second) elevation data, available on WGS-84, were reprojected to match the referencing of the other maps and images.

Table 1 Maps and images used in the study

Data type ^a	Source ^a	Particulars	Year of survey/date of pass	Resolution/scale
Survey of India 'one-inch' topographical maps	–	Six maps: 79I/13, 79 M/01, 02, 06, 09, 10	1931–34	1:63,360
Corona Photos	USGS: https://earthexplorer.usgs.gov	Three scenes: DS009048070DF268_b, DS009048070DF269_b, DS009048070DF267_b	1962-Nov-24	~2 m
Survey of India 'metric' topographical map	–	One map: 79 M/09	1974–75	1:50,000
Landsat-1 MSS Image	USGS: https://glovis.usgs.gov	One scene: Path-147, Row-43	1975-Mar-27	60 m
Resourcesat-2 LISS-4 fmx Images	NRSC: https://uops.nrsc.gov.in	Two scenes: Path-110, Row-55, Subscenes-B, -D	2017-Feb-12	5 m (resampled at source)
SRTM elevation data	USGS: https://glovis.usgs.gov	Two tiles: n23e90, n23e91	2000-Feb	90 m (3 arc-second)

Note ^afmx: full scene multi-spectral; LISS: Linear Imaging Self Scanner; MSS: Multi Spectral Scanner; NRSC: National Remote Sensing Centre; SRTM: Shuttle Radar Topography Mission; USGS: United States Geological Survey

It requires to be mentioned here that elevation models of finer resolutions could not be used for the Buri Basin due to several data inconsistencies.

The course of the Buri was digitised from the four datasets of 1931–34, 1962, 1975, and 2017 following the mid-line between riverbanks as channel mid-lines remain mostly unchanged even during floods (Friend and Sinha 1993). The 1974–75 Survey of India 'metric' topographical map covered only a part of the Buri Channel and was referred to as supplementary data of the 1975 MSS image.

The 2000 SRTM elevation data were utilised to bring out morphometric heterogeneity of the basin by bringing out the Buri's basin boundary, long profile shape, normalised stream length-gradient (SLk) index, and basin asymmetry factor (AF).

All georeferencing, mosaicing, and digitisation of the maps and images were carried out using Geomatica v2015 software. ArcGIS v10.3.1 was used for extraction of morphometric parameters from the elevation model. Presentation of all statistical data was done through Microsoft Excel v365.

3.3 Extraction of Morphometric Indices

3.3.1 Basin Boundary Extraction

The Buri's basin boundary was auto-extracted from the 2000 elevation data. Minor adjustments of the perimeter were done to preserve compatibility to drainage configuration close to its outfall locality.

3.3.2 Channel Reach Demarcation

Based on the breaks in the Buri's valley directions and adjacent topography, its course was divided into 37 reaches (Fig. 5). Among these, Reaches 1–4 represent the Buri's flow through the Baramura Hills, Reaches 5–28 through confined valleys, and Reaches 29–36 through the GBMD plains. The lowermost section of the Buri that got extended due to degeneration of the upper Pagla (see Sect. 2) was considered as Reach 37. This reach was not included in the comparative study of sinuosity indices.

3.3.3 Sinuosity Index

Sinuosity index is used for determining the degree of curvature of a channel. This work followed the relationship proposed by Schumm (1963):

$$\text{Sinuosity Index (SI)} = \text{Channel Length/Valley Length}$$

The channel length is measured along the midline of the riverbanks between two selected points and the valley length is the straight-line distance between the same two points. SIs were calculated for Reaches 1–36 for the four mapping years (Fig. 5). Changes in reach-specific values of SI obtained for these four years are shown in Fig. 6.

3.3.4 Profile Analysis

The long profile of the Buri was computed on the basis of its 2017 course and 2000 elevation data. The extracted profile line was smoothened by running 80-pixel ($\cong 7.2$ km) moving average. This is represented in Fig. 7, with the zones of convexity indicated in it.

3.3.5 Normalised Stream Length–Gradient Index

Stream Length–Gradient Index (SL) is used for identifying surface signature of tectonic activity and geology of a region. Hack (1973) proposed Stream Length–Gradient Index (SL) for a channel reach using the relationship:

$$SL = \frac{\Delta H \times L}{\Delta L}$$

where, ΔH is the change in elevation of the reach, L is the total channel length from the midpoint of the reach to the highest point on the channel, and ΔL is the length of the reach. $\Delta H/\Delta L$ is the reach slope or gradient.

However, SL Index, per se, often proves inappropriate for comparing rivers of different lengths, as its value depends on river length. Therefore, to normalise the SL index, the SL value of each reach is divided by the gradient index of the entire river profile (k), which returns more reliable results for identifying long profile anomalies (Seeber and Gornitz 1983; Pérez-Peña et al. 2009; McCleary et al. 2011). McCleary et al. (2011) used the following expression to determine k :

$$k = (h_s - h_f)/\ln(L_t)$$

where, h_s denotes the river head elevation, h_f is the elevation of the river mouth, \ln is natural logarithm, and L_t is the total length of the river. The values of normalised stream length–gradient index (SL k) are positively correlated with steepness of channel profiles. The SL k indices of the 37 reaches of the Buri were derived using its 2017 planform and 2000 elevation data.

3.3.6 Asymmetry Factor

Asymmetry Factor (AF) is used for determining topographic tilt of a drainage basin in order to understand its tectonic deformation (Hare and Gardner 1985). It uses the following formula:

$$AF = (A_r/A_t) \times 100$$

where, A_r is the drainage area right of the main channel facing downstream, and A_t is the total area of the drainage basin.

If AF is >50%, the channel is positioned close to the left divide of the drainage basin, length of the tributaries are usually longer in the right side of the basin than on the left, and the basin is left-tilted; AF < 50% reverses these observations. AF = 50% indicates little or no tilting perpendicular to the direction of the master stream (Keller and Pinter 2002). AF values vary significantly under the effects of tectonic renewal

or strong lithologic control (Ntokos et al. 2016). To obtain AF of the Buri, its basin boundary extracted from the 2000 elevation data and the 2017 channel configuration were used.

3.3.7 Chi Index

Willett et al. (2014) proposed the idea of landscape equilibrium through divide migration among drainage basins. The quantity χ (chi) is calculated from digital elevation data and it provides a measure of the length of a channel or the height of a point in the channel, normalised for basin area. In a tectonically active region having similar physical property, divides of a drainage basin having lower value of χ tends to move towards the drainage basin with larger χ value to reach equilibrium. The χ values of the Buri and its adjacent channel networks were retrieved from <https://www.nature.com/articles/sdata2018127#ref-CR33> (Giachetta and Willett 2018).

3.4 Analysis of Rainfall Trends

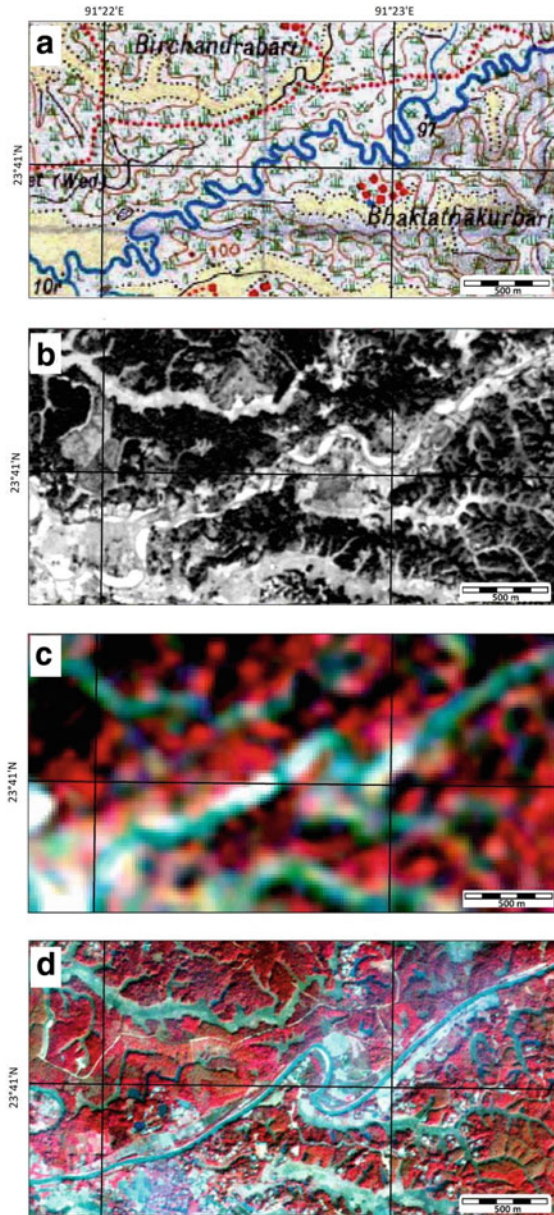
Annual rainfall records of the two nearest India Meteorological Department stations of the Buri Basin, at Agartala (14 km from basin, on the north) and Udaipur (15 km, on the south) were obtained for 1953–2013 (61 yr, $n = 56$) and 1938–2003 (66 yr, $n = 64$), respectively. These data were trend analysed to get some idea on long-term discharge variation of the Buri, because any information on discharge of the river was unobtainable.

4 Results

The results obtained from the analyses of the maps, images, elevation, and climatic data are presented in Figs. 4, 5, 6, 7, 8, 9, 10, 11, and Table 2.

Between 1931–34 and 2017 (84.5 yr), the Buri tended to shorten course by lowering its sinuosity in 25 out of 36 reaches (Figs. 5 and 6). E.g., in Reach 17 between Nabachandrabari and Gholaghati, its length decreased from 9.45 km to 5.64 km and sinuosity from 2.1 (meandering) to 1.2 (sinuous). In Reach 20 between Sipahijala and Kasba, length of the river reduced from 4.46 km to 3.09 km and sinuosity from 2.0 (meandering) to 1.3 (sinuous). In Reach 33 near Kutí, the channel shortened from 8.48 km to 4.37 km and the sinuosity from 2.15 (meandering) to 1.09 (straight). The shortening was most pronounced in its lower stretch over the GBMD plains. Increase in sinuosity, on the other hand, was detected near the source (Reaches 1–8) and in the mid-section (Reaches 23–25). Overall, the river decreased its length by 30.4% from 154 km (1931–34) to 107 km (2017). If looked into the interim imaging years of 1962 and 1975, sinuosity changes altered direction in a

Fig. 4 Changes in the Buri river sinuosity in Reach 17, represent the databases used in the study. Planforms in **a** 1931–34, **b** 1962, **c** 1975, and **d** 2017. Composite planform of all years and position of Reach 17 are shown in Fig. 5. Source See Table 1



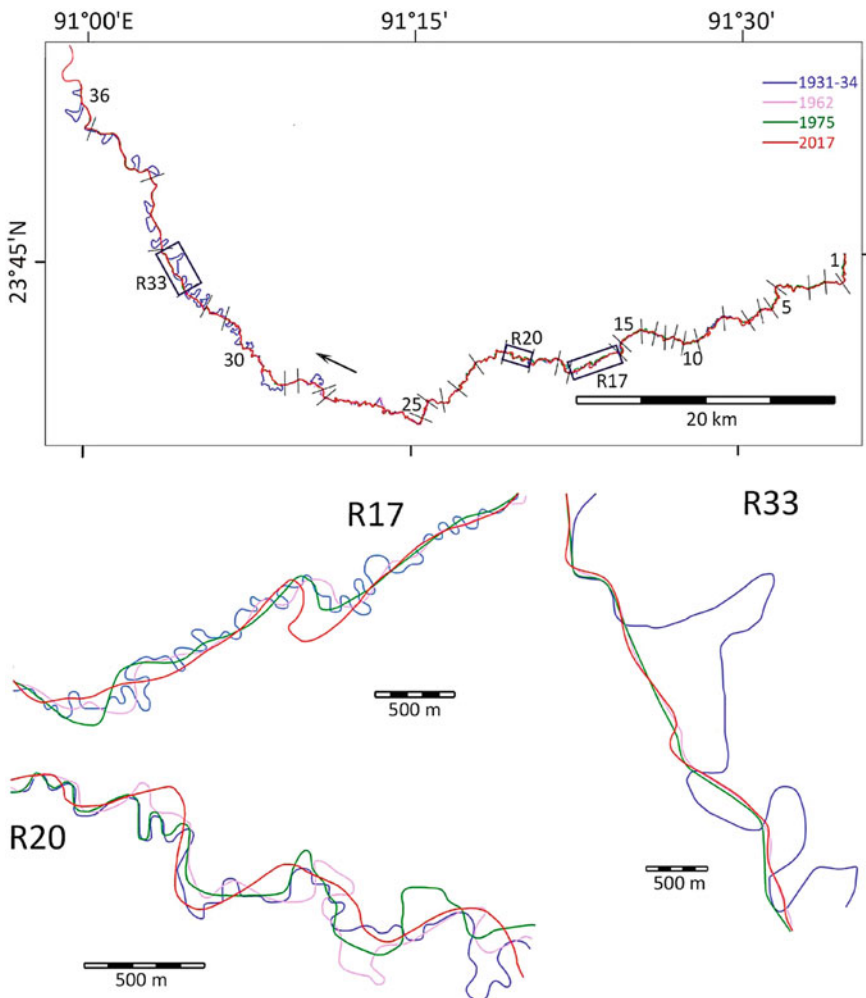


Fig. 5 Changes in the Buri river sinuosity from 1931–34 to 2017. ‘R’ stands for Reach. Numbers indicate Reach IDs. Details of Reaches 17, 20, and 33, indicated by black rectangles in the Buri’s course, are enlarged in the lower part of the diagram. Note the differences in scale in all four maps. *Source* see Table 1

number of sections; most notably in Reaches 5, 7–9, 11, 15, and 18 in the hills and in Reaches 19, 21, 23, and 27 in the plains. In the Buri’s lowermost stretch (Reaches 31–36), although drastic reduction in sinuosity, reducing up to 75% of reach lengths, was recorded between 1931–34 and 1962, slow and continuous rise in sinuosity was seen between 1962 and 2017. The 2017 reach-specific SI of the Buri, classified into very low (SI: < 1.05), low (1.05–1.25), medium (1.25–1.5), and high (>1.5), are shown in Fig. 8.

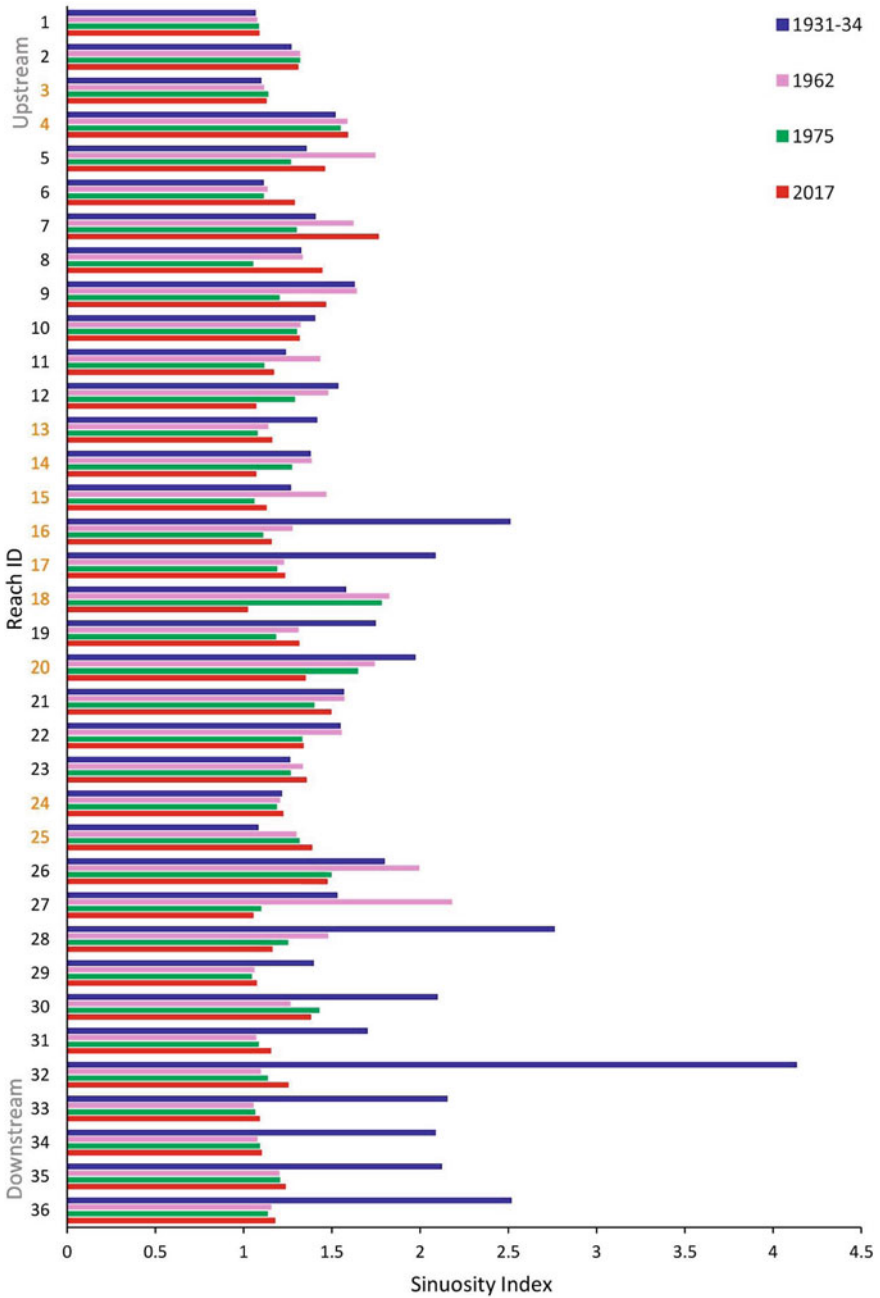


Fig. 6 Reach-specific sinuosity index values of the Buri between 1931–34 and 2017. Reach IDs falling in the four convexity zones of channel profiles are shown in orange. *Source* see Table 1

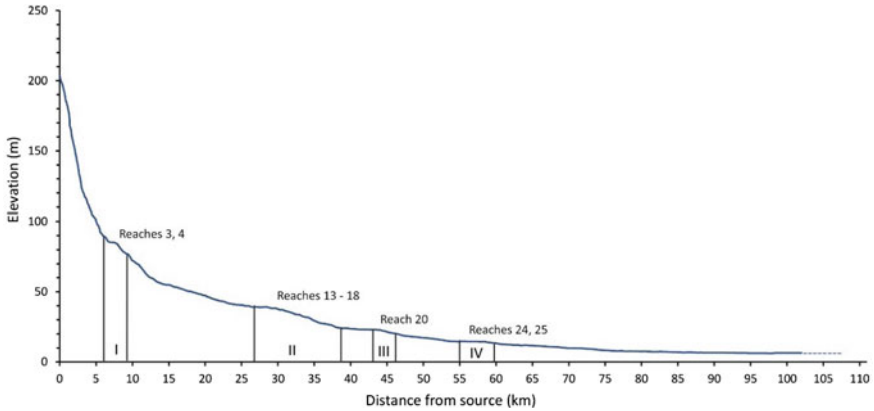


Fig. 7 Long profile of the Buri River. Zones I–IV represent profile convexity that may indicate presence of uplift. *Source* Based on SRTM data of 2000 and Resourcesat-2 LISS-4 fmx data of 2017. See Table 1 for details

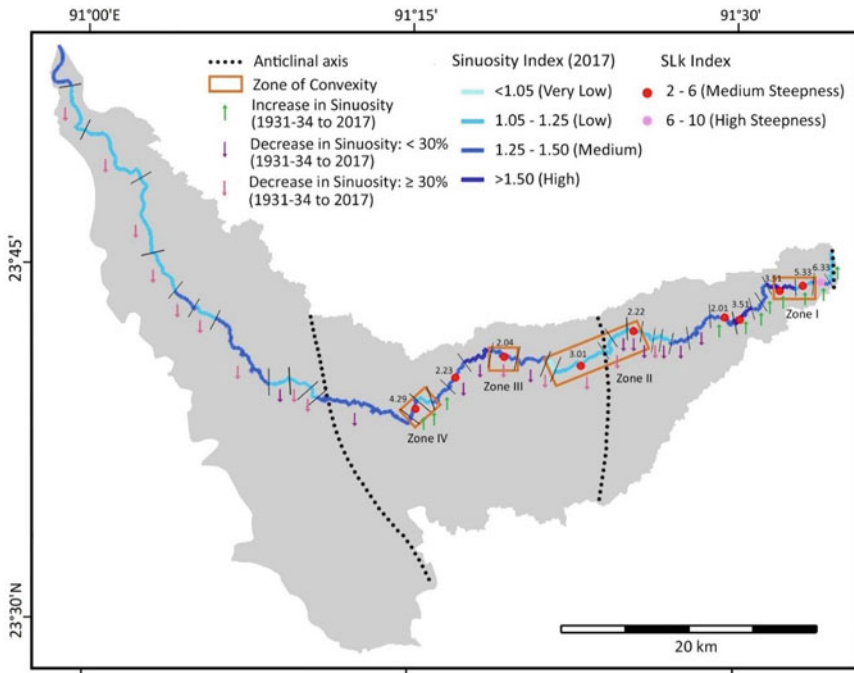


Fig. 8 Composite map of the Buri showing the four profile convexity zones, 2017 reach-specific sinuosity index ranges, SLk indices representing medium to high steepness, and known anticlinal axes. Trends of 1931–34—2017 change in sinuosity indices are shown by vertical arrows. Reach adjacent numbers indicate SLk index values. See text for further explanation. See Fig. 5 for reach IDs

Along the Buri’s long profile, four zones of convexity were detected that are represented by Reaches 3 & 4, 13–18, 20, and 24 & 25 (Fig. 7). Reach-specific SLk indices, as derived from the Buri’s profile analysis can be classified into the groups of <2 (low steepness), 2–6 (medium steepness), and 6–10 (high steepness). Table 2 summarises the main characteristics of the Buri’s reach-wise sinuosity with salient features of its profile convexity and SLk indices. Figure 8 spatially overlays these attributes over the Buri’s 2017 SI and trends of 1931–34—2017 SI change.

AF of the Buri Basin was found to be 31.02 (Fig. 9), which denotes that it is asymmetric and tilted towards the right (north).

Classification of the drainage networks of the Buri and its surrounding basins according to their χ values showed marked discrepancy between the headwaters of the Buri and the streams of the Khowai basin on their opposite side (Fig. 10). The higher values of the Buri (18.59–20.02) compared to the Khowai basin (12.37–14.30) designate the former as the ‘victim’ and the latter as the ‘aggressor’. This denotes that the drainage divide between the two basins is shifting westwards along the crest of the Baramura Range, towards the Buri’s direction.

Finally, long-term rainfall records of the Buri Basin region (Fig. 11) showed average decrease of 3.2 mm/yr towards the north of the basin (Agartala) and average

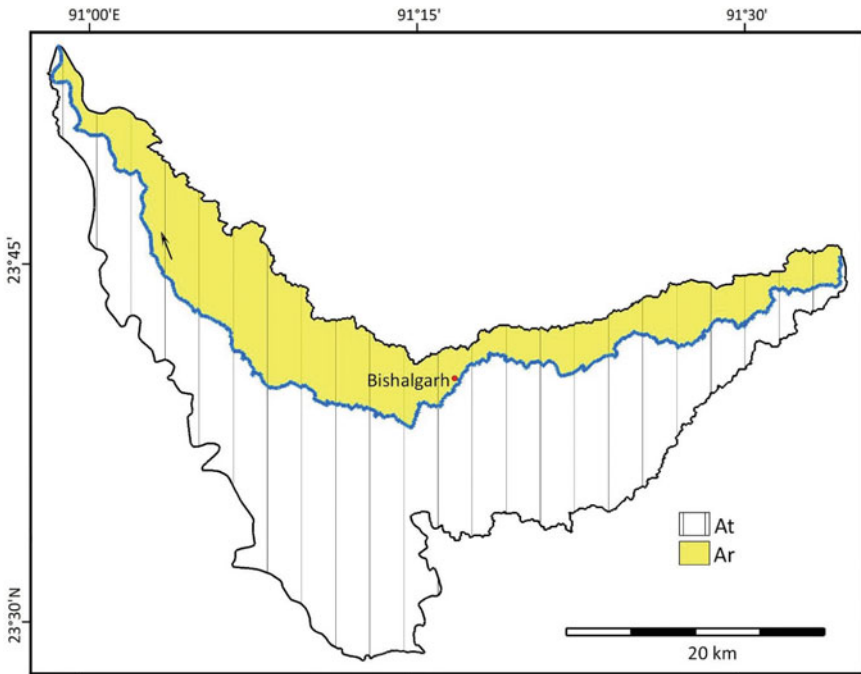


Fig. 9 Topographic asymmetry of the Buri Basin. ‘At’ and ‘Ar’ stand for total basin area and area of the basin to the right of the main channel facing downstream, respectively. *Source* Based on SRTM data of 2000 and Resourcesat-2 LISS-4 fmx data of 2017

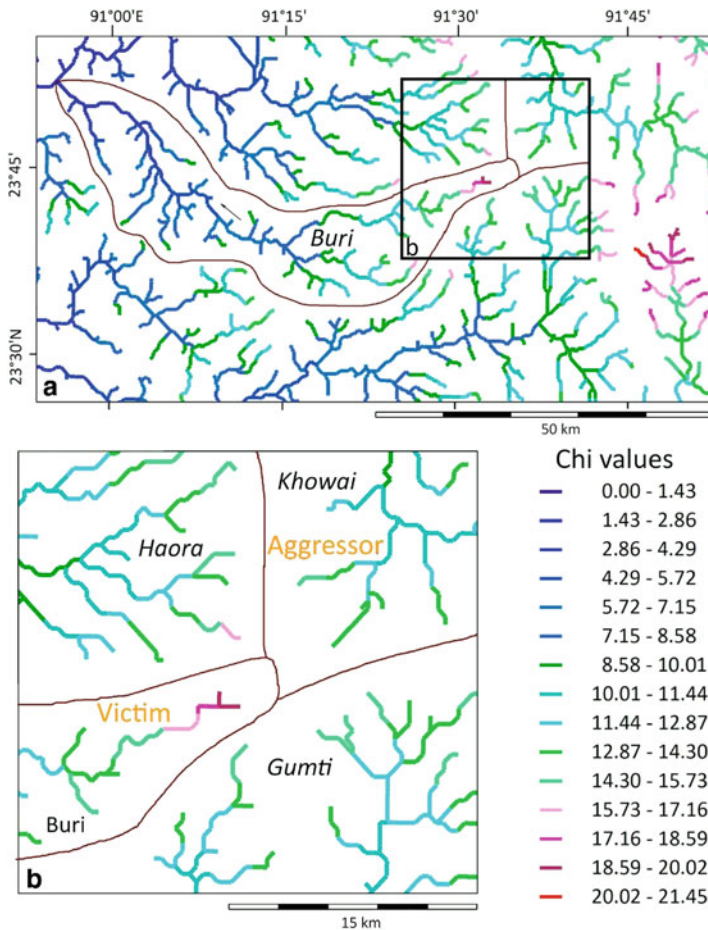


Fig. 10 χ values of Buri and its surrounding basin. See text for explanation. *Source* Data from <https://www.nature.com/articles/sdata2018127#ref-CR33>

increase of 6.2 mm/yr towards the south (Udaipur). Both trends, however, are statistically insignificant, but at $p = 0.053$, the trend for Udaipur is barely so. If these trends are projected to the timespan of data availability, the regions adjacent to northern and southern boundaries of the Buri basin register a net decrease of 187 mm (8.9% of average annual rainfall of 2102 mm) and net increase of 400 mm of rains (19.2% of average annual rainfall of 2080 mm), respectively.

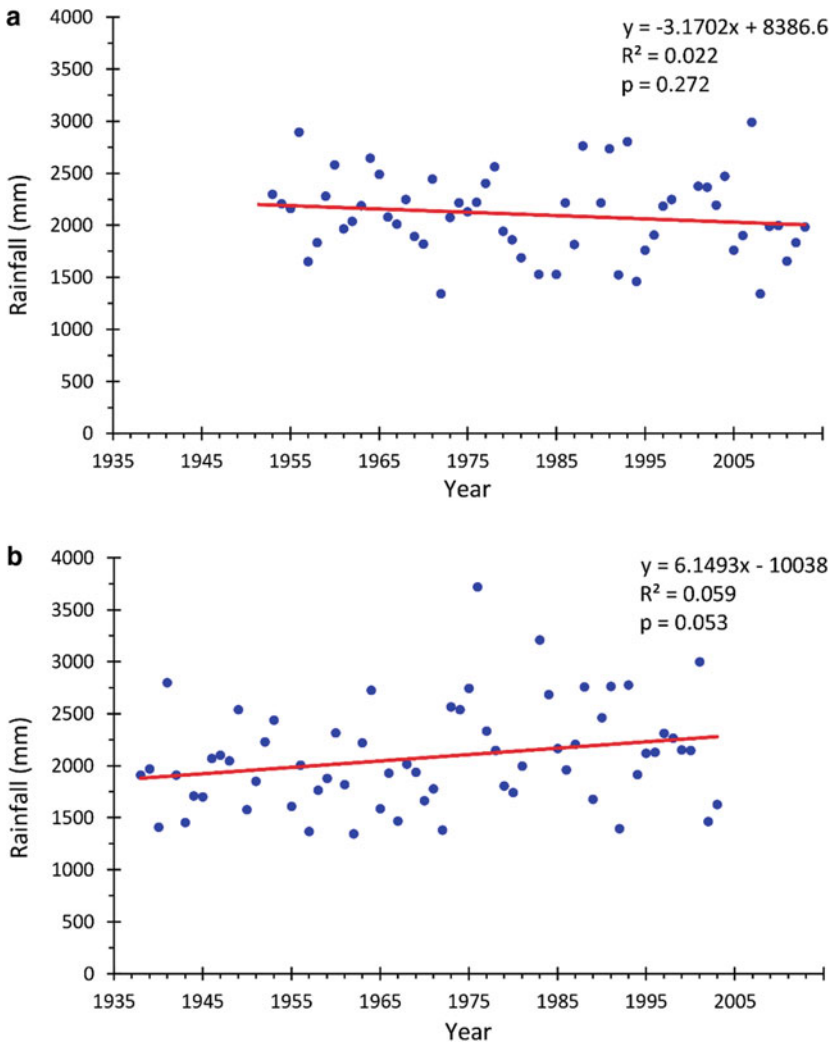


Fig. 11 Rainfall trends of **a** Agartala and **b** Udaipur from 1953–2013 (61 yr, n = 56) and 1938–2003 (66 yr, n = 64) respectively. *Source* India Meteorological Department

5 Discussion

Decrease in sinuosity of a channel is usually caused by reduction in its slope and discharge of water and sediments—acting separately or in unison (Knighton 1998; Holbrook and Schumm 1999). These, in turn, are regulated by tectonics, precipitation and land use transformation. Tectonic change of an area can be gradual as well as episodic, effected by earthquakes. In terrains with high relative relief, earthquakes also cause landslides that augment sediment loads of the channels.

Table 2 Morphometric parameters of the Buri: Reach-specific characteristics

Reach Id ^a	Overall change in sinuosity: 1931–34—2017	Long profile convexity zones	Reaches with medium and high steepness
1–4	Slight increase	Zone I: Reaches 3, 4	Reaches 2, 3, 4
5–8	General increase with decrease between 1962 and 1974–1975	–	Reaches 7, 8
9–22	Overall decrease in sinuosity, with increase in some stretches during 1931–34—1975, and 1962–2017	Zone II: Reaches 13–18, Zone III: Reach 20	Reaches 14, 17, 20, 22
23–25	Increase	Zone IV: Reaches 24, 25	Reach 25
26–28	Decrease	–	–
29–36	Major decrease between 1931–34 and 1962, followed by increase	–	–

Note ^aSee Fig. 5 for position of the reaches

Short-term vertical subsidence and uplift rates of the CTFB synclines and anticlines measured at six places during 2003/2007–2013 using Global Positioning System (Fig. 12) indicate that these rates vary between (–) 4 mm/yr and (+) 6 mm/yr (Reitz et al. 2015). Such high rates would have considerable influence on the rivers of the region. Earthquake records from the vicinity of the Buri Basin (GSI 2011) show occurrence of four events with magnitudes 4.6–5.4 between 1971 and 1985 (Fig. 3). The events within this magnitude range only cause minor damage, and can hardly have any direct or indirect impact on channel modification. There is no record of any other notable earthquake from the region during 1931–34—2017 or some years preceding 1931–34.

An ideal graded river produces a smooth, concave-upward curve without any irregularities (Morisawa 1968). Conversely, a river profile having convexities indicates topographic anomaly that generally suggests locations of neotectonic uplift, which decreases rate of channel downcutting in absolute terms. Because channel gradient and sinuosity are positively correlated, decrease in SI occurs on the upstream side of the uplift and increase on the downstream side (Ouchi 1985).

As shown in Figs. 1 and 3, the Buri flows transverse to the structural grain of the CTFB and its path is associated with three active anticlinal axes. The river originates at the Baramura anticline, crosses another minor anticline at the central part of its upland course and breaks through the Rakhia anticline into the GBMD plains. The reach-specific 2017 SI values, direction of changes in SI during 1931–34—2017, recent profile convexity zones (CZ), and SLk indices are overlaid on the anticline axes in Fig. 8.

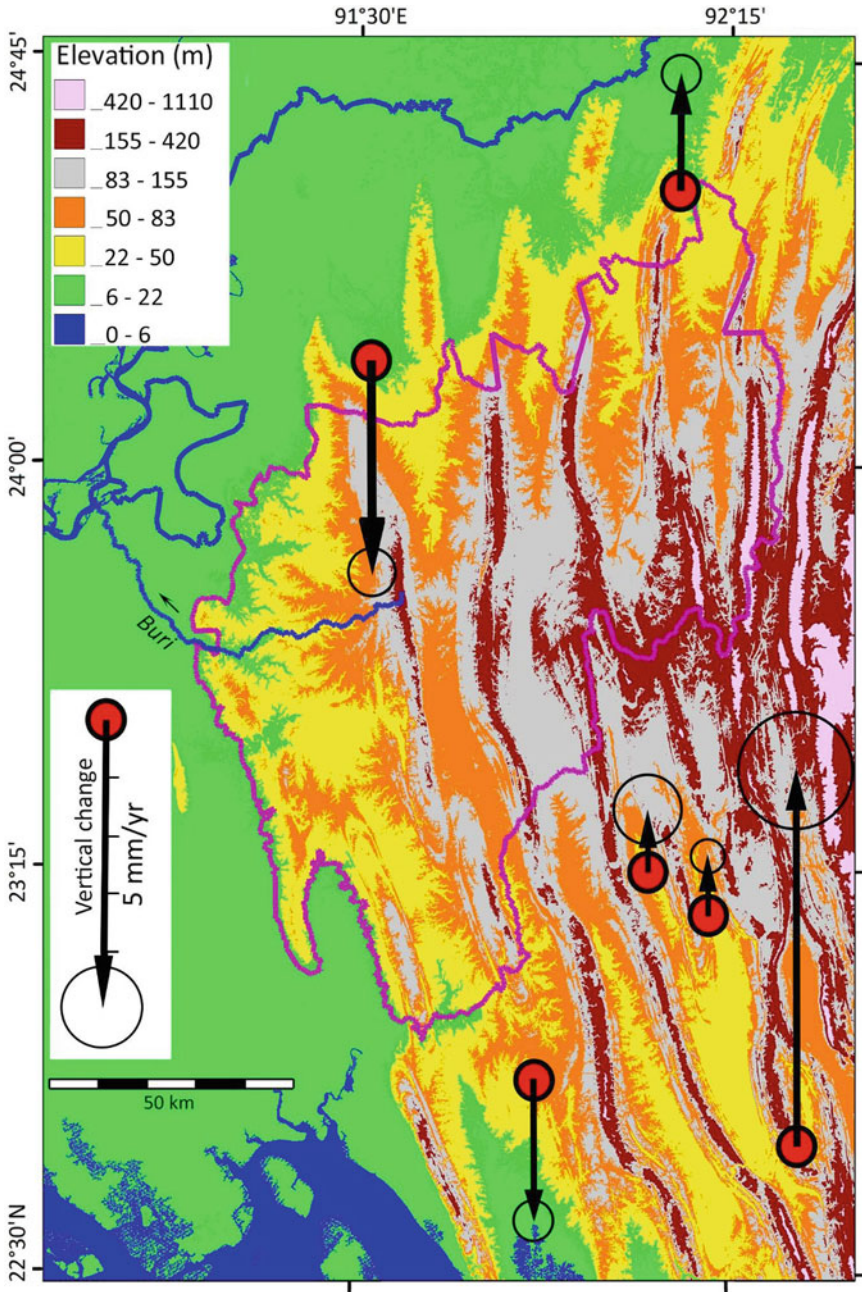


Fig. 12 Short-term subsidence and uplift rates in CTFB region measured from Global Positioning System observations from 2003/2007 to 2013. Hollow circles around the arrowheads represent 2σ uncertainty level. *Source* Elevation model from 2000 SRTM 3 arc second data, vertical change values from Reitz et al. (2015)

The reaches close to the Baramura anticline and the source region of the Buri show low but slightly increasing SI and high SLk values, as can be anticipated in the downstream of an active zone of uplift. The χ -map of this region indicates that the divide between the headwaters of the Buri and the Khowai is moving towards the former due to its steeper hydraulic gradient (Fig. 10). The overall alignment of the Buri shows structural control in its reach over the Baramura. It flows parallel to the strike for the first 2.4 km, before turning west. Valley development by differential erosion of soft sediments intercalated between two resistant strata in the western limb of the Baramura anticline was reported before (De and Bandyopadhyay 2011). Similar lineaments are also seen in the Buri Basin, with the course of the Buri deviated at one (greenish dashed line in Fig. 13), and flowing for 2.7 km along the boundary between the Bokabil and Tipam formations (black dashed line in Fig. 13).

The convexity zone-I (CZ-I) is located towards the lower elevations of the Baramura, over sediments accumulated at the slope break. CZ-II coincides with the central anticline, where the reaches display medium SLk indices, but contradictorily, very low to low SI values, all of which have decreased during 1931–34–2017 both in the upstream and downstream portions of the convexity (Figs. 4, 5 and 6). CZ-III and

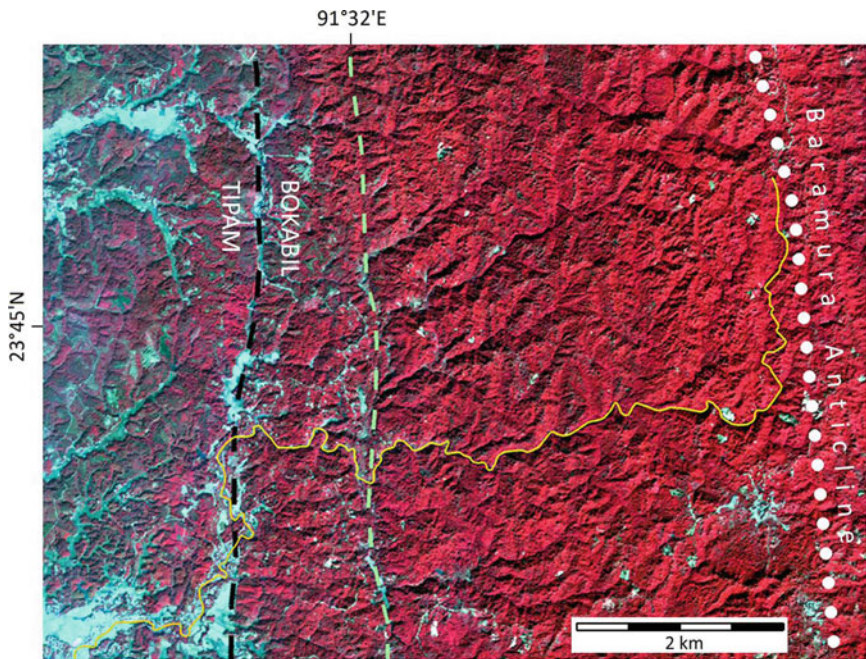


Fig. 13 Standard False Colour Composite of the Buri's stretch across the western flank of the Baramura range showing structural control. The dotted line denotes anticline axis; light green dashed line, a lineament; black dashed line, the boundary between Bokabil and Tipam formations. See Fig. 3 for location within the Buri basin. *Source* FCC from Resourcesat-2 LISS-4 fmx, Path-110, Row-55, Subscene-D; anticlinal axis and formation boundary from GSI (2011)

CZ-IV are comparatively more subtle, and both are associated with low to medium SI and medium SLk. Similar to CZ-II, the 1931–34—2017 SI also got lowered in CZ-III. In CZ-IV, however, the 1931–34—2017 SI changed positively, following decreasing values of the preceding reaches, as can be expected at a zone of uplift. The relatively lower 2017 SI in the upstream section of CZ-IV compared to its downstream part also connotes possibility of uplift in this region.

Thus, while the observed 2017 SI values and the trends of 1931–34—2017 SI change can be matched with CZ-I and -IV, they do not indicate presence of uplift in CZ-II and -III. This denotes that some local factors like channel modification and/or aggradation may have been responsible for the decrease in the SI in CZ-II and -III between 1931–34 and 2017. This also indicates that the anticlinal axis coinciding with CZ-II is inactive at least for the last ~ 85 yr (Figs. 3 and 8). The general decrease in SI in the zones outside the profile convexities in the Buri's upland section can similarly be related to reduction in gradient due to channel aggradation. It is, however, also plausible that the 90-m resolution of the elevation model was unable pick-up the actual channel altitude because of the Buri's narrow width in these reaches and recorded some portions of the surrounding heights. This may have inaccurately rendered convexity to the channel profile at CZ-II and -III.

On the western edge of its upland section, as the Buri crosses the Rakhia Antiform, SI is low and decreasing, but no profile convexity is detected. This connotes that its vertical erosion completely negated any effect of the anticline's uplift along the channel profile.

Downstream of this region, into the GBMD Plains, the drastic 1931–34—1962 changes in SI was due to channelisation of the Buri to steepen its gradient. This was probably undertaken to improve navigability and/or to make the river more efficient in draining floodwaters from the low-lying farmlands and homesteads of the lower basin. As continuous increase in the post-1962 SI of these reaches suggest, the river is again trying to return to its former equilibrium planform.

As stated earlier, age and elevation of the CTFB's anticlinal ridges decline from east to west (Sect. 2). The Buri seemed to have developed on the western flank of the Baramura as it uplifted and was antecedent to the more western anticlines. The westernmost Lalmai antiform of the CTFB (Fig. 3) is currently buried under the GBMD alluvium and has no surface expression except the Pleistocene residuals appearing at the southern edge of Fig. 3. However, it may have directed the northward orientation of the lower Buri that flows parallel to it, occupying a buried synform. GPS positioning showed that the rates of vertical movement vary throughout the CTFB (Fig. 12). The northward tilting of the Buri Basin, as indicated by its AF (Fig. 9), might be a manifestation of this.

This follows that the lower course of the Buri beyond Nayanpur is inherently younger and more transient in nature than its upland section. This is because, its existence depends on the position of the Meghna or one of its offshoots (e.g., the Titas) within its meander belt. An eastward migration of the Meghna would engulf most of the lower Buri, while westward shift of the Meghna would extend it.

The rainfall records from the north (Agartala) and the south (Udaipur) of the Buri Basin indicated conflicting results of fall at 3.2 mm/yr and rise at 6.2 mm/yr

(Fig. 11). If the trend to the south of the Buri (19.2% of the average rainfall in 71 yr) is considered in view of its low p-value (0.053), it would constitute a proxy of increasing runoff from the region, although with a pronounced yearly fluctuation. Rise in water and sediment discharge is positively related to SI change. Therefore, increase in rainfall cannot explain the decrease in SI along most of the Buri, except in the uppermost reaches. Finally, deforestation and spread of agriculture were not widespread in the Buri Basin during the study period, as seen in other areas of the CTFB; the influence of land use alterations is likely to be negligible on its channel planform.

6 Conclusion

The morphometric indices of the Buri—profile convexity, SLk values, AF, and χ -map—all indicated presence of active tectonics in the studied part of the CTFB. The river is antecedent to all anticlinal axes along its course. Association of profile convexity, high SLk values, and SI characteristics indicated uplift at the vicinity of the Baramura Range and ~3 km southwest of Bishalgarh. However, decrease in 1931–34—2017 SI and low 2017 SI downstream of the two profile convexity zones were found to be contradictory to expected relationship, and may have been caused either by recent aggradation / modifications of the channel, or by coarse resolution of the elevation model used. The observed SI changes also cannot be linked to rainfall and landuse alterations of the region. In its deltaic stretch, the drastic change in the Buri's SI was caused by channelisation between 1931–34 and 1962.

References

- Alam M, Alam MM, Curray JR, Chowdhury MLR, Gani MR (2003) An overview of the sedimentary geology of the Bengal Basin in relation to the regional tectonic framework and basin-fill history. *Sed Geol* 155:179–208
- Alam MK, Hasan AKMS, Khan MR, Whitney JW (1990) Geological map of Bangladesh. RF = 1:1,000,000. Geological survey of Bangladesh/United States Geological Survey
- Bandyopadhyay S, De SK (2009) Channel planform change in the northern Chattagram-Tripura Fold Belt, India. Abstracts Volume, 22nd Conference of the Indian Institute of Geomorphologists, University of Allahabad
- Bandyopadhyay S, Saha S, Ghosh K, De SK (2013) Channel planform change and detachment of tributary: a study on the Haora and Katakhal rivers, Tripura, India. *Geomorphology* 193:25–35
- Bandyopadhyay S (2007) Evolution of the Ganga Brahmaputra Delta. *Geograph Rev India* 69(3):235–268
- Beckinsale RP, Chorley RJ (1991) The history of the study of landforms (1896–1950), vol 3. Routledge, London, 496p
- Biswas SK, Agrawal A (1992) Tectonic evolution of the Bengal foreland basin since the Early Pliocene and its implication on the development of the Bengal fan. *Recent Geo-Scientific Studies in the Bay of Bengal and the Andaman Sea. Geolog Surv India Spec Publication* 29:5–19
- Burbank DW, Anderson RS (2012) Tectonic geomorphology. Wiley-Blackwell, Chichester, UK

- Chandra S (2012) Neotectonics and geomorphological regionalisation in India. In: Bandyopadhyay S, Bhattacharji M, Chaudhuri S, Goswami DC, Jog SR, Kar A (eds) *Landforms Processes and Environment Management*. ACB Publications, Kolkata, pp 3–12
- De SK, Bandyopadhyay S (2011) Morphological signatures of fault lines in an earthquake prone zone of southern Baromura hill, north-east India: a multisource approach for spatial data analysis—a critical review. *Environ Earth Sci* 63(2):437–441
- Dey S, Sarkar P, Debbarma C (2009) Morphological signatures of fault lines in an earthquake prone zone of southern Baromura hill, north-east India: a multi sources approach for spatial data analysis. *Environ Earth Sci* 59:353–361
- Friend PF, Sinha R (1993) Braiding and meandering parameters. *Geol Soc Lond Spec Publ* 75:105–111
- Gani MR, Alam MM (2003) Sedimentation and basin-fill history of the Neogene clastic succession exposed in the southeastern fold-belt of the Bengal Basin, Bangladesh: a high-resolution sequence stratigraphic approach. *Sediment Geol* 155:227–270
- Giachetta E, Willett SD (2018) A global dataset of river network geometry. *Sci Data* 5:180127. <https://doi.org/10.1038/sdata.2018.127>
- Goudie A, Viles H (2010) *Landscapes and geomorphology*. Oxford University Press Inc., New York
- GSI: Geological Survey of India (2011) District resource map of West Tripura District, Tripura. RF = 1:250,000
- Hack JT (1973) Stream-profile analysis and stream-gradient index. *J Res US Geol Surv* 1(4):421–429
- Hare PW, Gardner TW (1985) Geomorphic indicators of vertical neotectonism along converging plate margin, Nicoya Peninsula, Coast Rica. In: Morisawa M, Hack TJ (eds) *Tectonic geomorphology. Proceedings of the 15th Annual Binghamton geomorphology Symposium, September 1984*. Allen and Unwin, Boston, pp 123–134
- Holbrook J, Schumm SA (1999) Geomorphic and sedimentary response of rivers to tectonic deformation: a brief review and critique of a tool for recognizing subtle epeirogenic deformation in modern and ancient settings. *Tectonophysics* 305:287–306
- Keller EA, Pinter N (2002) *Active tectonics: earthquakes, uplift, and landscape*. Prentice-Hall Inc., New Jersey
- Kiss T, Blanka V (2012) River channel response to climate- and human-induced hydrological changes: case study on the meandering Hernád river, Hungary. *Geomorphology* 175–176:115–125
- Knighton D (1998) *Fluvial forms and processes: a new perspective*. Arnold, London
- Lawver LA, Scalter JG, Meinke L (1985) Mesozoic and Cenozoic reconstructions of the south Atlantic. *Tectonophysics* 114:233–254
- Maurin T, Rangin C (2009) Structure and kinematics of the Indo-Burmese Wedge: recent and fast growth of the outer wedge. *Tectonics* 28(2):1–21. <https://doi.org/10.1029/2008tc002276>
- McCleary RJ, Hassan MA, Miller D, Moore RD (2011) Spatial organization of process domains in headwater drainage basins of a glaciated foothills region with complex longitudinal profiles. *Water Resour Res* 47:W05505
- Morisawa M (1968) *Streams: their dynamics and morphology*. McGraw-Hill, New York
- Nandy DR (2001) *Geodynamics of Northeastern India and the Adjoining Region*. ACB Publications, Kolkata
- Ntokos D, Lykoudi E, Rondoyanni T (2016) Geomorphic analysis in areas of low-rate neotectonic deformation: South Epirus (Greece) as a case study. *Geomorphology* 263:156–169
- Obruchev VA (1948) Main features of the kinetics and plastics of neotectonics (in Russian). *Izvestiya Akademii Nauk SSSR, Seriya Geologycheskaya* 5:13–24
- Ouchi S (1985) Response of alluvial rivers to slow active tectonic movement. *Geol Soc Am Bull* 96:504–515
- Pedrerá A, Pérez-Peña JV, Galindo-Zaldívar JG, Azañón JM, Azor A (2009) Testing the sensitivity of geomorphic indices in areas of low-rate active folding (eastern Betic Cordillera, Spain). *Geomorphology* 105:218–231

- Pérez-Peña JV, Azañón JM, Azor A, Delgado J, González-Lodeiro F (2009) Spatial analysis of stream power using GIS: SLk anomaly maps. *Earth Surf Process Landforms* 34:16–25
- Persits FM, Wandrey CJ, Milici RC, Manwar A (2001) Digital Geologic and geophysical data of Bangladesh. United States geological survey open-file report 97–470-H. <https://doi.org/10.3133/ofr97470H>
- Reitz DM, Pickering LJ, Goodbred LS, Paola C, Steckler SM, Seeber L, Akhter HS (2015) Effects of tectonic deformation and sea level on river path selection: theory and application to the Ganges-Brahmaputra-Meghna river delta. *J Geophys Res* 120:671–689
- Schumm SA (1963) Sinuosity of alluvial rivers on the Great Plains. *Geol Soc Am Bull* 74(9):1089–1100
- Seeber L, Gornitz V (1983) River profiles along the Himalayan arc as indicators of active tectonics. *Tectonophysics* 92:335–367
- Steckler MS, Mondal DR, Akhter SH, Seeber L, Feng L, Gale J, Hill EM, Howe M (2016) Locked and loading megathrust linked to active subduction beneath the Indo-Burman Ranges. *Nat Geosci* 9:615–618. <https://doi.org/10.1038/NNGEO2760>
- Stewart JS (2004). Neotectonics. In: Goudie AS (ed) *Encyclopedia of geomorphology*, vol 1, Routledge, London, p 1156
- Valdiya KS, Sanwal J (2017) Orogenic belt of India–Myanmar border ranges. In: Valdiya KS, Sanwal J (eds) *Neotectonism in the Indian subcontinent: landscape evolution*. *Developments in Earth Surface Processes*, vol 22. Elsevier, pp 39–150. <https://doi.org/10.1016/B978-0-444-63971-4.00005-0>
- Wang Y, Sieh K, Tun ST, Lai K-Y, Myint T (2014) Active tectonics and earthquake potential of the Myanmar region. *J Geophys Res Solid Earth* 119(4):3767–3822. <https://doi.org/10.1002/2013jb010762>
- Willett SD, McCoy SW, Perron JT, Goren L, Chen CY (2014) Dynamic reorganization of river basins. *Science* 343:1248765

Morphotectonic Expressions of the Drainage Basins and Channel Long Profile Forms on a Selected Part of Sikkim-Bhutan Himalayas



Ujwal Deep Saha , Nilanjana Biswas , Sushonova Mondal ,
and Soma Bhattacharya 

Abstract This study is an endeavour for analysing the neotectonic signatures reflected at basin scale for few selected rivers in the eastern part of Himalayas through the application of morphotectonic indices. River catchments around the Jaldhaka re-entrant have been considered in this study due to its proven sensitivity to neotectonic perturbations. Since, the impact of neotectonics has already been sensed on the piedmont segment, the nature of sensitiveness of the fluvial forms at the entire catchment scale to tectonic deformations has been the focal theme of this study. The selection of the eleven morphotectonic indices was done pondering on three major geomorphic perspectives; basin form components, basin and valley relief components and channel long profile form parameters. The nature of the geomorphic signatures found at the basin scale, river valleys and along the river courses have steered towards an ongoing adjustment of the fluvial units with active tectonism. Invariably the catchments are experiencing a state of dynamic equilibrium where adjustment between the fluvial activity and tectonic upliftment along the major thrusts is characteristic of fluvial form modifications within the studied catchments. The neotectonic perturbations have its indentations reflected in the channel long profile form adjustments with characteristic differences of channel responses related to different expressions of surface warping. Spatial associations of the knick points has been observed in a close correspondence with the Himalayan thrusts and surface deformations, developed on the alluvial reaches of the foredeep plain are explicitly associated with the neotectonic twitching.

Keywords Drainage basin · Himalayas · Morphotectonics · Neotectonics · Long profiles

U. D. Saha
University of Calcutta, Kolkata 700073, India

N. Biswas (✉)
Vivekananda College for Women, Kolkata 700008, India

S. Mondal
SACT-I, Surendranath College for Women, Kolkata 700009, India

S. Bhattacharya
Vivekananda College for Women, Kolkata 700008, India

1 Introduction

Probing the geomorphological parameters of river catchments helps to analyse the modification of surface forms where alongside with different other factors, tectonics plays an important part (Holbrook and Schumm 1999). The morphotectonic indices have been proven to be a useful tool to extract the geomorphic expressions developed due to the tectonic impact at various geomorphic tiers within a river catchment (Keller and Pinter 1996). It helps to disclose the nature of continuous competition between the tectonic processes responsible for developing the topographical expressions and the surficial process that tends to modify the surface expressions (Burbank and Anderson 2012). The resultant effects of being tectonically sensitive are immediately reflected in catchment morphometry as well as channel forms. It is because the settings of regional tectonic features or local impact of surface deformations control the evolution process of the fluvial systems that traversing through (Schumm 1986). The basin shape perspective, terrain morphological expressions as well as the evolution stages of the fluvial system along with the long profile form adjustment are characteristically governed by the regional tectonic disposition (Bull and Mcfadden 1977; Cox 1994; Keller and Pinter 2002; Bull 2007). The most suitable spatial extent to apply these indices have been proved to be at the mountainous terrain with associated flat tracts experiencing an ongoing competition between the surface processes and underlying geometry of the active orogens at a catchment level (Bull 2007; Figueiredo et al. 2017; Flores-Prieto et al. 2015; Moussi et al. 2018; Altm 2012; Kashani et al. 2009).

Considering the above-mentioned attributes, the Himalayas are the first place that could strike first within the Indian sub-continent to apply the morphotectonic approach for extracting the signatures of the Quaternary tectonics. The ongoing development of the Himalayas due to the continuous submergence of the Indian plate at a differential rate over the period has been responsible for being pierced with tectonic wrapping and deformations during the Quaternary period (Valdiya 2002). It has resulted in controlling the fluvial systems both at catchment and fluvial scale (Nakata 1989; Valdiya et al. 1984; Valdiya 1986; Lave and Avouac 2000; Kumar and Thakur 2007). In the past couple of decades, several attempts have been conducted to study the tectonic imprints on the Himalayan terrain and its associated forelands using geomorphic indices. Whereas, the North-Western Himalayas has been at the foci of the majority of the initiatives (Sharma et al. 2017; Joshi et al. 2016; Bali et al. 2016; Chatterjee et al. 2019; Goswami and Pant 2008; Kaushal et al. 2017; Malik and Mohanty 2007; Philip and Suresh 2009; Dube and Satyam 2018; Pant and Singh 2017; Phartiyal and Kothyari 2011; Sharma et al. 2017; Singh and Tandon 2008; Viridi et al. 2007). In the recent past, the nature of surface deformations and markers of active tectonism in certain pockets of the Sub-Himalayan part of the Sikkim- Bhutan Himalayas have been attempted to study in detail (Goswami et al. 2012; Guha et al. 2007; Chakraborty and Mukhopadhyay 2013; Kar and Chakraborty 2014; Mukul et al. 2014; Ayaz et al. 2018) but not a single attempt was made to analyse the spatiality of channel responses at catchment tier to active tectonism on a continuous

stretch over this region. Although, the Jaldhaka re-entrant has been talked for its tectonic sensitiveness (Nakata 1972) and above-mentioned works were conducted to identify the tectonic activeness of the rivers mostly on the piedmont plain or mountain-piedmont juncture but not a single efforts being made to characterise the overall catchment scale sensitiveness of the rivers around this region in accumulation. Ayaz and Dhali (2019) had made an effort to analyse the longitudinal characteristics of a few of the rivers selected in this study but no significant relation being shown between the structural elements and relative channel longitudinal form adjustment. Thus, a significant research gap persists within this region in terms of an overall relationship between the Himalayan tectonic perturbations and adjustment of both the channel longitudinal form and catchment character.

In this study, neotectonic sensitiveness of the river catchments on a particular segment of the Eastern Himalayan has been tried to study using selected morpho-tectonic indices, efficient at river catchment scale and the resultant form adjustment of the fluvial systems were adhered by analysing the long profile forms of selected rivers. The regionality of the resultant surface warping due to tectonic impacts and its resultant effects as portrayed in the evolution and form adjustment of the fluvial system, located on a certain part of the Eastern Himalayas has been the focal theme of this work. The shape perspective of the catchment, the competition for dominance between tectonic disquiets and fluvial activity along the mountain front, the relief differentiation at the catchments and the responsive overall channel form were analysed in this study using the concerned geomorphic indices. The regional distribution of certain breaks in the river longitudinal profile as a resultant expression of differential upliftment of and along the mountain fronts, marked using relative slope extension method was considered as the portrayal of the direct response of the rivers to the active tectonism.

2 Study Area

This study deals with eleven selected river catchments located around the Jaldhaka re-entrant. All of these have been originated on the Sikkim-Bhutan Himalayas and drained two major physiographic regions in the eastern part of the Himalayas; i.e. Himalayan crystalline terrain and the associated piedmont surface (Fig. 1).

The Himalayan thrust loading during the process of Himalayan formation has given rise to prominent topographic regions and structural hegemonies over this area (Burbank et al. 1996). The Himalayan thrusts have separated the certain age-specific structural segments of the Himalayas into the specific tectono-geomorphic region along with the outflanking foredeep basin that occurred due to the flexural down buckling along the tertiary depo-centre called the Siwaliks (Yin 2006) (Table 1). Since the convergence between the Asian and Indian plates continues, the development of these tectono-geomorphic regions is still active and hence tectonically sensitive. The Main Boundary thrust has separated the crystalline lesser Himalayan succession from the Tertiary foreland basin succession. The foreland basin succession is partly

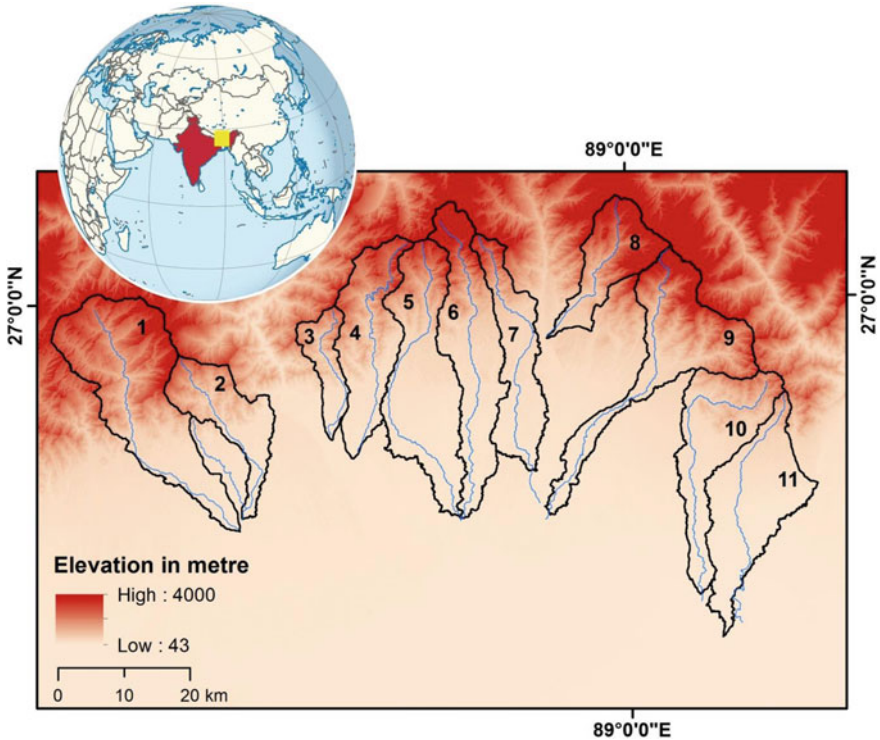


Fig. 1 Location of the study area

composed of the Neogene sedimentary succession called Siwalik (Chakraborty et al. 2020) (Fig. 2). The Himalayan Frontal Thrust has separated this fossiliferous sedimentary formation from the peripheral Quaternary sediment fill basin of the foreland depo region called the foredeep plains. The presence of the Siwalik formation is not continuous in the study area rather, certain gaps persist with the exposure of crystalline middle Himalayan succession to the Quaternary sediments, called the Siwalik Gap (Mallet 1875) (Fig. 3). These gaps were formed due to either the Siwalik being masked out by the Quaternary sediments and eventually the MBT has overridden it or due to lack of lithification that led to the absence of Siwalik formation (Gansser 1964). It has led to the presence of the crustal shortening with widespread sediment depositions called the Himalayan Reentrants (Dasgupta et al. 2013). The study area has been considered based on a prominent reentrant, the Jaldhaka Reentrant, designated by Nakata (1972). Channels originated on the mountain terrain and developed its courses around the axial part of the reentrants before entering the foredeep plain have been considered in this study. Broadly, this study area can be divided into four physiographic regions; the crystalline and sedimentary Himalayan Front or the lithified region, the Bhabar region with rock fragments and Quaternary valley-fill

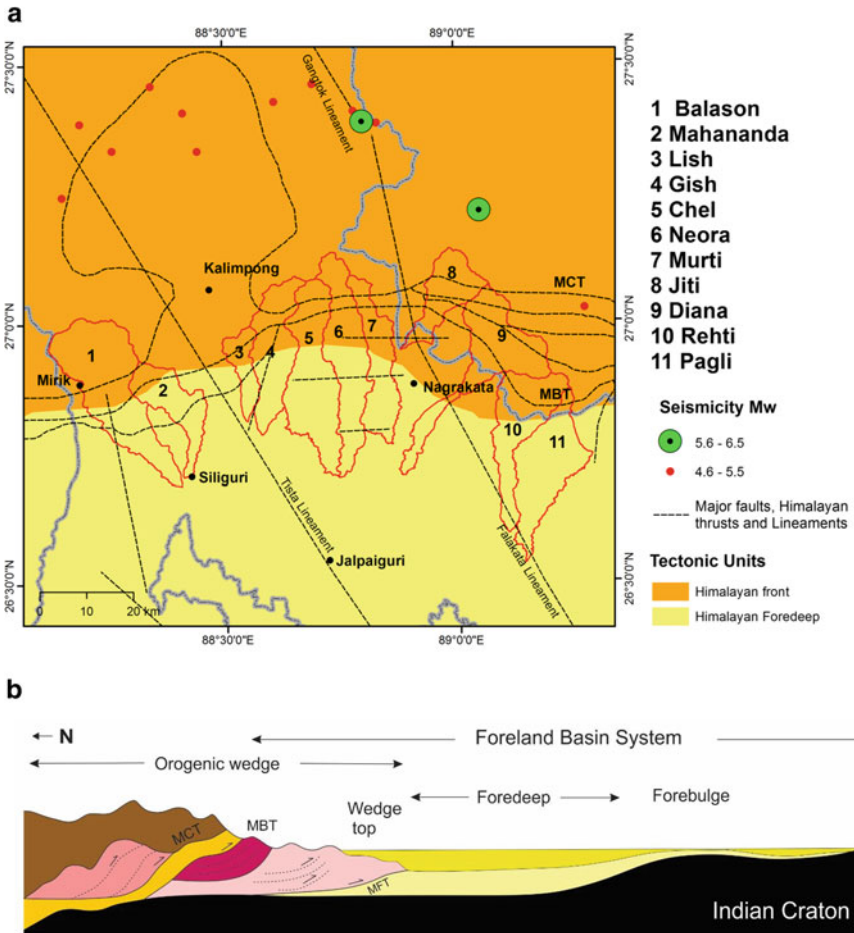


Fig. 2 a Structure and tectonic elements of the study area b Stratigraphic profile across the Himalayan belt and associated foreland (after DeCelles and Giles 1996)

deposits, the Terai region with moist alluvium, and the low lying alluvial plains with finer sediments (Chattopadhyay and Das 1979).

The Himalayan thrusts have impinged the development of the multiple thrust parallel faults on the Himalayan terrain while the Quaternary period has experienced reactivation of multiple thrust parallel and NNW-SSE oriented fault lines on the foreland segment. Thrust parallel topographic ridges with respective elevation drop towards the south, the south-dipping scarps, intraformational thrust faults and the river gorges are the characteristic tectono-geomorphic features on the orogenic wedge of the Himalayas. On the other hand, the association of blind thrusts, flexural deformations and uplifted sedimentary basins, south flanking scarps associated with



Fig. 3 **a** Quaternary fan deposits above the Middle Himalayan crystalline formation (Siwalik gap region) found at the mountain front in the Chel river basin; **b** Siwalik formation (conglomerate) with interbedded sand (Pliostocene fan deposits) found around the mountain-piedmont part of Murti River; DOC: a. 14.3.2019, b. 18.2.2017

the MBT and MFT along with the fault parallel drainage systems have been developed on the foredeep sedimentary basin in the study area (Starkel et al. 2008; Nakata 1972, 1989; Chattopadhyay and Das 1979).

3 Materials and Methods

In this study, the selected eleven drainage basins originated on the Himalayan complex have been studied for the required spatial properties of speckled dimensions. Shuttle Radar Topographic Mission (SRTM) Dem of 30 m and Landsat 8 images captured in 2019 were used for acquiring the elevation properties and concerned spatial parameters, both linear and areal respectively.

3.1 *Pre-processing of the Data Used and Application of Dem*

Correcting the radiometric property of Digital Elevation Model (DEM) and reducing its' elevation error are the essential practices before extracting spatial data from it (Hawker et al. 2018). The radiometry of the dem was corrected by removing the noises from the database using the smoothing technique in Geomatica v12. The radiometry of the dem was required to be corrected for lowering down the RMSE (Root Mean Squared Error). It was performed here by cross-referencing it with 235 ground control points taken from the bare part of the region to outcast the vegetation sensitivity of SRTM DEM. Before comparing the two point clouds, the Toposheet was resampled to WGS 84 datum. The RMSE of the prepared dem at z-direction lies at 0.52 m. Arc-Gis watershed module was used to delineate the basins, located around the Jaldhaka re-entrant. The void points found in the mosaicked dem surface were corrected by using the DEM Fill property in the Hydrology module. To delineate the drainage network, it was approximated by using the D8 algorithm where the flow direction was traced down by the flow away from each pixel to its 8 neighbourhood pixels. The DEM-derived drainage networks were furthered corrected using the Landsat 5 image acquired in 2000. Since the Dem determines the steepest possible path, sometimes it doesn't correspond to the actual river path on the plains. The use of satellite images acquired in 2000 has helped to identify the actual extensions of the channels on the piedmont and also in masking out the vegetation sensitiveness of the C band used in SRTM data.

3.2 *Morphotectonic Indices*

The morphotectonic approach has been a globally putative stream of analyzing the overall control of tectonics at the basin scale (Phartiyal and Kothiyari 2011; Partabian et al. 2016; Sharma and Sarma 2017; Ghosh and Shivakumar 2018; Moussi et al. 2018). In this study, the morpho-tectonic indices were selected based on three major dimension perspectives of the basin. For analyzing the basin shape, Basin shape factor (Bs), Form factor (Bf), Circularity ratio (Cr) and Elongation ratio (Re) was considered. To study the asymmetry perspective of the basin or basin tilt, Topographic

Symmetry Factor (TTSF) has been calculated. In the case for analyzing the basin topographic extremities, Relief ratio (Rr), Topographic Roughness Index (STD) and Hypsometric integral (HI) were computed (Table 1). The linearity and the relative fluvial dominance over the orogenic processes, the Valley floor width to valley height ratio (Vf) and Mountain front sinuosity (Mfs) were calculated. The indices have been elaborated in Table 1. A general understanding of basic geometric and altitude characteristics of the selected basins has been elaborated in Table 2.

3.3 River Longitudinal Profile and Related Indices

The longitudinal profile of a river represents a curve depicting the gradient of the valley with corresponding distances from the source to the mouth. It portrays the geomorphic history of a river basin (Sen 1993; Sinha and Parker 1996; Jain and Sinha 2006; Chen et al. 2006). The channel long profile has been crammed by many researchers to extract the tectonic upshots both at the basin scale and floodplain level (Hack 1957; McKeown et al. 1988; Lee and Tsai 2010; Seeber and Gornitz 1981; Lu and Shang 2015; Kale et al. 2013; Moussi et al. 2018). The form of long profiles has been studied using different indices to depict its nature and relative anomalies. The long profiles of the eleven selected rivers were extracted from the DEM after compartmentalising the path into 50 m segments and the downstream points of each segment were converted into a point vector. The x, y and z values of the point vector were converted into a file format that is suitable for MS Excel ('.csv' file format was used). The distances between the points were calculated using the Eq. 1

$$d = \sqrt{\{(x_2 - x_1)^2 + (y_2 - y_1)^2\}} \quad (1)$$

where, d = distance between points X1 and X2, X1 = X—coordinate (in meters) of point X1, Y1 = Y-coordinate (in meters) of point Y1, X2 = X-coordinate of point X2, Y2 = Y-coordinate of point Y2.

3.3.1 Mathematical Models

Curve fitting is one of the most common practices to evaluate the formation of river longitudinal profile. It can be a simple linear, logarithmic, exponential and, power regression models that feature a picture of ongoing processes. The Sum of Squared Errors (SSE) and the Coefficient of determination (R^2) determine the model's best fit with the curve (Lee and Tsai 2010).

$$\text{The Linear function } y = ax + b \quad (2)$$

Table 1 Maps and images used in the study

Properties	Index	Mathematical derivation	Explanations	Source
Basin form and symmetry	Shape factor	L/B Where L = Basin Length, B = Basin Width	Higher values indicate elongation whereas lower values indicate oval and round-shape catchments	After R.E. Horton (1932)
	Form factor (F_f)	$F_f = A/L^2$ Where A = Basin Area, L = Basin Length	Higher values indicate bulging and oval-shaped basin whereas lower values indicate elongated basin	After R.E. Horton (1932)
	Circularity Ratio (C_R)	$C_R = 4\pi A/P^2$ Where A = Basin Area, P = Area of a circle with same basin perimeter	$C_R > 1$; circular form $C_R < 1$; elongated or oval-shaped form	After Miller (1953)
	Elongation ratio (R_e)	$R_e = (2\sqrt{A/\pi})/L_b$ Where, A = Basin area, L_b = Maximum Length of the Basin	$R_e < 0.50$; tectonically active $R_e = 0.50$ to 0.70 ; slightly active $R_e > 0.70$; tectonically inactive	Bull and McFadden (1977)
	Topographic symmetry factor (T)	$T = Da/Dd$ Da is the distance from the channel to the basin midline. Dd is the distance from the lateral basin margin to the basin midline	$T = 0$; symmetric basin with no ambiguities $T > 0$ asymmetric basin	Cox (1994)
Basin relief	Relative relief (H)	$H = (H/P) \times 100$ Where H = Difference between highest and lowest point, P = Perimeter	Determine the degree of dissection	M.A. Melton (1957)
	Relief ratio (R_f)	$R_f = (E_{max} - E_{min})/L_b$ Where E_{max} Maximum = elevation of the basin, E_{min} = Minimum elevation of the basin, L_b = Longest length of the basin	High values of relief ratio indicate steep slope and high relief. In other side low values indicate small ridge with lower degree of slope	Panek (2004)

(continued)

Table 1 (continued)

Properties	Index	Mathematical derivation	Explanations	Source
	Topographic roughness index (STD)	Standard deviation of the elevation value	Magnitude of topographic variability; higher the value greater is the roughness	Klinkenberg (1992)
	Hypsometric integral (HI)	$HI = (H_{\text{mean}} - H_{\text{min}}) / (H_{\text{max}} - H_{\text{min}})$ Where H_{mean} = Average of elevation, H_{max} & H_{min} = Maximum and Minimum elevation of area respectively	$HI > 0.6$ characterise tectonic mobility $HI < 0.6$ indicates mature stage of development	Strahler (1952)
Mountain front	Mountain front Sinuosity (Mfs)	$S_{mf} = (L_{mf}/L_s)$ Where L_{mf} = Length along the edge of the mountain piedmont junction, L_s = Overall length of the mountain front	$S_{mf} < 1.4$ tectonically active areas $S_{mf} = 1.4-3$ slightly active areas $S_{mf} > 3$ inactive areas	Bull and McFadden (1977)
	Valley width to height ratio (Vf)	$V_f = 2V_{fw} / \{(E_{ld} - E_{sc}) + (E_{rd} - E_{sc})\}$ Where, V_{fw} = width of the valley floor, E_{ld} & E_{rd} = Elevation of left and right valley divides respectively, E_{sc} = Elevation of valley floor	$V_f < 1$ characterise active incision $V_f > 1$ active deposition into a broad valley	Bull and McFadden (1977)

$$\text{The Exponential function } y = ae^{bx} \quad (3)$$

$$\text{The Logarithmic function } y = a \ln x + b \quad (4)$$

$$\text{The power regression model } y = ax^b \quad (5)$$

Here, y stands for elevation and x is for length. The mathematical models of curve fitting are based on the relationship between the grain sizes of sediments with channel capacity. When the channel bed grain size is greater than the transportation capacity of the river, the long profile shows a low degree of concavity and best fit by linear function curve. If the deposition and transportation of a stream experiences a dynamic equilibrium state, the long profile would fit the exponential function. Whenever the profile is subjected to follow a graded shape, the sediment size of the stream would decrease downstream, and the logarithmic function would be the best fit. With the

Table 2 Linear and relief properties of the trunk stream and the catchments

Catchments	Basin area	Basin length	Basin perimeter	Width	Maximum elevation	Mean elevation	Minimum elevation	Relative relief	Length of the trunk stream
Balason	392.953	42.054	122.749	17.473	2614	1351.56	110	2504	42.05
Mahananda	157.199	26.701	84.738	9.641	2233	1168.72	133	2010	26.70
Lish	78.933	20.386	54.729	8.36	1887	984.47	116	1771	20.38
Gish	221.663	34.524	94.593	11.159	2359	1214.37	115	2244	34.52
Neora	324.683	42.343	132.833	12.795	3160	1624.51	94	3066	47.92
Chel	281.502	47.926	139.36	9.987	2464	1262.56	94	2370	42.34
Murti	188.542	37.015	110.933	8.395	2537	1295.57	105	2432	37.01
Jiti	149.302	24.44	74.249	11.902	3461	1805.89	231	3230	24.44
Diana	247.937	39.422	139.47	23.124	2546	1317.13	95	2451	39.42
Rehti	235.366	34.746	107.419	14.057	1820	903.63	64	1756	34.74
Pagli	270.063	38.187	115.328	17.17	1619	818.88	60	1559	38.18

additional rate of increase in concavity, the power function is most suitable (Lee and Tsai 2010).

3.3.2 Stream Length Gradient Index (SL)

The stream length gradient index is a parameter that evaluates the erosional resistance of the rocks and the relative intensity of tectonic activity (Rhea 1993). The SL index was proposed by Hack (1973) related to the hydrographic network and slopes of the river channel, is the function of the power of the stream per unit length and as a proportion to the total stream power available at a particular river reach (Summerfield 1991; Pérez-Peña et al. 2010). It is expressed as follows

$$SL = (\Delta H/\Delta L) \times L \tag{6}$$

where ΔH is the elevation change, ΔL is the horizontal length for a given channel reach, and L is the horizontal distance from the midpoint of the reach to the drainage divide (Fig. 4).

It can be obtained also from the semi-logarithmic form of the longitudinal profile, where gradient index is equal to the constant K , the slope of the profile and can be expressed as

$$K = (h_1 - h_2)/[\ln(d_2) - (d_1)] \tag{7}$$

where h is the elevation and d is the distance, 1 and 2 are the successive points.

The ratio of average SL value and the k of a certain river was proposed by Seeber and Gornitz (1981) as the Normalized Stream Gradient Index (NSL). It was considered by Lee and Tsai (2010) as the Channel Steepness Index that displays the rate of fluvial erosional process of a river. The values of $NSL \geq 2$ indicate significantly

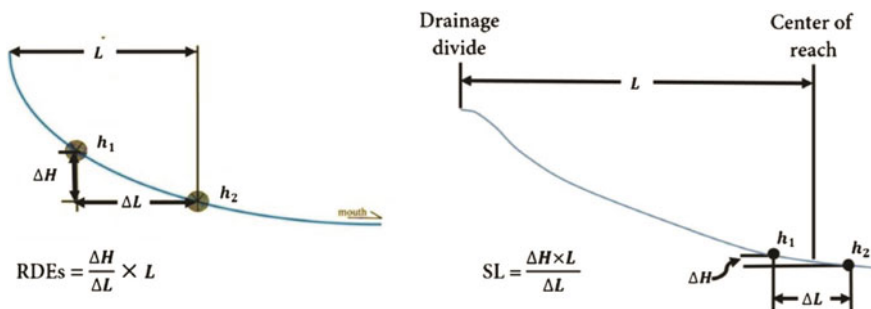


Fig. 4 Schematic sketch of the method used to calculate SL and Rdet (after Moussi et al. 2018)

steeper reaches whereas $NSL \geq 10$ is classified as highly steep reaches. The NSL index explains the instability of a particular area.

3.3.3 Relative Slope Extension Index (RDEt)

RDE index is an indicator that implies the relation between stream discharge energy and slope of a river channel. Etchebehere et al. in 2004 prepared the RDE index as derivatives of the SL index (Hack 1973). It is regarded as a useful tool to identify knick points in a river long profile (Moussi et al. 2018). The total RDE index refers to the total length of the river and the total slope of the channel with the logarithm of total channel length.

$$RDEt = (\Delta H / \Delta L) \times \ln(L) \quad (8)$$

where ΔH is the elevation difference between the extremes of given stream reach, ΔL is the length of the segment, and quantity and L is the stream length.

The existence of Knick points in the long profile demarcates the influence of tectonics and lithology on the development of river characteristics. The Knick points are identified by filtering of RDE index values and the interpolation of Knick points was done by using the RDEt values.

4 Neotectonic Movements and Channel Evolution

4.1 *Morphotectonic Characteristics of Different Geomorphic Tiers; River Catchment and Valley*

4.1.1 Basin Geometry

Drainage basin geometry is related to the form or shape of the basin controlled by structure, relief, slope, lithology, and precipitation (Singh 2005). Basin shapes vary from narrow elongated forms to oval and circular. The form factor value will always be 0.7857 for a river basin of compact massive circular shape (Sen 1989). Lower value of the form factor, less than 0.7857, represents a narrow elongated basin area. The values of selected catchments vary from 0.12 to 0.25, depicting an overall elongated nature (Table 3).

The index of shape ratio expresses the extreme elongation for higher values while the lower ones signify circular shape. The shape ratio of the rivers like Jiti, Pagli, Balason, Lish, Rehti, and Mahananda ranges from 2.05 to 2.77. While the values of Gish, Chel, Neora, and Murti are 3.09, 4.8, 3.31, and 4.41 respectively. Only river Diana is an exception, registering a value less than 2. On the other hand, the value

Table 3 Computation of the morphometric indices for the selected river basins

Catchment	Mfs	Form factor	Basin shape factor	Circularity ratio	Elongation ratio	Topographic symmetry factor	Vf ratio	Channel concavity	Mean SL	HI	STD	Relief ratio
Balason	1.92	0.22	2.41	0.33	0.53	0.30	0.15	0.020	106.84	0.28	717.2	0.06
Mahananda	1.52	0.22	2.77	0.28	0.53	0.59	0.1	0.059	164.54	0.22	610.1	0.08
Lish	2.07	0.19	2.44	0.33	0.49	0.50	0.28	0.043	112.42	0.20	508.7	0.09
Gish	1.83	0.19	3.09	0.31	0.49	0.43	0.19	0.027	142.15	0.28	635.4	0.06
Neora	2.01	0.18	3.31	0.23	0.48	0.30	0.28	0.342	170.01	0.15	883.9	0.06
Chel	1.77	0.12	4.80	0.18	0.40	0.26	0.07	0.034	152.36	0.20	675.6	0.06
Murti	1.74	0.14	4.41	0.19	0.42	0.44	0.14	0.035	167.51	0.15	688.3	0.07
Jiti	2.38	0.25	2.05	0.34	0.56	0.31	0.1	0.070	212.21	0.38	911.1	0.13
Diana	2.71	0.16	1.70	0.16	0.45	0.38	0.15	0.044	245.19	0.27	706.1	0.06
Rehti	2.32	0.19	2.47	0.26	0.50	0.44	0.24	0.011	61.22	0.18	486.9	0.05
Pagli	2.170	0.185	2.224	0.255	0.485	0.48	0.15	0.290	93.56	0.100	441.3	0.04

of the Circularity ratio (R_c) varies from 0 to 1, where a lower value indicates an oval or elongated shape. The Circularity ratio of the selected rivers ranges from 0.16 to 0.34, revealing the elongated shape of the drainage basins. Like R_c , the lower value (less than 1) of elongation ratio (R_e) also represents the elongated form of the basin, while the values approaching unity will indicate a rounded basin area. Here, the R_e varies from 0.4 to 0.53, demonstrating the shape of the basins is invariably oval to elongated. The geometry of the selected drainage basins reflects significantly elongated in shape, which points towards the prosecuted impact of the geologic structure and neotectonics of the concerned region.

4.1.2 Basin Asymmetry

The asymmetric factor of a drainage basin is an important measurement to detect tectonic tilting (Keller and Pinter 2002). When the Transverse Topographic Symmetry Factor (TTSF) is 0, it represents the basin in perfect symmetry, otherwise asymmetric or having a relative tilt towards a particular side. The TTSF, in this study varies between 0.3 and 0.59, indicating the more or less asymmetric character of the basins initiated by surface orogeny. The Balason River on the piedmont surface was found following a fault line lying NNW-SSE along the western flank of the basin. Apart from that formation of the Rakti-Rohini fan surface, covering the interfluvium of Balason and Mahananda River has created a local tilt towards the east, governing the development of the path along the eastern margin of the watershed (Fig. 5). Similarly, the development of the blind thrust across the Matiali fan surface has governed a flow deflection for the Chel River towards the west. The elevated terrace surface near Totopara has resulted in a local tilt of the said surface towards the east which has sidetracked the flow of Pagli significantly.

4.1.3 Relief Aspect

Relief aspect of a drainage basin highlights the influence of upliftment and erosional process in modifying the terrain character and its roughness. Relief Ratio (R_r) is a simple statistical tool to characterize the relief properties of a drainage basin (Schumm 1956). High values of the R_r are associated with steep slopes, while a low value indicates a gentler slope having resistant basement rock. Although the R_r values of the concerned catchments vary from 0.04 to 0.13, showing moderate to low relief features, R_r of the mountainous catchment separately, ranges from 0.09 to 0.95. On the HFB region due to the associations of low relief features, the values range between 0.01 and 0.03. Interestingly, Gish river basin has registered maximum R_r on the mountainous part and lowest R_r on the piedmont slope among the selected rivers (Table 4).

The topographic roughness (STD), pointing towards the terrain undulations ranges from 441.36 to 911.10 among the studied catchment. It was found comparatively higher for the river basins like Jiti (911.10) and Neora (833.90), whereas Rehti and

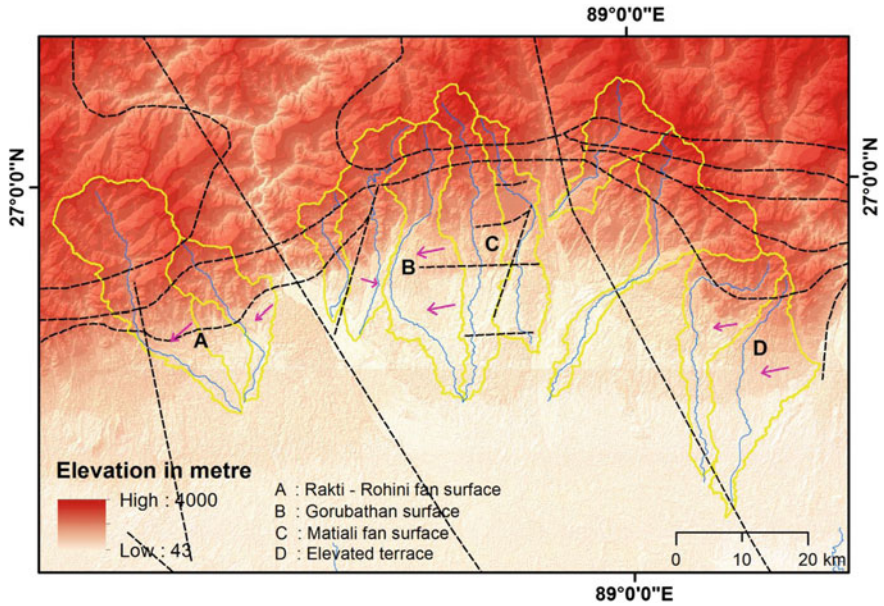


Fig. 5 Characteristic basin tilt within the study area and association of the major deformations and geomorphic units

Table 4 Distribution of the Relief ratio and Hypsometric integral values for the selected catchments on the mountainous part and on the HFB

Catchment	Relief ratio		Hypsometric integral	
	mountain	Piedmont	Mountain	Piedmont
Balason	0.089	0.019	0.50	0.50
Mahananda	0.14	0.014	0.50	0.47
Lish	0.13	0.016	0.49	0.45
Gish	0.95	0.012	0.48	0.49
Neora	0.14	0.02	0.50	0.49
Chel	0.15	0.010	0.50	0.50
Murti	0.18	0.015	0.49	0.45
Jiti	0.17	0.030	0.49	0.49
Diana	0.20	0.01	0.49	0.44
Rehti	0.14	0.01	0.50	0.49
Pagli	0.19	0.013	0.48	0.48

Pagli are sharing the lower values of 486.89 and 441.36 respectively. Higher STD signifies greater elevation anomaly within a concerned spatial extent. Since the STD is calculated as the standard deviation of elevation value from the mean elevation of the catchment, the catchments experiencing comparatively higher STDs illustrate relative skewness in the distribution of elevation values due to differential upliftments.

Valley floor width to height ratio (V_f) is a highly useful geomorphic tool to describe active tectonism. Any value, less than 1 indicates the deep and narrow valley, dominated by active incision associated with active tectonism, whereas a higher value shows the broad valley character, signifying stability. The V_f values of selected river basins range from 0.71 to 0.28, reflecting an overall dominance of incision close to the mountain fronts. Although, the different segments of the rivers were found with differences in intensity of dominance by the upliftment or fluvial action. Moreover, the mountain reaches for most of the rivers are being dominated by active tectonism as the V_f was found significantly lower than 1. On the Quaternary basin-fill segment, the formation of terraces, scarps and debris cones were found invoking valley confinements.

Hypsometric integral (HI) ranges between 0 to 1, where, usually value greater than 0.5 signifies the youthful stage, represents by a convex curve, any value between 0.4 to 0.5 displays a concave-convex slope, disclosing the mature stage. Lastly, any value lower than 0.40 represents the senile stage, showing a concave slope. The HI of the selected river basins varies between 0.47 and 0.51, indicating the basins are in the mature stage and attaining a state of dynamic equilibrium. There has not been any significant difference found while calculating the HI separately on the mountainous catchment and piedmont slope for the selected river basins. It suggests that the rivers are still going through a state of balance between heavy input of sediments that result in aggradation and on the other hand, active orogenic nature leads toward slope deformations (Table 4).

4.1.4 Mountain Front Sinuosity

Mountain front sinuosity (Mfs) was developed to measure the competition between the active surface upliftment and fluvial erosion (Bull 1977). The values of Mountain front sinuosity near to 1 or less than 1.4 usually signifies tectonically active fronts (Keller 1986) and higher than 3 indicates inactive fronts (Bull 2007). The mountain front sinuosity values of the selected rivers in the frontal zone of the Eastern Himalayas varies from 1.52 to 2.71. The SMF values of the rivers namely Balason, Mahananda, Gish, Chel, and Murti are found 1.92, 1.52, 1.83, 1.77, and 1.74 respectively, representing a moderately active frontal zone, while the rest of the rivers like Neora (2.01), Lish (2.07), Pagli (2.17), Jiti (2.38) and Diana (2.71) represent low to the moderate orogenic activity along the mountain front. Since the lesser Himalayan complex is composed of crystalline rocks, fragile to fluvial erosion, the fluvial action continues to perform beside the tectonic upliftment (Fig. 6).

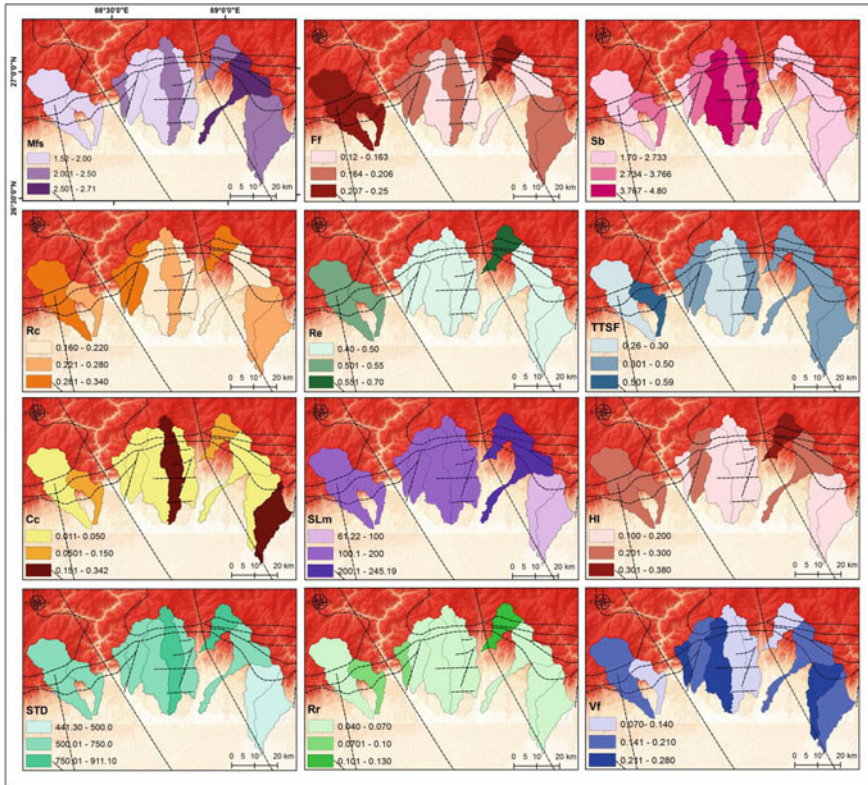


Fig. 6 Spatial representation of the geomorphic indices

4.2 Catchment Scale Adjustment and Localised Abnormalities of Channel Long Profile Forms to Neotectonic Movements

4.2.1 Mathematic Models

The best fit mathematical models for the corresponding normalised long profiles of the rivers has been shown in Table 5. Among the selected eleven rivers, the Mahananda (up to its confluence with Balason) and Pagli River were found best fitted with the logarithmic model. The mathematical curve fitting of the Chel river was the most interesting among all. Although it has registered the best fit with the exponential model but falls marginally separate from the logarithmic model. Except for the above-mentioned rivers, the remaining rivers were found best fitted with an exponential model. Since, the selected rivers although, originate on the mountain terrain but not in association with any large glaciers, not a single river was found fitted best with the power relation. Power relation corresponds to high discharge

Table 5 Curve fitting on the longitudinal profile of the rivers and its statistical significance; cells marked in yellow shows the most significant mathematical model

Rivers	Length	Gradient	No of samples	Coefficient of determination (R^2)			
				Linear	Exponential	Logarithmic	Power
Balason	52.065	48.09	202	0.83	0.98	0.82	0.66
Mahananda (up to confluence)	35.706	56.29	136	0.527	0.839	0.93	0.87
Lish	26.783	66.12	106	0.709	0.946	0.86	0.69
Gish	50.244	44.66	198	0.856	0.979	0.75	0.60
Chel	58.856	52.09	221	0.54	0.865	0.861	0.80
Neora	61.391	38.60	248	0.640	0.898	0.76	0.71
Murti	55.764	43.61	222	0.609	0.906	0.87	0.76
Jiti	31.136	103.73	126	0.777	0.964	0.81	0.65
Diana	63.563	38.56	255	0.52	0.87	0.83	0.79
Rehti	57.563	30.50	231	0.789	0.982	0.88	0.71
Pagli	48	32.47	198	0.595	0.888	0.94	0.77

rivers nearly achieving their graded form. The selected rivers are rainfall and run-off fed channels with a flashy discharge character during the dominant monsoon months. Even channel flow in a few of the rivers becomes so feeble that is hard to distinguish during the lean period (Soja and Sarkar 2008). Along with that, also not a single channel was found in correspondence with the linear function asserting the strong influence of surface upliftment and higher intensity of erosion. It is because these rivers are antecedent in nature, thus incised its paths on the lesser Himalayan terrain and the frontal plain segment (Goswami et al. 2012).

4.2.2 Standardised Long Profiles and Mean SL Index

The representation of the longitudinal profile in semi-logarithmic scale was done to characterise the nature of its deviation from the ideal graded profile. The semi-logarithmic profile or the Hack's profile of a river tends to be convex if it experiences surface warping and differential upliftment within its course. The graded profile in a semi-logarithmic scale seems to be a perfectly straight line, decaying downstream (Hack 1973). The convex nature of the profiles plotted on a semi-logarithmic scale signifies the role of active neotectonism and resultant channel slope deformation in the study area (Fig. 7). Stream Length Gradient Index (SL) targets the influence of lithological and tectonic activities that determines the changes in the long profile due to differential bulging of sediments and slope deformations. The current investigation is dealing with the overall SL value for the selected rivers, varying from 61.22 to 245.19. Diana and Jiti display comparatively higher SL values of 245.19 and 212.21

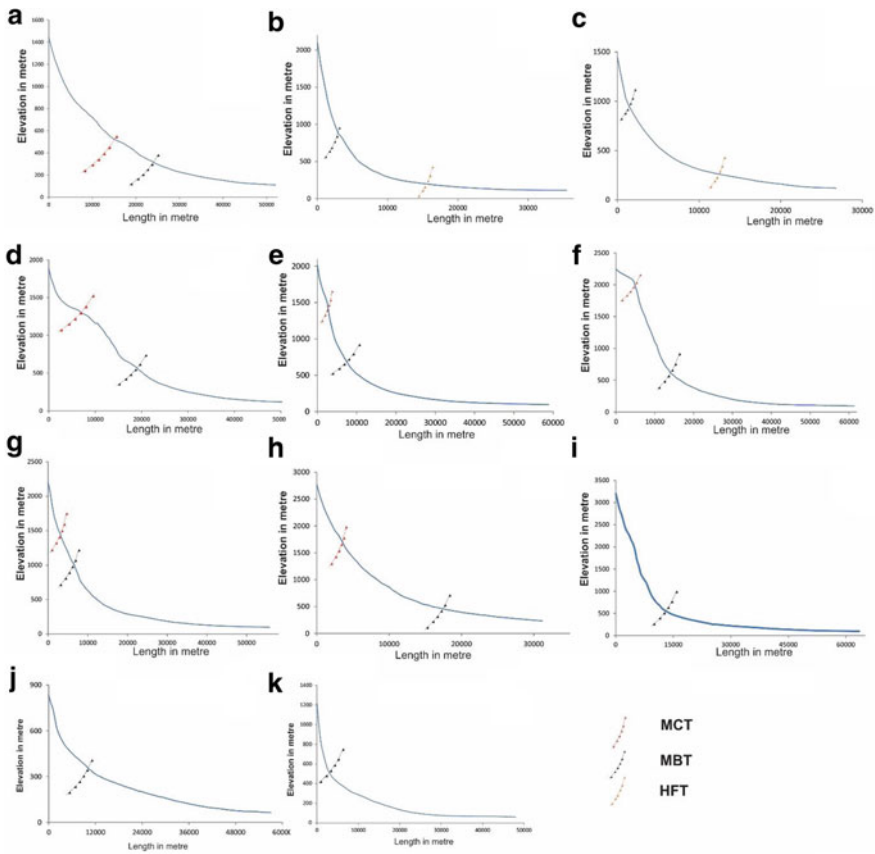


Fig. 7 Semi-logarithmic profiles of the selected rivers. Elevation values were derived from the SRTM 30 m DEM; the sequence of the rivers (in alphabets) is similar to that of mentioned in Fig. 2

respectively. On the other hand, Rehti and Pagli represent the lowest value of SL index among the eleven studied rivers (61.22 and 93.56 respectively). Higher values of average SL (SL_m) represents a greater fall in the gradient concerning its watershed margin.

4.2.3 Quantification of the Magnitude of Adjustment: Normalised Gradient Index (NSL)

The segment-specific SL values were divided by the corresponding average SL or the absolute K value to compute the channel steepness or the Normalised Gradient Index (NSL). The values were classified into five separate classes, where $NSL < 2$ was considered as near flat segments. The intensity of the steepness increases with values above 2, where channel segments with $NSL > 10$ can be considered as near

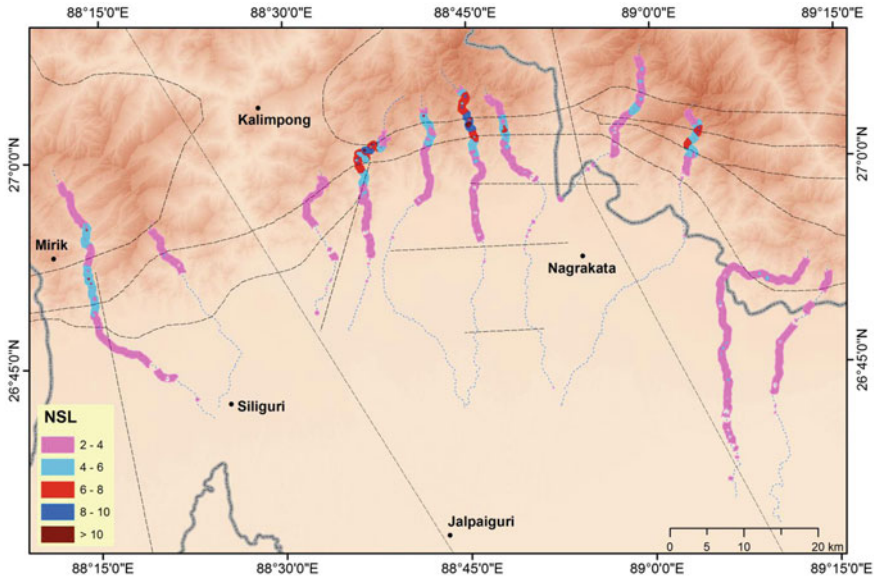


Fig. 8 Interpolation of the Normalised SL or channel steepness values of the selected rivers

vertical fall (Fig. 8). The mountainous reaches of all the rivers were found situated with considerable channel steepness. The reaches associated with the Himalayan thrusts in the Gish, Neora and Diana Rivers were found with maximum steepness and certain near-vertical falls in the river courses. On the alluvial foreland, for natural reasons the steepness went on decreasing in comparison with the mountain reach. Compared to other rivers on the piedmont slope, floe path of Neora and Rehti were found with relatively steeper segments associated with the blind thrusts and uplifted terraces along the neotectonic fault of the Totopara region respectively. Visual observations provide a close association of the relative departures in channel steepness along the Himalayan thrusts invariably for all the selected river courses. The average channel steepness was found interesting. Balason, Gish, Neora, Jiti and Rehti river has maintained an overall steep profile with local departures. On the other hand, Lish was found marginally on the steeper side with an overall steepness of 2.08. Diana river was observed with major departures in the relative steepness of the profile but overall it was found as a near flat river course since, on the piedmont, lesser confinements and lower degrees of disturbances in terms of endogenetic perturbations has led to developing a near flat middle to lower reach (Table 6).

4.2.4 Quantifying the Localised Anomalies; RDet Index

The Rdet index identifies the major slope anomalies in the river long profiles (Moussi et al. 2018). In this study, the Rdet has been portrayed in three different ways; one, extracting the major breaks at an interval of 100 m, starting from 200 m. It was started

Table 6 General statistics of the Normalised SL values for the selected river basins

	Balason	Mahananda	Lish	Gish	Chel	Neora	Murti	Jiti	Diana	Rehti	Pagli
Mean	3.44	3.09	2.75	4.567	3.344	4.712	3.433	3.259	4.324	3.036	2.474
Max	6.77	4.184	3.86	13.58	6.906	13.42	8.167	5.747	9.273	4.907	3.411
Min	2.16	1.678	2.05	2.036	2.015	1.412	2.067	1.736	2.138	1.327	2.003
St Dev	1.13	0.75	0.55	2.46	1.14	2.66	1.29	0.93	2.09	0.67	0.34
CV	32.8	24.38	20.06	53.94	34.21	56.61	37.86	28.75	48.38	22.18	13.85

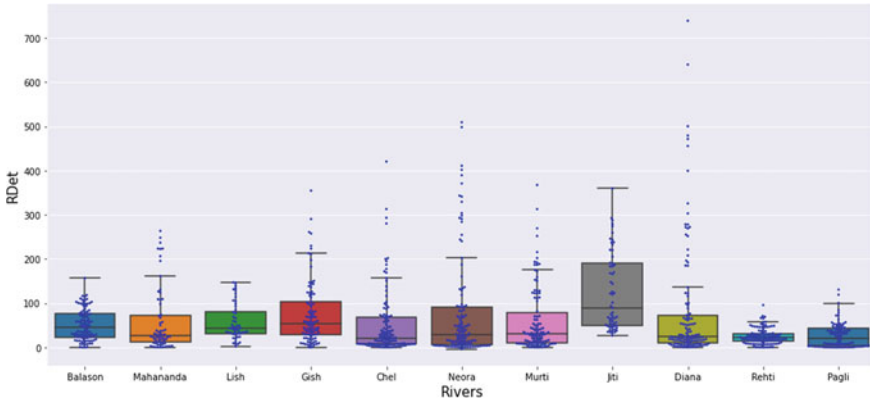


Fig. 9 River respective categorical distribution of the Rdet values

from 200 m because values less than 200 were found too ubiquitous to consider as an anomaly. Second, Rdet values computed at the random interval was interpolated using the IDW module in Arc-GIS and third, the categorical distribution of Rdet values within the major tectono-geomorphic domains of the Himalayas and the associated Quaternary alluvial fill basin. These perspectives add up cartography with simplified visualisation of the anomaly zones.

The Rdet values of the trunk streams of eleven selected basins have been illustrated in Fig. 9 where the highest value was found 764 m in the Diana River, around a segment associated with thrust faults. The river respective categorical distribution of the Rdet values portrays a non-uniform distributional scenario among the selected rivers. The distribution was found less skewed for Balason, Lish and Jiti River where no outliers were found. The distribution of the outliers depicts the issue of an anomaly in the slope of the river courses. It is evident in river courses like Diana, Chel and Neora where extreme outliers signify greater anomalies and the formation of major breaks in the longitudinal slope. The spatial distribution of the interpolated Rdet (Fig. 10) shows the exact locations of the outliers in the courses of Mahananda, Gish, Chel, Neora, Murti and Diana. In most of the state, the anomalous zone or the knick zones are associated with the thrust faults lying into the domain of lesser Himalayan complex (Fig. 11). The distribution of the Rdet values in the Greater Himalayan complex was found less anomalous compared to the lesser Himalayan complex (Fig. 12). Except in the course of Jiti and Neora, no other rivers have significantly registered anomalous values in the Greater Himalayan domain. Apart from that, the Siwalik pockets were found with lesser disturbances with comparatively lower skewness but the associated foreland region was found with greater anomalies. Except for an abrupt break in the Neora River at the junction of the mountains and plains, registering a Rdet value above 200 m, no other anomaly of considered intensity was found on the HFB in any of the river courses. Compared to the spatial distribution, the zone respective categorical distribution has outlined multiple anomalies on the foreland domain. Thus, the spatiality of the Rdet on the HFB was studied

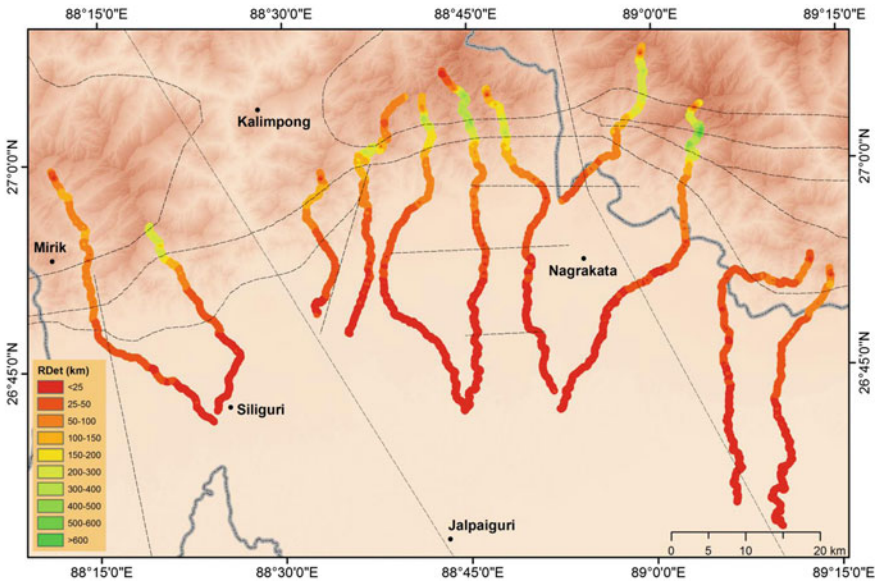


Fig. 10 Interpolation of the RDet values of the selected rivers

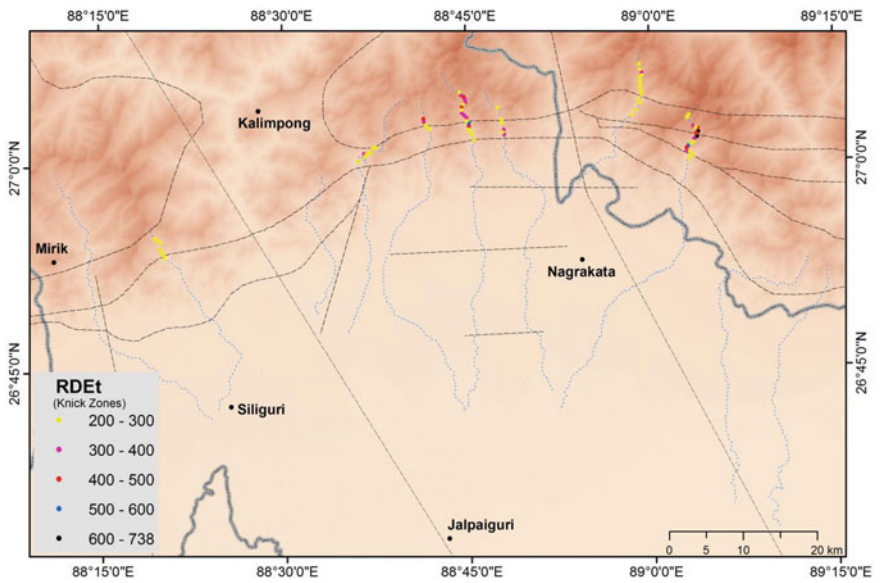


Fig. 11 Knick zones found in the study area. The values were selected based on a certain interval, starting from 200 m

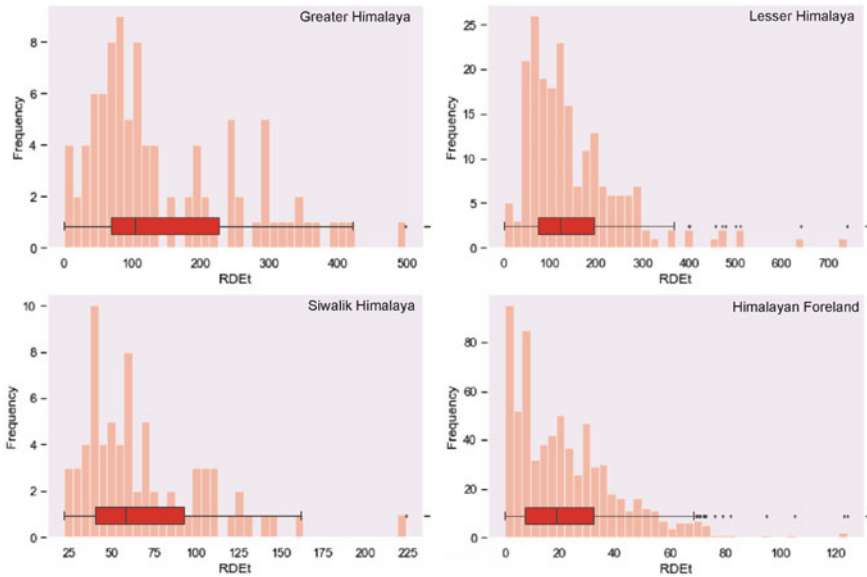


Fig. 12 Distribution of the Rdet values within distinct tectonogeomorphic zones in the study area. The outliers were considered as the slope anomaly in the river reaches

separately and the anomalous condition was mapped based on the boundary of its upper whisker (Fig. 13). Around the mountain front, the anomalous condition was found in rivers like Chel, Neora, Murti, Diana and Pagli. Among these five channels, the anomalous condition in Neora and Murti was found associated with the Matiali scarp (blind thrust) while a similar issue of slope anomaly was also associated in the Pagli River at intersection of the neotectonic fault. Since all the rivers has been originated on the Higher or Lesser Himalayas, these are antecedent to the faults. The abrupt surface warping had created an anomalous condition in the long profiles as the rivers continued to down cut during the surface upliftment.

4.3 Overview of Channel Responses to Neotectonic Perturbations

The geospatial approach applied in this study has helped to derive the nature of fluvial responses, collectively at the catchment form to its evolution phases through adjusting its longitudinal forms. The catchment forms have significantly portrayed coninity effects in its development which is usually governed by the tectonic perturbations that result in basin elongation (Bull and McFadden 1987). Surface warping and tectonism led surface deformations often create relief barriers for rivers. It is most common in the form of ridges that compel a river to deviate either due to physical contact or

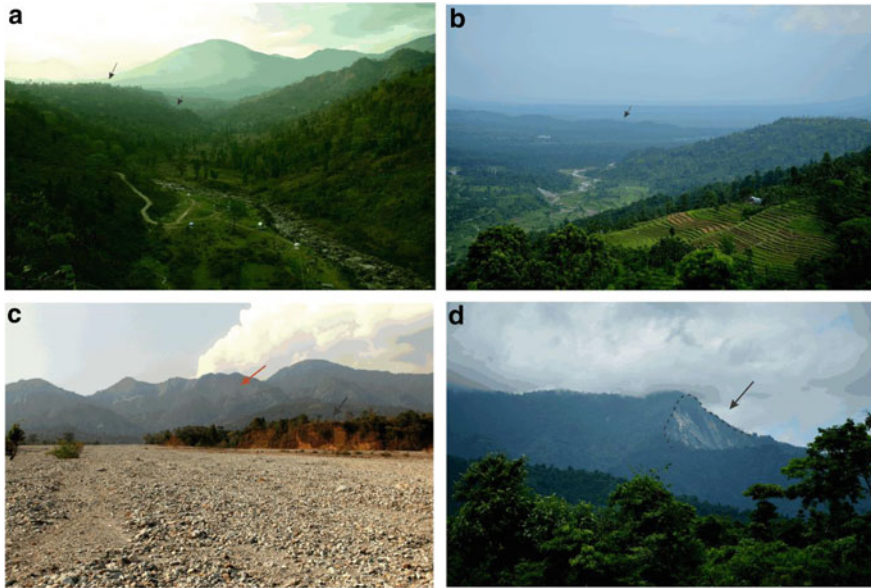


Fig. 13 a Unpaired terraces along the course of Murti River (viewing upstream); b Chasla scarp lying parallel to the mountain front (viewing downstream); c Uplifted terrace surface (Totopara surface) with exposed faultscarp of a neotectonic fault located on the east of Pagli River (viewing west); d Triangular facets developed around fault scarp near Pagli River (viewing north)

surface tilt through surface slope modification (Holbrook and Schumm 1999). The results of basin asymmetry of the selected river basins show significant tilting at varied directions but are found immediately associated with structural elements. Although the regional tilt on the eastern side of the Teesta river is towards SE but the effective local deformations concentrated at a certain part, have resulted in the basin tilting in varied directions. Here, the impact of the alluvial fan attitude cannot be overruled. It has significantly governed the channel direction around the mountain front as well as on the piedmonts (Chakraborty and Mukhopadhyay 2013). Similar findings were also encountered by Sharma and Sarma (2017) within the belt of Schuppen where local deformations have produced tilts in varied directions. At the mountain piedmont junctions, cessation of upliftment allows fluvial action to dominate which results into transformation of the linear and active mountain fronts into a zig-zag form. Although it requires less resistant lithological composition. In any intermediate state of action, upliftment and fluvial erosion go hand in hand (Bull 2007). Similarly, upliftment of the tectonically active frontal surface attracts intense downcutting, resulting into deeply incised valleys (Bull and McFadden 1977; Bull 2007). In this study, mountain fronts of the river basins seemed to be moderate to low tectonically active but still present with incised river valleys as a portrayal of ongoing upliftment. The less resistant lithological composition around the frontal part of the Himalayan complex allowed fluvial erosion to change the linearity of the front. The imprints

of simultaneously active Himalayan upliftment are also quite distinct as observed through Vf ratio which is invariably < 1 for all the selected courses around the corresponding mountain fronts. Thus, the process of Himalayan upliftment is neither dormant or rigorous along its frontal segment within the studied part.

Besides the location of structural elements, rock erodibility or certain litho-contacts and differential upliftment can also influence the essential drop in downstream channel slope (Troiani et al. 2014; Pavano et al. 2016; Moussi et al. 2018). The Himalayan complex, contemplated with multiple thrusts and intra-formational thrust sheets were found as the major zones of concentration of slope anomalies or knick points. Although the nature of concentration has varied throughout the extent. The formation of the knickpoints suggests differential upliftment of the surface where reconstruction of the river flow paths gets fragmented into multiple phases in response to these perturbations. The differential upliftment was within the Spiti River basin in the Westen Himalaya was found associated with spatially varying concentrations and intensity of breaks in the channel longitudinal slope (Phartiyal and Kothyari 2011). Apart from the spatial distribution of the knick points, for inferring the lithological and surface material composition on the knickpoints, it was categorically grouped interms of different tectono-geomorphic domains in the study area. The association of the anomalous zone was invariably concentrated into the zone with relatively highest density of the thrust faults or simpler to say, the region with maximum surface deformations due to faulting. The enclosed region of the MCT and MBT around the apex of the reentrant has been found with relatively higher values of NSL compared to other segments with a dominance of knickpoint clusters. Thus, it is being inferred that the higher rate of upliftment of the MCT and associated channel incision in order to adjust the upliftment pace has resulted in greater intensity of long profile deformation. The rate might have varied through out the extent. Apart from that, the topographic barriers of the Himalayas attracts greater rainfall which might have been another potential agent ignited the rapid incision compared to other topographic extents. Although the frontal part of the Himalayas acts as orographic front that helps in monsoon orography and a major difference in rainfall intensity usually found over the Greater Himalayas compared to the Middle Himalayas (Rees and Collins 2006). Moreover, the summer monsoon gets weaker as it moves towards west along the Himalayan front and a clear distinction can be made on the east and western part of Teesta. Thus, strengthening the rainfall intensity results in active erosion that perhaps influence the isostatic upliftment or tectonic upliftment (Bishop et al. 2002). These differential upliftment along between the MBT and MCT and continuing growth process of the intra-formational thrust sheets in this region has resulted in adjustment of the river long profile forms to surface ruptures. Here, we infer that since, the lithological composition of the Himalayan segment being analysed in this study are present with no such major distinguished variations in lithology, the tectonic impact and differential surface warping has compelled the fluvial system to adjust accordingly and resulted into major slope anomalies formed whenever scarps and fault lines were encountered.

5 Conclusion

The morphotectonic approach applied on a selected segment of the Eastern Himalayas has revealed a mutual association of fluvial action and epirogenic activity where the rivers are mostly antecedent to the recent developments of structural elements. Thus, the ongoing incision in order to accommodate the uplift is characteristic outcome of such association. The neotectonic activeness of the Quaternary alluvial fill basin of the foreland part has been significantly associated with flow paths of the trunk streams to the development of the landscape features. The overall tectonogeomorphic environment has significantly impacted the evolution of the fluvial systems, starting from its basin planimetric properties to valley form as well as longitudinal slope. The morphometric data has inferred that these basins are tilted, highly asymmetric, thoroughly confined to get the elongated form and tectonically deformed which have attracted terrain roughness to slope anomalies both a catchment scale and valley forms. Although, invariably for most of the rivers, the intensity of slope fall and deformation on the river longitudinal forms are found highly associated with the location of the Himalayan Thrusts but the dominance of the knick points on the mountainous tract is present around the apex of the reentrant. On the other hand, the channel slope deformation on the piedmont slope is significantly associated with neotectonic twitchings in case of Gish, Chel, Neora, Murti, Rehti and Pagli River (Fig. 13). Compared to all, channels located around the apex and eastern flank of the reentrant are more deformed due to the formation of sub-parallel thrusts to the Himalayan thrusts, translational thrust sheets and neotectonic scarps. The uniqueness of this work lies on the process-response approach, commenced to study the tectonic indentations and corresponding geomorphic responses at catchment scale to channel longitudinal form.

References

- Altın BT (2012) Geomorphic signatures of active tectonic in drainage basins in the Southern Bolkar mountain, Turkey. *J Indian Soc Remote Sens* 40(2):271–285. <https://doi.org/10.1007/s12524-011-0145-8>
- Ayaz S, Dhali MDK (2019) Longitudinal profiles and geomorphic indices analysis on tectonic evidence of fluvial form, process and landform deformation of Eastern Himalayan Rivers, India. *Geol Ecol Landscapes* 4(1):11–22. <https://doi.org/10.1080/24749508.2019.1568130>
- Ayaz S, Biswas M, Dhali MK (2018) Morphotectonic analysis of alluvial fan dynamics: comparative study in spatio-temporal scale of Himalayan foothill. India. *Arabian J Geosci* 11:41. <https://doi.org/10.1007/s12517-017-3308-2>
- Bali BS, Wani AA, Khan RA, Ahmad S (2016) Morphotectonic analysis of the Madhumati watershed, northeast Kashmir Valley. *Arabian J Geosci* 9:390. <https://doi.org/10.1007/s12517-016-2395-9>
- Bhattacharyya K, Mitra G (2011) Strain softening along the MCT zone from the Sikkim Himalaya: Relative roles of Quartz and Micas. *J Struct Geol* 33:1105–1121. <https://doi.org/10.1016/j.jsg.2011.03.008>

- Bishop MP, Shroder Jr JF, Bonk R, Olsenholler J (2002) Geomorphic change in high mountains: a western Himalayan perspective. *Global Planet Change* 32:311–329
- Bull WB, McFadden LD (1977) Tectonic geomorphology North and South Garlock fault, California. Eight annual geomorphology symposium, State University of New York, (pp. 115–138). Binghamton
- Bull W (2007) Tectonic geomorphology of mountains: a new approach to paleoseismology. Wiley-Blackwell, Oxford, p 328
- Burbank DW, Anderson RS (2012) Tectonic geomorphology. Blackwell publishing Ltd
- Burbank D, Leland J, Fielding E et al (1996) Bedrock incision, rock uplift and threshold hillslopes in the northwestern Himalayas. *Nature* 379:505–510. <https://doi.org/10.1038/379505a0>
- Chakraborty PP, Tandon SK, Roy SB, Saha S, Paul PP (2020) Proterozoic sedimentary basins of India. Switzerland AG: Springer Geology. <https://doi.org/10.1007/978-3-030-15989-4>
- Chatterjee RS, Nath S, Kumar SG (2019) Morphotectonic analysis of the Himalayan Frontal region of Northwest Himalaya in the light of geomorphic signatures of active tectonics. Singapore: Springer Nature
- Chen YC, Sung Q, Chen CN, Jean JS (2006) Variations in tectonic activities of the central and southwestern foothills, Taiwan, inferred from river Hack profiles. *Terrestrial, Atmosph Oceanic Sci* 17:563–578
- Cox RT (1994) Analysis of drainage basins symmetry as rapid technique to identify areas of possible quaternary tilt-block tectonics: an example from Mississippi Embayment. *Geol Soc Am Bull* 106:571–581
- Dasgupta S, Mukhopadhyay B, Mukhopadhyay M, Nandy D (2013) Role of transverse tectonics in the Himalayan collision: further evidences from two contemporary earthquakes. *J Geol Soc India* 81:241–247
- DeCelles Peter G, Giles Katherine A (1996) Foreland basin systems. *Basin Res* 8(2):105–123. <https://doi.org/10.1046/j.1365-2117.1996.01491.x>
- Dubey RK, Satyam GP (2018) Morphotectonic appraisal of Yamuna river basin in headwater region: a relative active tectonics purview. *Geological Soc India* 92:346–356. <https://doi.org/10.1007/s12594-018-1018-3>
- Figueiredo PM, Rockwell TK, Cabral J, Ponte LC (2017) Morphotectonics in a low tectonic rate area: analysis of the southern Portuguese Atlantic coastal region. *Geomorphology*. <https://doi.org/10.1016/j.geomorph.2018.02.019>
- Flores-Prieto, E., Quénéhervé, G., Bachofer, F., Shahzad, F., & Maerker, M. (2015). Morphotectonic Interpretation of the Makuyuni Catchment in Northern Tanzania using DEM and SAR data. *Geomorphology*. <https://doi.org/10.1016/j.geomorph.2015.07.049>
- Gansser A (1964) *Geology of Himalayas*. Interscience publishers, New York
- Ghosh S, Sivakumar R (2018) Assessment of morphometric parameters for the development of relative active tectonic index and its significant for seismic hazard study: an integrated geoinformatic approach. *Environ Earth Sci* 77:600. <https://doi.org/10.1007/s12665-018-7787-6>
- Goswami C, Mukhopadhyay D, Poddar BC (2012) Tectonic control on the drainage system in a piedmont region in tectonically active Eastern Himalayas. *Frontiers Earth Sci* 6(1):29–38. <https://doi.org/10.1007/s11707-012-0297-z>
- Goswami PK, Pant CC (2008) Tectonic evolution of Duns in Kumaun sub-Himalaya, India: a remote sensing and GIS based study. *Int J Remote Sens* 29(16):4721–4734
- Guha D, Bardhan S, Basir SR, De AK, Sarkar A (2007) Imprints of Himalayan thrust tectonics on the Quaternary piedmont sediments of the Neora-Jaldhaka Valley, Darjeeling-Sikkim Sub-Himalayas, India. *J Asian Earth Sci* 30:464–473. <https://doi.org/10.1016/j.jseaeas.2006.11.010>
- Hack JT (1957) Studies of longitudinal river profiles in Virginia and Maryland. U.S. Geological Survey Professional Paper (pp 249B-99)
- Hack JT (1973) Stream-profile analysis and stream-gradient index. *J Res U.S. Geol Surv* 1(4):421–429

- Hawker LP, Rougier J, Neal J, Bates P, Archer L, Yamazaki D, (2018) Implications of simulating global digital elevation models for flood inundation studies. *Water Res* 54:7910–7928. <https://doi.org/10.1029/2018wr023279>
- Holbrook J, Schumm SA (1999) Geomorphic and sedimentary response of rivers to tectonic deformation: a brief review and critique of the tools for recognizing subtle epeirogenic deformation in modern and ancient settings. *Tectonophysics* 305:287–306
- Jain V, Sinha R (2005) Response of active tectonics on the alluvial Baghmata River, Himalayan foreland basin, eastern India. *Geomorphology* 70:339–356. <https://doi.org/10.1016/j.geomorph.2005.02.012>
- Joshi LM, Pant PD, Kotlia BS, Kothyari GC, Luirei K, Singh AK (2016) Structural overview and morphotectonic evolution of a strike-slip fault in the zone of North Almora Thrust, Central Kumaun Himalaya, India. *J Geol Res*, 16. <https://doi.org/10.1155/2016/6980943>
- Kale VS, Sengupta S, Achyuthan H, Jaiswal MK (2013) Tectonic controls upon Kaveri river drainage, Cratonic Peninsular India: inferences from longitudinal profiles, morphotectonic indices, hanging valleys and fluvial records. *Geomorphology*. <https://doi.org/10.1016/j.geomorph.2013.07.027>
- Kar R, Chakraborty T (2014) Comment on “Geomorphology in relation to tectonics: A case study from the eastern Himalayan foothills of West Bengal, India” by Chandreyee Chakrabarti Goswami, Dhruva Mukhopadhyay, B. C. Poddar [Quaternary International, 298, 80e92]. *Quatern Int* 338:113–118. <https://doi.org/10.1016/j.quaint.2014.01.041>
- Kashani R, Partabian A, Nourbakhsh A (2009) Tectonic implication of geomorphometric analyses along the Saravan Fault: evidence of a difference in tectonic movements between the Sistan Suture Zone and Makran Mountain Belt. *J Mt Sci* 16(5):1023–1034
- Kaushal RK, Singh V, Mukul M, Jain V (2017) Identification of deformation variability and active structures using geomorphic markers in the Nahan salient, NW Himalaya, India. *Quat Int*, 1–17. <https://doi.org/10.1016/j.quaint.2017.08.015>
- Keller E, Printer N (1996) *Active tectonics: earthquakes, uplift and landscape*. Prentice Hall, New Jersey
- Keller E, Printer N (2002) *Active tectonics: earthquakes, uplift and landscape*. Prentice Hall, New Jersey
- Klinkenberg B (1992) Fractals and morphometric measures: is there a relationship? *Geomorphology* 5:5–20
- Lave J, Avouca JP (2000) Active folding of fluvial terraces across the Siwalik Hills, Himalaya of Central Nepal. *J Geogr Res* 105(B3):5735–5770
- Lee C-S, Tsai LL (2010) A quantitative analysis for geomorphic indices of longitudinal river profile: a case study of the Choushui River, Central Taiwan. *Environ Earth Sci* 59:1549–1558. <https://doi.org/10.1007/s12665-009-0140-3>
- Lu P, Shang Y (2015) Active tectonics revealed by river profiles along the Puqu fault. *Water* 7:1628–1648. <https://doi.org/10.3390/w7041628>
- Malik JN, Mohanty C (2007) Active tectonic influence on the evolution of drainage and landscape: Geomorphic signatures from frontal and hinterland areas along the Northwestern Himalaya, India. *J Asian Earth Sci* 29:604–618. <https://doi.org/10.1016/j.jseaes.2006.03.010>
- Mallet FR (1875) On the geology and mineral resources of the Darjiling district and western Duars. *Geol Surv India Memoirs* 11(1):1–50
- Moussi A, Rebail N, Chaieb A, Saadi A (2018) GIS-based analysis of the stream length-gradient index for evaluating effects of active tectonics: a case study of Enfidha (North-East of Tunisia). *Arab J Geosci* 11:123. <https://doi.org/10.1007/s12517-018-3466-x>
- Mukul M, Sridevi SJ, Ansari K, Abdul AM (2014) Seismotectonic implications of Strike-slip earthquakes in the Darjiling-Sikkim Himalaya. *Curr Sci* 106:198–210
- Nakata T (1989) Active faults of the Himalaya of India and Nepal. *Geol Soc America Special Paper* 232:243–264
- Pant CC, Singh SP (2017) Morphotectonic analysis of Kosi river basin in Kumaun Lesser Himalaya: an evidence of neotectonics. *Arab J Geosci* 10:421. <https://doi.org/10.1007/s12517-017-3213-8>

- Partabian A, Nourbakhsh A, Ameri S (2016) GIS-based evaluation of geomorphic response to tectonic activity in Makran Mountain Range, SE of Iran. *Geosci J*
- Pavano F, Pazzaglia FJ, Catalano S (2016). Knickpoints as geomorphic markers of active tectonics: a case study from northeastern Sicily (southern Italy). *Geol Soc America*. <https://doi.org/10.1130/L577.1>
- Pérez-Peña JV, Azor A, Azañón JM, Keller EA (2010) Active tectonics in the Sierra Nevada (Betic Cordillera, SE Spain): insights from geomorphic indexes and drainage pattern analysis. *Geomorphology*, 74–87. <https://doi.org/10.1016/j.geomorph.2010.02.020>
- Phartiyal B, Kothyari GC (2011) Impact of neotectonics on drainage network evolution reconstructed from morphometric indices: case study from NW Indian Himalaya. *Z Geomorphol* 56(1):121–140. <https://doi.org/10.1127/0372-8854/2011/0059>
- Philip G, Viridi NS, Suresh N (2009) Morphotectonic evolution of Parduni basin: an intradun Piggy-back basin in Western Doon Valley, NW outer Himalaya. *J Geol Soc India* 74:189–199. <https://doi.org/10.1007/s12594-009-0121-x>
- Rees GH, Collins DN (2006) Regional differences in response of flow in glacier-fed Himalayan rivers to climatic warming 20(10):2157–2169
- Rhea S (1993) Geomorphic observation of rivers in the Oregon coast range from a regional reconnaissance perspective. *Geomorphology* 6(2):135–150
- Schumm SA (1956) The evolution of drainage systems and slopes in bad lands at Perth, Amboi, New Jersey. *Geol Soc Ame Bull* 67 (5):597–646
- Schumm (1986) Alluvial river response to active tectonics. In: N.R. Council (ed) *Active tectonics*. National Academy Press, Washington (D.C.), pp 80–94
- Seeber L, Gornitz V (1981) River profiles along the Himalayan arc as indicators of active tectonic. *Tectonophysics* 92:335–367
- Sharma G, Ray PK, Mohanty S (2017) Morphotectonic analysis and GNSS observations for assessment of relative tectonic activity in Alaknanda basin of Garhwal Himalaya, India. *Geomorphology*
- Sharma S, Sarma JN (2017) Application of drainage basin morphotectonic analysis for assessment of tectonic activities over two regional structures of the Northeast India. *J Geol Soc India* 89:271–280
- Singh V, Tandon SK (2008) The Pinjaur dun (intermontane longitudinal valley) and associated active mountain fronts, NW Himalaya: tectonic geomorphology and morphotectonic evolution. *Geomorphology* 102:376–394. <https://doi.org/10.1016/j.geomorph.2008.04.008>
- Sinha SK, Parker G (1996) Causes of concavity in longitudinal profiles of rivers. *Water Resour Res* 32:1417–1428
- Soja R, Sarkar S (2008) Characteristics of hydrological regime. In: Starkel L, Sarkar S, Soja R, Prokop P (eds), *Present-day Evolution of Sikkimese-Bhutanese Himalayan Piedmont* (pp 37–46). Warszawa: Stanisława Leszczyckiego
- Starkel L, Sarkar S, Prokop P (2008) Present-day evolution of the Sikkimese-Bhutanese Himalayan Piedmont. *Polska Akademia Nauk, Instytut Geografii i Pezestrzennego Zagospodarowania*
- Summerfield MA (1991) *Global geomorphology: an introduction to the study of landforms development*. Longman, Harlow
- Troiani F, Galve JP, Piacentini D, Seta MD, Guerrero J (2014) Spatial analysis of stream length-gradient (SL) index for detecting hillslope processes: a case of the Gállego River headwaters (Central Pyrenees, Spain). *Geomorphology* 214:183–197. <https://doi.org/10.1016/j.geomorph.2014.02.004>
- Valdiya KS (2002) Emergence and evolution of Himalaya: reconstructing history in the light of recent studies. *Prog Phys Geogr* 26(3):360–399
- Valdiya KS (1986). Neotectonic activities in the Himalayan belt. *New tectonics in South Asia*, Surv., (pp 241–267). Dehradun
- Valdiya KS, Joshi DD, Sanwal RS, Tandon SK (1984) Geomorphologic development across the active Main Boundary Thrust: an example from the Nainital Hills in Kumaun Himalaya. *J Geol Soc India* 25:761–774

- Virdi NS, Philip G, Bhattacharya S (2007) Neotectonic activity in the Markanda and Bata river basins, Himachal Pradesh, NW Himalaya: a morphotectonic approach. *Int J Remote Sens* 27(10):2093–2099. <https://doi.org/10.1080/01431160500445316>
- Yin A (2006) Cenozoic tectonic evolution of the Himalayan orogen as constrained by along-strike variation of structural geometry, exhumation history, and foreland sedimentation. *Earth-Sci Rev* 76:1–131

Development of the Dharala River Course and Its Response to Neotectonic Indentations-Evidences from Old Data Inventory, Satellite Images and Sedimentary Architecture



Ujwal Deep Saha, Soma Bhattacharya, Harendra Nath Bhattacharya, and Sanjana Dutt

Abstract Himalayan Foreland Basin (HFB) has been a fluvio-geomorphic domain of hyper-avulsive rivers associated with numerous abandoned channels. This study contemplates the evolution of a presently abandoned channel named Dharala and the echoes of neotectonic controls in it. Analysing the old data inventory in the forms of old maps since 1767 and colonial literature along with fine resolution digital datasets and validation of those using geomorphic markers and sedimentary archives have been the major stance of this study during establishing the facts of channel development. While marking out the tectonic controls in the process of channel development morphotectonic approach was embarked using the indices related to channel planform; Regional Sinuosity, Topographical Sinuosity index, Meander Arc Angle and Meander Shape Index along with channel orientation parameters; channel parallelism to neotectonic confinement and meander bends direction. Dharala River, one of the major branches of Torsa River, was formed primarily through capturing palaeo channels of Jaldhaka River and later on reworked by the major share of discharge of Torsa River. The abnormality in the channel planform with respect to the locational extent, sudden deflections in channel direction around the points where Dharala had encountered lineaments or fault lines had certified the positive controls of neotectonic features. Precisely, intense meandering with sinuosity ranging from 1.20 to 3.12, possible deformations in channel long profile with relatively flatter middle segment, channel segments deflected along the lineaments and fault lines with 42% of the total number of major turns in channel direction that had encountered neotectonic

U. D. Saha (✉)

Department of Geography, Vivekananda College for Women, Barisha, Kolkata, India

S. Bhattacharya

Vivekananda College for Women, Barisha, Kolkata, India

H. N. Bhattacharya

Department of Earth Sciences, Techno India University, Sector V, Salt Lake, West Bengal, India

S. Dutt

Department of Geography, University of Calcutta, Kolkata, India

confinements, confined meandering with 21% of total bends oriented in the NNE-SSW direction and the existence of micro-terraces and entrenched channel segments had showcased neotectonic controls on the development of Dharala River.

Keywords Abandoned channel · Dharala River · Evolution · Himalayan Foreland Basin · Neotectonics · Planform

1 Introduction

Dharala River had once been the foremost flow-path for the Torsa River, situated in the Sub-Himalayan region of West Bengal. The presently abandoned channel of Dharala had been considered as one of the major waterways in the Sub-Himalayan part of West Bengal and its importance in the local economy and culture had been well documented in the colonial literature of Choudhury (1903), Hunter (1867–71), Gunning (1911). On the young alluvial formation of the Himalayan foreland basin (HFB) rivers are with a substantial history of flood and frequent avulsion (Wells 1987; Wells and Dorr 1977; Sinha 1996, 2009; Goswami et al. 1999; Jain and Sinha 2004; Mitra et al. 2005; Jana 2006; Chakraborty and Ghosh 2010; Soja and Sarkar 2008; Sinha et al. 2008; Mukhopadhyay 2014; Saha and Bhattacharya 2016, 2019, 2020). Vast extents of the floodplain deposits by the major rivers on the HFB contain several abandoned channels which used to carry a considerable amount of discharge in the past. HFB is well associated with the topographic transition where channel sedimentation often modifies the cross-valley slope character which is significantly responsible for frequent channel avulsion after any major flood event (Slingerland and Smith 2004; Aslan et al. 2006; Sinha 2009; Sinha et al. 2014b).

The hyper-avulsive rivers of HFB are often controlled by the strong stimulus of tectonic effects. Earlier works of Seeber and Gornitz (1983), Agarwal and Bhoj (1992), Goodbred and Kuehl (2000, Goodbred et al. 2003), Mazumdar et al. (2001), Jain and Sinha (2005), Malik and Mohanty (2007), Goswami et al. (2013), Lahiri and Sinha (2012), Rashid et al. (2016), Mandal and Sarkar (2016) on channel response to tectonic effects had accounted many rivers on the HFB as well as numerous tributaries of Brahmaputra River. Considering this typical feature, tectonic controls on any particular river in the lower Brahmaputra region in India have been less documented. Even the valuable documents and literature based on this region have had not been utilized to reconstruct any significant fluvial history. The reconstruction of the complex history of channel shifting in this region will be of much importance from the palaeo geomorphic perspective. Along with it, the associated tectonic stimulus on channel development should be showcased in any region which has been tectonically active since the Quaternary period (Kaushal et al. 2017). The Western branch of Torsa, Dharala River, had developed its course on a tectonically active margin along the Falakata Fault. The signatures left in its planform characteristics and orientation pings an inquisition for the tectonic control on channel development.

Considering the tectonic controls on channel development, this study is aimed towards a systematic reconstruction of the fluvial history of Dharala or 'Dhalla' on a tectonically active fault margin. Old data inventory in the form of old maps (since 1764–77) and literature (of Colonial period in India) has been utilized to prepare a database which requires incorporation with present-day analysis of remotely sensed data as well as topographic and sedimentological evidence.

2 Study Area: Structural Setup and Geomorphology

The HFB is immediately associated with the Rangpur platform which is the transitional tectonic province between the Bengal fan and Himalayan foredeep, lies towards the south of the study area (Khan 2002; Farhaduzzaman et al. 2015; Hossain et al. 2019). The basement uplift of the Rangpur platform centred among the piedmont on the north, Bengal fan in the south, Indian shield on the west and Shillong massif in the east. The sedimentary structure of HFB has become progressively younger towards the south where recent deposits have built up a significant floodplain that demarcates the belts of channel migration within it (Chattopadhyay and Das 1979; Kumar et al. 2016). Dharala had developed its course on the northern plain of West Bengal that lies above the Rangpur platform. The general surface gradient is quite low ranging from 0.91 to 0.21 m/km along with the elevation ranging from 49 to 31 m (see Fig. 1). The Dharala River system has been developed on a comparatively higher ground than other palaeo courses of Torsa because the altitudinal drop is from west to east due to the mega fan deposits and extension of distal fan segment flanking along the Jaldhaka River (see Fig. 2). The interfluvial region of Dharala and Torsa River is associated with several transverse and drainage parallel lineaments where Dharala had roughly flowed parallel to the N-S trending Falakata fault which roughly separates the elevated Jaldhaka valley on the west from the low lying historical migration corridor of Torsa River in the East (see Fig. 3). The slope-guided and fault line controlled plain-fed fluvial system of Dharala has been concentrated into a wandering path with tight meander bends and cut-offs. The Dharala River branched into two different channels after a bifurcation near Haldimohan and reunited downstream. The western branch is called Mara Dharala and the eastern branch is called Bura Dharala. The migration of Dharala River is well reflected in those cut-offs, meander scars and abandoned channels lying mostly on the west of the river. Few minor spill channels of Jaldhaka developed as abandoned courses and one of those; named Brahmi River has been flowing through the decayed course of Dharala. The meandering channel of Dharala with a history of channel recapture while developing its course and further reworked by minor channels has resulted in entrenched meandering conditions within a misfit fluvial system. Certain sections were identified with several tiers of terraces.

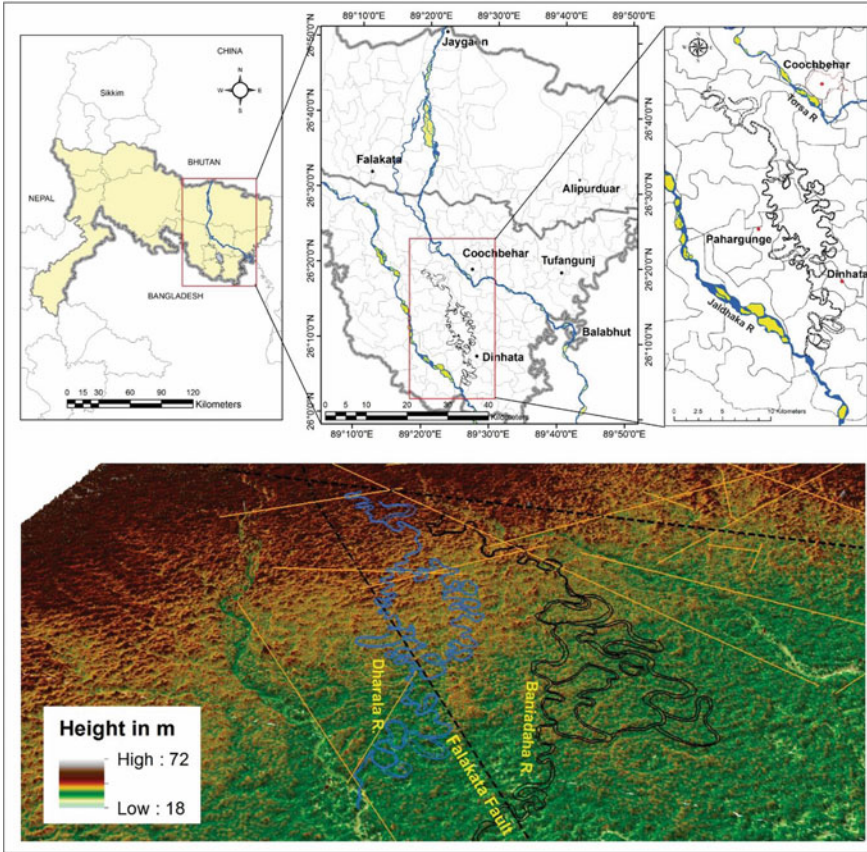


Fig. 1 Study area. 3d figure of the study area (elevation map (3d) was prepared from SRTM DEM 30 m)

3 Materials and Methods

The sedimentary archives (Miall 2014; Sinha 1996) studied along the abandoned courses and digital image processing (Bhuiyan et al. 2015; Laha and Bandyopadhyay 2013; Li et al. 2007) are the non-negotiable tools while studying palaeo-fluvial phenomenon.

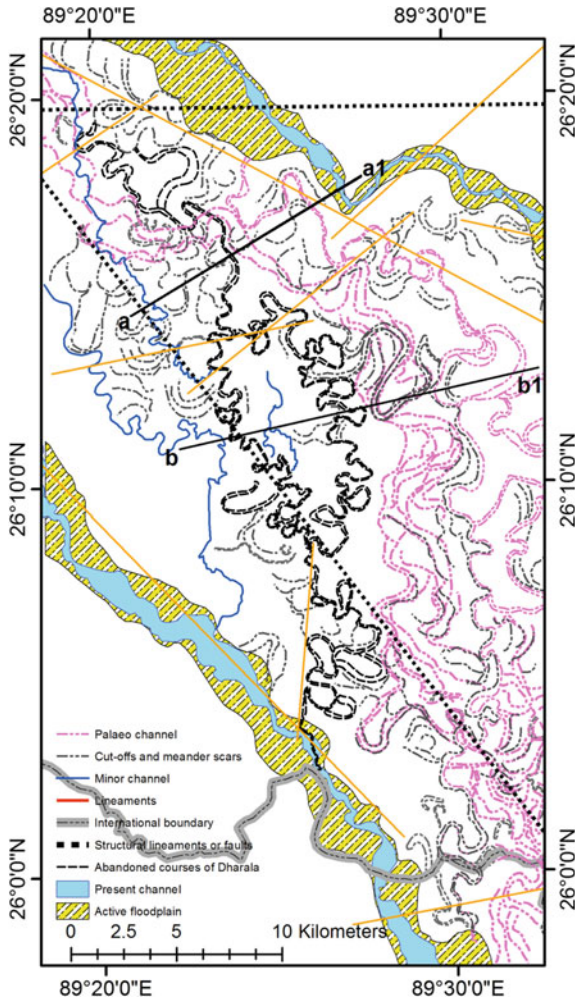


Fig. 2 Floodplain geomorphology and structural setup of the study area; compiled from Khandoker (1989), Alam et al. (1990), Khan (2002), Rashid et al. (2016)

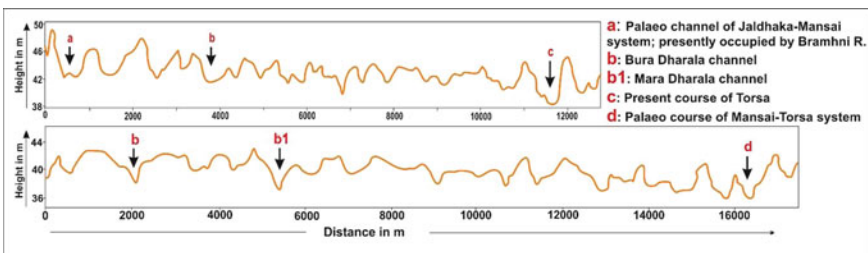


Fig. 3 Elevation profiles derived from DEM SRTM 30 m across the region demarcates Dharala on a comparatively higher elevation than the associated palaeo courses on the east

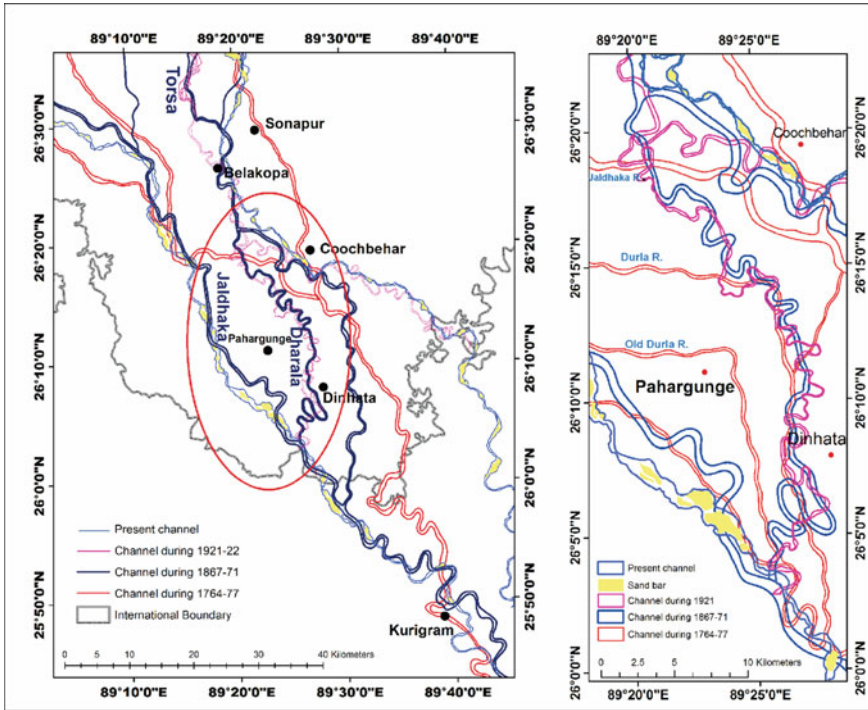


Fig. 4 Spatio-temporal characteristics of Jaldhaka-Torsa system and initiation of Dharala river course

3.1 Analysis of Old Data Inventories

The old data inventories in the form of literature of the colonial period in India and maps (since 1764–77) are of great use while drainage reconstruction (Bandyopadhyay 1996; Chakraborty et al. 2010; Rudra 2014; Scorpio et al. 2018). Georeferencing of the old maps was done using the affine transformation model based on 41 placemarks collected from Google Earth (Walz and Berger 2003). Valid placemarks on the old maps were only considered after a cross-check was performed based on relative locations i.e. distance and direction between two places, as well as the relative positions of those points from famous locations like Coochbehar and Jalpaiguri town. Root Mean Square Error (RMSE) was performed from the coordinate matching table prepared in the software domain following the works of Thapa (1992) and Klang (1996).

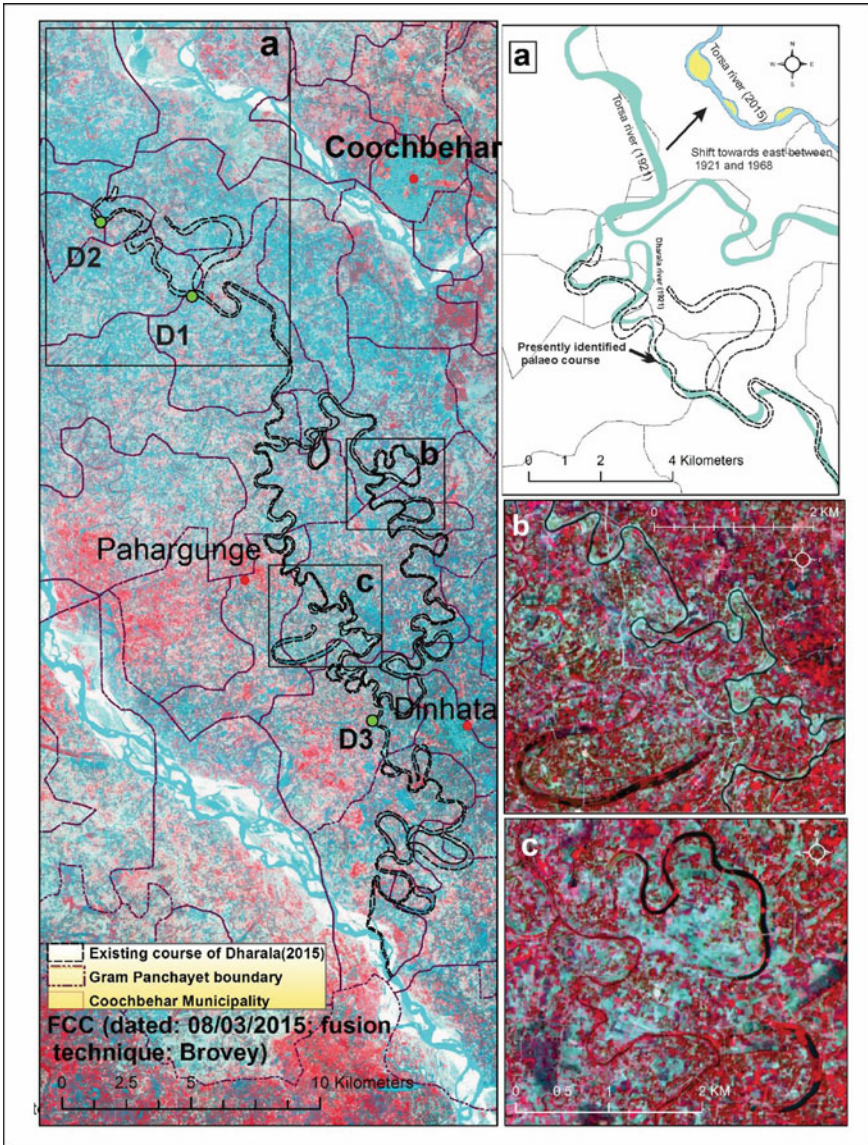


Fig. 5 Demarcation of the course of Dharala River and its present day characteristics. **a** Shifting of Torsa river towards east between 1921 and 1968; **b** present day characteristics of the misfit segment of Bura Dharala; **c** present day characteristics of the decayed course of Mara Dharala

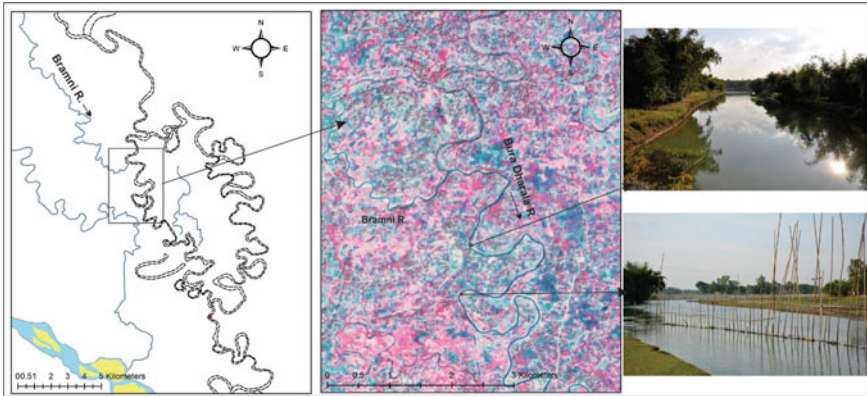


Fig. 6 On-field signature of the decayed course of Dharala

3.2 Identification of the Old Courses and Geomorphic Indicators

Landsat 8 image acquired during the pre-monsoon period of 2015 has been used to track down the courses of Dharala River. Image fusion technique was applied for the Landsat images using the Brovey method (Brovey 1990) where Band 3, Band 4, Band 5, Band 6 and Band 8 (Panchromatic) were fused to obtain comparatively higher resolution data (15 m). Geo-rectified Sentinel 2 data of March 2017 has also been used as an additional reference for the abandoned courses of Dharala. Geomorphic indicators like paleo-levee, scroll marks, paleo bank lines, cut-offs and oxbows were identified from the processed images (Saha and Bhattacharya 2019). Minor corrections were done by taking spatial references from Google Earth. Image processing and vector generation were done using Arc Gis v. 10.3 and TNT Mips 2014. Ground control points (Gcps) at 22 relevant sites were collected using Garmin eTrex 30 keeping the instrument at 1 m accuracy. A topographic study of the decayed channels was conducted in 2015 and 2016 as on-field verification of the vectors derived from digital datasets (Table 2). On the other hand, knowledgeable persons were interviewed to gather information regarding past fluvial activities around certain areas (Table 1).

3.3 Extraction of Neo-Tectonic Signatures

Rivers on the HFB, both on the piedmont and associated plain, are tectonically controlled where surface deformation in the form of lineaments, fault lines and upheaval or subsidence of certain blocks has thoroughly guided the direction of the channels (Rashid et al. 2016). On an alluvial plain tectonic signature and spatial

Table 1 Materials used

<i>Old maps</i>				
Material	Time period	Source	Scale	RMSE (m)
Map of Bengal and Bihar	1764–77	Bengal Atlas, 1777 by Major J. Rennell	60 geog. miles to 1 inch	18
Map of Rajshahi and Kuch Behar Division	1867–1871	Statistical Account of Bengal, 1875, vol 10 by Sir W. W. Hunter	1 inch to 16 miles	16
Toposheets 78F/5/6/7/8/11/12;	1917–18	Survey of India, 1931	1:63,360	6
<i>Satellite images</i>				
Satellite	Sensor	P/R	Resolution	Date of Acquisition
Landsat 8	OLI	139/42	30 m	15.03.2015
Sentinel 2	MSI	Coordinates: 26.6037653, 89.5593356	10 m	16.03.2017

visualization of surface, deformation are strenuous to identify. Although, a river through its mode of adjustment usually showcases the impact of surface displacement along a fault line implied on it (Ouchi 1985; Gregory and Schumn 1987; Boyd and Schumm 1995; Holbrook and Schumn 1999; Schumn et al. 2000; Barman et al. 2019). In this study morphotectonic approach was applied to analyse the tectonic implications on both channel morphology and orientation considering the changes in sinuosity parameters, parameters of meander geometry, and meandering intensity.

3.3.1 Channel Long Profile

Long profile of any channel is an immediate exhibition of the tectonic impact of the channel (Hack 1973; Seeber and Gornitz 1983; Sinha-Roy 2001; Troiani and Della 2008; Lee and Tsai 2010; Ambili and Narayana 2014; Lu and Shang 2015; Moussi et al. 2018). SRTM DEM derived long profile of the channel with an overlay of lineaments and fault was constructed and smoothed to extract the overall nature of the long profile. Channel gradient was calculated by collecting elevation values from the long profile at an interval of 4 km (from the N-S ranging straight line within the study area). The equation used was; $\text{Elevation of two extreme points (in m) / Length of the reach (in km)}$.

Table 2 On-field character and geomorphic signatures of old courses of Dharala at selected locations

Coordinates	Signatures from the digital dataset	On field signatures	Fluvio-geomorphic significance
26°18'4.85"N 89°23'14.03"E	Scroll marks and palaeo bank lines; palaeo levee was demarcated using the linear vegetation growth	Extremely degraded due to agricultural practices. although farm ponds have significant sand layers just beneath the floodplain mud and reclaimed portion	One of the off takes. got abandoned due to shifting of Torsa river
26°18'42.81"N 89°19'37.65"E	Minor channel within a comparatively wider valley marked by palaeo bank lines and levee	Misfit channel characteristics with entrenched meandering condition	Upstream portion of Dharala than was actually developed through capturing palaeo course of Jaldhaka river
26°17'6.51"N 89°21'28.64"E	Linear orientation of ponds and palaeo levee that was demarcated following the linear trend of vegetation	Both the levee and channel corridor was extremely degraded due to agricultural and aqua-culture practices. although the farm ponds were identified with distinct layers of massive sand and heterolithic surfaces beneath the floodplain deposits and reclaimed portion	Section of the abandoned course that was active during 1920's
26°16'56.23"N 89°23'20.97"E	Palaeo levee, scroll marks, feeble flow with a width of 12 m	Palaeo bank line, floodplain has been utilized for intensive agricultural practices. the high moisture content of the abandoned channel bed is utilized for wet paddy cultivation and the higher grounds were under cereals	Active during 1920's
26°13'49.28"N 89°23'56.11"E	Minor channel with a width of 23 m	Entrenched meandering condition. Minor channel engraved within a wider palaeo course. tiers of micro terraces	Abandoned course of Mara Dharala that was last active before 1864
26°13'48.07"N 89°24'18.24"E	Palaeo levee and scroll marks	Linear channel with no flow. the palaeo channel bed was under paddy cultivation	Abandoned course of Bura Dharala that was last active during 1920's

(continued)

Table 2 (continued)

Coordinates	Signatures from the digital dataset	On field signatures	Fluvio-geomorphic significance
26°12'32.66"N 89°23'32.85"E	Minor channel with a width of 19 m	Misfit fluvial characteristics with tiers of micro terraces	Abandoned course of Mara Dharala that was last active before 1864
26° 8'35.36"N 89°26' 12.56"E	Palaeo levee, scroll marks, prominent location of cut-offs and a feeble flow with a width of 18 m	Abandoned channel with high grounds as the remnants of palaeo bank lines	Abandoned course of Bura Dharala that was last active during 1920's
26° 7'58.43"N 89°25'54.84"E	Prominent channel with an active flow	Misfit channel characteristics. active flow was due to Brahmini River that has been flowing through the abandoned course. heterolithic structure with channel fill deposits during large floods	Abandoned course of Mara Dharala that was last active before 1864
26° 7'25.77"N 89°26'7.23"E	Prominent channel with an active flow, cut-offs and scroll marks	Misfit channel characteristics with a wider valley. palaeo bank lines over topped with marginal floodplain deposits. floodplain has been widely utilized by agricultural practices	Downstream section after the reunion of Bura Dharala and Mara Dharala

3.3.2 Sinuosity Parameter

Regional sinuosity was calculated for both the channels of Dharala River at an interval of 2 km using the ratio between channel distance and shortest path distance (Leopold et al. 1965). Adjustment of the meandering river under the influence of faulting can well be captured through regional variations in sinuosity (Holbrook and Schumm 1999; Zámolyi et al. 2010; Roy and Sahu 2015). The Topographic Sinuosity Index (TSI) suggests both the tectonic and topographic controls on a river. It was calculated as;

$$HSI = (CI - VI)/(CI - 1)$$

$$TSI = (VI - 1)/(CI - 1) * 100$$

VI (Valley Index) = VL (Valley length)/AL (Air length).

CI (Channel Index) = CL (Channel length)/AL (Air length).

3.3.3 Directional Attributes of Meander

The direction of the meander bend was calculated using the direction of the meander bend axis with reference to geographical north. All the existing meander loops (N = 77) of both the courses of Bura Dharala and Mara Dharala as well as of the associated minor channels were considered while measuring the bend orientation. Stress implied on the surface due to faulting can create several neotectonic obstructions for a river where the orientation of the meandering loops easily gets affected. Alongside, the angle of turn was measured along 19 major locations, wherever any striking change in channel direction has been noticed in both the channels of Dharala and minor channels. The downstream flow direction above the turn was considered as 0 degree.

3.3.4 Meander Intensity Attributes

Meandering intensity attributes were only considered for the courses of Dharala. Measuring the intensity is best suited for a particular river rather than applying for an intraregional trend, as apart from tectonic reasons meandering intensity is also derived by competence and capability of a river (Timár 2003). 63 loops of demarcated continuous channel segment (cut-offs were excluded) of Bura Dharala and Mara Dharala were only considered while analysing the meandering intensity.

The meander arc angle or tightness of a meandering loop was calculated by taking reference from the point of inflection on either side of the bends following the works of Williams (1987). The selected 63 loops were calculated in TNT Mips using the arc angle attribute in the Geo-tool box. This signifies the nature of bend tightness (Williams 1987). Smallest the arc angle greater the adjustment and vice versa.

The shape index of meanders is used to identify the intensity of bending. It is the ratio between the radius of curvature and amplitude (Das 2014). Following the ranges considered in the works of Das (2014) loops having a value less than 0.50 signify acute meandering while loops having a value ranging between 0.50–1 signify acute to open meandering and a value greater than 1 defines open meandering. The shape index of 48 loops of Mara Dharala and Bura Dharala was calculated.

3.4 Collection of Sedimentary Sequences

Migratory channels leave their imprint on the ground it used to flow as well as within the floodplain stratigraphy which is quite useful while identifying the depositional behaviour of courses during different phases of channel evolution (Schumn 1981, Abdullatif 1989; Jain et al. 2004; Miall 2014; Aslan et al. 2006; Sinha 1996; Toonen et al. 2012; Sinha et al. 2014a). Several past works on the HFB have been utilized sedimentary records while delineating phases of river evolution (Mohindra et al. 1992; Shukla et al. 2001; Singh et al. 2006; Chakraborty and Ghosh 2010; Lahiri and Sinha 2012; Sinha et al. 2005, 2014b). The typical depositional pattern on the alluvial

Table 3 Geomorphic significance of excavation sites

ID and location of excavated sites	Overall character	Fluvial significance
D1: 26°17'7.51"N; 89°21'28.17"E	Abandoned segment with no such channel reoccupation events	Around the off-take of Dharala
D2: 26°18'41.40"N; 89°19'39.11"E	Couple of channel abandonment and further reoccupation events	Palaeo course of Jaldhaka-Mansai system
D3: 26° 8'12.49"N; 89°26'2.09"E	floodplain depositions with inter-beddings channel fill deposits	Decayed course of Dharala, presently occupied by Brahmi River

fan surface usually dominates the nature of sedimentary records in this selected spatial extent. Along with this the frequent abandonment of the channel environment, channel filling during flood events had mostly influenced the sedimentary records in the low-lying flood plains in the south of HFB. The significance of all 5 excavations was judged based on their fluvial nature (see Table 3). The excavations were done by digging trenches either at the bank of the Dharala River or at the side of ponds parallel to palaeo flow directions within the decayed segments with no traces of continuity. Sites were selected based on accessibility and availability. Field chart and magnifying glass were used to find the textural characteristics of different sedimentary layers in each of the Litho sections.

4 Neotectonic Movements and Channel Evolution

The analysis of channel responses to neotectonic perturbations in this concerned fluvial system has been done in two different steps. Firstly, the evolution of the river course has been analysed and the nature of neotectonic controls on the evolution of the system has been incorporated thereafter.

4.1 Evolution of the River Course

Coochbehar state (presently in West Bengal) was a princely state before the independence of India. Developed road networks, major monuments from the era assisted in collecting GCPS and verifying it from the old maps. A well-traced history of the Coochbehar and Koch dynasty from several colonial literatures, survey records, historical articles and books had enriched the data inventory.

4.1.1 Pre-development Scenario; Late Eighteenth Century

Observations from the digital datasets had revealed that throughout the past, the present course of Torsa was not the main course that used to flush out the major share of discharge. In support of present-day observations, a map prepared during 1764–77 had concealed that Mujnai or Mansai which had a connection with Jaldhaka River near Matiarkuthi used to meet Torsa downstream around 16 km south of Coochbehar town (see Fig. 4). The united course of Torsa and Mujnai used to flow from the east of Dinjata in Coochbehar district. Flowing through the east of Kurigram (now in Bangladesh) it met Brahmaputra River further downstream. During 1764–77 Durla and old Durla were flowing through the south of the Mansai River with a sharp deflection towards the south before joining the united course of Torsa and Mansai near Kurigram (see Fig. 4).

4.1.2 Development of Dharala; Since Early Nineteenth Century to Early Twentieth Century

The westward movement of the Torsa River and forking out into two channels, Dharala (western branch) and Baniadaha river (eastern branch), during the late eighteenth century, were the most significant changes that occurred in the course of Torsa between 1777 and 1861–64. The floods of 1801, 1809 and 1820 had significant roles in the development of Dharala River (Hunter 1871; Choudhury 1903; Bandopadhyay 2007). Aggradation of the previous course and the westward shift of Torsa into Char Torsa near Hasimara invariably lead to the westward diversion of the entire flow. Besides the westward movement of Torsa River, Jaldhaka River also went shifted towards the west and developed its course through the Old Durla River during the late eighteenth century (see Fig. 4). This westward shift in the course of Jaldhaka abandoned a considerable stretch of the Jaldhaka-Mansai system on the east of the present course of the Jaldhaka River. Dharala or Dhalla River had expanded its course as it captured a certain segment of the palaeo courses of the Jaldhaka-Mansai system and the course of Durla River downstream. The share of flow that used to run through the western branch of Torsa followed the course of Bura Dharala (eastern channel) in 1867–71 as the course of Bura Dharala (western channel) was abandoned by then (Choudhury 1903; Gunning 1911). Until a westward shift due to morphometric changes around the bifurcation of the two feeders of Torsa River and Baniadaha, the eastern feeder of Torsa had been more powerful and it was the main branch of Torsa during the late nineteenth century. Later on a flow diversion towards the west, facilitated by morphometric changes around the bifurcation (see Fig. 5) of the two feeders diverted the major share of discharge into Dharala River (Majumder 1977; Choudhury 1903). Writings of Buchanan, 1830 and Hunter, 1867, have mentioned Dharala River as one of the most important and widest channels of Coochbehar in terms of the role played in local economy and transportation. The nature of channel migration of the Torsa River was not unidirectional at all rather certain sections had registered events of channel oscillation (Saha and Bhattacharya 2016). An eastward shift of

Torsa River around the off-take of Dharala between 1921 and 1968 left Dharala as a beheaded stream (see Fig. 5).

4.1.3 Channel Abandonment; After 1917–21

Presently, Brahmni River, a spill channel of Jaldhaka after a southward shift is flowing through the course of Bura Dharala which has given rise to a misfit fluvial character (see Fig. 5). Tiers of micro-fluvial terraces, the concentration of the flow into a distinct shallow channel segment within a broad floodplain were demarcated as the floodplain signatures of misfit channel characteristics (see Figs. 6). Around the bifurcation of Dharala with Torsa several abandoned courses were demarcated using the orientation of ponds, traces of palaeo-levee, and bank lines (see Table 2). Shifting of off-take point of Dharala was evident from the demarcated courses. In the downstream segment due to the flow of Brahmni into Bura Dharala and groundwater contribution to the Mara Dharala the downstream segments can be observed with the feeble flow but the upstream segment was observed with complete absence of flow except for water into few agricultural ponds excavated in the bed of the palaeo courses.

4.2 Present Geomorphic Characteristics and Pattern of Evolution

The abandoned channels of Dharala were surveyed for two different purposes; *i.* the present geomorphic character of the courses and *ii.* to validate the findings gathered from analysing the data inventory on the history of course development (see Table 2). Decayed course with traces of palaeo banks and levee was the on-field signatures around the off-take of Dharala. Besides that linear orientation of ponds, impounded cut-offs into mud excavation sites, and farm ponds hold the remnants of lost fluvial signature. In the downstream section, misfit channel characteristics portrayed by a narrow channel engraved into an incised valley within a wide floodplain flanked by palaeo bank lines were observed. Micro-terraces and sections with entrenched meandering have been directed toward multiple cycles in channel evolution due to tectonic effect and post abandonment fluvial actions. The near-surface sediment facies excavated along the palaeo-courses of Dharala has exposed a scenario of decayed fluvial conditions. The deposition of the active fluvial regime was well observed under the overlying floodplain associations.

4.2.1 D1; Decay of an Active Fluvial Regime

Deposition of sand, moderate to fine, and the intermediate laminations of mud, has clearly demonstrated a varying hydrological regime within an active fluvial environment. Massive bedding composed of moderate sand probably deposited immediately after high flood situations and the following drop in the energy flux brought down the corresponding finer sediments engraved to form a heterolithic condition. Association of the simple bed sets with a lack of erosional bounding surfaces has clearly showcased fewer disturbances in flow direction or channel orientation. A trend of fining upwards from sand to floodplain mud without any immediate contact had been due to a decaying condition of the river where the discharge of the channel got reduced with time. The overlying floodplain mud served as a validation for complete abandonment of the channel and few laminations of sand within the floodplain association were evident of low flood situations aided by run-off water (see Fig. 7). In the case of excavations at e1 and e2, both are located around off-take reaches displayed an immediate association of channel deposits with overlying mud which is significant of channel shifting. Lack of multiple facies of channel deposits also had justified the absence of channel reoccupation events. Shifting of off-take points of Dharala was evident from the traced down palaeo courses from the high-resolution satellite images and the sedimentary architecture also corresponded to that finding.

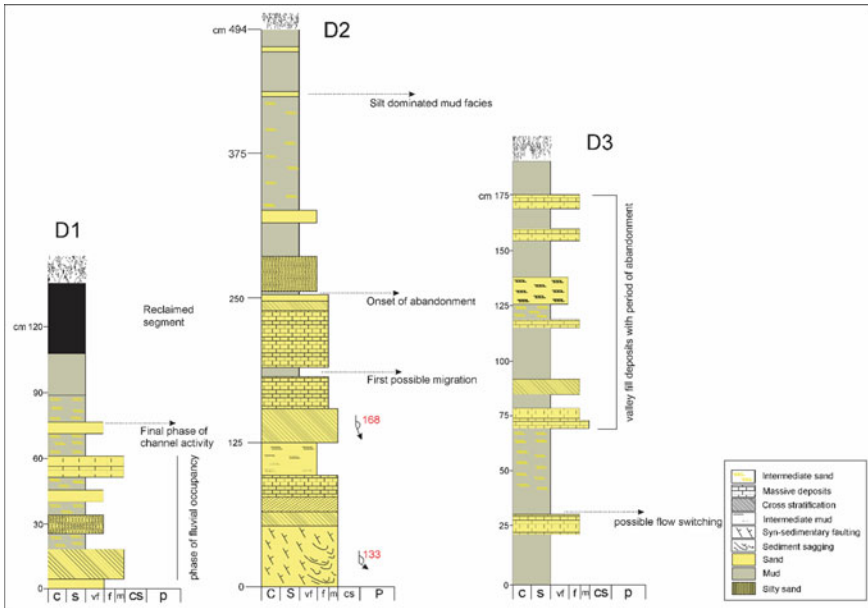


Fig. 7 Facies analysis at D1, D2 and D3 excavation site

4.2.2 D2; Recapturing the Paleocourse

The studied Litho-section on the upstream of Dharala was characteristics of episodic changes in the channel hydrological character (see Fig. 7). It has archived evidence of both channel abandonment and recapturing within a restricted river valley. The bottom-most part of this section signifies channel deposits of a comparatively lower energy regime with overlying oxidized massive sand facies. Above that, a thick layer of floodplain mud and contact of an oxidized layer of active channel deposits signify an event of channel abandonment for a concerned time span. After a while, the course was again recaptured as evaluated from the cross-stratified layer of sand. There have also been traces of massive sand deposition overlying the thick floodplain mud. This channel remained active for a shorter period of time or the rate of deposition of the captor stream was lower compared to the previous one. The textural character of sand in this segment is lower lesser in diameter than the section of the active fluvial regime at the bottom. It was probably captured by Dharala which was a branch of Torsa evidently weaker in terms of stream energy and the total amount of transported load compared to Jaldhaka or Mansai. Litho-stratigraphy of this kind is ideal for any wandering stream that has a tendency of frequent shifting but the competence of the deposited materials reveals the nature of the potential energy that the streams had. The soft deformation structure, syn-sedimentary faulting, found on the bottom of the sequence is evident of tectonic jerking (see Fig. 8).

4.2.3 D3; A Misfit Channel System

Another litho-section was studied downstream of the confluence of Mara Dharala and Bura Dharala. The layer of thick floodplain mud at the bottom was archived during an abandoned condition of the course. Layers of sand with inter-bedded mud signify a scenario of low energy regime associated with layers of massive sand deposited during high flow conditions as channel fill deposition. The alternate orientation of sand and mud associated with massive sand facies correspond to an active channel environment. Thick overlying layers of floodplain mud would be evident of complete channel abandonment but the inter-bedded fine sand to silt deposits signify a misfit character of the channel where these layers were deposited during extremely high flood situations in the captor channel later on. This particular segment of Dharala was previously serving as the active course of Durla River which was captured by Dharala later on. The significant association of fluvial facies with a thick concentration of mud at the bottom was probably due to the abandonment before it was captured by Dharala.

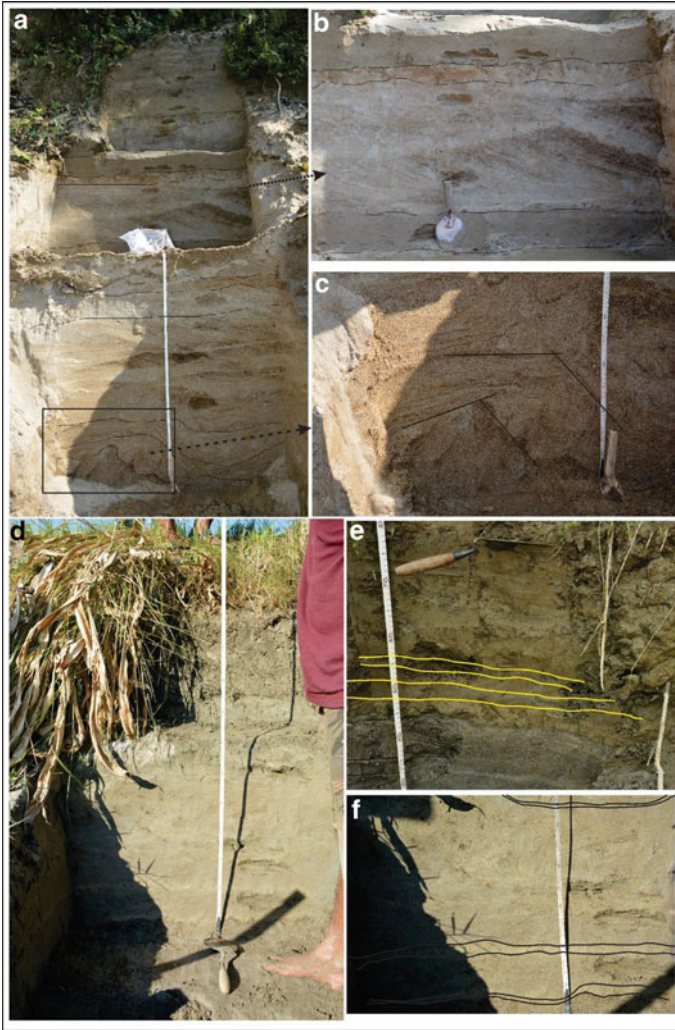


Fig. 8 a Trench excavated at D2; b floodplain mud located at the bottom most and top most section denotes a particular phase of fluvial activity; c Soft sedimentary deformation (SSD) in the form of syn-sedimentary faults were observed at D2; d trench excavated at D1; e Channel deposits underlying the mud facies, denotes event of channel abandonment; yellow lines demarcates thin sand beds deposited within floodplain deposits signifies the occasional high flood events during the period of active flow cessation; f inter-beddings of mud within active channel deposits signify low flow deposits within the active regime

4.3 Channel Morphological Responses to Quaternary Tectonics

4.3.1 Channel Long Profile Forms Adjustments

The long profile of the Bura Dharala corresponded to the quaternary fan sedimentation with several tiers of topographic expressions (see Fig. 9). The distal portion of the mega fan surface on the western part of the study area is well associated with several drops in elevation around its outflanking portions (see Fig. 2). The segment where Mara Dharala has strictly followed the fault line, an upheaval in its course corresponded to maximum depositional activity along the fault line buried under alluvium. This is quite common for rivers flowing along a sub-surface fault margin (Holbrook and Schumn 1999). The channel gradient also corresponded to the nature of the differential sedimentation. The segment of the channel along the fault margin has registered a drop in the gradient value compared to both the upstream and downstream segments. Channel distance from 10.49 to 19.39 km from the offtake had an average gradient of 0.22 m/km which is lower than both the upstream and downstream segment as well the average gradient of 0.55 m/km of the entire channel (see Fig. 9). Misfit channel characteristics with entrenched meaders were well observed in that particular segment (see Table 2 and Fig. 6).

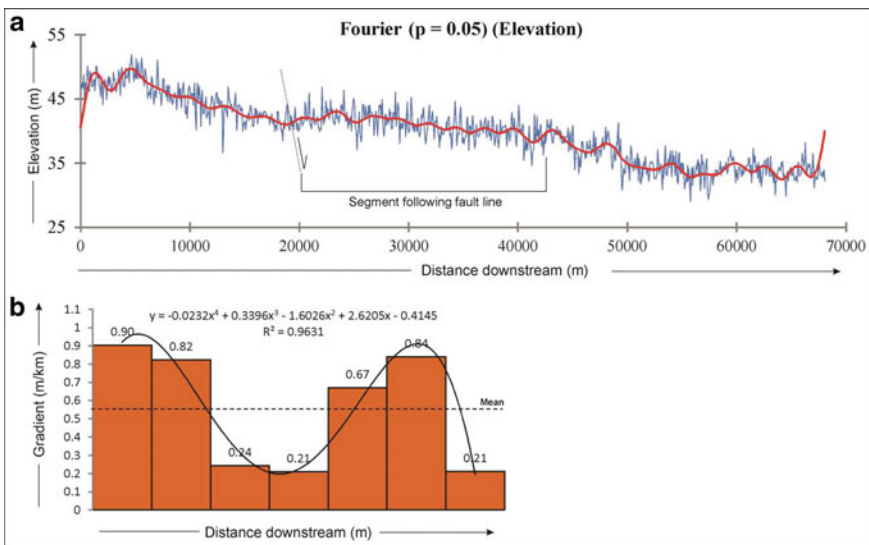


Fig. 9 Characteristics of the long profile of Dharala River. **a** higher amount of sediment deposition resulted in sediment bulging around the fault margin; **b** channel gradient of Bura Dharala

4.3.2 Channel Planform Adjustments

Compressed meanders, asymmetric meander bends and bends following lineaments transverse to the major fault line are the surface features of the tectonic influence on drainage development (Holbrook and Schumn 1999; Goswami et al. 2009; Rashid et al. 2016). Among many other palaeo courses of Torsa River, Dharala has been the most distinct one in terms of planform and associated geomorphic expressions (Saha and Bhattacharya 2016).

4.3.2.1 Sinuosity Parameters

The regional sinuosity value of Dharala River is quite high with a maximum and minimum value ranging from 3.12 to 1.20 for Bura Dharala, 2.81 to 1.36 for Mara Dharala (see Table 4). Sinuosity value increases with acute adjustment in channel planform. The channel of Bura Dharala, which follows the fault line, has registered an overall high SI value with the highest SI being in the segment which encounters lineaments (see Fig. 10). The neotectonic constrain was strong enough to hold the channels into particular valleys. 88% and 83% of the total length of the courses of Mara Dharala and Bura Dharala respectively has sinuosity value of more than 1.5. Besides neotectonic constraints and tectonic impulses partly cohesive surface material, nearly flat terrain and a change in slope over the quaternary fan sedimentation have compelled these channels to take an acute wandering path. The TSI values of Bura Dharala and Mara Dharala were all positive and close to 100. It ranges from 69.51 to 106.04 for Bura Dharala and 88.68 to 96.91 for Mara Dharala. The average TSI was 86.50 and 92.42 for Bura Dharala and Mara Dharala respectively (see Table 6). On average, the channel sinuosity of Dharala River has been under topographic control with developed floodplains and a misfit fluvial character (Table 5).

4.3.2.2 Meandering Intensity

The meander bend tightness or the arc angle value of Bura Dharala ranges from 7 to 84° with a mean of 28° (see Table 5) while the Arc angle value for Mara Dharala ranges from 96 to 11 with a mean of 27. The distribution of meander tightness value and high regional sinuosity value has been a clear example of intense adjustments done by the Dharala River through time (see Fig. 13). Alongside, the meander shape index has significantly showcased the high intensity of meandering with an average value of 0.40 where 81% of the meandering loops of both the courses of Dharala were observed to have acute meander loops (see Table 5 and Fig. 12). Although the course of Mara Dharala is on the flanking part of the elevated ground where a

Table 4 Regional sinuosity value

Statistic	Mara Dharala	Bura Dharala	Brahmni	Minor Channels
Average	1.87	2.34	1.56	1.54
SD	0.57	0.53	0.66	0.45
% of Segments SI \geq 1.5	88.23	83.33	33.33	50

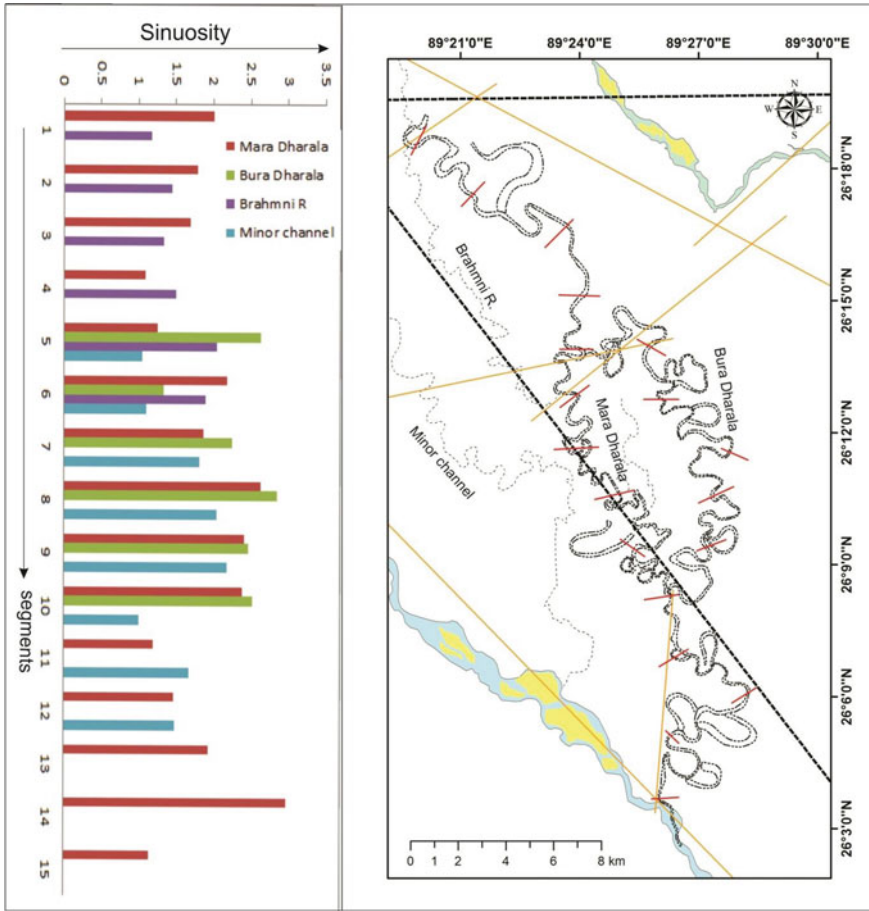


Figure10 Channel Sinuosity value

Table 5 Meandering parameter of selected bends

Courses	Arc angle			MSI			% Occupancy of Arc angles							% Occupancy of MSI		
	Max	Min	χ	Max	Min	χ	10	20	30	40	50	60	> 60	< 0.5	1	> 1
Mara Dharala	84	7	28	1.46	0.04	0.41	7.5	30	20	25	7.5	5	5	75	20	5
Bura Dharala	96	11	27	0.91	0.15	0.38	0	43	35	13	0	0	9	82.6	17.4	0

Table 6 Sinuosity parameter of the courses of Dharala River

Zone	CI		VI		TSI		HSI (TSI + HSI = 100)	
	Bura Dharala	Mara Dharala	Bura Dharala	Mara Dharala	Bura Dharala	Mara Dharala	Bura Dharala	Mara Dharala
1	2.08		1.99		91.81		8.18	
2	2.07		1.83		77.38		22.61	
3	1.76		1.70		93.10		6.89	
4	1.12		1.10		79.68		20.31	
5	1.25	2.84	1.24	2.67	94.22	90.44	5.77	9.55
6	2.33	1.35	2.17	1.39	87.70	96.91	12.29	3.08
7	2.40	2.35	1.99	2.28	70.87	94.92	29.12	5.07
8	2.30	2.90	2.38	2.79	106.01	94.14	-6.01	5.85
9	2.71	2.65	2.41	2.47	82.54	89.39	17.45	10.60
10	2.66	2.75	2.37	2.56	82.80	88.68	17.19	11.31
11	1.29		1.20		69.51		30.48	7.57
12	1.51		1.47		92.66		7.33	
13	2.06		1.94		88.88		11.11	
14	3.06		2.94		93.99		6.007	
15	1.15		1.13		86.36		13.63	
MEAN	1.98	2.47	1.86	2.35	86.50	92.42	13.49	7.57
MAX	3.06	2.90	2.94	2.79	106.01	96.91	30.48	11.31
MIN	1.12	1.35	1.10	1.33	69.51	88.68	-6.014	3.08

change in elevation and surface gradient could have played a significant role in the acute meandering condition of Mara Dharala, it has been estimated that the intensity of meandering and fault margin shows a neotectonic control on the acuteness of meandering (Fig. 11).

4.3.2.3 Channel Orientation

The direction of the meander bends is varied in direction. 20.63% of the total meander bends (N = 77) is oriented both towards NNE and WSW, 17.46% of the total is oriented towards ESE (see Table 5). All the eight directional quadrants have been experienced with the bend direction of Dharala River (see Fig. 13). The implied stress of Neotectonic event along the Falakata fault makes it a common feature of the channel morphometry to experience such drastic bends. Besides the neotectonic constraints, the fall in gradient and association of differential alluvial fan growth had allowed a preferable ground for Dharala river to develop its meandering loops on the fine sandy to the silty surface material. Moreover, the lineaments and the fault lines have played quite a significant role in case of deflecting the channels in the studied spatial extent. The minor channels on the west and Brahmini River have been flowing through certain palaeo courses. These were also characteristic of channel

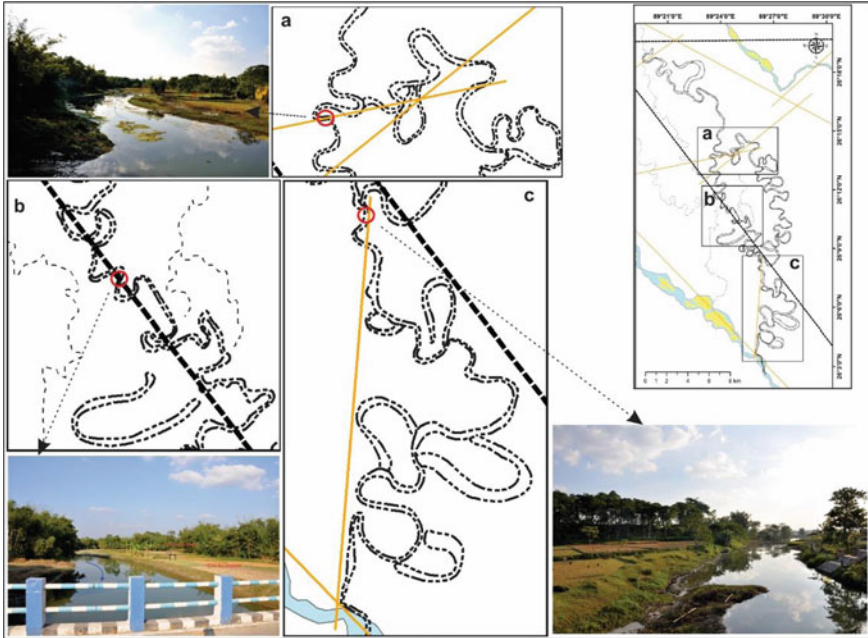


Fig. 11 Channel Parallelism of Dharala courses to lineaments and fault lines. Photographs depict the entrenched meandering character at the places of channel parallelism

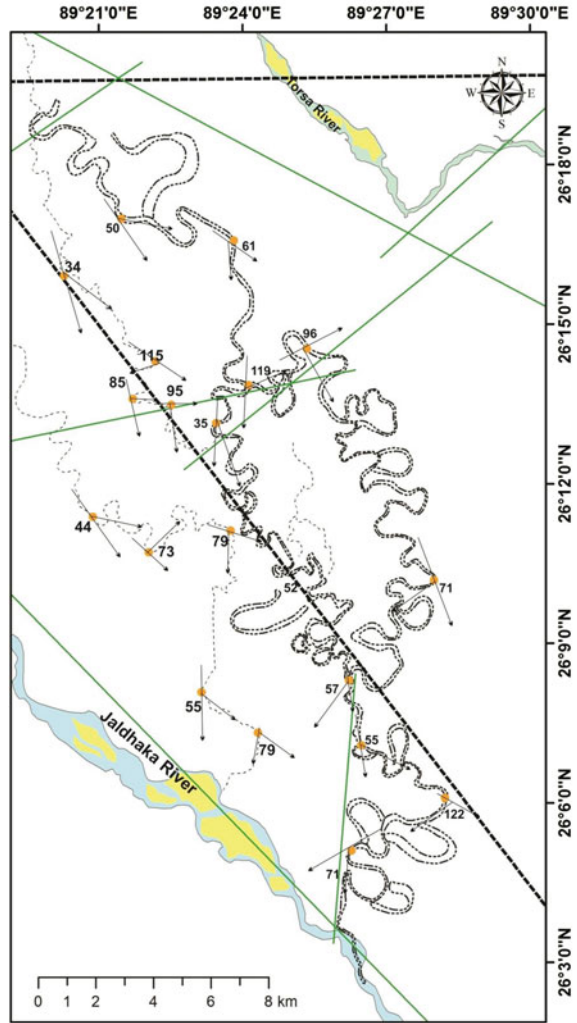
parallelism and neotectonic constraints at certain sections. Certain sections of Mara Dharala and Bura Dharala were distinctly observed flowing parallel to the neotectonic constraints (see Fig. 12). Significant turns along both the channels of Dharala River and nearby minor courses had been found corresponding to several lines transverse to the direction of the channel. 8 out of 19 major bends were deflected parallel to the lineaments or fault line (see Fig. 12). Within the entire reach at and around the divergence point of Bura Dharala effectiveness of the sudden turn in channel direction had registered more correspondence to lineaments and fault lines.

4.4 *Gestalt Linkage of Neotectonic Perturbations and Evolution of the Fluvial System*

4.4.1 Channel Capture

The Dharala River system has been developed on an elevated surface and concentrated within a zone of weakness along the Falakata fault. The incised character of the meandering river at certain places justifies the ongoing adjustment of the river system with surface deformation and sedimentation. Development of Dharala has ensued

Fig. 12 Major flow turn angles in the study area



flowing through a certain section of the abandoned course of Mansai (or Jaldhaka) and Durla river downstream. Possibly it was an over-spill channel that had made its way through these abandoned courses. This event of river capture was a century-old phenomenon. The westward shift of Jaldhaka between 1764 and 1871 was the major reason behind the expansion of the formidable circumstances for Dharala to come into existence. Fine resolution satellite images and placemarks on Rennell’s map were used to trace the palaeo course of Mansai which was once captured by Dharala (see Figs. 5 and 6) and within that particular stretch, litho-stratigraphic study also reveals coupling of channel abandonment and reoccupation (see Fig. 7). Presently

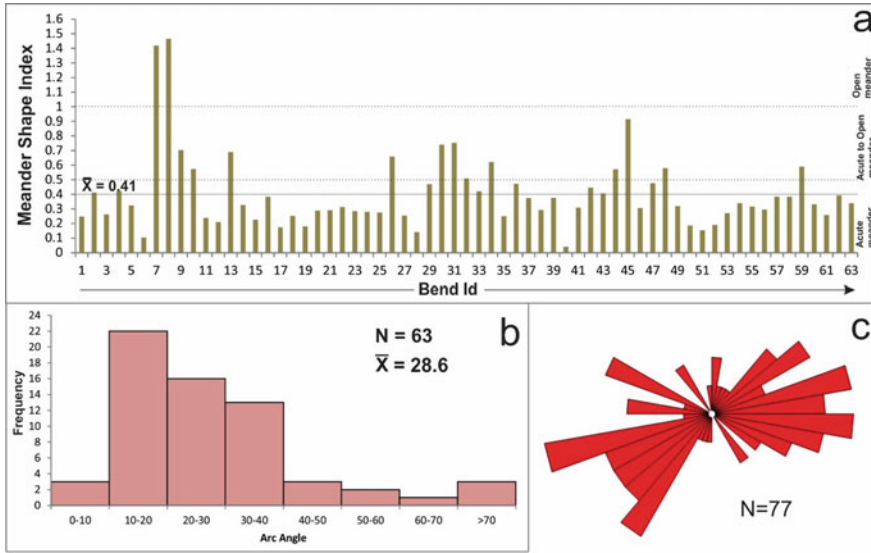


Fig. 13 a Meander shape index of selected bends from the courses of Dharala; b Meander arc angles of selected bends from the courses of Dharala; c Direction of meander bends

flowing Brahmini River through the abandoned course of Bura Dharala is a misfit in nature as it has been restricted into a narrow section within this wide river channel.

4.4.2 Active Tectonics and Channel Development

The development of Dharala was very much substantial in terms of the general avulsion model in the North Bengal plains (Mukhopadhyay 2014; Chakraborty et al. 2010; Holbrook and Schumm 1999). Development of a river course through capturing abandoned courses on and around a tectonically sensitive Quaternary surface was the evolutionary history of Dharala River. On a low relief surface, a minor change in relief can cause a significant change in meandering pattern (Boyd and Schumm 1995; Holbrook and Schumm 1999). The geomorphic signatures on the river planform and meander geometry clearly justify the controls of active tectonics on this drainage system. The compressed meanders, high regional sinuosity, tightened meandering loops and entrenchment at certain sections are the surficial projections of neo-tectonic imprints on the floodplain and channel morphology of Dharala River. The very same control was also reflected in the course of Durla and Old Durla back in 1764–77 through the formation of sharp turns towards the south. Few east-flowing minor rivers along with Durla and Bura Durla immediately turned towards the south as those rivers had encountered the fault zone (see Fig. 11). It was easier to erode the previously abandoned valley along the fault line of the N-S trending Falakata fault line. The average bend tightness value as well as the dominant club of intense

tightening of meander bends was very much significant for a river that is following a weaker zone. In the case of flow, turn angles, the direction, and intensity of bending was very much due to an imposed factor which is surface deformation. In the case of meander entrenchment, besides neo-tectonic reasons development of misfit channel characteristics within a wide floodplain and occupation of palaeo-channels was also responsible. The general trend of the regional slope in the northern part of Bengal is encountered by the Rangpur platform in the lower part of Jaldhaka and Torsa interfluvium and very gently dipping tectonic platform probably gave rise to the N-S slope that has been utilized by few small rivers like Dharala.

4.4.3 Abandonment of Dharala River

During the last 100 years, the course of Bura Torsa has been shifting towards the east and within the framework of such changes, few locations have been observed to oscillate along different nodes (Saha and Bhattacharya 2016). Shifting of the off-take point of Dharala was entirely dependent on the eastward migration of the present course of Torsa River or Bura Torsa. Such changes around the bifurcation were responsible for the complete abandonment of Dharala River. Sedimentary sequences of D1 and D3 had revealed a process of progressive channel decay of Dharala while stratigraphic sequences at D2 signified the reoccupation of the course of Jaldhaka or Mansai by Dharala later on. The studied lithofacies along various sections of the Dharala River have accurately justified the findings derived through analysis of data inventory and field observation. The formation of heterolithic structure of sand and mud along with flood deposition of the massive sand structure has been the characteristics of the active fluvial regime of Dharala. Abandonment of Dharala, eventually led to the clear absence of sand facies and the presence of thick floodplain mud deposition.

5 Conclusion

The major findings of this study have been listed as follows:

- a. Capturing left-out courses of the Jaldhaka-Mansai system and old courses of Durla Rivers have been the overall history of channel initiation of Dharala River as a branch of Torsa. With time eastward shift of Torsa River at a certain oscillation node around the Dharala off-take left the once active and economically significant Dharala River completely beheaded.
- b. Planform characteristics of Dharala River courses through its intensity and nature had reflected a strong control of the subsurface faulting along with Quaternary sedimentation.
- c. Channel orientation has showcased the significant control of lineaments and fault margins on the fluvial history of channel development of Dharala River.

The development of a river on an alluvial surface under the stimulus of neotectonics has been well documented in this study through the analysis of its fluvial history using a data inventory of past 250 years, on-field geomorphic signatures, and its fluvio-geomorphic indicators.

References

- Abdullatif OM (1989) Channel-fill and sheet-flood facies sequences in the ephemeral terminal River Gash, Kassala Sudan. *Sediment Geol* 63(1–2):171–184. [https://doi.org/10.1016/0037-0738\(89\)90077-8](https://doi.org/10.1016/0037-0738(89)90077-8)
- Agarwal RP, Bhoj R (1992) Evolution of Kosi fan, India: structural implications and geomorphic significance. *Int J Remote Sens* 13(10):1891–1901
- Alam MK, Hassan AKMS, Khan MR, Whitney JW (1990) Geological map of Bangladesh. Geol Surv Bangladesh, Dhaka, Scale 1:1 000 000
- Ambili V, Narayana A (2014) Tectonic effects on the longitudinal profiles of the Chaliyar River and its tributaries, Southwest India. *Geomorphology* 217:37–47
- Aslan A, Autin WJ, Blum MD (2006) Causes of River avulsion: insights from the late Holocene avulsion history of the Mississippi River, U.S.A.-reply. *J Sediment Res* 76(6):960–960. <https://doi.org/10.2110/jsr.2006.077>
- Barman SD, Islam A, Das BC, Mandal S, Pal SC (2019) Imprints of Neo-tectonism in the evolutionary record along the course of Khari River in Damodar Fan delta of Lower Ganga Basin. In: Das BC, Islam A, Ghosh S (eds) *Quaternary geomorphology in India*. Springer International Publishing. <https://doi.org/10.1007/978-3-319-90427-6>
- Bandopadhyay B (2007) *Coochbehar-Er Itihas*. Dey's Publishing, Kolkata
- Bandyopadhyay S (1996) Location of the Adi-Gannga palaeo channel, South 24- Parganas, West Bengal: a review. *Geogr Rev India* 58(2):93–109
- Bhuiyan MH, Kumamoto T, Suzuki S (2015) Application of remote sensing and GIS for evaluation of the recent morphological characteristics of the lower Brahmaputra-Jamuna River Bangladesh. *Earth Sci Inform* 8(3):551–568
- Boyd KF, Schumm SA (1995) Geomorphic evidence of deformation in the northern part of the New Madrid seismic zone. U.S. Geological Survey Professional Paper, 1538-R
- Chakraborty T, Kar R, Ghosh P, Basu S (2010) Kosi megafan: historical records, geomorphology and the recent avulsion of the Kosi River. *Quatern Int* 227(2):143–160. <https://doi.org/10.1016/j.quaint.2009.12.002>
- Chakraborty T, Ghosh P (2010) The geomorphology and sedimentology of the Tista megafan, Darjeeling Himalaya: implications for megafan building processes. *Geomorphology* 115(3–4):252–266
- Chattopadhyay GC, Das A (1979) Neotectonics in the Tista-Jaldhaka and Torsa interfluvial belt of North Bengal. In: GSI-record, vol 121, pp 101–109. Calcutta, GSI
- Choudhury HN (1903) *The Coochbehar State and its land revenue settlements*. C.E.S. Press. Cooch Behar. Reprint 2010. Edi. N. L. Paul. N. L. Pub. Siliguri. WB. India
- Das BC (2014) Two indices to measure the intensity of meander. In: Singh RB, Hassan MI (eds) *Advances in geographical and environmental sciences*, pp 233–246
- Farhadduzzaman M, Islam MA, Abdullah WH, Islam M (2015) Petrography and diagenesis of the tertiary surma group reservoir sandstones, Bengal Basin Bangladesh. *Univers J Geosci* 3(3):103–117. <https://doi.org/10.13189/ujg.2015.030304>
- Gregory DI, Schumm SA (1987) The effect of active tectonics on alluvial river morphology. In: Richards K (ed) *River environment and processes*, pp 41–68. Institute of British Geographers Special Publication, 18. Blackwell, New-York

- Goodbred SL Jr, Kuehl SL (2000) The significance of large sediment supply, active tectonism, and eustasy on margin sequence development: late quaternary stratigraphy and evolution of the Ganges-Brahmaputra delta. *Sed Geol* 133(3–4):227–248
- Goodbred SL Jr, Kuehl SA, Steckler MS, Sarker MH (2003) Controls on facies distribution and stratigraphic preservation in the Ganges-Brahmaputra delta sequence. *Sed Geol* 155:301–316
- Goswami C, Mukhopadhyay D, Poddar BC (2013) Tectonic control on the drainage system in a Piedmont region in tectonically active eastern Himalayas, pp 1–10. <https://doi.org/10.1007/s11707-012-0297-z>
- Goswami PK, Pant CC, Pandey S (2009) Tectonic controls on the geomorphic evolution of alluvial fans in the Piedmont Zone of Ganga plain, Uttarakhand India. *J Earth Syst Sci* 3:245–259
- Goswami U, Sarma JN, Patgiri AD (1999) River channel changes of the Subansiri in Assam India. *Geomorphology* 30(3):227–244. [https://doi.org/10.1016/S0169-555X\(99\)00032-X](https://doi.org/10.1016/S0169-555X(99)00032-X)
- Gunning JF (1911) Eastern Bengal and Assam District Gazetteers; Jalpaiguri. Government of West Bengal
- Hack JT (1973) Stream-profile analysis and stream-gradient index. *J Reseach US Geol Surv* 1(4):421–429
- Hunter WW (1871) Statistical account of Bengal. XI. Trübner & Company, London
- Holbrook J, Schunna SA (1999) Geomorphic and sedimentary response of rivers to tectonic deformation: a brief review and critique of a tool for recognizing subtle epeirogenic deformation in modern and ancient settings, vol 305, pp 287–306
- Hossain S Md, Khan SH, Chowdhury KR, Abdullah R (2019) Synthesis of the tectonic and structural elements of the Bengal basin and its surroundings. In: Mukherjee S (ed) *Tectonics and structural geology: Indian Context*, pp 135–218. Springer Nature, Switzerland. https://doi.org/10.1007/978-3-319-99341-6_6
- Jain V, Sinha R (2004) Fluvial dynamics of an anabranching river system in Himalayan foreland basin. *Baghmata River, North Bihar Plains, India* 60:147–170. <https://doi.org/10.1016/j.geomorph.2003.07.008>
- Jain M, Tandon SK, Bhatt SC (2004) Late Quaternary stratigraphic development in the lower Luni, Mahi and Sabarmati river basins, western India. *Proc Indian Acad Sci Earth Planet Sci* 113(3):453–471. <https://doi.org/10.1007/BF02716736>
- Jain V, Sinha R (2005) Response of active tectonics on the alluvial Baghmata River, Himalayan foreland basin, eastern India. *Geomorphology* 70(3–4 SPEC.ISS.):339–356. <https://doi.org/10.1016/j.geomorph.2005.02.012>
- Jana MM (2006) North Bengal Rivers, behavioural pattern and impact on development. In: Sengupta S (ed) *Rivers and riverine landscape in North East India*, Concept Publishing Company, New Delhi, pp 163–168
- Kaushal RK, Singh V, Mukul M, Jain V (2017) Identification of deformation variability and active structures using geomorphic markers in the Nahan salient, NW Himalaya, India. *Quat Int* 1–17. <https://doi.org/10.1016/j.quaint.2017.08.015>
- Klang D (1996) Experiences from the transformation, correction, revision and production of topographic orthophoto maps of the baltic states using SPOT data—the potential of semi-automatic data acquisition methods. *Int Arch Photogramm Remote Sens* 31(B4):454–459
- Khan MR (2002) Plate tectonics and Bangladesh. *J Asiat Soc Bangladesh Sci Gold Jubil Issue* 28(2):39–62
- Khandoker RA (1989) Development of major tectonic elements of the Bengal Basin: a plate tectonic appraisal Bangladesh. *J Sci Res* 7:221–232
- Kumar R, Ghosh SK, Mazari RK, Sangode SJ (2016) Tectonic impact on the fluvial deposits of Plio-Pleistocene Himalayan foreland basin: implication for tectonic and climatic decoupling Tectonic impact on the fluvial deposits of Plio-Pleistocene Himalayan foreland basin, India, (September). [https://doi.org/10.1016/S0037-0738\(02\)00267-1](https://doi.org/10.1016/S0037-0738(02)00267-1)
- Laha C, Bandyopadhyay S (2013) Analysis of the changing morphometry of River Ganga, shift monitoring and vulnerability analysis using space-borne Techniques: a statistical approach. *Int J Sci Res Publ* 3(7):1–10

- Lahiri SK, Sinha R (2012) Tectonic controls on the morphodynamics of the Brahmaputra River system in the upper Assam valley, India. *Geomorphology* 169:74–85. <https://doi.org/10.1016/j.geomorph.2012.04.012>
- Lee CS, Tsai LL (2010) A quantitative analysis for geomorphic indices of longitudinal river profile: a case study of the Choushui River, Central Taiwan. *Environ Earth Sci* 59:1549–1558. <https://doi.org/10.1007/s12665-009-0140-3>
- Leopold LB, Wolman M, Miller JP (1965) *Fluvial processes in geomorphology*. San Francisco and London, W.H. Freeman and Co.
- Li L, Lu X, Chen Z (2007) River channel change during the last 50 years in the middle Yangtze River, the Jianli reach. *Geomorphology* 85:185–196
- Lu P, Shang Y (2015) Active tectonics revealed by river profiles along the Puqu fault. *Water* 7:1628–1648. <https://doi.org/10.3390/w7041628>
- Majumder D (1977) *West Bengal District Gazetteers, Cooch Behar*. Government of West Bengal
- Malik JN, Mohanty C (2007) Active tectonic influence on the evolution of drainage and landscape: geomorphic signatures from frontal and hinterland areas along the Northwestern Himalaya, India. *J Asian Earth Sci* 29:604–618. <https://doi.org/10.1016/j.jseaes.2006.03.010>
- Mazumdar K, Sengupta R, Mishra MN (2001) Neotectonism in Brahmaputra Valley, Assam. National symposium on role of earth sciences in integrated development and related societal issues. *Geol Surv India Spec Publ* 65(3):227–230
- Miall AD (1996) *The geology of fluvial deposits*. Springer, Berlin
- Miall A (2014) *Fluvial depositional systems*. Springer International Publishing, Switzerland
- Mitra D, Tangri AK, Singh IB (2005) Channel avulsions of the Sarda River system, Ganga plain. *Int J Remote Sens* 26(5):929–936. <https://doi.org/10.1080/0143116031000102458>
- Mandal S, Sarkar S (2016) Overprint of neotectonism along the course of River Chel, North Bengal India. *J Palaeogeogr* 5(3):221–240. <https://doi.org/10.1016/j.jop.2016.05.004>
- Mohindra R, Parkash B, Prasad J (1992) Historical geomorphology and pedology of the Gandak megafan, Middle Gangetic plains, India. *Earth Surf Process Landf* 17:643–662
- Moussi A, Rebail N, Chaieb A, Saadi A (2018) GIS-based analysis of the stream length-gradient index for evaluating effects of active tectonics: a case study of Enfidha (North-East of Tunisia). *Arab J Geosci* 11:123. <https://doi.org/10.1007/s12517-018-3466-x>
- Mukhopadhyay SC (2014) Aspects of Hydro-geomorphology of North Bengal drainage, India and surroundings with an emphasis on the Torsa basin. *Indian J Landsc Syst Ecol Stud* 37(2):163–176
- Mueller JE (2015) An introduction to the hydraulic and topographic sinuosity indexes. *Ann Assoc Am Geogr* 58(2):371–385
- Ouchi S (1985) Response of alluvial river to slow active tectonic movement. *Geol Soc Am* 96:504–515
- Rashid B, Islam UI S, Islam B (2016) Evidence of neotectonic activities as reflected by drainage characteristics of the Mahananda River Floodplain. In: Evidence of neotectonic activities as reflected by drainage characteristics of the Mahananda River Floodplain and its adjoining are, (February)
- Roy S, Sahu A (2015) Quaternary tectonic control on channel morphology on over sedimentary low land: a case study in the Ajoy-Damodar interfluvium of Eastern India. *Geosci Front* 6:927–946
- Rudra K (2014) Changing river courses in the western part of the Ganga. *Geomorphology* 227:87–100
- Saha UD, Bhattacharya S (2016) A study of river induced major hydrogeomorphic issues and associated problems in Torsa basin West Bengal. *Geogr Rev India* 78(2):132–145
- Saha UD, Bhattacharya S (2019) Reconstructing the channel shifting pattern of the Torsa River on the Himalayan Foreland Basin over the last 250 years. *Bull Geogr Phys Geogr Ser* 16:99–114. <https://doi.org/10.2478/17088>
- Saha UD, Bhattacharya S (2020) Application of multi-criteria decision-making approach for ascertaining the avulsion potentiality of the Torsa River course. *Model Earth Syst Environ*
- Schumm SA, Dumont JF, Holbrook JM (2000) *Active tectonics and Alluvial Rivers*. Cambridge University Press, Cambridge

- Seeber L, Gornitz V (1983) River profiles along the Himalayan arc as indicators of active tectonics. *Tectonophysics* 92:335–367
- Scorpio V, Surian N, Cucato M, Prá ED, Zolezzi G, Comiti F, Zolezzi G (2018) Channel changes of the Adige River (Eastern Italian Alps) over the last 1000 years and identification of the historical fluvial corridor. *J Maps* 14(2):680–691. <https://doi.org/10.1080/17445647.2018.1531074>
- Shukla UK, Singh IB, Sharma M, Sharma S (2001) A model of alluvial megafan sedimentation: Ganga Megafan. *Sed Geol* 144:243–262
- Singh S, Parkash B, Rao MS, Arora M, Bhosle B (2006) Geomorphology, pedology and sedimentology of the Deoha/Ganga-Ghaghara Interfluvium, upper Gangetic plains (Himalayan Foreland Basin)—extensional tectonic implications. *CATENA* 67:183–203. <https://doi.org/10.1016/j.catena.2006.03.013>
- Sinha R (1996) Channel avulsion and floodplain structure in the Gandak-Kosi Interfan, North Bihar Plains, India. (K. H. Pfeffer, Ed.) *Zeitschrift für Geomorphologie. Supplementbände* 103:249–268
- Sinha R (2009) The great avulsion of Kosi on 18th August 2008. *Curr Sci* 97(3):429–433
- Sinha R, Bapalu GV, Singh LK, Rath B (2008) Flood risk analysis in the Kosi river basin, north Bihar using multi-parametric approach of Analytical Hierarchy Process (AHP). *J Indian Soc Remote Sens* 36(4):335–349. <https://doi.org/10.1007/s12524-008-0034-y>
- Sinha R, Gibling MR, Jain V, Tandon SK (2005) Sedimentology and avulsion patterns of the anabranching Bagmati River in the Himalayan foreland basin, India. In: Blum MD, Marriott SB, Leclair SF (eds) *Fluvial sedimentology*, pp 181–196. Special Publication, International Association of Sedimentologists
- Sinha R, Ahmad J, Gaurav K, Morin G (2014a) Shallow subsurface stratigraphy and alluvial architecture of the Kosi and Gandak megafans in the Himalayan foreland basin, India. *Sed Geol* 301:133–149. <https://doi.org/10.1016/j.sedgeo.2013.06.008>
- Sinha R, Sripriyanka K, Jain V, Mukul M (2014b) Avulsion threshold and planform dynamics of the Kosi River in north Bihar (India) and Nepal: a GIS framework. *Geomorphology* 216:157–170. <https://doi.org/10.1016/j.geomorph.2014.03.035>
- Sinha-Roy S (2001) Neotectonic significance of longitudinal river profiles: an example from the Banas drainage basin, Rajasthan. *J Geol Soc India* 58(2):143–156
- Slingerland R, Smith ND (2004) River avulsions and their deposits. *Annu Rev Earth Planet Sci* 35:257–285. <https://www.annualreviews.org/>. <https://doi.org/10.1146/annurev.earth.32.101802.120201>
- Soja R, Sarkar S (2008) Characteristics of hydrological regimes. In: Starkel L, Sarkar S, Soja R, Prokop P (eds) *Present-day evolution of Sikkimese-Bhutanese Himalayan piedmont*, pp 37–46. Warszawa, Stanisława Leszczyckiego
- Thapa K (1992) Accuracy of spatial data used in geographic information systems. *Photogramm Eng Remote Sens* 58(6):835–841
- Timár G (2003) Controls on channel sinuosity changes: a case study of the Tisza River, the great Hungarian plain. *Quatern Sci Rev* 22:2199–2207
- Toonen WHJ, Kleinmans MG, Cohen KM (2012) Sedimentary architecture of abandoned channel fills. *Earth Surf Proc Land* 37(4):459–472. <https://doi.org/10.1002/esp.3189>
- Troiani F, Della SM (2008) The use of the stream length-gradient index in morphotectonic analysis of small catchments: a case study from Central Italy. *Geomorphology* 102:159–168
- Walz U, Berger A (2003) Georeferencing and mosaicking of historical maps—basis for digital time span of landscape analysis. *Photogrammetrie, Fernerkundung, Geoinformation* 3(2003):213–219
- Weissmann GS, Hartley AJ, Scuderi LA, Nichols GJ, Owen A, Wright S, Anaya FML (2015) Geomorphology Fluvial geomorphic elements in modern sedimentary basins and their potential preservation in the rock record: a review. *Geomorphology* 250:187–219. <https://doi.org/10.1016/j.geomorph.2015.09.005>
- Wells NA, Dorr JA (1977) Shifting of the Kosi River, Northern India. *Geology* 15:204–207

Williams GP (1986) River meanders and channel size. *J Hydrol* 88:147–164

Zámolyi A, Székely B, Draganits E, Timár G (2010) Neotectonic control on river sinuosity at the western margin of the Little Hungarian plain *Geomorphology* Neotectonic control on river sinuosity at the western margin of the little Hungarian plain. *Geomorphology* 122(3–4):231–243. <https://doi.org/10.1016/j.geomorph.2009.06.028>

Preliminary Study of the Manabhum Anticline: A Possible Key to Better Understanding the Quaternary Tectonics of the Eastern Himalayan Syntaxial Zone



Chandreyee Goswami Chakrabarti, Belligraham Narzary, John C Weber, Prasun Jana, Somhrita Bhattacharjee, and Manoj Jaiswal

Abstract The NNW-SSE trending Manabhum Anticline is an impressive hill in the foredeep area of the Naga-Schuppen belt near Mishmi Hill on the southern bank of the Brahmaputra. We present a detailed geological study of this area to better establish its Quaternary tectonics. Rocks exposed in the core of the Manabhum anticline are Pleistocene in ages and Holocene sediments are also involved in the deformation. We have prepared a geological map at the 1:25,000 scale and for the first time dated nine representative samples of rocks and sediments from this area. Three distinct age ranges have been obtained; ~220 ka- ~130 ka, ~ 67 ka- ~36 ka, and less than 10 ka. We interpret the Manabhum Hill as an asymmetric antiformal fold that is actively developing in a compressive regime near the Eastern Himalayan Syntaxis (EHS) zone. We present evidence that it has been highly active tectonically during Pleistocene-Holocene time and maybe a key to understand how collision has accommodated and evolved in the eastern syntaxis.

C. G. Chakrabarti (✉) · S. Bhattacharjee
Department of Geology, University of Calcutta, 35 Ballygunge Circular Road, Kolkata 700,019, India

C. G. Chakrabarti
Department of Neotectonics and Thermochronology, Institute of Rock Structure and Mechanics, Prague, Czech Republic

B. Narzary · M. Jaiswal
Department of Earth Science, Indian Institute of Science Education and Research, Kolkata, India

J. C. Weber
Department of Geology, Grand Valley State University, 1 Campus Drive, Allendale, MI 49,401, USA

P. Jana
Geological Survey of India, Northern Region, Sector E, Lucknow 226,024, India

1 Introduction

The Eastern Himalayan Syntaxis (EHS) represents the juncture where the E-W-trending Himalayas meet or bend and transition into the NNE-SSW-trending Naga Schuppen belt. Both the Himalayas and the Naga-Schuppen (Imbricate) belts are active fold-thrust belts characterized by the belt-parallel thrust faults and transverse normal and strike-slip faults. The EHS is more poorly-studied than its western counterpart (e.g., Burg et al. 1997, 1998; Zeitler et al. 2001), yet deserves attention as it represents one of the most tectonically active areas in South East Asia.

According to Singh and Kumar (2013), the EHS appears to be a zone of weak crust as marked by its low crustal velocity; it is therefore potentially a zone of high ductile near-surface strain similar to that observed in the western syntaxis (Zeitler et al. 2001). Based on space geodesy, the EHS has also been suggested to be segmented into a number of blocks or microplates that move in response to the India-Eurasia collision (Jade et al. 2017). All of these blocks are rotating clockwise, but at slower rates than that of the Indian plate.

The EHS is encircled by three major regional thrust systems: the Himalayan Frontal Thrust, the Naga Thrust, and the Mishmi thrust (Gansser 1964; Thakur and Jain 1975; Acharyya 1980; Ningthoujam et al. 2015; Gururajan and Choudhuri 2003; Sarma et al. 2009). Within the EHS the upper Assam foreland basin contains 3–10 km thick of Paleocene-Eocene to Holocene sediments (Mandal 2013).

The Mishmi block is considered to act as a possible tectonic roof (Sarma et al. 2009) or a linkage (Nandy 1980) between the E-W trending Eastern Himalaya in the west and NNE-SSW trending Naga-Schuppen belt in the southeast (Fig. 1). Faults in the EHS are required to accommodate ~30% of the ~28 mm/yr convergence rate between the Shillong Plateau and Indo Burmese Arc (IBA) (Jade et al. 2017 and references therein). GPS measurements of the Mishmi block reveal slow motion (2.26 mm/yr with and the azimuth of 45.88°N) relative to Eastern Tibetan Block (6–11 mm/yr), China (14–20 mm/yr), and Burmese Arc (19 mm/yr).

Our study area is located southwest part of EHS within the Quaternary-Holocene foreland of Mishmi Thrust and within the Upper Assam Basin. We focus on examining the development of the impressive antiformal Manabhum Hill that rises out of a generally flat, broad alluvial plain. We studied the geological history of Manabhum Hill and its surroundings using satellite image analysis, an extensive field survey, and OSL dating of nine key sediment samples. We use these data to better understand the Quaternary stratigraphy and then relate that to Pleistocene-Holocene deformation that folded these units and produced Manabhum Hill's topography.

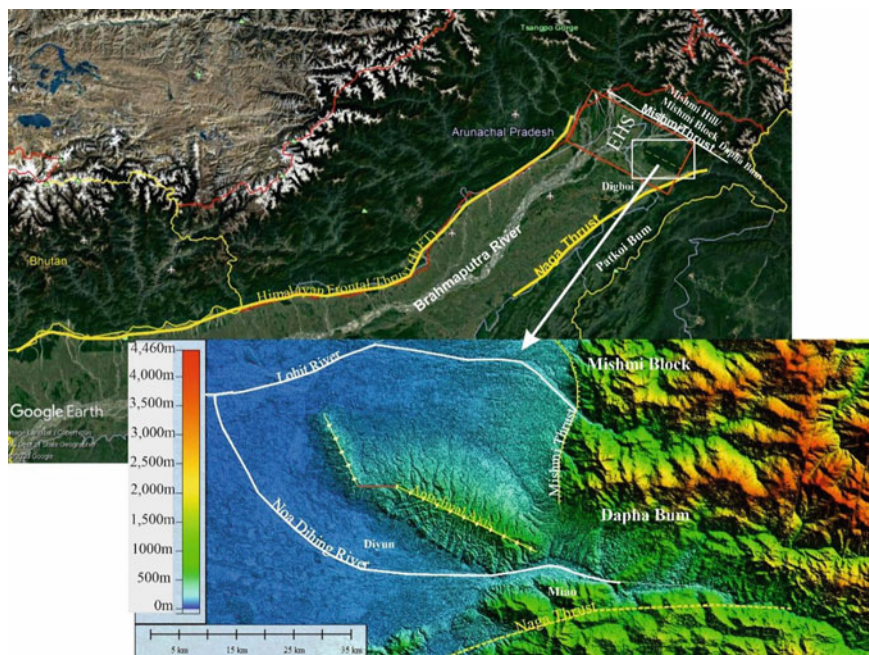


Fig. 1 Study Area is shown in Google Earth and Cartosat I DEM. All the major tectonic and geographic units are shown. Dotted orange lines denote axes of Manabhum anticline and Jaipur-Digoiboi anticline from east to west respectively

2 Geological Setting

The Upper Assam Basin is a contractile foreland basin filled with Paleogene and younger sediments that increase dramatically in thickness from northeast to southwest from 7000 to 10,000 m indicating deeper and more basinal conditions toward the southwest (Das gupta 1977). The environment of deposition of these sediments changed from marine to lagoonal, and then to deltaic, and finally to fluvial through Paleogene time. The overlying Neogene to Holocene sediments is mostly molasse that was deposited almost exclusively in a fluvial environment with only brief pulses of brackish to deltaic conditions (Nandy 2001). The thickness of the Neogene and Holocene sediments of the upper Assam basin increased to the north and northeast during Pliocene and Pleistocene time.

Two prominent structural trends dominate the immediate surroundings of the study area: the NE-SW trend of the Naga-Patko range and the NW-SE trend of the Mishmi hills (Fig. 1). Two anticlines occur within the generally undeformed Quaternary alluvial fill of the Dihing valley, the Manabhum anticline, and the Jaipur-Digoiboi anticline. We address the evolution and development of the former in this study.

In the unpublished report of GSI, the Quaternary units around the Manabhum Anticline are mentioned as with increasing age QHII, QHI, QPIII, QPII and QPI. Lithologically, QP I and QP II are comprised mainly of boulders and pebbles with silt and clay that are oxidized and are of limited areal extent. Unit QP III is made up of oxidized sand, silt, and clay. Unit QH I is comprised of pebbles, silt, and clay, and is very weakly oxidized. The youngest unit, QH II, is largely unoxidized and contains pebbles, sand, silt, and clay. Geomorphologically, the QP I and QPII units are located in high depositional terraces in the piedmont zone southwest of Mishmi Hill that extend up to the Noa-Dihing River. QP III is mapped in a vast low-lying alluvial tract compare to QP I and QPII. Unit QH I is also present in a low alluvial tract, and QH II is represented by the present-day flood plain, which includes channel bars and point bars (Shrivastava and Sharma, GSI Progress Report for the Field Season 1985–86).

Older stratigraphic units in and around Manabhum Hill are, according to Boral and Tiwari (1975): (i) the Pliocene Dihing Formation, which includes pebble and boulder beds, coarse to medium grained; soft, loosely consolidated sandstones, and (ii) the Miocene Tipam Formation, which includes fine- to medium-grained, bluish to greenish-grey sandstone alternating with grey and greenish grey and red and brown (in the upper part) clay and siltstone bands, intercalated with thin pebble beds.

Within the foredeep of the Naga-Schuppen belt, fold and thrust traces change strike from NE to ENE, which might have taken place due to the movement of the Mishmi block along the Mishmi thrust. Displacement and strain on the Naga thrust and related folds reduced eastward and constitute only a mild offshoot rather than forming an integral part of the zone of Schuppen in this region (Das Gupta 1977).

Manabhum Hill and its surroundings can be divided into two major geomorphic units: (i) Manabhum Hill, (ii) river terraces along the Noa-Dihing and tributary river banks. The main river in this area is Noa-Dihing, which originates from the southeast within the Naga Schuppen belt. It first flows north, then takes a westerly bend and cuts the southern end of Manabhum Hill. Then again it takes a sharp NNW'sterly bend and flows along the foothill and western flank of the Manabhum Hill. A well-developed terrace system is present along the Noa-Dihing River.

3 Materials and Methods

We analysed Resourcesat LISS IV MSS data from January 2015 together with Cartosat 1 DEM of 10 m resolution using the ERDAS 2014 and Global Mapper 15 software. We also did an extensive field survey, collected structural data, traced and mapped formation boundaries (contacts), and dated nine samples using the OSL method to determine the Quaternary stratigraphy. We combined these data into a digital geological map (1:25,000 scale) using the ArcGIS platform (Fig. 2).

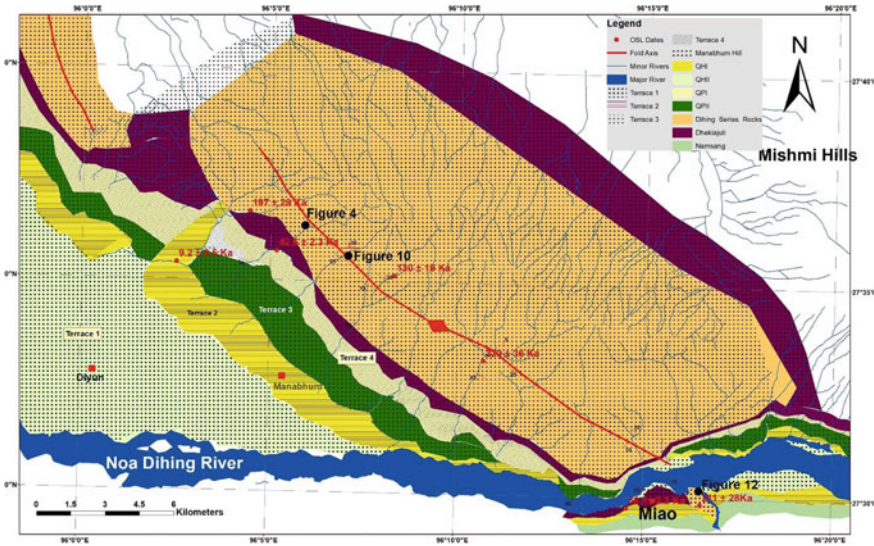


Fig. 2 Geological-Geomorphological Map of the study area around Manabhum

3.1 Description of the Terrace Material

In and around the Manabhum anticline, GSI mapped five Quaternary surfaces and morphostratigraphic units based on their relative heights, soil colour, and sediment below the corresponding surfaces. These are, in order of increasing antiquity: (i) QH II surface, (ii) QH I surface, (iii) QP III surface, (iv) QP II surface, and (v) QP I surface (in this nomenclature ‘Q’ stands for Quaternary, ‘H’ for Holocene and ‘P’ for Pleistocene).

Noa-Dihing and tributary river terraces are classified according to the increasing height as T₁, T₂, T₃ and T₄ terraces; the T₁ is the lowest and the T₄ is the highest. River terraces are characterized by the presence of soil horizons with different thickness and colour that, in general, reflect relative ages. These soil horizons are developed in and underlain by sand, pebble and boulder beds with occasional clay beds. The four terraces are corroborative with the QH II, QH I, QP II and QPI surfaces respectively with GSI report 1985. We could not differentiate between QP III and QP II and hence have shown both as QPII below T₃. We have not done a detailed sedimentological analysis on the terrace sediment. We simply present them as geomorphic terrace surfaces on our map (Fig. 2).

The generally horizontally to sub-horizontally bedded sub-terrace material can be distinguished using relative sediment character. Lithologically, the material below the T₁ terrace includes nearly horizontal beds of unoxidized, large boulders, pebbles, sand, silt, and clay. The material within individual beds is unsorted and coarse-grained and the beds generally lack clast preferred orientations. The T₂ terrace is covered with a light-yellow soil developed on beds of pebbles, silt, and clay, which are weakly



Fig. 3 T₂ terrace forms as a strath terrace over the Dihing Formation Rocks

oxidized. In many locations, the T₂ terrace occurs as a strath terrace cut into the lower Dihing Formation rock units that form the core of Manabhum Hill (Fig. 3). T₃ terrace material covers a major part of the study area and is made up of sand, silt, and clay that is moderately oxidized. The material comprising the T₄ terraces includes thick boulders and pebble beds, with subordinate silt and clay beds. T₃ boulder and pebble beds are markedly different from the boulder and pebble beds associated with T₄ terraces: they are highly oxidized and semi-lithified. Additionally, T₃ terraces are high depositional terraces in the piedmont zone and are of limited areal extent.

The pebble bed of T₄ terrace is steeply dipping over the uppermost pebble and sand beds of Dhekiajuli formation is separated by steeply dipping black clay bed (Fig. 4a). Pebble imbrications within the pebble bed of T₄ terrace are found to be opposite to the dip of the bedding in the southwestern limb (Fig. 4b). An unconformity was also seen in the same sedimentary sequence between T₄ pebble bed at the top and a sand bed of Dhekiajuli formation, dipping 15° → 150° (Fig. 4c).

3.2 *Material Constituting Manabhum Hill*

The principal rock constituent of the Manabhum Hill is thickly bedded sandstone and conglomerates overlain by terrace sediments rich in boulder beds. The grain size



Fig. 4 **a** Steeply dipping pebble beds below T_4 terrace over the uppermost pebble and sand beds of Dhekiajuli Sediments are separated by steeply dipping black clay bed. **b** Pebble imbrications within the pebble bed of T_4 terrace are opposite to the dip of the bedding. **c** An unconformity between T_4 pebble bed at the top and a sand bed of Dhekiajuli formation, (Fig. 4c). Shown in Fig. 2

of terrace sediments varies from very fine to coarse, and its colour varies is from yellow to gray.

The sandstone making up the core of Manabhum Hill likely belongs to the Miocene Dihing Formation according to GSI Reports (1985–86) and has locally been termed the “Luwang sand rock” (Nandy 2001). This sandstone is overlain by the less consolidated, thick, pebble beds with interbedded coarse-grained yellow sand thin clay beds. Based on GSI Reports (1985–86), we correlate the upper formation to the Dhekiajuli Formation and the lower formation with Dihing Formation rocks.

3.2.1 Dihing Formation Rocks

The comparatively compact and hard sedimentary rocks present in the core of the antiform are laminated gray arkosic sandstones with cross-bedding. The sandstone beds are approximately 3–4 m in thickness. Some have small mud balls and charcoal blocks. Bed thickness increases to about 5 m northward. Furthermore, northeastward, very thick laminated gray sandstone with an average thickness of approximately 3 m contains a very thin mud layer along with mud balls (greenish) and coal blocks (Fig. 5a). Along the northern bank of the Noa-Dihing River, a yellow-colored thick massive coarse-grained sandstone containing coal beds is present. Moving eastward



Fig. 5 **a** Easterly dipping arkosic grey sandstone with fossilised wood block and thin clay bed with mud balls. **b** Convolute laminations within the clay bed interlayered within Dihing Formation thick sand beds. **c** A clay layer of thickness 0.25 m overlies a less consolidated laminated coarse grained yellow sand layer with coal block

along the road the thickness of the bed reduces. Further, towards the northeast, the sand beds contain a fine-grained layer in between two coarse-grained layers. The thickness of the sand bed here varies from about 1–1.5 m. The sand layer contains an intermittent mud layer of thickness 20 cm with convolute laminations (Fig. 5b).

A clay layer of thickness of 0.25 m overlies a less consolidated laminated coarse-grained yellow sand layer with thickness of 0.25 m (Fig. 5c). Below these clay and sand layer lies another coarse-grained sand layer which is gray in colour and is more consolidated than the upper layer. This layer is about 0.5 m in thickness and contains charcoal. All these sandstones are interpreted as the Dihing Formation rocks.

Primary sedimentary structures present and observed within the constituent sediments and rocks include (i) Convolute laminations were seen within clay beds within the sandstone of the Dihing Formation rocks on the eastern limb at the southeastern



Fig. 6 Slump structures and convolute laminations below the T₃ terrace in the north western part of the Manabhum hill

part of the area (Fig. 5b). (ii) Slump structures and convolute laminations were seen below the T₃ terrace in the northwestern part of the hill (Fig. 6).

In the south bank of Noa-Dihing River at high elevations, the rocks are mainly gray to greenish-gray, medium to coarse-grained arkosic sandstone with salt-pepper appearance, and abundant coal fragments or fossilised wood associated with pebble and boulder beds (Fig. 7).

3.2.2 Dhekiajuli Formation

Sediments composed of boulders and pebbles embedded in silt and clay matrix is overlying the sandstones (Fig. 8). These are the Dhekiajuli formation rocks. It is highly oxidized and is deep reddish-brown in colour. The overlying pebble and boulder beds contain less clay matrix than below. Sand and silt beds with few coarse boulders overlie the pebble and boulder beds and are capped by clay. In some places there is a distinct clay horizon marked by ochre and black clay beds can be marked as unconformity and differentiate the pebble beds of terrace systems from the pebble beds forming the Dhekiajuli Formation (Fig. 4). The overlying boulder bed contains mainly sub-rounded pebbles mostly of gneissic type (Fig. 9). Pebble imbrications are common. These upper sand and pebble beds are associated with distinct black clay beds and sand beds with mud balls.



Fig. 7 General character of Dihing Formation rocks

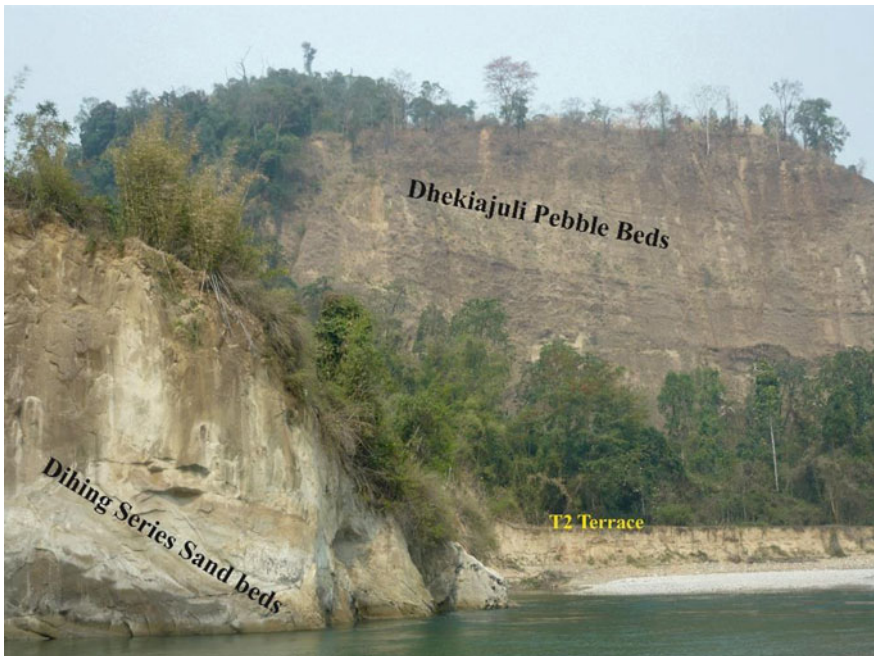


Fig. 8 Disposition of Dihing Formation rocks and Dhekiajuli sediments. The low dipping Dhekiajuli pebble and ssand beds are blanketed over high dipping Dihing Formation sand stones



Fig. 9 Subrounded gneissic boulder within the Dhekiajuli boulder bed

3.3 Structure

Deformation structures are evident from both the terrace sediments and the rocks constituting the Manabhum Hill.

We did reconnaissance structural mapping (Fig. 2) that shows that Manabhum Hill is an NNW-SSE trending antiformal hill that can be divided into two parts. The northernmost part has lower elevations than the higher southern part and gradually dies out towards the southern bank of the Lohit River in the north. Our work focuses on the southern part of the hill.

The geology in the core of the Manabhum Hill, as described above, is made up of Dhekiajuli and Dihing Formation units. The thick sandstone beds of the southwestern limb dip more than 400° in general towards southwest. Towards the core of the antiform, the sandstone dips more gently, less than 300° towards WSW. Towards the eastern limb of the antiform, the thickness of the sand bed reduces with dip varying from $35^\circ \rightarrow 210^\circ$ to $25^\circ \rightarrow 040^\circ$ (Fig. 10). Thus the Dihing Formation sand beds form a perfect antiform.

Boulder beds of the overlying Dhekiajuli formation mimic the folding observed in the older and structurally lower Dihing unit, but the beds dip gentler than those in the Dihing sandstone beds approximately $10\text{--}15^\circ$ (Fig. 11).

An E-W trending exposure of the consolidated hard sand and pebble bed in the southern bank of the Noa-Dihing river where a small northerly flowing stream meets

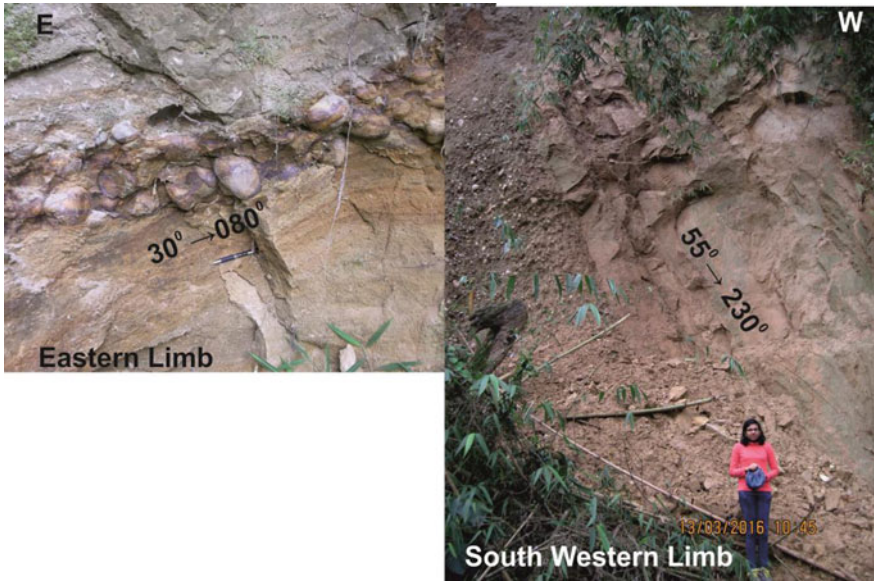


Fig. 10 Asymmetric fold within the Dihing Formation rocks showing two limbs dipping in opposite direction. The location of the photograph is shown in Fig. 2



Fig. 11 Easterly dipping sand and boulder beds of Dhekiajuli formation



Fig. 12 The older sand beds are thrust over the younger pebble beds near the confluence of a small northerly flowing stream and NoaDihing River. The position is shown in Fig. 2

at the Noa-Dihing River shows that the underlying sandstone beds have been thrust over younger pebble beds and abut against it (Fig. 12). The attitude of the contact of the sand and pebble beds is $5^\circ \rightarrow 100^\circ$ and this shallowly dipping surface is interpreted as thrust contact.

Our reconnaissance measured attitudes of the bedding of sandstones it is established that it is folded into an asymmetric anticline with the western limb dipping $45\text{--}55^\circ$ towards SW and the eastern limb dipping $20\text{--}35^\circ$ towards NE (Fig. 10). The observed limb dip asymmetry matches the hill's topographic asymmetry, suggesting that this is a young, probably active fold. We analyzed the strike and dip data we collected using Stereonet software (Cardozo and Allmendinger 2013). Our analysis of the thirty-three bedding measurements made during our field study shows that the Manabhum anticline plunges very gently to the NW (Figs. 13a, b).

3.4 *OSL (Optically Stimulated Luminescence) Methods and Results*

Optically Stimulated Luminescence (OSL) dating which dates the last daylight exposure of the sediments and provides the last depositional date (Huntley et al. 1985; Aitken 1998) has been widely used to date the Himalayan sediments. Quartz has been the more popular mineral among researchers due to the fact that the latent signal in Quartz resets faster and more efficiently than that of Feldspar. The poor luminescence intensity and lower level of luminescence saturation are the complications faced using Quartz as a dosimeter. Feldspar on the other hand has a brighter luminescence signal and its level of luminescence saturation is much higher, with a maximum age limit of up to 500 ka. However, feldspar grains are commonly affected by anomalous fading, which was first reported by Wintle (1973) and Spooner (1994) has reported most feldspar fade. This anomalous fading in feldspar has been attributed to the unstable electron traps which result in the shortfall of ages. There are several procedures and protocols which exist for correcting for anomalous fading. However,

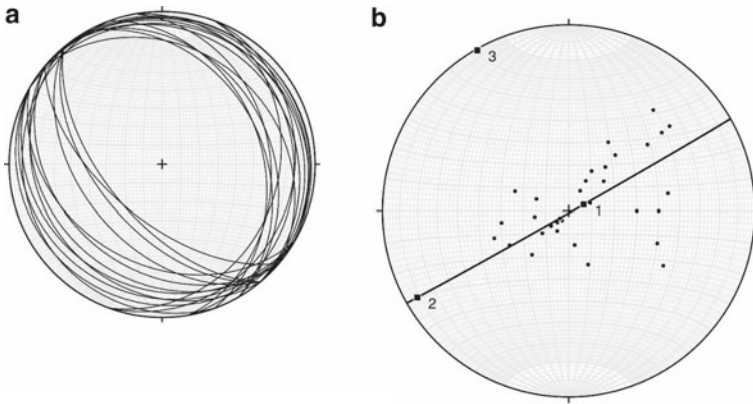


Fig. 13 **a** Stereonet showing strike and dip of all bedding planes observed in the core and on the flanks of the Manabhum anticline. $N = 33$. Plotted using Stereonet (Cardozo and Allmendinger 2013). **b** Stereonet showing poles to all bedding planes observed in the core and on the flanks of the Manabhum anticline, best-fit great circle (p-girdle) and eigenvectors. Eigenvector #3 is the best-fit microfold axis (b), which plunges 1° , 330 . $N = 33$. Plotted using Stereonet (Cardozo and Allmendinger 2013)

one of the most widely followed method of correcting for anomalous fading is by Huntley and Lamothe (2001).

In total nine samples were collected for OSL dating in galvanized iron tubes to avoid any exposure to sunlight. Five samples showed poor luminescence signal in quartz so feldspar was used for dating. All the experimental procedure was done in subdued red light environment. Approximately three centimetres from each end of the tubes were scraped away to avoid any sunlight exposed sediments during sampling and were used for water content and dose rate measurements. The samples were then routinely treated with 1 N HCl and 30% H_2O_2 to remove carbonates and organic matter respectively. These samples were then sieved to obtain the 90–150 μm size fraction which was followed by heavy liquid density separation using Sodium polytungstate (density = 2.58 gm/cm^3) to separate quartz and feldspar. The quartz grains were then etched with 40% HF for 80 min to remove any contribution from alpha irradiation followed by treatment with 12 N HCL treatments to remove the fluorides formed during etching. All the samples were checked for feldspar contamination using infrared stimulated luminescence (IRSL). The grains were mounted on 10 mm stainless-steel disc using Silko-Spray silicone oil. The OSL measurements were carried out on Lexsysmart TL-OSL reader (Freiberg Instruments, Germany) at Luminescence Dating Laboratory in the Department of Earth Sciences IISER Kolkata. The instrument was calibrated using calibration quartz supplied from the Riso National Laboratory, Denmark Technical University, Denmark. The instrument is equipped with blue light-emitting LEDs ($\lambda = 458 \text{ nm}$), the detection window consists of a combination of optical fibres Hoya U340 and Delta BP 365/50 EX mounted on a solid-state photomultiplier tube (PMT) designed to have very low background counts. A $90\text{Sr}/90\text{Y}$ beta source is used for irradiation.

The equivalent dose (ED) measurements for quartz separates were measured using the standard single aliquot regenerative (SAR) protocol (Murray and Wintle 2000). The OSL was measured at 125 °C and a pre-heat of 230 °C for 20 s for natural and regeneration dose was used.

For feldspar grains, IRSL was measured at 50 °C for the 60 s utilizing a pre-heat treatment of 250 °C for 60 s, for both the dose and test dose measurements (Lamothe et al. 2003; Blair et al. 2005; Auclair et al. 2003). For anomalous fading rate estimation, five aliquots from each of the five samples were used where natural luminescence was already measured. The Huntley and Lamothe (2001) model was used for estimation of g value and age correction. The anomalous fading which leads to the shortfall ages is a phenomenon caused by short-term leakage of an electron from traps at room temperature. Quantum–mechanical tunnelling of the trapped electrons to the nearby acceptors has been the most commonly accepted explanation (Visocekas 1985; Aitken 1985). This anomalous fading can be quantified as g value where g corresponds to the percentage loss per decade of time (Aitken 1985). The signal loss due to the recombination of electron and hole as a result of quantum–mechanical tunnelling follows a logarithmic decay curve over the laboratory time scale. A graph of IRSL intensities versus the log of the time elapsed since irradiation can be plotted. The g value can be then estimated from the regression line that connects the points in this graph.

The expression for the decrease in luminescence by Huntley and Lamothe (2001) is

$$I = I_c \left[1 - \frac{g}{100} \log_{10} \left(\frac{t}{t_c} \right) \right]$$

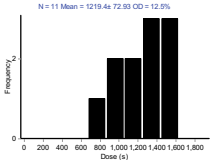
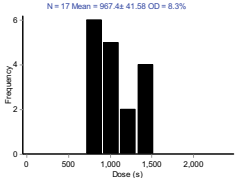
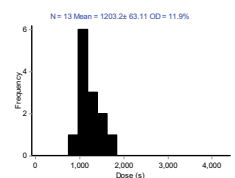
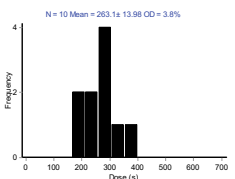
where I is the IRSL intensity measured at time t after the irradiation and I_c is the Intensity when t = t_c.

The OSL reluts are given in Tables 1, 2 and 3.

4 Results and Discussion

According to Ramesh (1988), the material making up the T₁ terrace represents the youngest QH II formation whereas the T₂ terrace is comprised of the QH I Formation. The material in the T₃ terraces corresponds to the QP III Formation, which is a low-lying alluvial tract covering a major part of the mapped area. The T₄ terraces mainly belong to the QP I and QP II formations. Our new OSL dates corroborate this stratigraphic scheme. Sand collected from below the T₂ terrace in the northern end of the main Manabhum Hill, around 1.5 m from the riverbed dates to ~9.2 Ka (QHI), and that of the sand bed just above the clay beds marked as the unconformity between the terrace material and the Dhekiajuli formation dates to ~42 Ka (Fig. 2). A sand bed in the southern bank of NoaDihing below the T₄ terrace dated to ~36 Ka. This is the oldest material from the terrace system (Fig. 2).

Table 1 Shows the equivalent dose and the distribution of the doses

Sl no	Sample name	ED (Gy)	Histogram
1	MIAO-1/14-1	184.6 ± 11	
2	MIAO-2 Terrace-1/14-2	146.5 ± 6.3	
3	OSL 17/1	182.2 ± 9.6	
4	OSL 17/2	39.8 ± 2.1	

Our dating shows that the older sandstone in the core of the Manabhum hill dates to within a range of ~220 to ~130 Ka from south to north (Fig. 2). It indicates that the core of the hill exposes rock that was formed in the late Pleistocene time. This is not consistent with the sandstone in the core of Manabhum hill belonging to the Miocene-Pliocene Dihing Formation of rock as mapped by the Geological Survey of India (GSI Reports, 1985–86). The age of the Dihing Formation rock is much younger and we assign it a Late Pleistocene age.

This sandstone unit is overlain by less consolidated thick pebble beds with interbedded coarse-grained yellow sand and thin clay beds that have been assigned to the Dhekiajuli Formation by the Geological Survey of India (GSI Reports 1985–86). Again unlike the GSI report our age data does not support its Pleistocene age, rather it shows Holocene age.

As there is no published absolute age data of Dhekiajuli or Dihing Formation rocks, we stick to these nomenclatures assigning younger ages. So, we conclude

Table 2 Shows the Equivalent Dose, dose distribution and the g value plot

Sl no	Sample name	ED (Gy)	Histogram	Normalised IRSL intensities plotted versus the log of time elapsed since the end of irradiation. One aliquot from each experimental routine is presented
1	MR-1	332.9 ± 13.4		
2	MR-3	372.9 ± 18.9		
3	OSL 18-1	466.7 ± 35		
4	OSL 15-2	539.4 ± 23.4		
5	OSL 16-3	551.5 ± 28.6		
6	MR-1	332.9 ± 13.4		

(continued)

Table 2 (continued)

Sl no	Sample name	ED (Gy)	Histogram	Normalised IRSL intensities plotted versus the log of time elapsed since the end of irradiation. One aliquot from each experimental routine is presented
7	MR-3	372.9 ± 18.9	<p>N = 15 Mean = 2463.0s 124.76% OD = 9.7%</p>	<p>MSWD = 0.012 Prob = 99 G_{decay} = 5.15 1/decade</p>
8	OSL 18-1	466.7 ± 35	<p>N = 13 Mean = 2062.8s 231.0% OD = 22.2%</p>	<p>MSWD = 0.062 Prob = 94 G_{decay} = 6.25 1/decade</p>
9	OSL 15-2	539.4 ± 23.4	<p>N = 14 Mean = 15863.4s 688.25% OD = 0.0%</p>	<p>MSWD = 0.0022 Prob = 96 G_{decay} = 7.25 1/decade</p>
10	OSL 16-3	551.5 ± 28.6	<p>N = 18 Mean = 3642.8s 183.62% OD = 14.5%</p>	<p>MSWD = 0.041 Prob = 96 G_{decay} = 2.15 1/decade</p>

that the Dihing Formation and Dhekiajuli rocks and sediments formed during Late Pleistocene to the Early Holocene time.

It is difficult to differentiate the Dhekiajuli boulders from the boulders of the T₄ terrace. The upper Dhekiajuli boulder beds imitate the same folding but the beds dip more gently than the Dihing Formation beds. The black and yellow clay bed just above the T₄ terrace at a high angle (Fig. 4) may be interpreted as a result of a thrusting event. These clay beds have formed in between two pebble beds of different formations. The lower pebble beds are at a high angle like the clay beds where the upper pebble beds are gentler. The low energy condition that prevailed to form such a thick clay horizon indicates a bogging of a somewhat energetic river for some time

Table 3 The ages of the sample collected, both uncorrected and the ages calculated after anomalous fading correction is shown in the table. The ages of four samples calculated using BSL is also shown in the table

Sl no	Sample name	U(ppm)	Th(ppm)	K(%)	ED (Gy)	No of discs	Dose rate (Gy/Ka)	Age (ka) (Uncorrected)	$g_{2\text{days}}$ (%/decade) (Average)	Age (Ka) (Corrected)	OSL
1	MR-1	2.7 ± 0.1	17.9 ± 0.9	3.8 ± 0.2	332.9 ± 13.4	22	6.4 ± 0.3	52 ± 3	9.8 ± 0.3	211 ± 28	IRSL
2	MR-3	2.8 ± 0.1	24.3 ± 1.2	4.2 ± 0.2	372.9 ± 18.9	15	7.2 ± 0.3	52 ± 4	2.7 ± 0.03	67 ± 8	IRSL
3	OSL 18-1	3.1 ± 0.2	21 ± 1.1	2.4 ± 0.1	466.7 ± 35	12	5.5 ± 0.3	85 ± 8	7.1 ± 0.0	197 ± 29	IRSL
4	OSL 15-2	3.3 ± 0.2	15.1 ± 0.8	1.7 ± 0.1	539.4 ± 23.4	14	4.4 ± 0.2	122 ± 8	5.6 ± 0.1	220 ± 36	IRSL
5	OSL 16-3	2.8 ± 0.1	18 ± 0.9	0.9 ± 2.6	551.5 ± 28.6	18	5.4 ± 0.3	103 ± 7	2.5 ± 0.0	130 ± 19	IRSL
6	MIAO-1/14-1	3.8 ± 0.2	29.7 ± 2	1.9 ± 0.1	184.6 ± 11	11	5.1 ± 0.1	36.1 ± 2.3			BSL
7	MIAO-2	3.6 ± 0.2	9.9 ± 0.5	1.1 ± 0.1	146.5 ± 6.3	17	2.7 ± 0.1	55.4 ± 2.8			BSL
8	OSL 17/1	3.5 ± 0.2	19.7 ± 1	2.3 ± 0.1	182.2 ± 9.6	13	4.3 ± 0.1	42.6 ± 2.5			BSL
9	OSL 17/2	3.6 ± 0.2	19 ± 1	2.2 ± 0.1	39.8 ± 2.1	10	4.3 ± 0.1	9.2 ± 0.5			BSL

may be due to a thrusting event. The sand beds between the ochre clay and pebble bed of T₄ terrace dates ~42 ka.

In the southern bank of Noa-Dihing River, arkosic sandstones with charcoal are reported as belonging to the Miocene Tipam Sandstone in the earlier literature (Shrivastava and Sharma 1986), but according to Mandal (2013) these might be of Dhekiajuli, Girujan or Namsang Formations of Plio- Pleistocene age. Exposures are scanty but are characterized by greenish grey coloured, coarse sand with large coal blocks and are identified as Tipam Beds by Boral and Tiwari (1975) and the Namsang Beds by Nandy (2001). In our opinion, as the character of these rocks are similar to the Dihing and Dhekiajuli Formation rocks we observed on the north bank of the NoaDihing, the rocks on the south bank of the NoaDihing River also of the Dihing Formation and Dhekiajuli, and not as old as Namsang or Tipam formations. So all these rocks and sediments formed and deformed during the Pleistocene Holocene time.

The thick sand beds in the anticlinal core show gentle dip when compared to the much steeper dip on the limbs of the anticline. This suggests that the anticline has a broad, open hinge zone. Our stereonet analysis (Figs. 13a and b) shows that the fold is subcylindrical and plunges very gently, 1°, 330. The western limb of the anticline is steeper than the eastern limb. The asymmetry of dips in the oldest units exposed that we measured matches the topographic asymmetry of the hill. This basic observation argues for active fold formation. This sort of fold shape is supported by the seismic reflection study of Borthakur et al. (2013). The asymmetric Manabhum anticline thus resembles a piggy-back structure of a ramp anticline that is actively developing over a blind thrust fault (Fig. 14). Manabhum anticline is forming in a complex foreland of both the Schuppen belt and the Mishmi thrust.

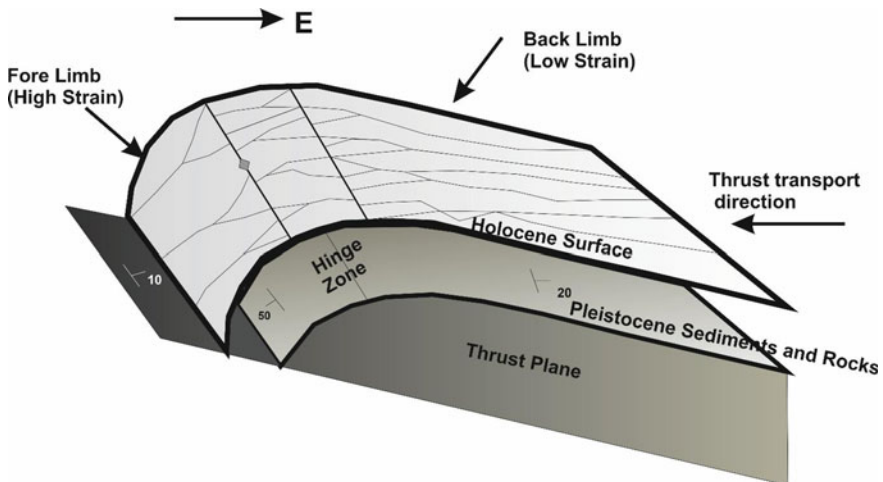


Fig. 14 The model showing the development of Manabhum anticline over an easterly dipping thrust

5 Conclusion

We interpret that the formation of Manabhum Hill has experienced two distinct processes: deposition of sediment and deformation. Three broad episodes are inferred. The first episode involved the creation of the foredeep in front of the Mishmi block by the deposition of the Dihing Formation or the Late Pleistocene rock, basically a large thick coarse sand unit with occasional pebble beds. Then, a small antiformal structure developed as a ramp anticline over an easterly dipping thrust parallel to the Mishmi thrust around 220 ka. This was followed by the deposition of a thick conglomerate blanketing the Dihing Formation rocks and uplift during Early Holocene -Late Pleistocene time. These are the sediments of the Dhekiajuli Formation. The newly formed pebbly sand sediments of Dhekiajuli then deformed and uplifted along a thrust plane around ~46 ka. The Manabhum Hill thus started growing. The third episode involves the formation of piedmont terrace system in the foothill of the Manabhum Hill, which shows episodic uplift evident from the subsequent older ages of terraces with increasing height from T_1 to T_4 .

A detailed geomorphological and seismological work is needed to understand the kinematics of formation of this anticline and also to understand the regional tectonic scenario as well as disaster management in this area.

Acknowledgements The present study is part of the Women Scientists Project (WOS-A) granted to CCG by the Department of Science and Technology, Government of India (Grant No. SR/WOS-A/EA-13/2018) and executed in the Department of Geology, University of Calcutta. CCG thanks the Head of the Department of Geology, University of Calcutta for providing infrastructural support. Belligraham thanks the HOD, Department of Earth Science, IISER, Kolkata for infrastructural support. We thank Basudha Goswami for her constant support during field work and sacrificing her time and studies for our work during the manuscript preparation. We are grateful to Prof. D Mukhopadhyay and Sri Bikash Chandra Poddar for the discussion and support all through the work.

References

- Acharyya SK (1980) Structural framework and tectonic evolution of the eastern Himalaya. *Himal Geol* 10:412–443
- Aitken MJ (1985) Thermoluminescence dating: past progress and future trends. *Nucl Tracks* (10):3–6
- Aitken MJ (1998) Introduction to optical dating: the dating of Quaternary sediments by the use of photon-stimulated luminescence. Clarendon Press
- Auclair M, Lamothe M, Huot S (2003) Measurement of anomalous fading for feldspar IRSL using SAR. *Radiat Meas* 37(4–5):487–492
- Blair MW, Yukihara EG, McKeever SWS (2005) Experiences with single-aliquot OSL procedures using coarse-grain feldspars. *Radiat Meas* 39(4):361–374
- Boral MC, Tiwari M (1975) Traverse mapping of the Area South of NoaDihing Valley, Tirap District, Arunachal Pradesh, Progress Report to 1974–75. Unpublished report, GSI
- Borthakur AN, Ahmed JP, Singh SP (2013) 10th Biennial International Conference & Exposition, 370p

- Burg JP, Davy P, Nievergelt P, Oberli F, Seward D, Maurin JC, Diao Z, Meier M (1997) Exhumation during crustal folding in the Namche-Barwa syntaxis. *Terra Nova* 9(2):53–56. <https://doi.org/10.1111/j.1365-3121.1997.tb00001.x>
- Burg JP, Nievergelt P, Oberli F, Seward D, Davy P, Maurin JC, Diao Z, Meier M (1998) The NamcheBarwasyntaxis: evidence for exhumation related to compressional crustal folding. *J Asian Earth Sci* 16(2–3):239–252. [https://doi.org/10.1016/S0743-9547\(98\)00002-6](https://doi.org/10.1016/S0743-9547(98)00002-6)
- Cardozo N, Allmendinger RW (2013) Spherical projections with OSX Stereonet. *Comput Geosci* 51:193–205. <https://doi.org/10.1016/j.cageo.2012.07.021>
- Das Gupta AB (1977) Geology of Assam-Arakan region quarterly. *J Geogical Mineral Metall Soc India* 49:1–53
- Gansser A (1964) *Geology of the Himalayas*. Intersci, Wiley, New York, p 289p
- Gururajan NS, Choudhuri BK (2003) Geology and tectonic history of the Lohit Valley, Eastern Arunachal Pradesh, India. *J Asian Earth Sci* 21:731–741
- Huntley DJ, Lamothe M (2001) Ubiquity of anomalous fading in K-feldspars and the measurement and correction for it in optical dating. *Can J Earth Sci* 38(7):1093–1106
- Huntley DJ, Godfrey-Smith DI, Thewalt ML (1985) Optical dating of sediments. *Nature* 313(5998):105–107
- Jade S, Shrungeswara TS, Kumar K, Choudhury P, Dumka RK, Bhu H (2017) India plate angular velocity and contemporary deformation rates from continuous GPS measurements from 1996 to 2015. *Scientific reports* 7:11439. <https://doi.org/10.1038/s41598-017-11697-w>
- Lamothe M, Auclair M, Hamzaoui C, Huot S (2003) Towards a prediction of long-term anomalous fading of feldspar IRSL. *Radiat Meas* 37(4–5): 493–498. [https://doi.org/10.1016/S1350-4487\(03\)00016-7](https://doi.org/10.1016/S1350-4487(03)00016-7)
- Mandal KL (2013) Upper Assam basin and its basinal depositional history. *South East Asian J Sediment Basin Res* 1.3–10
- Murray AS, Wintle AG (2000) Luminescence dating of quartz using an improved single-aliquot regenerative-dose protocol. *Radiat Meas* 32(1):57–73
- Nandy DR (1980) Tectonic pattern in NE India. *Indian J Earth Sci* 7:103–107
- Nandy DR (2001) *Geodynamics of Northeastern India and the adjoining region*. ABC Publications, Calcutta, p 209
- Ningthoujam PS, Dubey CS, Lolee LK, Shukla DP (2015) Tectonic studies and crustal shortening across Easternmost Arunachal Himalaya. *J Asian Earth Sci* 111:339–349
- Ramesh NR (1988) RGeoenvironmental appraisal of BurhiDihing and NoaDihing valleys in parts of Upper Assam and Arunchal Pradesh. *J Eng Geol* XVII(3&4)
- Sarma KP, Nandy S, Devi NR, Konwar P (2009) Is Mishmi block a tectonic roof? Some observations. In: Kumar S (ed) *Magmatism, tectonism and mineralization*. Macmillan Publishers India Ltd., New Delhi, India, pp 167–178
- Shrivastava RN, Sharma SK (1986) GSI progress report for the field season 1985–86. GSI portal
- Singh MD, Kumar A (2013) Active deformation measurements at mishmi complex of eastern Himalayan syntaxis. *Int J Geosci* 4:746–758. <https://doi.org/10.4236/ijg.2013.44068>
- Spooner NA (1994) The anomalous fading of infrared-stimulated luminescence from feldspars. *Radiat Meas* 23(2–3):625–632
- Thakur VC, Jain AK (1975) Some observations of deformation and metamorphism in the rocks of some parts of Mishmi Hills, Lohit district (NEFA). *Arunachal Pradesh. Himalayan Geol.* 5:339–364
- Visocekas, 1985. Visocekas R (1985) Tunnellingradiative recombination in labradorite: its association with anomalous fading of thermoluminescence. *Nucl Tracks Radiat Meas* (1982), 10(4–6):521–529
- Wintle AG (1973) Anomalous fading of thermo-luminescence in mineral samples. *Nature* 245(5421):143–144
- Zeitler PK, Koons PO, Bishop MP, Chamberlain CP, Craw D, Edwards MA, Shroder JF (2001) Crustal reworking at Nanga Parbat, Pakistan: metamorphic consequences of thermal-mechanical coupling facilitated by erosion. *Tectonics* 20(5):712–728. <https://doi.org/10.1029/2000tc001243>

Assessment of Neotectonic Effect on Quaternary Deposits in Darjeeling Himalayas



Sunipa Mandal and Pinaki Roy

Abstract A quantitative assessment of landform and sediment in Quaternary deposits, focusing upon the Mountain Front Thrust (MFT) manifests neotectonics in the aftermath of the orogeny, is intended in the Darjeeling Sub-Himalayas, to feel the ever-fecund pulses of ground tremors. The Sub-Himalayan hilly terrain, generally without sediment cover, has a distinctive character on two sides of the Mountain Front Thrust in terms of drainage pattern and density, stream order, 1st order stream gradient, and shape and size of watershed basins. The sinuosity of MFT <1.4 elicits tectonic deformation. Comparatively smaller and more elongated watershed basins residing at the southern flank of MFT suggest steepness along with tectonic imprints. Significantly more frequent occurrence of parallel drainage patterns, comparatively lower stream orders, and consequent reduction in drainage density on this thrust front are well anticipated. The River Tista in the area achieves minimum gradient on the crest of the MFT eliciting uplift. Frequent changes in river gradient around MFT without any correlation with lithologic changes testify tectonic effect. The valley floor-width/height ratios (<0.5) derived from this river bear clear attestation to the tectonic youthfulness of the studied terrain. This uplift of the MFT recorded the basin subsidence in fluvial sequence building with thinning of valley cycles through vertical stacking of warped and tilted multi-generated terraces along River Tista in the Sub-Himalayan region. A concomitantly progressive increment of clast sizes and distal crystalline rocks in a vertical succession of sediment piles with southward migration on thrust shoulder along with enhancement of sedimentation rate upstream and channel incision suggests the directive measurements of tectonism, not climatic effect. The common presence of penecontemporaneous deformational structures in the pile is also suggestive of intermittent tectonic disturbances.

Keywords Neotectonism · Mountain Front Thrust · Landform · Sediment · Fluvial sequence building · Basin subsidence · Upliftment · Sedimentation rate · Darjeeling Sub-Himalayas

S. Mandal (✉)

Department of Geological Sciences, Jadavpur University, Kolkata 700032, West Bengal, India

P. Roy

Department of Geology, Durgapur Government College, Durgapur 713214, West Bengal, India

1 Introduction

Tectonism creates and surficial processes that modify the earth's surface relief. The vertical component of plate-related movement is antecedent to topography, while erosion–deposition remoulds it. Exogenous sedimentary processes thus tend to obliterate the topographic signature of tectonism. The extent of obliteration depends on the climate-related rate of erosion and how frequently tectonism interrupts the drift. The compression has engendered successive thrusts, all dipping northward (Gansser 1964; Valdiya 1993), and has the potential to be reactivated. The latest among them, the Main Frontal Thrust (MFT; Gansser 1964, 1981; Nakata 1989) or the Himalayan Frontal Fault (HFF; Nakata 1972, 1989) still rises. A study across the precipice raised by the Himalayan Main Frontal Thrust or Himalayan Frontal Fault separating the rugged mountain range and the piedmont on its south is most apt for testing this percept. MFT being the youngest among all the major thrusts in the Himalayan region, any transect across it is likely to highlight the changing balance between tectonism and exogenous processes most explicitly (Fig. 1a). So, this paper focuses upon the hilly terrain mostly encompassing MFT both in the northern and southern part in the Sub-Himalayan zone having a little cover of Quaternary and Recent sediments and concentrates to work out the quantitative or semi-quantitative assessment of the geomorphic characteristics by using various indices derived from landforms and drainages along the course of the River Tista across the Sevok-Rangpo transect in the Darjeeling-Jalpaiguri districts, West Bengal (Fig. 1a). Notwithstanding, drainage and sedimentation are cogently affected. The signature of neotectonism is, however, expected to be more readily obliterated in the chosen area because of the wet climate. The River Tista encompassed in slices within the hilly region between the tectonically active MBT and MFT which had not yet been attested; except the documentation of genetic classification of finer sediments of the same river in the piedmont by Chakraborty and Ghosh (2010). A long-awaited demand for a specialist sedimentological analysis of Quaternary fluvial deposits in the context of neotectonism and climate change has largely been meted out through the present study. The present study also aims to address the reconstruction of the sequence building by a high-resolution process–product relationship with river base profile i.e., the profile of the imaginary slope on which the equilibrium between erosion and deposition is achieved, fluctuations by rapid subsidence, and consecutive basin upliftment. Vertical stacking of valley cycles records the subsidence. At least five terraces measuring around 15 m on average in height on these sediment piles have been recorded. The imperative is thinning of valley cycles with coarsening up the succession of sediment piles and the presence of maximum clast size along with the percentage of granite boulders in valley floor conglomerates increases up the succession. Besides, supportive documentation has been taken recourse by the presence of a conspicuous concentration of soft sedimentary deformational structures along some deformed and tilted beds.

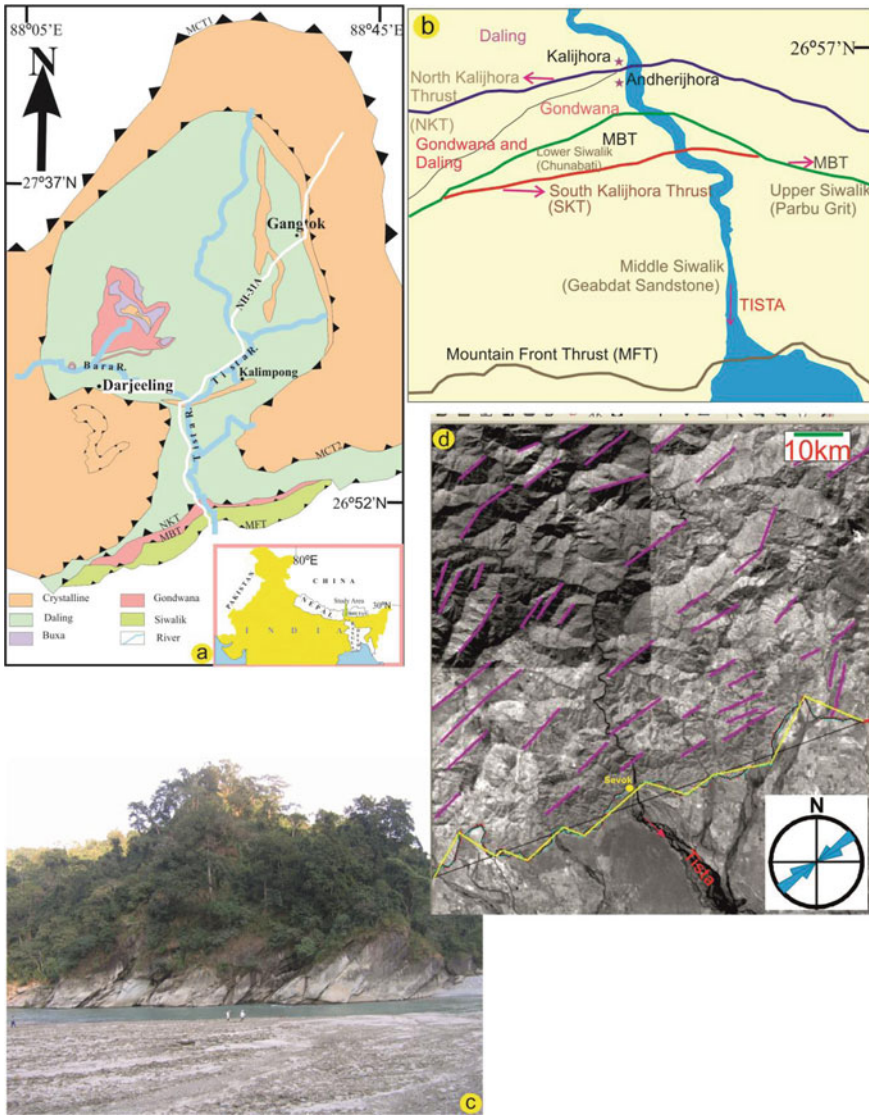


Fig. 1 Geological map of the north–south elongated eastern section of the Himalayan belt that includes the studied segment. The map highlights the major thrust sheets, four regional and one local, and the formations exposed between them. Location of the study area at the north-eastern fringe of India is indicated within the inset (modified after Ray et al. 2011) (a). Enlarge view of the area showing broad lithologies and their respective ages, indicated along with major tectonic elements within the studied part of the hilly terrain (modified after Ray et al. 2011) (b). Lower Siwalik Formation with northward dipping slivers along the River Tista in between SKT and MFT across Sevok-Rangpo transect (c). Lineament map generated through the combination of LISS-III and PAN images; rose diagram in inset depicts NNE-SSW trend (d)

2 Geological Background

Successive east–west elongated and southward verging thrusts dissect the ~2000 km-long Himalayan belt lengthwise in consequence to the plunge of the Indian plate under the Asian plate and resultant shortening of the low-density sediment cover on it (Fig. 1a). The Main Central Thrust (MCT 1) is the oldest among them and it extends from Nepal on the west up to the eastern end of the Himalayan belt. The Main Central Thrust (MCT 2), North Kalijhora Thrust (NKT), Main Boundary Thrust (MBT), South Kalijhora Thrust (SKT), and Mountain Front Thrust (MFT) have occurred progressively southward in succession (Fig. 1b and c). But the NKT and SKT (Matin and Mukul 2010 and references therein) among them are localized and confined almost entirely to the present study area, while the remaining three extend all over the Himalayan belt (Gansser 1964; Valdiya 1993; Decelles et al. 2001). North of the MCT2 high-grade crystalline massifs are exposed, they are mostly of Palaeoproterozoic age (Fig. 1a; Acharyya 1971; Ray and Neogi 2011; Long et al. 2011 and references therein). The area between the MCT2 and NKT exposes the Proterozoic metasediments, viz., the Daling and Buxa Groups of rocks. The NKT and MBT confine the Daling and Permo-Carboniferous Gondwanas, while the Lower Siwalik Formation (Chunabati) is confined between the MBT and SKT and the Upper and Middle Siwalik Formation are confined between SKT and MFT (Matin and Mukul 2010) of Mio-Pliocene Siwalik Group. The youngest of these thrusts at the south creates the high-relief mountain-front (MFT) bordering the Indo-Gangetic plain (Horton and DeCelles 2001 and references therein) (Fig. 1b). In the chosen area of study, a significant strike-slip displacement has made the tectonic history of the MFT complex (Gansser 1981; Nakata 1989). The major lineaments in the area align NNE-SSW, NW-SE, and E-W (Roy 1976; Acharyya 1976) (Fig. 1d). The River Tista negotiates this steep mountain front, emanating sudden enhancement in sedimentation rate that underscores significant hydraulic jump across the MFT. It is noteworthy that the river course of Tista on the mountainous region of the Himalayas was not demarcated in pre-1787 maps (Miall 1978; Islam and Higano 1999). The pre-1787 Tista could have been fed by rainwater only and emerge out from the mountain front, later on, it joined with the glacier-fed mountain-interior drainage system (Rennel 1794; Arrowsmith 1804; Carry 1811; Bahuguna et al. 2001; Chakraborty and Ghosh 2010) and thereby the discharge amount has been raised immensely followed by the devastating flood in the river in the year 1787 (Chakraborty and Ghosh 2010) and it has been directly linked with a major seismic event (Islam and Higano 1999).

Several related studies have been carried out in the foothills of the NE Himalayas, for example: geological (Medlicott 1864; Pilgrim 1913), geomorphological (Nakata 1972), neotectonic/active tectonic/morphotectonic (Delcaillau et al. 2006 and references therein; Mukul et al. 2007), seismic (Malik et al. 2003), and structural (Acharyya 1982; Basu and Sarkar 1990; DeCelles and Cavazza 1999; Mukhopadhyay and Mishra 2004, 2005; Ghosh et al. 2005; Meetei et al. 2007; Guha et al. 2007). However, only a few studies have focused on landscape development, conjunctively with the underlying relationship between landscape and structures (e.g. Nakata 1972).

The upliftment rate of the MFT was measured (Lavé and Avouac 2001) by using river incision on the piedmont at the immediate west of the present study area. The highest rate of uplift in the Himalayan belt along the MFT was recorded by Merritts and Hesterberg (1994). The drainage systems also characterize the early works on eastern Himalaya (Nakata 1989 and references therein), although no quantitative assessment has been invoked.

3 Methodology

For remote sensing studies LISS-III with a spatial resolution of 23.5 m and PAN images of National Remote Sensing Agency of India, while toposheets of Survey of India, digitized, served as the basic tools. Satellite imageries were further enhanced by standard image processing techniques such as contrast stretching, filtering, band rationing, colour composite, etc. The remotely sensed images were georeferenced with the help of Survey of India toposheets no. 78 A/8, A/12, B/5, B/9 (surveyed in 1932, 1962–63) on 1: 50,000 scales. Watersheds on two sides of the MFT ridge were outlined and GIS platforms were deployed to estimate areas covered by each of the watershed basins and to quantify the geomorphic attributes. Classical Sedimentology was the mainstay for the study of the Quaternary deposits.

Maximum clast size is determined in valley floor conglomerates following the usual practice of taking averages from the 10 largest clasts in every valley cycle of river terraces considered (Pettijohn et al. 1972).

4 Results

4.1 Geomorphic Neotectonic Elements

The study area is delimited by NKT, MBT, SKT, and MFT, which are tectonically active major thrust planes (Fig. 1b). As a result, the landslide debris caused by the rejuvenation of these older lineaments during the Quaternary has been observed in many places. Seismically induced deformational structures are present in Quaternary sediments. The Quaternary sediments affected by the splay-faults related to NKT, MBT, SKT, and MFT indicate that the area is tectonically active (Fig. 1c).

4.1.1 Sinuosity of MFT

Many workers have used the qualitative aspect of MFT to make general assessments of the degree of tectonic activity present (Burbank and Anderson 2001 and references therein). All geomorphic indices apart, the sinuosity index of MFT has been preferred

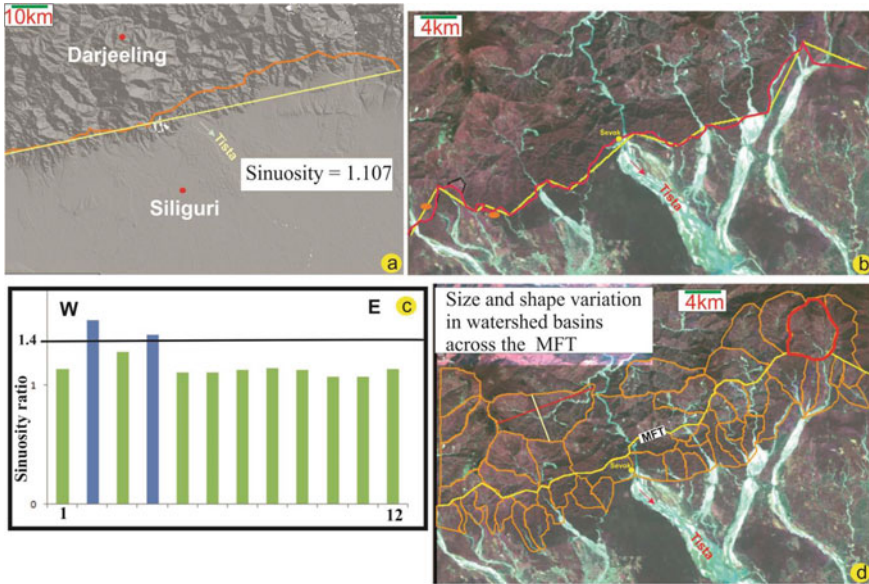


Fig. 2 Contrasting topographic relief in the Sub-Himalayan hilly-terrain and the piedmont on the foothills of the entire Eastern Himalayan belt well documented on the SRTM DEM. Note that the mountain front sinuosity separates the rugged hilly-terrain from the smoothed piedmont. MFT/MFRC (Mountain Front Ridge Crest) is marked by solid orange line on SRTM DEM in the present study area and showing overall sinuosity of the region (a). The segment wise sinuosity (marked by red line) for successive directional segments from west to east along MFRC (b). Segment wise sinuosity ratios of the MFT in study area from west to east. Note the ratio is slightly higher than 1.4 in only two segments which are pointed as orange circle in Fig. 2b (c). The size and shape variation in watershed basins across the MFT (d)

because of its prominent revealing of tectonic activity. The sinuosity of the ridge crest (S_{mf}) is measured as the ratio of the actual length of the chosen ridge (L_{mf}) to the length of a straight line joining its two ends (L_s) utilizing satellite imageries (Bull 1977, Bull and Mc Fadden 1977, Keller and Pinter 1996) (Fig. 2a, b). The sinuosity of the entire ridge crest in the study area is ~ 1.4 in all but two of its unidirectional near-straight constituent segments it is >1.4 (Fig. 2c).

4.1.2 Watershed Area, Size and Shape

Morphometric analysis of a watershed provides a quantitative description of the drainage system, which is an important aspect for the characterization of watersheds (Strahler 1964). The Watershed system-related attributes were erected through the combination of GIS software namely TNT mips and Global mapper 10 and analysed a digital elevation model (DEM). According to Schumm (1956) elongation ratio of the watershed basin is defined as the ratio of the diameter of a circle of the same

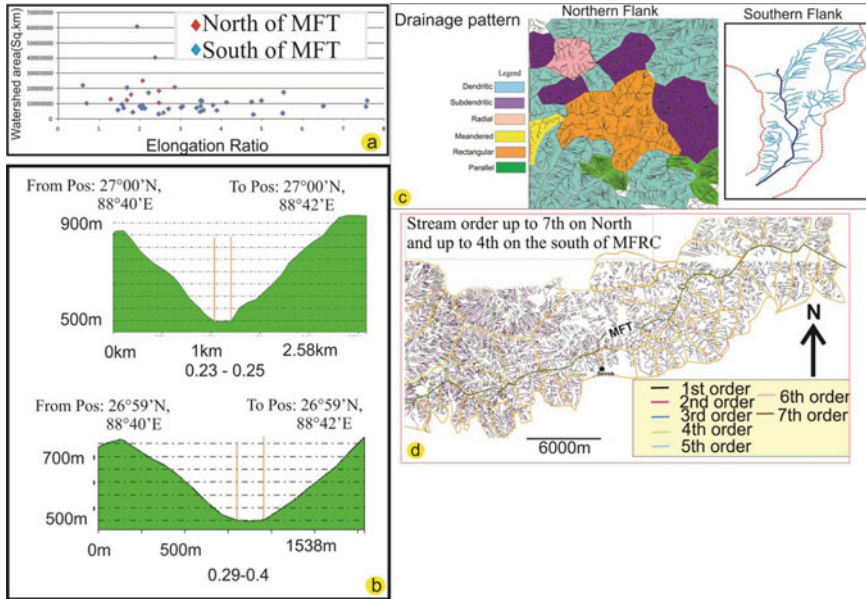


Fig. 3 Variation in elongation ratio of successive watershed from west to east along the studied stretch of the MFT on two sides of the thrust (north in Red and south in Blue) (a). V_f values along the River Tista on both sides of the MFT (b). Drainage pattern on both sides of MFT/MFRC (c). Stream orders within confinement of individual watershed basins on two sides of the MFT/MFRC. Note that higher stream orders are present on the northern flank of the MFT (d)

area as the basin to the maximum basin length. The elongation ratio of the watershed in the northern flank of the MFT and southern flank of the MFT are 2.85 and 7.59 respectively (Figs. 2d and 3a). Besides, the elongation ratio B_s (Ramírez-Herrera 1998), which is also used to describe the basin shape in horizontal projection and may be expressed by equation $B_s = B_l/B_w$, where B_l is the length of the basin, measured from its outlet to the most distal point in the drainage divide and B_w is the width of the basin measured across the short axis (Fig. 2d). The width vs. length ratio of the basins ranges from 0.59 to 0.86 on the northern flank, but never exceeds 0.43 on the southern scarp. The basins on the southern flank of the ridge are distinctly smaller and more elongated than those on its northern flank (Fig. 2d).

4.1.3 Valley Floor Width to Height Ratio (V_f)

The V_f (Bull 1977; Bull and McFadden 1977) of the River Tista have been quantified from the SRTM DEM (Fig. 3b). The location of the cross-valley transect within a drainage basin affects the values of V_f . Valley floors tend to become progressively narrower upstream from the mountain front and for a given stream system the values of V_f tend to become progressively larger downstream from the headwaters. The river

valley floor width to height ratio V_f in the River Tista on the north of the Mountain Front Ridge Crest (MFRC) 0.24 and 0.31 on the southern scarp face (Fig. 3b).

4.1.4 Drainage Pattern

Under confinement of individual watershed sub-basins within the River Tista system, the drainage pattern is predominantly dendritic, but may also be trellis, semi-parallel, parallel, rectangular, and rarely radial on the northern flank of the Mountain Front Ridge Crest (c.f. Howard 1967). In contrast, there is a clear dominance of parallel, semi-parallel and rectangular patterns on the southern flank of the same ridge (Fig. 3c).

4.1.5 Stream Order

Stream order is a measure of the position of a stream in the hierarchy of tributaries. Stream order that sorts out successive downstream convergence of streams, irrespective of the methodology adopted (Gravelius 1914; Horton 1945; Strahler 1952; Scheidegger 1965; Shreve 1967), shows higher orders on the northern flank than on the southern scarp of the MFT ridge (Fig. 3d).

4.1.6 Stream Frequency or Drainage Density

The cumulative length of all streams shown in the drainage basin of the River Tista has been measured on a mosaic of georeferenced toposheets simply by tracing the stream lengths by using GIS Platforms (Fig. 4a). The density of the drainage is given by the quotient of the cumulative length of the stream and the total drainage area. So the stream frequency or drainage density (Horton 1932, 1945; Faniran 1969) calculated based on the ratio between the total length of the streams versus the total area of the watershed basins is distinctly higher on immediate north than on the south of the MFT ridge crest (Fig. 4a).

4.1.7 Longitudinal Gradient of Major Stream

The gradient in degrees (θ) is derived from Atan of elevation difference/horizontal distance between the two ends of a studied stretch. Derivation of gradient of the River Tista in the study area run across the MFT was conducted in successive straight channel segments from those adjacent to MFT, upstream and downstream in this way. The gradient turns out to be the minimum at the MFT ridge crest (Fig. 4b).

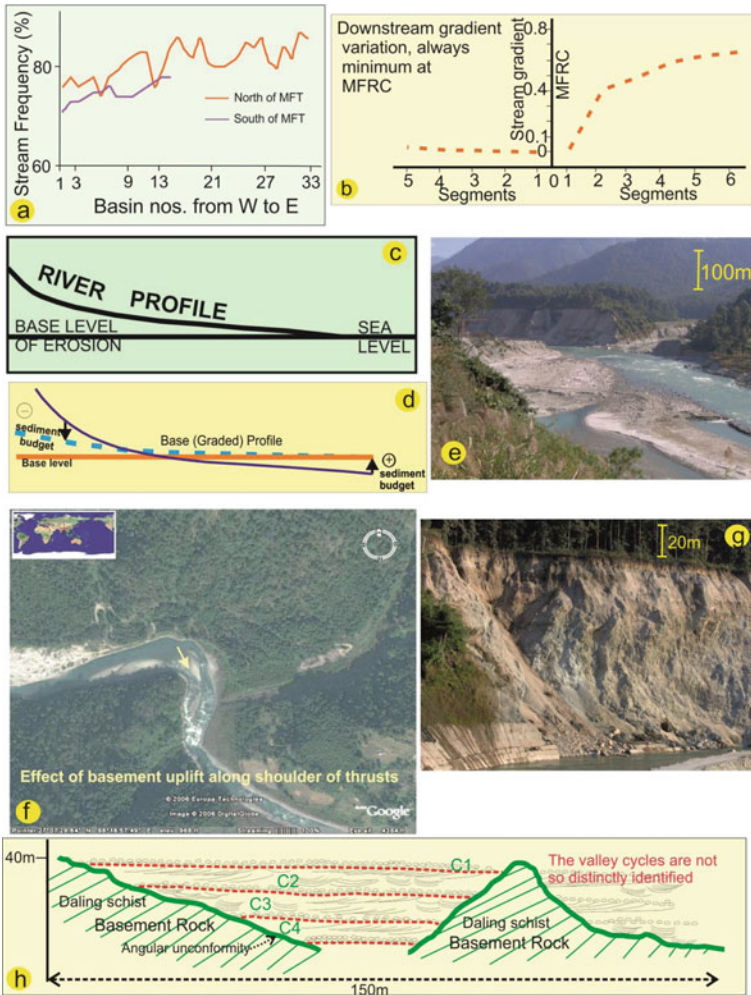


Fig. 4 The curves document frequency in occurrence of first order streams in successive watershed basins adjacent to the MFT/MFRC. Note that the frequency increases from west to east on both sides of the MFT/MFRC (a). Stream gradient variation in successive straight segments (numbered 1–5 or 6), on two sides of the MFT with reference to the River Tista in the hilly-terrain. Note that minimum gradient attains at the MFT/MFRC (b). Schematic diagram showing riverine erosion–deposition equilibrium is determined by the position of base profile (c); deeper channel incision (degradation) denotes basin uplift (sediment budget positive) whereas sediment layer stack up (aggradation) delineates basin subsidence (sediment budget negative) and sediment accumulation related with base profile (d). A substantially thick aggradational succession between two thrusts, basin subsided at a greater rate and created accommodation space (e). Effect of basement uplift along shoulder of thrust: opposite stratigraphic trends would arise—river base profile drops at incision point, but rises where ponding takes place (f). Sediment filled the valley, even spilled over—erched terrace (g). Sketch derived out of field data showing fluvial sequence building pattern and flood-plain amalgamation during aggradation due to basin subsidence; Note individual channel succession marked by C-horizon and channel floor (thalweg) covered with conglomerate (h)

4.1.8 River Terraces

Two terraces among the multilevel terraces have been observed in the Kalijhora and Rambhi sections representing the older alluvium, which are nearly 100 and 80 m high respectively. The valley cycles (for definition see Sect. 4.2) in the terrace marked as G1–G11, are overall coarsening upward, though individual valley cycles are showing fining upward trend, which is quite unusual in the fluvial regime. The clast size is gradually increasing in younger valley cycles.

4.1.9 Tilted Bed

The beds within quaternary succession are tilted in two opposite directions.

4.1.10 Interpretation

The ruggedness of topography itself is a measure of tectonic activity in the studied hilly terrain. Less than 1.4 sinuosities in all but two of its directional segments manifest the neotectonic imprint (Bull and McFadden 1977; Keller and Pinter 1996) (Fig. 2b and c). Strahler (1952) states that the elongation ratio runs between 0.6 and 1.0 over a wide variety of climatic and geologic types. The regional slope can be derived from the size along with the elongation ratio of the watershed basins; the higher the tectonic effect greater would be the slope, in general (Figs. 2d and 3a). With continued evolution or less active tectonic processes, the elongated shape tends to evolve into a more circular shape (Bull and McFadden 1977). Relatively young drainage basins in active tectonic areas tend to be elongated in shape normal to the topographic slope of the mountain. The considerably higher ratios on the MFT scarp are the direct consequences of ground steepness. The primarily tectonically induced watershed basins, at the northern flank of the MFT, have become larger due to the integration of watersheds through progressive denudation. The distinctly more elongated and smaller watershed basins derived from the southern flank of the MFT indicate that the southern flank is steeper than the northern one and the tendency of shortening of the watershed basins adjacent to the MFT denote the neotectonic rejuvenation of the MFT ridge crest.

The tectonic imprint has been testified through the quantitative measurements of V_f on both sides of MFT speaks eloquently about the neotectonism from the threshold value of V_f (Fig. 3b) with allowing little net sedimentation and deep incision of river valley resulting due to either basement uplift or climatic shift to aridity (Blum and Tornqvist 2000). The valley incision develops successive multilevel terraces bearing oppositely directed tilted beds which can again delineate gradual upliftment of the MFT ridge crest. The loss of channel gradient must have caused widening of valley floor widths and that, in turn, explains the somewhat higher values of V_f immediate downstream of the MFT ridge crest or the southern flank of the MFT. The tectonic effect is likely to be obliterated at a faster rate in the case of a larger river like

the River Tista for its greater erosive power. Tectonic induced activity generates relief and thereby imparts an order in drainage distribution; slope determines river flow direction. Hence dendritic, trellis, parallel, semi-parallel, rectangular, and radial drainage patterns bespeak tectonic effect on the hilly terrain (Fig. 3c).

More pronounced lower ordering of stream and dominance of parallel and semi-parallel drainage pattern in the southern flank of the MFT and in consequence, drainage density is comparatively higher, 1st order streams have considerably lower gradients on the northern flank of the MFT ridge further corroborates steeper slope on its southern flank (Figs. 3d and 4a). So, the tectonic overprint is apparent. From the successive measurement of the overall stream gradient, it has been noticed that the gradient is found to attain the minimum value around the MFT (Fig. 4b). So, it denotes the upliftment of MFT and it negates the erosional activity of the river.

4.2 Sediments

4.2.1 Facies Analysis and Sequence Building

A multipronged approach with special emphasis on detailed high-resolution facies analysis, recognition of fluvial architectural elements with the temporal and spatial variability of deposits along the River Tista across a series of thrust planes merging southward have been synthesized. All together 16 facies have been identified and presented in Table 1. The proper analysis of facies of fluvial deposit also helps to understand the sequence building pattern through base-level fluctuations.

The Tista river course at the north of the MFT is quite a meandering type, controlled and restricted by canyons whereas the River Tista has become braided at the south of the MFT (Figs. 1b, 4c, d). In between the thrusts i.e. MBT and MFT, the valley was filled up with the sediment that even spilled over the valley shoulder (Fig. 4e–g). A 100 m thick pile of Tista sediment has accumulated between thrust sheets (NKT and MBT) encompassing the Dalings and the Gondwanas (Fig. 4h). Terraces, at least four in number coexist amongst which three are most spectacularly exposed through the present river channel flowing below the youngest terrace (Figs. 5a–d and 6a–c). The terraces are very large in dimension and the oldest terrace or T4 of the total vertical height of nearly 110 m, containing 11 valley cycles and nearly 75 channel cycles (Figs. 6c, d and 7a–c). Here the fluvial succession shows mainly three types of facies architectural elements (Fig. 8a–l). They are mainly of (1) Channel fills, (2) Bank attached bars, (3) Ripple flood plains. Several large-sized boulders (more than 3–4 m in dimension) of irregular shape are seen scattered in the vicinity of the River Tista valley in different terraces.

The channel fills facies exhibit lenticular bedforms, with cross-sets of pebble to sand-sized grains with fining upward sequence (Fig. 8c). Trough cross-stratification is very common (Fig. 8c). The bank attached bar facies is identified by epsilon cross-stratification (Fig. 8b and d). Sand silt alternation is common. Here sandstone unit

Table 1 Quaternary fluvial sedimentary facies motif along the River Tista across Sevok-Rangpo transect

Facies designation	Facies name	Facies description	Facies interpretation
Gcm	Clast-supported massive gravel	The facies is characterized by haphazardly oriented clast-supported fabric. Body geometry is typical wedge-like and often the wedges pass laterally into cross-stratified sediment (Fig. 8a)	The down wedge fining and cross-stratification are attributable to reworking of scree deposits
Gcm	Clast-supported imbricated stratified gravel	Poorly sorted, clast-supported gravel having the tabular clasts imbricated though profoundly of clast imbrication may decrease laterally, in the direction of clast imbrications (Fig. 8b)	The facies represents gravel bars, possibly bank-attached. The majority of clasts constituted sliding bed load driven by flow of high velocity
Gsmx	Matrix-supported crudely cross-stratified gravel grading upward into sand	The facies bodies have flat bases, but slightly convex upward tops. Its texture is generally matrix-supported, but concentration of pebbles greater at the bottom of the beds effecting a coarse-tail frequency grading. The top part of the beds is almost entirely sandy within which faint cross-strata are often discernible. (Fig. 8c)	Upward decrease in frequency of occurrence of pebbles or in other words, upward increase in sand content may be attributed to increasing settling and infiltration of sand on waning of the flow. Such sand infiltration caused formation of sieve deposits as the water percolates rapidly downward through the under-saturated sediment (Todd 1989). They are coupled together spatially, might have been deposited within channels, the relatively coarser sediments on the bars and the finer ones within the interbar small channels. Repeated upward transitions from trough cross-strata to planar laminae within individual channel-fills suggest ephemeral nature of the river (Olsen 1989)

(continued)

Table 1 (continued)

Facies designation	Facies name	Facies description	Facies interpretation
Gmg	Normally graded poorly sorted gravel	This facies is dominated by matrix content but the base of the bed defined as clast-supported and clast-size decreases gradually towards up of the section (Fig. 8c)	The fluidal flow created from debris flow
Gmx	Cross-stratified clast to matrix-supported gravel	The facies is characterized by clast to matrix-supported gravel with steeply imbricated pebbles, manifested by cross-strata (Fig. 8d)	This facies may be depicted as the bar within channel thalweg
Gmm	Matrix-supported massive gravel	Its body geometry is lenticular, generally having flat base and convex top, but some having concave-up channel-form too. In this matrix-supported conglomerate the grain-size distribution is broadly bimodal, but both the pebble and sand fractions are poorly sorted. The clasts are randomly distributed and oriented, some standing almost vertical (Fig. 8e)	The matrix-supported fabric with chaotically arranged clasts, locally subvertical, points to high matrix strength of the parent flow that froze instantaneously as its shear strength exceeded shear stress applied on it (Blair and McPherson 1994). It is safe to assume that the flow had been a debris flow, at least, immediately prior to deposition

(continued)

Table 1 (continued)

Facies designation	Facies name	Facies description	Facies interpretation
Sm	Massive pebbly sand	This sand dominantly massive or faintly cross-stratified and have sparsely distributed floating over-sized pebbles (Fig. 8e-g)	The facies is a likely product of flash flood
SGt	Trough x-stratified pebbly sand	It is a poorly sorted coarse to medium grained sandstone. Individual facies units are internally characterized by a single co-set of trough cross-strata. They are broadly lenticular in shape having sharp bases with pebble tending to be concave-up. (Fig. 8c)	Relatively thinner isolated channel-fills, therefore, indicate shallowing of the channels as the distance from the main channels increased
Sr	Compound x-stratified sand	Pebble-free sandstone, coarse-grained and poorly sorted. The large but low angle cross-strata enclosed small scale steeper cross-strata; both have roughly the same direction of inclination. The facies bodies generally have flat bases, but discernibly convex upward tops (Fig. 8h)	The facies apparently represents longitudinal bars
Sh	Planar laminated sand	Planar laminated sand with sheet-like or tabular geometry generally overlying cross-stratified sandy gravel and gray mud interbedded silt with sand and the sandy beds have sharp lower contact with gutters (Fig. 8i)	Sheet flow product, possibly generated by reworking of bar-top sediment during falling water stage

(continued)

Table 1 (continued)

Facies designation	Facies name	Facies description	Facies interpretation
Shg	Planar laminated graded sand	This facies is characterized by sets of planar/low angle laminae, locally topped by small scale ripple laminae. Each couplet are encased below and above by reddish silt/mud laminae. The bed geometry is laterally wedging with flat base (Fig. 8j)	This facies is obviously a product of a high flow shear. Coarse grain-size suggests it can be of channel-base origin, either a linguoid bar or a cross-channel bar. However, atop a bar it suggests reworking of already settled sediment, winnowing out the fines, during low water stage
Sl	Planar laminated fine-grained sand periodically interrupted by silt stringers	This facies, very coarse grained within the sand grade, is characterized by sheet-like geometry, and laterally discontinuous, crude planar laminae inside. This facies in majority of cases overlies a major erosion surface. Locally, however, a relatively finer grained counterpart has been seen on top of bars (Fig. 8i)	This facies possibly formed close to the channel bank as the fine grain size of the sediment suggests. The body geometry, internal structure and intermittent inclined mud laminae cumulatively identifies the facies as of levee
St	Trough cross-stratified sand	This facies characterized by trough co-sets in a poorly sorted sandstone whose average grain size is smaller than that of longitudinal bar facies with which they are closely associated. The bed geometry is lenticular with bases commonly distinctively concave upward and top flat. (Fig. 8d)	The facies presumably represents channel fill sediments, between bars or between banks. The facies geometry corroborates its contention. The upward concomitant reduction in grain size with co-set thickness is possibly due to gradual reduction in depositional slope with channel filling

(continued)

Table 1 (continued)

Facies designation	Facies name	Facies description	Facies interpretation
Sp	Tabular cross-stratified sand	This facies is internally characterized by normally graded tabular cross-strata. Cross-strata azimuths are at high angle between the sand and the encasing gravel deposits (Fig. 8d, k, l)	The geometry of the beds reveals identity of the facies as bars. Because of the tabular nature of the cross-strata, the bars are likely to be bank-attached in braided river
Fcl	Climbing Ripple laminated silt	This facies is characterized by a set of climbing ripples in sand. The small scale cross strata migrate in direction opposite to the inclination of the set boundaries enclosing them. The bed geometry is indeterminable (lenticular?). (Fig. 8k)	Since the ripple migrates opposite to the direction of the set boundaries cross-strata, the ripples can be interpreted to have back-flow origin. However, laterally uniform thickness of the sets of small scale cross-strata defies this contention. The more likely interpretation is that ripples climbed along upstream face of a bar, possibly longitudinal ones. The accretion on the upstream face of a longitudinal bar indicates relatively high rate of sedimentation
Frl	Ripple laminated silt and mud	This facies is defined by mud bodies having tabular geometry and also characterized by fine planar laminae. Rootlets often concentrate along the top surfaces of the beds. Multiple units of this facies may stack up vertically (Fig. 8f, k)	The facies elements along with the presence of root-casts; presumably denote it as the low energetic product of overbank deposit. Preferred concentration of iron encrustation suggests existence of omission surfaces which points to intervals between successive floods. Consequently, the vertical stacking of beds denotes basin subsidence

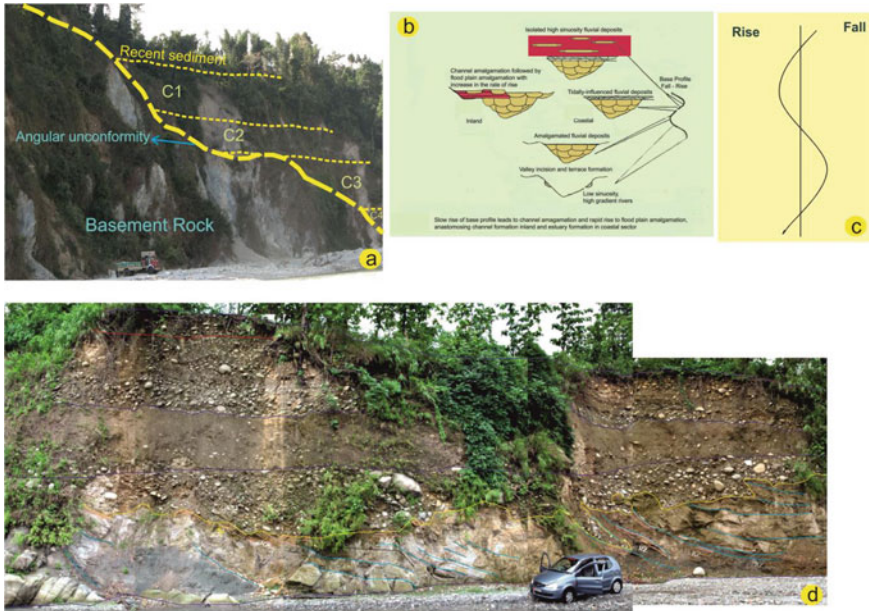


Fig. 5 Field photograph showing aggradational record points to basin subsidence that followed, sediment filled the valley as well as negative sedimentation budget and the angular unconformity (yellow dotted line) placed between basement rock (Daling Schist) and channel sediments (a). Slow rise of base profile leads to channel amalgamation and rapid rise to flood plain (high accommodation space) amalgamation. Schematic diagram showing fluvial sequence building pattern changes with base profile fluctuations (b). A sinuous curve representing the record of base profile fluctuations (c). The Quaternary aggradational fluvial sediments overlies on the Siwalik sandstone, the contact (yellow) being very sharp but highly irregular. The Siwaliks is constituted by imbricated thrust slivers (blue bordered) at variable angles with the contact. The thrust slivers, at places, are topped by fragments of oxidized bands encrusted by iron (pink bordered) immediately overlying rootlet zones (RZ), together probably representing an unconformity (d)

trapped along parallel-sided coarse sand to finer material. The bank attached bars are usually made up of planar laminated beds (Fig. 8i, j and l). But other bar deposits occur as patches and are characterized by rippled flats (Fig. 8f and k).

Thick sand bodies of lenticular geometry juxtaposed one upon another laterally and vertically. Lenticular channel bodies floored by small pebbles are stacked up one over another and laterally variable thickness is defined as channel cycle and their succession is intermittently intercepted by large pebble conglomerates of comparatively greater lateral persistence defining the valley cycles which consist of various types of crystalline rocks (Figs. 7a–c, 9a–c). Mainly they comprise the clasts of (a) White crystalline granitic gneiss and Para gneisses of Paro/Kanchanjhanga/Darjeeling gneisses, (b) Daling schist, (c) Arkosic Gondwana Sandstone, (d) Quartzite of Gondwana, (e) Coarse and fine-grained Siwalik Sandstone. Each of the valley cycles is an individually fining upward sequence (Fig. 7c). But a thick unit of overall coarsening upward with individual fining upward valley

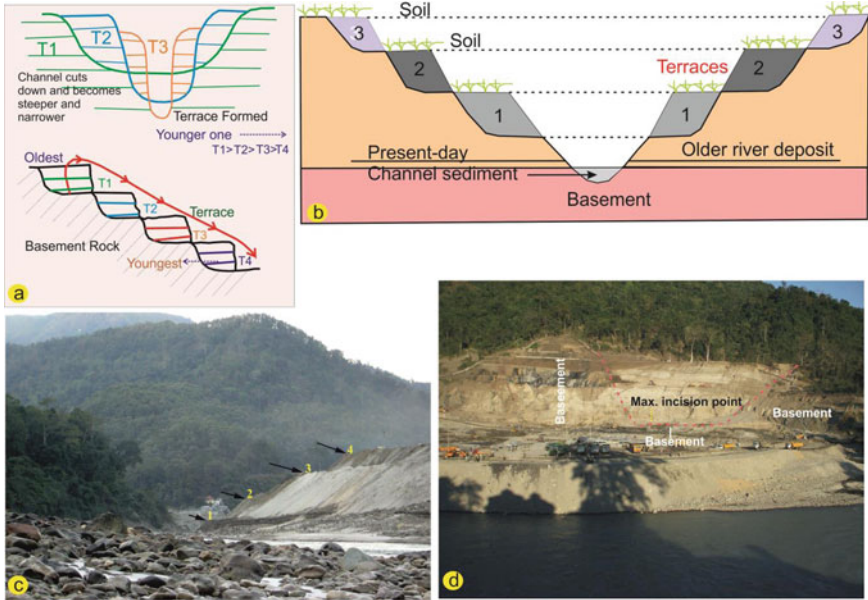


Fig. 6 Drop in base profile tends to remove the previous record of fluvial deposition, if there is any. Residues may, however, be retained at the channel margin because the channel becomes increasingly narrower as it turns deeper, step by step. Terraces are formed, successive younger ones at lower levels (a). The schematic diagram showing the river cannibalizes its own sediments, digs and may penetrate the basement as well (b). Field photograph showing discrete terraces of several generations record the course of basin uplift (c). Valley (red dotted line) incised to the level of maximum incision point during previous basement uplift phase. The present river channel is incised all through the sediment pile and into the Gondwana-Siwalik basement (d)

cycle is very well exposed along the course of River Tista (Fig. 7a). In all the places alternate appearance of clast supported gravel-boulder beds are identified as similar to the first-order cycle while gravel-pebble-coarse to moderate sand fill cycles are 2nd order cycle, though they are genetically unrelated. But overall thinning of valley cycles up the succession has been distinctly recognized (Figs. 7a and 9a). Maximum clast size in valley floor conglomerates increases up the succession and the hallmark of sediment source is most apparent in clast composition. A progressive increment in contribution from crystalline rocks reflects a temporal increase (Fig. 9b). The laterally extensive conspicuous concentration of soft deformation structures like fluid-escape, single-lobated, multi-lobated, and imbricated convolutes, contorted laminae, and load structures are found within the sediment piles.

4.2.2 Interpretation

The fluvial sediment cannot be part of the geological record unless going beneath the base level of erosion; thereby removing the previous record of fluvial deposition, if

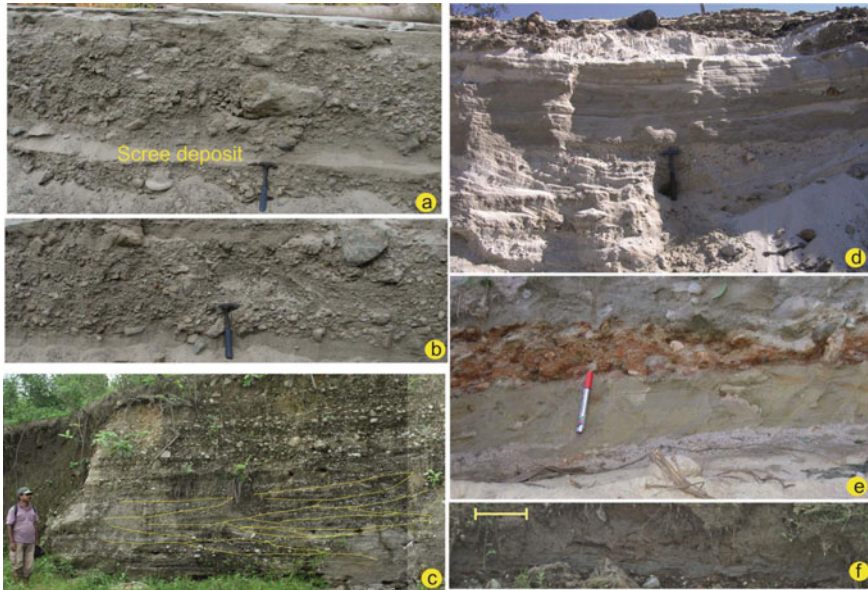


Fig. 8 Clast-supported massive gravel; scree deposits (a). Clast supported imbricated stratified gravel and upper part of the succession showing protrusion of vertically large sized gravel (b). Matrix-supported crudely cross-stratified gravel grading upward into sand and lower part of the deposits showing trough cross-stratified pebbly sand (c). Cross-stratified clast to matrix-supported gravel and also showing tabular cross-stratified sand (d). Matrix-supported massive gravel (e). Ripple laminated silt and mud (f). Massive pebbly sand (g). Compound cross-stratified sand (h). Planar laminated sand; Gray mud interbedded silt with sand and the sandy beds have sharp lower contact with gutters (i). Planar laminated graded sand (j). Climbing Ripple laminated silt (k). Planar laminated fine-grained sand periodically interrupted by silt stringers (l). Bar = 30 cm

Tornqvist 2000), cause ponding and sediment trapping. A thick pile of accumulation of sediment (100 m) in between thrust sheets (NKT and MBT) indicates the tectonic movement or upliftment is denoted by such a huge pile of sediment that could not accumulate over the base profile. But, here the sediment has accommodated such a huge height (100 m), which is now above the base level of erosion but once in the recent past, it was below the base unit of erosion (Fig. 6b–d). So, this can be sought again the source was uplifted or the accumulation site was subsided (Fig. 5a and d). Actually, it is more appropriate to assure that the accumulation site once gets subsided, forming an aggradational fluvial sequence of substantial thickness which has been grown up (Fig. 4e–h) due to the gradual increment in valley width with the progressive rise of base profile and depositing huge sediment pile in isolated pockets bounded between the thrusts namely MBT and MFT which is subjected to form the piggyback basins with rapid basin subsidence (Figs. 1b and 4f).

At a point in time, the trend was reversed and the basement of the depositional site started to rise (Fig. 4e–g). So, the sediment budget is positive and the pattern of the

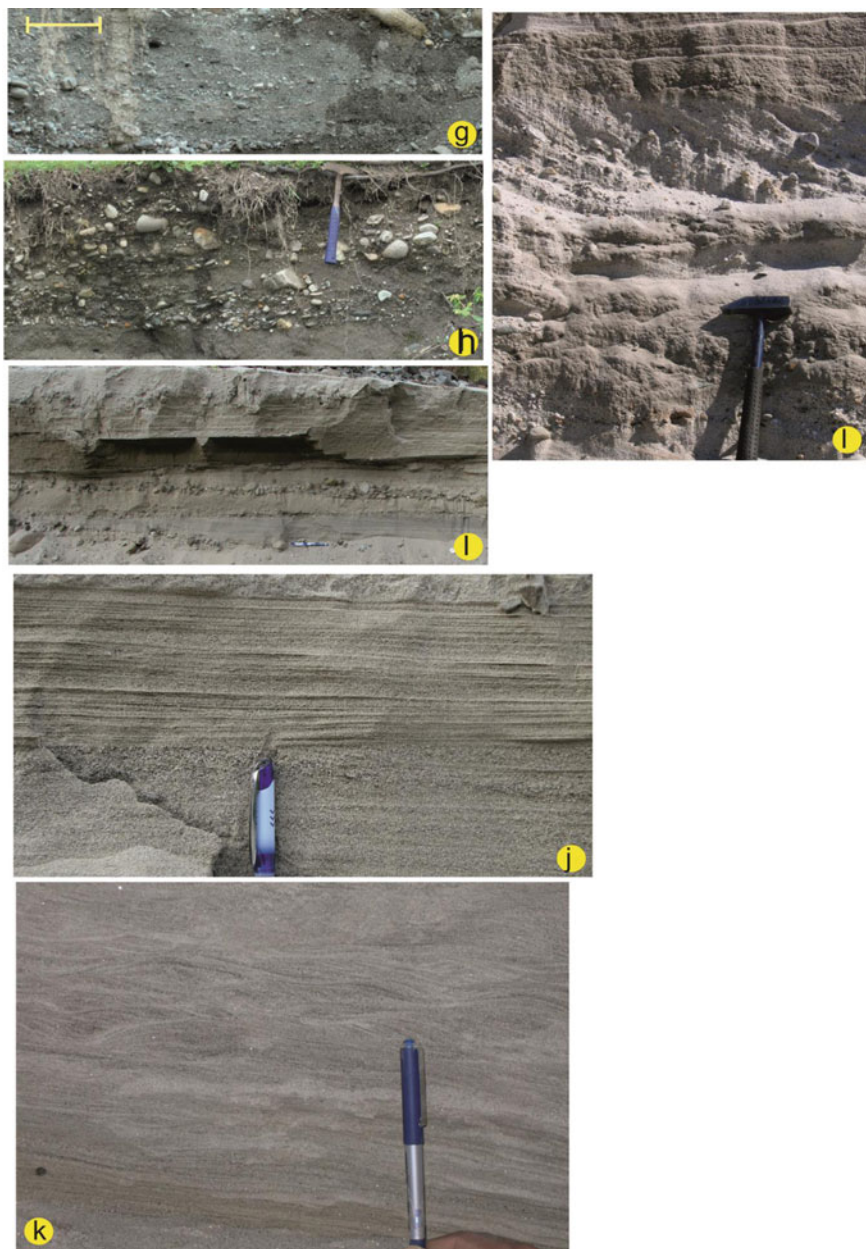


Fig. 8 (continued)

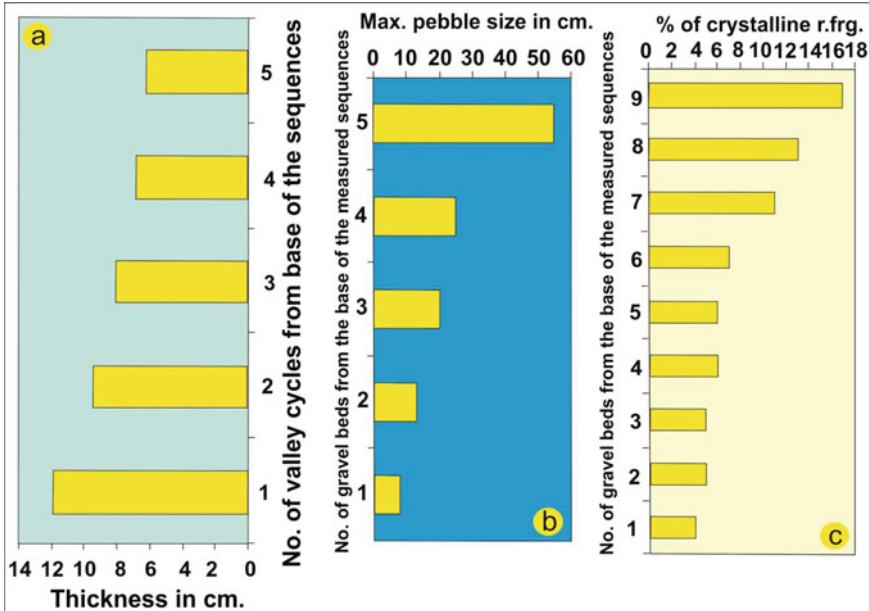


Fig. 9 Up section decrease in valley cycle thickness indicate progressive decrease in the rate of subsidence of the small basin reducing the accommodation space (a). Up section increase in maximum clast size in successive coarser gravel beds implying upliftment (b). Up section increase in percentage of crystalline rock fragments in successive coarser gravel beds indicate progressive uplift of crystalline basement far north (c)

River Tista has become braided at the south of the MFT (Figs. 1b and 4f). Again, it has got uplifted forming degradation with fall in base profile so, the river cannibalized its own accumulated sediment, digs and may penetrate the basement as well (Figs. 5a and d, 6b–d); however, may be retained at the channel margins, and on the other hand, valley walls get eroded and terraces formed due to degradation at the southern flank of the MFT. More so over, it happened in more than one generating several terraces in Sevok-Rangpo transect along the River Tista onto the Gondwana basement rock (Fig. 6c and d). The absence of in-situ exposures of these rocks in the nearby vicinity, which are exposed beyond Boundary Thrust delineates upliftment. The deep concave-up geometry of the basement sediment contact indicates channel incision in a previous phase of basement uplift (Fig. 6d). Thinning of valley cycles up the succession indicates a gradual drop in the rate of base profile rise creating a progressively lesser and lesser amount of accommodation space (Figs. 7a and 9a). Consequently, an increase in maximum clast size in valley floor conglomerates renders the succession coarsening upward and this unusual trend of fluvial aggradations further support the gradual uplift of the source area (Figs. 7a and 9a). But the overall coarsening up successions indicates a faster effect of basement uplift along the shoulder of thrusts (Fig. 9b). In consonance with this, more distant sources contributed to a greater frequency in occurrence of plutonic rock clasts in this large pebble population records

progressive uplift of the granitic terrain far upstream (Fig. 9c), besides the rate of erosion enhanced at source through time.

The deformed beds oppositely directed and laterally persistent have been found in Quaternary sediments that may be formed due to tectonic jerking (Fig. 10a–d). The same manifestation has been further corroborated by soft deformational structures like contorted laminae, single and multi-lobated convolute structure, pseudonodule, load-structures/sagging, and fluid-escape structures, within the same sediment contents (Fig. 11a–e).

5 Conclusion

The documentations attest to the imprints of neotectonism along the River Tista along the Sevoke-Rangpo transect. In the topography, river valley configurations, watershed basin characters, lateral variations in drainage patterns in general, sediment characters, and records of repeated subsidence at places testimony to neotectonics continue in the Quaternary period. The entire study area achieves a minimum channel gradient on top of the ridge of MFT documenting its uplift. Basement uplift causing migration of base profile below the depositional surface compels the river to incise deeper. In consequence, the river valley becomes progressively narrower leaving out successive residual terraces at its margins, till the stratigraphic trend reverses with subsidence of the basin. The migration of the base profile above the depositional surface in consequence of the subsidence of the basin induces aggradation of river sediment and obliteration of the previously formed terraces during its course. Aggradational fluvial succession is fining upward even when the rate of rising of the base profile is steady; nonetheless, increasing rate leads to a transition from low to high accommodation stage, channel amalgamation rapidly giving way to flood plain amalgamation. Large pebble gravel beds intercepting the pile with increasing frequency and maximum clast size with the occurrence of plutonic rock clasts point to source uplift. Upward thinning of the valley cycles defined by these large pebble gravel beds, however, indicates a progressive decrease in the rate of accommodation space creation in the small basin and incising through a number of terraces of successive generations implies that eventual switching over of aggradation to degradation in consequence to neotectonic basin-floor uplift.

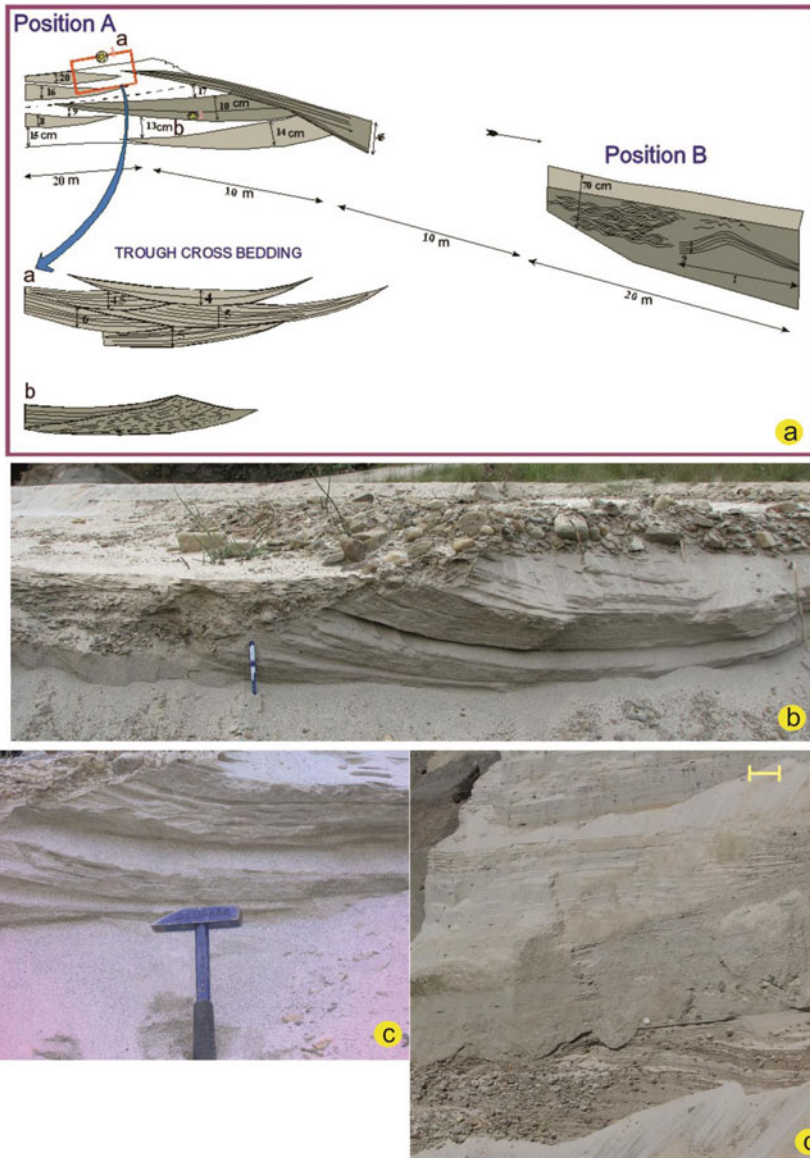


Fig. 10 Diagram traced from field exposure showing tilted and deformed beds, oppositely directed within terraces; a panel of tilted beds in the two given positions shown in the diagram: **Position A** (orientation of bed— $342^{\circ}/15^{\circ}$ W orientation of cross-lamination— $15^{\circ}/10^{\circ}$ 285°) and **Position B** (orientation of bed— $20^{\circ}/10^{\circ}$ 110° orientation of cross-lamination— $30^{\circ}/17^{\circ}$ 120°) (a). Warped and tilted beds in fluvial terrace along the River Tista in Sevok-Rangpo transect near Andherijhora (b). Field photograph showing ripple laminae with mud drape followed by massive and deformed beds (c). As the top most part of the deformed layer is completely homogenous in nature, it is unlikely that the downward bending of the laminae below is the result of loading and cross stratified nature of the sandy unit over major erosional surface (d)

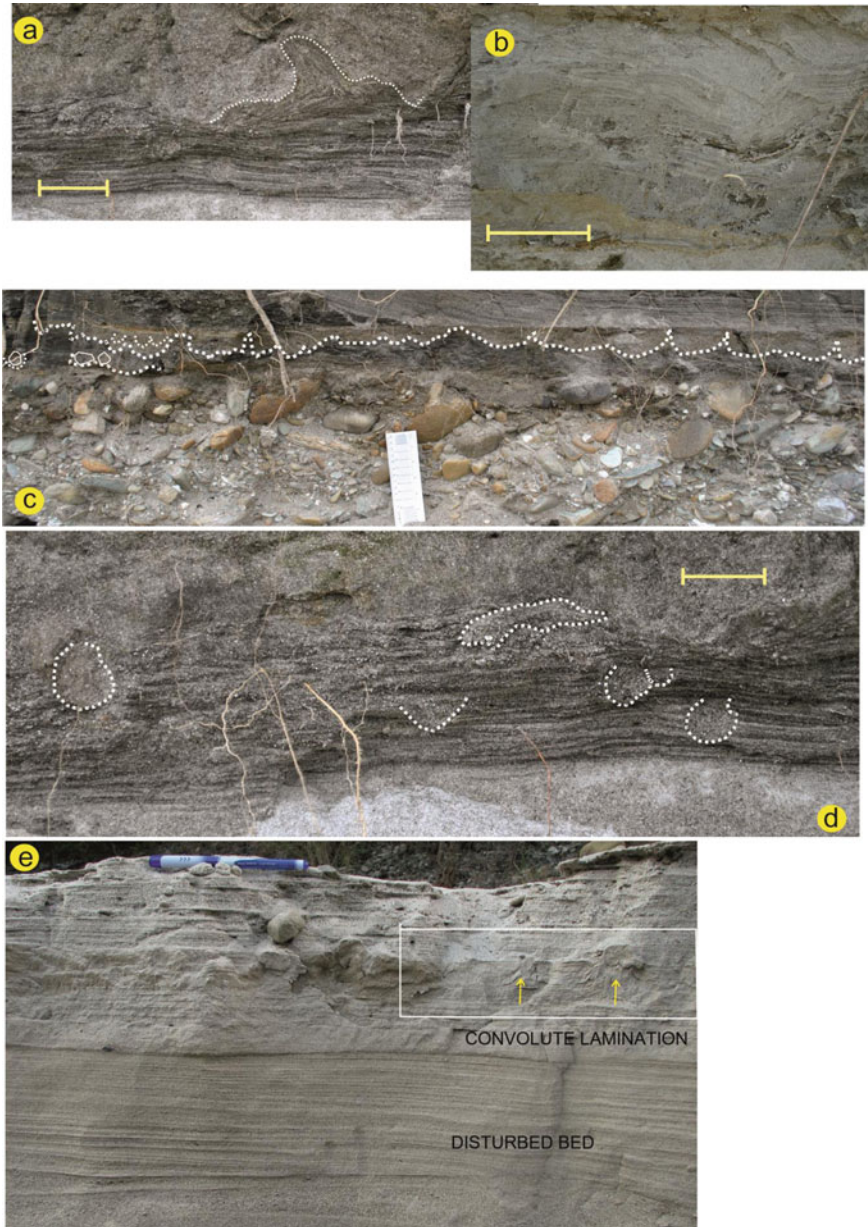


Fig. 11 Various types of Soft-deformational structures along the River Tista within Quaternary sediments as imprint of tectonic jerking: Fluid escape (a). Contorted laminae (b). Single-lobated and multi-lobated convolute (c). Pseudonodule and sagging (d). Deformed laminae and convolute laminanae with fluid-escape structure (marked by yellow arrow) (e). Yellow bar in the diagram depicts 30 cm

Acknowledgements SM acknowledges to UGC, Extension Activity under XII Plan General Development Assistance, Govt. Of India (R-11/406/15) for financial support. All the authors express gratitude to Jadavpur University, Kolkata, India for infrastructural facilities.

References

- Acharyya SK (1971) Structure and stratigraphy of the Darjeeling Frontal zone, eastern Himalaya. In: Recent geological studies in the Himalaya, Geological Survey of India, vol 24, no 1. Miscellaneous Publication, pp 71–90
- Acharyya SK (1976) On the nature of the Main Boundary Fault in the Darjeeling sub Himalaya. Geological Survey of India, vol 24. Miscellaneous Publications, pp 395–408
- Acharyya SK (1982) Structural framework and tectonic evolution of the Himalaya. *Himalayan Geol* 10:412–439
- Arrowsmith A (1804) *Hindoostan: from Arrowsmith's map of Asia*. David Rumsey Digital
- Bahuguna IM, Kulkarni AV, Arrawatia ML, Shresta DG (2001) Glacier atlas of Tista basin (Sikkim Himalaya). (SAC/RESA/MWRG-GLI/SN/16/2001) Space Application Centre, Ahmedabad
- Basu SR, Sarkar S (1990) Development of Alluvial Fans in the Foothills of the Darjeeling Himalayas and their geomorphological and pedological characteristics. In: Rachocki AH, Church M (eds) *Alluvial fans: a field approach*. Wiley.
- Blair TC, McPherson JG (1994) Alluvial fans and their natural distinction from rivers based on morphology, hydraulic processes, sedimentary processes, and facies assemblages. *J Sediment Res* A64:450–489
- Blum MD, Tornqvist TE (2000) Fluvial responses to climate and sea level change: are view and look forward. *Sedimentology* 47(Suppl. 1):2–48
- Bull WB (1977) The alluvial fan environment. *Prog Phys Geogr* 1:222–270
- Bull WB, McFadden LD (1977) Tectonic geomorphology north and south of the Garlock Fault, California. In: Doehring DO (ed) *Geomorphology in Arid Regions*. State University of New York, Binghamton, NY, pp 115–138
- Burbank DW, Anderson RS (2001) *Tectonic geomorphology*. Blackwell Scientific, Oxford, p 270
- Carry M (1811) An accurate map of Hindostan or India from best authorities. David Rumsey Digital map collection. University of California, Berkeley
- Chakraborty T, Ghosh P (2010) The geomorphology and sedimentology of the Tista megafan, Darjeeling Himalaya: implications for megafan building processes. *Geomorphology* 115:252–266
- DeCelles PG, Cavazza W (1999) A comparison of fluvial megafans in the Cordillarians (Upper Cretaceous) and modern Himalayan foreland basin systems. *Bull Geol Soc Am* 111:1315–1334
- DeCelles PG, Robinson DM, Quade J, Ojha TP, Garzzone CN, Copeland P, Upreti BN (2001) Stratigraphy, structure and tectonic evolution of the Himalayan fold thrust belt in western Nepal. *Tectonics* 20:487–509
- Delcaillau B, Carozza JM, Laville E (2006) Recent fold growth and drainage development: the Janauri and Chandigarh anticlines in the Siwalik foothills, northwest India. *Geomorphology* 76:241–256
- Faniran A (1969) The index of drainage intensity a provisional new drainage factor. *Austr J Sci* 31(9):328–330
- Gansser A (1964) *Geology of the Himalayas*. Interscience, Wiley, New York, pp 1–289
- Gansser A (1981) The geodynamic history of Himalaya. In: Gupta HK, Delany FM (eds) *Zagros–Hindukush–Himalaya: geodynamic evolution*, vol 3. American Geophysics Union, Geodynamic Series, Washington, pp 111–121

- Ghosh P, Chakraborty C, Chakraborty T (2005) Quaternary deposits of the Tista Valley: implications for foredeep sedimentation, tectonism and climate. Abstract Volume, Symposium on "Geoscientific aspects of landscape evolution of North Bengal– Sikkim: environmental problems and developmental perspectives. West Bengal Academy of Science and Technology, pp 6–7
- Gravelius H (1914) Grundrifi der gesamten Gewisserkunde. Band I: Flufkunde (Compendium of Hydrology, vol I. Rivers, in German). Goschen, Berlin, Germany
- Guha D, Bardhan S, Basir SR, De AK, Sarkar A (2007) Imprints of Himalayan thrust tectonics on the Quaternary piedmont sediments of the Neora-Jaldhaka Valley Darjeeling Sikkim Sub-Himalayas, India. *J Asian Earth Sci* 30:464–473
- Horton RE (1932) Drainage basin characteristics. *Trans Am Geophys Union* 13:350–361
- Horton RE (1945) Erosional development of streams and their drainage basins: hydrophysical approach to quantitative morphology. *Geol Soc Am Bull* 56:275–370
- Horton BK, DeCelles PG (2001) Modern and ancient fluvial megafans in the foreland basin system of the central Andes, southern Bolivia: implications for drainage network evolution in fold-thrust belts. *Basin Res* 13:43–63
- Howard AD (1967) Drainage analysis in geologic interpretation: a summation. *Bull Am. Assoc Petrol Geol* 51:2246–2259
- Islam MF, Higano Y (1999) International environmental Issue between India and Bangladesh: environmental and socio-economic effects on the Teesta River Area. European Regional Science Association, ERSA conference papers
- Keller EA, Pinter N (1996) Active tectonics: earth-quakes, uplift and landscape. Prentice Hall, New Jersey, p 338
- Lavé J, Avouac JP (2001) Fluvial incision and tectonic uplift across the Himalayas of central Nepal. *J Geophys Res* 106(B11):26561–26591
- Long S, McQuarrie N, Tobgay T, Rose C, Gehrels G, Grujic D (2011) Tectonostratigraphy of the lesser Himalaya of Bhutan: implications for the along-strike stratigraphic continuity of the Northern Indian margin. *Geol Soc Am Bull* 123(7/8): 1406–1426
- Malik JN, Nakata T, Philip J, Virdi NS (2003) Preliminary observations from a trench near Chandigarh, NW Himalaya and their bearing on active faulting. *Curr Sci* 85:1793–1799
- Matin A, Mukul M (2010) Phases of deformation from cross-cutting structural relationships in external thrust sheets: insights from small-scale structures in the Ramgarh thrustsheet, Darjiling Himalaya, West Bengal. *Curr Sci* 99(10):1369–1377
- Medlicott HB (1864) On the geological structure and relationship of the southern portion of the Himalayan range between the river Ganga and Ravee. *Geol Surv India Memoirs* 3:1–212
- Meetei LI, Pattanayak SK, Bhaskar A, Pandit MK, Tandon SK (2007) Climatic imprints in quaternary valley fill deposits of the middle Teesta valley, Sikkim Himalaya. *Quatern Int* 159:32–46
- Merritts D, Hesterberg T (1994) Stream networks and long term surface uplift in the New Madrid Seismic Zone. *Science* 265:1081–1084
- Miall AD (1978) Tectonic setting and syndepositional deformation of molasse and other nonmarine-paralic sedimentary basins. *Can J Earth Sci* 15:1613–1632
- Mukhopadhyay DK, Mishra P (2004) The main frontal thrust (MFT), Northwestern Himalayas: thrust trajectory and Hangingwall fold geometry from balanced cross sections. *J Geol Soc India* 64:739–746
- Mukhopadhyay DK, Mishra P (2005) A balanced cross section across the Himalayan frontal fold-thrust belt, Subathu area, Himachal Pradesh, India: thrust sequence, structural evolution and shortening. *J Asian Earth Sci* 25:735–746
- Mukul M, Jaiswal M, Singhvi AK (2007) Timing of recent out of-sequence active deformation in the frontal Himalayan wedge: insights from the Darjiling sub-Himalaya, India. *Geology* 35(11):999–1003
- Nakata T (1972) Geomorphic history and crustal movements of the Himalayas. Institute of Geography, Tohoku University, Sendai, p 77

- Nakata T (1989) Active faults of the Himalaya of India and Nepal. *Geol Soc Am Spec Pap* 232:243–264
- Olsen H (1989) Sandstone-body structures and ephemeral stream processes in the Dinosaur Canyon Member, Moenave Formation (Lower Jurassic), Utah, U.S.A. *Sediment Geol* 61:207–221
- Pettijohn FJ, Potter PE, Siever R (1972) *Sand and sandstone*. Springer, New York, 618p
- Pilgrim GE (1913) The correlation of the Siwaliks with the mammalian horizons of Europe. *Rec Geol Surv India* 43:264–325
- Ramirez-Herrera MA (1998) Geomorphic assessment of active tectonics in the Acambay Graben, Mexican Volcanic Belt. *Earth Surf Proc Land* 23:317–332
- Ray SK, Neogi S (2011) Extent and analogues of the Rangit window in the Sikkim Himalaya. *Indian J Geosci* 65(4):275–286
- Rennel J (1794) *An actual Survey of Bengal, Bahar etc.* Laurie and Whittle, London
- Roy KK (1976) Some problems of stratigraphy and tectonics of the Darjeeling and Sikkim Himalayas. *Misc Pub Geol Surv India* 24(2):379–394
- Scheidegger AE (1965) The algebra of stream-order numbers. *U.S Geol Surv Prof Pap* 525B:B187–B189
- Schumm SA (1956) The evolution of drainage systems and slopes in badlands at Perth Amboy, New Jersey. *Geol Soc Am Bull* 67:597–646
- Shreve RL (1967) Infinite topologically random channel networks. *J Geol* 75:17886
- Strahler AN (1952) Dynamic basis of geomorphology. *Geol Soc Amer Bull* 63:923–938
- Strahler AN (1964) Quantitative geomorphology of drainage basins and channel networks. In: Te Chow V (ed) *Handbook of applied hydrology*. McGraw-Hill, New York
- Todd SP (1989) Stream-driven, high-density gravelly traction carpets: possible deposits in the Trabeg Conglomerate Formation, SW Ireland and some theoretical considerations of their origin. *Sedimentology* 36:513–530
- Valdiya KS (1993) Uplift and geomorphic rejuvenation of the Himalaya in the Quaternary period. *Curr Sci* 64:873–885

Himalayan Foredeep Neotectonics and Deformed Riverscape Landforms: An Integrated Discussion, West Bengal, India



Adrija Raha and Mery Biswas

Abstract This book chapter provides immense documentation of Himalayan fore-deep neotectonics and evolutionary processes that focus on landform deformation and channel succession in terms of morphotectonic discussion at a glance. The Himalayan foredeep foothill is composed of successive sediment deposition of 16.0–0.5 Ma BP i.e. Middle Miocene–Middle Pleistocene and late Quaternary Siwalik, which is overlain by young thick sandy to loamy sediments of Holocene near surface (Jain AK, Banerjee DM, Kale SV (2020) *Tectonics of Indian subcontinent*, society of earth scientists series, ISSN 2194-9204 ISSN 2194-9212 (electronic), ISBN 978-3-030-42844-0 ISBN 978-3-030-42845-7 478 (eBook), 111–433. 10.1007/978-3-030-42845-7). This elongated section is formed by series of alluvial fans, which are deformed and restructured by the neotectonic activities evident by earthquake magnitude in the last 120 years with the presence of Matiali scarp (MBT) 34 ka, Chalsa scarp (MFT) 11–6 ka (Kar et al. *Geomorphology* 227:137–152, 2014). The MIS-3 (marine isotope stage 3) of 34 ka (Mukul M, Singh V (2016) *Active tectonics and geomorphological studies in India during 2012–2016*. In: *Proceedings of the Indian national science academy*, p 82 10.16943/ptinsa/2016/48480) initiated the alluvial fan formation (Matiali fan) which had been interrupted by repeated tectonic activities and accompanied by hydrological flow alteration due to climate change as the emergence of LGM (Last Glacial Maximum) and MIS-2 in Holocene (Martinson et al. *Quatern Res* 27:1–29, 1987). Upliftment and erosion sequences assemblaged by slope differentiation and flow/velocity alteration prompted the reframed alluvial fans and two tier river terraces. The alluvial fan in a fan formation extended towards the south with distinctly identified three geomorphic units as apex, mid fan, and lobes. These fans are cast around as mega fans and meso to micro-scale dimensions. The outcome of the study is recapitulated in one pictorial image to make a clear understanding of its morphological units. In the field, artificially initiated water flow in varying discharge (Q) has been experimented to set an idea of expanded coverage area in both monsoon and flood seasons. The morphotectonic indices on River Kaljani specify the active tectonics over the area where fans have developed in an elongated

A. Raha · M. Biswas (✉)

Department of Geography, Presidency University, 86/1 College Street, Kolkata, West Bengal 700073, India

e-mail: mery.geog@presiuniv.ac.in

shape with changed SL and concavity along the channel. It is a comprehensive study of foreland active tectonics of North Bengal foothill. It clarifies the mechanism of deformed landforms and modification of channel succession in response to the active tectonics.

Keywords Neotectonics · Deformed alluvial fans · Channel geometry

1 Introduction

The collision of the Indian plate with Asia is well known as the highest, youngest one continental collision orogenic belt where the Siwalik foredeep basin along the southern west- the east boundary of the Lesser Himalaya specify the erosional history of the uplift and exhumation of the Himalaya since collision (Garzanti 2019). The northward progression of the Indian plate into the Eurasian plate is evident, as we study topography, geology, earthquake events, and deformation (Wesnousky et al. 1999) mechanism over time. The Himalayan thrust sheets shingled together since ~58 Ma consist of South Tibetan detachment (STD), Main Central Thrust (MCT), Main Boundary Thrust (MBT), and Main Frontal Thrust (MFT) from north to south (Fig. 1a) (Saha 2013 and DeCelles et al. 2016). In the Late Pleistocene to Holocene, along the active fault lines in the southernmost foredeep section of the Himalayan arc, the geomorphic deformation took place. The East–West trending Himalayan hillslope is diversely delineated from north to south by major thrust lines as MCT, MBT, and MFT. The tectonic anomalies transport Upper Pliocene—Lower Pleistocene Siwalik succession over the Middle Pleistocene—Holocene sediments of the Indo-Gangetic plains (Nakata 1972) in the foreland area.

According to Mukul (2000), Chaudhri and Chaudhri (2001), Valdia (2003), Thakur (2013), Srivastava et al. (2016), the most deformed Quaternary deposits are found between the Main Boundary Thrust (MBT) and Main Frontal Thrust (MFT) are significantly deformed resulting landforms like fans and terraces due to active tectonics (Biswas and Paul 2020) and surface rupture. The softer sediments detached from the basement in terms of basal decollement due to the slipped MFT plane into the Himalayan edges during folding (Lave and Avouac 2000; Kumar et al. 2012). The thin-skinned model define that the faults are initiated from the basal decollement and accumulated strains that released during the earthquakes (magnitude >7.89). It is defined by Lave and Avouac (2000), Mugnier et al. (2013), that such an earthquake unlocks the trapped MFT sediment sequences and insists mobilization towards the foreland Himalayan ranges. Therefore, the development of foreland basin with landform deformation are associated with Holocene tectonic activities near MFT and MBT (Saha 2013; De Celles et al. 2016) (Fig. 1b).

The foreland topography dissected by foothill rivers bears the neotectonic evidence which is also accompanied by seismological attestation. The Holocene neotectonics have deformed the alluvial fans forming T3/T2 (T=Terrace) along the active parts of the rivers where T4 is fan surface. The Quaternary active fault scarps

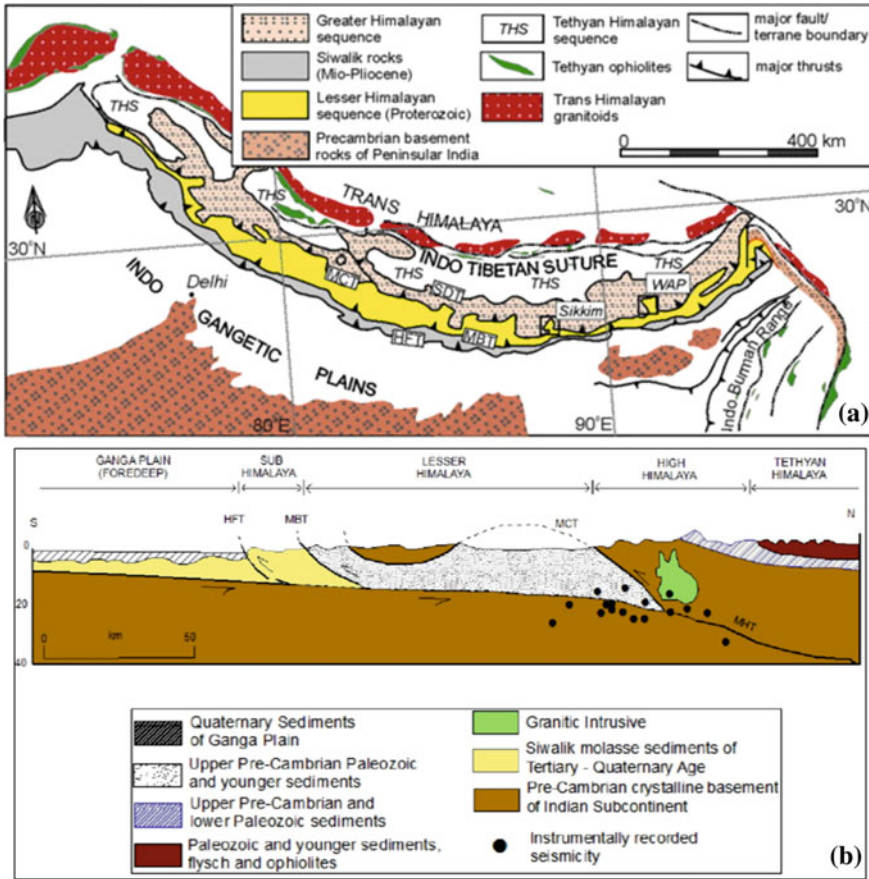


Fig. 1 a Arc shaped Himalayan mobile belt with major sections from North to South (Saha 2013). STD-South Tibetan detachment, MCT-Main Central Thrust, MBT-Main Boundary Thrust, HFT-Himalayan Frontal Thrust. b North-South geological cross-section with major Thrusts and expanded foreland area towards south of the MFT (Main Frontal Thrust)

are exposed as the sediment sequences of conglomerate which is overlain by recent sediments and studied during fieldwork. After river Torsa, MFT and MBT are abrupt, visualized and channels are successively incised that may be re-examined by morpho-tectonic analysis (Biswas et al. 2021). The MFT and MBT are widely spaced until Torsa and later they share a very narrow space between them. The flat synformal axial zone between MBT and MFT is characterized by deformed landforms due to Quaternary tectonics. Landforms like alluvial fans and river terraces have developed (Kar et al. 2014) in this area in between Matiali fault (MBT) and Chalsa Fault (MFT). The formation of such scarp surfaces along the foothills suggests the orogenic movement.

The foothill river systems flow down huge sediments with a compilation of gravel and boulders carried out from the outer Himalayan ranges at the beginning

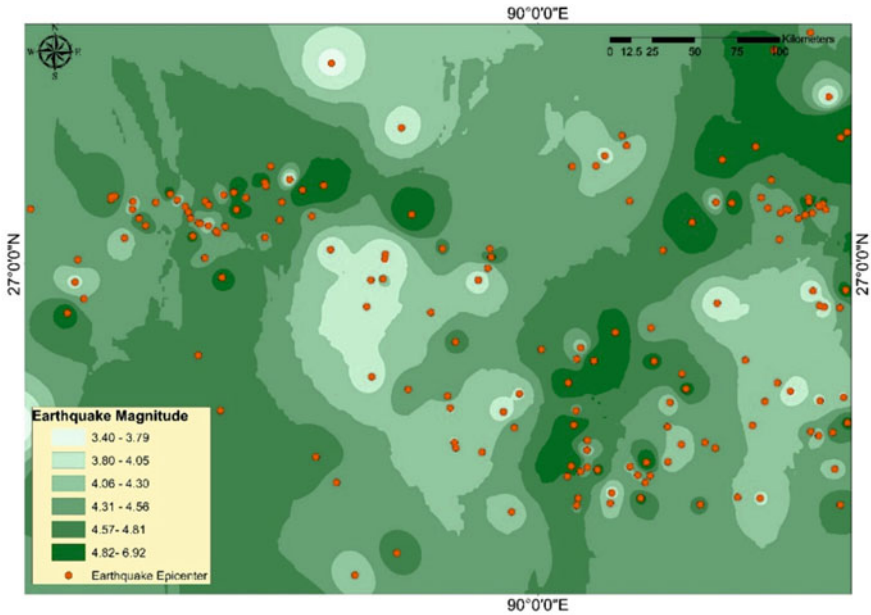


Fig. 2 Interpolated Earthquake magnitude map of North Bengal foot hill and its adjacent Hilly terrain of Himalaya. Based on earthquake magnitude data from (USGS Bulletin, 1900–2019) <https://earthquake.usgs.gov/earthquakes/search/>

of the Quaternary period insisting to the formation of alluvial fans. Thereafter, the active orogenesis insisted the upliftment/incision process led to the further deformed morphological layout of the area. Such active (Gansser 1964) belt of the Himalaya address an interlinking between uplift, erosion, climatic variation, etc. (Lave and Avouac 2000; Bookhagen et al. 2005; Wobus et al. 2006; Srivastava et al. 2016; Singh et al. 2016) that have controlled the syn-depositional and post-depositional tectonic events. It correlates the erosional cycle and valley deepening of the Pleistocene to Holocene. The foredeep neotectonics is evident as assimilation of uplift-erosion sequence of channels that dissect the alluvial fans with the progression of river terraces.

The present study is an attempt to decipher the effect of active tectonics of the North Bengal foredeep area and development of deformed alluvial fan surfaces (Biswas 2014) with topographic dynamics of the Himalayan edge of the foreland area in the context of active faults and lineaments. Secondly, a case study of River Kaljani (Torsa system) has been analyzed in an integrated way that elucidates the geomorphic, linear, and basin-scale parameters.

2 Study Area

2.1 Location

The entire foredeep area is drained and dissected by a number of parallel N-S flowing rivers and their tributaries. Broadly, they are under the Brahmaputra River system with several sub-systems, based on particular major river such as the Teesta, Jaldhaka, Torsa, Raidakh and Sonkosh. All the rivers are originated from the middle or higher Himalaya and flow down slope to meet the Brahmaputra.

2.2 Regional Geology

Unlike the continuous range of Himalaya of North Bengal, the foothill sediments are the part of a sub-Himalayan tectonic zone (Gansser 1964; Naldtiyal et al. 1964; Jangpangi 1974, Kale et al. 2014) delineated by MBF. Regarding the geological formations like Baikunthapur and Chalsa formation over the entire piedmont zone, there is no remnant of glacial action, but Mallet (1975) and Bisaria (1980) noted massive aggradations, which is uncommon in the Eastern Himalayan rivers. Later on, the fluvial channels (Jain et al. 2016) transport an investigation on the prominence of rock fragments. In Fig. 2, the spatial distribution of earthquake magnitude (3–4) reveals the paleoseismic occurrences from 1900 to 2019 in the North-Eastern part of the Himalaya. It shows a low contour value trending W-E portraying seismic gap thus implying large magnitude earthquake in future.

In general, the rivers flowing down to the lower floodplains of North Bengal have deposited the fine grain sediments, originated due to the denudation process of catchment rocks. It is also associated with the deposits ranging from cobble to clay size materials that overlie the area during the high flow and low flow period. Besides, the scarp faces (terrace scarps) cut by fluvial activity, another set of scarps (piedmont scarps) are observed towards the south, due to the presence of local fault scarp like Baradighi.

These run across the trend of the rivers and impart a step like appearance to the landscape. The intensive interaction of endogenic (related to Himalayan upheaval), mesogenic (reactivation of lineaments) and exogenic (surficial morpho-dynamic processes including accommodated landmass) factors during the Quaternary period has resulted in the formation of six aggradation terraces in the area i.e. the terrace sediment accumulation has happened mainly during the floods as huge sediments are discharged accompanied by flood scourge and filling (Biswas and Banerjee 2018; Paul and Biswas 2019). The southern flank of the Himalayan orogeny is highly affected by the MBT that has carried the Gondwana series and overlain the Tertiary Siwalik sedimentary layers at its foothills (Gansser 1964; Yin 2006; Mukherjee et al. 2015). The quaternary deposits near MFT is under the Siwalik group and composed of recent alluvium sediment sequences of different grain size (Nakata 1972, 1982, 1989;

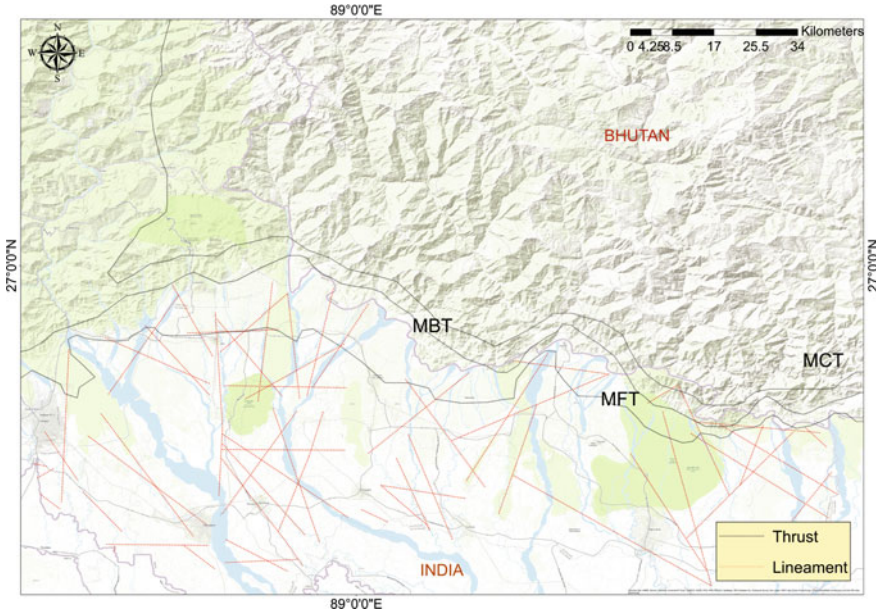


Fig. 3 Major thrusts and lineaments over the Himalaya and its foreland basin of North Bengal foothill. (Modified from Hossain et al. 2020 and Gupta 2008)

Hodges 2000; Yin 2006; Jain et al. 2020). This area comprises the Main Boundary Thrust (MBT) and the Main Frontal Thrust (MFT) with a number of lineaments having both geomorphic and structural linkages (Fig. 3). Along with the major E-W aligned fault lines, there are faults like Gish transverse fault, Madhupur fault, Dhubri fault that are transverse to the Himalaya and these have revised the channel morphometric indicators to be an intended anomalies along the channel (Srivastava et al. 2016; Ayaz et al. 2018).

The MBT and the MFT from the Lish to Diana are widely spaced towards the east along the E-W trend thrust lines on the foredeep area, which are confined and exposed in northward dipping MBT near Matiali and the MFT near Chalsa (Kar et al. 2014). Besides these two, there is east–west trend GT (Garubathan Thrust) in the north of the Matiali thrust, near Samsing which is successively overlain by Matiali formation near Matiali bazar (left bank of Kurti river, downward side of Shiva temple). Towards east, MBT is continued into two lines, as Jiti fault in north and Thaljhora thrust in south. Though, both Matiali and Thaljhora thrust belong to the MBT (Nakata 1982), but the Matiali is a fore thrust blind fault dipping towards the north and the Thaljhora is the back thrust, dipping towards the south (Chakrabarti Goswami et al. 2019). Between MBT and MFT exists a deformed landscape (Kar et al. 2014) of synformal zone that developed between the Mal and Murti River and distinctly observed near the Kurti (near Matiali school) and the Murti River (polo ground) as mentioned before.

The Neotectonics of this foreland basin comprises drainage modifications and valley incision (Biswas 2015). This area is also characterized by the overlapping of fan surfaces, promoted by sediments carried by individual rivers and channels. Nevertheless, during 24–18 ka with the substantial decrease of discharge, some fans were abandoned (Mukul and Singh 2016) and lobes have become stable as there was no such aggradation process taking place. There are some meso level fans that are active and proceed in response to slope and their hydro-sediment flow behaviour (Ayaz et al. 2018) and deformed by Quaternary tectonics like activation of Chalsa fault (~90 m elevated) during 11–6 ka (Mukul and Singh 2016).

Broadly, the Himalayan belt had been formed between 65 and 55 Ma or more specifically 53.3 ± 97 Ma when the genesis was accompanied by subduction of the Indian lithosphere beneath the Asian plate (Jain et al. 2020). The foreland strip from the Teesta to Kameng river is under the Miocene–Pliocene Siwalik group and is composed of sediments during 13–7 Ma and <2.6 Ma (Jain et al. 2020). However, the Quaternary deformation mechanism is evident over the foredeep area with the geomorphic processes, controlled by Himalayan tectonics has propagated to great extent (Guha et al. 2007).

This riverscape is manifested by surface rupture, which is caused by the tectonic events and the active faults (MBT and MFT) that act as the respondent (Singh et al. 2016). De Celles et al. 2016 argued that the Himalayan front evolved like a bowl-shaped sedimented basin being characterized by low gradient foredeep. The mountain foredeep section is overlapped with meso level alluvial fans, (Ayaz et al. 2018) fed by parallel rivers originated from the Himalayan. The MBT and MFT are the two asymmetrical folds with blind faults which have not yet been exposed on the surface (Goswami et al. 2013). Indeed, only the minor displacement and cross-bedding of sediment, flow is noticeable in the exposed part. Kar et al. (2014) and Ayaz et al. (2018) depicted the alluvial fan morphology through the morphotectonic analysis of both fans and channels including Quaternary evolution where the entire foredeep area encompasses the deformed landscape as terraces (Ghosh and Paul 2020).

The Himalayan active neotectonics is strongly related to the seismic activity in the study area (Starkel et al. 2008). The N-E trending contours of negative Bouguer gravity anomaly (–180 to –160 m Gal) pass-through this area (Dasgupta et al. 2000). The seismic activity is associated with the MBT and tear faults. It focuses on the Nepal-Bihar earthquake in 1934 and 1988 indicating the thrusting with a strike-slip component. Study of microearthquakes are intimated with the seismic gap transverse to the MBT (Gupta and Srivastava 1992; Srivastava et al. 1976; Ichikawa et al. 1972). The high convergence rate of the Higher and the Frontal Himalaya including the active Gish transverse fault zone specifies the tendency to stimulate earthquake (Mullick and Mukhopadhyay 2011). This active foreland basin is also marked by the recorded evidence of a great earthquake around A.D. 11 which was reinterpreted around A.D. 1255 (Mishra et al. 2016). Pierce and Wesnousky (2016) argued that the earthquake of A.D. 11 was an indication of active tectonics along the MFT and MBT zone of Chalsa fault displacement as the fore thrust and Thaljhora as the back thrust (Chakrabarti and Goswami et al. 2019).

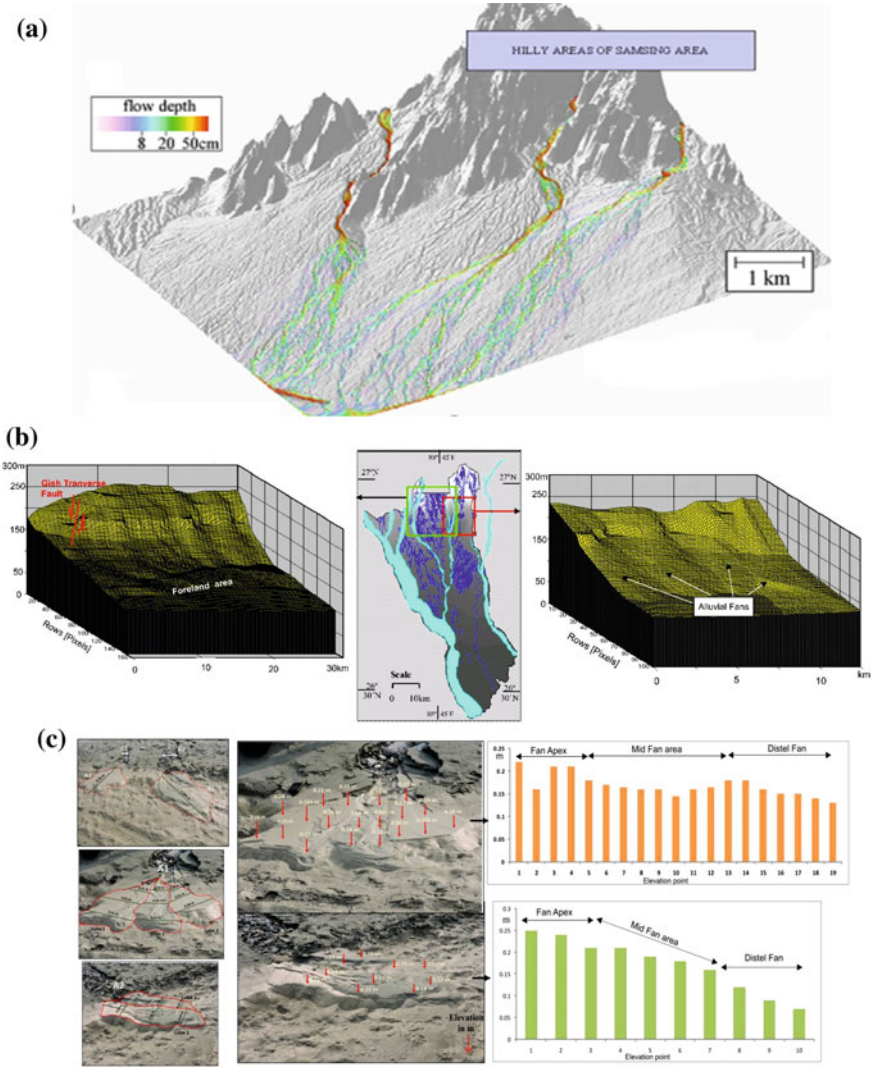


Fig. 4 a Expanded Alluvial fan formation in the part of foreland area (Biswas 2009). b Undulation Foreland basin with Gish Transverse Fault and Alluvial fans with distinct lobes in Neora-Murti interfluvial area (Biswas 2009). c Field based (2018) Micro scale Fan modelling with lobe identification and graphical representation of different morphological parts of fan. d Understanding of flow behaviour on fan shaped micro landscape through an application of manual flow modelling using soluble Potassium Permanganate with water in respective time gap. (Based on field experiment). e Elongated shaped Alluvial Fan of Kaljani River with 5 identified lobes as 1–5 (marked in red colour); extracted from SRTM data and faults/lineaments are based on Saha and Bhattacharaya 2019

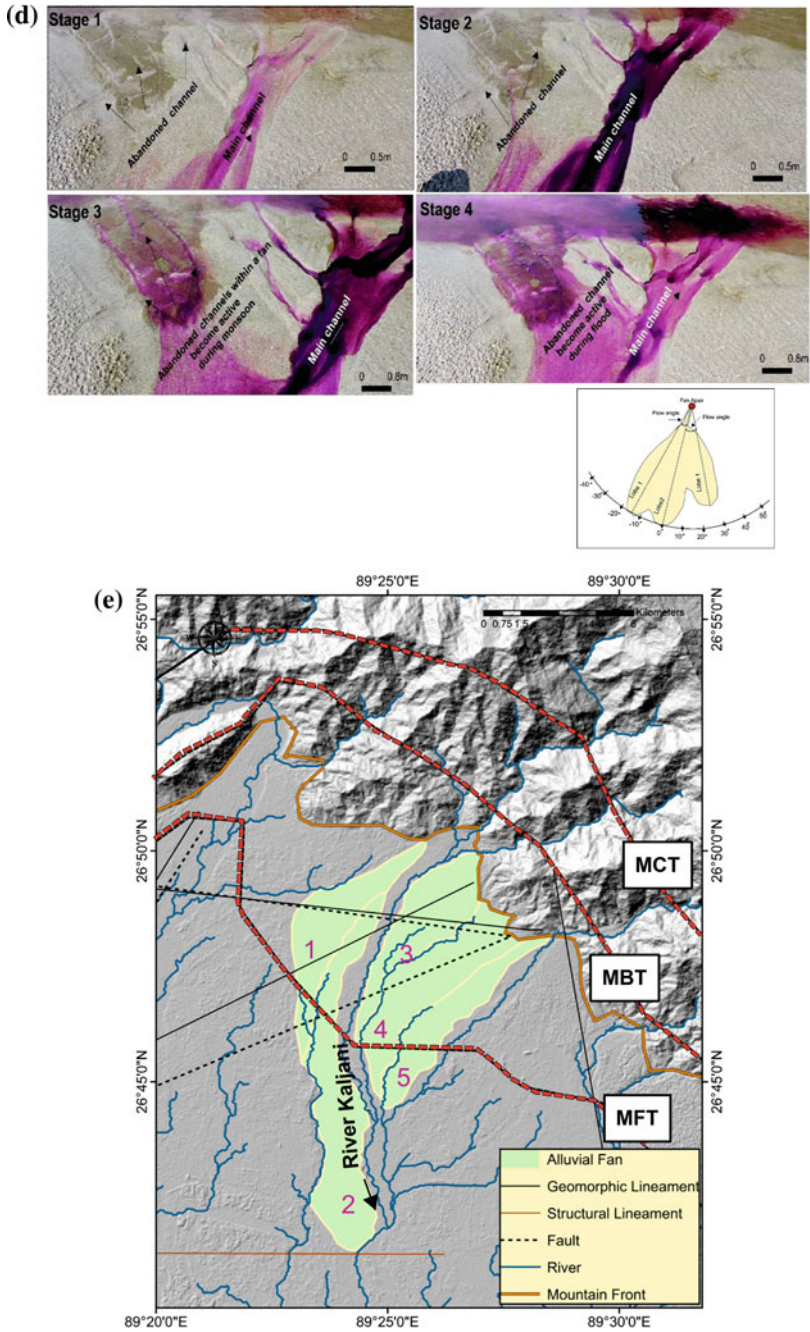


Fig. 4 (continued)

3 Materials and Methodology

This book chapter has been formulated on the basis of three broad sections of data sets.

- The basic geological setup of the area has been studied from the geological map, the broad geological section from the Geological Survey of India, Quaternary Division, Kolkata as well as from published secondary sources. The tectonic setup has been analysed with the help of faulting and folding of the area along with fault scarp delineation. Accumulated data and modified figures from secondary sources as literature, reports, documents, published papers have been re-examined. Seismological magnitude data have been collected from USGS Bulletin, 1900–2019.
- Field based data collection, physical modeling and micro scale understanding of landform have been incorporated during 2015 and 2018 field trips.
- For morphotectonic analysis of the concerned basin, SRTM 90 m resolution DEM has been considered. We obtained the DEM as a Geo Tiff raster file and clipped according to the basin area. Each error of the ICPs was considered by converting the C30 geoidal heights to ellipsoidal heights (Mukul et al. 2014 and Mukul and Singh 2016).

Subtracting them from the corresponding ICP RTK ellipsoidal heights, the obtained errors were then subjected to correction for maintaining accuracy and uncertainty of C30 DEMs in the study area. The mean error (ME), mean absolute error (MAE) and root mean square error (RMSE) have been calculated to analyze the accuracy of the C30 data. Then the re-sampled mean corrected 30 m resolution SRTM data have been used to delineate the Kaljani Basin as well as the considered foredeep section of the Himalaya where the distinct drainage orientation of the area is well distinguished. Apart from the geological and tectonic setup, other selective morphometric indices have been calculated accordingly to analyse the imprint of neotectonism over the study area in a simplified manner. To assess the active tectonic channel, morphotectonic analysis has been adopted using the parameters on both linear scale and basin scale.

Linear indicators such as a longitudinal profile in terms of the linear, logarithmic, exponential, power curve, concavity, SL index, SI and T (Transverse topographic symmetry factor). Table 1a and basin-scale parameters as Hypsometric Integral (Hi), Form Factor (Rf), Elongation ratio (Er), Circulatory ratio (Cr), Tilt angle, and Ruggedness number have been calculated (Table 1b). Selected parameters have been applied to the basin of River Kaljani, the left side (East) tributary of the Torsa. All the layout of the analysed data have been reframed using different platforms as Arc GIS 10.4.1, Surfer 11 and Mat lab 15.

Table 1a Detail methodology for calculating linear scale and basin scale indices to examine tectonic vicinity of Kajjani River basin

Linear scale indices						
Indices	Long profile analysis	Concavity index (θ) (e.g., Whipple et al. 2007; Wobus et al. 2006)	Stream gradient index (SL)	Sinuosity index (SI)	Transverse topographic symmetry factor (T)	Hack profile (Hack 1957, Chen et al. 2006; Magar and Magar 2016)
Geometric calculation	<p>The linear function $y = ax + b$</p> <p>The exponential function $y = aebx$</p> <p>The logarithmic function $y = alnx + b$</p> <p>The power regression model $y = axb$</p> <p>Where, y is the elevation (H/H₀), H = elevation of each point, H₀ = elevation of the source), x is the length of the river (L/L₀; L = distance of the point from the source, L₀ = total length of the stream), a and b are the coefficients derived independently from each profile. The R² value determines the best fit. The curve with highest R² value is the best fit curve</p>	<p>$S = k_s A^{-\theta}$</p> <p>Where, θ is referred to as the concavity index since it describes how concave a profile is; the higher the value, the more rapidly a channel's gradient decreases downstream</p>	<p>$SL = \frac{f}{\ln D_2 - \ln D_1}$</p> <p>Where, f = fall in elevation (e₂-e₁)</p> <p>ln = Natural logarithm of the cumulative distance</p> <p>*Higher SL value indicated tectonic control over stream</p>	<p>$SI = \frac{\text{Channel Length}}{\text{Valley length}}$</p> <p>Straight channel values <1.05</p> <p>Sinuosity values between >1.05 and <1.50</p> <p>Meandering channel indicates >1.50</p>	<p>$T = \frac{D_a}{D_d}$</p> <p>D_a = distance between the midline of the drainage basin and the active meander belt midline and D_d = distance between the midline and the basin divide</p> <p>If the river flows through the midway of the basin, the resulting (T) would be '0' indicates symmetric basin. If the value is >0, the river basin is asymmetric</p>	<p>$H = C - K \times \log(L)$</p> <p>H is altitude of the profile resembling the change in slope demonstration tectonic activity and topography of the river. C is constant (regression of y). K is the SL index and L is the length of the stream from its source</p>

Table 1b Detail methodology for calculating linear scale and basin scale indices to examine tectonic vicinity of Kaljani River basin

Basin scale indices							
Hypsometric integral (Hi) (Pike and Wilson 1971; Schumm 1956; Andreani et al. 2014)	Form factor (Rf) (eg. Brzezińska-Wójcik et al. 2010)	Elongation ratio (Re) (Schumm 1956)	Circulatory ratio (C _c) (Horton 1945)	Relief ratio (Schumm 1956)	Slope	Tilt angle (Pinter and Keller 1995)	Ruggedness number (Schumm 1956)
$Hi = \frac{(H_{mean} - H_{min})}{(H_{max} - H_{min})}$ Where, Hmean = Mean elevation of the basin, Hmin = Minimum elevation of the basin, Hmax = Maximum elevation of the basin Hi value ≤ 0.30 states tectonically stable basin and ≥ 0.30 indicated tectonically unstable basin	$Rf = A / Lb^2$ Where, A = Area of the watershed Lb = Maximum basin length	$Re = 1.128 \sqrt{A} / Lb$ Where, A = Area of the watershed Lb = Maximum basin length	$Rc = 4\pi A / P^2$ Where, A = Area of the watershed P = Perimeter of the watershed	$Rh = \frac{R}{Lb}$ Where, R = Basin Relief Lb = length of the basin	Processed from DEM on ArcGIS 10.4.1 platform	$\beta = \arccos \sqrt{\left(\frac{b}{a}\right)^2 \sin^2 \alpha + \cos^2 \alpha}$ Where, b = Minimum half-length of fan a = Maximum half-length of fan α = Original depositional slope of fan	$Hd = Rz * Dd$ R = Basin Relief Dd = Drainage Density of the Basin

4 Neotectonic Movements, Landform Genesis and Channel Evolution

The entire drainage pattern of the foreland basin is a constituent of series of alluvial fans which are successively formed by the huge sediment aggradations. Quaternary tectonic activity has deformed the fan surfaces initiating the valley incision process resulting in the genesis of river terraces where the Fan surfaces remain as T4. Indeed, the upliftment and valley incision process enforced the formation of river terraces. Both the linear channel morphometry and basin-scale areal aspects display the anomalies and specify the active tectonics.

4.1 Deformed Landforms and Micro-scale Physical Modelling of Alluvial Fans

This tectonic imprint in landform deformation among the other factors is well observed along the entire foothill that encompasses meso level fans, formed by the transportation and aggradation mechanism of individual rivers having their own water and sediment discharge capacity (Fig. 4a, b) in respect of climate change. The sediment flow and depositional history of Matiali fan area initiated in 34 ka (Mukul and Singh 2016) that coincided with the emergence of the Indian Monsoon as MIS-3 (marine isotope stage 3). But, during 24–18 ka, the rainfall decreased enormously in LGM (Last Glacial Maximum) having an effect on the nature of the hydro-sediment flow of the rivers. In MIS-2 and post-glacial Holocene MIS-1 (Martinson et al. 1987), substantial increase of rainfall-induced the volumetric change of water and sediments that initiated the vertical valley incision forms, the T2 and T1, near 12 ka (Mukul and Singh 2016). Regarding the hydrological and morphological alterations, fans were reframed and developed in a wide shaped poplar with a number of lobes, being incorporated as undulated foreland fan-in-a fan formation (Fig. 4a, b).

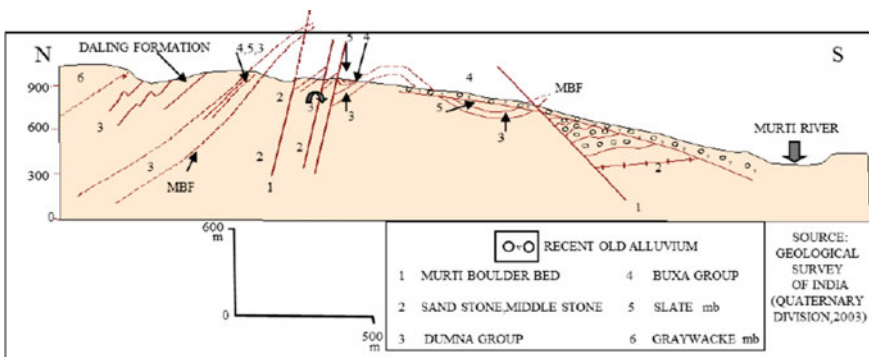


Fig. 5 North to south Geological Section of Murti Boulder Bed, West bank of Murti River based on GSI Quaternary Division 2003, (Biswas 2009)

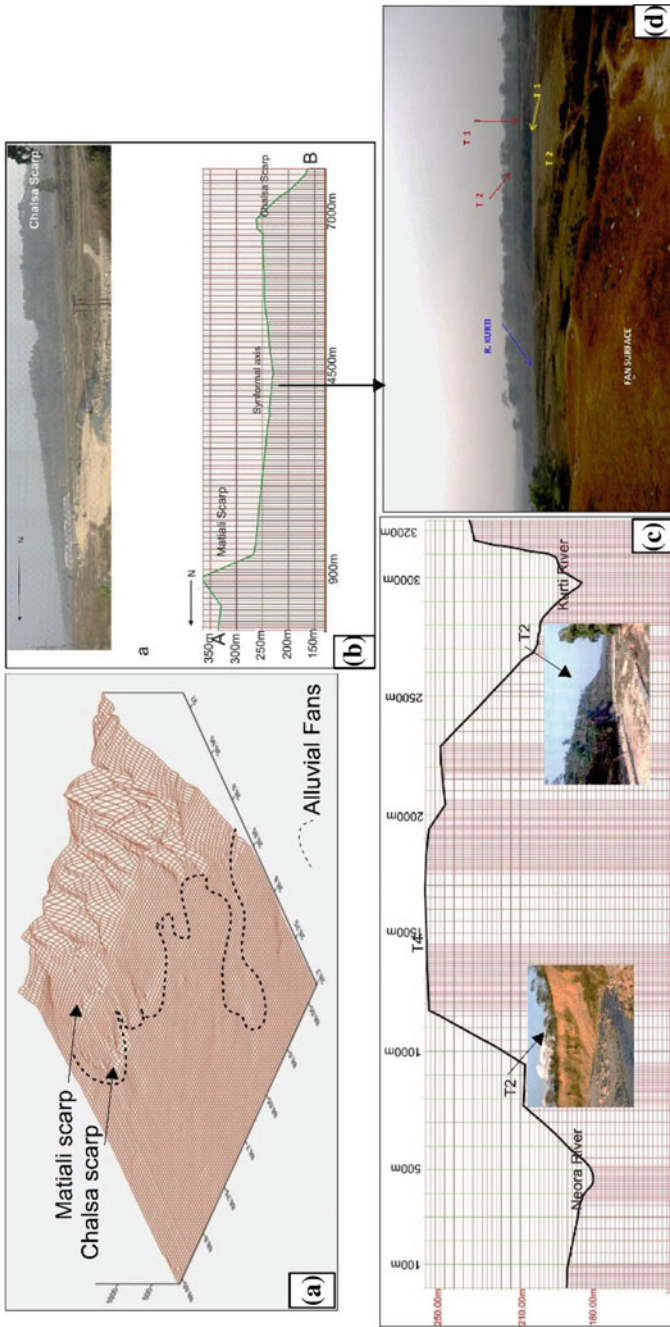


Fig. 6 a SRTM base formulation of 3D mesh of the Foreland area with distinct identification of Alluvial fans with Maitiali scarp (MBT) and Chalsa Scarp (HFT). b Photographic evidence of synformal zone before Chalsa scarp with northerly sloped T4 (fan surface) between Maitiali and Chalsa scarp. (Goswami et al. 2013). c East-West transverse profile from Neora to Kurti River showing both T4 and T2 (Goswami et al. 2013) embedded with photographic evidences of T2. d Identified River terraces as T 2 and T1 in both side of River Kurti near Maitiali High School with Fan surfaces

This discussion further includes the micro-scale fan identification and their conceptual understanding through a physical model. During the fieldwork, the present workers have identified micro-scale fan formation in the left side of Khuji Diana River where two minor non-permanent channels as C1 and C2 (Fig. 4c) have developed their individual fans distinctly. Through the measurement and quantification in two consecutive fans identified as A1 and A2 in Fig. 4c have a number of lobes with a maximum length of 1.079 m and 1.336 m. In A1 fan, there are three lobes as Lobe 1, 2 and 3 respectively having different widths from apex to lobe. Similarly, in Fan A2, only two lobes are prominent in an elongated shape with varying widths from apex to lobe. The physical micro-scale entities may be considered as the conceptual model of common fan series that have been developed in the concerned section of the foredeep area. In Fig. 4c, individual lobes have been marked focusing on fan apex, mid area and distal part. Massive aggradation mechanism has been enhanced by the flow behaviour of the channels and their tributaries over time; especially during the monsoon and extreme climatic condition like flood, when huge sediments were carried by the rivers that developed the fans and active lobes.

During the fieldwork, another physical flow modelling technique was adopted using potassium permanganate with water manually to understand the fan formation (Fig. 4d) in different stages. The results show that water coverage area during monsoon has increased as well as during flood period in stages 4. The alluvial fans in the entire Himalayan Foothill have been developed in this sequence and Quaternary tectonic activities have deformed the fans. The quantification of fan lobe geometry includes the measurement of flow angle, gradient of each lobe considering its maximum length and width that may be discussed under fan morpho-geometry (Fig. 4d). In respect of the above discussion, five fan lobes have been delineated from the Kaljani River Basin where each tributary having their own hydro-sediment discharge contributed in shaping the lobe orientation and eventually they are associated with lineaments and faults in the foredeep section resulting in channel anomalies (discussed later) (Fig. 4e).

The elongated North Bengal foothill area gives immense progressive knowledge about the deformed landforms. In this active area, southerly sloped alluvial fans are dissected by north to south flowing rivers and interrupted by east–west trend Matiali scarp in the north and the Chalsa scarp in the south. Towards the western part of the Murti River, lineament is better to understand as N-S trending Murti Boulder Bed and the geological section depicts the antiformal folding with blind fault, which is not exposed on the surface (Fig. 5). Here, the MBT and the MFT are widely spaced having a synformal axis between them (Kar et al. 2014) where the fan surface got deformed and terraces formed on both sides of the River Kurti near the Matiali high school (Fig. 6a). However, the alluvial fans are less deformed where MBT and MFT are closely spaced and no synformal axis has developed. But river like the Kaljani is strongly controlled by the E-W aligned lineaments and N-S trend transverse to the Himalaya fault line as the Madhupur fault (Saha and Bhattacharya 2019). According to Goswami et al. (2013) apart from these E-W MBT and MFT, there are two other scarps; one is near the Neora River (East bank) and another NNE–SSW scarp as the Murti lineament. During the fieldwork, it has been noticed at the East bank scarp of

Neora river near the railway bridge is a part (Western) of Chalsa scarp (Fig. 6b, 6c embedded image near Neora River) where sediment facies are distinctly displayed.

4.2 *Morphotectonic Analysis*

The computed results of geomorphic indices from re-sampled and corrected SRTM have been discussed in a conjugative manner. Figure 7 shows the major fault lines

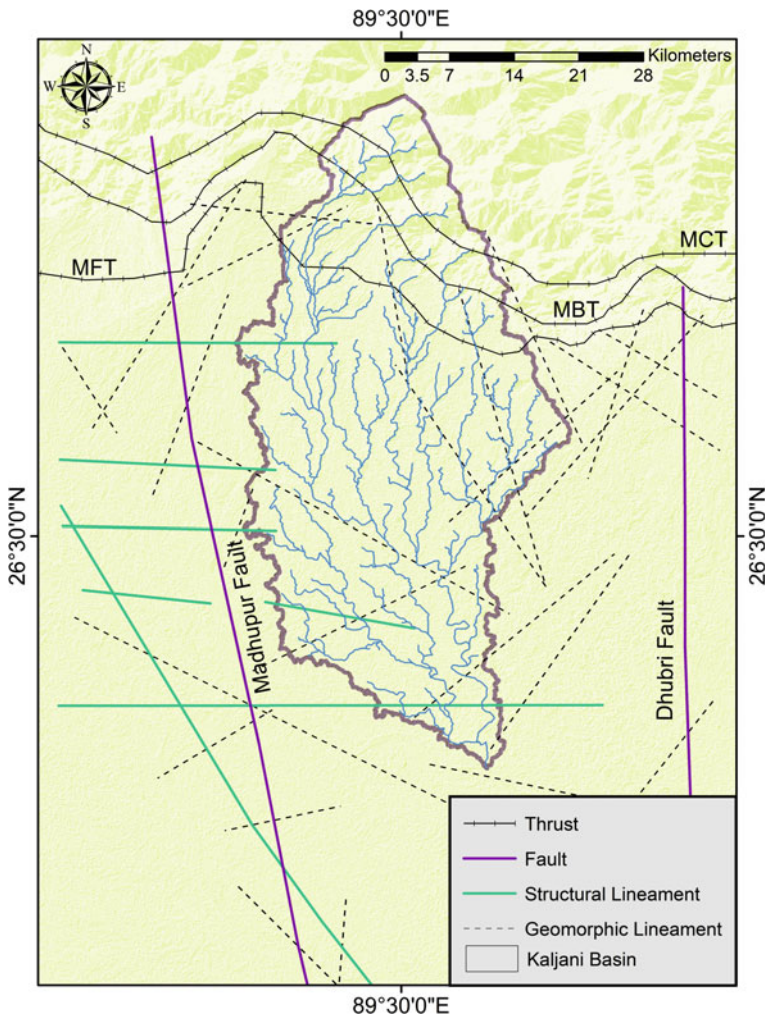


Fig. 7 Major lineaments and thrusts over the considered Kaljani Basin. (Based on Saha and Bhattacharya 2019)

(Madhupur and Dhubri fault having south to north orientation and MBT, MFT and MCT having east to west orientation), the number of lineaments of the basin, and those adjacent to the basin area where both geomorphic and structural lineaments are present. The structural lineaments are mostly having orientation from east to west and the geomorphic lineaments exist in different directions. These faults and lineaments are accompanied by eleven recognized geological formations (Fig. 8) where Baikunthapur and Chalsa formations are under the foredeep Quaternary section and consist of a number of lineaments with their substantive imprint on both channel and basin morphometry.

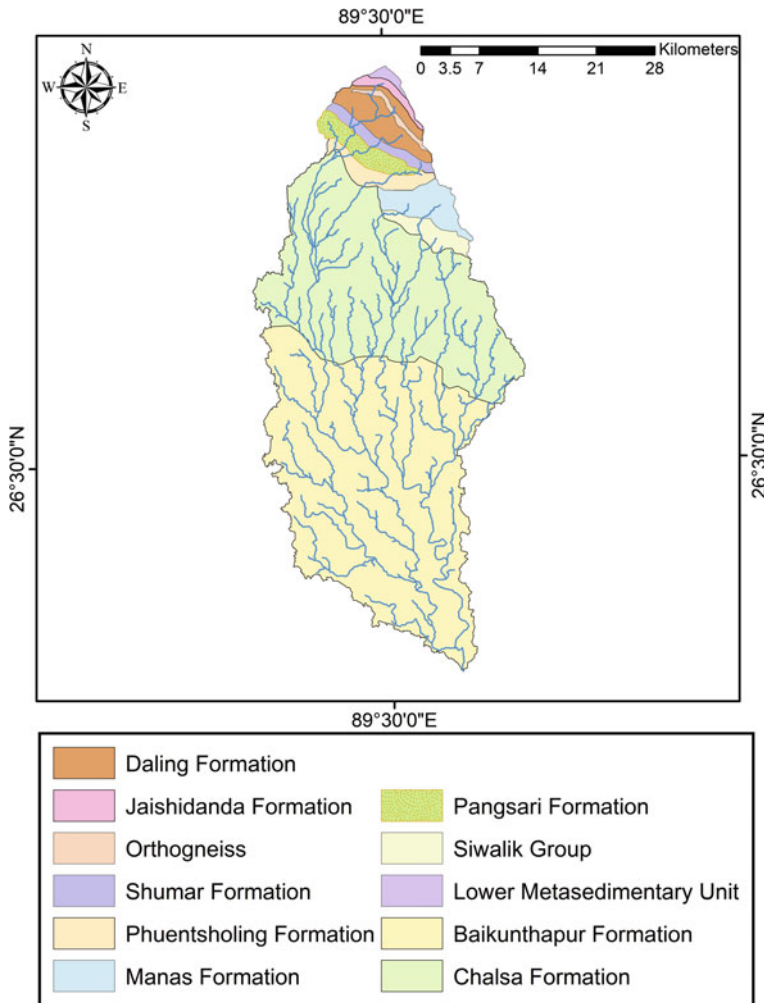


Fig. 8 Major Geological formations of Kaljani Basin. (Modified from Long et al. 2011)

- **Elevation profile:** The extracted elevation profile shows the existence of Quaternary fault scarps in the foreland basin. If the drainage area from Chel to Torsa and Torsa to Sankosh is differentiated, the North to south aligned elevation profile distinctly displays the MFT and the MBT in the form of fault scarps; though they both are blind antiform between Mal and Murti River. Figure 5 illustrates the above fault scarps between the Matiali and the Chalsa scarp; both being northerly dipping and blind in nature. The distinctly identified scarps define the intermediate Synformal axis where river terraces have formed in upliftment/incision mechanism near Matiali School on the River Kurti.
- **Long profile and Hack profile analysis:** Long Profile of the river along with various trend lines with calculated R^2 values also assess tectonism. The positive R^2 of logarithmic, exponential and power curves (Fig. 9) denote the active tectonics affecting the channel morphometry. The overlaying of actual and computed curves after 40 km from the source that makes an outline of the erosion/deposition alteration mechanism of the channel itself. The active tectonism of the region is evident in Hack profile where the channel is convex in shape (R^2 0.777) determining the erosive nature of the channel and also signifying some disturbances of the particular region due to neotectonic activity (Fig. 10). The lower reach of the river is typically characterized by a gentler gradient as it is representing a concave up profile as shown in the Hack Profile signifying depositional activity.
- **SL and Concavity:** Fig. 11 is a combined diagrammatic representation of SL index and concavity. SL index was used by Keller and Printer in 2002 to assess the relative tectonics of any area. Here, the values vary from 317.742 to -5.8967 along the long profile in different studied points of Kaljani River. Random alteration of values denotes the active tectonics. The recent tectonics is marked by the higher values as observed in the upper part of the Kaljani River due to the presence of MCT and MBT. Inconsistently, the lower values in the downstream section pertain to the presence of joints, cracks, faults and lineaments along the stream or transverse the river flow path. It is also associated with concavity index that specifically refers to the tectonic activity in accordance with the gradient and erosion probability of the River Kaljani. Both the indices indicate that the fore-deep area is tectonically active and broadly under the Baikunthapur and Chalsa formations are dominated by steep channel gradient and debris flow.
- **Sinuosity Index (SI):** Changes in channel orientation with tectonic disturbances and valley slope change enhance the channel pattern as straight to sinuous, sinuous to meandering and etc. to encounter its threshold. Pike and Wilson in 1971 applied the Hypsometric Integral (Hi) and Relief Ratio in discussing tectonics in a basin area. Near foothill, the SI value decrease (1.0) and further downstream it increases substantially up to 2.4 i.e., meandering. The SI values indicate down cutting where the channel in a straight manner due to incision. It is depicted by the SI that the channel is regulated by its changing flow pattern and volume when it passes through the weak zone termed as faults, lineaments or fractures. Such slope alteration induces vertical incision of the channel with higher velocity than lateral erosion resulting in straight to sinuous channel.

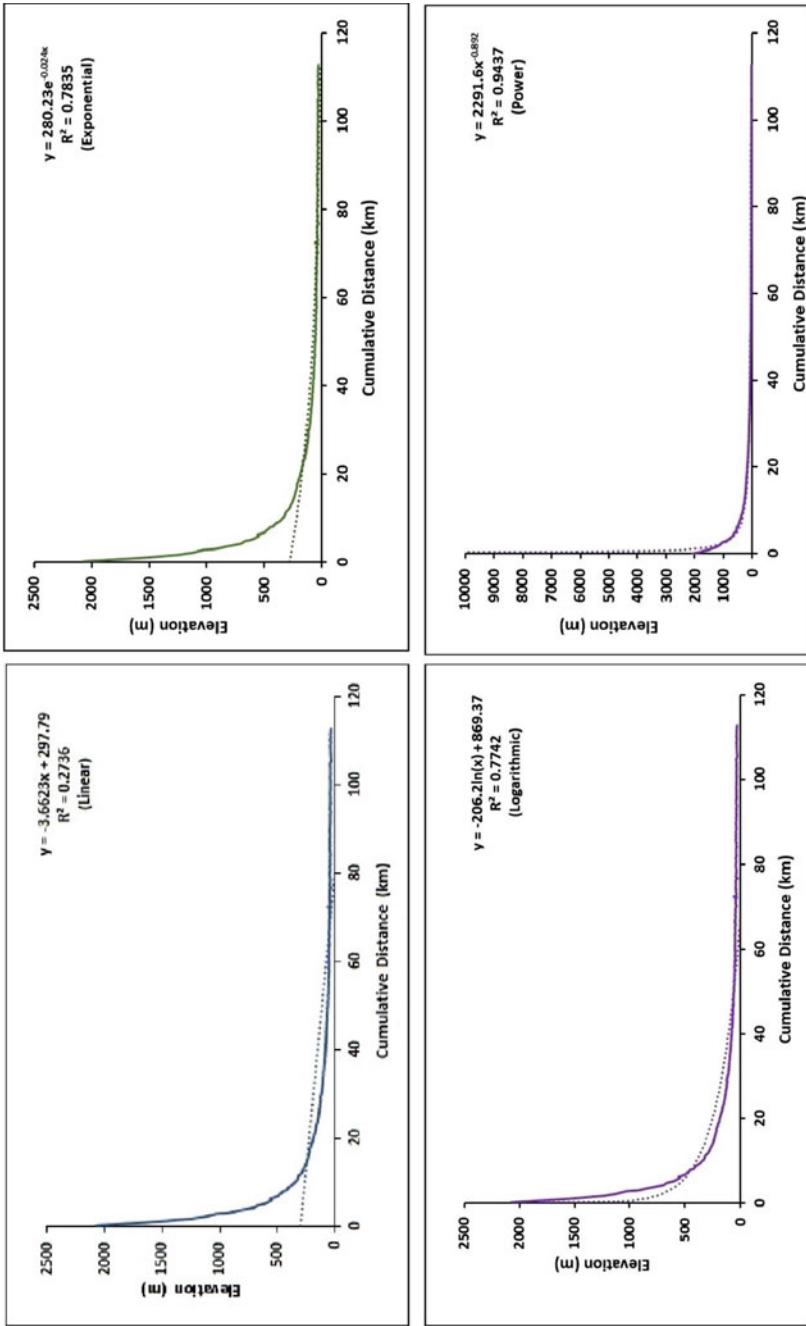


Fig. 9 Longitudinal Profile of Kaljani River with Linear, Exponential, Logarithmic and Power curves where the R² value of exponential, logarithmic and power curves are highly positive that specify the active tectonics

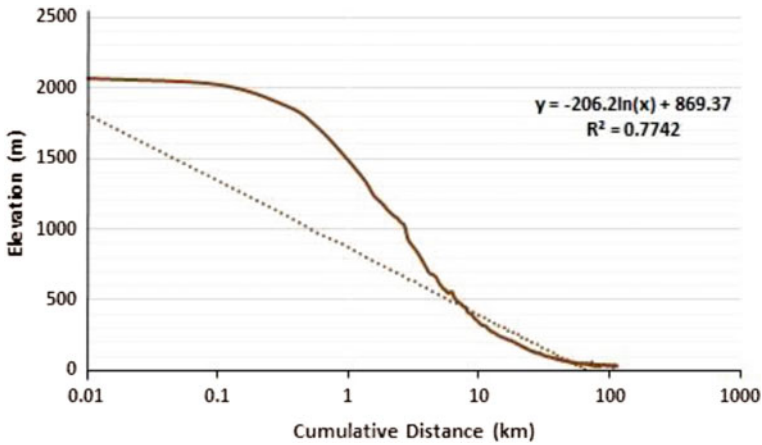


Fig. 10 Hack Profile of Kaljani River shows the convex shape that depict the erosional tendency of the river

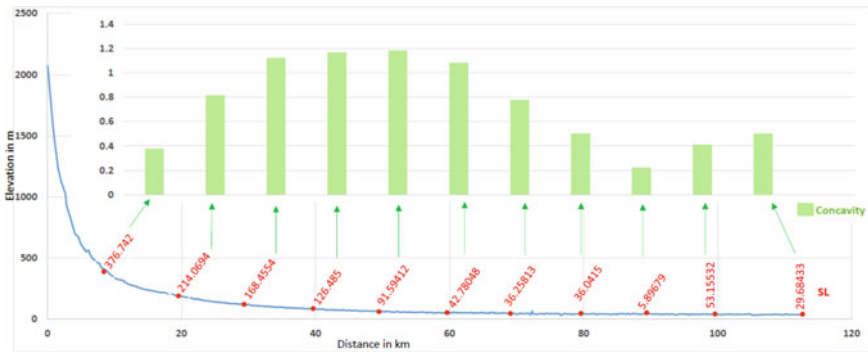


Fig. 11 Assessment of SL index and concavity of River Kaljani along the long profile to determine the anomalies. (Data extracted from SRTM data)

- **T (Transverse topographic symmetry factor):** It is a basin morphometric indicator that portrays the symmetry of the basin in reference to its midline. It is applicable to measure the perfect symmetry to asymmetry (0–1) of the basin. Considering the studied points in Kaljani basin up to 26.55 N/89.41E, the values are higher indicating river oscillation and maximum shifting in response to tectonic tilt after which the values have decreased due to minimum tilt. But in 26.39 N/89.56E, 26.35 N/89.57E and 26.27 N/89.58E alteration of higher values encompasses the asymmetric nature of the basin. These results bespeak the tectonic imprint of the entire basin, especially in the lowermost foreland area.
- **Elongation Ratio, Form factor and Circulatory Ratio:** According to Pareta and Pareta 2011; value >0.7 refers to elongated, 0.7–0.8 as less elongated, 0.8–0.9 oval and 0.9–1.0 as circular. The Kaljani river basin is elongated in nature as the value is

0.57 which again suggests the basin as active. The value of the form factor is 0.25 that positively matched with the elongation ratio indicating as positive feedback system. Continuing such quantification, elongated basins become circular when tectonic activities diminish and with time topographic evolution takes place. It is noticed when channel widths increase, indeed, the circularity value as low as 0.28 indicates active tectonics.

- Hypsometric integral (Hi) and Tilt angle: Hypsometric integral (Hi) correlates height (h/H) versus relative area (a/A). The Hi value ≤ 0.30 states tectonically stable basin and ≥ 0.30 indicated tectonically unstable basin according to Pike and Wilson (1971). The Kaljani is tectonically unstable as the calculated Hi value is 0.44 and it is strongly comparable with tilt angle value of 5.88 and Ruggedness Index as 1.67. The morphometric analysis along with geo-tectonic characteristics of the basin elucidates the tectonic instability of the foredeep basin and resultant deformed landforms.

5 Conclusion

The above discussion centers around the Himalayan foreland area which is affected by Quaternary tectonics. The entity of spatial earthquake magnitude distribution layout connects the tectonic evidence significantly. The morphotectonic analysis, seismological evidence, and major fault lines/lineaments propose the North Bengal foredeep section as tectonically active. The field-based application and experiment of alluvial fan physical modelling disclose the mechanism of fan formation due to change of discharge (Q). The fan-in a fan topography over the piedmont strip (Banerjee and Biswas 2021) of undulating riverscape land surfaces on a larger scale that has been enhanced by the dynamic river hydrological behaviour and sediment aggradation mechanism with time. The elaborate study defines the formation of fan surfaces that deformed by the active tectonics and formed the river terraces in the Holocene time. The study took into account the tectonic uplift/incision sequence that modified the channel morphometry and the results of morphotectonic analysis of the Kaljani River Basin as a case study advocates the tectonic proximity of the area.

References

- Ayaz S, Biswas M, Dhali K (2018) Morphotectonic analysis of alluvial fan dynamics: comparative study in spatio-temporal scale of Himalayan foothill, India. *Arab J Geosci* 11:41, 1–16
- Andreani L, Stanek K, Gloaguen R, Krentz O, Domínguez-González L (2014) DEM-based analysis of interactions between tectonics and landscapes in the ore mountains and eger rift (East Germany and NW Czech Republic). *Remote Sens* 6:7971–8001. <https://doi.org/10.3390/rs6097971>
- Bisaria BK (1980) Report on geomorphological mapping of a part of the foothills of Darjeeling Himalayas, West Bengal, Geological survey of India report, 1–16
- Biswas M (2009) Impact of landforms on land use of the tista-jaldhaka interfluvium, PhD thesis, Department of Geography, University of Calcutta, Kolkata, West Bengal, India

- Biswas M (2014) Development of alluvial fans and associated land use problems of himalayan foot hills, west bengal. *Res Inventy Int J Eng Sci* 4(2), 28–35 Issn(e): 2278–4721, Issn(p):2319–6483
- Biswas M (2015) Impact of neotectonism in the discussion of geomorphological processes as a feedback system: North Bengal foothills, West Bengal. *GSTF J Geol Sci* 2. https://doi.org/10.5176/2335-6774_2.1.22
- Biswas M, Banerjee P (2018) Bridge construction and river channel morphology—a comprehensive study of flow behaviour and sediment size alteration of the River Chel, India. *Arab J Geosci* 11. <https://doi.org/10.1007/s12517-018-3789-7>
- Biswas M, Paul A (2020) Application of geomorphic indices to Address the foreland Himalayan tectonics and landform deformation- Matiali-Chalsa- Baradighi recess, West Bengal, India, *Quaternary International*, vol 585, 2021, pp 3–14. ISSN 1040-6182. <https://doi.org/10.1016/j.quaint.2020.12.012>
- Biswas M, Paul A, Jamal M (2021) Tectonics and channel morpho-hydrology—a quantitative discussion based on secondary data and field investigation structural geology and tectonics field guidebook—vol 1. Springer Geol. https://doi.org/10.1007/978-3-030-60143-0_16
- Banerjee P, Biswas M (2021) Application of habitat modification score and fluvial functioning index in discussion of eco-hydrological behavior and flood risk zonation of Himalayan foothill rivers, West Bengal, India. *Acta Geophys*. <https://doi.org/10.1007/s11600-021-00570-0>
- Bookhagen B, Thiede RC, Strecker MR (2005) Latequaternary intensified monsoon phases control landscape evolution in the northwest Himalaya. *Geology* 33:149–152. <https://doi.org/10.1130/G20982.1>
- Brzezińska-Wójcik T, Lukasz C, Leszek G (2010) Neotectonic mobility of the Roztocze region, Ukrainian part, Central Europe: Insights from morphometric studies. *Ann Soc Geologorum Poloniae* 80
- Chakrabarti Goswami C, Jana P, Weber JC (2019) Evolution of landscape in a piedmont section of Eastern Himalayan foothills along India-Bhutan border: a tectono-geomorphic perspective. *J Mt Sci* 16. <https://doi.org/10.1007/s11629-018-5208-7>
- Chaudhri RS, Chaudhri AR (2001) Plate tectonics and sedimentation model of the cenozoic sediments of western and central himalaya. In: Gupta LN, Kumar R, Gill GS (eds) *Structure and tectonics of the Indian plate*. Spl vol, Bull. Indian Geol Assoc, v.34, pp 127–138
- Chen Y, Sung Q, Chen C, Jean J (2006) Variations in tectonic activities of the central and southwestern foothills, Taiwan, inferred from river hack profiles. *Terr Atmos Ocean Sci* 17(3):563–578
- Dasgupta S, Pande P, Ganguly D, Iqbal Z, Sanyal K, Venkatraman NV, Sural B, Harendranath L, Mazumdar K, Sanyal S, Roy A, Das LK, Misra PS, Gupta H (2000) *Seismotectonic atlas of India and its environs*. Geol Surv India, p 29
- De Celles PG, Carrapa B, Gehrels GE, Chakraborty T, Ghosh P (2016) Along-strike continuity of structure, stratigraphy, and kinematic history in the himalayan thrust belt: the view from northeastern India, *American geophysical union* 35(12):1–71. <https://doi.org/10.1002/2016TC004298>
- Gansser A (1964) *Geology of himalayas*, vol 56(3). Inter Science, Wiley, New York, 275–370
- Ghosh S, Paul A (2020) Tectonic control over drainage basin of South Andaman Island: study toward hydro-morphometric analysis. *Appl Water Sci*. <https://doi.org/10.1007/s13201-019-1055-0>
- Garzanti E (2019) The himalayan foreland basin from collision onset to the present: a sedimentary–petrology perspective. In: Treloar PJ, Searle MP (eds) *Himalayan tectonics: a modern synthesis*. Geological Society, London, Special Publications, 483. First published online January 4, 2019. <https://doi.org/10.1144/SP483.17>
- Goswami C, Mukhopadhyay D, Poddar BC (2013) Tectonic control on the drainage system in a piedmont region in tectonically active eastern Himalayas. *Front Earth Sci* 6(1), 29e38. <https://doi.org/10.1007/s12517-017-3308-2>
- Guha D, Bardhan S, Basir SR, De AK, Sarkar A (2007) Imprints of Himalayan thrust tectonics on the Quaternary piedmont sediments of the Neora-Jaldhuka Valley, Darjeeling-Sikkim Sub-Himalaya, India. *J Asian Earth Sci* 30:464–473

- Gupta GD, Srivastava HN (1992) Onearthquake risk assesment in the himalayan region. Himalayan Seismity by Gupta, G. D. Mem Geol Soc India 23:175–182
- Gupta N (2008) Geoinformatics for inter basin water transfer assessment-a study in parts of Ganga-Brahmaputra Basin, Eastern India (Master of Science (MSc)). International Institute for Geo-information science and earth observation
- Hack J (1957) Studies of longitudinal stream profiles in Virginia and Maryland. Geological survey professional paper, 294–B, 45–95
- Hodges K (2000) Tectonics of the Himalaya and Southern Tibet from two perspectives. Geol Soc Am Bull 112:324–350. [https://doi.org/10.1130/0016-7606\(2000\)112%3c0324:TOTHAS%3e23.CO;2](https://doi.org/10.1130/0016-7606(2000)112%3c0324:TOTHAS%3e23.CO;2)
- Horton R (1945) Erosional development of streams and their drainage basins; hydrophysical approach to quantitative morphology. Geol Soc Am Bull 56(3):275. [https://doi.org/10.1130/0016-7606\(1945\)56\[275:edosat\]20.co;2](https://doi.org/10.1130/0016-7606(1945)56[275:edosat]20.co;2)
- Hossain M, Xiao W, Khan M, Chowdhury K, Ao S (2020) Geodynamic model and tectono-structural framework of the Bengal Basin and its surroundings. J Maps 16(2):445–458. <https://doi.org/10.1080/17445647.2020.1770136>
- Ichikawa M, Srivastava HN, Drakopoulos JC (1972) Focal mechanism of earthquakes occurring in and around the Himalayan and Burmese mountain belt. Papers Meteor Geophys Tokyo 23:149
- Jain A, Dasgupta S, Bhargava ON, Israil M, Perumal R, Patel R, Mukul M, Parcha SK, Adlakha V, Agarwal K, Singh P, Bhattacharyya K, Pant N, Banerjee D (2016) Tectonics and evolution of the Himalaya. In: Proceedings of the Indian national science academy, p 82. <https://doi.org/10.16943/ptinsa/2016/48469>
- Jain AK, Banerjee DM, Kale SV (2020) Tectonics of Indian subcontinent, society of earth scientists series, ISSN 2194-9204 ISSN 2194-9212 (electronic), ISBN 978-3-030-42844-0 ISBN 978-3-030-42845-7 478 (eBook), 111–433. <https://doi.org/10.1007/978-3-030-42845-7>
- Jangangi BS (1974) Stratigraphy and tectonics of parts of eastern bhutan: Himalayan geology, vol 4, 117–136
- Kale VS, Sengupta S, Achyuthanc H, Jaiswald KM (15 December 2014) Tectonic controls upon Kaveri River drainage, cratonic Peninsular India: Inferences from longitudinal profiles, morphotectonic indices, hanging valleys and fluvial records. Geomorphology 227:153–165
- Kar R, Chakraborty T, Chakraborty C, Ghosh P, Tyagi AK, Singhvi AK (2014) Morpho-sedimentary characteristics of the Quaternary Matiali fan and associated river terraces, Jalpaiguri, India: implications for climatic controls. Geomorphology 227:137–152
- Kumar M, Hazarika P, Prasad S, Singh A, Saha S (2012) Tectonic implications of the September 2011 Sikkim earthquake and its aftershocks. Curr Sci 102
- Lave and Avouac (2000) Active folding of fluvial terraces across the Siwaliks Hills, Himalayas of central Nepal. J Geophys Res Atmos 105(B3):5735–5770
- Long S, McQuarrie N, Tobgay T, Grujic D, Hollister L (2011) Geologic map of Bhutan. J Maps 7(1):184–192. <https://doi.org/10.4113/jom.2011.1159>
- Magar PP, Magar NP (2016) Application of Hack's stream gradient index (SL Index) to longitudinal profiles of the rivers flowing across Satpura-Purna plain, Western Vidarbha, Maharashtra. J Geomorphol 4:65–72
- Mallet FR (1975) On the geology and mineral resources of darjeeling and western Duars. Mem.G.S.I. 11:1–50
- Martinson DG, Pisias NG, Hays JD, Imbrie J, Moore TC Jr, Shackleton NJ (1987) Age dating and the orbital theory of the ice ages: development of a high resolution 0 to 300,000-year chrono stratigraphy. Quatern Res 27:1–29
- Mishra RL, Singh I, Pandey A, Rao PS, Sahoo HK, Jayagondaperumal R (2016) Paleoseismic evidence of giant medieval earthquake in the eastern Himalaya
- Mugnier et al (2013) Structural interpretation of the great earthquakes of the last millennium in the central Himalaya. Earth-Sci Rev 127:30–41

- Mukherjee S, Carosi R., van der Beek PA, Mukherjee BK, Robinson DM (2015) Tectonics of the Himalaya: an introduction. In: Mukherjee S, Carosi R, van der Beek P, Mukherjee BK, Robinson D (eds) Geological society, vol 412. Special Publications, London, pp 1–3
- Mukul M, Jade S, Ansari K, Matin A (2014) Seismotectonic implications of strike-slip earthquakes in the Darjeeling-Sikkim Himalaya. *Curr Sci* 106:198
- Mukul M, Singh V (2016) Active tectonics and geomorphological studies in India during 2012–2016. In: Proceedings of the Indian national science academy, p 82. <https://doi.org/10.16943/ptinsa/2016/48480>
- Mukul M (2000) The geometry and kinematics of the Main Boundary Thrust and related Neotectonics in the Darjiling Himalayan fold-and-thrust belt, West Bengal, India
- Mullick M, Mukhopadhyay D (2011) An analysis of GPS-derived velocities in the Bengal basin and the neighbouring active deformation zones. *Curr Sci* 101:423–426
- Nakata T (1972) Geomorphologic history and crustal movements of foothills of the Himalaya, Sendai. Institute of Geography, Tohoku University, p 77
- Nakata T (1982) A photogrammetric study on active faults in the Nepal Himalayas. *J Nepal Geol Soc* 2:67–80
- Nakata T (1989) Active faults of the Himalaya of India and Nepal. *Geol Soc Am Spec Pap* 232:243–264
- Nalditryal SP, Jangpangi BS, Singh P, Guha Sarkar TK, Bhate BD, Raghavan MR (1964) A preliminary note on geology of Bhutan Himalaya. Report of 22 international geological congress, Vol.11, pp 1–14
- Pareta K, Pareta U (2011) Quantitative morphometric analysis of a watershed of Yamuna basin, India using ASTER (DEM) data and GIS. *Int J Geomat Geosci* 2(1):248–269. <https://www.researchgate.net/publication/260319314>
- Paul A, Biswas M (2019) Changes in river bed terrain and its impact on flood propagation—a case study of River Jayanti, West Bengal, India. *Geomat Nat Haz Risk* 10(1):1928–1947. <https://doi.org/10.1080/19475705.2019.1650124>
- Pierce I, Wesnousky SG (2016) On a flawed conclusion that the 1255 A.D. earthquake ruptured 800 km of the Himalayan Frontal Thrust east of Kathmandu. *Geophys Res Lett* 43. <https://doi.org/10.1002/2016GL070426>
- Pike RJ, Wilson SE (1971) Elevation-relief ratio, hypsometric integral and geomorphic area—altitude analysis. *Geol Soc Am Bull* 82:1079–1084
- Pinter N, Keller EA (1995) Geomorphological analysis of neotectonic deformation, northern Owens Valley, California. *GeolRundsch* 84:200–212
- Saha D (2013) Lesser Himalayan sequences in Eastern Himalaya and their deformation: Implications for Paleoproterozoic tectonic activity along the northern margin of India. *Geosci Front* 4:289–304. <https://doi.org/10.1016/j.gsf.2013.01.004>
- Saha U, Bhattacharya S (2019) Reconstructing the channel shifting pattern of the Torsa River on the Himalayan Foreland Basin over the last 250 years. *Bull Geog Phys Geogr Ser* 16(1):99–114. <https://doi.org/10.2478/bgeo-2019-0007>
- Schumm SA (1956) The evolution of drainage systems and slopes in bad lands at Perth, Amboi. *New Jersey Geol Soc Am Bull* 67(5):597–646
- Singh A, Bhushan K, Singh C, Steckler MS, Akhter SH, Seeber L, Kim WY, Tiwari AK, Biswas R (2016) Crustal structure and tectonics of Bangladesh: new constraints from inversion of receiver functions. *Tectonophysics* 680:99–112. <https://doi.org/10.1016/j.tecto.2016.04.046>
- Srivastava HN, Chatterjee SN, Chaudhury HM (1976) Assessment of the earthquake potential of a Region. *Bull Indian Soc. Earq. Tech* 13:93–99
- Srivastava P et al (2016) River in the Himalaya: responses to neotectonics and past climate. *Proc Indian Natn Sci Acad* 82(3):763–772
- Starkel L, Sarkar S, Soja R, Prokop P (2008) Present-day evolution of the Sikkimese-Bhutanese Himalayan piedmont, PL ISSN 0373-6547, ISBN 978-83-61590-095, PL ISSN-0373-6547
- Thakur V (2013) Active tectonics of Himalayan Frontal Fault system. *Int J Earth Sci* 102(7). <https://doi.org/10.1007/s00531-013-0891-7>

- Valdia KS (2003) Reactivation of Himalayan frontal fault: implication. *Curr Sci* 85(7):1031–1044
- Wesnousky SG, Kumar S, Mohindra R, Thakur VC (1999) Upliftand Convergence along the Himalayan frontal thrust. *Tectonics* 18(6):967–976
- Whipple K, Wobus C, Crosby B, Kirby E, Sheenan D (2007) New tools for quantitative geomorphology: extracting and interpretation of stream profiles from digital topographic data. GSA annual meeting, Boulder, USA
- Wobus C, Whipple K, Kirby E, Snyder N, Johnson J, Spyropoulou K, Crosby B, Sheehan D (2006) Tectonics from topography: procedures, promise, and pitfalls. In: *Tectonics, climate, and landscape evolution*. Special Paper Geol Soc Am 398:55–74
- Yin A (2006) Cenozoic tectonic evolution of the Himalayan orogen as constrained by along-strike variation of structural geometry, exhumation history, and foreland sedimentation. *Earth Sci Rev* 76(1–2):1–131. <https://doi.org/10.1016/j.earscirev.2005.05.004>

Evaluating the Relative Tectonic Response of the Fluvial Systems Using Multicriteria Entropy Method: A Case Study of the Rangit Catchment, Eastern Himalayas, India



Lopamudra Roy , Somasis Sengupta , Sayantan Das ,
and Arindam Sarkar 

Abstract The Rangit catchment is nestled within the active tectonic region of the Eastern Himalayas in the mountainous state of Sikkim, India. The role of tectonics in this catchment is visibly indicated by the presence of fluvial systems under the erosional regime and associated geomorphic features, along with frequent seismic activities. The streams in the Rangit Basin and their associated catchments were extracted from the ortho-corrected ALOS PALSAR DEM. To assess the tectonic response in the fluvial systems, several indices such as the asymmetric factor, hypsometric integral, elongation ratio, stream gradient index and valley width-height ratio have been calculated for all 16 sub-catchments along with the trunk-stream of the Rangit River. Besides, morphometric indices such as relief ratio, relative relief, plan-form curvature, dissection index, ruggedness number and stream power index have been evaluated for these drainage units. These attributes have been collated and further analysed by the multi-criteria Entropy Method. Finally, the Index of Active Tectonics (IAT) values for individual sub-catchments were mapped to determine the intra-basin variation of relative tectonic activity in the Rangit Basin. Before performing the analysis, the parameters were checked for redundancy by the Variance Inflation Factor-induced multicollinearity diagnostics. It can be summarized that the concerned region has extremely rugged topography and characterised by high relative relief, steep gradient and highly dissected segments. Furthermore, it is observed that the left bank tributaries display a higher degree of tectonic control than the right bank tributaries. The Main Central Thrust (MCT), which is located between the Greater Himalayas and the Lesser Himalayas, roughly divides the catchment into

L. Roy

Department of Geography, Pakuahat Degree College, Malda 732138, India

S. Sengupta (✉)

Department of Geography, The University of Burdwan, Bardhaman 713104, India

e-mail: ssengupta@geo.buruniv.ac.in

S. Das

Department of Geography, Dum Dum Motijheel College, Kolkata 700074, India

A. Sarkar

Department of Geography, P.K.H.N. Mahavidyalaya, Howrah 711410, India

right and left bank tributaries. The notable difference in tectonic activity across two flanks of the MCT suggests that the MCT is active during the Holocene.

Keywords Himalayas · Tectonics · ALOS PALSAR DEM · Main Central Thrust · Entropy

1 Introduction

Rivers are the most dynamic elements of the landscapes around the world. Any river system represents a complex interplay between system attributes such as topography, structure, tectonics, climate, biosphere, etc. that operate on different spatio-temporal scales (Clarke 1966; Phillips 1988; Mesa 2006; Evans 2012). A river basin or drainage basin or catchment refers to the entire region which collects surface water from rain, snowmelt, hail, sleet, as well as groundwater underneath the earth's surface, eventually providing runoff to the mainstream and its tributaries (Lambert 1997). The shape and other physical attributes of the catchment determine various geomorphic and hydrologic processes functioning within it. Alterations in the climatic and tectonic conditions affect these processes, and the consequences are eventually reflected in the landscape morphology of the catchment. To understand the processes and related changes, morphometry-based landform studies have become important in recent geomorphic studies (Florinsky 2017). General geomorphometry refers to the quantitative analysis of different surficial morphological parameters of a river catchment by considering it as a complete areal unit (Goudie 2004; Evans 2012). The morphometry-based approach has been popular in geomorphology ever since the publication of classical papers on drainage basin morphometry by Horton (1932, 1945) and Strahler (1957). Following this well-accepted approach, a large number of studies were carried out even in the last decade (Ferraris et al. 2012; Burian et al. 2015; Clarke and Romero 2017; Asfaw and Workineh 2019). Several studies in the last few decades have shown that morphometry-based indices are useful for ascertaining the presence of active tectonics (Pike and Wilson 1971; Hack 1973; Bull and McFadden 1977; Keller and Pinter 1996; Kale and Shejwalkar 2007; El Hamdouni et al. 2008; Shtober-Zisu et al. 2008; Valensise et al. 2013; Jacques et al. 2014; Habibi and Gharibreza 2015). These morphotectonic indices include basin asymmetric factor, hypsometric integral, basin elongation ratio, stream gradient index, valley width-height ratio etc., which directly determine the degree of tectonic control on a river catchment.

The largest mountain chain in the world—the Himalayas—covers a large area in the northern and north-eastern parts of India. The collision of the northward-moving Indo-Australian Plate and the relatively static Eurasian Plate since the Middle Eocene (44 Ma BP) caused the emergence of the Himalayas (Curry et al. 1982; Chen et al. 1993). The process of mountain formation is still active and has undergone many alterations in the geological past (Sinha-Roy 1977; Klootwijk et al. 1985; Jade et al. 2007; Roy and Purohit 2018). Characterised by the tropical montane ecosystem, the

Eastern Himalayas has a rich geological history and prevalent topographic features (Quanru et al. 2006; Choudhuri et al. 2009), where the concerned catchment is located. As the uplift of the Himalayas still continues, the role of tectonics needs to be evaluated at a catchment scale, as any change would have rippling effect on the geomorphic processes and features within it. This is where neo-tectonics becomes important, which is basically a closely related offshoot of tectonics and deals with the geological and geomorphologic processes that are operating in recent geological time.

Although a number of tectonics-related studies were carried out in the Western and Central Himalayas (Jain and Sinha 2005; Malik and Mohanty 2007), systematic investigations related to the tectonic effects on the drainage systems are palpably few (Seeber and Gornitz 1983). In a recent study, a mathematical model-based analysis of the stream longitudinal profiles in the Rangit catchment was done by Das et al. (2020). However, it did not incorporate the morphotectonic indices to assess the role of active tectonics. In fact, very few of the previous studies on tectonic geomorphology have analysed the direct indices of tectonic activity in a fluvial domain. The studies in this field have mostly taken the components in isolation, especially in the Indian context. So, the prevailing research gap in this domain is that the morphotectonic indices as signatures of fluvial response to tectonics have not been much explored. In the present study, along with the direct morphotectonic indices, basin morphological parameters such as relief ratio, dissection index, ruggedness number, stream power index etc. were calculated to assess the relative neo-tectonic response of the fluvial systems within a catchment snuggled inside a mountainous landscape. This paper treats the channel response to neo-tectonics as a multicriteria problem, wherein a new composite parameter named Index of Active Tectonics (IAT) is proposed to ascertain the degree of tectonic activity in this part of the Eastern Himalayas in recent geological time. For calculating the IAT, the Information Entropy Method proposed by Shannon (1948) was applied. Finally, the IAT values for individual sub-catchments were mapped to determine the intra-basin variation of relative tectonic activity in the Rangit Basin.

2 Study Area

2.1 Location

The Rangit River emanates from a glacial lake near the Rathong Glacier snout (27.560°N, 88.125°E), located in the southern slopes of the Kabru South Peak in the Indian state of Sikkim (Fig. 1). The principal channel, which is also the main tributary of the Tista River, has a catchment area of ~2132 km² and merges with the Tista near Melli at the border of Sikkim and West Bengal States of India (27.080°N, 88.433°E; Fig. 1). The principal channel, characterized by deep gorges and steep tributary valleys, has carved out a 97.5 km-long course through the Eastern Himalayas.

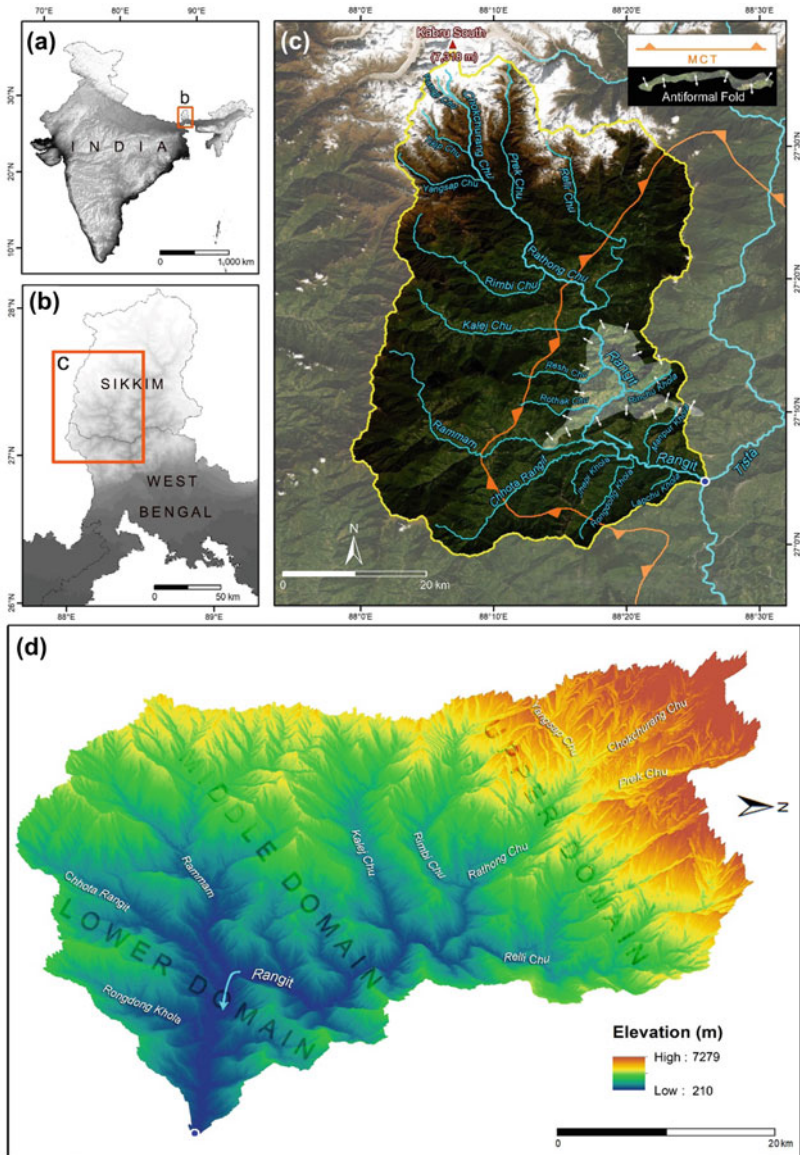


Fig. 1 The Rangit River, its tributaries and catchment area in the Eastern Himalayas. Streams were generated from the ALOS PALSAR DEMs (12.5 m) of 2007 and overlaid on November 2018 GeoEye image (c panel). The catchment is delineated by yellow. The line MCT depicts the position of the underlying Main Central Thrust. The position of MCT is shown following Thakur et al. (2012). The dyed region on the eastern part of the basin shows the existence of antiformal fold (c panel). A DEM-generated 3-dimensional illustration of the catchment is shown in d panel. The arrows indicate principal flow direction, whereas the blue dots represent the confluence between the Rangit and Tista Rivers (c and d panels)

The streams of the Rangit catchment are mainly fed by melting snow during the summer months and heavy rains in the monsoon season between June and October. While snowfall occurs at higher elevations during the winter season, the rest of the catchment receives trace rainfall due to western disturbances. Most places of the catchment receive more than 275 cm of rainfall annually, about 80% of which occurs during the monsoons (IMD 2018).

As observed from the ALOS PALSAR digital elevation model (DEM), the average elevation of the Rangit catchment is 2367 m AMSL, and the mean basinal slope is about 28.98°. Almost half of the total area is located above 2000 m AMSL. In total, 16 major tributaries can be identified in the Rangit catchment—12 of which are located on the right (western) bank of the principal channel, while four meet the mainstream on the left (eastern) bank (Fig. 1). The mainstream is only referred to as the Rangit after the convergence between the Rathong Chu and Relli Chu. Incidentally, it is known as the Chokchurang Chu near its headwaters. The Rangit catchment, on the basis of runoff sources, can be divided into three Major domains—upper, middle and lower. The snowmelt runoff-fed tributaries that drain into the main channel upstream of the Rimbi Chu confluence, can be considered as part of the *upper domain* (Rangit main channel reach: 0–41 km). The downstream segment of the main channel till the Rammam confluence can be identified as the *middle domain* (Rangit main channel reach: 41–77 km). The tributaries meeting the main channel in this domain are mostly rain-fed. The flow directions of the main channel through the aforementioned domains are south-eastward and southward, respectively (Fig. 1). The Rangit River takes an abrupt turn toward the east from the Rammam confluence and meets the Tista River 21 km downstream. This portion, characterized by the presence of rain-fed ephemeral tributaries, can be defined as the *lower domain*.

2.2 Geology

The Rangit Channel traverses through two major tectonic zones—the Central Himalayan Domain and the Lesser Himalayas (Le Fort and Cronin 1988; Roy and Purohit 2018). These two zones are divided by the Main Central Thrust (MCT; Figs. 1 and 2), separating the higher elevation areas in the western half (underlain by the Kanchenjunga–Darjeeling Gneiss and Chungthang Formation of the Central Crystalline Gneissic Complex), and relatively low lying areas of the eastern portion (underlain by the Precambrian Daling Series of quartzites and phyllites) of the basin (Sinha-Roy 1974, 1977; Acharya and Ray 1977; GSI 2012; Thakur et al. 2012; Basu 2013; Roy and Purohit 2018). In the eastern part of the catchment, an antiformal fold exposes the conglomerate and phyllite-dominated Gondwana Formation (Fig. 1), which overlies the Buxa Formation of the Lesser Himalayas (Acharya and Ray 1977; GSI 2012; Basu 2013). The northern portion of this fold is superimposed by the Daling Formation, which is again overlain by the gneissic Darjeeling Formation along the MCT (Thakur et al. 2012). The major lithologic groups of the basin along with the lineaments are shown in Fig. 2. These lithological groups are generally

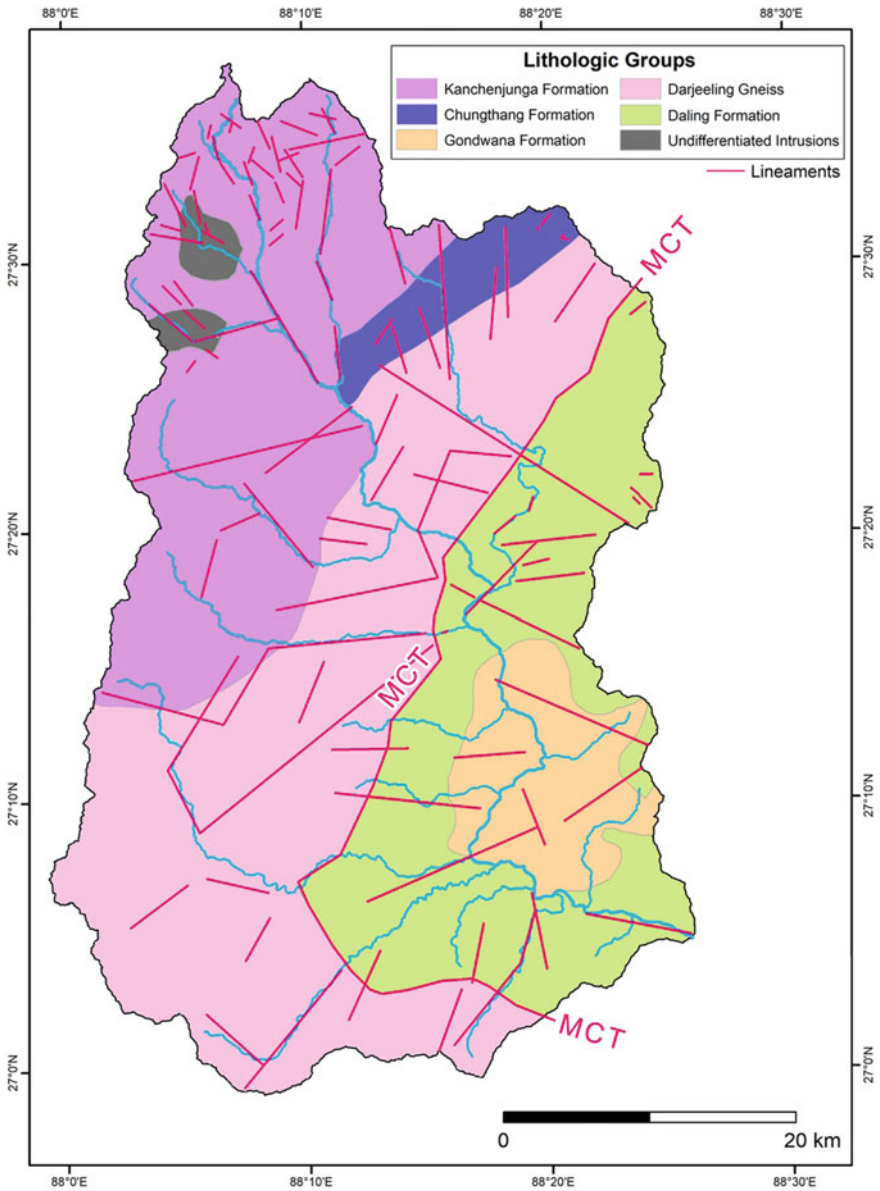


Fig. 2 Geological map of the Rangit Basin showing major lineaments along with the MCT. The lineaments were derived from the ALOS PALSAR DEMs (12.5 m) of 2007 and overlaid on the map of the major lithologic groups of the basin (reproduced map from Sarkar et al. 2021)

buried under the sandy loam and silty loam-based materials of varying thickness (CGWB 2018). This part of the Himalayas has experienced a number of earthquakes in the past (Bilham 1995; de la Torre et al. 2007; Singh et al. 2010; Thakur et al. 2012; Pradhan et al. 2013). Continuous seismic activities coupled with abundant rainfall during the monsoons, along with the presence of rocks viz. conglomerate, phyllite etc. make this catchment a landslide hazard-prone.

3 Materials and Methods

3.1 Datasets

The present study is based on the ALOS PALSAR DEM data (Scene 1: ALPSRP055230540, Path-505, Frame-540; Scene 2: ALPSRP055230530, Path-505, Frame-530; acquisition date of the DEMs: 6 February 2007; *downloaded from the Alaska Satellite Facility Distributed Active Archive Center*). This freely available dataset can provide information at a finer resolution (12.5 m) as compared to the coarse-resolution datasets (Niipele and Chen 2019). It is also pertinent to mention here that the acquired DEMs exhibit elevation above the local ellipsoidal surface (Das et al. 2015). Due to this, the datasets were converted into orthometric heights by using the Earth's Gravity Model of 2008 (EGM 2008, available from https://earth-info.nga.mil/GandG/wgs84/gravitymod/egm2008/egm08_wgs84.html), which is a spherical harmonic model of the earth's gravitational potential obtained from a global set of gravity anomalies (Pavlis et al. 2012). The geoidal elevation is subtracted from the ellipsoidal elevation associated with a DEM pixel to get the orthometric elevation of that pixel.

The corrected DEMs were further processed for filling the data voids and finding outlet cells in a repetitive manner (O'Callaghan and Mark 1984; Jenson and Domingue 1988; Das et al. 2016). Subsequently, the void-free DEMs were used to extract the drainage network and catchment of the Rangit main channel and its 16 major tributaries. This entire process was executed through ArcGIS 10.3.1.

3.2 Indices for Quantifying Direct Effect of Tectonic Activity

In the present study, five indices of active tectonics were derived from the ALOS PALSAR DEM datasets (Table 1). The indices are—hypometric integral (HI), stream length-gradient index (SL), valley width-height ratio (V_f), basin elongation ratio (R_e) and the basin asymmetry factor (A_f). In order to understand the spatial distribution of these proxy indicators, index-wise maps are presented in this paper (Fig. 3). As there were significant inter-catchment variations in the index values, the results were further analyzed in a multi-criteria domain so as to identify specific zones of potential tectonic activity.

Table 1 Morphotectonic indices and their formulae

Sl. no	Index	References	Formulae	Variables
1	Hypsometric integral (HI)	Bull and McFadden (1977)	$HI = (H_m - H_{min}) / (H_{max} - H_{min})$	H_m = Mean Elevation, H_{max} = Maximum Elevation, H_{min} = Minimum Elevation
2	Stream length-gradient index (SL)	Hack (1973)	$SL = (H1 - H2) / (\ln L2 - \ln L1)$	H1 and H2 are the elevations of upper and lower ends of a given reach, respectively. L1 and L2 are the distances from each end of the reach to the channel source
3	Valley width-height ratio (V_f)	Bull and McFadden (1977)	$V_f = V_{fw} / ((E_{ld} - E_{sc}) + (E_{rd} - E_{sc})) / 2$	V_{fw} = Width of the valley floor, E_{ld} = Elevation of the left valley divide, E_{rd} = Elevation of the right valley divide, E_{sc} = Elevation of the valley floor
4	Basin elongation ratio (R_e)	Bull and McFadden (1977)	$R_e = 2 * (A / \pi)^{0.5} / L_b$	A = Area of the basin, L_b = Distance between the two most distant points in the basin or length of the basin
5	Basin asymmetry factor (A_f)	Keller and Pinter (1996)	$A_f = 100(A_r / A_t)$	A_r = Area of the basin to the right side of the trunk stream, A_t = Total area of the drainage basin

3.2.1 Hypsometric Integral (HI)

Hypsometric integral (HI) is often recognized as a powerful indicator to differentiate between tectonically active and relatively inactive areas (Keller and Pinter 1996; Goudie 2004; Kale and Shejwalkar 2007; El Hamdouni et al. 2008). The index is defined as the area below the hypsometric curve or the area-height curve (Table 1), and thus expresses the proportion of the basin that has not been eroded. Therefore, HI is a direct measure of the degree of fluvial dissection in a landscape (Kale and Shejwalkar 2007). The values of HI range from 0 to 1. Usually higher values of HI (close to 1) indicate that a large proportion of the area in the basin is in the high-elevation category, which is typically observed in the actively uplifting regions or in areas of significant structural control. On the contrary, basins exhibiting lower

Jacques et al. 2014 and the references therein). Normally, it is expected that the SL index will increase in reaches associated with resistant rocks or and/active tectonic deformation.

3.2.3 Valley Width-Height Ratio (V_f)

Valley width-height ratio (V_f) is a measure to quantitatively determine the shape of a valley (Table 1). It is defined as the ratio between the valley floor width to the mean depth of the valley (Bull and McFadden 1977). Besides indicating whether the river is actively downcutting (Kale and Shejwalkar 2007), this ratio can be used to differentiate between wide and narrow valleys (El Hamdouni et al. 2008). The valley profile morphology can be associated with the rate of incision in a tectonically active area. Because uplift and incision are nearly harmonized in a state of dynamic equilibrium, this index is often recognized as a surrogate for active tectonics (El Hamdouni et al. 2008). The higher the rate of uplift, the valleys tend to become narrower and deeper. Hence, lower values of V_f are suggestive of deep and narrow valleys, which are commonly witnessed in the regions undergoing rapid tectonic uplift such as the Himalayas. In contrast, higher values of V_f highlight the presence of wide and shallow valleys, suggesting the dominance of lateral erosion in a tectonically stable landscape (Kale and Shejwalkar 2007). Normally, V_f of a river basin tends to increase downstream in accordance with the decrease in stream energy and increase in lateral erosion. For each of the selected sub-catchments, multiple valley profiles (about 20) perpendicular to the drainage basin axis were drawn. The requisite data for valley width and valley height were extracted and then the V_f for each cross-profile was obtained by employing the standard formula (Table 1). The average ratio was then taken as the representative of each sub-basin.

3.2.4 Basin Elongation Ratio (R_e)

The planimetric shape of a catchment can be quantitatively expressed by an aerial morphometric variable known as basin elongation ratio (R_e). This index is often used as a proxy indicator for active tectonics (Kale and Shejwalkar 2007; Bhatt et al. 2008; El Hamdouni et al. 2008). The R_e is defined as the ratio between the area of the catchment to the area of a circle having the same perimeter of the catchment (Table 1). The catchments located in the tectonically active regions are usually elongated in shape, whereas the shape becomes circular if there is a cessation of uplift (Bull and McFadden 1977).

3.2.5 Basin Asymmetry Factor (A_f)

The basin asymmetry factor (A_f) is an aerial morphotectonic index that is used to detect the presence or absence of regional tilt in the catchment (Kale and Shejwalkar

2007). It is defined as the ratio between the area of the catchment to the right of the trunk stream and the total catchment area (Keller and Pinter 1996; Table 1). A catchment grossly unaffected by regional tilt is generally symmetric with the A_f value around 50, indicating that the areas on both sides of the main channel are more or less similar. A_f values significantly above or below 50 indicate tilting due to tectonic processes operating across the trunk stream course.

3.3 Basin Morphological Indices

Alongside the indices of active tectonics, basin morphological indices such as relative relief (R_1), relief ratio (R_r), basin gradient (S), planform curvature (P_{curv}), dissection index (DI), ruggedness number (R_n) and stream power index (SPI) for the Rangit catchment and its sub-catchments were calculated to further substantiate the obtained results. Alike the direct indices, index-wise maps were made for the catchments (Fig. 5).

One of the most commonly used basin morphological indices is the relative relief (R_1), which can be derived from a DEM as the difference between the maximum and minimum altitudes within a certain cell (Oguchi 1997). For the present study, maximum and minimum altitudes of a catchment are considered to obtain R_1 . In addition to this, the relief ratio (R_r) of a catchment can be calculated by dividing its relative relief with the length of the catchment (L_b). Devised by Schumm (1956), the dimensionless ratio is positively correlated with the erosion potential and rate of sediment loss. Thus, it may be used as an indicator of potential sediment yield from a catchment. High R_r indicates the presence of steep slope and high relief that are generally associated with highly resistant rocks, which further specifies a higher degree of tectonic activity.

Primary topographic attributes such as the mean basin slopes were computed in the ArcGIS environment. The obtained values were converted into gradients to measure the ratio of altitude drop per unit of horizontal distance (Leopold et al. 1964). A high gradient indicates a steeper slope characterised by the rapid flow of water through narrow V-shaped valleys with high erosion potential. On the other hand, planform curvature is the rate of change of topographic slope and it is expressed in degrees/100 m (Goudie 2004). This parameter is used to classify the terrain as concave, convex, or rectilinear on the basis of negative, positive, or zero value of curvature, respectively. Negative curvature implies that the slope decreases downstream, which suggests a concave region characterised by uniform lithology and a lower rate of erosion. Whereas, positive curvature indicates a convex area associated with topographic and drainage abnormality. Incidentally, zero curvature implies a rectilinear surface. Planform curvatures of the catchments are derived to see if the surficial flow converges (concave curvature, indicated by negative values) or diverges (convex curvature, indicated by positive values) in the landscape (Zevenbergen and Thorne 1987).

Dissection index (DI), a popular morphometric parameter put forward by Nir (1957) in its present form, is used for understanding morphometry, physiographic attributes, and vertical erosion of terrain (Schumm 1956). DI is basically the ratio of relative relief to absolute relief. The value of DI ranges between 0 (absence of dissection) and 1 (totally dissected). Ruggedness number (R_n) combines terrain steepness and length, indicating the degree of the instability of land surface (Strahler 1957). The structural complexity of the terrain in association with relief and drainage density can be known from R_n (Altaf et al. 2013). R_n is derived from the product of maximum relief and drainage density within a particular catchment (Melton 1965). The product is divided by 1000 to get the actual R_n . It has a positive relationship with erosional regime, with high R_n values imply greater relative relief and drainage density.

Stream Power Index (SPI) can be used as a proxy to estimate the potential capacity of a fluvial system to cause erosion. SPI is the product between catchment area size and tangent of the slope in degrees (Moore et al. 1993). Stream Power Index is calculated based on the following formula:

$$SPI = \ln(A_s \times \tan \beta) \quad (1)$$

where, A_s is the specific catchment's area and $\tan \beta$ is local gradient measured in degrees.

SPI is extremely useful in areas where discharge data is not available. As the catchment size and slope increase, the discharge proportion from upstream areas and flow velocity also increase, therefore stream power tends to be escalated in areas under intense erosional regime (Moore and Burch 1986; Moore et al. 1991; Vijith and Dodge-Wan 2019). Whereas, lack of stream power indicates increased sedimentation within the river system.

3.4 Multicollinearity Diagnostics

The next step involved checking of any evidence of multicollinearity in the dataset obtained for morphotectonic and morphological indices. Multicollinearity or non-linear dependence is a statistical phenomenon in which two or more predictor variables in multivariate statistical analysis are highly correlated (Daoud 2012). Multicollinearity gets introduced due to a very high degree of correlation between the attributes which are considered in the analysis (Keat et al. 2009; Vommi 2017). Multicollinearity often introduces redundant variables in the data and may result in the introduction of bias (Mela and Kopalle 2002). Therefore, one of the prerequisites of multi-criteria decision making (MCDM) is the detection of multicollinearity. This exercise can be performed by calculating the Variance Inflation Factor (VIF) for a number of variables, which calculates the severity of multicollinearity. This is a quotient of the variance in a multi-criteria model by the variance of a model with one criterion alone (James et al. 2017).

The VIF is calculated by the following formula (Jensen and Ramirez 2012; Dupuis and Victoria-Feser 2013 and the references therein):

$$VIF_j = \frac{1}{1 - R_j^2} \quad (2)$$

where, VIF_j is the Variance Inflation Factor of the i th variable against all other predictor variables, R_j is the correlation coefficient of the j th independent variable on the remaining $(k-1)$ independent variable.

Under this scenario, the VIF for each parameter was calculated from multiple regression coefficients by treating one variable as the dependent and all other predictor variables as the independent variables. This process was reiterated for all other variables. The variables exhibiting a $VIF > 10$ were excluded from the MCDM analysis (Hair et al. 1995).

3.5 Data Normalization

After checking for the multicollinearity diagnostics, some of the parameters with VIF_j greater than 10 were removed and the rest were used for calculating the Index of Active Tectonics (IAT) for the Rangit Basin. It must be mentioned here that the units and the range of data for different factors are different. For example, whereas relative relief ranges from 1700 to 7000 m, hypsometric integral is unit less and ranges from 0 to 1. Hence, all the parameters were normalized to facilitate easy comparison. Normalization refers to a pre-processing stage when the raw values of all parameters are transformed according to a definite algorithm to get a new range of values (from 0 to 1) (Al Shalaby et al. 2006).

Amongst a myriad methods of data normalization, the Min–Max normalization has been taken for normalizing all the morphotectonic and morphological variables in the Rangit River Basin. This method was found to be of greater efficiency as compared to the other data normalization methods (Milligan and Cooper 1988). This method takes into account both the beneficial and non-beneficial factors. Beneficial factors represent the predictor variables that are favourable for the dependent factor. An area under active tectonics is characterized by higher values of basin asymmetry, hypsometric integral, stream gradient index, relative relief, relief ratio and slope. These factors were normalized by using the following expression:

$$X_{norm} = \frac{X - X_{min}}{X_{max} - X_{min}} \quad (3)$$

whereas the non-beneficial factors (predictor variable unfavourable for the dependent variable) for tectonics include elongation ratio and valley width-height ratio. These variables were normalized by Eq. (3).

$$X_{norm} = \frac{X_{max} - X}{X_{max} - X_{min}} \quad (4)$$

In Eqs. (2) and (3), X_{norm} is the normalized value for variable X , while X_{max} and X_{min} are the maximum and minimum values for variable X , respectively.

So, the normalized matrix is derived as follows:

$$\begin{bmatrix} X_{norm1} & \cdots & X_{normN} \\ \vdots & \ddots & \vdots \\ X_{normM} & \cdots & X_{normM} \end{bmatrix}$$

3.6 Index of Active Tectonics by Entropy Method

After normalizing the variables, the combined effect of all the causal factors was ascertained to differentiate the river basins on the basis of tectonic deformation. For this purpose, multi-criteria decision-making was applied to derive a combined Index of Active Tectonics (IAT) for the studied basin and its major tributaries. For multi-criteria problems, the determination of the variable weights is of prime importance. Amongst a number of MCDM techniques available in the literature, this study has incorporated the Information Entropy Method, for the determination of the weight of each of the predictor variables. This method is widely applied in studies on water resource monitoring (Li et al. 2011; Amiri et al. 2014; Chen et al. 2015 and the references therein). This method was devised by Shannon (1948) in the realm of information science. Entropy has been suggested as a measure of information or uncertainty in predicting the outcome of a probabilistic event.

The formula for weight determination by Information Entropy Method is given as follows (Amiri et al. 2014; Chen et al. 2015):

$$E_j = -h \sum_{i=1}^m x_{ij} \cdot \ln x_{ij} \quad (5)$$

where, E_j is the entropy parameter of the j th predictor variable, x_{ij} is the normalized value for each predictor variable for sub-basin i . The parameter h can be expressed as $h = 1/\ln(m)$ where m is the number of observations (sub-basins in this case). Then the weightage of each parameter (W_j) is calculated by using Eq. (6).

$$W_j = \frac{1 - E_j}{\sum (1 - E_j)} \quad (6)$$

After deriving the weightage of each predictor variable, the weightages of each parameter were multiplied with the normalized value of the corresponding parameter for individual sub-basins. These were summed up to get the Index of Active Tectonics (IAT) for each sub-basin as per the following formula:

$$IAT_i = \sum_{j=1}^n W_j * x_jnorm \quad (7)$$

where, IAT_i is the Index of Active Tectonics (IAT) for basin i , W_j is the weightage assigned to parameter j , x_jnorm is the normalized value (obtained from Eqs. 3 and 4) of the predictor variables for each morphotectonic and morphological attribute.

The IAT values for each sub-basin were then mapped in ArcGIS environment for deriving spatial variations in the relative tectonic activity for the Rangit Basin.

4 Neo-tectonic Movements and Channel Evolution

4.1 Inferences from Direct Morphotectonic Indices

The direct morphotectonic indices were calculated and mapped for all the sub-catchments of the Rangit Basin, as well as for the entire catchment (Table 2, Fig. 3).

It is evident that the values of HI for the studied sub-catchments are below 0.5, except for the Rammam (0.551), Prek Chu (0.514) and Manpur Khola (0.500). This implies that, by and large, the area-height relationships in the Rangit catchment depict concave patterns. This is typically observed in the catchments having modest tectonic and structural control (El Hamdouni et al. 2008). Incidentally, no specific pattern can be observed in the distribution of catchments possessing higher than 0.5 HI value, as each domain contains one such catchment. Interestingly, none of the sub-catchments have less than 0.339 HI value (the Rungji Chu), indicating that there is a significant proportion of area in the high-relief category. The average HI for the entire catchment is 0.304, which does not appear to be indicating intense erosion. However, all the sub-catchments are displaying values higher than the entire basin. The HI values are not as high as expected in the sub-catchments of the upper domain, which may point toward passive erosional regime.

As from Table 2, the average SL indices for the streams in the Rangit catchment range from 184 (Lapchu Khola) to 1530 (Rangit main stream). The average of these SL indices is 512. Higher than average SL values can be found for the large tributaries such as the Relli Chu (1142), Rammam (799), Rimbi Chu (796) and Prek Chu (663), besides the Rangit itself. Otherwise, all domains of the concerned study unit are characterized by the average SL Index value of less than 300 (the Rungji Chu and Tikip Chu in the upper domain; the Rothak Chu and Rinchu Khola in the middle

Table 2 Calculations of direct morphotectonic indices

	Rivers	Basin area (km ²)	HI	SL	V _f	R _e	A _f
Right bank tributaries	Rungji Chu	12.3	0.339	255	3.05	0.97	72.9
	Tikip Chu	23.6	0.498	294	3.04	0.60	67.7
	Yangsap Chu	55.1	0.490	302	2.43	0.73	49.0
	Rimbi Chu	161.9	0.476	796	2.81	0.75	51.3
	Kalej Chu	208.7	0.444	471	2.52	0.67	68.5
	Reshi Chu	45.0	0.437	389	3.09	0.58	53.3
	Rothak Chu	41.3	0.397	293	2.42	0.62	31.5
	Rammam	379.4	0.551	799	3.07	0.76	63.4
	Chhota Rangit	157.8	0.436	508	5.18	0.58	63.0
	Jhepi Khola	24.6	0.429	251	5.68	0.63	55.1
	Rongdong Khola	66.2	0.452	366	2.68	0.67	58.9
	Lapchu Khola	11.5	0.525	184	2.76	0.67	73.1
Left bank tributaries	Prek Chu	125.6	0.514	663	3.84	0.59	44.6
	Relli Chu	374.2	0.407	1142	2.33	0.82	20.8
	Rinchu Khola	29.8	0.482	235	1.94	0.78	30.2
	Manpur Khola	37.2	0.500	227	2.56	0.64	51.1
	Rangit Main Basin	2132.1	0.304	1530	2.51	0.76	63.5

domain; the Jhepi Khola, Manpur Khola and Lapchu Khola in the lower domain). Besides, the SL index values cannot be related to the position of the MCT, as sub-catchments possessing both high and low values are found on both flanks of the MCT.

From Table 2, it is evident that none of the tributaries in the catchments under consideration possess average V_f values of more than 6.0, which is certainly an indicator of rapid tectonic uplift (Kale and Shejwalkar 2007). The relatively lower values of V_f suggest dominance of vertical erosion over lateral erosion. Average V_f values for the left bank tributaries such as the Rinchu Khola (middle domain; 1.94) and Relli Chu (upper domain; 2.33), and the right bank tributaries viz. the Rothak Chu (middle domain; 2.42) and Yangsap Chu (upper domain; 2.43) are lower than other sub-catchments and the main channel of the Rangit River. This indicates the presence of narrower valleys in these tributaries. However, domain-wise, no systematic pattern can be observed for this valley shape parameter. Considering different segments of each tributary under consideration, the individual V_f values have never crossed 6.0 mark barring the Rimbi Chu, Reshi Chu, Chhota Rangit and Jhepi Khola (all right bank tributaries) (Fig. 4).

From the obtained results of R_e, it is clear that none of the catchments can be referred as extremely elongated as none of the values are below 0.5 (Table 2, Fig. 3). The right bank catchments of the Chhota Rangit (lower domain; 0.58), Reshi Chu

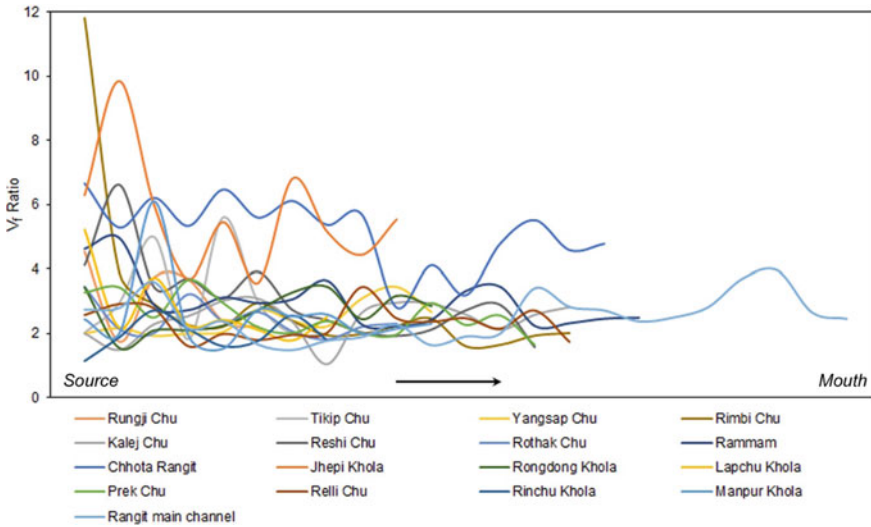


Fig. 4 Downstream variation of V_f for all streams of the Rangit Basin

(middle domain; 0.58) and Tikip Chu (upper domain; 0.60), and the left bank catchment of the Prek Chu (upper domain; 0.59) are significantly more elongated than the other catchments under study. Whereas, two upper domain catchments like the Rungji Chu (right bank; 0.97) and Relli Chu (left bank; 0.82) have comparatively higher R_e values, as there are significantly circular in shape. Interestingly, presence of lower number of elongated catchments is anomalous to the area supposedly going through active tectonic deformation. Incidentally, except the Rammam and Relli Chu, the tributaries under study have catchment area below 300 km² (Table 2). In a tectonically active region, the streams have a tendency to elongate through headward erosion with an increase in catchment area (Mulder and Syvitski 1996). This might be the reason behind relatively circular form of the catchments having smaller areal extents.

Barring the Rothak Chu (middle domain; 31.5) and Yangsap Chu (upper domain; 49.0), all the other right bank tributaries of the Rangit possess the A_f value above 50 (Table 2). This implies that the basin area to the right of the main channel is comparatively higher than the area to the left in most of the right bank tributaries. The situation is different for the left bank tributaries as only the Manpur Khola (lower domain) has the A_f value above 50, indicating more basin area to the left of the main channel in case of the other left bank tributaries. Notable examples of unidirectional catchment asymmetry can be seen for the Rungji Chu, Tikip Chu, Kalej Chu and Lapchu Khola (right bank tributaries), which have significantly more area to the right, and the Rothak Chu (right bank tributary), Relli Chu and Rinchu Khola (left bank tributaries), which have significantly more area to the left (Fig. 3). In fact, for the trunk-stream, the Rangit, the A_f value is 63.5, which signifies notably more area to the right than the left. The tributaries like the Yangsap Chu, Rimbi Chu, Reshi Chu and

Jhepi Khola (right bank tributaries), and the Manpur Khola (left bank tributary) do not show much deviation from the line of perfect symmetry, with A_f values ranging between 45.0 and 55.0. The characteristic unidirectional asymmetry that one would associate with tilting is mostly visible in the upper and middle domains. Subtle variations of A_f values for the other catchments can be attributed to local factors.

4.2 Inferences from Basin Morphological Indices

The relief-based morphological parameters were calculated and mapped for all the sub-catchments of the Rangit Basin, including the entire catchment (Table 3, Fig. 5).

The spatial variation in the relative relief of the Rangit Catchment is shown in Fig. 5. The average R_l across the catchments is 2798 m. This catchment is characterized by significantly higher R_l values for the left bank tributaries (the Relli Chu and Prek Chu; $R_l > 4000$ m) in the upper domain. Considerably high R_l values (R_l : 3000–4000 m) can be found in the middle domain catchments like the Rimbi Chu, Kalej Chu and Rammam (right bank tributaries). Interestingly, barring the Prek Chu, all these catchments are cut across by the MCT, and therefore can be related to the higher R_l values. Low R_l values ($R_l < 2000$ m) can be observed for the Lapchu Khola and Jhepi Khola catchments located in the lower domain. This is expected as these are two of the smallest catchments in the Rangit Basin. However, the relief ratio of these catchments reveals a different scenario (Table 3, Fig. 5). Higher R_r values ($R_r > 0.25$) are associated with some of the smaller catchments like the Rungji Chu, Tikip Chu and Lapchu Khola (right bank tributaries), and the Rinchu Khola (left bank tributary). This indicates higher potential sediment yield from these catchments comprised of highly resistant rocks, which indirectly specifies continuing tectonic activity. Conversely, relatively larger right bank tributaries like the Chhota Rangit, Rammam and Kalej Chu exhibit lower R_r values ($R_r < 0.15$), hinting toward less potential sediment yield.

An examination of the spatial variation across the catchments reveal that the average slope (gradient) is expectedly high ($S > 0.575 \text{ m}^{-1}$) for the upper domain tributaries like the Rungji Chu, Relli Chu and Kalej Chu (Table 3, Fig. 5). Whereas, relatively lower gradient ($S < 0.525 \text{ m}^{-1}$) is a characteristic of the middle and lower domain catchments on the right bank of the Rangit like the Reshi Chu, Rammam, Chhota Rangit, Jhepi Khola, Rongdong Khola and Lapchu Khola. In fact, the gradient map has substantial similarities with the relative relief map (Fig. 5). It appears that the lithological groups on both sides of the MCT have some influence on the differential gradient values across the mentioned domains. In addition to this, the average planform curvature is mostly positive across the catchments under study, with the exceptions of the Rongdong Khola and Lapchu Khola (Table 3). Higher P_{curv} values are related with the upper domain catchments like the Rungji Chu, Tikip Chu and Yangsap Chu (right bank tributaries), and the Prek Chu (left bank tributary), indicating greater flow divergence from these areas (Table 3, Fig. 5).

Table 3 Calculations of basin morphological indices

	Rivers	R _l	R _r	S	P _{curv}	DI	R _n	SPI
Right bank tributaries	Rungji Chu	2237.4	0.55	0.638	0.0199	0.324	1.096	-0.412
	Tikip Chu	2403.5	0.27	0.501	0.0300	0.395	1.541	-0.674
	Yangsap Chu	2473.6	0.21	0.527	0.0170	0.451	1.290	-0.417
	Rimbi Chu	3705.7	0.19	0.598	0.0027	0.803	0.947	-0.101
	Kalej Chu	3356.4	0.14	0.529	0.0045	0.864	0.788	-0.109
	Reshi Chu	2397.4	0.18	0.522	0.0044	0.845	0.716	-0.064
	Rothak Chu	2480.1	0.21	0.555	0.0082	0.877	0.728	0.076
	Rammam	3353.3	0.12	0.506	0.0042	0.915	0.723	-0.268
	Chhota Rangit	2762.5	0.11	0.511	0.0042	0.903	0.808	-0.170
	Jhepi Khola	1891.1	0.21	0.494	0.0028	0.873	1.215	-0.104
	Rongdong Khola	2302.3	0.17	0.495	-0.0002	0.895	0.619	-0.047
	Lapchu Khola	1748.9	0.31	0.511	-0.0047	0.883	1.080	0.056
Left bank tributaries	Prek Chu	4317.6	0.20	0.559	0.0119	0.666	1.154	-0.413
	Relli Chu	5087.6	0.19	0.617	0.0012	0.890	1.110	-0.115
	Rinchu Khola	2236.3	0.28	0.642	0.0028	0.851	0.812	0.335
	Manpur Khola	2008.4	0.19	0.569	0.0039	0.891	0.733	0.065
	Rangit Main Basin	7069.8	0.10	0.554	0.0054	0.972	0.928	-0.152

In the Rangit System, dissection amount ranges from 0.324 (low dissection) in the Rungji Chu catchment to 0.915 (high dissection) in the Rammam catchment (Table 3). Extremely high DI values are found in the larger tributary catchments of the middle and lower domains (Fig. 5). Surprisingly, these are not the areas possessing high relative relief. On the other hand, moderate to high DI values can be found in the upper domain tributaries (the Prek Chu and Relli Chu) having high relative relief. Significantly low DI values are found in the smaller catchments of the upper domain like the Rungji Chu, Tikip Chu and Yangsap Chu, which implies modest rates of erosion in these areas. In addition to this, it is found that the topography is more rugged in the smaller catchments on the right bank of the Rangit viz. the Rungji Chu, Tikip Chu, Yangsap Chu, Jhepi Khola and Lapchu Khola, and in the larger catchments on the left bank of the Rangit viz. the Prek Chu and Relli Chu (Table 3, Fig. 5). While the areas having greater R_n values are more erosion-prone, comparatively lower R_n values can be found in the larger catchments like the Rammam and Chhota Rangit, which are surprisingly more dissected.

In the concerned study area, more stream power is observed in the smaller catchments of the middle and lower domains like the Rothak Chu and Lapchu Khola

(right bank tributaries), and the Rinchu Khola and Manpur Khola (left bank tributaries), indicating that these areas are currently under strong erosional regime. On the contrary, low SPI values are associated with the upper domain tributaries like the Rungji Chu, Tikip Chu and Yangsap Chu (right bank tributaries), and the Prek Chu (left bank tributary). Interestingly, all these upper domain catchments also possess low DI values. This confirms the absence of intense erosional activities in these areas.

4.3 Multicollinearity Diagnostics

As stated earlier, the multicollinearity of variables is assessed by means of the Variance Inflation Factor (VIF). In various studies, it has been repeatedly pointed out that a VIF of 10 or greater indicates high degree of multicollinearity amongst the predictor variables (Wang et al. 2008; Dormann et al. 2013). Therefore, the VIF was performed for each of the morphological and morphotectonic attribute so as to ascertain the redundant variables in the Rangit Basin. The results are outlined in Table 4. It is clear from the table that the Variance Inflation Factor for relative relief, slope and dissection index are above 10. This is understandable as relative relief; dissection index and ruggedness number are mutually interrelated, as evident from the formulae for these parameters. Similarly, slope and stream power index are mutually interrelated (Table 1). Therefore, the parameters of relative relief, dissection index and slope are removed from the final analysis for computation of the IAT. Therefore, the total number of variables is reduced to nine, which are listed as following: morphotectonic indices viz. hypsometric integral (HI), stream gradient

Table 4 VIF outcomes for different parameters

	Parameters	VIF	Entropy weights	Relative importance (%)
Direct morphotectonic indices	HI	3.73	0.1232	12.32
	SL	6.12	0.1236	12.36
	V _f	3.47	0.1015	10.15
	R _e	6.29	0.0165	1.65
	A _f	2.80	0.0791	7.91
Basin morphological indices	R _l	33.33	NA	NA
	R _r	9.75	0.1296	12.96
	S	12.50	NA	NA
	P _{curv}	9.50	0.1630	16.30
	DI	41.67	NA	NA
	R _n	4.48	0.1329	13.29
	SPI	7.68	0.1360	13.60

NA = Parameters not considered for the analysis

index (SL), valley width-height ratio (V_f), elongation ratio (R_e) and basin asymmetric factor (A_f), and basin morphological attributes viz. relief ratio (R_r), profile curvature (P_{curv}), ruggedness number (R_n) and stream power index (SPI). These nine parameters went through the mathematical operation as per Eq. (7) to derive the IAT for all the sub-basins in the Rangit Basin.

4.4 Index of Active Tectonics (IAT) of the Rangit Basin

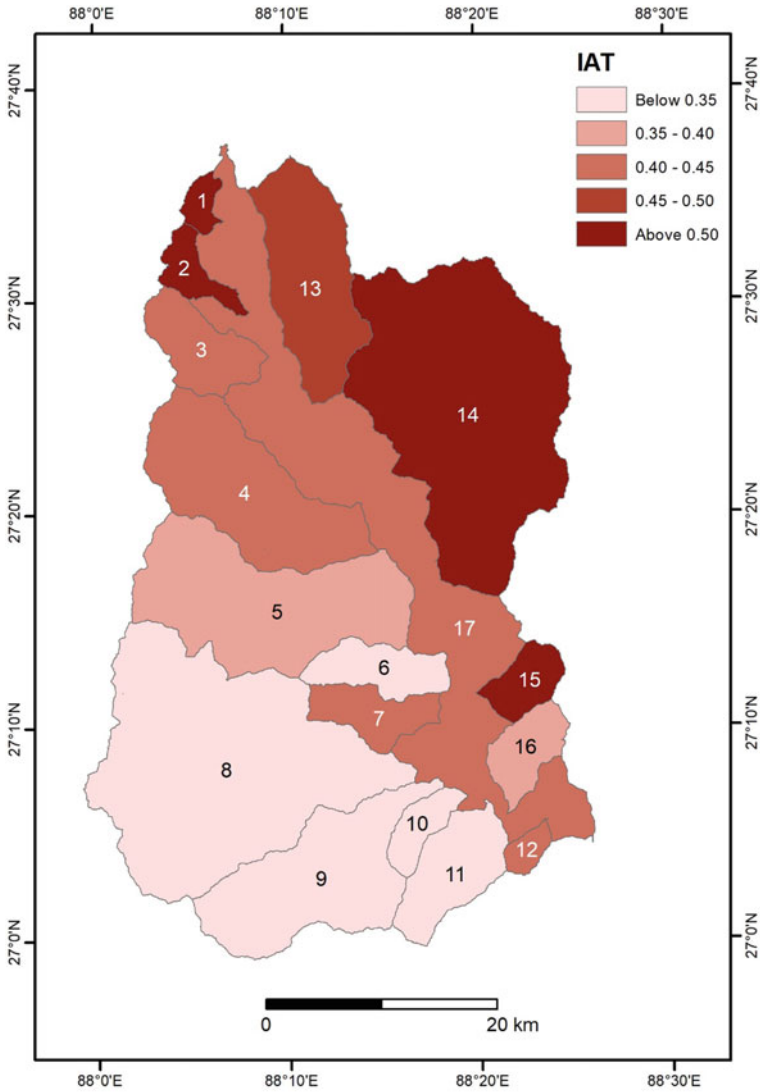
Unequal weightages to the morphotectonic and basin morphological parameters of the Rangit Basin were assigned on the basis of the Entropy analysis. As revealed from Table 4, the most influencing factor in this area is the profile curvature (16.30%), followed by stream power index (13.60%) and ruggedness number (13.29%). Among the morphotectonic attributes, average SL Index (12.35%) influences the most, followed by hypsometric integral (12.32%) and valley width-height ratio (10.15%).

The spatial variation of IAT along the Rangit Basin has been mapped and displayed in Fig. 6. It is evident that the left bank tributaries of the Rangit River viz. Relli Chu (0.54), Rinchu Khola (0.52), Prek Chu (0.48) etc. display higher magnitudes of IAT as compared to the right bank tributaries. Notable exceptions of high IAT values in the right bank tributaries include the Rungji Chu (0.52) and the Tikip Chu (0.51). Therefore, the occurrence of strong regional skewness with respect to the left bank tributaries gives an impression of regional tilt towards the right bank. This is corroborated by the fact that the basin asymmetric factor of the Rangit Basin as a whole is about 63.5, suggesting more areas to the right as compared to the left.

Another notable observation that cannot be ignored is the presence of an inter-domain difference in the IAT. Even a cursory examination of the map depicting the spatial variation of IAT in the studied basin reveals that the IAT values are higher in the upper and middle domains as compared to the lower domain of the Rangit Basin (Fig. 6). This is applicable for both the right and the left bank tributaries. Therefore, it would be reasonable to assume that whereas the upper and middle domains of the Rangit Basin display numerous evidences of tectonically-controlled drainage, the lower domain is characterized by rather depositional environment as revealed by subdued values of IAT.

5 Conclusion

This study was carried out to ascertain the relative effects of surficial geomorphic processes to recent tectonic activity. Since fluvial systems are recognized to be one of the most sensitive expressions to tectonic diastrophism, it is expected that the rivers will swiftly respond to underlying tectonic activity in the form of morphological changes, both at the reach scale and the basin scale. Fluvial morphotectonic and morphological indices of such streams will, therefore, be highly elevated as compared



- 1. Rungji Chu
- 2. Tikip Chu
- 3. Yangsap Chu
- 4. Rimbi Chu
- 5. Kalej Chu
- 6. Reshi Chu
- 7. Rothak Chu
- 8. Rammam
- 9. Chhota Rangit
- 10. Jhepi Khola
- 11. Rongdong Khola
- 12. Lapchu Khola
- 13. Prek Chu
- 14. Relli Chu
- 15. Rinchu Khola
- 16. Manpur Khola
- 17. Rangit

Fig. 6 Variations in the index of active tectonics (IAT) observed for the sub-catchments of the Rangit Basin. The IAT value associated with the Rangit (Basin ID: 17) represents the IAT for the entire catchment

to those under long-term tectonic quiescence. The Himalayas are universally recognized to be under active tectonic regime as revealed by various researchers (Seeber and Gornitz 1983; Brookfield 1998 etc.). So, it is expected that the rivers draining this orogenic belt must reflect anomalous values of geomorphic indices. Hence, this study was conducted to verify whether the much-talked about active tectonic diastrophism in the Himalayas in general, and Eastern Himalayas in particular is reflected in the fluvial morphology of the rivers flowing across this region.

The fluvial indices investigated here include the morphotectonic (hypsometric integral, stream length-gradient index, valley width-height ratio, basin elongation ratio, and basin asymmetry factor) as well as morphological ones (relative relief, relief ratio, slope, planform curvature, dissection index, ruggedness number, and stream power index). This paper treats tectonic activity as a multi-criteria problem and a composite index based on the Information Entropy Method, termed as Index of Active Tectonics (IAT), is proposed to assess the degree of tectonic activity in the Rangit catchment.

Analysis reveals that the left bank tributaries of the Rangit River are characterized by relatively higher degree of tectonic activity as compared to the right bank tributaries. Isolation of lithology on the tectonic effects was done by considering the geological map displayed in Fig. 2. Even a quick comparison of the lithologic groups (Fig. 2) and the obtained sub-basin wise IAT values (Fig. 6) reveals no direct role of lithology and IAT. This is exemplified by the fact that the tributaries such as the Relli Chu and Rinchu Khola, which display higher values of IAT, are more or less concentrated in the crystalline belts of Darjeeling Gneiss and Daling Formation. However, the same belts comprise the rivers such as the Rammam, Chhota Rangit, etc. which are characterized by relatively subdued rates of tectonic activity. So, lithology does not appear to be an important factor in the spatial variation of IAT values. It may be mentioned that the Main Central Thrust (MCT) sandwiched between the Greater and the Lesser Himalayas, roughly as a demarcating line between the left and right bank tributaries. Although it is well-recognized that the Himalayas are currently under active tectonic deformation, the status of the MCT has not been solved yet. Whereas the Evolutionary Model proposes that the MCT has attained stability after the formation of the Main Boundary Thrust (MBT) in the Plio-Pleistocene (Sinha-Roy 1982; Chemenda et al. 2000; Mukhopadhyay et al. 2017), the Steady-State Model assumes that the MCT is currently active in the Holocene (Seeber and Armbruster 1981; Ni 1989). The tributaries such as the Prek Chu, Relli Chu and Rinchu Khola, which exhibit higher degree of tectonic deformation, are situated to the east of the MCT, whereas to the west of the MCT, the tributaries such as the Kalej Chu, Rammam, Chhota Rangit and Jhepi Khola are characterized by relatively lower degree of tectonic activity and control. Therefore, it may be stated with a reasonable degree of certainty that there is substantial displacement along the MCT which is reflected in the differences in IAT between the tributaries to the east and west of the MCT. Therefore, this study substantiates the Steady-State Model which proposes faulting and displacement along the MCT. Apart from the fluvial indices, numerous seismic activities in the vicinity of this region suggests tectonic resurgence along the MCT.

References

- Acharya SK, Ray KK (1977) Geology of the Darjeeling-Sikkim Himalaya. In: Fourth international gondwana symposium, India, Report, 22 p
- Al Shalaby L, Shaaban Z, Kasasbeh B (2006) Data mining: a preprocessing engine. *J Comput Sci* 2(9):735–739. <https://doi.org/10.3844/jcssp.2006.735.739>
- Altaf F, Meraj G, Romshoo SA (2013) Morphometric analysis to infer hydrological behaviour of Lidder Watershed, Western Himalaya, India. *Geogr J* 178021:1–14. <https://doi.org/10.1155/2013/178021>
- Amiri V, Rezaei M, Sohrabi N (2014) Groundwater quality assessment using entropy weighted water quality index (EWQI) in Lenjanat, Iran. *Environ Earth Sci* 72:3479–3490. <https://doi.org/10.1007/s12665-014-3255-0>
- Asfaw D, Workneh G (2019) Quantitative analysis of morphometry on Ribb and Gumara watersheds: implications for soil and water conservation. *Int Soil Water Conserv Res* 7:150–157. <https://doi.org/10.1016/j.iswcr.2019.02.003>
- Basu SK (2013) Geology of Sikkim State and Darjeeling District of West Bengal. Geological Society of India, Bangalore, pp 37–81
- Bhatt CM, Litoria PK, Sharma PK (2008) Geomorphic signatures of active tectonics in Bist Doab interfluvial tract of Punjab, NW India. *J Indian Soc Remote Sens* 36:361–373. <https://doi.org/10.1007/s12524-008-0036-9>
- Bilham R (1995) Location and magnitude of the 1833 Nepal earthquake and its relation to the rupture zones of contiguous great Himalayan earthquake. *Curr Sci* 69:101–128
- Brookfield ME (1998) The evolution of the great river systems of southern Asia during the Cenozoic India–Asia collision: riverdraining southwards. *Geomorphology* 22:285–312. [https://doi.org/10.1016/S0169-555X\(97\)00082-2](https://doi.org/10.1016/S0169-555X(97)00082-2)
- Bull WB, McFadden LD (1977) Tectonic geomorphology north and south of the Garlock fault, California. In: Doehring DO (ed) *Geomorphology in arid regions*. Proceedings of the 8th annual geomorphology symposium, State University of New York, Binghamton, pp 115–138
- Burian L, Mitusov AV and Poesen J (2015) Relationships of attributes of gullies with morphometric variables. In: Jasiewicz J, Zwoliński Z, Mitasova H (eds) *Geomorphometry for Geosciences*. Poznań, Poland: Institute of Geoecology and Geoinformation, pp 111–114
- CGWB: Central Ground Water Board (2018) South Sikkim district. Ground Water Information Booklet. http://cgwb.gov.in/District_Profile/Sikkim/South_sikkim.pdf Accessed 6 Apr 2020
- Chemenda AI, Burg JP, Mattauer M (2000) Evolutionary model of the Himalaya-Tibet system: geopoem: based on new modelling, geological and geophysical data. *Earth Planet Sci Lett* 174(3–4):397–409. [https://doi.org/10.1016/S0012-821X\(99\)00277-0](https://doi.org/10.1016/S0012-821X(99)00277-0)
- Chen Y, Courtillot V, Cogné JP, Besse J, Yang Z, Enkin R (1993) The configuration of Asia prior to the collision of India: cretaceous palaeomagnetic constraints. *J Geophys Res* 98(B12):21927–21942. <https://doi.org/10.1029/93JB02075>
- Chen J, Zhang Y, Chen Z, Nie Z (2015) Improving assessment of groundwater sustainability with analytical hierarchy process and information entropy method: a case study of Hohhot Plain, China. *Environ Earth Sci* 73:2353–2363. <https://doi.org/10.1007/s12665-014-3583-0>
- Choudhuri B, Gururajan N, Bikramaditya RK (2009) Geology and structural evolution of the eastern Himalayan Syntaxis. *Himal Geol* 30:17–34
- Clarke KC, Romero BE (2017) On the topology of topography: a review. *Cartogr Geogr Inf Sci* 44:271–282. <https://doi.org/10.1080/15230406.2016.1164625>
- Clarke JJ (1966) *Morphometry from map*. Essays in geomorphology, Elsevier, New York, pp 235–274
- Curry JR, Emmel FJ, Moore DG, Raitt RW (1982) Structure, tectonics and geological history of the northeastern Indian ocean. In: Nairn AEM, Stehli FG (eds) *Ocean basins and margins*. Springer, Boston, MA, pp 399–450. https://doi.org/10.1007/978-1-4615-8038-6_9
- Daoud JI (2012) Multicollinearity and regression analysis. *J Phys: Conf Ser* 949:012009. <https://doi.org/10.1088/1742-6596/949/1/012009>

- Das A, Agrawal R, Mohan S (2015) Topographic correction of ALOS-PALSAR images using InSAR-derived DEM. *Geocarto Int* 30(2):145–153. <https://doi.org/10.1080/10106049.2014.883436>
- Das S, Patel PP, Sengupta S (2016) Evaluation of different digital elevation models for analyzing drainage morphometric parameters in a mountainous terrain: a case study of the Supin-Upper Tons Basin Indian Himalayas. *Springerplus* 5(1544):1–38. <https://doi.org/10.1186/s40064-016-3207-0>
- Das S, Roy L, Sarkar A, Sengupta S (2020) Mathematical modelling of long profiles in a tectonically active area: observations from the DEM-based geomorphometry of the Rangit River, India. In: Alvioni M, Marchesini I, Melelli L, Guth P (eds) *Proceedings of the geomorphometry 2020 Conference*, pp 124–127. https://doi.org/10.30437/GEOMORPHOMETRY2020_35
- de la Torre TL, Monslave AF, Sheehan S, Sapkota S, Wu F (2007) Earthquake processes of the Himalayan collision zone in eastern Nepal and southern Tibet plateau. *Geophys J Int* 171:718–738. <https://doi.org/10.1111/j.1365-246X.2007.03537.x>
- Demoulin A (1998) Testing the tectonic significance of some parameters of longitudinal river profiles: the case of the Ardenne (Belgium, NW Europe). *Geomorphology* 24(2–3):189–208. [https://doi.org/10.1016/S0169-555X\(98\)00016-6](https://doi.org/10.1016/S0169-555X(98)00016-6)
- Dormann CF, Elith J, Bacher S, Buchmann C, Carl G, Carre G, Garcia Marquez JR, Gruber B, Lafourcade B, Leitao PJ, Munkemuller T, McLean C, Osborne PE, Reineking B, Schroder B, Skidmore AK, Zurell D, Lautenbach S (2013) Collinearity: a review of methods to deal with it and a simulation study evaluating their performance. *Ecography* 36:27–46. <https://doi.org/10.1111/j.1600-0587.2012.07348.x>
- Dupuis DJ, Victoria-Feser M (2013) Robust VIF regression with application to variable selection in large data sets. *Ann Appl Stat* 7(1):319–341. <https://doi.org/10.1214/12-AOAS584>
- El Hamdouni R, Irigaray C, Fernández T, Chacón J, Keller EA (2008) Assessment of relative active tectonics, southwest border of the Sierra Nevada (southern Spain). *Geomorphology* 96(1–2):150–173. <https://doi.org/10.1016/j.geomorph.2007.08.004>
- Evans IS (2012) Geomorphometry and landform mapping: What is a landform? *Geomorphology* 137(1):94–106. <https://doi.org/10.1016/j.geomorph.2010.09.029>
- Ferraris F, Firpo M, Pazzaglia FJ (2012) DEM analyses and morphotectonic interpretation: the Plio-Quaternary evolution of the eastern Ligurian Alps, Italy. *Geomorphology* 149–150:27–40. <https://doi.org/10.1016/j.geomorph.2012.01.009>
- Florinsky IV (2017) An illustrated introduction to general geomorphometry. *Prog Phys Geogr* 41(6):723–752. <https://doi.org/10.1177/0309133317733667>
- Goudie AS (2004) *Encyclopedia of geomorphology*, vol 1. Routledge, London, pp 434–439
- GSI: Geological Survey of India (2012) *Geology and Mineral Resources of the States of India*, Pt. 1: Sikkim, Miscel Pub 30(XIX), 55p
- Habibi A, Gharibreza M (2015) Estimation of the relative active tectonics in Shahriary basin (Central Iran) using geomorphic and seismicity indices. *Nat Environ Change* 1(1):71–83
- Hack JT (1973) Stream profile analysis and stream-gradient index. *J Res US Geol Surv* 1(4):421–429
- Hair JF Jr, Anderson RE, Tatham RL, Black WC (1995) *Multivariate data analysis*, 3rd edn. Macmillan, USA
- Horton RE (1932) Drainage basin characteristics. *Trans Am Geophys Union* 13:350–361. <https://doi.org/10.1029/TR013i001p00350>
- Horton RE (1945) Erosional development of streams and their drainage basins: hydrophysical approach to quantitative morphology. *Geol Soc Am Bull* 56(3):275–370. <https://doi.org/10.1177/030913339501900406>
- IMD: India Meteorological Department (2018) Customized Rainfall Information System (CRIS). Hydromet Division, India Meteorological Department, Ministry of Earth Sciences, New Delhi. [http://hydro.imd.gov.in/hydrometweb/\(S\(uw4ptqehyw3huc452eqfpi55\)\)/DistrictRaifall.aspx](http://hydro.imd.gov.in/hydrometweb/(S(uw4ptqehyw3huc452eqfpi55))/DistrictRaifall.aspx). Accessed 16 Mar 2020

- Jacques PD, Salvador ED, Machado R, Grohmann CH, Nummer AR (2014) Application of morphometry in neotectonic studies at the eastern edge of the Parana Basin, Santa Catarina State, Brazil. *Geomorphology* 213:13–23. <https://doi.org/10.1016/j.geomorph.2013.12.037>
- Jade S, Mukul M, Bhattacharyya AK, Vijayan MSM, Jagannathan S, Kumar A, Tiwari RP, Kumar A, Kalita S, Sahu SC, Krishna AP (2007) Estimates of interseismic deformation in Northeast India from GPS measurements. *Earth Planet Sci Lett* 263(3–4):221–234. <https://doi.org/10.1016/j.epsl.2007.08.031>
- Jain V, Sinha R (2005) Response of active tectonics on the alluvial Baghmati River, Himalayan foreland basin, eastern India. *Geomorphology* 70:339–356. <https://doi.org/10.1016/j.geomorph.2005.02.012>
- James G, Witten D, Hastie T, Tibshirani R (2017) *An introduction to statistical learning*, 8th edn. Springer Science and Business Media, USA
- Jensen DR, Ramirez DE (2012) Variance Inflation in regression. *Adv Decis Sci* 2013(671204):1–15. <https://doi.org/10.1155/2013/671204>
- Jensen SK, Domingue JO (1988) Extracting topographic structure from digital elevation data for geographic information system analysis. *Photogramm Eng Remote Sens* 54:1593–1600
- Kale VS, Shejwalkar N (2007) Western ghat escarpment evolution in the deccan basalt province: geomorphic observations based on DEM analysis. *J Geol Soc India* 70(3):459–473
- Kale VS, Sengupta S, Achyuthan H, Jaiswal MK (2014) Tectonic controls upon Kaveri River drainage, cratonic Peninsular India: inferences from longitudinal profiles, morphotectonic indices, hanging valleys and fluvial records. *Geomorphology* 227:153–165. <https://doi.org/10.1016/j.geomorph.2013.07.027>
- Keat PG, Young PKY, Banerjee S (2009) *Managerial Economics*, 6th edn. Pearson Education Inc.
- Keller EA, Pinter N (1996) *Active tectonics: earthquakes uplift and landscapes*. Prentice Hall, New Jersey, p 338
- Klootwijk CT, Conaghan PJ, Powell CMcA (1985) The Himalayan arc: large-scale continental subduction, oroclinal bending and back-arc spreading. *Earth Planet Sci Lett* 75(2–3):167–183. [https://doi.org/10.1016/0012-821X\(85\)90099-8](https://doi.org/10.1016/0012-821X(85)90099-8)
- Lambert D (1997) *The field guide to geology*. Checkmark Books, pp 130–138
- Le Fort P, Cronin VS (1988) Granites in the tectonic evolution of the Himalaya, Karakoram and Southern Tibet. *Phil Trans R Soc Lond A* 326(1589):281–299. <https://doi.org/10.1098/rsta.1988.0088>
- Leopold LB, Wolman MG, Miller JP (1964) *Fluvial processes in geomorphology*. W.H. Freeman & Company, San Francisco, USA, 544 p
- Li X, Wang K, Liu L, Xin J, Yang H, Gao C (2011) Application of the entropy weight and TOPSIS method in safety evaluation in coal mines. *Procedia Eng* 26:2086–2091. <https://doi.org/10.1016/j.proeng.2011.11.2410>
- Malik JN, Mohanty C (2007) Active tectonic influence on the evolution of drainage and landscape: geomorphic signatures from frontal and hinterland areas along the northwestern Himalaya, India. *J Asian Earth Sci* 29:604–618. <https://doi.org/10.1016/j.jseaes.2006.03.010>
- Mela CF, Kopalle PK (2002) The impact of collinearity on regression analysis: the asymmetric effect of negative and positive correlation. *J Appl Econ* 34(6):667–677. <https://doi.org/10.1080/00036840110058482>
- Melton MA (1965) The geomorphic and paleoclimatic significance of alluvial deposits in Southern Arizona. *Geol Soc Am Bull* 73(1):1–38. <https://doi.org/10.1086/627044>
- Mesa LM (2006) Morphometric analysis of a subtropical Andean basin (Tucuman, Argentina) *Environ Geol* 50(8):1235–1242. <https://doi.org/10.1007/s00254-006-0297-y>
- Milligan GW, Cooper MC (1988) A study of standardization of variables in cluster analysis. *J Classif* 5:181–204. <https://doi.org/10.1007/BF01897163>
- Moore ID, Burch G (1986) Physical basis of the length-slope factor in the Universal Soil Loss Equation. *Soil Sci Soc Am J* 50(5):1294–1298. <https://doi.org/10.2136/sssaj1986.0361599500500050042x>

- Moore ID, Grayson RB, Ladson AR (1991) Digital terrain modeling: a review of hydrological, geomorphological, and biological applications. *Hydrol Process* 5(1):3–30. <https://doi.org/10.1002/hyp.3360050103>
- Moore ID, Gessler PE, Nielsen GA, Peterson GA (1993) Soil attribute prediction using terrain analysis. *Soil Sci Soc Am J* 57(2):443–452. <https://doi.org/10.2136/sssaj1993.03615995005700020026x>
- Mukhopadhyay DK, Chakraborty S, Trepmann C, Rubatto D, Anczkiewicz R, Gaides F, Dasgupta S, Chowdhury P (2017) The nature and evolution of the Main Central Thrust: structural and geochronological constraints from the Sikkim Himalaya, NE India. *Lithos* 282–283:447–463. <https://doi.org/10.1016/j.lithos.2017.01.015>
- Mulder T, Syvitski J (1996) Climatic and morphologic relationships of rivers: implications of sea-level fluctuations on river loads. *J Geol* 104(5):509–523. <https://doi.org/10.1086/629849>
- Ni JF (1989) Active tectonics of the Himalaya. *Proc Indian Acad Sci (Earth Planet Sci)* 98(1):71–89
- Niipele JN, Chen J (2019) The usefulness of alos-palsar dem data for drainage extraction in semi-arid environments in the Iishana sub-basin. *J Hydrol Reg Stud* 21:57–67. <https://doi.org/10.1016/j.ejrh.2018.11.003>
- Nir D (1957) The ratio of relative and absolute altitudes of Mt. Carmel: a contribution to the problem of relief analysis and relief classification. *Geogr Rev* 47(4):564–569. <https://doi.org/10.2307/211866>
- O’Callaghan JF, Mark DM (1984) The extraction of drainage networks from digital elevation data. *Comput Gr Image Process* 28(3):323–344. [https://doi.org/10.1016/S0734-189X\(84\)80011-0](https://doi.org/10.1016/S0734-189X(84)80011-0)
- Oguchi T (1997) Drainage density and relative relief in humid steep mountains with frequent slope failure. *Earth Surf Proc Land* 22(2):107–120. [https://doi.org/10.1002/\(SICI\)1096-9837\(199702\)22:2%3c107::AID-ESP680%3e3.0.CO;2-U](https://doi.org/10.1002/(SICI)1096-9837(199702)22:2%3c107::AID-ESP680%3e3.0.CO;2-U)
- Pavlis NK, Holmes SA, Kenyon SC, Factor JK (2012) The development and evaluation of the Earth Gravitational Model 2008 (EGM 2008). *J Geophys Res* 117:B04406. <https://doi.org/10.1029/2011JB008916>
- Phillips JD (1988) The role of spatial scale in geomorphic systems. *Geogr Anal* 20(4):308–317. <https://doi.org/10.1111/j.1538-4632.1988.tb00185.x>
- Pike RI, Wilson SE (1971) Elevation-relief ratio, hypsometric integral, and geomorphic area altitude analysis. *Geol Soc Am Bull* 82:1079–1084. [https://doi.org/10.1130/0016-7606\(1971\)82\[1079:ERHIAG\]2.0.CO;2](https://doi.org/10.1130/0016-7606(1971)82[1079:ERHIAG]2.0.CO;2)
- Pradhan R, Prajapati SK, Chopra S, Kumar A, Bansal BK, Reddy CD (2013) Causative source of Mw 6.9 Sikkim-Nepal border earthquake of September 2011: GPS baseline observations and strain analysis. *J Asian Earth Sci* 70–71:179–192. <https://doi.org/10.1016/j.jseas.2013.03.012>
- Quanru G, Guitang P, Zheng L, Chen Z, Fisher RD, Sun Z, Ou C, Dong H, Wang X, Li S, Lou X, Fu H (2006) The Eastern Himalayan syntaxis: major tectonic domains, ophiolitic mélanges and geologic evolution. *J Asian Earth Sci* 27(3):265–285. <https://doi.org/10.1016/j.jseas.2005.03.009>
- Roy AB, Purohit R (2018) The Himalayas: evolution through collision. Indian shield: precambrian evolution and phanerozoic reconstitution, pp 311–327. <https://doi.org/10.1016/B978-0-12-809839-4.00018-7>
- Sarkar A, Roy L, Das S, Sengupta S (2021) Fluvial response to active tectonics: analysis of DEM-derived longitudinal profiles in the Rangit River Basin, Eastern Himalayas India. *Environ Earth Sci* 80:258. <https://doi.org/10.1007/s12665-021-09561-2>
- Schumm SA (1956) Evolution of drainage systems and slopes in badlands at Perth Amboy, New Jersey. *Geol Soc Am Bull* 56:275–370. [https://doi.org/10.1130/0016-7606\(1956\)67\[597:EOD SAS\]2.0.CO;2](https://doi.org/10.1130/0016-7606(1956)67[597:EOD SAS]2.0.CO;2)
- Seeber L, Armbruster JG (1981) Great detachment earthquakes along the Himalayan Arc and long-term forecasting. In: Simpson DW and Richards PG (eds) *Earthquake prediction: an international review*. Maurice Ewing series, vol 4. American Geophysical Union, Washington DC, pp 259–277. <https://doi.org/10.1029/ME004p0259>.

- Seeber L, Gornitz V (1983) River profiles along the Himalayan arc as indicators of active tectonics. *Tectonophysics* 92(4):335–337, 341–367. [https://doi.org/10.1016/0040-1951\(83\)90201-9](https://doi.org/10.1016/0040-1951(83)90201-9)
- Shannon CE (1948) A mathematical theory of communication. *Bell Syst Tech J* 27(379–423):623–656. <https://doi.org/10.1002/j.1538-7305.1948.tb01338.x>
- Shtober-Zisu N, Greenbaum N, Inbar M, Flexer A (2008) Morphometric and geomorphic approaches for assessment of tectonic activity, Dead Sea Rift, Israel. *Geomorphology* 102:93–104. <https://doi.org/10.1016/j.geomorph.2007.06.017>
- Singh A, Kumar MR, Raju PS (2010) Seismic structure of the underthrusting Indian crust in Sikkim Himalaya. *Tectonics* 29(6):TC6021. <https://doi.org/10.1029/2010TC002722>
- Sinha-Roy S (1974) Polymetamorphism in the Daling rocks from a part of the Eastern Himalayas and the problems of Himalayan metamorphism. *Himal Geol* 4:74–101
- Sinha-Roy S (1977) Metamorphism and tectonics of the Himalayas as illustrated in the Eastern Himalayas. *Geotectonics* 11:120–124
- Sinha-Roy S (1982) Himalayan main central thrust and its implications for Himalayan inverted metamorphism. *Tectonophysics* 84:197–224. [https://doi.org/10.1016/0040-1951\(82\)90160-3](https://doi.org/10.1016/0040-1951(82)90160-3)
- Strahler AN (1957) Quantitative analysis of watershed geomorphology. *Trans Am Geophys Union* 38:913–920. <https://doi.org/10.1029/TR038i006p00913>
- Thakur VC, Mahajan AK, Gupta V (2012) Seismotectonics of 18 September 2011 Sikkim earthquake: a component of transcurrent deformation in eastern Himalaya. *Himal Geol* 33(1):89–96
- Valensise G, Burbank DW, Anderson RS (2013) Tectonic geomorphology. *J Seismol* 17:1355–1356. <https://doi.org/10.1007/s10950-013-9376-1>
- Vijith H, Dodge-Wan D (2019) Modelling terrain erosion susceptibility of logged and regenerated forested region in northern Borneo through the Analytical Hierarchy Process (AHP) and GIS techniques. *Geoenviron Disast* 6:8. <https://doi.org/10.1186/s40677-019-0124-x>
- Vommi VB (2017) TOPSIS with statistical distances: a new approach to MADM. *Decis Sci Lett* 6(1):49–66
- Wang H, Wang G, Wang F, Sassa K, Chen Y (2008) Probabilistic modelling of seismically triggered landslides using Monte Carlo simulations. *Landslides* 5:387–395. <https://doi.org/10.1007/s10346-008-0131-6>
- Zevenbergen LW, Thorne CR (1987) Quantitative analysis of land surface topography. *Earth Surf Proc Land* 12:47–56. <https://doi.org/10.1002/esp.3290120107>

Role of Active Tectonism and Geomorphic Drivers on Channel Oscillation of the Raidak-I River in the Eastern Himalayan Foothills, India



Md. Hasanuzzaman, Pravat Kumar Shit, and Aznarul Islam

Abstract The dynamicity of the channel is the main characteristic of the Raidak-I River in the eastern Himalayan foothill. The present study evaluates riverbank migration in association with erosion–deposition changes along the river Raidak-I using DSAS models. The present work intends to evaluate the relationship between the riverbank erosion–deposition and geomorphological and tectonic adjustment. For the study, earth observatory data like MSS, TM, ETM+ and OLI datasets of 1972, 1979, 1987, 1995, 2003, 2011, and 2020 have been used to demarcate the bankline position. Temporal analysis reveals that the river has changed its bank position by extensive erosion-accretion processes and modified its floodplain area uses significantly. The historical positions of both banklines indicate that a large portion of the floodplain area depicts an erosion-accretion sequence with time. In the timeframe of the last 48 years, the Raidak-I River has an average erosion–deposition at -0.23 m/year on the right bank and 1.57 m/y on the left bank. A general observation from this research is that the most dynamic or migrant part of the river is zone A and zone B compared to zone C which is relatively stable. In this study, the river course in zone C (both banks) is the most dynamic part of this entire river. The changes by the direct effect of banking migration have a bad impact on the dwellers of the floodplain adjacent village area of the river. The results of this study can represent an important indicator of the vulnerability of the Raidak-I River buffer area and also provide information about the geomorphological instabilities of the study area.

Keywords DSAS · Erosion–deposition · Himalayan foothill · Alluvial channel · Remote sensing

Md. Hasanuzzaman · P. K. Shit (✉)

PG Department of Geography Raja N. L. Khan Women's College (Autonomous), Midnapore 721102, India

A. Islam

Department of Geography, Aliah University, 17 Gora Chand Road, Kolkata 700014, India

1 Introduction

The foothills region of an active orogenic belt such as the Himalayas is characterized by active faults and complex alluvial morphology with fluvial erosion and deposition (Burbank and Anderson 2001). The eastern Himalayan foothills, east of the Tista River in West Bengal depicted a large piedmont area, which is drained by numerous major and minor rivers. These rivers brought immense load from the Himalayas in form of boulders, gravels, sand, and silt, and deposit the coarser ones at the foothills in the extreme north due to lesser slopes (Starkel et al. 2008) while accrete the finer particles in the south (parts of Darjeeling, Jalpaiguri and Alipurduar districts and entire Coochbehar district) to form and shape their wide, flat and almost monotonous floodplains subjected to inundation for multiple times even in a single monsoon season hampering the livelihoods of the floodplain dwellers. An alluvial river floodplain area of the Himalayan foothills experiences frequent periodical and seasonal variations as a result of channel migration through erosion deposition (Bastawesy et al. 2013). The channel migration, high sediment load, frequent floods, and anthropogenic interventions have caused morphological changes in the river course (Kuehl et al. 2005; Kummur et al. 2008; Guchhait et al. 2016). Meandering rivers signify channel dynamicity which reveals frequent changes in channel patterns through bank erosion, deposition, down cutting, etc. (Uddin et al. 2011). River meander and channel shifting are very complex processes of river floodplains that are triggered by different factors in the fluvial system (Hooke 2013; Islam and Guchhait 2017a). Channel migration is one of the significant characteristics that can change the morphology of river buffer areas, with major problems for human life (Gurnell et al. 2012; Islam and Guchhait 2017b). River geomorphological factors are important indicators to investigate environmental changes and are especially related to changes in river buffer areas (Dai et al. 2008). These geomorphological changes are associated with changes in sediment load and river discharge variation (Cserkés-Nagy et al. 2010). Therefore, the Himalayan foothill rivers are generally dynamic and riverbank erosion–deposition is strongly related to the formation and shifting of meander bends. Channel migrations of alluvial rivers are the most common geomorphological features all over the earth's surface. Channel migration is the movement of the river channel within the valley over the historical time period (Kesel 2003). An alluvial channel migration in terms of time and space is controlled by both natural and anthropogenic factors (Rhoads et al. 2016). These controlling factors have shaped the physical form of the channel morphology (Chakraborty and Mukhopadhyay 2014). Due to decreased river gradient and discharge, lateral erosion becomes the most significant cause behind river migration (Ahmed et al. 2018). The river channel is subject to be eroded and deposited to reach the state of equilibrium (Xia et al. 2014). The mapping of changed channel position is significant for archiving the erosion hazards and changes in LULC, as well as for finding the causes of those changes (Debnath et al. 2017). Anthropogenic activities such as the construction of dams, channel straightening, removal of riparian vegetation, bridges across the rivers, alteration of bank materials, sand-gravel mining, intruding land

use, etc. are the most influential factors that lead to river channel migration. (Rhoads et al. 2016). Besides channel morphology is controlled by sediment load, channel resistance, nature of bedrock, discharge variability, embankment stability, floods, the slope of the river bed, and vegetation (Dhariet al. 2014).

For measuring, mapping, representing, and monitoring the morphodynamic features, effective tools, and techniques are very important. At present, remote sensing (RS) and geographical information systems (GIS) have enormous importance for change detection and mapping in rivers and their buffer zone dynamics at a different strategic scale (Wang and Mei 2016; Wang and Xu 2018). RS and GIS tools and techniques with field verification can accurately and quickly map and investigate river morphological changes (Rinaldi et al. 2013; Langat et al. 2018). In GIS-based spatial analysis, attributes both linear (here river bank) and areal (here floodplain area) segments of the study area have been considered for assessing the temporal trends. Therefore, the digital shoreline analysis system (DSAS) is a highly acceptable method, developed by the United States Geological Survey (USGS), capable to accurately measure the rate and predication of different river bankline positions (right and left bank separately) (Thieler et al. 2009; Ashraf and Shakir 2018; Jana 2019). Generally, the DSAS model has been used in the context of the sea shoreline. However, in the study of the river, the right and the left bank can be separately mapped with a higher degree of accuracy.

The area under study being situated in the seismo-tectonically unstable foothill terrain (Bhutan Himalaya) has produced an array of magnificent landscapes both physical and cultural involving multiple cycles of fluvial migration. The Raidak-I River is very important in terms of ecological variation. However, the previous literature indicates a relative vacuum of work in the geomorphological domain. This research is unique in terms of dynamic river studies in the geological and geomorphologically active or highly vulnerable areas of the Himalayan foothills of West Bengal. Especially, the effort to measure channel migration, erosion–deposition, and meander geometry parameters of the Raidak-I River buffer area is almost absent at the national level or local level. Therefore, this work attempts to measure the channel migration and erosion–deposition in the last 48 years timeframe. This work has been developed for estimating the historical bankline. Moreover, calculating channel migration, erosion–deposition, channel width, and channel sinuosity, is attempted using geospatial techniques coupled with field verification. Thus, the work intends to address the following objectives to study the morphodynamic changes of the Raidak-I River.

- (i) To estimate the nature of bankline oscillation using the DSAS method, and
- (ii) To relate the channel oscillation with geomorphological and neotectonic controls.

2 Study Area

2.1 Location

A total of 81.9 km river stretch of Raidak-I River is selected for the present study which is the leftmost branch of the Raidak River that originates from the Himalayas and eventually meets Brahmaputra River in Bangladesh (Fig. 1). Spatially, River Raidak-I falls under two districts of West Bengal namely Cooch Behar and New Alipurduar. The latitudinal and longitudinal extent of the river is $26^{\circ} 34' 30.18''$ N to $26^{\circ} 12' 57.58''$ N and $89^{\circ} 43' 12.12''$ E to $89^{\circ} 41' 38''$ E. The Raidak River is amongst the main right bank tributaries of the Brahmaputra River. It is a trans-boundary river and flows through countries like Bhutan, India, and Bangladesh (Hasanuzzaman and Mandal 2020). River Raidak has three courses: (1) the middle one is old Raidak, (2) western flow is named Raidak-I or Dipa-Raidak, and (3) the eastern one is named as Raidak-II. The studied river Raidak-I or Dipa-Raidak flows through Alipurduar District and enters in Tufanganj Subdivision in Cooch Behar District. Then it passes through the entire C.D. Block TufanganjI. During the path in Tufanganj Subdivision, the river is flowing through Balabhut, Bansraja, Debogram, Dhalpal,

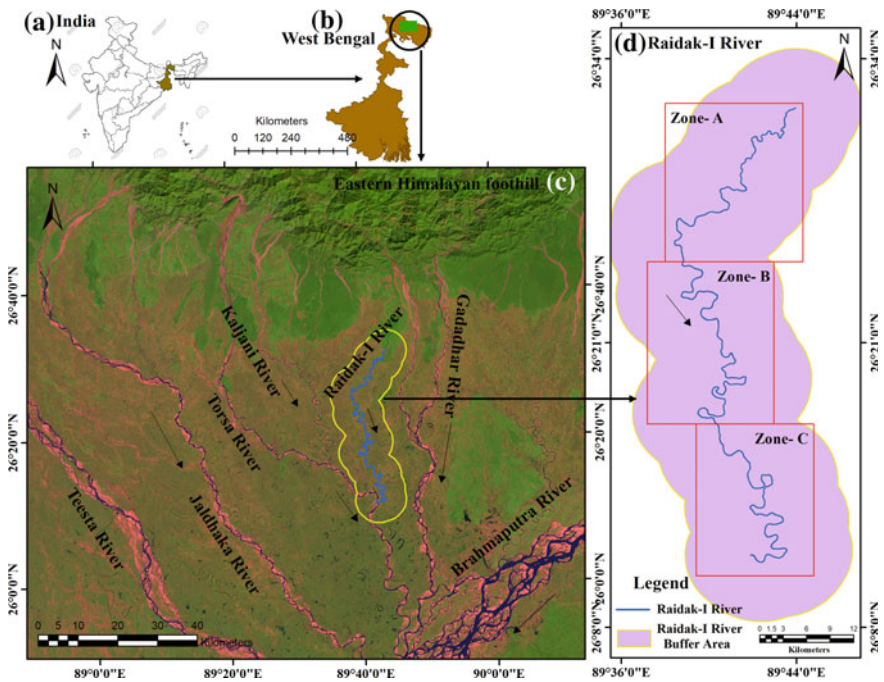


Fig. 1 Location map of the study area. **a** India. **b** West Bengal. **c** Eastern Himalayan foothill with study area. **d** Raidak-I River buffer area

Rajarkuthi, Shalbari, Dwiparpar, Andaranfulbari, Nakkatigachh, Kamatfulbari, and Chamta villages of the C.D. Block Tufanganj I. and enters Bangladesh to meet the Brahmaputra River.

2.2 Geology

The study area is a part of the extra-peninsula region, built up of rocks of ages ranging from Precambrian to Quaternary in various sections of the Himalaya Mountain and Ganga-Brahmaputra plain in eastern Himalaya (Banerji and Banerji 1979). The Quaternary deposits of the study area occur just south of the Siwalik group of formation and are constituted of boulders, gravels, pebbles, sands, and silts in the higher reaches forming alluvial fans and fluvial depositional terraces while mainly sands, silts, and clays in the lower reaches forming fluvial terraces of flood plain facies. Aggregates of boulders, pebbles and finer elastics exit on the levelled hilltops of BuxaDuar (Chattopadhyay and Das 1991). The rivers in this area are controlled by tectonism that gave rise to thrusting and normal faulting. The rivers change their slopes to adjust to geomorphic changes caused by the thrusts (Goswami et al. 2012). The study area is tectonically very active as it has experienced few earthquake events. According to Alam and Dominey-Howes (2016), seventeen above high to medium magnitude earthquake events were recorded during 1601–1984 in this region.

3 Materials and Methodology

3.1 Database

In this study, MSS, TM, ETM+ , and OLI datasets collected for 1972, 1979, 1987, 1995, 2003, 2011 and 2020 were used to demarcate the channel banklines (Table 1). All the satellite images were projected in the Universal Transverse Mercator (UTM) projection with zone 45 north and world geodetic survey 1984 (WGS84) datum and resampled in the ArcGIS environment. To maintain the data quality, all the images have been co-registered using the first-order polynomial model with the accuracy of root mean square error (RMSE) of less than 0.5 pixels with a minimum number (here it is 5) of ground control points (GCPs). Afterward, around 741 transects (on the left banks) and 922 (on the right bank) are generated for the estimation of riverbank shifting/erosion-accretion rate. Copernicus aerial imagery has also been used for river bank primary data verification.

Table 1 Characteristics of selected satellite images

Satellite images	Acquisition date	Path/row	Spatial resolution (in m)	Source
Landsat-1 MSS	21.12.1972	129/043	60	http://earthexplorer.usgs.gov
Landsat-1 MSS	16.12.1979	129/043	60	
Landsat-5 TM	08.12.1987	129/043	30	
Landsat-5 TM	19.12.1995	129/043	30	
Landsat-7 ETM+	16.01.2003	129/043	30	
Landsat-7 ETM+	05.01.2003	129/043	30	
Landsat-8 OLI-TIRS	27.12.2020	129/043	30	
ASTER DEM	2011		30	

3.2 Banklines Extraction

This process has been adopted for the assessment of earlier bankline positions with the help of selected satellite images. The bankline extraction is the process of transformation of the image, into a vector layer from raster data structure to determine right and left banklines separately on particular imagery (Jana 2019). We have used the normalized difference water index (NDWI) after McFeeters (1996), Haque et al. (2020) and modified normalized difference water index (MNDWI) (Xu 2006) for bankline extraction based on Eqs. (1) and (2) which employed green and NIR bands for segregation of land from water. Where pixels for water features are assigned as ‘1’ and for land as ‘0’ to achieve a binary image.

$$NDWI = \frac{Green - NIR}{Green + NIR} \quad (1)$$

To estimate the MNDWI, the MIR band of Landsat 7 and SWIR band of Landsat 5 and 8 along with the green band are also used. The technique for calculating the MNDWI was given by Xu (2006) as follows.

$$MNDWI = \frac{Green - MIR}{Green + MIR} \quad (2)$$

$$MNDWI = \frac{Green - SWIR}{Green + SWIR} \quad (3)$$

The output of these two ratios (NDWI and MNDWI) were further multiplied to generate another new image where the isolated pixel of the product image was nullified through the filtering technique of local mean matching (de Bethune et al. 1998) for detection of bankline position.

3.3 Estimation of Erosion–Deposition Rate

In the present work, the Digital Shoreline Analysis System (DSAS) extension tool of ArcGIS was used to assess the rate of bankline erosion-accretion by using the reference extracted baselines and auto-generated transects (Mandal et al. 2021). For the DSAS based statistical output, one further model has been employed such as the End Point Rate (EPR) model for computing present bankline erosion-accretion or shifting rate.

3.3.1 EPR Model for Calculating the Bankline Erosion-Accretion Rate

In the EPR model, based on the availability of data the considering period is divided into four temporal datasets i.e., 1973–1987, 1987–1997, 1997–2007, and 2007–2020. For each dataset, superimposed bankline positions have been portrayed and achieved a final line of overlapping visualization and this line is traced out as a composite line. Afterward, a buffer of 5 km distance from the composite line is drawn towards the right for the right bank and left for the left bank to demarcate the baselines. Therefore, several transects have been placed at a 50-m gap on the baseline which is created at the acute angle to the baseline up to 15 km distance away from both banks, and transects are auto-generated with ± 0.5 m uncertainties depending on the orientation of the baselines. Moreover, around 1347 transects (on the left banks) and 1456 (on the right bank) are placed along the baseline with 50 m spacing to cover the entire selected tract of the Raidak-I River (about 84.7 km) (Fig. 2).

$$EPR = \frac{\text{Distance of bankline movement}}{\text{Time between oldest and most recent}} \tag{4}$$

In the EPR model, previous and recent data of two banklines are needed for this calculation and do not require any earlier knowledge regarding hydraulic interference or sediment transport. Moreover, this model is applied for two years of a data set viz. 1973–1987, 1987–1997, 1997–2007, and 2007–2020 for calculating the riverbank erosion-accretion rate which depicts the shifting trend over time.

The result of EPR is applied to calculate the rate of bankline migration and to understand the erosion-accretion nature (Mukhopadhyay et al. 2012; Jana 2019) using the ‘Y’ for positions of earlier (Y_{ob}) and recent (Y_{rb}) bankline. In this attempt, it is used as ‘Y’ to denote the projected bankline position which is estimated by Eq. (5).

$$Y = \alpha_{EPR} + \beta_{EPR}X \tag{5}$$

where, X is the time interval ($X_{ob} - X_{rb}$) between earlier bankline (X_{ob}) and recent bankline (X_{rb}), α_{EPR} is model intercept, β_{EPR} denotes the rate of riverbank shifting (slope or regression coefficient).

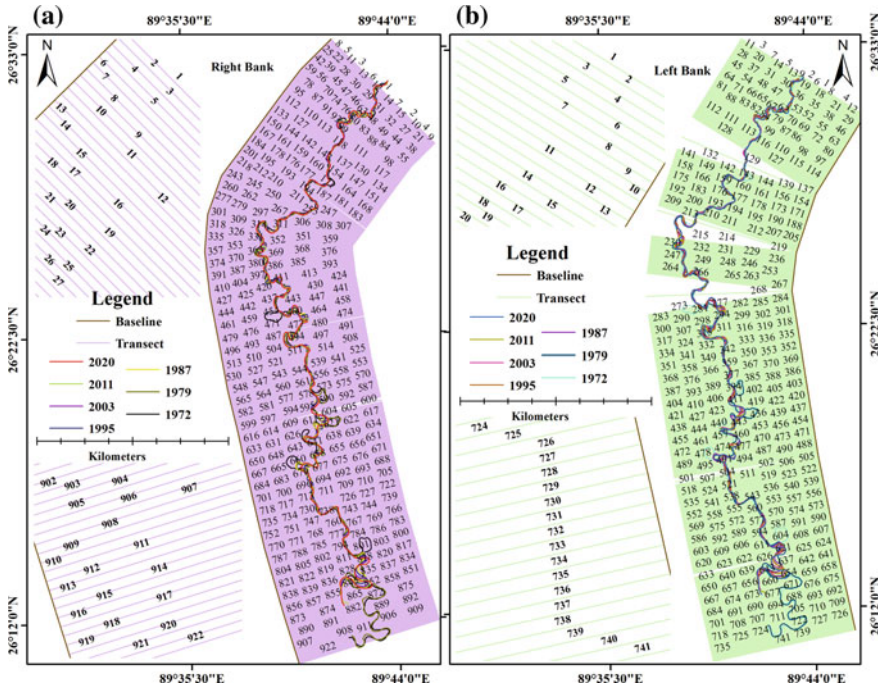


Fig. 2 Different banklines (1972–2020) are positioned along the baseline. All transects are oriented at angle with the corresponding baselines

On the other hand, the EPR intercept is calculated by Eq. (6).

$$\alpha_{EPR} = Y_{ob} - \left\{ \frac{Y_{ob} - Y_{rb}}{X_{rb} - X_{ob}} \right\} X_{ob} = Y_{rb} - \left\{ \frac{Y_{ob} - Y_{rb}}{X_{rb} - X_{ob}} \right\} X_{rb} \quad (6)$$

The rate of bankline migration for a given set of transects, the β_{EPR} is calculated by Eq. (7).

$$\beta_{EPR} = \left\{ \frac{Y_{ob} - Y_{rb}}{X_{rb} - X_{ob}} \right\} \quad (7)$$

3.4 Uncertainties and Errors

Potential errors are associated with satellite image-derived maps including datum changes, different surveying standards, projection errors, and distortions from uneven shrinkage, etc. (Anders and Byrnes 1991; Moore 2000). In the present study, four

different errors are identified for measuring the rate change and it may be of both positional and calculation-related errors. Calculation uncertainties are related to the skill and approach such as pixel error E_p , digitizing error E_d , and rectification error E_r and positional uncertainties are related to the features and phenomena that reduce the precision and accuracy of defining a bankline (both) position from a given data set such as; seasonal error E_s (Kankara et al. 2015). Finally, the total uncertainty value was estimated for each banklines by accounting for both positional and measurement uncertainties as follows.

$$E_t = \pm \sqrt{E_p + E_d + E_r + E_s} \quad (8)$$

The weighted linear regression rate (WLR) is 2.4 m/yr for transect number 1347 (on the left bank) and 1456 (on the right bank) and the 87 percent confidence interval is 0.79 (Fig. 2). The band of confidence around the reported rate of change is -2.6 ± 0.78 . In other words, it can be 87% confident that the true rate of change is between 3.25 and 1.78 m/yr. Also, R^2 (0.813) value justifies the acceptance of the work.

4 Channel Oscillation, Hydro-Geomorphic Drivers, and Active Tectonism

4.1 Channel oscillation

The riverbank shifting trend is estimated (Figs. 3 and 4) by considering the entire 48 years of data (1972–2020). As stated, the studied river stretch was segmented into the three distinct zones (A, B, and C) by spacing about 27 km based on the magnitude of meander geometry and the axial length of the river stretch in the middle-lower course. Moreover, around 247 transects (on the left banks) and 307 transects (on the right bank) are generated in the zone of A and B for estimation of riverbank shifting. However, in zone C, the number of transects is varied for different temporal spans due to spatio-temporal inconsistency of dynamic in the mouth of the river estuary. The temporal variation of river erosion–deposition for the year 1972–1979, 1979–1987, 1987–1995, 1995–2003, 2003–2011, and 2011–2020 are depicted in Fig. 8, that illustrates channel shifting of the Raidak-I River.

The result from 1972 to 1979 depicts that the average rate of bankline shifting in zone ‘A’ was -2.06 m/y at the left bank and 4.44 m/y at the right bank respectively. In zone ‘B’, the average rate of bankline shifting was -6.66 m/y (left bank) and 11.54 m/y (right bank). The rates of average bankline shifting in zone ‘C’ was 12.76 m/y and 14.47 m/y for the left and right bank, respectively. In this period, the overall average shifting of the left and right bank was 1.09 m/y and 10.04 m/y, respectively. The erosion–deposition rate and number of affected transects indicate that channel narrowing is caused by sediment accretion on bed areas of both the banks. Therefore, the dynamicity of the river was very high, especially in zone ‘B’ compared to other

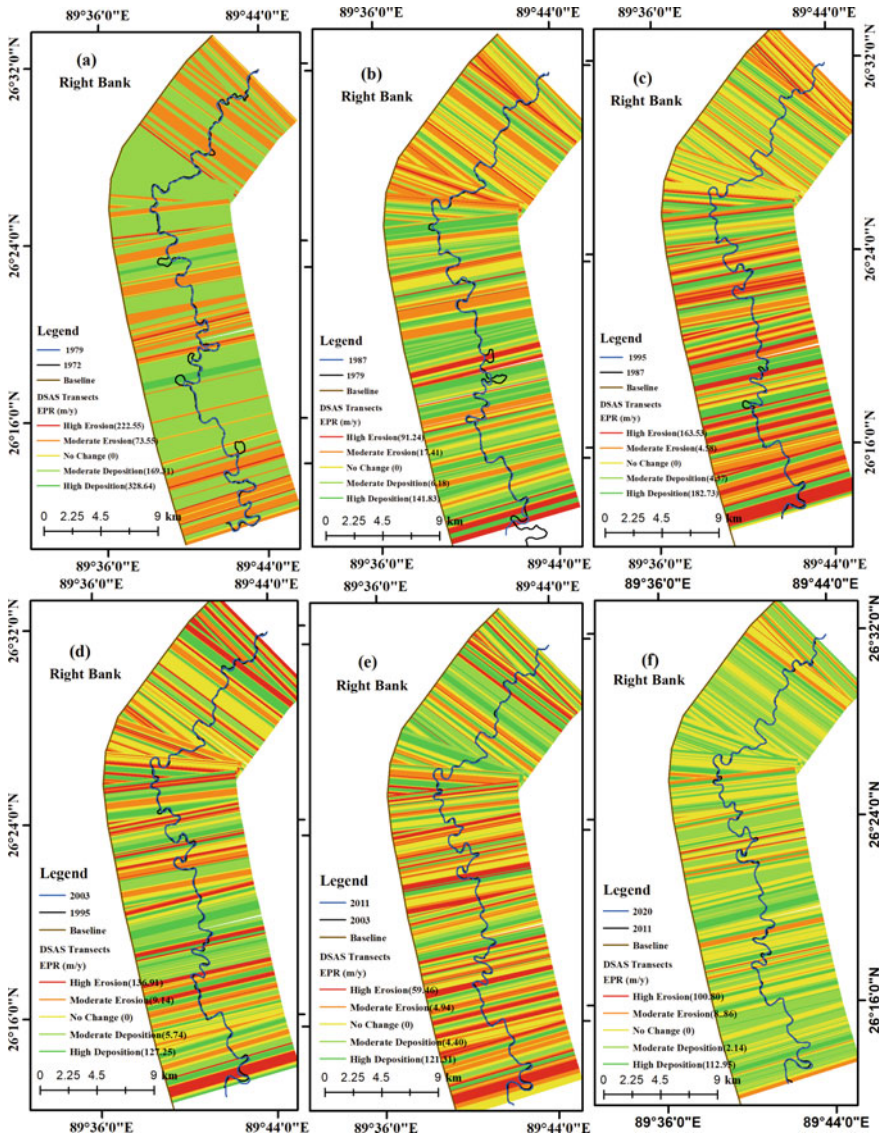


Fig. 3 Distribution of DSAS model derived riverbank erosion and deposition rate along transects during the different study periods, **a** 1972–1979, **b** 1979–1987, **c** 1987–1995, **d** 1995–2003, **e** 2003–2011, and **f** 2011–2020 at the right bank and **g** 1972–1979, **h** 1979–1987, **i** 1987–1995, **j** 1995–2003, **k** 2003–2011, and **l** 2011–2020 at the left bank

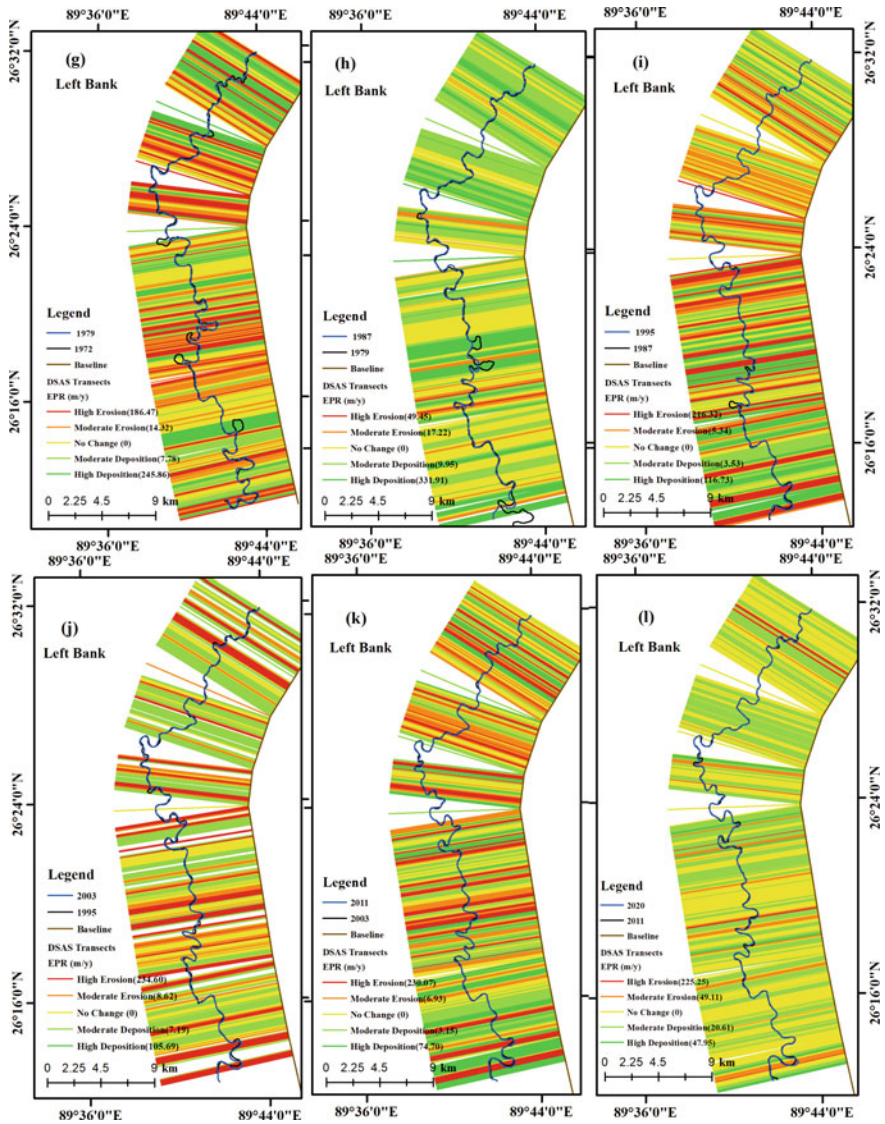


Fig. 3 (continued)

zones. From 1979 to 1987, zone ‘A’ was observed a higher rate of erosion–deposition on both banks (3.42 m/y at left bank and -5.20 at the right bank). On the other hand, in zone ‘B’ high deposition (10.35 m/y) was recorded in the left bank and also the high erosion (-2.24 m/y) in the right bank. Zone ‘C’ shows a rightward shifting of the river course with an average shifting rate of -5.54 m/y at the right bank and 8.26 m/y at the left bank. In general, during the period 1979 to 1987, the overall

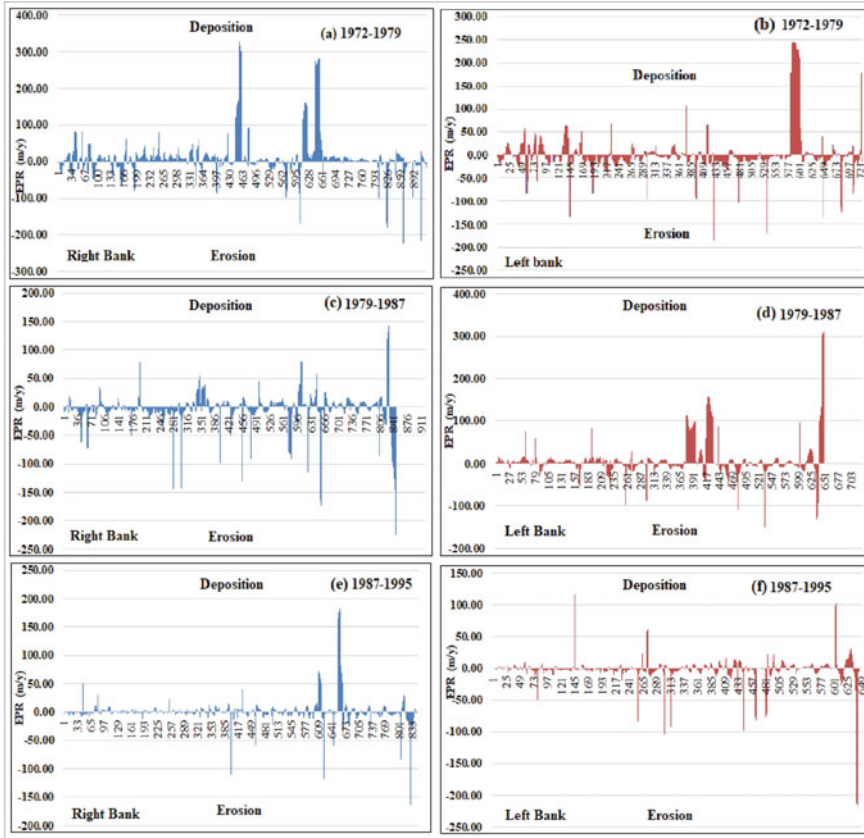


Fig. 4 DSAS model derived riverbank accretion-erosion during the periods of **a** 1972–1979, **c** 1979–1987, **e** 1987–1995, **g** 1995–2003, **i** 2003–2011, and **k** 2011–2020 at the right bank and **b** 1972–1979, **d** 1979–1987, **f** 1987–1995, **h** 1995–2003, **j** 2003–2011, and **l** 2011–2020 at the left bank

outward shifting rate was 7.22 m/y at the left bank and -4.12 m/y inward at the right bank, which indicates the rightward shifting of the river channel with its shrinking nature. As a result, the river channel migrates towards the right bank with a large extent of sedimentation at the left bank.

During 1987–1995, the average shifting rate in zone ‘A’ was -0.72 m/y for the left bank and 0.62 m/y for the right bank. In zone ‘B’, the rate of average shifting was -2.80 m/y for the left bank and 1.35 m/y for the right bank. Zone ‘C’ resulted in an average rate of channel migration with -1.71 and 0.75 m/y for the left and right bank, respectively. In this time frame, the average channel migration rate was -1.76 m/y (left bank) and 0.92 m/y (right bank), respectively. In this analysis, the left bank experienced extensive erosion. In this time period, the river has changed shifting direction from the right bank to the left bank. From 1995 to 2003, zone ‘A’

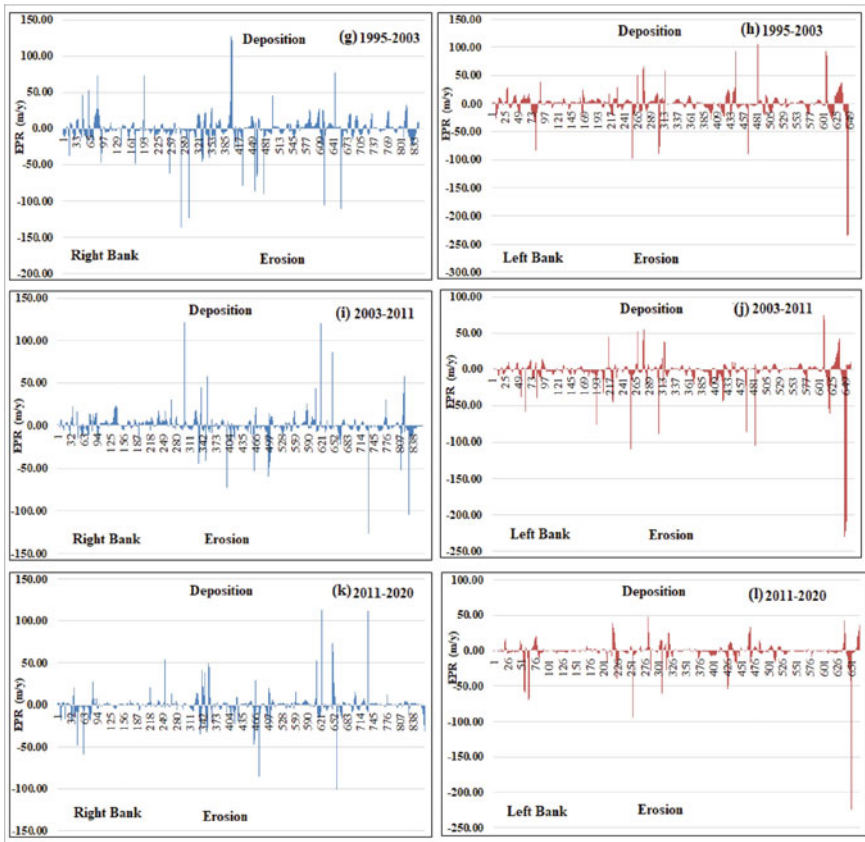


Fig. 4 (continued)

shows a high shifting rate (0.56 m/y) on the left bank and a high erosion rate on the right bank at -2.96 m/y. However, zone ‘B’ comprises significant erosion on both the left bank (-0.59 m/y) and the right bank (-0.42 m/y). Zone ‘C’ also passes through a relatively higher rate of erosion and it was estimated at -3.10 and -0.68 m/y on the left and right bank, respectively. In this time frame, the average channel migration rate was -0.73 m/y (left bank) and -1.32 m/y (right bank), respectively. The result from 2003 to 2011 depicts that the average rate of bankline shifting in zone ‘A’ was -3.04 m/y at the left bank and 2.40 m/y at the right bank respectively. In zone ‘B’, the average rate of bankline shifting was -3.55 m/y (left bank) and -1.05 m/y (right bank). The rates of average bankline shifting in zone ‘C’ were -3.52 and -1.86 m/y for the left and right bank, respectively. In this period, the overall average shifting of the left and right bank was -3.35 m/y and -0.05 m/y, respectively. In this observation, both bank experienced extensive erosion. During 2011–2020, the average shifting rate in zone ‘A’ is -0.79 m/y for the left bank and -1.09 m/y for the right bank. In zone ‘B’, the rate of average shifting is –

0.57 m/y for the left bank and -1.05 m/y for the right bank. Zone 'C' resulted in an average rate of channel migration with a figure of -1.60 and 0.14 m/y for the left and right bank, respectively (Fig. 4). In this time frame, the average channel migration rate is -0.92 m/y (left bank) and -0.65 m/y (right bank), respectively. The correspondence of high erosion at both banks is indicating channel widening. In this period (2003–2020), the overall negative (erosion) trend was observed for both banklines. This result indicates a widening river course triggered by persistent erosion on both banks. A general observation emanating from the present research is that the most dynamic or migrant part of the river is zone A and zone B compared to zone C which is relatively stable. In zone A, very active villages are Bakla, Chipra, Paschim, and PurbaKhalishamari for erosion and PurbaChikliguri, Uttar Parokata, and ChhotoChakirbas for deposition. In zone B, very active villages are Dhalpal, Chikliguri Dwitiakhanda, Guriarpur, and Basaraja Dwitia Khanda for erosion and Sikdarkerkhata and Haripur for deposition. Kamat Phulbari, Balabhut, Dwiparpar, Debgram, Rajarkuthi, and Boalimohan Dwitia Khanda of zone C are very active for erosion-accretion and channel migration. In the timeframe of the last 48 years, the Raidak-I River has an average erosion–deposition at -0.23 m/year in the right bank and 1.57 m/y in the left bank. However, periodical migration values are regular and very considerable in terms of shifting. This investigation of the historical datasets has depicted the clear picture that the previous day deposition activity and present-day erosion activity are dominated. The Raidak-I River course has a high dynamic adjustment for their need and this changed channel behavior is very dramatic.

4.2 Hydro-Geomorphic Drivers and Active Tectonism

The riverbank erosion in the Himalayan foothill river course is triggered by a high gradient, high discharge of water and sediment load, meander geometry, bank material composition, and human interferences. However, the most crucial driving factors in the Raidak-I River are involved in fluid flow, which creates a significant impact on the flow regime of the river during the monsoon flood. Almost the entire amount of average annual rainfall (about 3444.04 mm) within the basin is received during the monsoon (June to September) (District Disaster Management Report 2009, Government of West Bengal, India). Thus, the bank margin allows rightward shifting the course and formed a dry gap with shrubs and grasses at the place of the former active channel. Also, near Dhalpal (zone B), the right bank has shifted about 224 m on the landward side (rightward) and 1 km distance along the bank through eroding agricultural land and embankment breaching. Such a condition is demonstrated by the EPR model-based riverbank shifting.

The geomorphological and tectonic adjustment in terms of channel migration and erosion–deposition can be undoubtedly depicted in terms of the changes of the river buffer zone that took place over space and time (Wallick et al. 2007; Bolton and Shellberg 2001). The Raidak-I River is bearing the imprint of active tectonics of the region as they lie in the zone of Himalayan Frontal Fault, the most active thrust belt

of the Himalayas (Das 2004; Goswami et al. 2012). Tectonic changes are depicted by the responses made in the adjoining morphology of this river behavior. Channel shifting and erosion–deposition may be modified directly or indirectly by an increase or decrease in slope imposed by areal uplift or subsidence. Sufficiently decreased slopes may cause rivers to transform along the path of meandering to the braided channel. The most commonly observed of these adjustments is for a meandering channel to increase its sinuosity in response to the increased slope, or decrease its sinuosity as an adjustment to the decreased slope (Holbrook, and Schumm 1999). Among the various causes, one of the most important causes of this river dynamicity is tectonic activity. In our analysis, the total erosion is greater than the deposition which indicates that this river is still actively engaged in fluvial erosion.

The hypsometric curve represents the different stages of the evolution of erosional landform (Strahler 1952). The basin age can be estimated through the value of the hypsometric integral (HI). The value of HI close to 1 indicates its youthfulness of topography with the active pace of erosion while HI close to 0 denotes the old stage with the negligible rate of erosion (Schumm 1956; Strahler 1952). We have calculated the hypsometric integral as 0.15 which indicates that the Raidak-I River basin now falls into mature to the old stage.

The basin relief and size variations are represented in the long profiles of the river and stream length gradient index (SL Index). The distances and elevations were divided by maximum basin relief and the total stream length respectively to define the long profile (Lee and Tsai 2009). Thus, the presence of breaks in the river long profile depicts that a strong structural effect is somehow present in the river course. The long profile represents that the maximum portion of the river basin is included in plainland (Fig. 5). The SL Index is considered as a significant tool to detect local uplift as well as the incipient local response to regional processes (Troiani and Della Seta 2008). The SL Index was recorded high at the upper part of the river (Fig. 5). In this case, the union of morphological and morphometric evidence allows us to distinguish a sector in the Raidak-I River basin affected by active tectonic deformation. The hypsometric

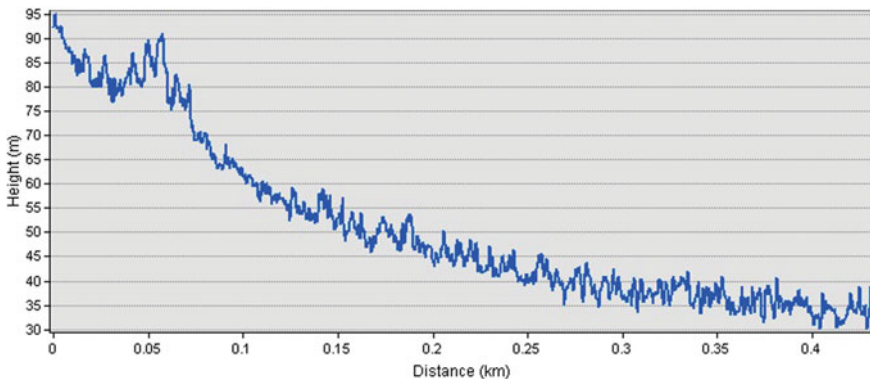


Fig. 5 a Long profile of the Raidak-I River Basin. b Stream Length Gradient Index (SL Index)

curve value, the SL Index, and the long profile properties provide adequate evidence of this river’s low energy but the study result is different. This may be due to the energy boost-up that takes place in the river during extreme rainfall and floods. Moreover, the Bhutan Himalayas boulders, sand, and detritus are continuously deposited in these rivers causing the river beds to gradually rising (Saha and Bhattacharya 2019). This large sedimentation has choked the channel by the formation of countless islands and bars forcing the river to collapse the river banks and thus promoting continuous channel migration.

The hydrogeological map depicts that various formations of different ages and rock types have controlled the riverbank erosion–deposition activity of the Raidak-I River Basin (Fig. 6). The geological map depicts that Jalpaiguri and Shaugoan formations are the major control factors for the dynamicity of the river (Fig. 7). The geomorphological map of the study basin represents that piedmont and younger alluvial plain are dominant of the basin, which indicates that Raidak-I River is geomorphologically very unstable (Fig. 7). In our study, continuous channel adjustments have occurred in the Raidak-I River buffer area and the construction of various river regulation works along the river. In this analysis, both these processes such as natural (floods, geological activity), and anthropocentric activity (construction embankment and bridges) are playing an important role in geomorphological instability and various natural

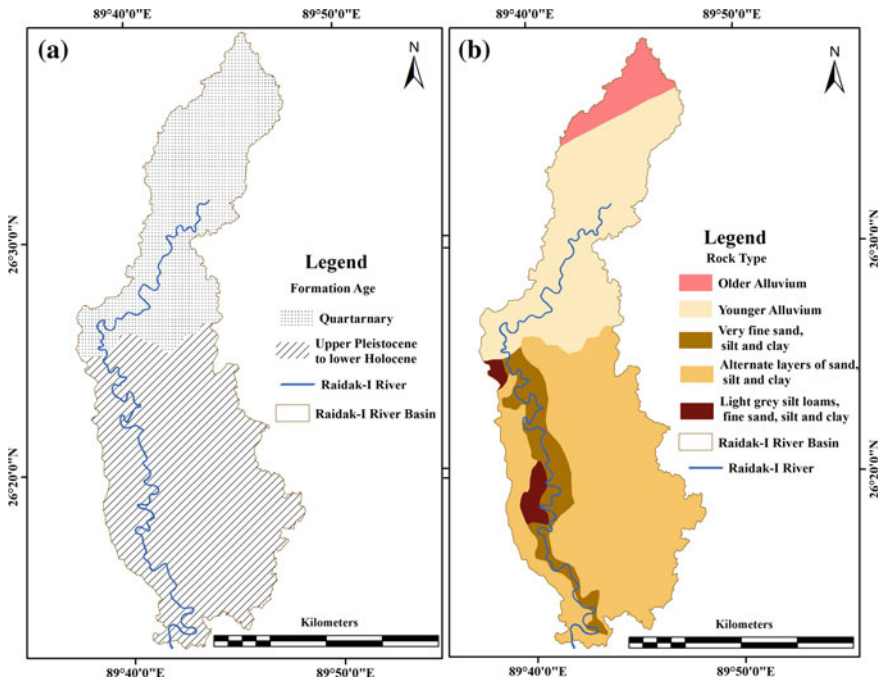


Fig. 6 Hydrogeological map of Raidak-I Basin. **a** Formation age, **b** Rock-type, *Source* Central Ground Water Board, India (CGWB and GIS)

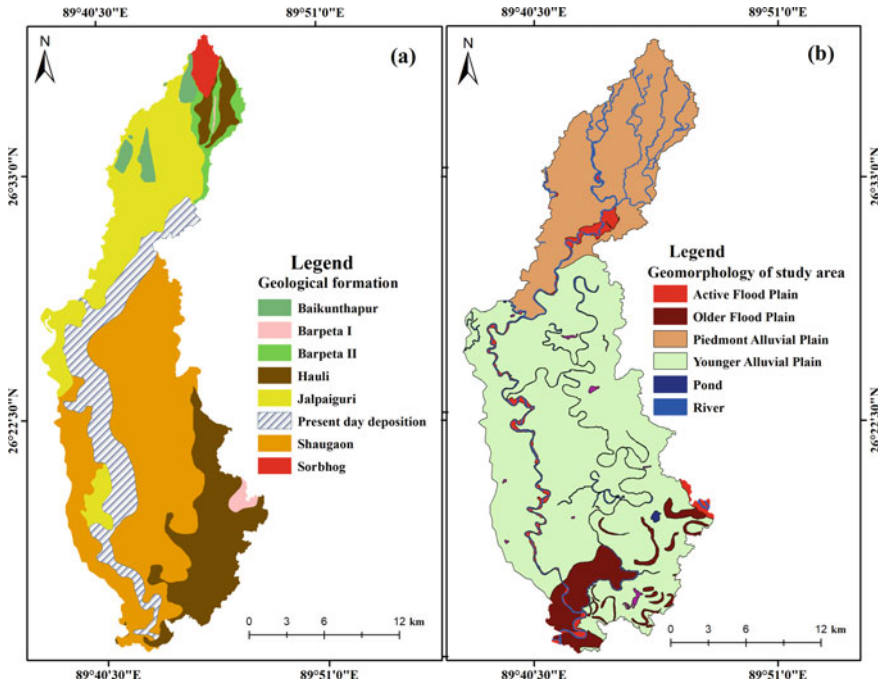


Fig. 7 Geomorphological and geological map of Raidak-I Basin. **a** Geological formation. **b** Geomorphology of the study area. *Source* Geological Survey of India

hazards. Therefore, this analysis has made a circumspect effort to provide insight into the historical channel migration and erosion–deposition of the study river in the sub-Himalayan piedmont region. It could help the administrators for understanding the relation between river migration and geomorphological adjustment.

4.3 Role of Embankment

The immense population pressure in the river corridor is exaggerated by controlling the natural channel flow pattern. The erosive meandering stretches are protected by strong embankment structures that are also able to divert the channel flow pattern. The diverted flow creates a harsh impact on the opposite bank through a severe rate of land erosion. Intensive sand mining activities also exaggerate the extensive riverbank erosion. Therefore, the riverbank shifts towards the left or right just after the embankment protected positions and adjusts its course with hydrodynamic behaviour. Thereafter, another new embankment is constructed at the recently exposed erosive section and robust controls the channel flow pattern which leads to channel narrowing. Also, at the positions of the bridge (across the river), the bridge protecting embankments

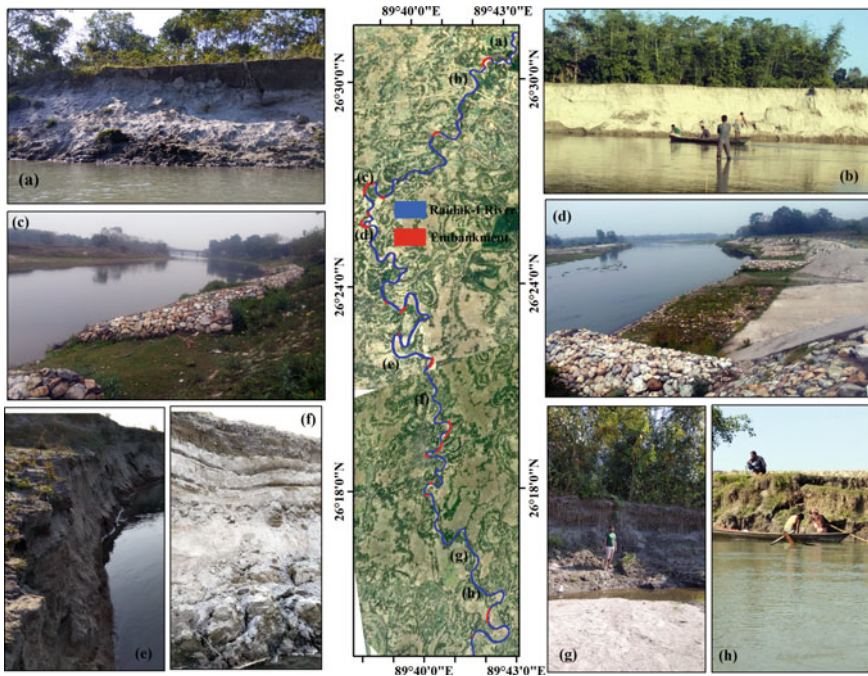


Fig. 8 Bridges and embankment along the Raidak-I River with field validation photos

are constructed along a concentrated part of the channel, is also insists on channel narrowing. The length of the river is 81.9 km in the present study, out of which 7.95 km long is attributed to embankments (Fig. 8). However, the channel hydraulic pattern has changed immediately after the bridge site by the widening of the channel. The overall result of erosion–deposition shows that to heavy extent erosion will take place in the inward position of the meander bend at the left bank and sediment deposition will occur in the straight course of the right bank. These will create a harsh impact on sediment feeding processes and resultant riverbank erosion/accretion in the course of the river. The riverbank erosion-accretion observation is a very important variable to planners, environmentalists, policymakers for understanding and formulating the needed and appropriate channel design schemes of vulnerable areas of the Raidak-I River.

5 Conclusion

This study has demonstrated the application and capability of earth observatory technology and generated a detailed evaluation of temporal and spatial changes in

river channel dynamics and adjustment of the Raidak-I River buffer area. The multi-temporal data analysis reveals that the Raidak-I River has continuously changed its bankline positions due to extensive erosion-accretion processes. In the timeframe of the last 48 years, the Raidak-I River has an average erosion-deposition at -0.23 m/year in the right bank and 1.57 m/y in the left bank. A general observation from this whole research is that the most dynamic or migrant part of the river is zone A and zone B compared to zone C which is relatively stable. The study assesses the significant study regarding the dynamic change of river bankline positions in vulnerable areas and the endangered condition of the nearby settlements and infrastructures due to high bank erosion. Most hydrogeomorphological studies are focused on identifying factors causing the riverbank migration and erosion-accretion and its present situation. This work is a small effort to calculate the historical river bankline migration through an automated computational platform. Field validation and continuous monitoring are imperative for such types of automated approaches. Therefore, in the present research, the DSAS based automated approach is employed as an alternative way that successfully and accurately measures geomorphic processes (erosion-accretion) at an appropriate spatio-temporal scale. Moreover, it will be helpful for engineers, planners and administrators to take the appropriate management plans to save the river adjacent villages which are at the risk of severe bank erosion.

References

- Ahmed I, Das N, Debnath J, Bhowmik M (2018) Erosion induced channel migration and its impact on dwellers in the lower Gumti River, Tripura, India. *Spatial Information Research*. <https://doi.org/10.1007/s41324-018-0196-9>
- Alam E, Dominey-Howes D (2016) A catalogue of earthquakes between 810BC and 2012 for the Bay of Bengal. *Nat Hazards* 81(3):2031–2102. <https://doi.org/10.1007/s11069-016-2174-7>
- Anders FJ, Byrnes MR (1991) Accuracy of shoreline change rates as determined from maps and aerial photographs. *Shore Beach* 59:17–26
- Ashraf M, Shakir AS (2018) Prediction of river bank erosion and protection works in a reach of Chenab River, Pakistan. *Arab J Geosci* 11(7). <https://doi.org/10.1007/s12517-018-3493-7>
- Banerji I, Banerji S (1979) A coalescing alluvial fan model of the Siwalik sedimentation a case study in the eastern Himalaya. *Geol Surv India Miscellaneous Publ* 41(1):1e12
- Bastawesy M, White KH, Gabr S (2013) Hydrology and geomorphology of the Upper White Nile Lakes and their relevance for water resources management in the Nile basin. *Hydrol Process* 27:196–205. <https://doi.org/10.1002/hyp.9216>
- Bolton S, Shellberg J (2001) Aquatic habitat guidelines white paper: ecological issues in floodplains and riparian corridors. Prepared for WA State Dept of Fish and Wildlife and others
- Burbank DW, Anderson RS (2001) *Tectonic geomorphology*. Blackwell Publishing, 287 pp
- Chakraborty S, Mukhopadhyay S (2014) An assessment on the nature of channel migration of River Diana of the sub-Himalayan West Bengal using field and GIS techniques. *Arab J Geosci*. <https://doi.org/10.1007/s12517-0141594-5>
- Chattopadhyay GS, Das A (1991) Quaternary geology and geomorphology of the Tista-Torsha interfluvial area—a brief review. *Geol Surv India Rec* 118(pt 3–8):115–124
- Cserkés-Nagy Á, Tóth T, Vajk Ö, Sztanó O (2010) Erosional scours and meander development in response to river engineering: middle Tisza region, Hungary. *Proc Geol Assoc* 121:238–247

- Dai SB, Yang SL, Cai AM (2008) Impacts of dams on the sediment flux of the Pearl River, Southern China. *Catena* 76:36–43
- Das JD (2004) Active tectonics of the Eastern Himalayan foothills region and adjoining Brahmaputra Basin based on satellite images. *Int J Remote Sens* 25(3):549–557. <https://doi.org/10.1080/0143116031000148070>
- de Bethune S, Muller F, Donnay JP (1998) Fusion of multispectral and panchromatic images by local mean and variance matching filtering techniques. *Fus Earth Data* 28–30
- Debnath J, Das (Pan) N, Ahmed I, Bhowmik M (2017) Channel migration and its impact on land use/land cover using RS and GIS: a study on Khowai River of Tripura, North-East India. *Egypt J Remote Sens Space Sci* 20(2):197–210. <https://doi.org/10.1016/j.ejrs.2017.01.009>
- Dhari S, Arya DS, Murumkar AR (2014) Application of remote sensing and GIS in sinuosity and river shifting analysis of the Ganga River in Uttarakhand plains. *Appl Geomat.* <https://doi.org/10.1007/s12518-014-0147-7>
- Goswami C, Mukhopadhyay D, Poddar BC (2012) Tectonic control on the drainage system in a piedmont region in tectonically active eastern Himalayas. *Front Earth Sci* 6(1):29–38. <https://doi.org/10.1007/s11707-012-0297-z>
- Guchhait SK, Islam A, Ghosh S, Das BC, Maji NK (2016) Role of hydrological regime and flood-plain sediments in channel instability of the Bhagirathi River, Ganga-Brahmaputra Delta, India. *Phys Geogr* 37(6):476–510
- Gurnell AM, Bertoldi W, Corenblit D (2012) Changing river channels: the roles of hydrological processes, plants and pioneer fluvial landforms in humid temperate, mixed load, gravel bed rivers. *Earth Sci Rev* 111(1–2):129–141. <https://doi.org/10.1016/j.earscirev.2011.11.005>
- Haque SM, Kannaujia S, Taloor AK, Keshri D, Bhunia RK, Champati Ray PK, Chauhan P (2020) Identification of groundwater resource zone in the active tectonic region of Himalaya through earth observatory techniques. *Groundw Sustain Dev* 10. Elsevier. <https://doi.org/10.1016/j.gsd.2020.100337>
- Hasanuzzaman M, Mandal S (2020) A Morphology-independent Methodology to Assess Erosion, accretion and lateral migration of an alluvial channel using geospatial tools: a study on the Raidak-I River of Himalayan Foothills. *Sustain Water Resourc Manag* 6(3). <https://doi.org/10.1007/s40899-020-00393-9>
- Holbrook J, Schumm SA (1999) Geomorphic and sedimentary response of rivers to tectonic deformation: a brief review and critique of a tool for recognizing subtle epeirogenic deformation in modern and ancient settings. *Tectonophysics* 305(1–3):287–306. [https://doi.org/10.1016/s0040-1951\(99\)00011-6](https://doi.org/10.1016/s0040-1951(99)00011-6)
- Hooke JM (2013). *River meandering, Treatise on geomorphology*. Elsevier Ltd. <https://doi.org/10.1016/B978-012-374739-6.00241-4>
- Islam A, Guchhait SK (2017a) Analysing the influence of Farakka Barrage Project on channel dynamics and meander geometry of Bhagirathi river of West Bengal, India. *Arab J Geosci* 10(11):1–18
- Islam A, Guchhait SK (2017b) Search for social justice for the victims of erosion hazard along the banks of river Bhagirathi by hydraulic control: a case study of West Bengal, India. *Environ dev sustain* 19(2):433–459
- Jana S (2019) An automated approach in estimation and prediction of riverbank shifting for flood-prone middle-lower course of the Subarnarekha River, India. *Int J River Basin Manag* 1–49. <https://doi.org/10.1080/15715124.2019.1695259>
- Kankara RS, Selvan SC, Markose VJ, Rajan B, Arockiaraj S (2015) Estimation of long and short term shoreline changes along Andhra Pradesh coast using remote sensing and GIS techniques. *Procedia Engineering* 116:855–862. <https://doi.org/10.1016/j.proeng.2015.08.374>
- Kesal RH (2003) Human modifications to the sediment regime of the Lower Mississippi River flood plain. *Geomorphology* 56:325–334
- Kuehl SA, Allison MA, Goodbred SL, Kudrass H (2005) The Ganges-Brahmaputra Delta. *Soc Sediment Geol* 83:413–434

- Kummu M, Lu XX, Rasphone A, Sarkkula J, Koponen J (2008) Riverbank changes along the Mekong River: remote sensing detection in the Vientiane–NongKhai area. *Quatern Int* 186(1):100–112
- Langat PK, Kumar L, Koech R (2018) Understanding water and land use within Tana and Athi River Basins in Kenya: opportunities for improvement. *Sustain Water Resourc Manag* 1–11
- Lee C, Tsai LL (2009) A quantitative analysis for geomorphic indices of longitudinal river profile: a case study of the Choushui River, Central Taiwan. *Environ Earth Sci* 1549–1558
- Mandal BK, Islam A, Sarkar B, Rahman A (2021) Evaluating the spatio-temporal development of coastal aquaculture: an example from the coastal plains of West Bengal, India. *Ocean Coast Manage* 214:105922
- McFeeters SK (1996) The use of the Normalized Difference Water Index (NDWI) in the delineation of open water features. *Int J Remote Sens* 17(7):1425–1432
- Moore LJ (2000) Shoreline mapping techniques. *J Coastal Res* 16:111–124
- Mukhopadhyay A, Mukherjee S, Mukherjee S, Ghosh S, Hazra S, Mitra D (2012) Automatic shoreline detection and future prediction: a case study on Puri Coast, Bay of Bengal, India. *Eur J Remote Sens* 45(1):201–213
- Rhoads BL, Lewis QW, Andresen W (2016) Historical changes in channel network extent and channel planform in an intensively managed landscape: natural versus human-induced effects. *Geomorphology* 252:17–31. <https://doi.org/10.1016/j.geomorph.2015.04.021>
- Rinaldi M, Surian N, Comiti F, Bussetini M (2013) A method for the assessment and analysis of the hydromorphological condition of Italian streams: the Morphological Quality Index (MQI). *Geomorphology* 180:96–108
- Saha UD, Bhattacharya S (2019) Reconstructing the channel shifting pattern of the Torsa River on the Himalayan Foreland Basin over the last 250 years. *Bulletin of geography. Physical geography series*, no 16, pp 99–114 <https://doi.org/10.2478/bgeo-2019-0007>
- Schumm SA (1956) Evolution of drainage systems and slopes in badlands at perthamboy, New Jersey. *Geol Soc Am Bull* 67(5):597. [https://doi.org/10.1130/00167606\(1956\)67\[597:eodsas\]2.0.co;2](https://doi.org/10.1130/00167606(1956)67[597:eodsas]2.0.co;2)
- Starkel L, Sarkar S, Soja R, Prokop P (2008) Present-day evolution of the Sikkimese-Bhutanese Himalayan Piedmont, vol 219. *Polska Akademia Naukinstytut Geografii i Przestrzennego Zagospodarowania, Prace Geograficzne*, Warsaw, pp 62–70
- Strahler AN (1952) Dynamic basis of geomorphology. *Geol Soc Am Bull* 63:923–938
- Thieler ER, Himmelstoss EA, Zichichi JL, Ergul A (2009) Digital Shoreline Analysis System (DSAS) version 4.0—an ArcGIS extension for calculating shoreline change: U.S. Geological Survey Open-File Report 2008-1278
- Troiani F, Della Seta M (2008) The use of the stream length–gradient index in morphotectonic analysis of small catchments: a case study from Central Italy. *Geomorphology* 102(1):159–168. <https://doi.org/10.1016/j.geomorph.2007.06.020>
- Uddin K, Shrestha B, Alam MS (2011) Assessment of morphological changes and vulnerability of river bank erosion alongside the river Jamuna using remote sensing. *J Earth Sci Eng* 1:29–34
- Wallick JR, Grant GE, Lancaster ST, Bolte JP, Denlinger RP (2007) Patterns and controls on historical channel change in the Willamette River, Oregon, USA. In: Gupta A (ed) *Largerivers: geomorphology and management*. Wiley, pp 492–516
- Wang S, Mei Y (2016) Lateral erosion/accretion area and shrinkage rate of the Linhe reach braided channel of the Yellow River between 1977 and 2014. *J Geog Sci* 26(11):1579–1592
- Wang B, Xu YJ (2018) Dynamics of 30 large channel bars in the Lower Mississippi River in response to river engineering from 1985 to 2015. *Geomorphology* 300:31–44
- Xia J, Zong Q, Deng S, Xu Q, Lu J (2014) Seasonal variations in composite riverbank stability in the lowerJingjiang reach China. *J Hydrol* 519:3664–3673
- Xu H (2006) Modification of normalised difference water index (NDWI) to enhance open water features in remotely sensed imagery. *Int J Remote Sens* 27(14):3025–3033

Morphotectonics of the Chel River Basin, Eastern Himalaya, India: Insights from Shuttle Radar Topography Mission Digital Elevation Model- Based Geomorphic Indices



Sonam Lama  and Ramkrishna Maiti

Abstract The Morphotectonic characteristics of Chel river was examined through the analysis of Shuttle Radar Topography Mission (SRTM) DEM-based geomorphic indices to investigate the effects of neotectonics on channel characteristics and landform development. The individual and cumulative analysis of geomorphic indices such as Relief Ratio (Rh), Drainage basin asymmetry (Af), Stream length gradient index, Mountain front sinuosity, Basin Shape, Valley floor width to height ratio signify adjustment of Chel river basin to the prevailing tectonics. The elongated basin shape and the derived hypsometric integral value of 0.15 indicate that the basin is in the senile stage and only 15% of the actual landmass is present to be denuded by the erosion agents. The Basin asymmetry factor suggests that the basin is tilted significantly towards the south-west direction in the middle reach but is tilted towards the east in its upper and lower reach. The basin has an irregular mountain front and the derived Smf value of 2.02 implies that the basin falls under the moderate tectonics category. Lower Vf values <0.7 from its source up to mountain front (10 kms approx) suggest the presence of V-shaped valleys due to accelerated vertical erosion induced by landform upliftment. The sudden increase of SL index values even in uniform lithology further indicates the greater role of relative tectonics over lithology. Cross-examination of assessed geomorphic indices with geology confirms the adjustments of river Chel to the differential effects of ongoing tectonic processes over the channel and basin as a whole which has shaped the evolution of the basin to its present-day morphology.

Keywords SRTM DEM · Geomorphic indices · Neotectonics · Chel River

S. Lama (✉)

Department of Geography, Darjeeling Govt. College, Darjeeling, West Bengal 734101, India

R. Maiti

Department of Geography, Vidyasagar University, Medinipur, West Bengal 721102, India

1 Introduction

The Earth's landscape is shaped by a complex interplay between the endogenic or tectonic and exogenic or erosion-related processes (Andermann and Gloaguen 2009; Harkins et al. 2005; Perez-Pena et al. 2009; Whittaker 2012). The highest mountain range of the world, Himalayas is mainly a direct consequence of ongoing convergence between the Indian Plate and the Eurasian Plate. The underthrusting of the Indian plate below the Eurasian plate resulted in N-S contraction of the lithosphere and development of the foreland-ward migrating fold and thrust belt (FTB) of the Himalayas during the Cenozoic Era (Gansser 1964; Nakata 1989). The Main Central thrust (MCT) and the Main Boundary Thrust (MBT) are considered to be two main expressions of the FTB whereas the Main Frontal Thrust (MFT) is considered as the southernmost expression of the FTB in the Sub-Himalayan foreland (Gansser 1981). These thrusts divide the Himalayas into three orographic belts from north to south, viz., the Higher Himalayas, the lesser Himalayas, and the Sub-Himalayas (Gansser 1981; Nakata 1989; Guha et al. 2007). Apart from these major thrusts, there are numerous smaller and regional level faults, folds, and lineaments in diverse orientation which adds to the complexity and makes the Himalaya, in terms of tectonics and seismicity, also one of the most active mountain ranges in the world (Acharyya et al. 1976; Valdiya et al. 1992).

The drainage pattern in tectonically active regions is very sensitive to processes such as upliftment, folding, faulting, and tilting—which are responsible for river incision, basin asymmetry, drainage geometry, and river deflections (Cox 1994). The study of active tectonics, and in particular those areas with relatively high activity, in the Holocene and late Pleistocene, is important to evaluate the earthquake hazard (Keller and Pinter 2002). Neotectonics and geomorphic parameters exert great control over the drainage basin dynamics of a channel and their studies, therefore, are important in watershed prioritization and management studies (Vijith et al. 2015). The geomorphic indices are important indicators capable of decoding landform responses to active deformation processes and have been widely used as a reconnaissance tool to differentiate zones influenced by active tectonics (Keller 1986; Azor et al. 2002; Keller and Pinter 2002; Chen et al. 2003; Kale 2014). The information about geomorphic indicators of active tectonics can be retrieved through the analysis of topographic maps, aerial photographs, satellite images, digital elevation models, and quantification of morphotectonic features (Horton 1945; Keller and Pinter 1996, 2002; Mukul et al. 2017; Sharma et al. 2018).

Recent rapid development in Spatial information technologies, especially the availability of high-resolution satellite DEMs which are mostly freely available and enormous increase in the capability of personal computers and Geographical Information systems, has given a great impetus for the growth of morphotectonic analysis studies using geomorphic indices (Jain et al. 2006; Garrote et al. 2008; Kale and Shejwalkar 2008; Ferraris et al. 2012; Vijith et al. 2015). Geomorphologists today are much capable of carrying out more precise morphotectonic studies and earth modelling to identify and assess the degree of tectonic disturbance in a basin

(Dehbozorgi et al. 2010; Giaconia et al. 2012; Mahmood and Gloaguen 2012 and Vijith et al. 2015).

The Himalaya has been a center of attention for tectonic studies for more than a century mainly because of active tectonics and seismicity (Heim and Gansser 1939; Hodges and Silverberg 1988; Valdiya 1995; Yin 2006). Rivers in the eastern Himalayas are numerous due to higher rainfall, yet there are fewer studies on them as compared to the number of studies done on rivers of the western Himalaya (Seeber and Gornitz 1983; Mandal and Sarkar 2016). There is a further dearth of studies analyzing and evaluating the response of the channels and basins to the recent tectonic activities, using geomorphic indices through spatial analysis techniques. Though few but very significant studies have been done using geomorphic indices recently (Mukul et al. 2017; Mandal and Sarkar 2016), the documentation and advancement of knowledge are still too few to comprehend the drainage and landform evolution in response to regional neotectonics in Darjeeling-Sikkim Himalaya and its foreland.

Rivers originating in the Eastern Himalaya and draining towards north Bengal plains are characterized by highly incised mountainous courses with elongated, asymmetric drainage basins and low sinuous mountain fronts. All these drainage and basin characteristics indirectly point towards the adjustments of rivers and whole watersheds to the prevailing neotectonics. The present work tries to analyze and elucidate the response of channel and basin as a whole of Chel river to the neotectonics of the region, through some selected geomorphic indices computed from SRTM DEM.

2 Regional Geological Setting and Tectonic Sensitivity of the Study Area

Chel lies to the left of river Tista after Lish and Gish and joins Neora to become Dharala Nadi at 88° 44' 13"E, 26° 41' 45.6"N which ultimately merges with mighty Tista about 13kms downstream. The catchment extends between 26° 41' 30" and 27° 5'15" north latitudes and longitudes 88° 37'00" and 88° 45' 15" east (Fig. 1c) with an entire watershed area of 321 km² and a watershed perimeter of 115.21 km. Elevation ranges from 92 to 2449 m. Geomorphologically the basin comprises the lesser Himalayan surfaces, piedmont surface, terrace surfaces, alluvial plain, etc.

The northern mountainous portion of Chel basin lies to the east of Lesser Himalayan Duplex (LHD) and Gish Transverse zone (GTZ), a sinistral strike-slip transverse fault (Mukul et al. 2017). The major portion of the Chel basin south of the mountain front is a part of the Gorubathan recess wherein the absence of Siwalik and Damuda series of rocks and consequent minimal North–South width of the Himalayan arc makes it unique in the Eastern Himalayan belt (Heim and Gansser 1939; Goswami et al. 2013; Srivastava et al. 2017). Further, the Ramgarh Thrust (RT) rather than the Mountain Front Thrust (MFT) defines the mountain front here (Matin and Mukul 2010). The northernmost part of the catchment drains Chungthang formation of Proterozoic age, followed by Lingtse Granite Gneiss of Proterozoic-II

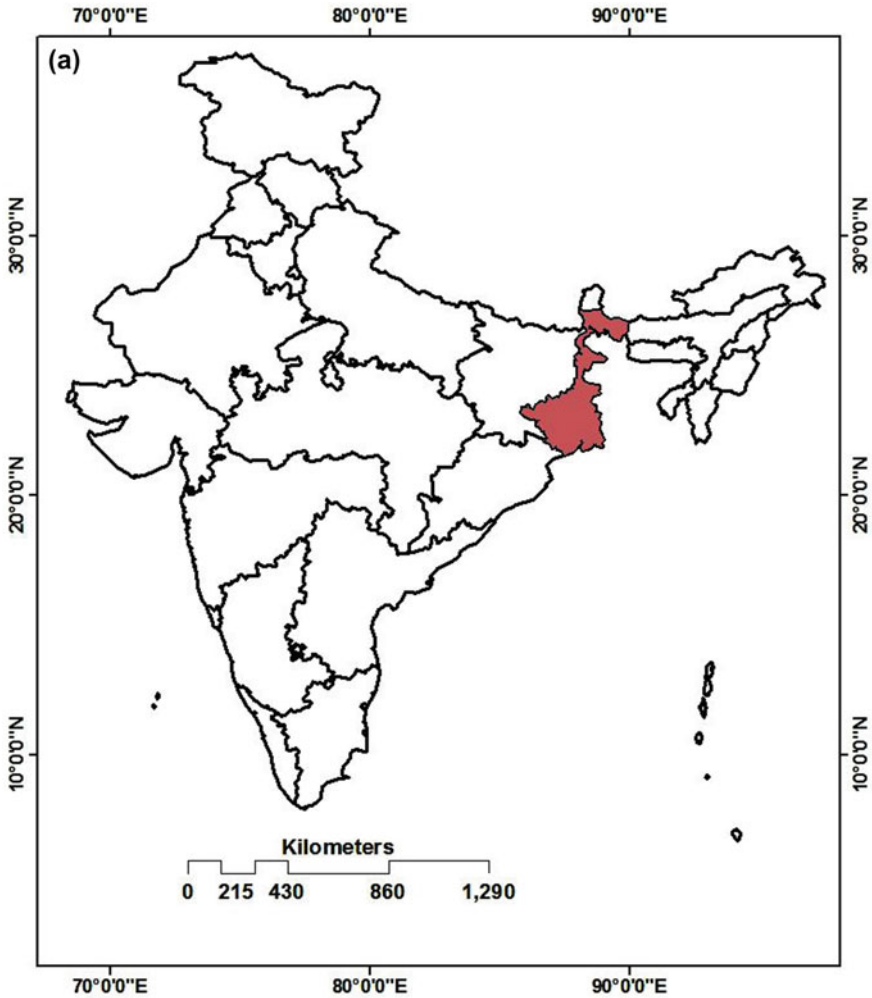


Fig. 1. a-c India with the state of West Bengal (a), West Bengal with Chel river Basin (b) and Chel River Basin (Study Area) (c)

and Reyang formation of again Proterozoic age. Downstream, the river crosses over a narrow strip of Buxa formation of Proterozoic age again. Further downstream from the near mountain front, the remaining part of the basin is over Quaternary sediments of Baikunthapur formation of the very recent Holocene epoch and Chalsa formation (middle to upper) of Pleistocene epoch (Table 1 and Fig. 12).

The Chel basin area falls within the meizoseismal zone of 1934 Bihar-Nepal, the 1950 Assam Earthquakes and belongs to zone-IV in the seismotectonic map of India (Kumar et al. 2010; De and Kayal 2003; Goswami et al. 2013). The 18th September 2011 Sikkim earthquake and 2015 Nepal earthquake had epicenters in the north

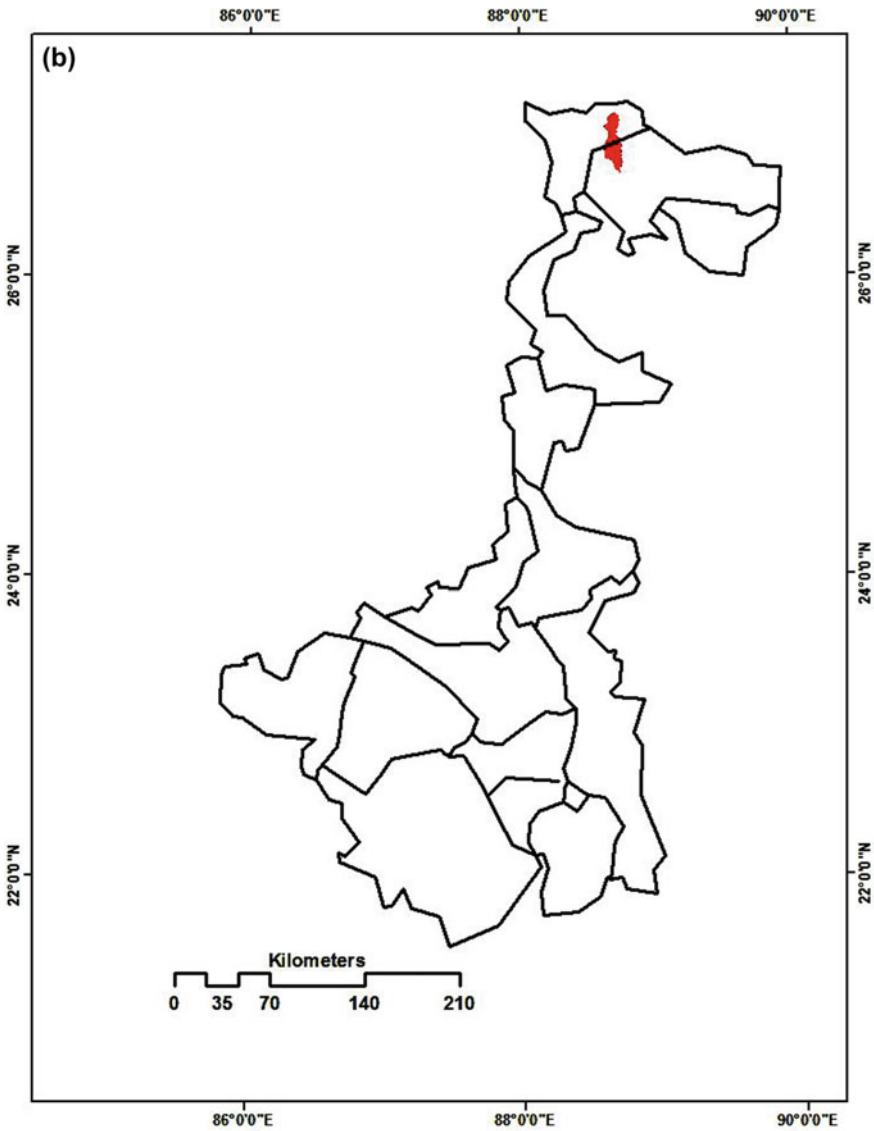


Fig. 1. (continued)

of this meizoseismal zone. In the vicinity, geological mapping of the Darjeeling-Sikkim sub-Himalayan foothill region reveals the presence of discontinuous strands of tectonically active Quaternary thrust faults (Guha et al. 2007).

With its upper portion flanked on the outer Himalayan surface and rest on the Himalayan foreland, Chel River basin has a typical straddle-like situation and is tectonically disturbed due to its proximity to major Himalayan faults. Besides these,

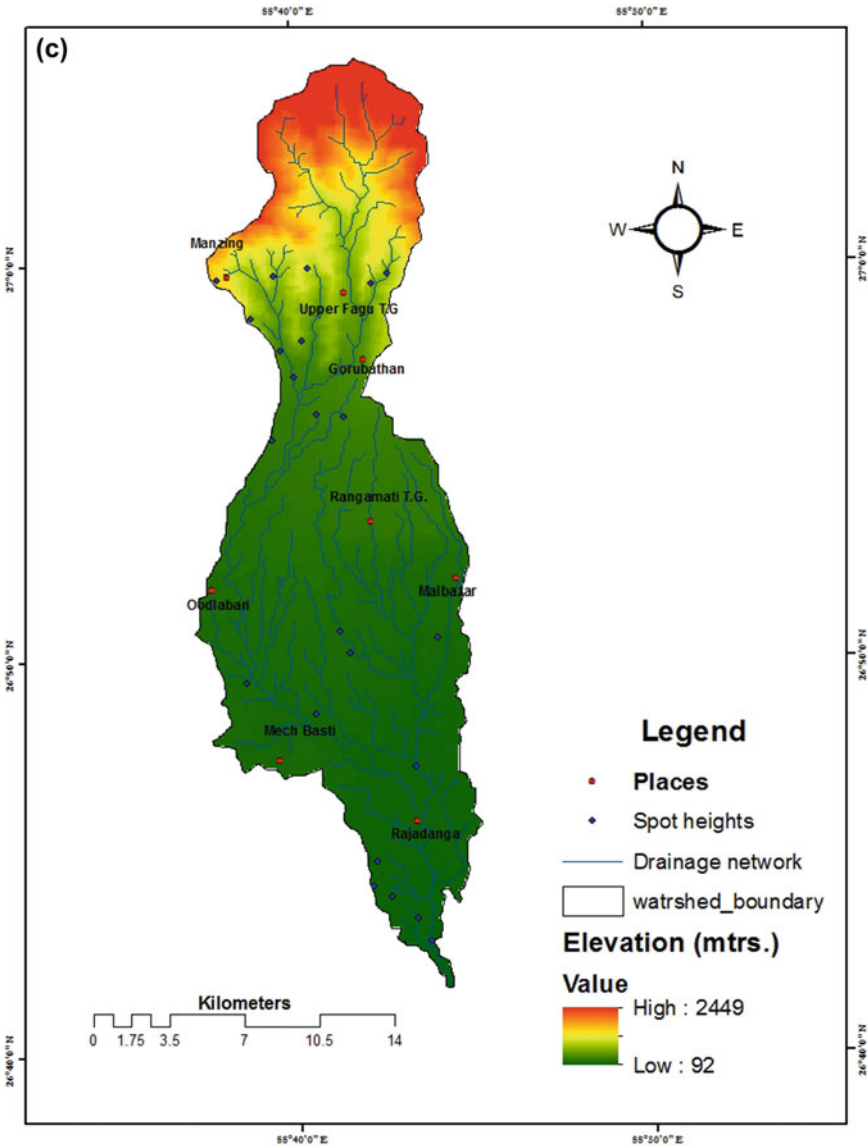


Fig. 1. (continued)

the Rajmahal Fault, the Malda-Kishanganj fault, the Tista lineament, the Dhubri fault, the Gangtok lineament, the Kanchanjunga lineament, are the major faults and lineaments which are transverse to the E-W trending major Himalayan faults in the region. In fact, the Chel basin falls on the northern portion of the Bengal basin which along with above-listed faults and lineaments, is also characterized by other major

Table 1 Geological and Lithostratigraphic units of Chel basin, compiled from Geological and Mineral map of West Bengal, GSI (1999) and Mitra et al. (2010) and references therein

Abbreviation	Units & age	Group	Lithology
Q2b	Baikunthapur Formation (Holocene)	-----	Sand, silt & clay
Q1c	Middle to Upper Chalsa Formation (Pleistocene)	-----	Boulders, Gravels, pebbles, sands and silts
Ptb	Buxa Formation (Proterozoic)	Daling	Predominantly dolostone, cherts and variegated slates
Ptr	Reyang Formation (Proterozoic)	Daling	Ortho-, and protoquartzite variegated slates ancrphyllites
Ypt2l	Lingse Granite Gneiss (Proterozoic-II)	Darjeeling Gneiss	Sheared, streaky, porphyritic biotite gneiss
Ptd2	Chungthang Formation (Proterozoic)	Daling	Calc-gneiss, calc-granite, augen gneiss, marble, sillimanite gneiss, graphite schists; etc

faults like the Garhmoyna-Khandaghosh Fault, the Jangipur-Gaibandha Fault, the Pingla Fault, the Debogram-Bogra Fault, the Rajmahal Fault, the Malda-Kishanganj Fault, the NE–SW-trending Eocene Hinge Zone (EHZ), the Sainthia-Bahmani Fault, the Purulia Shear Zone, and the Purulia Lineament and is itself tectonically very unstable. The incidents of devastating earthquakes around the region like the great 1897 Shillong earthquake of M_W 8.1, the 1934 Bihar-Nepal earthquake of M_W 8.1, the 1950 Assam earthquake of M_W 8.7, the 2011 Sikkim earthquake of M_W 6.9 were all felt well in the basin (Nath et al. 2014). Along with above mentioned large earthquake events, the M_W 7.9–36 km E of Khudi, Nepal earthquake of 25.04.2015 of 06:11:25 (UTC) depth-8.2 km and the most recent 05.04.2021 20.49.57 (UTC + 05.30) earthquake of M_W 5.0 having epicenter at 33 km NNW of Samtse Region, Bhutan from a depth of 8.4 km was felt across Bhutan, Sikkim, North Bengal and Upper Assam (usgs.gov). North Bengal was again shaken by M_W 4.1 earthquake having epicenter at Jalpaiguri with a depth of 10 km on 06.04.2021 at 07.07.02 (IST) (Official Website of National Center of Seismology, MES, GOI). Both of these earthquake events of 05.04.2021 and 06.04.2021 had epicenters within 30 km from the basin (Fig. 2). These frequently recorded earthquake events are thus testimony of the tectonically active nature of the region (Fig. 2).

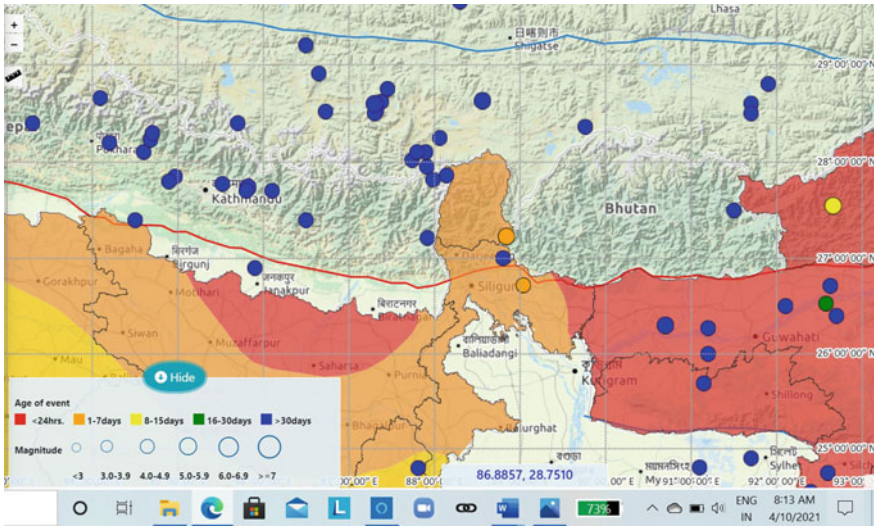


Fig. 2 Screenshot of Earthquake frequency and intensity (>4Mw) map of the region. Note-Circle sizes represent intensity of the earthquakes and circle color represent age of the events for last 10 years (01.01.2001–10.04.2021). There are four events of less than one month’s age wherein two events have epicenters very close to the basin and have occurred within one week of procurement of this screenshot (10.04.2021). (Source- Website, National Center of Seismology, MOES, GOI)

3 Materials and Method

3.1 Preparation of Digital Elevation Models (DEMs)

In the present study, two SRTM DEM 1 Arcsec (n26_e088_1arc_V3 and n27_e088_1arc_V3) with 30 m resolution were used for extraction of geomorphic indices to access the implications of tectonic activities in the Chel river basin. The DEMs were downloaded from the U.S. Geological Survey website using the Earth explorer interface: <http://earthexplorer.usgs.gov/>. as GeoTiff raster files, mosaicked them into one and then our watershed was clipped out from. Other relevant and related information was collected from SOI toposheets (Sheet no. 73B/9 and 73B/10 having R.F -1:50,000). The geological map published by the Geological Survey of India (1990) was consulted. ArcGIS 10.1 along with many DEM processing extensions were used for the analysis.

3.2 Accuracy Assessment and Reliability Test

Since the accuracy and usability of resultant geomorphic indices values for the Chel river basin depend highly on the accuracy of the DEM used, its accuracy measurement

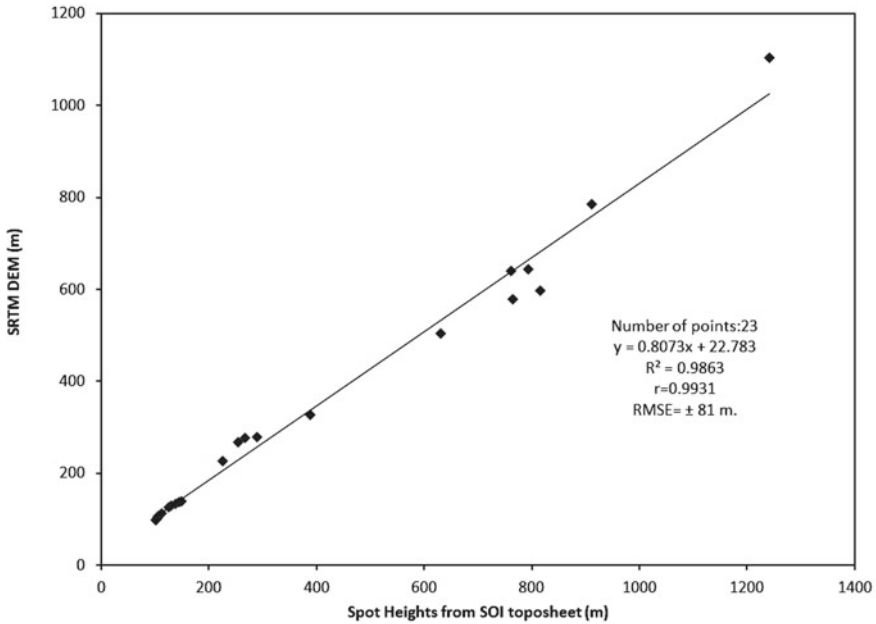


Fig. 3 Correlation plots of spot heights derived from SOI toposheets and corresponding points on SRTM DEM

becomes imperative. Thus, the accuracy of SRTM DEM was cross-checked and tested before the generation of geomorphic indices for the Chel basin. Therefore, elevation values of 23 spot heights were collected from SOI toposheet (1:50,000) and corresponding values were extracted from SRTM DEM to perform a linear regression analysis. The analysis resulted in a best-fit plot with a correlation coefficient of 0.99 (Fig. 3) and root mean square error of ± 81 m. The result is further corroborated by the findings of greater accuracy of C30N SRTM data in comparison to C90, owing to its better vertical accuracy and therefore has been suggested for all future geomorphic studies (Mukul et al. 2017). This validates the use of SRTM DEM 1Arc sec (30 m resolution) in the extraction of geomorphic indices for the present study.

3.3 Computation of Geomorphic Indices

The following geomorphic indices that are typically used to identify neotectonics in river basins: relief ratio, drainage basin asymmetry, basin elongation ratio, hypsometric curve and integral, stream length gradient index, mountain front sinuosity index, and valley floor width-to-height ratio (Bull and McFadden 1977; Strahler 1952; Schumm 1956; Pike and Wilson 1971; Hack 1973; Gardner et al. 1987; Burbank and Anderson 2001) has been computed for the Chel river basin. Geomorphic indices

which need elevation for their computation are Relief ratio, Stream length gradient index, valley floor width-to-height ratio, hypsometric integral etc. whereas drainage basin asymmetry, transverse topographic symmetric factor, basin elongation ratio (Re) are few geomorphic indices that require length or area for its computation (Mukul et al. 2017) (Table 2).

4 Results

4.1 Relief Ratio (*Rh*)

The relief ratio (*Rh*) is computed from the elevation of the river source (*ZS*), river mouth (*ZM*), and the maximum watershed length (*L*). Schumm (1956) describes relief ratio as the grade of the river and is derived as follows:

$$\text{Relief Ratio (Rh)} = \frac{ZS - ZM}{L} \quad (1)$$

The *ZS* and *ZM* values for Chel River are 1918.9 m and 95.5 m respectively. The maximum watershed length (*L*) is 42.6 km. From the above values, the relief ratio (*Rh*) was computed ~0.043.

4.2 Drainage Basin Asymmetry (*AF*)

The drainage basin asymmetry is used to show asymmetry of drainage networks and basin as a result of tectonic tilting at both local and regional scale (Keller and Pinter 2002; Garrote et al. 2008; Hare and Gardner 1985; Cox 1994; Özkaymak and Sözbilir 2012; Giaconia et al. 2012).

The asymmetry factor (*AF*) can be represented as the percent of the area of the basin that is found on the right bank side of the mainstream (while looking downstream) to the whole area of the basin (Vijith et al. 2015) and is defined as:

$$AF = \left(\frac{A_r}{A_t} \right) \times 100 \quad (2)$$

where *A_r* is the area of the basin to the right of the trunk stream and *A_t* is the total area of the drainage basin. *AF* is applied over a relatively large area or at the scale of a drainage basin (Hare and Gardner 1985). *AF* value close to 50 shows that the basin has developed under stable conditions with little or no tilting. Parameter *Af* factor above or below 50 may result from basin tilting, which may be attributed to active tectonics or differential erosion owing to lithological variations (El et al. 2007). With *A_r* = 129.4 km². and *A_t* = 321 km² the drainage basin asymmetry factor for

Table 2 List of geomorphic indices used with results from the Chel river basin

Geomorphic indices	Equation	Explanations	Results
Relief ratio (Rh), Schumm (1956)	$Rh = ZS-ZM/L$	ZS- elevation of the river source ZM- elevation of the river mouth L- maximum watershed length	0.043
Drainage basin asymmetry (Af)	$Af = ((Ar/At) \times 100)$	Ar—area of the basin to the right side of the major river At—total area of the drainage basin	40.31
Basin elongation ratio (Re), Schumm (1956)	$Re = 2x \frac{\sqrt{AT/\pi}}{L}$	diameter of the circle having the same area as the basin (AT), and the maximum basin length (L)	0.47
Hypsometric Integral (HI), Strahler (1952)	$HI = (hmean - hmin)/(hmax - hmin)$	hmean—average height, hmin and hmax are the minimum and maximum height of the catchment	0.15
Stream length gradient index (SL), Hack (1973)	$SL = (\Delta H/\Delta L) \times L$	ΔH —change in elevation of the reach ΔL —change in length of the reach L—total length of the channel to the point where the SL index is being calculated	23–950
Valley floor width-to-height ratio (Vf), Bull and McFadden (1977)	$Vf = 2Vfw/Eld + Erd - 2Esc$	Erd and Eld are elevations of the right and left valley divides respectively, Esc the valley floor elevation, and Vfw the valley floor width	0.1–3.67
Index of mountain front sinuosity (Smf), Bull and McFadden (1977)	$Smf = Lmf/Ls$	Lmf- length of the mountain front along the foot of the mountain where a change in slope from the mountain to piedmont occurs; and Ls- straight-line length of the mountain front	2.02
Transverse topographic symmetry factor (T)	$T = Da/Dd$	Da—distance between the midline of the drainage basin and the active meander belt midline Dd—distance between the midline and the basin divide	0.15–0.91
Longitudinal profile	Elevation—distance plot	X, Y plot of elevation and distance along the river channel from head water to mouth	–

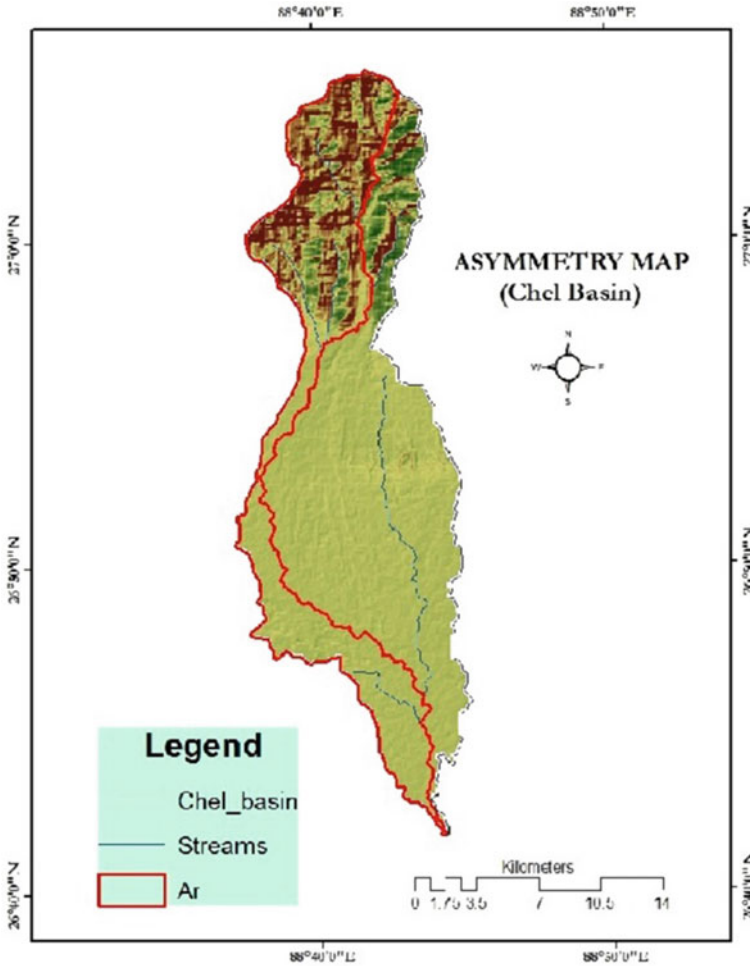


Fig. 4 Tectonic tilting of Chel Basin, 40.31% area of basin is to the right side of trunk stream

the Chel basin is 40.31 which implies the basin is tilted towards the right (looking downstream) (Fig. 4).

4.3 Basin Elongation Ratio (Re)

The basin elongation ratio (Re) is defined as the ratio of the diameter of the circle having the same area as the basin (AT) and the maximum basin length (L ; Schumm 1956) and is computed using the following equation (Schumm 1956):

$$\text{Basin Elongation Ratio (Re)} = 2x \frac{\sqrt{AT/\pi}}{L} \quad (3)$$

Based on Re, the basins are classified as circular ($\text{Re} > 0.9$), oval ($0.8 < \text{Re} < 0.9$), less elongated ($0.7 < \text{Re} < 0.8$), and elongated ($\text{Re} < 0.7$; Strahler 1964). The basin elongation ratio for the Chel river basin is computed to 0.47.

4.4 Hypsometric Curve and Hypsometric Integral (HI)

Hypsometry is the computation of the relation between area and corresponding elevation slab of a basin (Strahler 1952; Langbein 1947). Thus, hypsometric curve facilitates the comparison of areas of varying sizes and elevations and consists of a normalized cumulative area along the x-axis and normalized elevation along the y-axis. The consequent shape of the curve obtained, gives an indication of the geomorphic processes operating in a watershed (Strahler 1952). A convex curve indicates a young basin categorized by irregular relief demonstrating active tectonics, whereas a concave curve is related to an old basin where alluvial or fluvial processes dominate. A concave-convex curve (S-shape) is an indication of a mature basin where tectonics and erosion work in near equilibrium (Strahler 1952). A basin's relief can be quantified easily by the hypsometric integral (HI). The HI can be calculated from the area under the curve, and it expresses, in percentage, the volume of the original basin that remains unaltered. Hypsometric curves are obtained by plotting the proportion of the total height (h/H) against the proportion of the total area (a/A) of the basin, where H is the total relative height, A is the total area of the basin and "a" is the area of the basin above a given line of elevation h (Keller and Pinter 2002). Following Pike and Wilson (1971), HI can be calculated as follows:

$$\text{HI} = \frac{h_{\text{mean}} - h_{\text{min}}}{h_{\text{max}} - h_{\text{min}}} \quad (4)$$

where h_{mean} , h_{min} , and h_{max} are the mean elevation, minimum elevation, and maximum elevation of the watershed respectively. The HI values range between 0 and 1 with values close to 0 indicating the basin to be at an old-age stage and values close to 1 indicating a youthful stage (Strahler 1964). The basin at the youthful stage is characterized by rugged relief and deep incision, whereas old-age basins have subdued relief (Keller and Pinter 2002; Strahler 1964). Mature basins are the intermediate stage where the geomorphic progression occurs at near stability. The HI is expressed as a percentage and is an indicator of the remaining volume of the original basin (Ritter et al. 2002). The hypsometric integral is also an indication of the 'cycle of erosion' (Strahler 1952; Garg 1983). The higher H.I. values indicate much area under the hypsometric curve that is still to be eroded and thus indicate a young landform and vice-versa. The Hypsometric Integral (H.I.) of Chel basin is

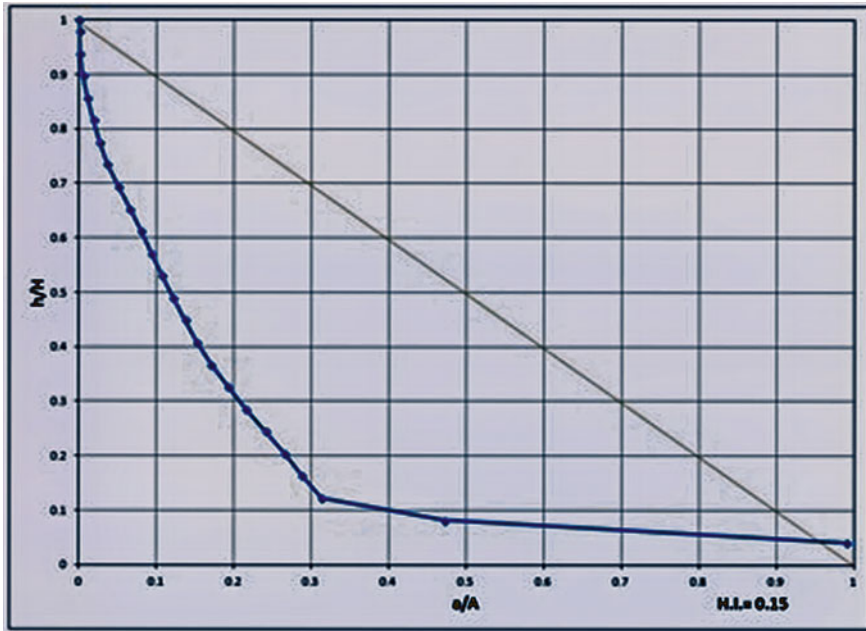


Fig. 5 Hypsometric curve of chel basin

0.15 indicating the basin is in the senile stage and only 15% of the original landform is yet to be removed by the erosion agents (Fig. 5).

4.5 Stream Length Gradient Index (SL)

Stream Length-Gradient Index (SL Index) is considered as one of the quantitative geomorphic parameters incorporated in the morphotectonic analysis (Hack 1973). Tectonic upliftment of a basin and consequent higher vertical erosion and stream profiles changes can be attributed to the SL gradient Index (Vijith et al. 2015).

Lithology, erosional process, and tectonic forces greatly affect the morphology of a drainage basin (Keller and Pinter 2002; Dehborzogi et al. 2010; Hack 1973; Giaconia et al. 2012). For areas with abrupt changes in stream profiles, stream pattern and slope, the SL index has proved to be an excellent method to evaluate the ongoing processes of uplift (Štěpančíková et al. 2008; Toudeshki and Arian 2011). Nevertheless, the effectiveness of the parameter in detecting local active structures has not been confirmed for small catchments and/or in regions where tectonic activity is subtle (Chen et al. 2003 and references therein); (Troiani and Della Seta 2008). In small river basins, the contribution of the lithological effect to anomalous values of the SL Index seems indistinguishable from the tectonic one (Troiani and Della Seta

2008). However, in spite of all the difficulties, the SL index has been widely used as a proxy to identify areas of anomalous uplift within a landscape (Kale and Shejwalkar 2008). In tectonically active regions, and at the basin scale of investigation, the SL index can be a useful tool to detect tectonic displacement (Keller and Pinter 2002; Chen et al. 2003; Zovoili et al. 2004).

The stream length gradient index (SL) also shows the association between tectonics, stream power, and rock resistance (Hack 1973; Keller and Pinter 2002) and is computed using the following equation:

Stream Length Gradient Index,

$$SL = \frac{\Delta H}{\Delta L} \times L \quad (5)$$

where ΔH is the difference in elevation, and ΔL the length of the stream reach where the index is to be computed. Thus $(\Delta H/\Delta L)$ is the gradient of the stream reach. The L is the channel length from the drainage divide to the center of the reach. Stream power is a function of water, slope, and discharge.

Thus, any alter in slope induced by tectonic deformation or differential rock resistance from lithological variation leads to a change in stream power and gets reflected in abnormal SL values.

We calculated the values of SL along the river Chel through demarcation of the watershed, generation of contour at equal intervals OF 2kms, measurement of the values of H and L using ArcGIS 10.1 on a mosaic of SRTM DEM. The SL values thus generated along the river Chel range widely from 23 to 950 (Table 3 and Fig. 9).

4.6 Valley Floor Width-To-Height Ratio (Vf)

The U- and V-shaped valleys can be identified by the valley floor width-to-height ratio, Vf; (Wells et al. 1988) geomorphic index, which is defined as:

$$Vf = \frac{2Vfw}{Eld + Erd - 2Esc} \quad (6)$$

where Erd and Eld are elevations of the right and left valley divides respectively, Esc the valley floor elevation, and Vfw the valley floor width. Values closer to 0 are signifying the presence of V-shaped valleys and those close to 1 or above 1 indicate U- shaped valleys. The V-shaped valleys indicate the presence of areas affected by tectonic uplift. The U-shaped valleys indicate the attainment of erosion at the base level (Keller 1986; Keller and Pinter 2002). The Vf for the Chel river basin was computed for every 2 kms of the channel length at SL computation points from its near-source up to the mountain front. The Vf values range from 0.1 to 3.67 within this stretch of 14 km (Fig. 6).

Table 3 Stream Length Gradient Index, computed along the main channel of Chel river

Distance (Kms)	SL index (m)
2	180
4	575
6	950
8	700
10	453
12	465
14	390
16	330
18	300
20	292
22	280
24	180
26	120
28	310
30	130
32	140
34	85
36	280
38	132
40	86
42	102
44	71
46	73
48	23
50	36
52	25
54	31
56	33
58	28

4.7 Index of Mountain Front Sinuosity (*Smf*)

Bull and McFadden (1977) and Bull (1978) defines Index of mountain front sinuosity, *Smf* as

$$Smf = \frac{Lmf}{Ls} \quad (7)$$

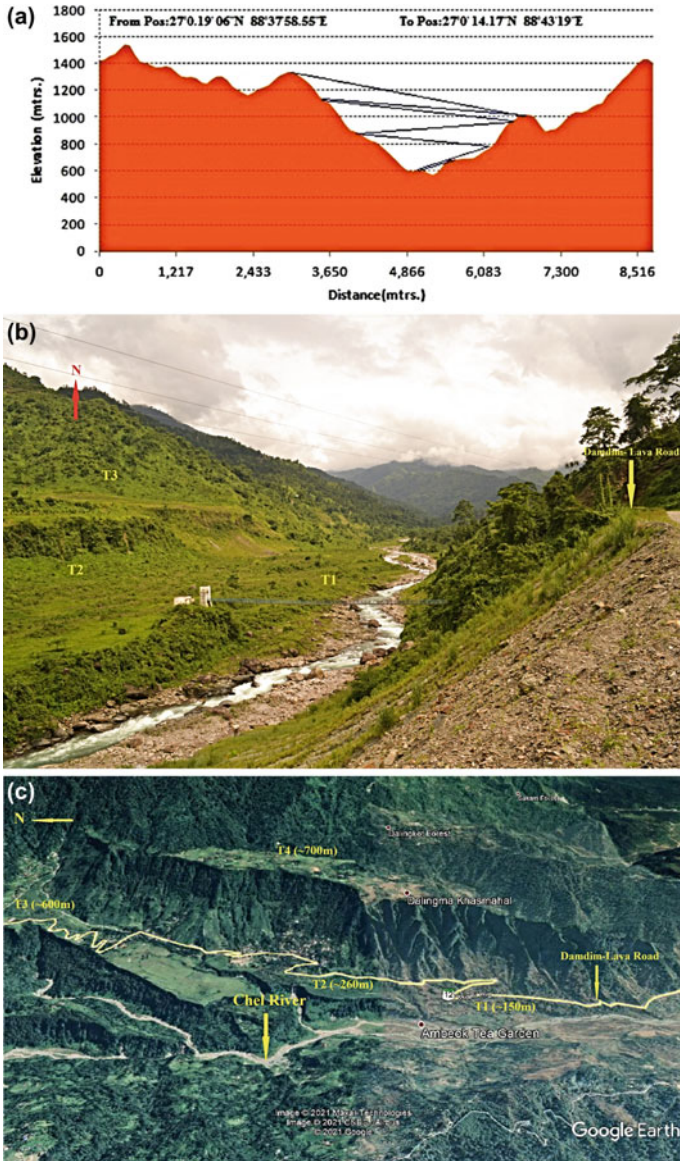


Fig. 6 a–c Transverse valley profile of the Chel River, sculpted by unpaired terraces connected by blue line (a), Field photograph showing steep and highly incised valley floor of Chel with multiple terrace development on the right side of flow in the upper course around 4kms upstream of Gorubathan (view towards north) (b), Google Earth image showing highly incised valley floor with multiple terrace development on the left side of flow in the upper course near Ambik T.E. (view towards north east) (c)

where L_{mf} is the length of the mountain front along the foot of the mountain where a change in slope from the mountain to piedmont occurs; and L_s is the straight-line length of the mountain front.

S_{mf} shows a relationship between erosive processes that tend to erode a mountain front, making it more sinuous through rivers, and active vertical tectonics that tend to produce straight mountain fronts, which are often coincidental with active faults or folds (Keller 1986; Bull and McFadden 1977). That is, mountain fronts with active tectonics and active uplift are straight giving the lower value of S_{mf} whereas the regions which have lower or no active tectonics and consequent low rate of upliftment, the erosional processes along the mountain front will dominate and thus will produce more sinuous mountain front resulting in higher S_{mf} .

This index is used to evaluate the relative tectonic activity along mountain fronts (Keller and Pinter 2002; Silva et al. 2003). Active mountains yield a straight front with low S_{mf} values; whereas along less active fronts, erosional processes generate irregular or sinuous fronts with high S_{mf} values. The mountain front sinuosity index is generally applicable to all fault-bounded mountain fronts (Sharma et al. 2018).

S_{mf} can be easily calculated from topographical maps or aerial photographs. But the accuracy of value depends upon the scale (Bull and McFadden 1977). Large-scale maps such as Topographical maps and aerial photography which generally have higher resolution give a higher level of accuracy compared to small-scale maps (>1:250,000) which give approximate values of S_{mf} due to the lower resolution. Lower the value of S_{mf} higher is the level of active tectonics and vice-versa. S_{mf} approach 1.0 for the most tectonically active mountain front whereas as the rate of upliftment decreases, the erosional processes carve a much broad and sinuous mountain front leading to a higher S_{mf} value. S_{mf} values lower than 1.4 signifies tectonically active (Keller 1986; Rockwell et al. 1985) whereas inactive mountain fronts where the initial mountain front may be more than 1 km away from the present erosional front are usually associated with higher S_{mf} values (>3) (Bull and McFadden 1977).

Silva et al. (2003) have calculated the index of mountain front sinuosity using a topographical map at a scale 1:50,000 in the two most prominent crustal-scale structures of the Mediterranean sector of Spain: The Eastern Betic Shear Zone (EBSZ) and the Valencia Trough. The authors have divided mountain fronts into three classes on the basis of S_{mf} values:

Class-I (Active Tectonics)—Linear Mountain Fronts ($S_{mf} < 1.5$).

Class-II (Moderate Tectonics)—Irregular Mountain Fronts (S_{mf} ranges from 1.8–2.3).

Class-III (Inactive)—Highly Sinuous Mountain Fronts ($S_{mf} \geq 2.8$).

Here the mountain front sinuosity Index of Chel basin has been attempted from SOI toposheet no 73 B/9 at 1:50,000 scale (Fig. 9b) and with $L_{mf} = 8.9$ km and $L_s = 4.4$ km, the S_{mf} value so calculated is 2.02. So based on (Keller 1986; Silva et al. 2003; Rockwell et al. 1985), the mountain front of Chel basin falls under Class-II of moderate tectonics characterized by irregular mountain front (Fig. 7a–b).

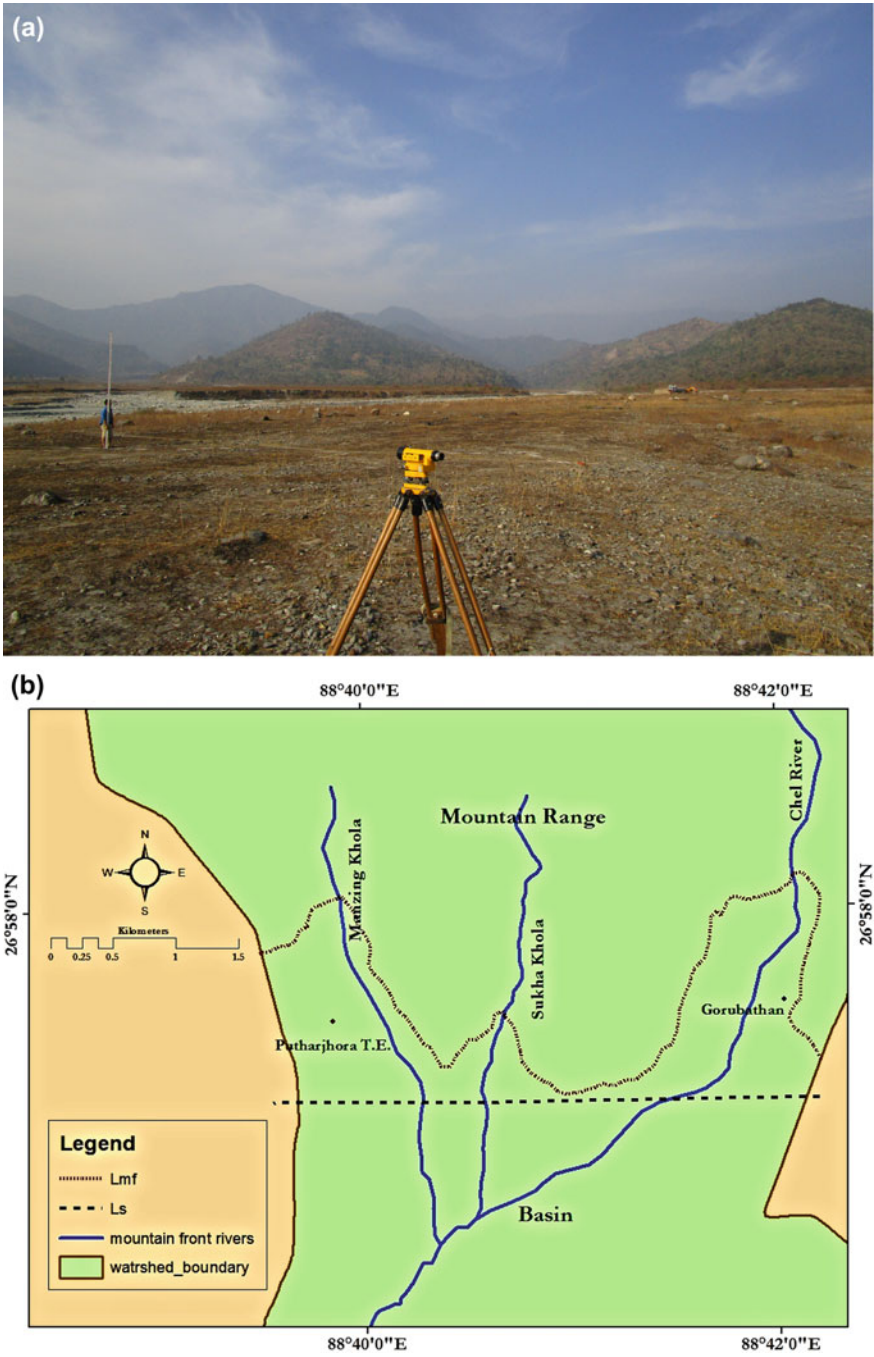


Fig. 7 a-b Field photograph showing Mountain front of Chel Basin (View towards North-west) **a**, Mapping of mountain front, Lmf and Ls of Chel basin **b**

4.8 *Transverse Topographic Symmetry Factor (T)*

The transverse topographic symmetry factor is another important quantitative geomorphic parameter for the evaluation of the tilt of a basin. The T factor can be calculated using the equation:

$$T = D_a/D_d \quad (8)$$

where D_a is the distance from the midline of the drainage basin to the midline of the active meander belt. D_d is the distance from the basin midline to basin divide. Generally, the value of T ranges from 0 to 1 and the values close to 0 indicate an absolute symmetric basin, while values close to 1 indicate a highly asymmetric basin. Thus, the T value approaches 1 as the asymmetry of the basin increases. This method was first devised by Cox (1994) in the year 1994 and applied to the southwestern Mississippi Embayment infer west-southwestward as preferred stream migration. The observed T values for the Chel basin range 0.15–0.91 implying ground tilting of the basin (Figs. 8 and 9).



Fig. 8 Multiple terrace in the Piedmont near the confluence of the Chel River and the Sukha River, North-east of Putharjhora T.G, T3 is the oldest and T1 is the youngest

4.9 Longitudinal Profile

The longitudinal profile of a stream can provide clues to underlying materials as well as an insight into the geologic processes and geomorphic evolution of the area (Giaconia et al. 2012; Jain et al. 2006; Hack 1957; Ambili and Narayana 2014). The longitudinal profile of a stream channel can be drawn graphically by a plot of altitude in (ordinate) as a function of horizontal distance in (abscissa). Longitudinal river profiles can be interpreted as arising from the balance between erosion and uplift rates. This profile provides an interpretation of the surface history of the river channel as they depict the origin of the river channel and it can be interpreted based on the shape of the curves (Ferraris et al. 2012). Concave profiles represent a long-term equilibrium between uplift and erosion rates, while concave-convex profiles with erosion steps in the middle reach indicate a long-term predominance of erosional processes. Convex profiles are characteristic of the areas where the uplift is dominant (Giaconia et al. 2012). The prepared longitudinal profile indicates the non-uniform and undulating nature of the longitudinal profile with the presence of few knick points at the steeper mountainous reach of the river (Fig. 11).

5 Discussion

Analysis of selected geomorphic indices derived from freely available SRTM DEMs were made to assess the impact of neotectonics on the drainage and landform development of the Chel river basin. The accuracy measurement performed to assess the usability of the DEM, validated the use of SRTM DEM 1Arc sec (30 m resolution) for the extraction of geomorphic indices in the present study.

The Relief ratio (Rh) computed for the Chel basin indicates that the river's gradient is steep (~ 0.043). The drainage basin asymmetry factor (AF) suggests possible regional tectonic tilting or any structural anomalies. The deviation of AF from the central value of 50 indicates basin asymmetry due to tectonic tilting. The AF calculated for the Chel basin is 40.31 (< 50) indicates the basin is tilted towards the right (looking downstream). It has been further corroborated by the values and directional vectors of tilting calculated by assessing the transverse topographic symmetric (T) factor, which was computed at 2 km interval along the main channel. The observed T values for the Chel basin range 0.15–0.91 implying a lateral shift of stream and basin from symmetrical to asymmetrical. The basin is tilted significantly towards the southwest direction in the middle reach but is tilted towards the east in its upper and lower reach. This tilt or asymmetry of the basin is getting well manifested through the progressive westward migration of Chel river (Fig. 10) on the piedmont zone resulting in longer eastern tributaries compared to the western tributaries (Fig. 1c).

The elongation ratio (Re) 0.47 for Chel basin indicates basin as an elongated one (Strahler 1964) and tectonically active (Re range < 0.5 ; e.g., Cuong and Zuchiewicz 2001). According to (Bull and McFadden 1977), the basins draining tectonically

active areas are generally more elongated and become more circular with the ending of uplift. The reason behind such transformation is due to the fact the stream energy is mostly directed towards the down cutting in the drainage basins near the tectonically active mountain fronts whereas the slow rate of uplift permits widening of basins near the mountain fronts. Molin et al. (2004) opine that elongated basin shapes are also associated with high local relief and steep valley slopes.

The mountain front sinuosity index (Smf) value of 2.02 implies that the Chel basin falls under moderate tectonics, characterized by irregular mountain front (Keller 1986; Silva et al. 2003; Rockwell et al. 1985). Whereas it is under the category of slightly active and inactive regions (Smf range 1.4–3.0; e.g., Cuong and Zuchiewicz, 2001) and thus point to relatively high tectonic activity. In general, the mountain fronts in tectonically active areas are generally irregular and vice-versa because of the fact that stream energy is mostly directed towards the down cutting in the drainage basins near the tectonically active mountain fronts whereas the slow rate of uplift permits widening of basins near the mountain fronts making it more regular. The presence of V-shaped valleys at the mountain front (as evident from field photograph; Fig. 7a) and irregular mountain front (Fig. 7b) of Chel basin seem to be the result of an ongoing process of a higher rate of valley floor downcutting in response to the tectonic uplift near the mountain front.

The Hypsometric curve shows a relationship between the degree of erosion, dominant hillslope processes and landscape evolution. The hypsometric curve of river Chel shows a steep initial fall with increasing distance from the equilibrium line then followed by long gentle gradient and finally becoming almost parallel to the abscissa (Fig. 5). This resultant curve indicates very high stream power and a thus higher rate of erosion which denuded the basin to a large extent and gave the basin characteristics of an old stage of the erosion cycle. This is supplemented by a hypsometric integral (H.I.) value of 0.15 which implies that very little (only 15%) of the total basin area is present to be removed by the erosion agents. The very steep nature of the hypsometric curve with undulations and HI value of 0.15 can be attributed to the tectonically induced higher rate of erosion rather than the normal fluvial processes.

SL gradient index for Chel River was calculated for its whole length at every 2 km unit length extracting corresponding elevation values from the DEM. The SL gradient values thus computed for every 2 km unit length for 28 segments range widely from 23 to 950. SL index can be used to recognize recent tectonic activity by identifying irregularly high index values of a particular rock type, as the value of the SL index increases as rivers flow over active uplifted areas (Keller and Pinter 2002; Troiani and Della Seta 2008). The sudden increase in SL gradient index values can also be attributed to zones of lithological transition. Whereas the observed sudden changes in the SL gradient Index values of Chel river even on homogeneous lithology suggest greater role of tectonics over lithology (Fig. 9).

The valley floor width-to-height ratio (Vf) is considered to be a robust proxy of active tectonics. The Vf values for the Chel basin were computed from its source up to the mountain front i.e. only for the mountainous part at the 2 km interval for a total length of 14 km. The Vf values thus computed are all <0.7 till 10 km indicating vertical erosion in response to uplift resulting in tectonically induced V-shaped river valleys

which indicates a younger stage of valley development and ongoing deformation. The Vf values at 12 km and 14 km are 3.67 and 3.5 respectively suggesting broader river floors than onwards (10 km downslope) due to the comparatively greater lateral erosion of valley sides over weak tectonics. On its upper mountainous course, the main river is found to be flanked by multiple unpaired terraces on both sides and many of them are tilted (Fig. 6a–c).

A longitudinal profile for the river Chel was prepared by extracting and placing elevation values against the length. The profile thus obtained was subjected to smoothing technique available in MS Excel to avoid any unnecessary large misleading fluctuations. The prepared longitudinal profile is non-uniform and undulating in nature along with the presence of knick points at the steeper mountainous reach of the river (Fig. 11). According to Crosby and Whipple (2006), the presence of knickpoints in the steeper reaches of the longitudinal profile is caused either by the change in lithology (resistant or non-resistant) or structural disturbance in the area (uplift or fault), where the stream tries to adjust to the terrain characteristics. In the case of Chel river, all the knick points are close to different lithological transition zones and also to major thrusts (both surface and blind). So there seems coupled reason of lithology and tectonics for the location of knick points. Whereas the non-uniform and undulating longitudinal profile suggests occasional changes in the gradient of the Chel river and can be attributed to the structural disturbances caused by the tectonic activities in the region (e.g. reactivation of Munsiri thrust in the vicinity; Mukul et al. 2017, Quaternary deformation of the Gorubathan recess; Srivastava et al. 2017) that seems to have caused multiple fractures and changes in the base level of the river channel.

The combination of assessed indices with the lithology of the basin gives an elaborate picture of the influence of neotectonics and its implications on the basin morphology and consequent river characteristics (Fig. 12). This includes SL, T, and AF which shows the variation of SL values along the river, direction of channel shifting from the basin midline, and direction of tilt. This allows for the assessment of the role of varying lithology over the development of SL index values. Since the maximum variation of SL values is observed above the mountain front in the multi-lithozone of the transitional boundary between Ptd2, YPt2l, and Ptr whereas the largest variation is observed in a single unit of rock (Q2b), it seems there is coupled impact of tectonics and lithology in the evolution of river characteristics in the Chel basin where tectonics slightly dominates over the lithology. These findings are further substantiated by the deep incisions made by the main channel on Quaternary sediments (Q2b and Q2c) of piedmont and the lower course with unpaired terraces which indicates the response of the channel to the ongoing tectonics (Fig. 8). Mandal and Sarkar (2016) also describe the fact that the present-day Chel river, incises deep through the sediment pile leaving the fan system dormant and opines basement uplift to be the cause of this incision.

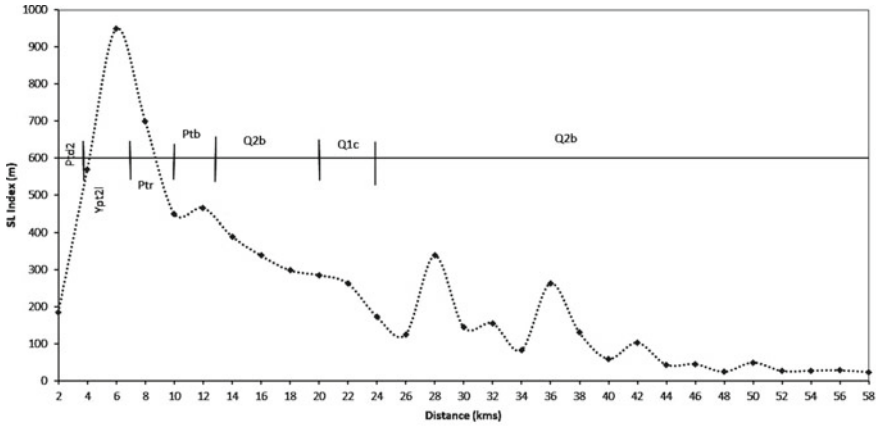


Fig. 9 SL Index of Chel river with lithological boundaries. Note the sudden increase in SL values in uniform lithology. (Consult Table-1 for details of litho units)

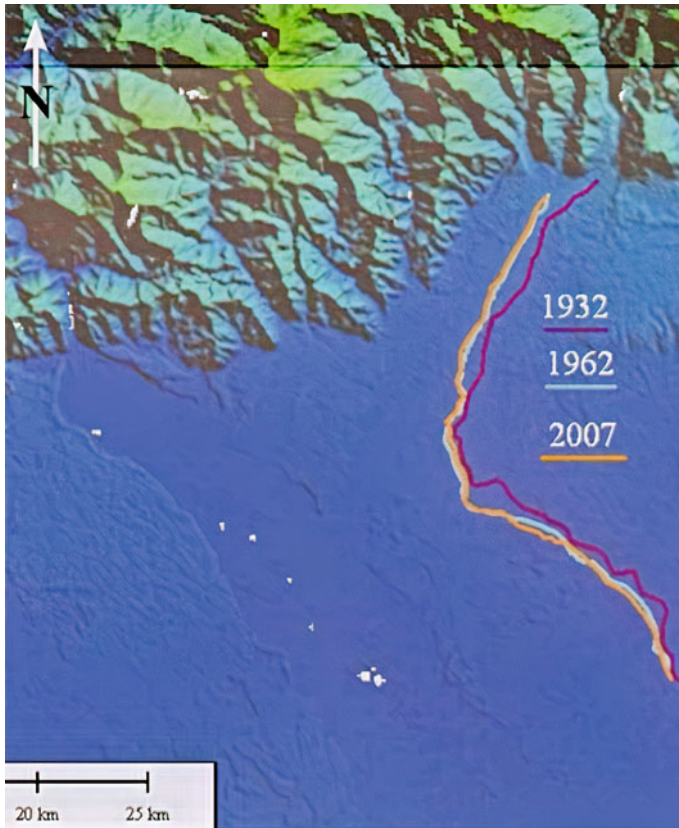


Fig. 10 Progressive westward migration of River Chel. (Source- Mandal and Sarkar 2016)

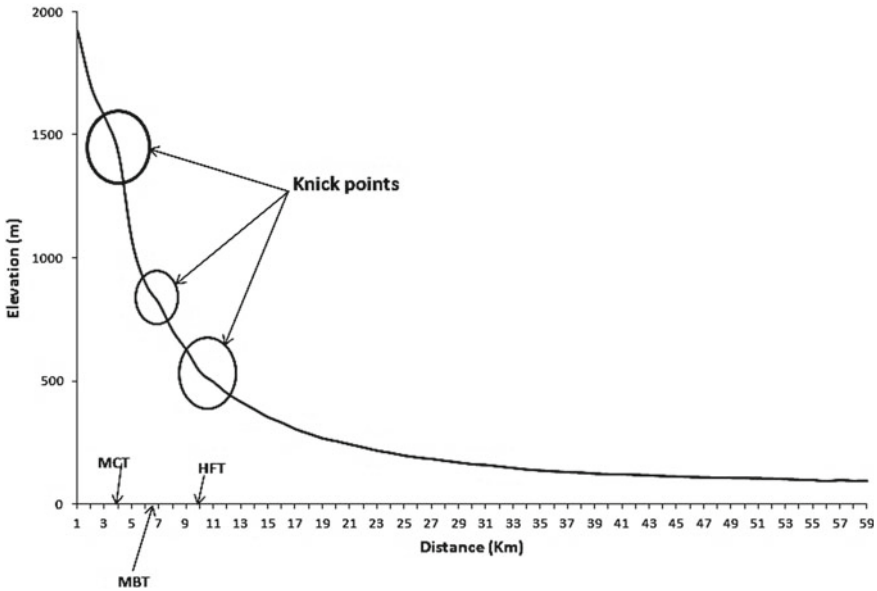


Fig. 11 Longitudinal profile of the Chel river with Knick points

6 Conclusion

Neotectonics exerts significant control on landforms and the rivers flowing over it. Thus, an attempt was made to understand the extent of tectonic influence over the Chel river and its basin characteristics through analysis of spatially derived SRTM DEM-based geomorphic indices. The reliability and accuracy of geomorphic indices depend heavily on the accuracy of DEM used, therefore the SRTM DEM used was first subjected to accuracy assessment. The linear regression analysis resulted in a best-fit plot with a correlation coefficient of 0.99 and RMSE of ± 81 m. Thus, the results derived confirmed the usability of SRTM 30 m DEM. Relief Ratio (Rh) of 0.043 indicates high gradient of the river. The basin is asymmetric and is tilted towards the southwest direction as suggested by the drainage basin asymmetric factor (Af) of 40.31 and the transverse topographic symmetric factor (T) values ranging from 0.15 to 0.91. The basin elongation (Re) of 0.47 implies an elongated active basin. Further, a sigmoidal or a concave-convex hypsometric curve with an integral value of 0.15 indicates an active but mature basin. The longitudinal profile of the Chel river approximates an equilibrium, concave profile with few knick points on the steep mountainous course which further corroborates the active but mature nature of the basin. The computed valley floor width-to-height ratio (Vf) values < 0.7 from its source till 10 km of length indicates the presence of tectonically induced V-shaped valleys in the upper course of the river. In this zone, the main river is flanked with multiple terraces on both sides and many of them are tilted. Further, the mountain

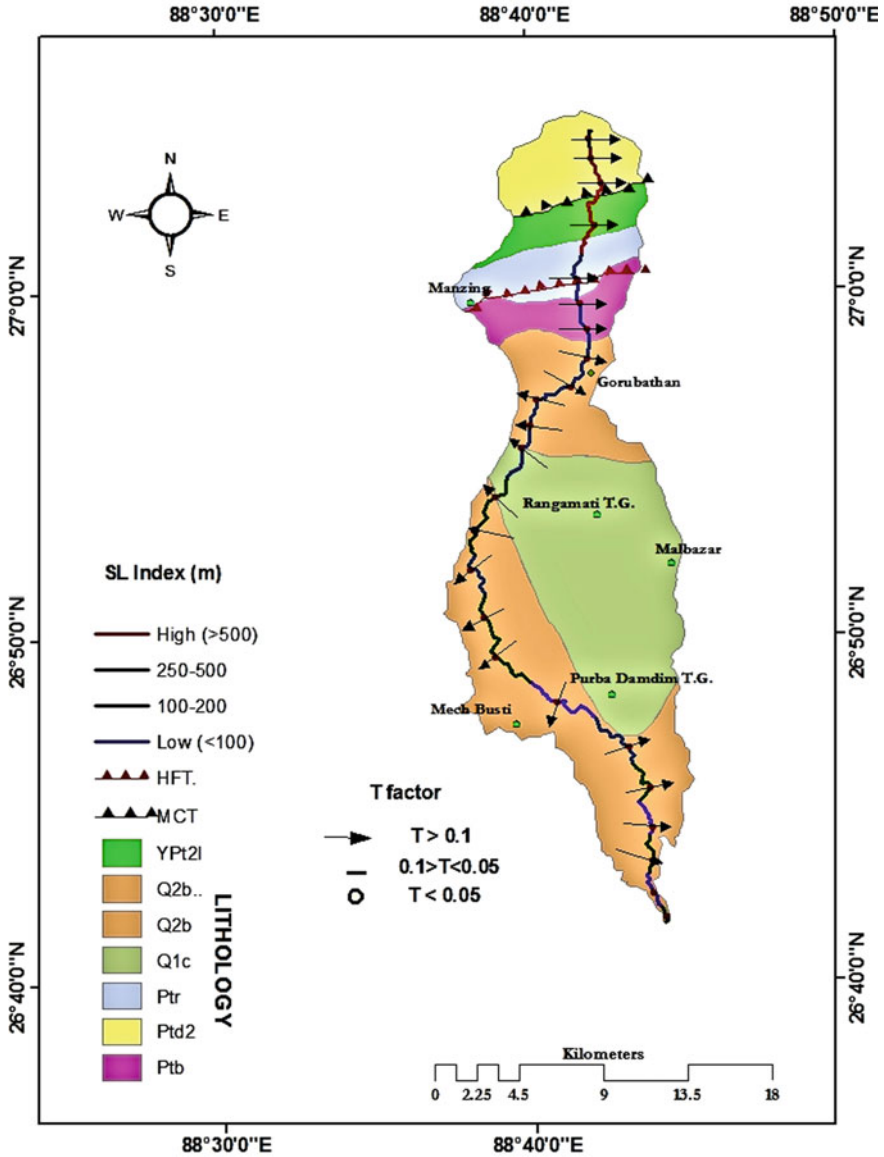


Fig. 12 Map showing cumulative effect of lithology, transverse topographic symmetric factor (T), SL gradient index and major structural features present in the Chel river basin. YPt2l-Lingtse Granite Gneiss (Proterozoic-II), Q2b = Baikunthapur Foration (Holocene), Q1c = Middle to upper Chalsa formation (Pleistocene), Ptr = Reyang formation (Proterozoic), Ptd2 = Chungthang Formation (Proterozoic), Ptb = Buxa Formation (Proterozoic)

front sinuosity index (Smf) value of 2.02 implies that the basin falls under moderate tectonics characterized by irregular mountain front. The abrupt changes in the SL gradient index suggest differential uplift of the basin, in response to the ongoing tectonics. Thus, from the analysis of geomorphic indices, it can be inferred that the Chel river basin has undergone the differential level of neotectonics activity and the trend of severity generally decreases from north to south. Consequently, the river has adjusted with the ongoing tectonics and the evolution has led to the present-day basin morphology. Lastly, the study also underscores the huge potentiality of SRTM DEMs or any other satellite-based DEMs in morphotectonic studies.

Acknowledgements The first author would like to acknowledge the financial assistance received from the University Grants Commission (UGC), through letter no. F.PHW-135/15-16(ERO) dated: 02/12/2016. First author would also like to thank friends Mr. Lenin Rai and Miss Asha Lama from Gorubathan and Malbazaar respectively for taking care of his lodging, fooding and introducing the study area during the initial phase of the field study. We also would like to convey our gratitude to two anonymous reviewers for their critical comments which greatly helped to improve the quality of this manuscript.

References

- Acharyya SK (1976) On the nature of the main boundary fault in the Darjeeling sub-Himalaya. Geol Survey India, Misc Publ 24:395–408
- Ambili V, Narayana AC (2014) Tectonic effects on the longitudinal profiles of the Chaliyar River and its tributaries, southwest India. *Geomorphology* 217:37–47
- Andermann C, Gloaguen R (2009) Estimation of erosion in tectonically active orogenies. Example from the Bhotekoshi catchment, Himalaya (Nepal). *Int J Remote Sens* 30, 3075e3096
- Azor A, Keller EA, Yeats RS (2002) Geomorphic indicators of active fold growth: South Mountain-Oak Ridge Ventura basin, southern California. *Geol Soc Am Bull* 114:745–753
- Bull WB, McFadden LD (1977) Tectonic geomorphology North and South of the Garlock Fault, California, Geomorphology in Arid Regions. In: Proceedings of the eighth annual geomorphology symposium. State University of New York, Binghamton, pp 115–138
- Bull WB (1978) Geomorphic tectonic activity classes of the south front of the San Gabriel Mountains, CA. Unpublished Final Rep., U.S. Geol. Survey, Contract No. 14–08- 0001-G-394, p 59
- Burbank DW, Anderson RS (2001) *Tectonic Geomorphology*. Blackwell Scientific, Oxford, p 270
- Chen YC, Sung Q, Cheng KY (2003) Along-strike variations of morphotectonic features in the Western Foothills of Taiwan: tectonic implications based on stream gradient and hypsometric analysis. *Geomorphology* 56:109–137
- Cuong NQ, Zuchiewicz WA (2001) Morphotectonic properties of the Lo River Fault near Tam Dao in North Vietnam. *Nat Hazards Earth Syst Sci* 1:15–22
- Cox RT (1994) Analysis of drainage basin symmetry as a rapid technique to identify areas of possible quaternary tilt-block tectonics: an example from the mississippi embayment. *Geol Soc Am Bull* 106:571–581
- Crosby BT, Whipple KX (2006) Knickpoint initiation and distribution within Fluvial Networks: 236 waterfalls in the Waipaoa River, North Island, New Zealand. *Geomorphology* 82:16–38
- De R, Kayal JR (2003) Seismotectonic model of the Sikkim Himalaya: constraint from microearthquake surveys. *Bull Seismol Soc Am* 93:1395–1400

- Dehbozorgi M, Pourkermani M, Arian M, Matkan AA, Motamedi H, Hosseiniasl A (2010) Quantitative analysis of relative tectonic activity in the Sarvestan area, central Zagros. *Iran Geomorphol* 121(2010):329–341
- Ferraris F, Firpo M, Pazzaglia FJ (2012) DEM analyses and morphotectonic interpretation: the plio-quaternary evolution of the Eastern Ligurian Alps, Italy. *Geomorphology* 149–150:27–40
- Gansser A (1964) *Geology of the Himalayas*. Interscience, Wiley, New York, p 289
- Gansser A (1981) The geodynamic history of Himalaya. In Gupta HK, Delany FM (eds) *Zagros–Hindukush–Himalaya: Geodynamic Evolution*, 3. American Geophysics Union, Geodynamic Series, Washington, pp 111–121
- Gardner TW, Back W, Bullard TF, Hare PW, Kesel RH, Lowe DR, Troester JW (1987) Central America and the Caribbean. *Geomorphic systems of North America: Boulder, Colorado. Geological Society of America*, 2, 343–401 (Centennial Special)
- Garg SK (1983) *Geology-the science of the earth*. Khanna Publishers, New Delhi
- Garrote J, Heydt GG, Cox RT (2008) Multi-Stream order analyses in basin asymmetry: a tool to discriminate the influence of neotectonics in Fluvial Landscape Development Madrid Basin, Central Spain. *Geomorphology* 102:130–144
- Gehrels GE, DeCelles PG, Martin AT, Ojha P, Pinhasi G, Upreti BN (2003) Initiation of the Himalayan orogen as an early Paleozoic thin-skinned thrust belt. *Geol Soc Am Today* 13(9):4e9
- Giaconia F, Booth-Rea G, Martínez-Martínez JM, Azañón JM, Pérez-Peña JV, Pérez-Romero J, Villegas I (2012) Geomorphic evidence of active tectonics in the Sierra Alhamilla Eastern Betics, SE Spain. *Geomorphology* 145–146:90–106
- Goswami CC, Mukhopadhyay D, Poddar BC (2013) Geomorphology in relation to tectonics: a case study from the eastern Himalayan foothills of West Bengal, India. *Quat Int* 298(2013):80–92
- GSI (1999) *Geological and Mineral map of West Bengal*
- Guha D, Bardhan S, Basir SR, De AK, Sarkar A (2007) Imprints of Himalayan thrust tectonics on the Quaternary piedmont sediments of the Neora-Jaldhaka Valley, Darjeeling-Sikkim Sub-Himalayas, India. *J Asian Earth Sci* 30(2007):464–473
- Hack JT (1957) Studies of longitudinal stream profiles in Virginia and Maryland (No. 294-B). Geological Survey Professional Paper 294-B
- Hack JT (1973) Stream-profiles analysis and stream-gradient index. *J Res U.S. Geol Surv* 1(4):421–429
- El HR, Irigaray C, Fernández T, Chacón J, Keller EA (2007) Assessment of relative active tectonics, southwest border of Sierra Nevada (southern Spain). *Geomorphology* 96:150–173
- Hare PH, Gardner TW (1985) Geomorphic indicators of vertical neotectonism along converging plate margins, Nicoya Peninsula, Costa Rica. In: Morisawa M, Hack JT (eds) *Tectonic geomorphology*. Allen and Unwin, Boston, pp 75–104
- Harkins NW, Anastasio David J, Pazzaglia Frank J (2005) Tectonic geomorphology of the Red Rock fault, insights into segmentation and landscape evolution of a developing range front normal fault. *J Struct Geol* 27:1925–1939
- Heim A, Gansser A (1939) Central Himalaya geological observations of swiss expedition. *Mem Soc Helv Sci Nat* 73:1–245. In: Keller EA, Pinter N (eds) *Active tectonic earth quake—uplift and landscape*. Prentice Hall Inc., Upper Saddle River, p 337
- Hodges KV, Silverberg DS (1988) Thermal evolution of the Greater Himalaya, Garhwal, India. *Tectonophysics* 7:583–600
- Horton RE (1945) Erosional development of streams and their drainage basins: hydrophysical approach to quantitative morphology. *Geol Soc Am Bull* 56:275–370
- Jain V, Preston N, Fryirs K, Brierley G (2006) Comparative assessment of three approaches for deriving stream power plots along longitudinal profile in the upper Hunter River catchment, New South Wales, Australia. *Geomorphology* 74:297–317
- Kale VS (2014) Geomorphic history and landscape of India. In: Kale VS (ed) *Landscapes and landforms of India*. Springer-Verlag, Heidelberg, pp 25–37
- Kale VS, Shejwalkar N (2008) Uplift along the Western Margin of the Deccan Basalt Province: is there any geomorphometric evidence? *J Earth Syst Sci* 1176:959–971

- Keller EA (1986) Investigation of active tectonics: use of sacrificial Earth processes. In: Wallace RE (ed) *Active Tectonics*. Studies in Geophysics, National Academy Press, Washington, DC, pp 136–147
- Keller EA, Pinter N (1996) *Active tectonics: earthquakes, uplift, and landscape*, 1st edn. Prentice Hall, New Jersey
- Keller EA, Pinter N (2002) *Active tectonics: earthquakes, uplift, and landscape*, 2nd edn. Prentice Hall, New Jersey
- Kumar S, Wesnousky SG, Jayangondaperumal R, Nakata T, Kumahara Y, Singh V (2010) Paleoseismological evidence of surface faulting along the northeastern Himalayan front, India: timing, size, and spatial extent of great earthquakes. *J Geophys Res* 115:B12422
- Langbein WB (1947) Topographic characteristics of Drainage Basins. Geological Survey Water-Supply paper 9, 68-C, Washington
- Mahmood SA, Gloaguen R (2012) Appraisal of active tectonics in Hindu Kush: insights from DEM derived geomorphic indices and drainage analysis. *Geosci Front* 3:407–428
- Matin A, Mukul M (2010) Phases of deformation from cross-cutting structural relationships in external thrust sheets: insights from small-scale structures in the Ramgarh thrust sheet, Darjeeling Himalaya, West Bengal. *Curr Sci* 99:1369–1377
- Mandal S, Sarkar S (2016) Overprint of neotectonism along the course of River Chel, North Bengal, India. *J Paleogeogr* 5(3):221–240
- Mitra G, Bhattacharya K, Mukul M (2010) The Lesser Himalayan Duplex in Sikkim: Implications for variations in Himalayan shortening. *J Geol Soc India* 75:289–301
- Molin P, Pazzaglia FJ, Dramis F (2004) Geomorphic expression of active tectonics in a rapidly-deforming forearc, Sila massif, Calabria, southern Italy. *Am J Sci* 304:559–589
- Mukul M, Srivastava V, Mukul M (2017) Out-of-sequence reactivation of the Munsiri thrust in the Relli River basin, Darjiling Himalaya, India: Insights from Shuttle Radar Topography Mission digital elevation model-based geomorphic indices. *Geomorphology* 284:229–237
- Nakata T (1989) Active faults of the Himalaya of India and Nepal. *Geol Soc Am Spec Pap* 232:243–264
- Nath SK, Adhikari MD, Maiti SK, Devaraj N, Srivastava N, Mohapatra LD (2014) Earthquake scenario in West Bengal with emphasis on seismic hazard microzonation of the city of Kolkata, India. *Nat Hazards Earth Syst Sci* 14:2549–2575
- Official Website of National Center of Seismology, MES, GOI. Accessed 10.04.2021
- Özkaymak C, Sözbilir H (2012) Tectonic Geomorphology of the Spiladağ High Ranges, Western Anatolia. *Geomorphology* 173–174:128–140
- Perez-Pena JV, Azanon JM, Azor A, Delgado J, Gonzalez FL (2009) Spatial analysis of stream power using GIS: SLk anomaly maps. *Earth Surf Process Landf* 34:16–25
- Pike RJ, Wilson SE (1971) Elevation-relief ratio, hypsometric integral and geomorphic area-altitude analysis. *Geol Soc Am Bull* 82:1079–1084
- Ritter DF, Kochel RC, Miller IR (2002) *Process geomorphology*. McGraw Hill, Boston
- Rockwell TK, Keller EA, Johnson DL (1985) Tectonic geomorphology of alluvial fans and mountain fronts near Ventura, California. In: Morisawa M (ed.) *Tectonic Geomorphology*. In: *Proceedings of the 15th Annual Geomorphology Symposium*. Allen and Unwin Publishers, Boston, MA, pp 183–207
- Schumm SA (1956) (1956) Evolution of drainage systems and slopes in badlands at Perth Amboy, New Jersey. *Geol Soc Am Bull* 67(5):597–646
- Seeber L, Gornitz V (1983) River profiles along the Himalayan arc as indicators of active tectonics. *Tectonophysics* 92:335e367
- Sharma G, Champati ray PK, Mohanty S (2018) Morphotectonic analysis and GNSS observations for assessment of relative tectonic activity in Alaknanda basin of Garhwal Himalaya, India. *Geomorphology* 301:108–120
- Silva PG, Goy JL, Zazo C, Bardajm T (2003) Fault generated mountain fronts in Southeast Spain: geomorphologic assessment of tectonic and earthquake activity. *Geomorphology* 250:203–226

- Srivastava V, Mukul M, Mukul M (2017) Quaternary deformation in the Gorubathan recess: insights on the structural and landscape evolution in the frontal Darjiling Himalaya. *Quat Int* XXX, 1–24
- Strahler AN (1952) Hypsometric (Area-Altitude) analysis of erosional topography. *Geol Soc Am Bull* 11:1117–1142
- Strahler AN (1964) Quantitative geomorphology of drainage and channel networks. In: Te Chow V (eds) *Handbook of applied hydrology*. Mc Graw Hill Book Company. New York, pp 4–39–4–76
- Štěpančíková P, Stemberk J, Vilímek V, Košťák B (2008) Neotectonic development of drainage networks in the East Sudeten Mountains and Monitoring of recent fault displacements (Czech Republic). *Geomorphology* 102:68–80
- Toudeshki VH, Arian M (2011) Morphotectonic analysis in the Ghezel Ozan River Basin, NW Iran. *J Geogr Geol* 31:258–265
- Troiani F, Della Seta M (2008) The use of the stream length-gradient index in morphotectonic analysis of small catchments: a case study from central Italy. *Geomorphology* 102:159–168 (usgs.gov). Accessed 06.04.2021
- Valdiya KS, Joshi DD, Sharma PK, Dey P (1992) Active Himalayan frontal fault, main boundary thrust and Ramgarh thrust in southern Kumaun. *J Geol Soc India* 40:509–528
- Valdiya KS (1995) Proterozoic sedimentation and Pan-African geodynamic development in the Himalaya. *Precambrian Res* 74:35–55
- Vijith H, Prasannakumar V, Ninu Krishnan MV, Pratheesh P (2015) Morphotectonics of a small river basin in the South Indian granulite terrain: An assessment through spatially derived geomorphic indices, Georisk: assessment and Management of Risk for Engineered Systems and Geohazards
- Wells SG, Bullard TF, Menges TM, Ritter JB, Wesling JR (1988) Regional variations in tectonic geomorphology along segmented convergent plate boundary, Pacific coast of Costa Rica. *Geomorphology* 1:239–265
- Whittaker AC (2012) How do landscapes record tectonics and climate? *Lithosphere* 4(2):160–164
- Yin A (2006) Cenozoic tectonic evolution of the Himalayan orogen as constrained by along strike variation of structural geometry, exhumation history, and foreland sedimentation. *Earth Sci Rev* 76:1–131
- Zovoili E, Konstantinidi E, Koukouvelas IK (2004) Tectonic geomorphology of escarpments: the cases of Kompotades and Nea Anchialos faults. *Bull. Geol. Soc. Greece* 36:1716–1725

Influence of Neotectonics on Channel Evolution of Kameng River, North–East Himalaya



Balai Chandra Das, Suman Deb Barman, and Aznarul Islam

Abstract In this study, we addressed the impact of neotectonics on channel evolution of the Kameng River of North–East Himalaya. To the end we used ArcGIS software and derived information on the basin’s asymmetry factor, bearing of lineaments and streamlines and hypsometric variables. Information gathered from images and other secondary sources were processed using basin’s asymmetry factor (AF) and revised asymmetry factor (RAF), variance (R^2) for bearing of channel lines explained by bearing of tectonic lineaments, and hypsometric integral (HI) methods. We conclude that neotectonics caused the Kameng basin and its sub-basins tilted and channel links of the Kameng system are evolved following the fault, crack, and joint lines.

Keywords Kameng river · Neotectonics · Revised asymmetry factor · Fault · Fold-thrust

1 Introduction

Landform is the function of structure, process and time (Davis 1899), and most part of the earth’s surface bears the imprints of fluvial processes on its landscapes. Therefore, the evolution of the river channel is the function of the substrate (geological structure and lithology), process, and time. Tectonics have a significant role in the processes and forms of a river system by the control on geology and lithology of the substrate upon which a river flows. In tectonically active areas, where uplift rates keep pace with the erosion rates, rivers are in a dynamic equilibrium state and constantly tries to ‘catch up’ with tectonically driven changes (Charlton 2008). ‘Tectonic style produces the macro-architectural framework and influences the behaviour of rivers at a meso-architectural scale’ (Leeder 1993). The magnitude, position, and development of

B. C. Das (✉)

Department of Geography, Krishnagar Government College, Krishnagar, West Bengal, India

S. D. Barman

Independant Researcher, Barasat, India

A. Islam

Department of Geography, Aliah University, Kolkata, West Bengal, India

the drainage basin are controlled by tectonics which combining with climate and anthropogenic interventions controls the sediment flux of a drainage basin (Islam et al. 2021). Individual channels are highly susceptible to gradient change, channel incision, and avulsion caused by tectonic forces (Islam and Guchhait 2020).

It takes time for a concave profile to develop, so the overall shape of long profiles in tectonically active regions tends to be straight rather than convex. Parallel and trellis drainage patterns tend to develop on acute fault dip. The rectangular component of joints promotes a typical type of drainage pattern with right-angular bends. Lateral tilting causes channel migration and affects sedimentation patterns. In an erosionally graded landscape (Hack 1960, 1973), the longitudinal profile of a stream can provide clues to underlying materials as well as insights into geologic processes and the geomorphic history of an area (Barman et al. 2019). For example, Cox (2014) found control of northwest-trending tilting on drainage patterns of southwestern Mississippi Embayment. Similarly, Coleman (1969) pointed out the effect of seismicity and active subsidence along the eastern margin of the Bay of Bengal and supports an argument for westward ground tilting along the southern reach of the Brahmaputra River.

Kameng River basin in north-eastern India is one of the most tectonically unrest regions of the Eastern Himalaya and it is obvious that the channel network morphology of the river is carrying the prominent imprints of tectonic controls. Srivastava and Misra (2008) studied morpho-sedimentary record of active tectonics at the Kameng River exit and pointed that the river incised 95 m in the span of ~8 ka between 14 and 6 ka BP, and calculated the uplift rate of Siwaliks as 7.5–11.9 mm/year. Chirouze et al. (2014) presented Nd and Hf isotopic data as well as apatite and Zr fission-track analyses from the Miocene–Pliocene Siwalik Group along the recently dated Kameng River section and uncovered the late Neogene exhumation history of the eastern Himalaya. Taral et al. (2019) examined the sedimentology of the Siwalik succession of the Kameng River valley and suggested that sediment transport pathways and deposition took place in open shallow marine to the deltaic environment. In these works, issues of geotectonic and geological evolutions of the discrete parts of the basin have been addressed (Chirouze et al. 2014; Shrivastava and Misra 2008; Taral et al. 2019). However, basin-scale studies from the viewpoint of tectonic control on fluvial geomorphology were found absent in the available literature. Thus, the present chapter intends to address the following objectives.

- (1) To trace out the seismotectonic imprints over the Kameng River Basin.
- (2) To relate the tectonic forces with the trajectories of the basin evolution and fluvial dynamics.

2 Study Area

2.1 Location

The Kameng River (Jia Bharali in Assam) is a river of eastern Himalayan mountains (Fig. 1). The river originates in Tawang district from the glacial lake below snow-capped Gori Chen mountain at $27^{\circ}48'36''$ N and $92^{\circ}26'38''$ E at an elevation of 6300 m, on the *Indo-Tibet border* in South Tibet (Wikipedia 2021). Then the river flows through the states of Arunachal Pradesh and Assam and joins the Brahmaputra River at Tezpur near Koila Bhomora Setu. The river is 264 km long and drains a basin of 11,843 km². The major tributaries are Pachi Para-Keniya-, Wadha, Pakke Bung and Pachuk river (Saha et al. 1989).

2.2 Geology

The surface geological expression of the basin is portrayed by the complex lithology and structure. North–West marginal part of the basin is formed of *Crystalline Complex Overprinted by Himalayan Fold-Thrust Movement [(F)F]* while most of the basin is under *Older Folded Cover Sequence Overprinted by Himalayan Fold-Thrust Movement [(F)FC]*. Both *Older Folded Cover Sequence Overprinted by Himalayan Fold-Thrust Movement* and *Older Cover Sequence Folded During Himalayan Fold Thrust Movement [(F)C]* are characterized by faulting and thrust and strike-slip (Fig. 2). Southern small tract is of *Pre To Syntectonic Granitoid* and *Alluvial Fill in Intra-Tectonic Linear Depression (cl)*.

Northwest–Southeast Bomdila lineament is passing through the basin. A very small tract of basic volcanic formation [(a) BV] is there in the border of *(F)FC* and *(F)C*. East–West oriented southern belt of *Cover rocks of frontal belt affected by fold–thrust movement during the terminal phase of Himalayan Orogeny [(F)Cr]* forms the foothill front of the basin (Fig. 3). Except for namable major lineaments and faults (gravity fault), there are numerous tectonic thrusts and faults and geomorphic lineaments governing the morpho-tectonic look of the basin (Fig. 3).

3 Materials and Methodology

3.1 Materials

ALOSPALSAR radiometric terrain corrected DEM (12.5 m × 12.5 m) was obtained from the Alaska Sattelite facility (*ASF Data Search (alaska.edu)*). Path 498 and frame 530, path 497 and frame 520, 530, 540, path 496 frames 520, 530, 540 were used for

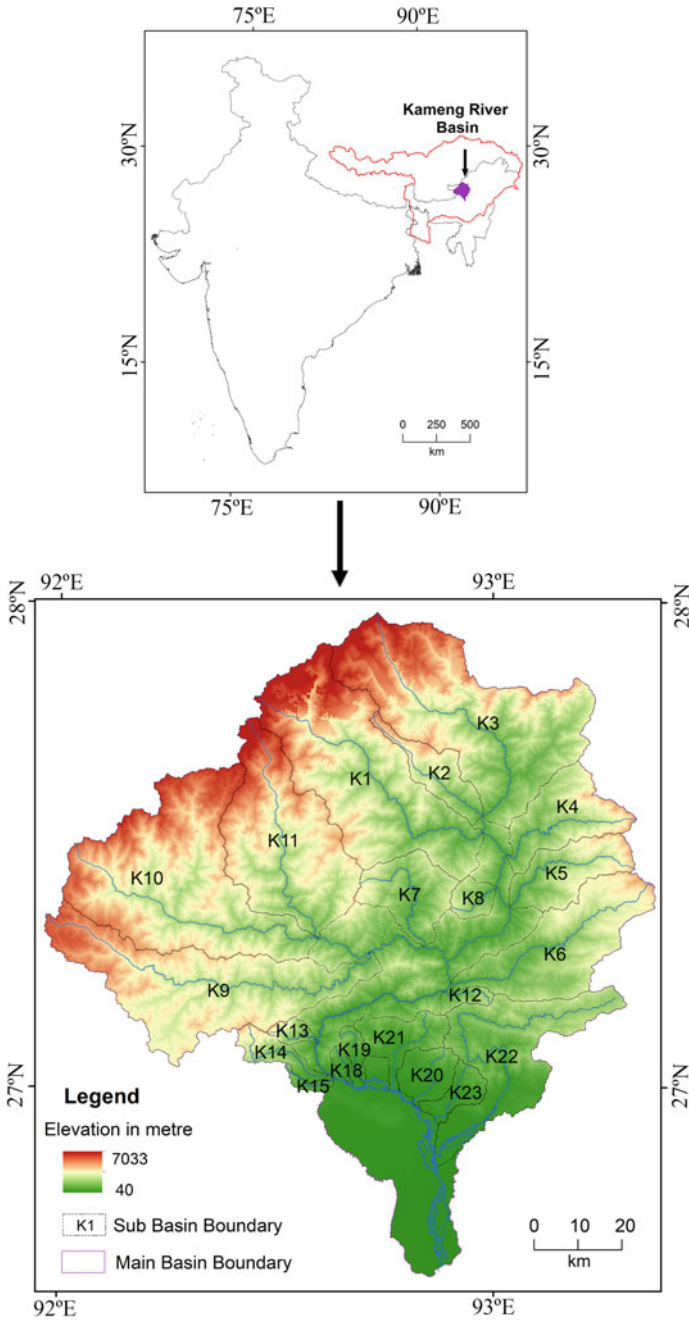


Fig. 1 Location of the Kameng River basin

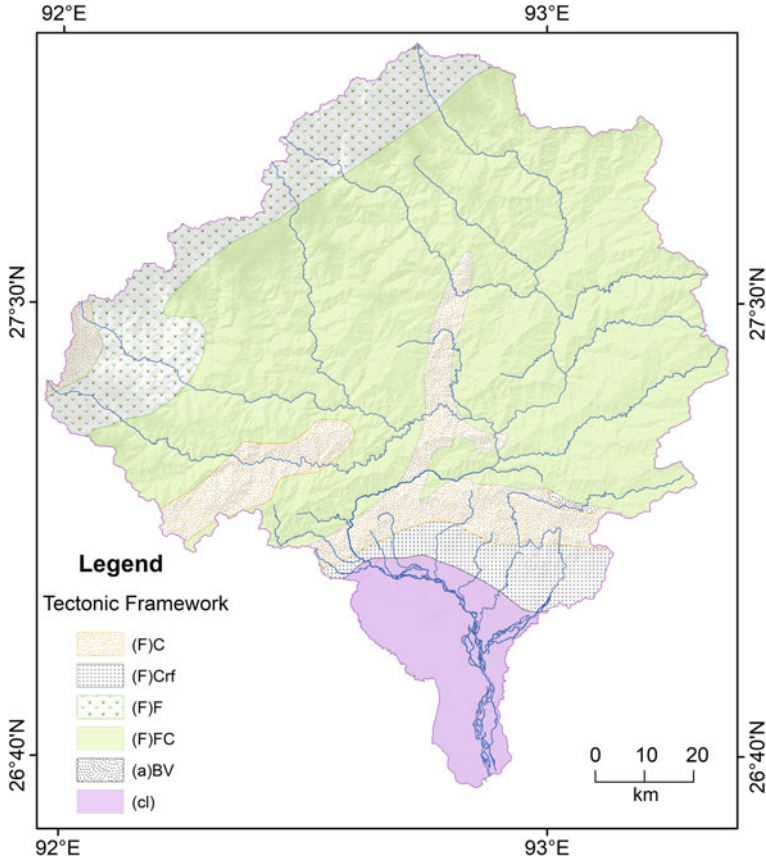


Fig. 2 Tectonic framework of the Kameng basin. (F)C for Older Cover Sequence folded during Himalayan Fold Thrust movement; (F)CrF for Cover rocks of frontal belt affected by fold-thrust movement during terminal phase of Himalayan Orogeny; (F)F for Crystalline complex overprinted by Himalayan fold-thrust movement; (F)FC for Older folded cover sequence overprinted by Himalayan fold-thrust movement; (a)BV for Basic Volcanics; (cl) for Alluvial fill in intracratonic linear depression

the present study. Besides, seismotectonic maps have been collected from the ‘Seismotectonic Atlas Of India And Its Environment’ bearing the sheet number SEISAT 14, 16 (Dasgupta et al. 2000). Moreover, SENTINEL 2 (TILES No. T46RDQ) dated 10 February 2021 has been used for the portrayal of the fault lines. The lithology maps (83A/3,4,7,8,11,12,15,16, 83E/3,4,7,8 83F/1,83B/9,10,13,14) have been taken from the Geological Survey of India (GSI). Moreover, the earthquake databases have been obtained from United States Geological Survey (USGS 2021) and GSI.

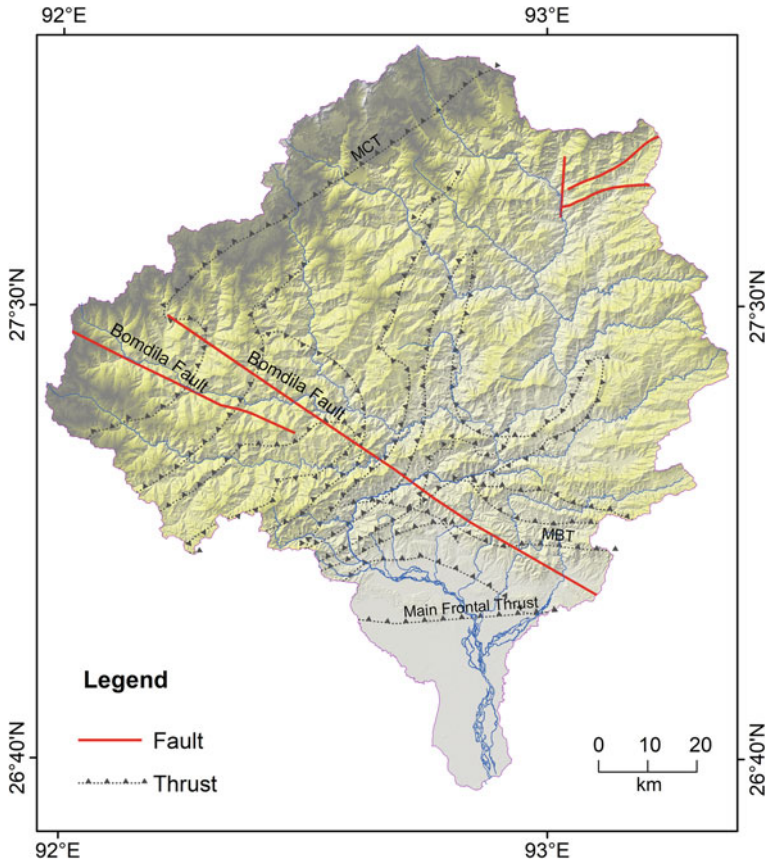


Fig. 3 Distribution of Thrust and Fault lines over the Kameng River basin

3.2 Methodology

3.2.1 Processing of Geospatial Data and Extraction of Information

We have corrected ellipsoidal height into the orthogonal height of ALOS PALSAR DEM with Earth Gravitational Models (EGM-1996) in Arc GIS 10.4 software. Then we processed DEM for Sub-Basin extraction of Kameng River basin with the help of Hydrology tool in Arc GIS Spatial toolbox. Regarding the calculation of the hypsometric Curve using ArcGIS 10.4, the area under the different elevation of each sub-basin has been extracted from the DEM by 'Reclassify Raster' tool in the 3D analyst Arc toolbox and then converted 'Reclassifying Raster to polygon' feature using 'Raster to Polygon conversion' tool. Regrading Basin Asymmetry Factor, each sub-basins polygon has been divided into 2 polygons—one on the left bank and another on the right bank using 'Feature tool' under 'Data Management' toolbox and

area of each side has been measured by using ‘*Calculate geometry*’. For measuring lineament-channel direction, a polyline feature has been drawn parallel to lineament along the meander axis of the channel, and then meander axis bearing has been measured by using the ‘*add geometry*’ attribute tool under ‘*Data management*’ of the Arc toolbox.

3.2.2 Tectonic Indices

Tectonic activities that control drainage and channel patterns and river behaviour (Holbrook and Schumm 1999; Sinha-Roy 2001; Valdiya and Narayana 2007) are described both qualitatively and quantitatively (Hare and Gardner 1985; Keller and Pinter 2002). Various indices are used as a reconnaissance tool to describe the tectonics-morphologies interplay of the drainage basin (Bull and Mc Fadden 1977; Burbank and Anderson 2001). However, amongst these following tools are used in this present study.

Basin Asymmetry Factor

Basin Asymmetry Factor (AF) is described as one of the rapid tools for identifying the ground tilting due to tectonics. The Asymmetry Factor is defined as

$$AF = 100 \left(\frac{Ar}{A} \right) \quad (1)$$

where Ar = Area of the basin to the right side of the trunk stream while facing downstream and A = Total basin area. Each sub-basins polygon was divided into two polygons—left bank and right bank sides using Feature tool under Data Management toolbox and measured area of Each side by using Calculate geometry.

However, this formula is commonly and widely used (Keller and Pinter 1996) and explains that $AF = 50$ describes a symmetrical basin on a stable substrate with no tectonic tilting while both $50 < AF < 50$ indicate asymmetric basin on the tectonically tilted unstable substrate (Keller and Pinter 1996).

But this formula does not bother about the direction of the tilting in which the river migrated. To address this directional parameter of tilting, in this present study, we cloned Knighton’s (1981) channel asymmetry index with a minor modification. In this index, –ve value indicates tilting towards the left side and +ve value indicates tilting towards the right side of the trunk stream. The *revised asymmetry factor* (RAF) is formulated as:

$$RAF = \frac{A_l - A_r}{A} \quad (2)$$

where, A_r = Area of the basin to the right side of the trunk stream while facing downstream, A_l = Area of the basin to the left side of the trunk stream while facing downstream and A = total basin area. The value of the RAF ranges from -1 to $+1$ in cases of extremely leftward and rightward tilted basins respectively while $RAF = 0$ indicates a symmetrical basin on a stable substrate with no tectonic tilting.

Lineament-Channel Directions Correlation

To find out the directions of imprints of tectonics on channel network orientation, a bivariate correlation coefficient was derived using Microsoft office excel. The significance of the correlation was determined by R^2 and the linear trend of correlation is expressed as follows.

$$y = a + bx \quad (3)$$

where y = bearing of channel lines, a = y intercept, b = slope of the line or rate of change of y on unit change of x , x = bearing of lineaments.

Hypsometric Integral

The hypsometric curve was first introduced by Langbein et al. (1947) for topographic characterization, later its properties and applications were added by Strahler (1952). In the hypsometric analysis of erosional topography, Strahler (1952) suggested the high Hypsometric Integral ($HI = 0.54$) is the reflection of accelerated stream erosion as a result of the southward tilting of Louisiana Gulf Coastal Plain. A high value of HI of a basin implies that the basin has been influenced by tectonic activities (Bhadran et al. 2018). Ohmori's (1993) study on Japanese mountains reveals that it is not necessary to have a convex curve for the youthful stage of landscape evolution and mountain building due to concurrent tectonics and denudation rather produce concave or s-shaped curves.

For calculating HI, we used the formula

$$HI = \frac{\sum(X_i Y_{i+1}) - (Y_i X_{i+1})}{2} \quad (4)$$

X = Ratio of the area of the basin above given contour (a) to the total area of the basin (A)

Y = Ratio of the height of a given contour from the base plane (h) to the maximum basin elevation (H).

Transverse Topographic Symmetry

Cox (2014) provided a quick-look tool for identifying possible tilting elements in neotectonic regions using even only topographic maps or satellite images. Like RAF and AF, this technique is of greatest utility where active faults are concealed or poorly exposed. Cox's (2014) algorithm of Transverse topographic symmetry (T) was given as:

$$T = \frac{D_a}{D_d} \quad (5)$$

where D_a = the distance from the active meander-belt midline to the basin midline; D_d = the distance from the basin divide to the basin midline. The value of T ranges between 0 and 1 indicating perfect symmetry and extreme asymmetry of the basin. $T = 0.5$ indicates that $\frac{3}{4}$ of the basin is to the one side of the main channel and $\frac{1}{4}$ is to the other side. This type of asymmetric distribution of the basin is attributed to tectonic tilting. We used this tool also.

4 Neotectonic Movements and Channel Evolution

4.1 Seismotectonic Movements

Kameng basin had gone through several tectonic movements of such scale producing faults, joints, cracks, and thrusts of hefty magnitude. According to GSI published information, 126 earthquakes of magnitudes ranging from 3.2 to 5.7 are recorded during the period 1941–2014 while USGS recorded 80 events of earthquakes of magnitude up to 6 during last 71 years (1950–2021). Therefore, the frequency of seismotectonic events in the Kameng basin is nearly 2 per annum. An interesting observation is that magnitudes of earthquakes as in GSI and USGS records, showing a gradual declining trend with time and depth of the centre of seismic events (Fig. 4).

A normal fault along the course of the Kameng River, hence named Kameng Fault, is interpreted from the litho-contact trends (Saha et al. 1989). The litho units of the two sides of this fault show a difference in altitude of about 200 m. Along the sub-vertical fault plane, the western block has been thrown down. NW–SE oriented trans basin Bomdila Fault, Main Central Thrust (MCT), and Main Boundary Thrust (MBT) faults and Main Frontal Thrusts are other namable tectonic indenture on the basin (Fig. 5a).

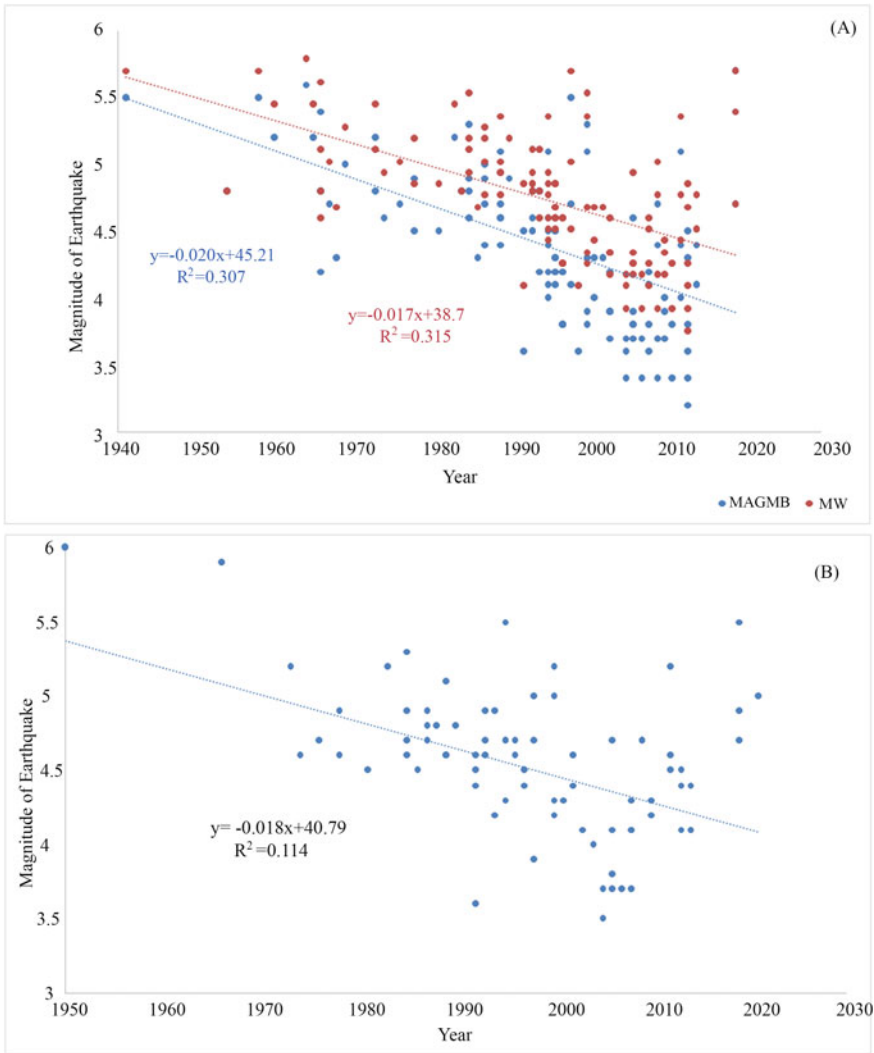
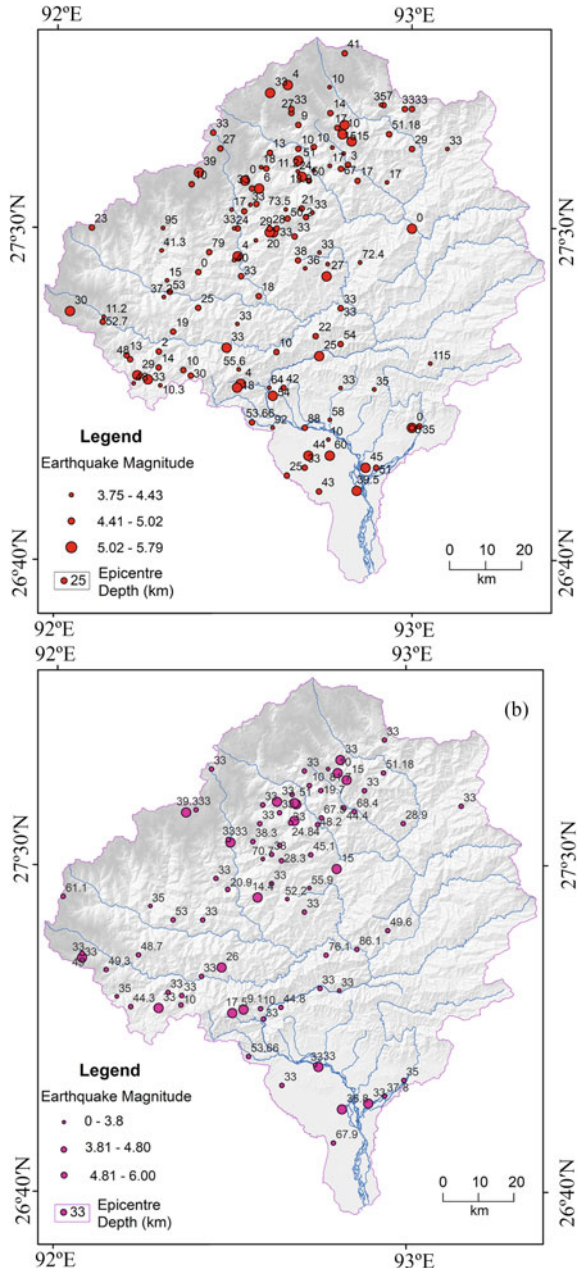


Fig. 4 Declining trend of magnitude of earthquakes. a GSI and b USGS data base

4.2 Neotectonics and Basin Asymmetry

The sinuous trunk stream and basin asymmetry of the river Kameng indicate tectonic controls on channel pattern and basin shape. The unusual hairpin bend of the river to the east of Lower Bhalukpong indicates tectonic controls of Main Boundary Thrust, Kameng Fault, Himalayan Frontal Thrust-1, and Bhalukpong Thrust (Yin et al. 2006; Burgess et al. 2012; Goswami et al. 2018; Srivastava and Misra 2008). The asymmetry factor (AF) of the river basin is 64.82% meaning the area of the right

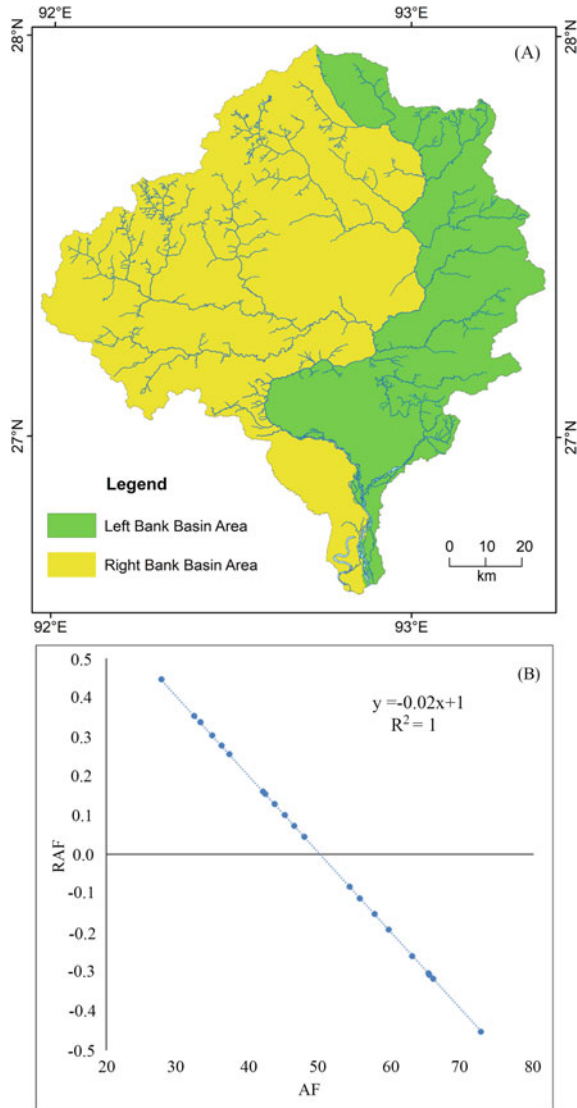
Fig. 5 Seismotectonic movements. **a** GSI. **b** USGS



side of the basin covers 64.82% area of the total area (Fig. 6). Revised asymmetry factor (RAF) -0.30 indicates the leftward tilting of the basin with a very small basin area to the left side of the trunk stream.

To decode the magnitude and direction of neotectonics and to estimate the impact of neotectonics on channel evolution of the Kameng River basin, we analyzed 21 sub-basins of the river Kameng using two simple but effective tools of asymmetry factor (AF) and revised asymmetry factor (RAF). Out of 21 sub-basins, 9 sub-basins are tilted leftward and $>50\%$ area of the basin area is to the right side of the trunk

Fig. 6 a Unequal distribution of left and right part of the Kameng River basin. b Correlation between AF and RAF methods of asymmetry measurement of basin



stream (Fig. 7, Table 1). Rest 12 sub-basins are tilted towards the right and >50% of the basin area is to the left side of the trunk stream. The highest AF 72.53% and RAF -0.45 (K15) indicates that the sub-basin is tilted to the left and the major area of the

Fig. 7 **a** Asymmetry factor of 21 sub-basins and **b** Revised asymmetry of 21 sub-basins of Kameng basin

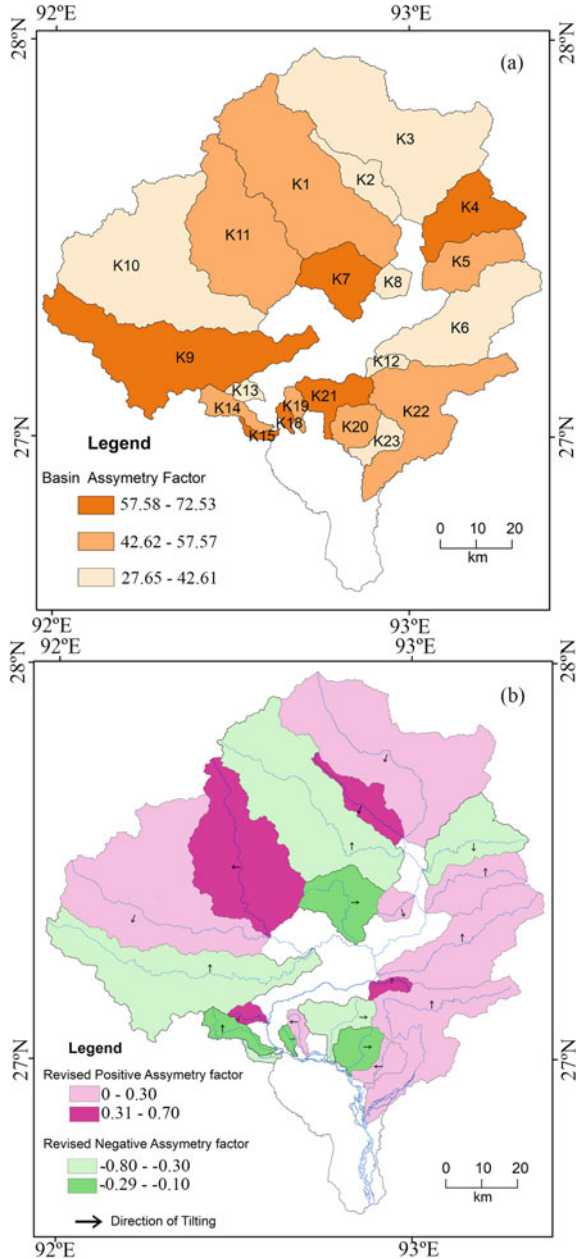


Table 1 Bearing of tectonic lineaments and channel segments nearest to the lineaments

Lineament type	Lineament	Bearing of lineament (degree)	Bearing of channel axis (degree)
Structural lineaments	Fault	68.58	69.26
Structural lineaments	Fault	107.16	109.26
Structural lineaments	Fault	117.09	121.53
Structural lineaments	Fault	212.69	216.43
Structural lineaments	Fault	245.41	256.41
Structural lineaments	Fault	220.34	221.73
Structural lineaments	Fault	269.85	266.49
Structural lineaments	Fault	225.93	225.06
Structural lineaments	Joint/fracture	85.87	82.88
Structural lineaments	Joint/fracture	201.16	203.93
Structural lineaments	Joint/fracture	249.50	252.34
Structural lineaments	Joint/fracture	203.68	205.48

basin lies to the right side of the main river of the sub-basin. The lowest AF 27.66% (K12) indicates that only a minor share of the basin area is to the right side of the trunk stream of the sub-basin. But the RAF 0.45 indicates that the magnitude of symmetry of the K12 sub-basin is equal to that of the K15 (RAF = 0.45) but in opposite direction. Another interesting feature appears from the haphazard arrangement of left tilted sub-basins (colored green and pale blue) and right tilted sub-basins (colored pink and pale pink) that there is no orderliness in the directions of tilting. This observation decodes the crisscrossed pattern of faults and lineaments and subsequent tilting below the surface controlling sub-basins asymmetry. Sub-basin orders, sizes, and perimeters did not affect the values of AF or RAF.

4.3 Lineament-Channel Directions Correlation

We studied the bearing of 12 tectonic lineaments (8 fault-lines and 4 crack and joint lines) and the bearing of channel lines nearest to those tectonic lineaments. It was observed that, in most of the cases, where there is a fault or joints or crack, there is a streamline oriented along that tectonic lineament (Fig. 8). Srivastava and Misra (2008) presented a reach of the Kameng River was flowing along the Kameng Fault downstream to Bhalukpong (Fig. 8b). The regression equation ($y = 0.9996x + 2.476$) of bearings of fault-lineaments and streamlines shows a strong association between the two. The correlation value ($R^2 = 0.9967$) between the two also indicates a strong impact of fault-lineaments on the orientations of stream paths (Fig. 8a).

We studied bearings of 4 cracks/joints and streamlines nearest to those tectonic lineaments. In this case, also, the regression equation ($y = 1.0382x - 5.9553$) and the correlation coefficient ($R^2 = 0.9999$) indicate the firm signature of neotectonics on the orientation of the channel lines. Under this category, we also studied bearings of 253 geomorphic lineaments and 253 streamlines nearest to those lineaments. Here we also found very strong correlation ($R^2 = 0.9003$; $y = 0.9547x + 8.66$) between bearings of lineaments and channel lines (Fig. 9).

4.4 Neotectonics and Basin Altitude-Area Relation

We analyzed 21 minor sub-basins, 4 major sub-basins (Fig. 10a), and the whole basin of the Kameng River using tools of the hypsometric curve, HI and results are shown in Table 2 and Fig. 10b. From Table 2, and Fig. 10 it is apparent that HI of all the major (M1–M4) and minor sub-basins (K1–K22) ranges from 0.25 (K15) to 0.50 (K8). If the whole basin is considered as a single unit, HI of the Kameng River basin is 0.45 and higher than HI values of M1 (0.28), M2 (0.39), M3 (0.42) and M4 (0.36). Minor sub-basin K8 belongs to the major sub-basin M1. There is no such trend of decreasing HI with increasing order of sub-basin within a system of river basin rather we found a very minute positive trend! It is apparent from the seismotectonic framework of the basin that tectonic activities are very common in the upper reaches and lower ordered streams are located in higher altitudes. But we did not find any significant correlation between basin order and HI values of the basins.

4.5 Neotectonics and Transverse Topographic Symmetry (T) of Basins

We analyzed Kameng basin and three sub-basins under the beam of T. It was found that like RAF and AF, T also reveals a significant asymmetric nature of the Kameng basin ($T = 0.450316$) which is probably the manifestation of tectonic tilting of the

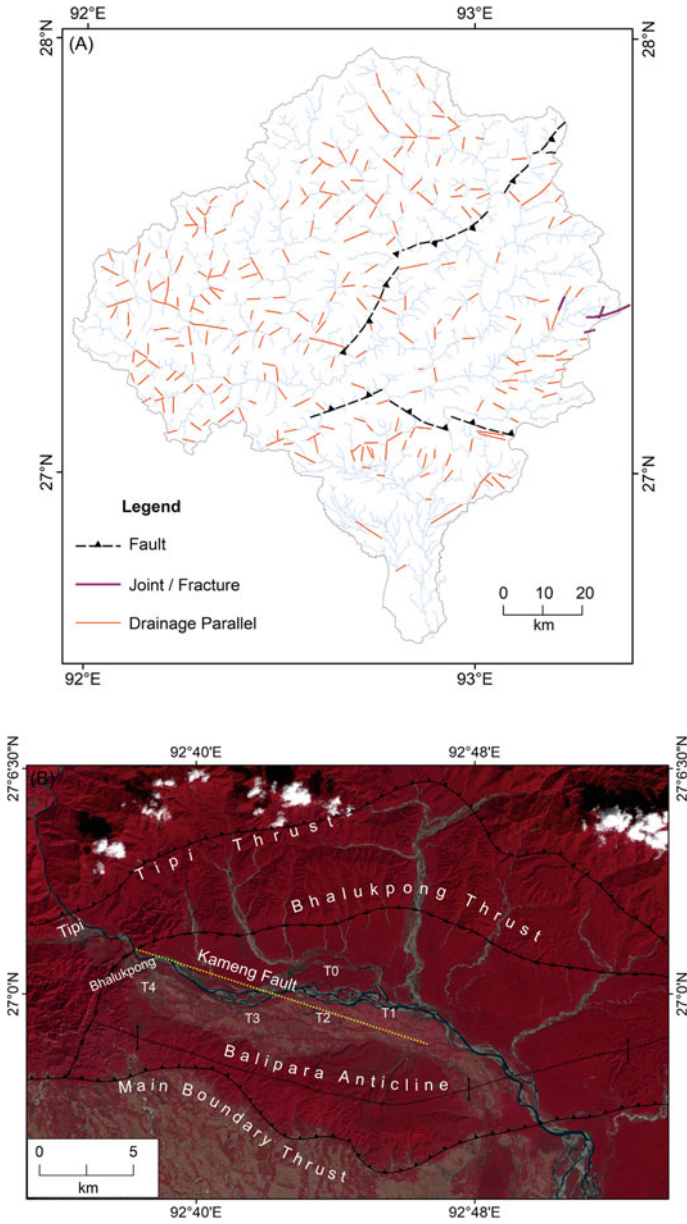


Fig. 8 a Orientation of lineaments and channel links. b Fault-guided channel of the Kameng River near Bhalukpong (After Srivastava and Misra 2007)

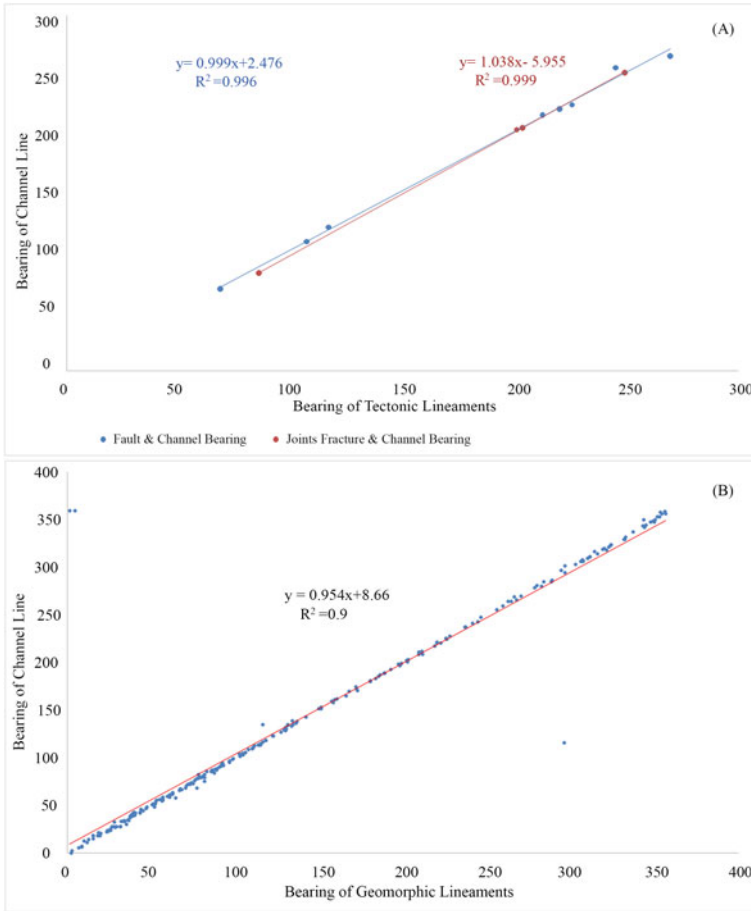


Fig. 9 Variance of bearing of channel line on **a** bearings of tectonic lineaments and **b** bearings of geomorphic lineaments

basin. Nearly 3/4th part of the basin lies to the right side of the main channel keeping only a little above 1/4th part to the left. This massive asymmetry of the basin indexing to the tilting elements of the basin is due to neotectonic events. Amongst sub-basins, K2 has $T = 0.433907$ which is near the average T value of the Kameng basin ($T = 0.450316$). Basin K3 has $T = 0.3202$ while for K6, $T = 0.3322$. So average T value of the Kameng basin is the higher than T values of its sub-basins.

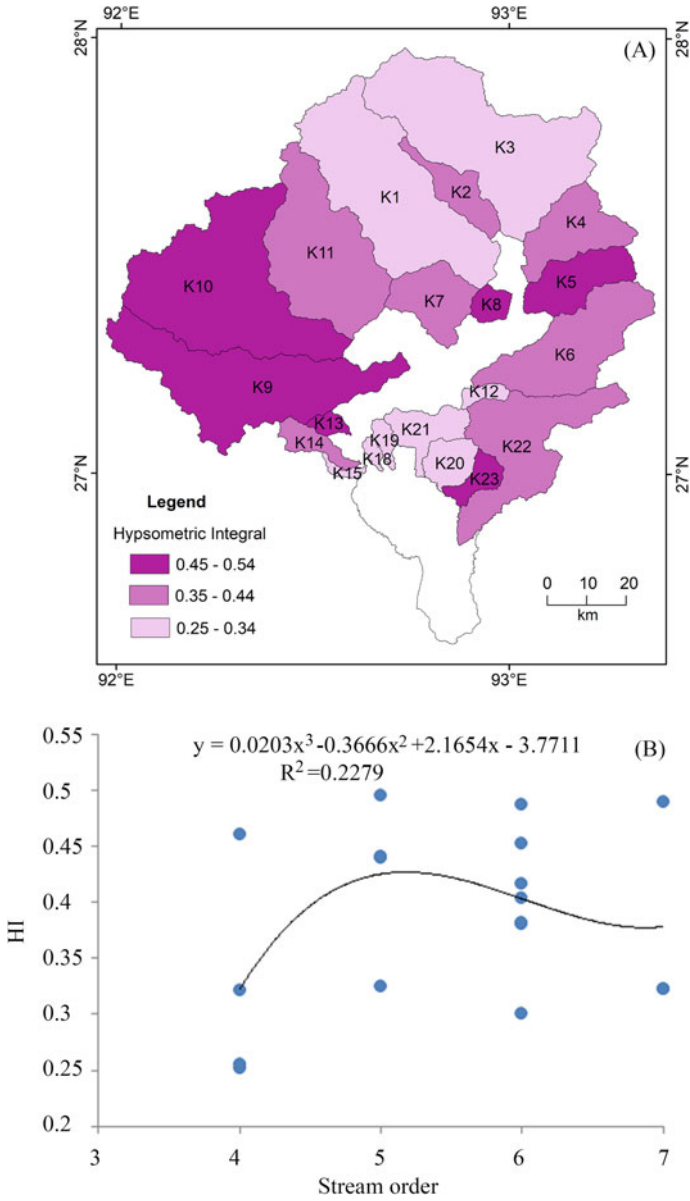


Fig. 10 a Sub-basins of the Kameng River basin and b correlation between stream order and HI values

Table 2 Sub-basin orders, HI values, AF and RAF of Kameng River basin

Sl no	Sub-basin name	Basin order	Hypsometric Integral (HI)	Left bank area km ² (Al)	Right bank area km ² (Ar)	$AF = 100\left(\frac{Ar}{Al}\right)$	$RAF = \frac{Al - Ar}{A}$
1	K1	7	0.32	557.27	191.29	54.09	-0.08
2	K2	5	0.44	127.65	87.85	33.09	0.34
3	K3	7	0.32	847.93	218.26	37.21	0.26
4	K4	6	0.40	123.71	91.67	65.14	-0.30
5	K5	6	0.45	162.88	86.68	44.97	0.10
6	K6	6	0.42	367.92	154.02	42.25	0.15
7	K7	6	0.38	108.35	76.08	62.88	-0.26
8	K8	5	0.50	47.56	35.97	36.08	0.28
9	K9	6	0.49	371.60	221.65	65.28	-0.31
10	K10	7	0.49	882.50	209.10	34.83	0.30
11	K11	6	0.38	487.32	154.84	46.29	0.07
12	K12	4	0.27	33.42	38.17	27.66	0.45
13	K13	4	0.46	29.54	38.10	32.28	0.35
14	K14	5	0.44	45.64	63.35	55.54	-0.11
15	K15	4	0.25	6.86	35.28	72.53	-0.45
16	K18	4	0.26	10.07	26.58	59.56	-0.19
17	K19	4	0.32	25.80	41.87	43.58	0.13
18	K20	5	0.32	58.36	47.16	57.54	-0.15
19	K21	6	0.30	61.86	66.03	65.84	-0.32
20	K22	6	0.36	351.03	211.21	47.73	0.05
21	K23	5	0.54	55.15	52.31	41.93	0.16

5 Conclusion

The Kameng River is located in the north-eastern Himalaya, one of the most tectonically unrest parts of the Indian subcontinent. The channel of the river system and landscape forms are significantly carrying signatures of neotectonics. The basin and its sub-basins are significantly tilted due to neotectonics movements and a number of channel links are oriented along paths of faults, joints, and cracks directed by neotectonics. The pattern of channel evolutions of the region directs towards the interest-avenue of studying meso and micro-scale fluvial forms using morpho-tectonic tools.

References

- Barman SD, Islam A, Das BC, Mandal S, Pal SC (2019) Imprints of Neo-tectonism in the evolutionary record along the course of Khari River in Damodar fan delta of lower Ganga basin. In: Das B, Ghosh S, Islam A (eds) Quaternary geomorphology in India. Geography of the physical environment. Springer, Cham, pp 105–126
- Bhadran A, Vijesh VK, Gopinath G, Girishbai D, Jesiya NP, Thrivikramji KP (2018) Morphohypsometric evolution of the Karuvannur river basin, a Tropical river in Central Kerala, Southwestern Peninsular India. *Arab J Geosci* 11:430. <https://doi.org/10.1007/s12517-018-3794-x>
- Bull W, McFadden L (1977) Tectonic geomorphology north and south of the Garlock Fault, California. In: Doehring DO (ed) Geomorphology in arid regions. Publications in Geomorphology, State University of New York, Binghamton, pp 115–138
- Burbank DW, Anderson RS (2001) Tectonic geomorphology. Blackwell Scientific, Oxford, p 270
- Burgess WP, Yin A, Dubey CS, Shen ZK, Kelty TK (2012) Holocene shortening across the Main Frontal Thrust zone in the eastern Himalaya. *Earth Planet Sci Lett* 357–358(2012):152–167. <https://doi.org/10.1016/j.epsl.2012.09.040>
- Charlton R (2008) Fundamentals of fluvial geomorphology. Routledge, London, p 234
- Chirouze F, Huyghe P, Beek P, Chauvel C, Chakraborty T, Dupont-Nivet G and Bernet M (2014). Tectonics, exhumation, and drainage evolution of the eastern Himalaya since 13 Ma from detrital geochemistry and thermochronology, Kameng River Section, Arunachal Pradesh, *GSA Bulletin*, March/April 2013; vol 125, no 3/4, pp 523–538. <https://doi.org/10.1130/B30697.1>
- Coleman JM (1969) Brahmaputra river: channel processes and sedimentation. *Sediment Geol* 3:129–239
- Cox RT (2014) Analysis of drainage-basin symmetry as a rapid technique to identify areas of possible Quaternary tilt-block tectonics: an example from the Mississippi Embayment. *Geol Soc America Bull* 106:571–581, 7 figs., May 1994. [https://doi.org/10.1130/0016-7606\(1994\)106<0571:AODBSA>2.3.CO;2](https://doi.org/10.1130/0016-7606(1994)106<0571:AODBSA>2.3.CO;2)
- Davis WM (1899) The geographical cycle. *Geogr J* 14:481–504
- Dasgupta S et al (2000) Seismotectonic Atlas of India and its environs. *Geol Surv India Spec Publ* 59:87p
- Goswami TK, Bezbaruah D, Mukherjee S, Sarmah RK, and Jabeed S (2018) Structures and morphotectonic evolution of the frontal fold–thrust belt, Kameng River section, Arunachal Himalaya, India. *J Earth Syst Sci* 127:88. <https://doi.org/10.1007/s12040-018-0984-6>
- Hack JT (1960) Interpretation of erosional topography in humid temperate regions: *Am J Sci* 258-A(Bradley Volume):80–97
- Hack JT (1973) Stream-profile analysis and stream-gradient index. *J Res US Geol Surv* 1(4), July–Aug 1973:421–429
- Hare PH, Gardner TW (1985) Geomorphic indicators of vertical neotectonism along converging plate margins, Nicoya Peninsula, Costa Rica. In: Morisawa M, Hack JT (eds) Tectonic geomorphology. Allen and Unwin, Boston, pp 75–104
- Islam A, Guchhait SK (2020) Characterizing cross-sectional morphology and channel inefficiency of lower Bhagirathi River, India, in post-Farakka barrage condition. *Nat Haz* 103(3):3803–3836
- Islam A, Das BC, Mahammad S, Ghosh P, Barman SD, Sarkar B (2021) Deforestation and its impact on sediment flux and channel morphodynamics of the Brahmani river basin, India. In: Shit PK, Pourghasemi HR, Adhikary PP, Bhunia GS, Sati VP (eds) Forest resources resilience and conflicts. Elsevier, pp 377–415
- Holbrook J, Schumm SA (1999) Geomorphic and sedimentary response of rivers to tectonic deformation: a brief and critique of a tool for recognizing subtle epeirogenic deformation in modern and ancient settings. *Tectonophysics* 305:287–306
- Keller EA, Pinter N (1996) Active tectonics, vol 338. Prentice Hall, Upper Saddle River, NJ
- Keller EA, Pinter N (2002) Active tectonics: earthquakes, uplift and landscape. Prentice Hall, New Jersey

- Knighton AD (1981) Asymmetry of river channel cross-sections: Part I. Quantitative indices. *Earth Surf Proc Land* 6(6):581–588
- Langbein WB et al (1947) Topographic characteristics of drainage basins. *US Geol Surv W.-S. Paper* 968-C, 125–157
- Leeder MR (1993) Tectonic controls upon drainage basin development, river channel migration and alluvial architecture: implications for hydrocarbon reservoir development and characterization. *Geol Soc London, Spec Publ* 173: 7–22. <https://doi.org/10.1144/GSL.SP.1993.073.01.02>
- Ohmori H (1993) Changes in the hypsometric curve through mountain building resulting from concurrent tectonics and denudation. *Geomorphology* 8:263–277
- Saha AK, Singh BK, Keddy KVS, Sharma R, Rao KK, Srivastava JK (1989) Geology of Bameng-Pipu-Chayang Tajo area, East Kameng and lower Subansiri districts, Arunachal Pradesh
- Sinha-Roy S (2001) Neotectonic significance of longitudinal river profiles: an example from the Banas drainage basin, Rajasthan. *J. Geol Soc India* 58:143–156
- Srivastava P, Misra DK (2008) Morpho-sedimentary records of active tectonics at the Kameng River exit, NE Himalaya. *Geomorphol* 96:187–198. <https://doi.org/10.1016/j.geomorph.2007.07.019>
- Strahler AN (1952) Hypsometric (area-altitude) analysis of erosional topography. *Geol Soc Am Bull* 1952(63):1117–1142
- Taral S, Chakraborty T, Huyghe P, Beek P, Vogeli N, Dupont-Nivet G (2019) Shallow marine to fluvial transition in the Siwalik succession of the Kameng River section, Arunachal Himalaya and its implication for foreland basin evolution. *J Asian Earth Sci* 184(2019):103980. <https://doi.org/10.1016/j.jseaes.2019.103980>
- USGS (2021) Earthquake data. United States of America. <https://www.usgs.gov/programs/earthquake-hazards/science/earthquake-data>. Accessed 4 Apr 2021
- Valdiya KS, Narayana AC (2007) River response to neotectonic activity: example from Kerala, India. *J Geol Soc India* 70:427–443
- Wikipedia (2021) Kameng River. From Wikipedia, the free encyclopedia. https://en.wikipedia.org/wiki/Kameng_River. Accessed 27 Mar 2021
- Yin A (2006) Cenozoic tectonic evolution of the Himalayan orogen as constrained by along-strike variation of structural geometry, exhumation history, and foreland sedimentation. *Earth Sci Rev* 76(1–2):1–131